eCAM Evidence-Based Complementary and Alternative Medicine

Application of Complementary and Alternative Medicine on Neurodegenerative Disorders: Current Status and Future Prospects

Guest Editors: Paul Siu-Po Ip, Karl Wah-Keung Tsim, Kelvin Chan, and Rudolf Bauer

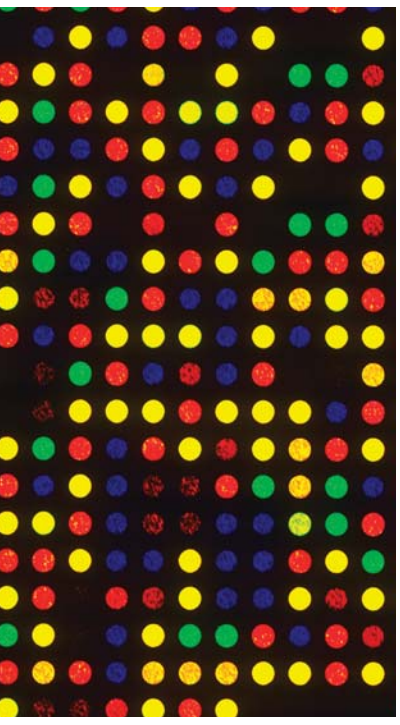

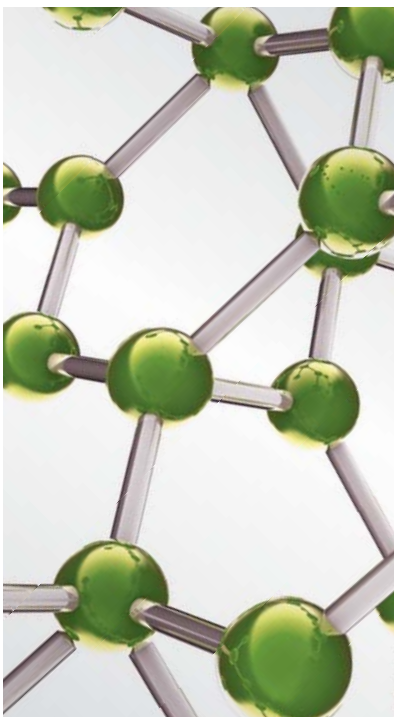


Application of Complementary and Alternative Medicine on Neurodegenerative Disorders: Current Status and Future Prospects

Evidence-Based Complementary
and Alternative Medicine

Application of Complementary and Alternative Medicine on Neurodegenerative Disorders: Current Status and Future Prospects

Guest Editors: Paul Siu-Po Ip, Karl Wah-Keung Tsim, Kelvin Chan, and Rudolf Bauer

Editorial Board

Contents

Hindawi Publishing Corporation
Evidence-Based Complementary and Alternative Medicine
Volume 2012, Article ID 930908, 2 pages
doi:10.1155/2012/930908

Editorial

Application of Complementary and Alternative Medicine on Neurodegenerative Disorders: Current Status and Future Prospects

Paul Siu-Po Ip,[1] Karl Wah-Keung Tsim,[2] Kelvin Chan,[3,4] and Rudolf Bauer[5]

[1] *School of Chinese Medicine, The Chinese University of Hong Kong, Hong Kong*
[2] *Division of Life Science, The Hong Kong University of Science and Technology, Hong Kong*
[3] *Faculty of Pharmacy, The University of Sydney, Sydney, NSW 2006, Australia*
[4] *Centre for Complementary Medicine Research, University of Western Sydney, Sydney, NSW 2560, Australia*
[5] *Department of Pharmacognosy, Institute of Pharmaceutical Sciences, University of Graz, 8010 Graz, Austria*

Correspondence should be addressed to Paul Siu-Po Ip, paulip@cuhk.edu.hk

Received 6 November 2012; Accepted 6 November 2012

Neurodegenerative disorders are defined as hereditary and sporadic conditions which are characterized by progressive loss of structure or function of neurons in sensory, motor, and cognitive systems. Alzheimer's disease, Parkinson's disease, and depression are well-known examples of neurodegenerative disorders. The World Health Organization estimates that, by 2040, neurodegenerative diseases will surpass cancer as the principal cause of death in industrialized countries. Despite various advances in the understanding of the diseases, pharmacological treatment by conventional medicine has not obtained satisfactory results. Therefore, complementary and alternative medicine (CAM) can be a potential candidate for the preventative treatment of the disorders. The aim of this special issue is to demonstrate the clinical evidence and explore the acting mechanisms of CAM in treating neurodegenerative disorders.

Alzheimer's disease is a well-recognized neurodegenerative disease characterized by a progressive deterioration of cognitive function and memory. At present, there are no effective treatments that can stop or reverse the progression of the disease. Pharmaceutical interventions that aim to delay the deterioration of this disease have been extensively studied. Although cholinesterase inhibitors and an N-methyl-D-aspartate receptor antagonist have been widely used for treating the syndromes of the disease, these drugs have not shown promising results and their uses are always limited by their undesirable side effects. In this special issue, several studies have shown that CAM can be useful for the management of the disease.

Although the pathological cause of Alzheimer's disease has not been fully understood, the deposition of beta-amyloid is believed to be one of the risk factors. Therefore, neurotoxicity induced by beta-amyloid is commonly used as a cellular or animal model of Alzheimer's disease. In this issue, an animal study showed that oral administration of Yi-Chi-Tsung-Ming-Tang (Table 1) ameliorated beta-amyloid injection-induced learning and memory impairments. Further investigation by biochemical analysis showed that the herbal decoction decreased amyloid accumulation and reversed acetylcholine decline in the hippocampus of the animals treated with beta-amyloid.

There are two studies on cellular model of Alzheimer's disease with *Flemingia macrophylla* and *Uncaria rhynchophylla*, respectively. Beneficial effects of both medical herbs have been suggested for the management of Alzheimer's disease. By using bioassay-guided fractionation, rhynchophylline and isorhynchophylline have been identified as the active ingredients of *Uncaria rhynchophylla*. The neuroprotective effect of these chemical ingredients has been suggested to be mediated by inhibiting intracellular calcium overloading and tau protein hyperphosphorylation.

Depression is a chronic mental disorder clinically characterized by a pervasive low mood, loss of interest or pleasure in daily activities, low self-esteem, and a high suicidal tendency.

Table 1: Composition of herbal formulae.

Herbal formulae	Component herbs[#]
Yi-Chi-Tsung-Ming-Tang	Astragali Radix, Cimicifugae Rhizoma, Ginseng Radix, Glycyrrhizae Radix et Rhizoma, Paeoniae Radix Alba, Phellodendri Chinensis Cortex, Puerariae Lobatae Radix, and Viticis Fructus.
Shu-Yu-San	Albiziae Flos, Acori Tatarinowii Rhizoma, Bupleuri Radix, Curcumae Radix, Gardeniae Fructus, Menthae Herba, Polygalae Radix, Poria, and Ziziphi Spinosae Semen.
Kai-Xin-San	Acori Tatarinowii Rhizoma, Ginseng Radix et Rhizome, Polygalae Radix, and Poria.
Baihe-Dihuang-Tang	Lilii Bulbus and Rehmanniae Radix.
Danggui-Shaoyao-San (Toki-Shakuyaku-San)	Alismatis Rhizoma, Angelicae Sinensis Radix, Atractylodis Macrocephalae Rhizoma Chuanxiong Rhizoma, Paeoniae Radix Alba, and Poria.

[#]Official name listed in Pharmacopoeia of China (2010 Edition), Chinese Medical Science and Technology Press, Beijing, China.

Although the monoamine theory of depression has been extensively investigated, it is unable to fully explain the pathophysiology of depression. In recent years, a huge amount of evidences suggesting a causal relationship between the incidence of major depressive disorders and neurodegenerative processes such as the decreased neurotrophic factors, altered neuronal plasticity, neuronal atrophy, or destruction in the hippocampus and cortex has been published.

At present, there are several types of antidepressants available for pharmaceutical management of the disease including tricyclic antidepressants, monoamine oxidase inhibitors, selective serotonin reuptake inhibitors, noradrenergic reuptake inhibitors, serotonin, and noradrenaline reuptake inhibitors. However, due to the multiple pathogenic factors involved in depression, many antidepressant drugs show low response rates and may cause adverse side effects such as cardiotoxicity, hypertensive crisis, sexual dysfunction, and sleep disorder. Therefore, a number of herbal remedies have been suggested to be safe, better tolerated, and efficacious antidepressants. In this issue, several research articles have shown that herbal prescriptions, including Shu-Yu-San, Kai-Xin-San, Baihe-Dihuang-Tang, and Danggui-Shaoyao-San (Table 1), are effective antidepressants on animal model of depression.

In this special issue, we have collected a couple of clinical studies on the application of CAM in treating neurodegenerative diseases. Although the scale of these studies is small, all of them have demonstrated a promising effect of CAM on neurodegenerative diseases. For example, a study of Toki-Shakuyaku-San (Danggui- Shaoyao-San in Chinese phonetic name), a six-herb Chinese medicine (Table 1), on patients with mild cognitive impairment and Alzheimer's disease showed that treatment with Toki-Shakuyaku-San for eight weeks significantly increased regional cerebral blood flow in the posterior cingulate and tended to improve cognitive impairment in these patients. Another randomized clinical trial showed that Saffron (flower of *Crocus sativus*) supplement improved retinal flicker sensitivity in patients with early age-related macular degeneration and the beneficial effect of the herbal drug was extended over a 14-month follow-up study.

In this special issue, a large amount of evidences have shown that CAM can be an efficacious treatment for neurodegenerative disorders. However, a large-scale, double-blind, and placebo-controlled trial is still needed to demonstrate the clinical effect of CAM on these diseases.

Acknowledgments

We thank the authors of this special issue for their contributions. We would like to express our sincerely gratitude to all reviewers for their valuable comments in the peer review.

Paul Siu-Po Ip
Karl Wah-Keung Tsim
Kelvin Chan
Rudolf Bauer

Hindawi Publishing Corporation
Evidence-Based Complementary and Alternative Medicine
Volume 2012, Article ID 381278, 16 pages
doi:10.1155/2012/381278

Research Article

Xiaoyaosan Decoction Regulates Changes in Neuropeptide Y and Leptin Receptor in the Rat Arcuate Nucleus after Chronic Immobilization Stress

Shao-Xian Wang, Jia-Xu Chen, Guang-Xin Yue, Ming-Hua Bai, Mei-Jing Kou, and Zhong-Ye Jin

School of Preclinical Medicine, Beijing University of Chinese Medicine, P.O. Box 83, No. 11, Beisanhuan Donglu, Chaoyang District, Beijing 100029, China

Correspondence should be addressed to Jia-Xu Chen, chenjiaxu@hotmail.com

Received 25 April 2012; Revised 29 August 2012; Accepted 20 September 2012

Academic Editor: Paul Siu-Po Ip

The arcuate nucleus (ARC) in the basal of hypothalamus plays an important role in appetite regulation and energy balance. We sought to investigate the central neuroendocrine mechanism of appetite decrease and weight loss under chronic stress by observing the regulatory effects of Xiaoyaosan decoction in the expression of leptin receptor (*ob-R*) and neuropeptide Y (NPY) in the ARC. Our results showed that bodyweight and food intake of rats in the 21-day stress group increased slower than those of the normal group. Higher contents of Leptin and *ob-R* were noted in the 21-day stress group compared with control rats, while NPY expression was not statistically different. Xiaoyaosan powder can significantly downregulate the contents of leptin and *ob-R* in the hypothalamus of stressed rats. These findings suggest that increase of *ob-R* expression in the ARC is possibly one key central neuroendocrine change for the somatic discomfort. Weight loss and decreased food intake in rats caused by the binding of leptin to *ob-R* in hypothalamus do not appear to utilize the NPY pathway. This study also suggests that *ob-R* in the ARC may act as the target of Xiaoyaosan in regulating the symptoms such as appetite decrease and bodyweight loss under chronic stress.

1. Introduction

The body needs timely adjustment of physiological status to adapt to stress. Moderate stress is beneficial to the body; while excessive stress can influence the body's mental and physical health. Studies show that stressful events significantly affect body's feeding behaviors [1] and that, long-term, chronic, and repeated stresses can cause decreased food intake and bodyweight loss in rats [2–6]. Previous experiments of this research team also suggested that chronically stressed rats presented abnormalities of emotions and behaviors such as depression and anxiety, which were mostly accompanied by slow increases of food intake and bodyweight along with other changes [7, 8]. At present, most research focuses on the central neuroendocrine mechanisms of abnormalities of emotions and behaviors such as stress-induced depression and anxiety; while there are few studies on the mechanisms underlying food intake and bodyweight changes under stress.

The hypothalamic nucleus group is required for the regulation of energy balance. Specifically, the ARC in the basilar part of hypothalamus plays an important role in appetite regulation and energy balance. Neuropeptide Y (NPY) is a polypeptide with biological activity composed of 36 amino acids that is widely distributed in the mammalian central and peripheral nervous systems. In hypothalamus, NPY content is the highest; while expression of NPY neurons in hypothalamus is the most in the ARC [9]. Leptin receptor (*ob-R*) belongs to a family of cytokines. The hormone receptor *ob-R* plays a role by binding with specificity of leptin to regulate many physiological functions. Also, *ob-R* is widely distributed in the central nervous system of normal rats and hypothalamus nucleus groups such as the ARC, paraventricular nucleus, ventromedial nucleus,

and orsomedial [10, 11]. Studies show that *ob-R* and NPY coexist in the ARC [12–14] and that the binding of *ob-R* with leptin can influence the synthesis and secretion of NPY and, thus, regulate food intake and energy metabolism [15–17]. Specifically, NPY can enhance appetite and promote food intake. Conversely, binding of *ob-R* can inhibit appetite and decrease food intake. In energy metabolism, feeding behavior and bodyweight, NPY and *ob-R* oppose and assist each other.

Studies showed that NPY can regulate emotional and behavioral changes caused by stress and can induce antistress and antianxiety effects in multiple-stress animal models [18, 19]. The hypothalamic-pituitary-adrenal (HPA) axis and NPY influence each other [20–23], and NPY is regarded as the "stress molecule" [24, 25], which plays an important role in the common core mechanism of psychological and somatic stress responses. However, there is still no systematic study on the mechanism of *ob-R* change in central nervous system under stress and the mechanism of how NPY and *ob-R* regulate appetite and energy metabolism under stress.

The Xiaoyaosan prescription originated from the book *Taiping Huimin Heji Jufang* in the Song Dynasty (960–1127 A.D.) and was composed of eight crude drugs, such as Radix Angelicae Sinensis, Radix Paeoniae Alba, Radix Bupleuri, Rhizoma Atractylodis Macrocephalae, Radix Et Rhizoma Glycyrrhizae, Poria, Rhizoma Zingiberis Recens, and Herba Menthae Haplocalycis. Xiaoyaosan is prescribed to sooth the liver, tonify spleen, and nourish blood. The finished products (pill, decoction, etc.) were always used to treat mental diseases such as depression for centuries in China [26, 27]. Now, they are being used for multiple-system diseases such as mental disorders, neurological diseases, digestive system diseases, respiratory diseases, endocrine diseases, and gynecologic diseases [28–30]. The reliability of the therapeutic effect of Xiaoyaosan in relieving symptoms of chronic stress has been widely proved. For example, Xiaoyaosan can influence the expression of the genes encoding proopiomelanocortin (POMC), corticotropin releasing factor (CRF), encephalin, and preprodynorphin [31, 32]. Xiaoyaosan also reversed chronic immobilization stress-(CIS-) induced decreases in brain-derived neurotrophic factor(BDNF) and increases in tyroxine hydroxylase (TrkB) and neurotrophin 3 (NT-3) in the frontal cortex and the hippocampal CA1 subregion [7]. Xiaoyaosan can interfere with metabolic network abnormalities of chronic unpredictable mild stress or CIS model animals, and we should further seek or elucidate the targets or receptor of characteristic metabolic molecules of antistress effect of drugs [33–35].

Based on the regulating effect of *ob-R* and NPY in the ARC on appetite and energy metabolism and the defined anti-stress effect of Xiaoyaosan, we studied changes in NPY and *ob-R* in the ARC of rats stressed by chronic immobilization in order to elucidate the possible mechanisms of appetite decrease and bodyweight loss under chronic stress. At the same time, we also studied the regulating effect of Xiaoyaosan decoction on the above changes.

2. Materials and Methods

2.1. Animals. The healthy male Sprague Dawley (SD) rats with bodyweight of 180 ± 20 g were purchased from Beijing Vital River Laboratory Animal Technology Limited Company. Standard animal feeding room: room temperature: 21 ± 1°C; relative humidity: 30% to 40%; Light condition: (light for 12 h: 07:00 to 19:00, darkness for 12 h: 19:00 to 07:00); *ad libitum* purified water. The rats were randomly divided into 4 groups, namely, the control group, the 7-day stress group, the 21-day stress group, and the Xiaoyaosan-treated group, which were also stressed. In each group, there were 24 rats in 8 cages and 3 rats in each cage. The rats in the normal control group were fed routinely for 21 days; continuous immobilization stress for 3 h/day for 7 days was conducted for the rats in the 7-day stress; continuous immobilization stress for 3 h/day for 21 days was conducted for the rats in the 21-day stress groups; while continuous immobilization stress for 3 h/day was conducted for the rats in the Xiaoyaosan-treated group for 21 days. Xiaoyaosan was intragastrically administered 30 min before chronic immobilization stress. The rats were fed and provided with water *ad libitum*. All the animals in the study were maintained in accordance with the guidelines of China legislations on the ethical use and care of laboratory animals. All efforts were made to minimize animal suffering and the number of animals needed to produce reliable data.

2.2. Preparation of Extracts of Xiaoyaosan. Composition proportions of Xiaoyaosan prescription: *Poria : Radix Paeoniae Alba : Radix Et Rhizoma Glycyrrhizae: Radix Bupleuri : Radix Angelicae Sinensis : Rhizoma Atractylodis Macrocephalae: Herba Menthae Haplocalycis : Rhizoma Zingiberis Recens* equaled to 3 : 3 : 1.5 : 3 : 3 : 3 : 1 : 1. All 8 crude drugs were purchased from Beijing Tongrentang (Bozhou) Decoction Pieces Limited Company and authenticated by Dr. B. Liu, Department of Botany, and Beijing University of Chinese Medicine. All crude drugs were extracted by the Chinese medicine preparation room of China-Japan Friendship Hospital as previously described [7]. Extraction steps were performed as follows: *Poria, Radix Paeoniae Alba, and Radix Rhizoma Glycyrrhizae* were boiled and extracted three times with 10 volumes (2 h), 8 volumes (1 h), and 8 volumes (1 h) of water to obtain the extraction liquid (A). *Radix Bupleuri, Radix Angelicae Sinensis, Rhizoma Atractylodis Macrocephalae, Herba Menthae, and Rhizoma Zingiberis Recens* were soaked with 10 volumes of water for 12 h to obtain the volatile oil, drug liquid (B), and drug residue (C). Subsequently, C was boiled in 8 volumes of water for 1 h and extracted twice to obtain the extraction solution (D). Extraction solutions A, B, and D were mixed to form the water extraction liquid (E). Next, E was filtered and centrifuged (3000 r/min for 40 min). The supernatant was collected and vacuum dried at 70°C. Then, the dried product and the volatile oil were processed into dry decoction for use. The extraction rate was 18.8%. Xiaoyaosan (was dissolved in deionized water and administered by intragastric injection at a dose of) was 3.854 g/kg·d, and deionized water was used in all groups.

2.3. Chronic Immobilization Stress (CIS) Procedure. A previously described chronic constraint method [31] was used in which rats were bound to a binding rack (type T binding platform: the base: width of 10 cm, length of 20 cm, thickness of 2.8 cm; the upper part of binding platform for rat binding: length of 22 cm, maximum width of 6.6 cm; the front end had small frames for fixing the head and small grooves suitable for placing limbs; the upper binding platform had two adjustable soft belts which could, respectively, fix the chest and abdomen of animal) for 3 h every day. Binding time points were randomly selected from 7:00 am to 16:00 pm in an effort to avoid the animal adaptation to a fixed binding time. Moreover, before administration, bodyweight and food intake of rats (including those at 0 day) were weighed. Daily food intake was calculated by subtracting the intraday surplus food amount from the feeding amount at the last one day.

2.4. ELISA for Measurement of Leptin, NPY, and ob-R Content in Hypothalamus. On the 22nd day of the trial, 6 rats in the normal control group, the 21-day stress group, and the Xiaoyaosan-treated group were anaesthetized with an intraperitoneal injection 10% chloral hydrate (0.35 to 0.40 mL/100 g bodyweight). Subsequently, the hypothalamus was removed and placed a 2 mL EP tube, immediately frozen on liquid nitrogen (http://www.iciba.com/liquid nitrogen) and stored below −20°C. To create a hypothalamus homogenate: the hypothalamus specimen was boiled in 1 mL normal saline for 3 min. Then, 0.5 mL of 1 N glacial acetic acid was added, and the mixture was homogenized with hand-held electric homogenizer. Next, 0.5 mL of 1 N NaOH was added for neutralization. The solution was mixed uniformly and centrifuged at 3500 ×g for 20 min at 4°C. The supernatant was collected and stored at −20°C. According to the kit instructions, leptin, *ob-R*, and NPY contents in hypothalamus were detected by ELISA method.

2.5. Double-Labeling Immunofluorescence for NPY and ob-R in the ARC of Hypothalamus. On the 8th day of the trial for the 7-day stress group and on the 22nd day of the trial for the normal control group, the 21-day stress group and Xiaoyaosan-treated group, samples were acquired (the same as following test). 6 rats in each group were anaesthetized with an intraperitoneal injection of 10% chloral hydrate (0.35 to 0.40 mL/100 g bodyweight), and the left ventricular ascending aortic perfusion fixation of the heart was carried out. Firstly, the samples were quickly washed with 0.9% NaCl solution (precooled to 4°C in advance) by perfusion, and then 4% paraformaldehyde solution was perfused with continuously. Perfusion was stopped when the tail tip hardened. Rats were sacrificed by decapitation and the whole brain was taken out. The whole brain was placed into 4% paraformaldehyde solution, stored at 4°C, and fixed for 12 h. Brain tissues were transferred into sucrose solutions with concentration of 20% and 30% for dehydration and stored at 4°C. The constant temperature freezing microtome (Leica CM1900) was used for sectioning, and section thickness was about 30 μm.

The main steps of double-labeling immunofluorescence were as follows: (1) washed with 0.05 M TBS three times, 5 min once; (2) incubated in 0.05 M TBS containing 0.5% TritonX-100 for 1 h in the incubator at 37°C; (3) washed with 0.05 M TBS three times, 5 min each; (4) added 0.05 M TBS blocking liquid containing 10% donkey serum (Millipore Corporation, USA) and 0.5% TritonX-100 and incubated for 1 h at room temperature; (5) removed blocking liquid and adding 1 : 500 of rabbit antineuropeptide Y polyclonal antibody (Millipore Corporation, USA) diluted with 0.05 M TBS containing 2% donkey serum and 0.5%TritonX-100 and incubated at 4°C overnight; (6) washed with 0.05 M TBS containing 2% donkey serum and 0.5% TritonX-100 for three times, 5 min each; (7) added 1 : 200 of Alexa Fluor@ 594 donkey anti-rabbit IgG (Invitrogen, USA, dilution liquid, the same as antibody I) and incubated for 4 h at room temperature, protected from light; (8) washed with 0.05 M TBS for three times, 5 min each; (9) added the blocking liquid (the same as step (4)) and incubated for 1 h at room temperature; (10) removed the blocking liquid and adding 1 : 50 of Goat anti-*ob-R* polyclonal antibody (Santa Cruz Biotechnology, Inc., USA) diluted with 0.05 M TBS containing 2% donkey serum and 0.5% TritonX-100. The mixture was incubated for 40 h at 4°C; (11) washed for three times, 5 min each (the same as step (6)); (12) added 1 : 200 of Alexa Fluor@ 488 donkey anti-goat IgG (Invitrogen, USA, dilution liquid, the same as antibody I). The mixture was incubated for 4 h at room temperature, protected from light; (13) washed with 0.05 M TBS for three times, 5 min each; (14) mounted the section on glass slide, and HardSet Mounting Medium with DAPI (Vector H-1500, USA) was used for sealing. Tris was purchased from Sigma Company; TritonX-100, paraformaldehyde, NaCl, and sucrose were purchased from Beijing Chemical Reagent Limited Company.

ZEISS LSM510 META laser scanning confocal microscope was used for imaging and analysis of 10 slices in each group. The integral optical density (IOD), NPY and *ob-R* colocalization area, and NPY or *ob-R* weight colocalization coefficient were calculated and selected for statistics from analytic results. weight colocalization coefficient represents sum of intensities of colocalizing pixels in channel 1 or 2, respectively, as compared to the overall sum of pixel intensities above threshold and in this channel. Value range of 0-1 (0: no colocalization, 1: all pixels colocalization). The number of positive neurons was measured with Image Pro Plus.

2.6. In Situ Hybridization for NPY mRNA and ob-R mRNA in the ARC. Six rats in each group were injected intraperitoneally with 10% chloral hydrate (0.35 to 0.40 mL/100 g bodyweight), left ventricular ascending aortic perfusion prefixation was carried out, and postfixation of 4% paraformaldehyde was conducted (3 to 8 h). Subsequently, brain tissues were transferred into sucrose solutions with concentration of 20% and 30% for dehydration. The specific steps were the same as in the double-labeling immunofluorescence experiment described above. 0.9% NaCl solution, post-fixation solution of 4% paraformaldehyde, and 20% and 30% sucrose solutions were prepared with

RNase-Free water. Constant temperature freezing microtome (Leica CM1900) was used for sectioning, and section thickness was about 14 to 15 μm.

In situ hybridization assay kits of rat NPY and *ob-R* were purchased from Wuhan Boster Biological Engineering Limited Company. (1) mRNA sequences of rat *ob-R* target gene: (a) 5′-ATTTT CCACC CAAAA TTCTG ACTAG TGTTG-3′; (b) 5′-ATCTG GCTAT ACAAT GTGGA TCAGG ATCAA-3′; (c) 5′-AAGTT CCTAT GAGAG GGCCT GAATT TTGGA-3′. (2) mRNA sequences of rat NPY target gene: (a) 5′-TACCC CTCCA AGCCG GACAA TCCGG GCGAG-3′; (b) 5′-CTGCG ACACT ACATC AATCT CATCA CCAGA-3′. According to the kit instructions, *in situ* hybridization staining was conducted. All the used solutions were prepared with RNase-Free water. Elite ABC Kit was purchased from Vector, USA; DEPC, Tris, and DAB were purchased from Sigma, USA.

ZEISS Primo Star microscope was used for imaging, and Image-Pro Plus 6.0 Image Analysis System was used for image analysis. Nine slices in each group were selected from the ARC positions (area of 150 μm × 150 μm). In addition, the number of positive cells (cells) and integral optical density (IOD) were counted. IOD = measured value of IOD/total measured area.

2.7. RT-qPCR for NPY mRNA and ob-R mRNA in the ARC. Six rats in each group were anaesthetized with intraperitoneal injected 10% chloral hydrate (0.35 to 0.40 mL/100 g bodyweight). Brain tissues were rapidly taken out, immediately frozen on liquid nitrogen, and stored at −80°C. Solutions were prepared with DEPC-treated water, and vessels were soaked in DEPC water and sterilized at high temperature.

Oven temperature of the constant temperature freezing microtome (Leica, Germany) was adjusted to −10°C. The section thickness was set as 60 μm (the maximum setting), and shook the hand shank of frozen section to turn back 5 rings with forward 1 ring, then, 300 μm brain tissue was sectioned, and effective tissue slices were selected and placed onto clean glass slides. The ARC was taken out on dry ice with a flat needle, placed into RNase-Free 1.5 mL EP tube, immediately frozen in liquid nitrogen, and stored at −80°C.

Brain tissues were completely homogenized with a handheld electric homogenizer (KONTES, USA), and the total RNA of the ARC was extracted by using the Trizol method and stored at −70°C. According to the instructions of GoTaq@ 2-Step RT-qPCR System kit (Promega Corporation, USA), reverse transcription reaction and quantitative determination of cDNA were conducted.

According to Genebank sequences and the literatures [36, 37], NPY, *ob-R*, β-actin primers were designed. Among them, And β-actin acted as the internal reference. Beijing AuGCT DNA-SYN Biotechnology Co., Ltd. was entrusted to synthesize the primers. Primers: NPY, Forward: 5′-TGTGGACTG-ACCCTCGCTCTAT-3′101, Reverse: 5′-TGTAGTGTC-GCAGAGCGGAGTA-3′239, NM_012614.1, 139 bp; *ob-R*, Forward: 5′-TCTGCCTGAAGTTATAGATGATTTG-3′492, Reverse: 5′-GTCACTCCAGACTCCTGAGCCATCC-3′957, NM_012596.1, 466 bp; β-actin, Forward: 5′-GCTTCTCTT-TAATGTCACGCACG-3′24, Reverse: 5′-CCATCCAGGCTG TGTTGTCC-3′266, NM_031144.2, 243 bp.

According to GoTaq@ 2-Step RT-qPCR System and "Primed Synthesis Report Sheet" of AuGCT, 25 μL GoTaq@ qPCR Master Mix reaction system was prepared and mixed uniformly. Real-time fluorescent quantitative PCR instrument (Bio-rad Chromo4 CFB-3240, USA) was used for fluorescent quantitative PCR amplification. Optimum conditions of qPCR: NPY & β-actin: 95°C 2 min; 95°C 15 s, 60°C 1 min, 40 cycles; 60 to 95°C. *ob-R* & β-actin: 95°C 5 min; 95°C 30 s, 59°C 40 s, 72°C 1 min, 30 cycles; 72°C 10 min.

DEPC (diethyl pyrocarbonate), agarose, and Trizol reagent were purchased from Sigma Company, USA; chloroform, isopropyl alcohol, and anhydrous alcohol were purchased from Beijing Chemical Reagent Limited Company.

Fluorescent quantitative PCR results were used to calculate relative expressions of NPY mRNA and *ob-R* mRNA using the previously described of $2^{-\Delta\Delta CT}$ method [38, 39]. $^{\Delta\Delta}$CT = (mean target gene CT value − mean internal reference gene CT value) − (mean reference gene CT value − mean internal gene CT value). Also, β-actin acted as the internal reference gene. To calculate the relative expression of each sample (CT), the beta-actin CT value was subtracted from each sample gene CT value. $2^{-\Delta\Delta CT}$ was used for variance analysis and histogram.

2.8. Statistical Processing. Data were expressed as mean ± standard error of mean ($\bar{x} \pm$ SEM). Using SPSS 17.0 software and one-way ANOVA was applied for general data. In addition, LSD method was adopted for the comparisons between groups. Repeated measurement process of general linear model (GLM) in SPSS17.0 was used to conduct one-way ANOVA analysis for repeated measured data (bodyweight and food intake), and multivariate analysis process of variance was used to make comparisons between groups on each time point (LSD method). $P < 0.05$ was considered statistically significant.

3. Results

3.1. Bodyweight and Food Intake of Rats with Constraint Stress for 21 Days Significantly Reduced; While Xiaoyaosan Prevented This Effect. Before constraint stress, there was no significant difference in bodyweight and food intake among the 3 groups of rats (Table 1). From the 2nd day of constraint stress, bodyweight of simple stress rats was significantly lower than that of the normal control group at the same time point ($P < 0.05$ or $P < 0.01$). From the 6th day of constraint stress, bodyweight of the Xiaoyaosan-treated group was significantly lower than that of the normal control group at the same time point ($P < 0.05$ or $P < 0.01$). From the 16th day to 21st day, bodyweight of the Xiaoyaosan-treated group was significantly higher than that of simple stress rats at the same time point ($P < 0.05$ or $P < 0.01$).

Table 2 shows that from the 2nd day of constraint stress, food intake of stress rats was significantly lower than that of the normal control group at the same time point ($P < 0.05$ or

Table 1: Changes of bodyweight (g, $\bar{x} \pm$ SEM).

Day	The control group	The 21-day stress group	The Xiaoyaosan group
Day 0	211.167 ± 1.989	210.750 ± 2.122	213.080 ± 2.256
Day 1	222.375 ± 2.302	219.208 ± 2.430	223.560 ± 2.619
Day 2	228.083 ± 2.417	220.125 ± 2.366*	226.520 ± 2.684
Day 3	236.458 ± 2.685	224.958 ± 2.401**	229.480 ± 2.331*
Day 4	244.625 ± 2.985	230.417 ± 2.969**	237.400 ± 2.682
Day 5	245.167 ± 3.170	233.833 ± 3.002**	241.080 ± 2.666
Day 6	255.417 ± 3.033	239.250 ± 2.928**	246.280 ± 2.846*
Day 7	263.667 ± 3.154	245.208 ± 3.092**	252.440 ± 3.181*
Day 8	265.250 ± 3.168	242.625 ± 3.139**	250.040 ± 3.098**
Day 9	277.250 ± 3.227	255.083 ± 3.528**	262.640 ± 3.550**
Day 10	283.125 ± 3.483	259.708 ± 3.470**	263.160 ± 4.052**
Day 11	290.708 ± 3.685	265.917 ± 3.782**	270.720 ± 3.954**
Day 12	295.375 ± 3.978	267.917 ± 3.618**	275.040 ± 4.121**
Day 13	300.042 ± 3.999	272.167 ± 4.720**	279.280 ± 4.336**
Day 14	306.333 ± 4.059	274.792 ± 4.113**	285.360 ± 4.331**
Day 15	310.167 ± 4.370	279.167 ± 4.039**	289.800 ± 4.115**
Day 16	316.208 ± 4.258	282.708 ± 4.206**	297.040 ± 4.112**▲
Day 17	320.958 ± 4.519	286.458 ± 4.276**	302.880 ± 4.151**▲
Day 18	324.875 ± 4.473	290.792 ± 4.391**	310.120 ± 4.278*▲▲
Day 19	329.542 ± 4.592	295.625 ± 4.455**	316.200 ± 4.279*▲▲
Day 20	336.375 ± 4.996	297.125 ± 4.804**	322.680 ± 4.165*▲▲
Day 21	344.083 ± 4.132	302.208 ± 4.942**	326.920 ± 4.209*▲▲

$N_{\text{the control group}} = 24$, $N_{\text{the 21-day stress group}} = 24$, $N_{\text{the xiaoyaosan group}} = 24$.
*$P < 0.05$, **$P < 0.01$ versus the control group; ▲$P < 0.05$, ▲▲$P < 0.01$ versus the 21-day stress group.

Table 2: Changes of food intake ($N = 8$, g, $\bar{x} \pm$ SEM).

Day	The control group	The 21-day stress group	The Xiaoyaosan group
Day 0	22.556 ± 0.733	23.794 ± 1.160	24.188 ± 0.715
Day 1	23.825 ± 0.498	19.856 ± 0.551**	20.594 ± 0.575**
Day 2	25.162 ± 1.067	22.200 ± 0.359*	21.981 ± 0.736**
Day 3	25.963 ± 1.165	22.056 ± 0.908**	23.138 ± 0.445*
Day 4	25.000 ± 0.678	21.940 ± 0.592**	22.456 ± 0.488**
Day 5	26.744 ± 1.293	22.248 ± 0.602**	21.681 ± 0.608**
Day 6	25.794 ± 0.978	22.950 ± 0.391**	21.831 ± 0.563**
Day 7	27.806 ± 1.011	23.088 ± 0.409**	23.275 ± 0.548**
Day 8	23.644 ± 1.631	19.440 ± 0.725*	20.119 ± 0.672*
Day 9	24.163 ± 1.570	23.502 ± 0.476	22.975 ± 0.832
Day 10	26.531 ± 1.032	24.279 ± 0.660	24.337 ± 1.153
Day 11	26.094 ± 1.173	22.575 ± 0.567*	23.250 ± 0.802*
Day 12	26.669 ± 1.093	24.115 ± 0.540*	23.631 ± 0.860*
Day 13	27.131 ± 0.977	23.877 ± 0.968*	23.919 ± 0.871*
Day 14	26.575 ± 1.394	23.502 ± 0.707*	23.931 ± 0.342
Day 15	25.544 ± 0.877	22.771 ± 0.544*	24.113 ± 0.656
Day 16	26.631 ± 1.198	23.954 ± 0.986	24.194 ± 0.876
Day 17	26.538 ± 0.751	22.403 ± 0.673**	24.544 ± 0.622▲
Day 18	26.713 ± 0.811	23.081 ± 0.660**	24.812 ± 0.606
Day 19	26.381 ± 0.943	22.103 ± 0.793**	24.337 ± 0.425▲
Day 20	26.988 ± 1.000	22.125 ± 1.338**	24.079 ± 0.757
Day 21	26.281 ± 1.008	21.719 ± 1.164**	24.763 ± 0.528▲

*$P < 0.05$, **$P < 0.01$ versus the control group; ▲$P < 0.05$ versus the 21-day stress group.

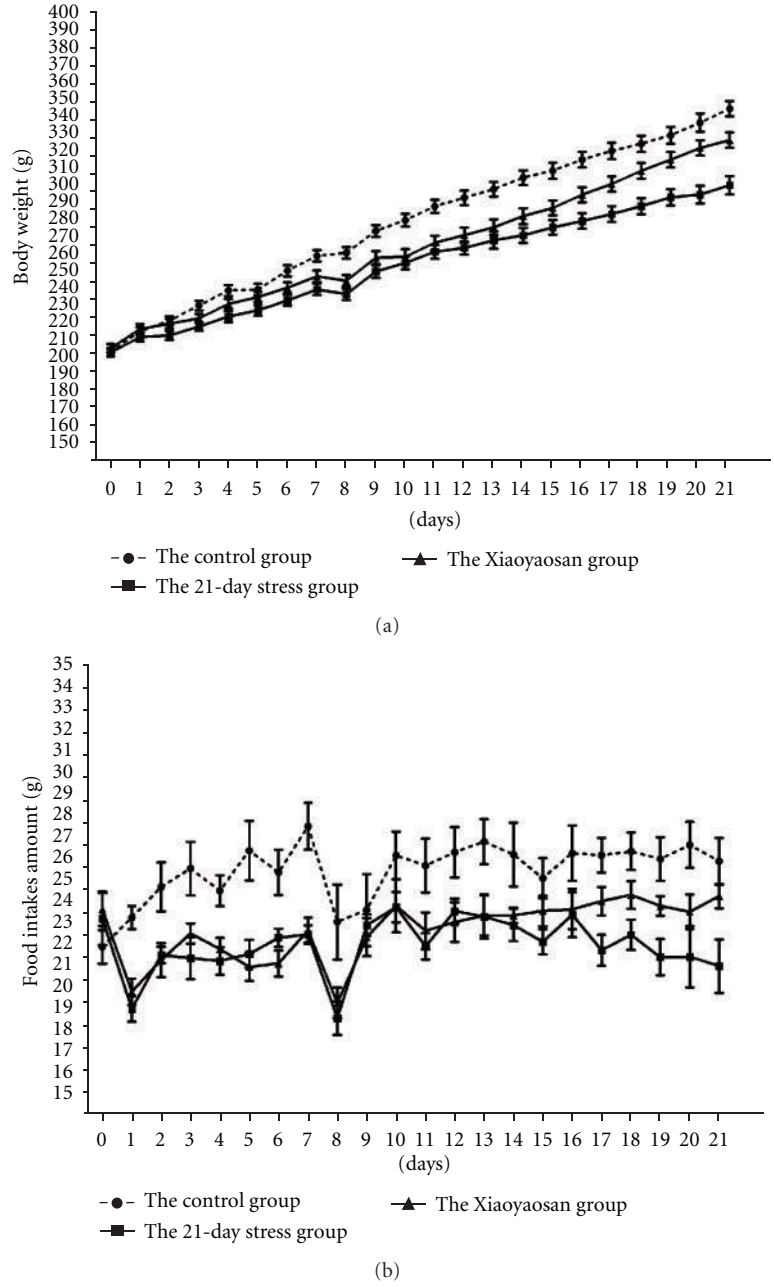

Figure 1: Changes in bodyweight and food intake in three groups. Each point represents the mean values and vertical bars represents SEM.

$P < 0.01$). From the 2nd day to 13th day of constraint stress, food intake of the Xiaoyaosan-treated group was significantly lower than that of the normal control group at the same time point ($P < 0.05$ or $P < 0.01$); while in the 3rd week of constraint stress, the food intake showed an increasing trend. Compared with the control group, there was no significant difference. Particularly on the 17th day, 19th day, and 21th day, the food intake of the Xiaoyaosan-treated group was significantly higher than that of stress rats ($P < 0.05$).

Figure 1 shows that in the 3rd week of constraint stress, bodyweight and food intake of simple stress rats were significantly lower than those of the normal group and the Xiaoyaosan-treated group. In the 1st week and 2nd week of constraint stress, the bodyweight and food intake of the Xiaoyaosan-treated group was lower than that of the normal control group. In the 3rd week, the bodyweight and food intake significantly increased and showed a trend close to those of the rats of the normal control group.

3.2. Hypothalamic Leptin and ob-R Protein Expression in the 21-Day Constraint Stress Group Is Significantly Increased; While NPY Expression Shows No Obvious Change. For NPY content in rat hypothalamus, among the normal control group (23.715 ± 1.964 ng/L), the 21-day stress group

(27.071 ± 1.053 ng/L) and the Xiaoyaosan-treated group (23.463 ± 1.517 ng/L), there were no significant differences ($P > 0.05$) (see Figure 2(a)). *ob-R* expression in rat hypothalamus of the 21-day stress group (10.644 ± 0.311 μg/L) was significantly higher than that of the normal control group (8.798 ± 0.230 μg/L) ($P < 0.01$); while *ob-R* content in rat hypothalamus of the Xiaoyaosan-treated group (5.938 ± 0.421 μg/L) was significantly lower than that of the 21-day stress group and the normal control group, with obvious statistical significance ($P < 0.01$) (see Figure 2(b)). The Leptin content in rat hypothalamus of the 21-day stress group (1.506 ± 0.049 μg/L) was significantly more than that of the normal control group (1.231 ± 0.031 μg/L) ($P < 0.01$); while the Xiaoyaosan-treated group (1.322 ± 0.022 μg/L) was significantly lower than that of the 21-day stress group ($P < 0.01$) (see Figure 2(c)).

3.3. Double-Labeling Immunofluorescence Results Show That ob-R Protein Expression in the ARC of the 21-Day Group Is More Than That of the Normal Group; While NPY Protein Expression Has No Obvious Change. NPY neurons were labeled with red fluorescence (II), widely distributed in the form of granules or block mass; while *ob-R* neurons were labeled as green fluorescence (I). Yellow staining sites were double-staining neurons of *ob-R* and NPY (III). Microscopic observation shows that compared to the control group, *ob-R*-positive cells in the ARC of the 7-day stress group and the 21-day stress group are increased; while positive expression neurons of NPY are reduced. Compared to the stress groups, *ob-R*-positive expression cells in the ARC of the Xiaoyaosan-treated group are reduced; while positive expression neurons of NPY are increased (see Figure 3).

Semiquantitative statistical analysis shows that for NPY IOD and positive neurons number in the ARC, the 7-day stress group (IOD: 91.452 ± 23.361, ×106; positive neurons number: 319.500 ± 31.201) and the 21-day stress group (IOD: 109.685 ± 15.836, ×106; positive neurons number: 323.700 ± 37.392) are different from the normal control group (IOD: 128.389 ± 33.972, ×106; positive neurons number: 372.000 ± 42.848) and the Xiaoyaosan-treated group (IOD: 134.692 ± 36.194, ×106; positive neurons number: 411.400 ± 31.219), but there is no significant difference ($P > 0.05$) among the 4 groups. The *ob-R* IOD and positive neurons number in the ARC of the 21-day stress group (IOD: 15.710 ± 1.683, ×106; positive neurons number: 76.100 ± 6.602) is significantly higher than that of the normal control group (IOD: 10.734 ± 1.444, ×106; positive neurons number: 49.400 ± 8.275) and the Xiaoyaosan-treated group (IOD: 11.114 ± 1.734, ×106; positive neurons number: 46.200 ± 8.779), $P < 0.05$.

Among 4 groups of double-labeling immunofluorescence staining, there is no significant difference ($P > 0.05$) in colocalization area (the normal control group: 36.995 ± 5.089, ×102, μm^2; the 7-day stress group: 28.073 ± 5.100, ×102, μm^2; the 21-day stress group: 27.291 ± 3.098, ×102, μm^2; the Xiaoyaosan-treated group: 44.237 ± 9.341, ×102, μm^2), NPY weighted colocalization coefficient (the normal control group: 0.071 ± 0.011; the 7-day stress group: 0.091 ± 0.009; the 21-day stress group: 0.088 ± 0.009; the Xiaoyaosan-treated group: 0.071 ± 0.009) or *ob-R* weighted colocalization coefficient (the normal control group: 0.654 ± 0.066; the 7-day stress group: 0.548 ± 0.099; the 21-day stress group: 0.616 ± 0.056; the Xiaoyaosan-treated group: 0.656 ± 0.082) (see Figure 3).

3.4. In Situ Hybridization Results Show That Compared with the Control Group, Positive Expression of ob-R mRNA in the ARC of Stress Rats Is Significantly Increased; While Positive Expression of NPY mRNA Is Unchanged with Stress Time. Combination of *in situ* hybridization staining image analysis and semiquantitative statistical analysis shows that the positive expression of NPY mRNA of the 7-day stress group is obviously more than that of the normal control group. However, among the 4 groups, there is no significant difference between positive expression IOD and cells of NPY mRNA (see Figure 4). NPY mRNA IOD: the normal control group 0.035 ± 0.006, the 7-day stress group 0.042 ± 0.011, the 21-day stress group 0.045 ± 0.010, and the Xiaoyaosan-treated group 0.029 ± 0.006. NPY mRNA cell numbers: the normal control group 24.333 ± 5.427, the 7-day stress group: 25.500 ± 5.513, the 21-day stress group 26.278 ± 3.896, and the Xiaoyaosan-treated group 23.722 ± 3.761.

ob-R mRNA localized to the cytoplasm and nucleus of the normal control group and the Xiaoyaosan-treated group, while the 7-day stress group and the 21-day stress group mainly have nucleus expressions, especially for rats with constraint stress for 21 days. Semiquantitative analysis suggests that the positive expression IOD of *ob-R* mRNA of the 7-day stress group (0.044 ± 0.005), 21-day stress group, (0.034 ± 0.005), and the Xiaoyaosan-treated group (0.032 ± 0.005) is significantly more than that of the normal control group (0.019 ± 0.002) ($P < 0.05$ or $P < 0.01$). The positive *ob-R* mRNAs in the 7-day stress group (40.333 ± 5.014) and the 21-day stress group (30.889 ± 4.191) were significantly increased, compared with those of the normal control group (16.111 ± 4.470), $P < 0.05$ or $P < 0.01$; while those of the Xiaoyaosan-treated group (25.500 ± 3.623) were significantly reduced, compared than those of the 7-day stress group ($P < 0.05$) (see Figure 5).

3.5. RT-qPCR Results Show That Compared with the Normal Control Group, Relative Expression of NPY mRNA in the ARC of Stress Rats Is Significantly Reduced; While Relative Expression of ob-R mRNA Is Significantly Increased. Relative expression of NPY mRNA and *ob-R* mRNA was calculated using the $2^{-\Delta\Delta CT}$ method. As for relative expression of NPY mRNA, compared with the normal control group, the relative expression of the 7-day stress group was 0.113 (coefficient of variation (CV): 0.021 to 0.593), the 21-day stress group was 0.038 (CV: 0.009 to 0.156), and the Xiaoyaosan-treated group was 0.213 (CV: 0.098 to 0.463). Compared with the 21-day stress group, the relative content of NPY mRNA of the Xiaoyaosan-treated group was 5.540 (CV: 1.535 to 20.000). This suggests that compared with the normal control group, relative expression in NPY mRNA of the 7-day stress group, the 21-day stress group, and

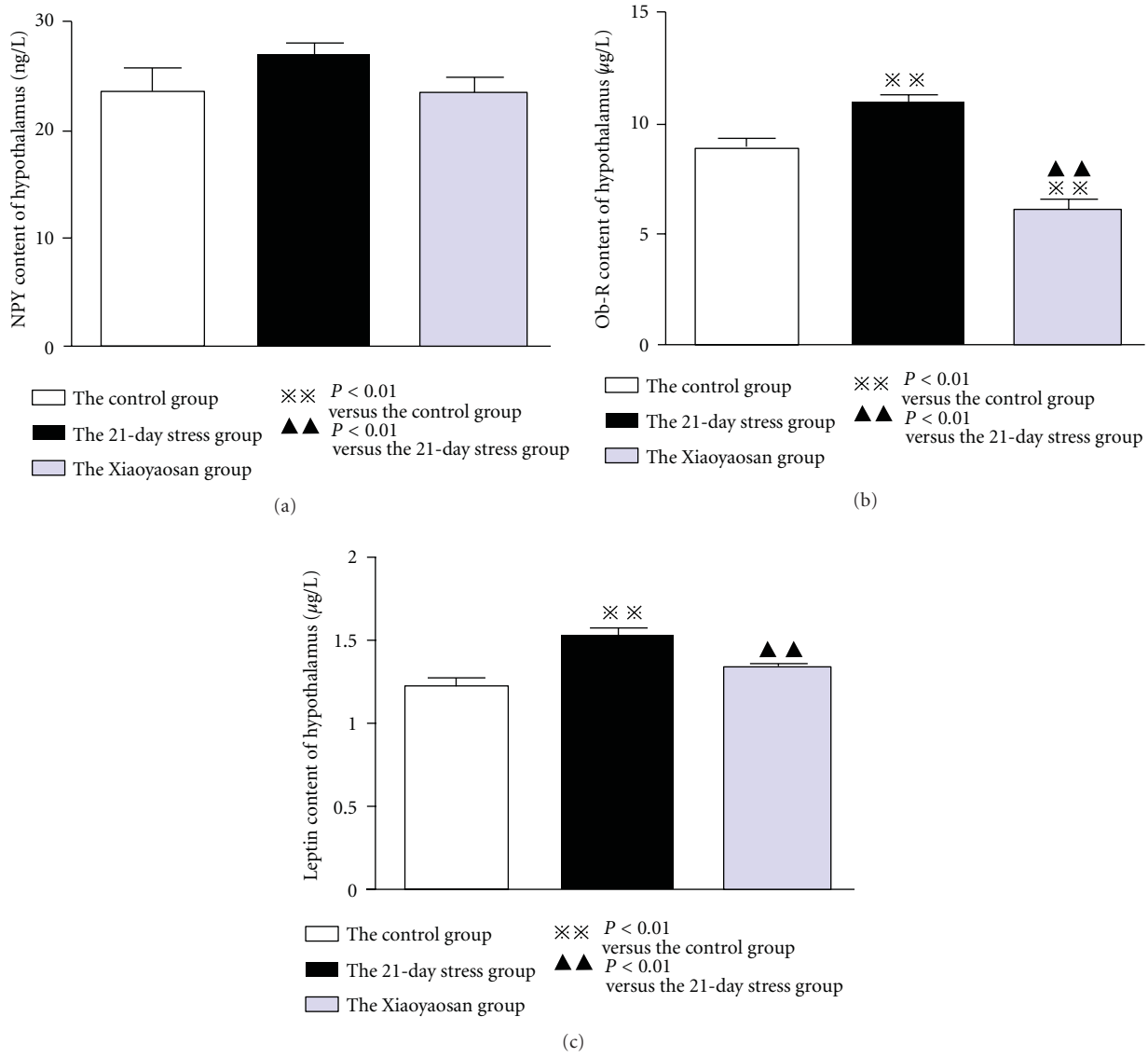

Figure 2: Differences in Leptin, NPY, and *ob-R* contents in hypothalamus. Each bar represents the mean values and vertical bars represent SEM. $^{**}P < 0.01$ as compared with the control group; $^{▲▲}P < 0.01$ as compared with the 21-day stress group.

the Xiaoyaosan-treated group was significantly reduced as shown in Figure 6 ($P < 0.01$).

Compared with the normal control group, relative content of *ob-R* mRNA in the 7-day stress group was 0.950 (CV: 0.287 to 3.150), that in the 21-day stress group was 2.969 (CV: 1.161 to 7.595), and that of the Xiaoyaosan-treated group was 1.286 (CV: 0.480 to 3.447). Compared with the 21-day stress group, relative content of *ob-R* mRNA of the normal control group was 0.337 (CV: 0.132 to 0.862), that of the 7-day stress group was 0.320 (CV: 0.130 to 0.786), and that of the Xiaoyaosan-treated group was 0.433 (CV: 0.241 to 0.778). Figure 6 shows that relative expression of *ob-R* mRNA of the 21-day stress group was significantly increased compared with that of the normal control group ($P < 0.05$); while relative expression of the Xiaoyaosan-treated group was significantly reduced compared with that of the 21-day stress group ($P < 0.05$).

4. Discussion

In this study, bodyweight and food intake of stressed rats increased more slowly than the normal rats with lengthening of chronic immobilization stress, in compliance with previous literatures and the previous research results of this research team [2–8]; while Xiaoyaosan can ameliorate the above changes.

The hypothalamus contains massive neuropeptide nervous pathways that promote appetite (NPY/Agouti-related peptide (AgRP)) and neuropeptide nervous pathways that inhibite appetite (POMC/Cocaine-amphetamine regulated

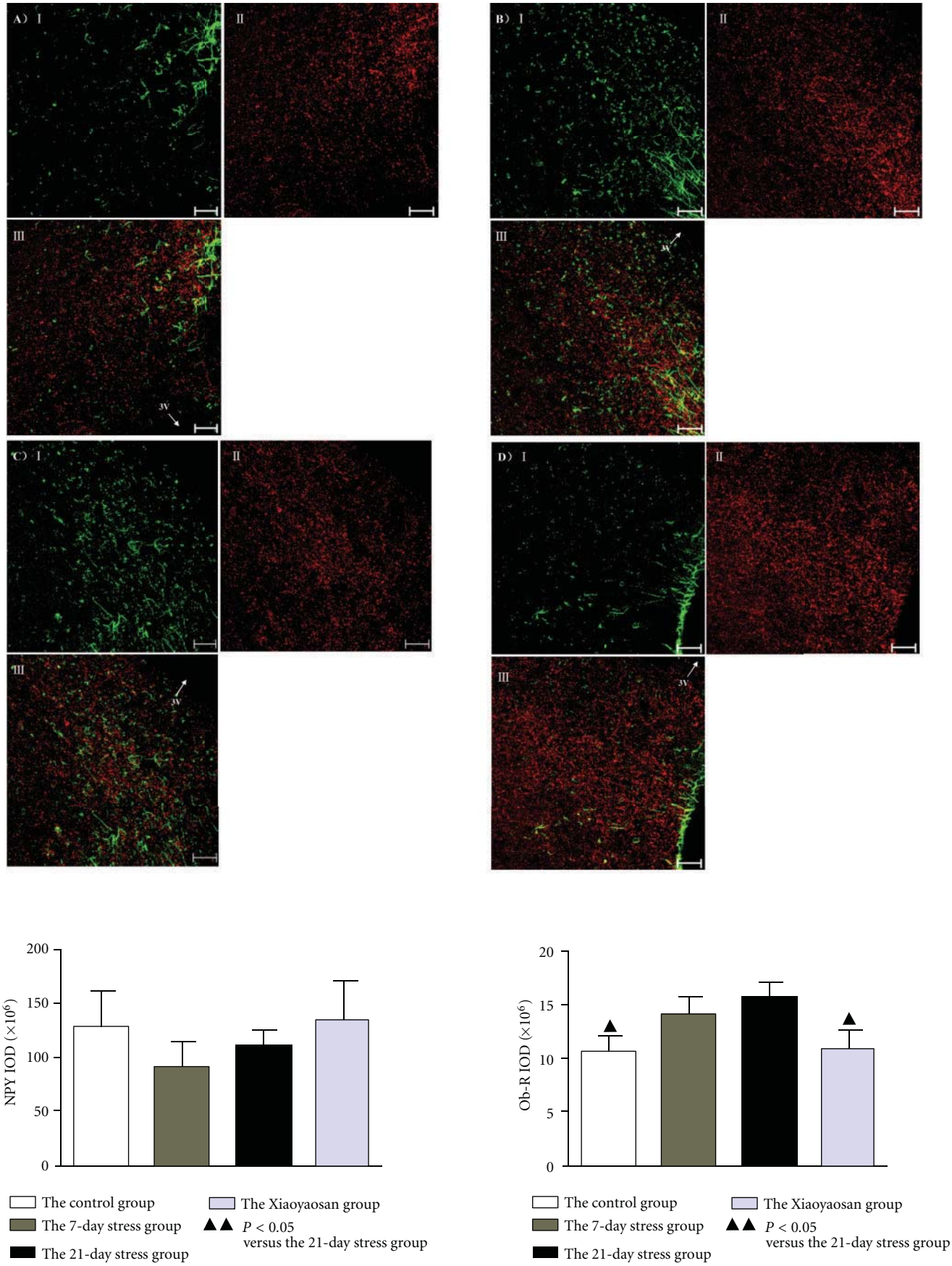

Figure 3: Continued.

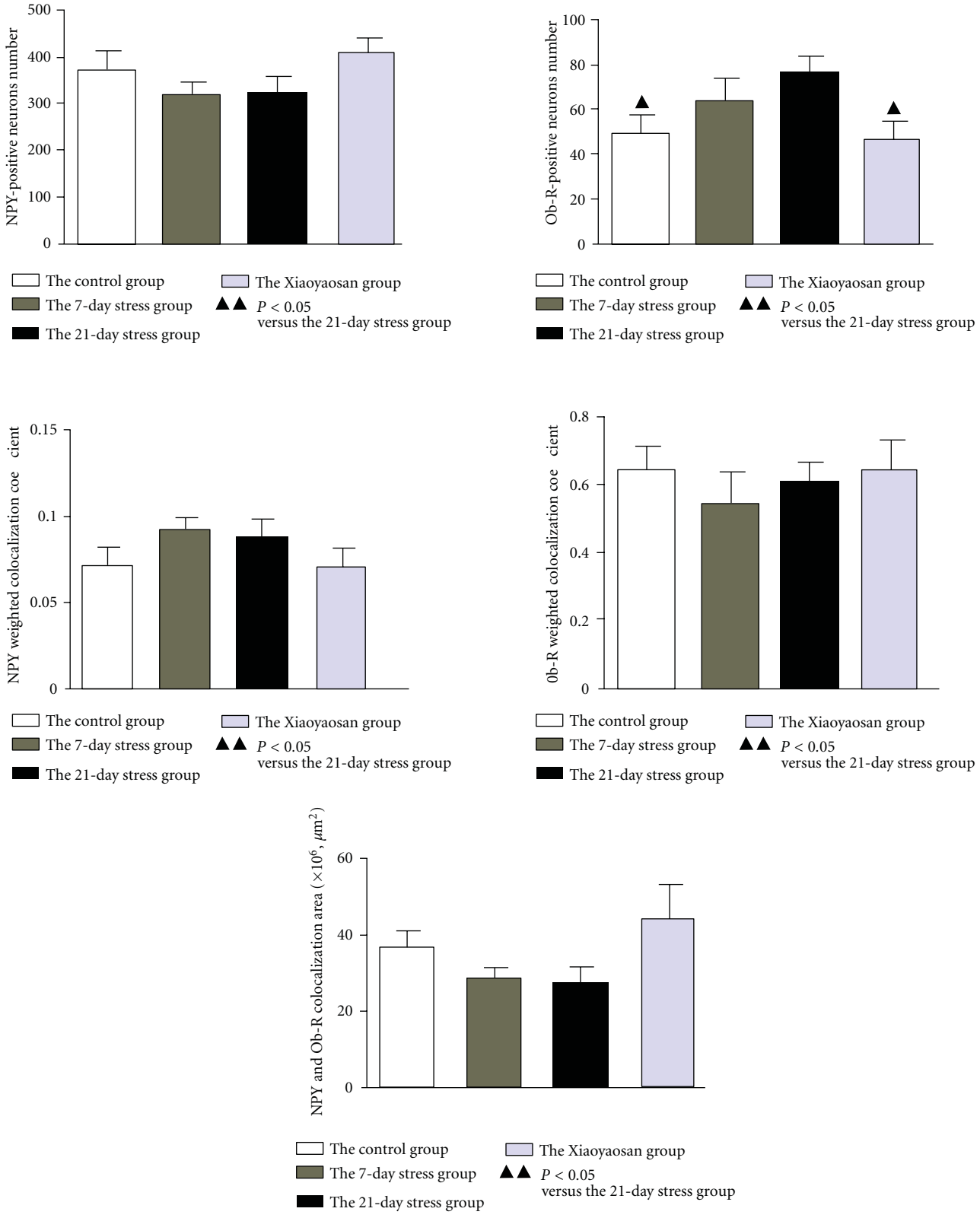

Figure 3: Double immunofluorescence for NPY and *ob-R* in the ARC. (A–D) Representative images of NPY, *ob-R*, and colocalization in ARC. (A) The control group. (B) The 7-day stress group. (C) The 21-day stress group. (D) The Xiaoyaosan-treated group. In each figure, *ob-R* was labeled with green fluorescence (I), NPY was labeled with red fluorescence (II), and co-loalization of NPY and *ob-R* was double-labeled in yellow (III). Scale bars = 50 μm for all images. NPY and *Ob-R* colocalization area, NPY or *Ob-R* IOD, and weighted colocalization coefficient were analyzed with Zeiss LSM Image Examiner, and the number of positive neurons was measured with Image Pro Plus. Each bar represents the mean values and vertical bars represent SEM. $^{\blacktriangle}P < 0.05$ as compared with the 21-day stress group. 3V means the third ventricle.

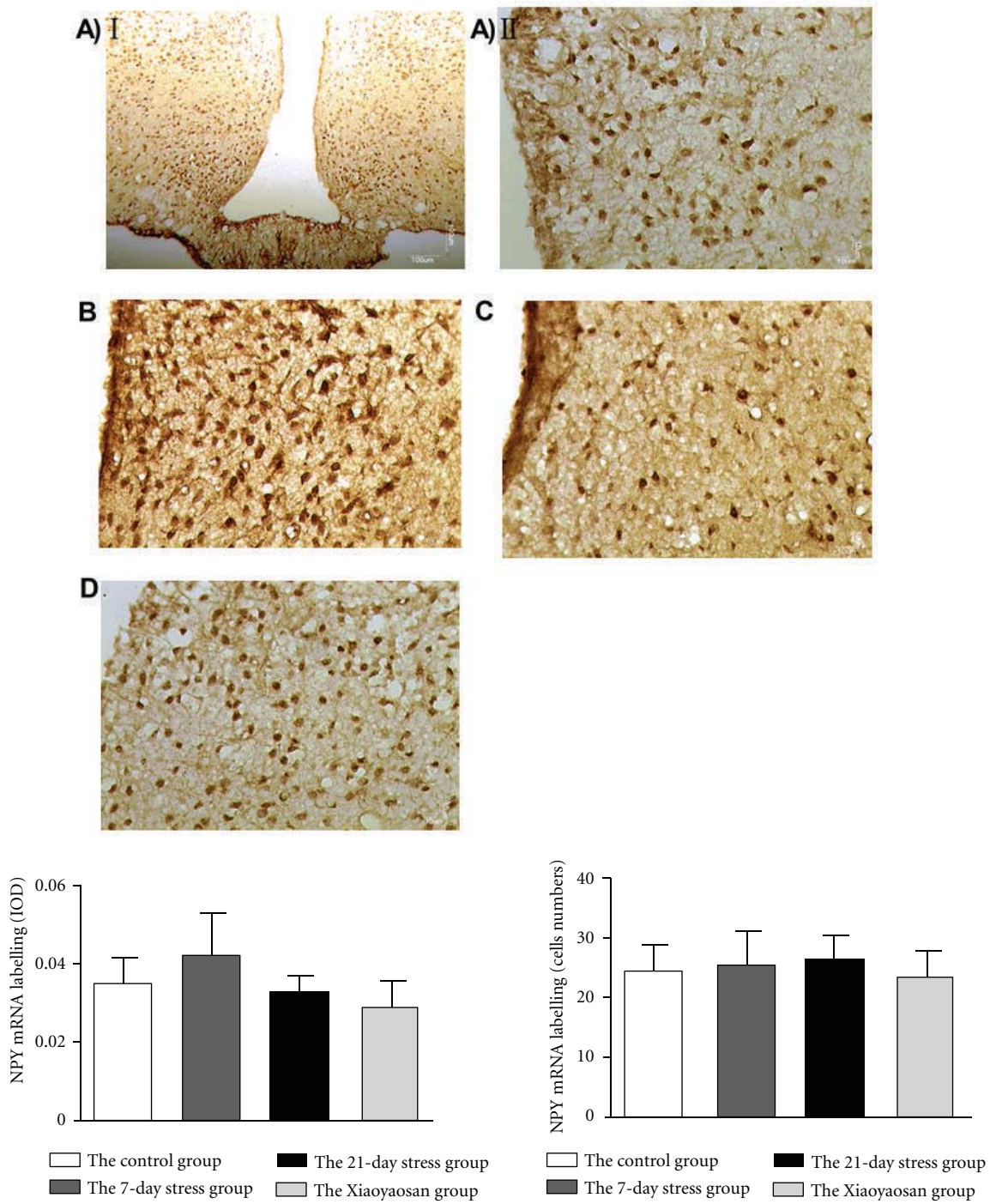

Figure 4: *In situ* hybridization for NPY mRNAin the ARC. (A–D) Representative images of NPY mRNA in ARC. (A) The control group. (B) The 7-day stress group. (C) The 21-day stress group. (D) The Xiaoyaosan-treated group. Scale bars = 100 μm for A (I) and 10 μm for other images. IOD of NPY mRNA labeling and cells of NPY mRNA labeling were measured with Image Pro Plus. Each bar represent the mean values and vertical bars represent SEM.

transcript (CART)). These nerves that promote appetite and inhibit appetite are sent by the ARC and projected onto other nucleus groups/brain areas of the hypothalamus, such as the lateral hypothalamic area (LHA), ventromedial nucleus (VMN), dorsomedial nucleus (DMN), and paraventricular nucleus (PVN), constituting the "appetite regulation network" (ARN) [40–42]. The ARN is the key the central system regulating food intake and bodyweight balance. Peripherally secreted appetite regulation signals, such as leptin, can cross the blood-brain barrier to reach hypothalamus nucleus group and influence appetite by affecting these two types of peptides [43].

Leptin is a polypeptide hormone secreted mainly by white adipose tissues. A number of electrophysiological and

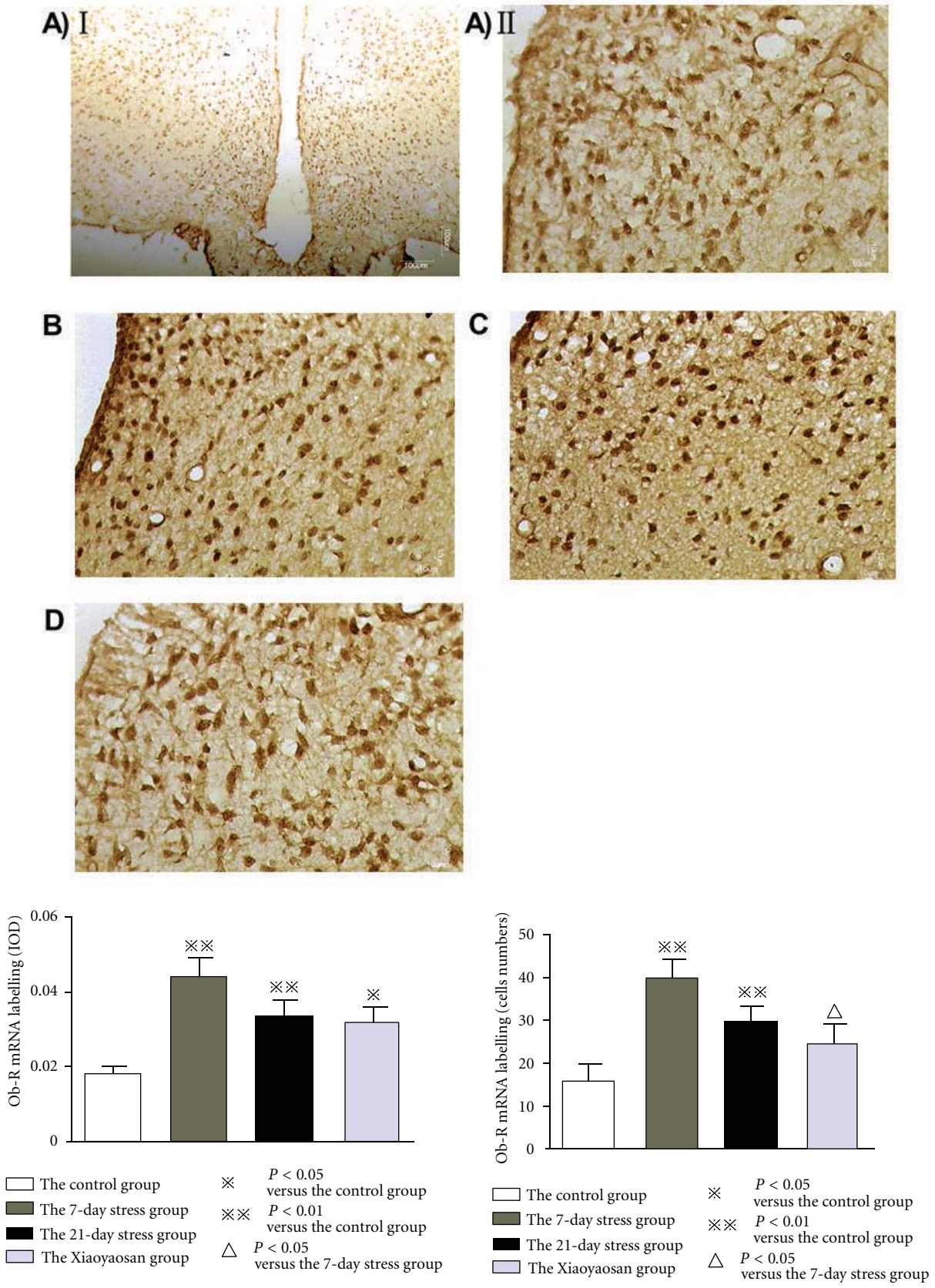

Figure 5: *In situ* hybridization for *ob-R* mRNAin the ARC. (A–D) Representative images of *ob-R* mRNA in ARC. (A) The control group. (B) The 7-day stress group. (C) The 21-day stress group. (D) The Xiaoyaosan-treated group. Scale bars = 100 μm for A (I) and 10 μm for other images. IOD of *ob-R* mRNA labeling and cells of *ob-R* mRNA labeling were measured with Image Pro Plus. Each bar represent the mean values and vertical bars represent SEM. $^{*}P < 0.05$ or $^{**}P < 0.01$ as compared with the control group; $^{\Delta}P < 0.05$ as compared with the 7-day stress group.

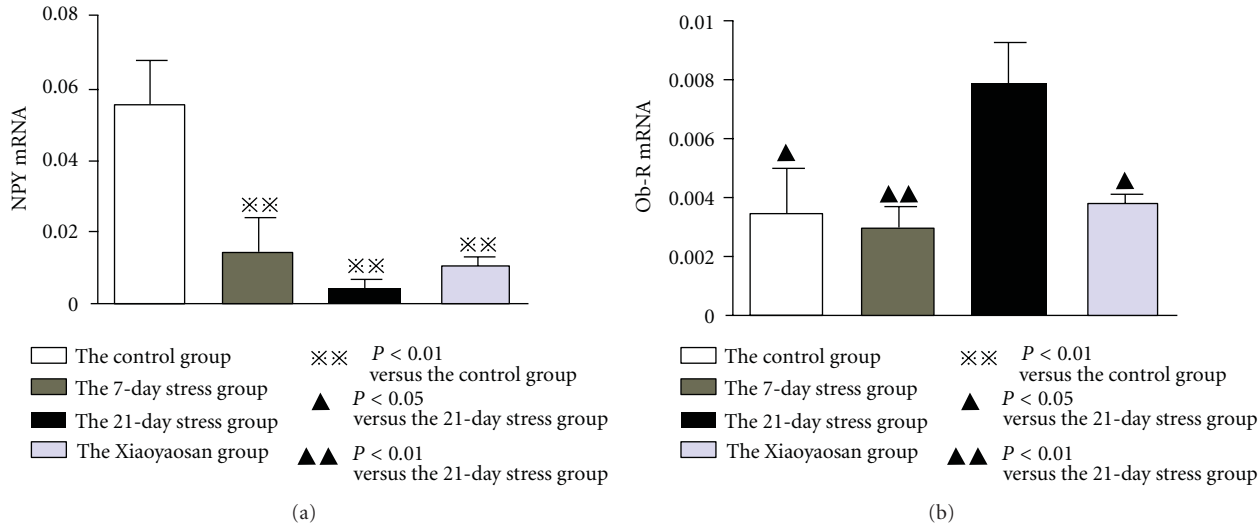

Figure 6: RT-qPCR detection of NPY mRNA and *ob-R* mRNA in the ARC. To calculate the relative amount of NPY or *ob-R* gene expression the formula ($\Delta CT = CT_{\text{target gene}} - CT_{\text{internal reference}}$) is used and analyzed with $2^{-\Delta CT}$ for statistics. Each bar represent the mean values and vertical bars represent SEM. $^{**}P < 0.01$ as compared with the control group; $^{\blacktriangle}P < 0.05$ or $^{\blacktriangle\blacktriangle}P < 0.01$ as compared with the 21-day stress group.

behavioral studies show that leptin regulates food intake and energy homeostasis mainly by means of the central nervous system (especially hypothalamus) [41, 44]. Also, hypothalamus is the main target of leptin [45].

ob-R is a high-affinity receptor of leptin, belonging to the class I cytokine super family. Current studies suggest that *ob-R* gene has at least 6 (a to f) splicing isomers [46]. Among them, *ob-R*b is a long receptor, and it is the main functional receptor. *ob-R*b is mainly expressed in the hypothalamus, and it has limited expression in peripheral tissues [47, 48]. Therefore, *ob-R*b is the main action receptor of leptin.

Leptin binds with *ob-R* in the hypothalamus, which can play a role in inhibiting appetite, reducing energy intake and increasing energy expenditure. Therefore, this study firstly detected leptin and *ob-R* contents in hypothalamus. The results show that compared with the control group, leptin and *ob-R* contents in the hypothalamus of the 21-day stress group are significantly increased, which suggests that CIS can increase Leptin levels in the hypothalamus and stimulate an increase in *ob-R* (mainly *ob-R*b) expression, and the combination specificities of the two damages the balance of hypothalamus "appetite regulation network."

As *ob-R* (mainly *ob-R*b) is widely expressed on the ARC, VMN, DMN, PVN, periventricular nucleus. and neurons in the lateral hypothalamic area [10, 11]; these areas are the main areas for regulating food intake and bodyweight. Among them, the ARC in the bottom of the third ventricle plays an important role in energy metabolism regulation by leptin [49]. For NPY/AgRP neuron and POMC/CART neuron in the ARC, the former can promote appetite, inhibit energy expenditure, and inhibit degradation of alpha-melanocyte-stimulating hormone (α-MSH); the later-secreted POMC can inhibit appetite and promote energy expenditure. The binding of leptin and *ob-R* can inhibit generation of NPY/AgRP neurons and release of NPY and AgRP. On the other hand, it can promote generation of POMC neuron and release of POMC and thus regulates the body's energy metabolism [50]. This study further detected *ob-R* protein and gene expressions in the ARC of stress rats. The results show that constraint stress (especially stress for 21 days) can induce *ob-R* protein and gene expressions in the ARC to be significantly higher than those of normal rats, which suggests that greatly increased leptin in the hypothalamus binding to *ob-R* in the ARC disrupts the homeostasis of NPY/AgRP-expressing neurons and POMC/CART-expressing neurons that regulate food intake and energy metabolism.

NPY is one of the most expressed neuropeptides in central nervous tissues, distributed in brain tissues and spinal cord but not the cerebellum. As a neurotransmitter, neurohormone, and neuromodulator, NPY is involved in the complexity of stress response. It not only regulates the emotional and behavioral changes caused by stress, such as anxiety and depression, but also promotes appetite mainly by means of the hypothalamus. Also, NPY neurons are abundant in the hypothalamus, especially in the ARC [9, 51].

Studies show that after 8 weeks of moderate psychological stress, NPY expression in the hypothalamus paraventricular nucleus, arcuate nucleus, and other areas of rats is significantly reduced [19], and NPY expression in the hippocampus area and ARC of rats receiving CIS for 21 days is reduced [52]. This study detected NPY content in the hypothalamus of rats receiving constraint stress by ELISA and observed NPY protein and gene expression in the ARC of restrained rats by means of immunofluorescence and *in situ* hybridization. Although there were changes in NPY protein and gene expressions, compared with the normal rats, the differences were not statistically significant. While RT-qPCR results show that NPY mRNA expression in the ARC of CIS rats is significantly reduced, in line with previous results

[19, 52]. We hypothesize that after chronic stress, the binding of leptin with *ob-R* in the ARC possibly causes a decrease in NPY expression and inhibits appetite to reduce food intake and thus reduces the increase in bodyweight.

However, many studies show that while food intake of chronically stressed rats is reduced, NPY mRNA expression in the arcuate nucleus is increased. For example, Sergeyev et al. [53] investigated the rats exposed to repeated, unpredictable, and mild stress for 3 weeks. As a result, NPY mRNA expression in the arcuate nucleus significantly increased; while the expression on hippocampal dentate gyrus was reduced [53]. Makino et al. proved that for acute stress (2 h) or chronic repeated immobilization stress (2 h daily, for 14 days), NPY mRNA expression in the arcuate nucleus was significantly increased [54]. The inconsistent results of NYP mRNA expression in the ARC induced by chronic stress: (1) As a "stress molecule" [24, 25], NPY and the HPA axis interact [20–23]. Psychological stress can activate the HPA axis to promote an increase in glucocorticoid secretion. *In vitro* and *in vivo* experimental studies show that glucocorticoid can stimulate the neurons in ARC to synthesize NPY, and there are response fragments upstream of the NPY gene encoding region carrying glucocorticoid [55]. This could possibly explain the significant increase of NPY mRNA expression in the hypothalamus after psychological stress. (2) Additional reports show that increases in blood glucose can upregulate NPY expression in hypothalamus [56]. Therefore, an increase in the of body's blood glucose after stress is possibly another explanation for the significant increase of NPY mRNA in hypothalamus. (3) The significant increase of NPY mRNA in hypothalamus after psychological stress is possibly associated with a neuropeptide and neurotransmitter secretion disorder caused by psychological stress, but it is necessary to carry out further research.

The results of this study from double-labeling immunofluorescence, *in situ* hybridization, and RT-qPCR demonstrate that *ob-R* protein and gene expression in the ARC of CIS rats are significantly increased. While various observation methods show that NPY protein and gene expressions have inconsistent changes (there were differences only for RT-qPCR assay), suggesting that the intermediate link of rat bodyweight is decreased and food intake loss of rats caused by the binding of leptin with *ob-R* in hypothalamus does not mainly pass through the NPY nervous inhibition pathway, but it possibly passes through another nerve pathway (possibly POMC, etc.).

Immobilization is a widely used method of nerve stimulation in stressed animal models. Immobilization stress deprives an animal of freedom of activity and is similar to the human psychosomatic disease process. It is an example of psychological frustration stress [57], mainly embodied in body's emotional disorder and behaviors such as depression, anxiety, and abnormal changes in appetite and bodyweight. Traditional Chinese prescription Xiaoyaosan is used to treat emotional disorders such as depression, anxiety, and irritation, and some symptoms such as dizziness, head fullness, dry eye, sense of pharyngeal foreign body, chest and hypochondrium distending pain, two-hypochondrium distending pain, chest and hypochondrium dull pain, breast distending pain, epigastric fullness discomfort after eating, spiritlessness, languidness, sigh, premenstrual irritability, menstrual abdominal distending pain, sexual dysfunction, bad sleep, stool dry pond, lusterless complexion (http://dict.cnki.net/dict_result.aspx?searchword=%E9%9D%A2%E8%89%B2%E5%B0%91%E5%8D%8E&tjType=sentence&style=&t=lusterless+complexion), premenstrual breast distending pain, premenstrual chest and hypochondrium distending pain, menstrual breast distending pain, and small and wiry pulse and has functions of dispersing stagnated liver Qi for relieving Qi stagnation and nourishing blood and strengthening spleen, suitable for liver depression and spleen deficiency syndrome [30, 58]. It has been proven through systematical evaluation that for the treatment of depression, Xiaoyaosan is effective and has no side effects [28]. Therefore, Xiaoyaosan has become a prescription preferred by domestic scholars for resisting chronic stress, and its chronic stress resistance has been widely researched. Also, a certain progress has been achieved [7, 31–35]. Therefore, we studied the effectiveness of selected extraction of Xiaoyaosan as an intervention to regulate NPY and *ob-R* in the ARC of stress rats. We show through immunofluorescence staining, *in situ* hybridization, or RT-qPCR, that Xiaoyaosan decreases *ob-R* protein and gene expression in the ARC of stressed rats.

5. Conclusion

The results of this study show that for somatic discomfort symptoms such as appetite decrease and bodyweight loss under chronic stress, increase of *ob-R* expression in the ARC is possibly a central neuroendocrine mechanism. Also, leptin signaling through *ob-R* in hypothalamus does not appear to utilize the NPY nervous inhibition pathway, and we presume that it possibly passes through another nervous pathway (possibly POMC, etc.). Therefore, the molecular basis of decreased regulation of *ob-R* expression in the ARC and intracellular signal transduction pathway requires further research. In addition, the results of this study suggest that a decrease in *ob-R* in the ARC is possibly the target of Xiaoyaosan, regulating somatic discomfort states with appetite decrease and weight loss induced by chronic stress.

Acknowledgments

This research was supported by the National Natural Science Foundation of China (nos. 30672578, 81202644) and National Natural Science Funds for Distinguished Young Scholar (no. 30825046). The authors thank the NIH Fellows Editorial Board for offering confidential scientific document editing service. Shao-xian Wang is now working at TCM College of Hebei Medical University, Shijiazhang 050000, China.

References

[1] S. Fryer, G. Waller, and B. S. Kroese, "Stress, coping, and disturbed eating attitudes in teenage girls," *International Journal of Eating Disorders*, vol. 22, no. 4, pp. 427–436, 1997.

[2] F. Monteiro, M. E. Abraham, S. D. Sahakari, and J. F. Mascarenhas, "Effect of immobilization stress on food intake, body weight and weights of various organs in rat," *Indian Journal of Physiology and Pharmacology*, vol. 33, no. 3, pp. 186–190, 1989.

[3] I. I. Rybkin, Y. Zhou, J. Volaufova, G. N. Smagin, D. H. Ryan, and R. B. S. Harris, "Effect of restraint stress on food intake and body weight is determined by time of day," *American Journal of Physiology*, vol. 273, no. 5, part 2, pp. R1612–R1622, 1997.

[4] A. Vallès, O. Martí, A. García, and A. Armario, "Single exposure to stressors causes long-lasting, stress-dependent reduction of food intake in rats," *American Journal of Physiology*, vol. 279, no. 3, pp. R1138–R1144, 2000.

[5] A. Alterman, R. Mathison, C. E. Coronel, M. M. Stroppa, A. B. Finkelberg, and R.V. Gallará, "Functional and proteomic analysis of submandibular saliva in rats exposed to chronic stress by immobilization or constant light," *Archives of Oral Biology*, vol. 57, no. 6, pp. 663–669, 2012.

[6] S. Makino, K. Asaba, M. Nishiyama, and K. Hashimoto, "Decreased type 2 corticotropin-releasing hormone receptor mRNA expression in the ventromedial hypothalamus during repeated immobilization stress," *Neuroendocrinology*, vol. 70, no. 3, pp. 160–167, 1999.

[7] J. X. Chen, W. Li, X. Zhao, and J. X. Yang, "Effects of the Chinese traditional prescription Xiaoyaosan decoction on chronic immobilization stress-induced changes in behavior and brain BDNF, TrkB, and NT-3 in rats," *Cellular and Molecular Neurobiology*, vol. 28, no. 5, pp. 745–755, 2008.

[8] L. F. Yue, J. Ding, J. X. Chen et al., "Establishment and review of rat model of syndrome of liver depression with spleen insufficiency," *Journal of Beijing University of Traditional Chinese Medicine*, vol. 31, no. 6, pp. 369–400, 2008.

[9] C. L. Boguszewski, G. Paz-Filho, and L. A. Velloso, "Neuroendocrine body weight regulation: integration between fat tissue, gastrointestinal tract, and the brain," *Endokrynologia Polska*, vol. 61, no. 2, pp. 194–206, 2010.

[10] H. X. Wang, Z. H. Lei, F. Ding, and X. L. Tan, "Localization of long form leptin receptor mRNA in the hypothalamus in the pig studied by *in situ* hybridization," *Journal of Nanjing Agricultural University*, vol. 25, no. 1, pp. 80–84, 2002.

[11] J. Wu and D. J. Zou, "Progress in the study of leptin receptor," *Progress in Physiological Sciences*, vol. 31, no. 2, pp. 143–146, 2000.

[12] D. G. Baskin, M. W. Schwartz, R. J. Seeley et al., "Leptin receptor long-form splice-variant protein expression in neuron cell bodies of the brain and co-localization with neuropeptide Y mRNA in the arcuate nucleus," *Journal of Histochemistry & Cytochemistry*, vol. 47, no. 3, pp. 353–362, 1999.

[13] M. L. Håkansson, H. Brown, N. Ghilardi, R. C. Skoda, and B. Meister, "Leptin receptor immunoreactivity in chemically defined target neurons of the hypothalamus," *The Journal of Neuroscience*, vol. 18, no. 1, pp. 559–572, 1998.

[14] D. G. Baskin, T. M. Hahn, and M. W. Schwartz, "Leptin sensitive neurons in the hypothalamus," *Hormone and Metabolic Research*, vol. 31, no. 5, pp. 345–350, 1999.

[15] S. J. Konturek, J. W. Konturek, T. Pawlik, and T. Brzozowki, "Brain-gut axis and its role in the control of food intake," *Journal of Physiology and Pharmacology*, vol. 55, no. 1, part 2, pp. 137–154, 2004.

[16] G. J. Morton and M. W. Schwartz, "The NPY/AgRP neuron and energy homeostasis," *International Journal of Obesity*, vol. 25, supplement 5, pp. S56–S62, 2001.

[17] T. L. Horvath, "Synaptic plasticity in energy balance regulation," *Obesity*, vol. 14, supplement 5, pp. 228S–233S, 2006.

[18] L. E. Kuo and Z. Zukowska, "Stress, NPY and vascular remodeling: implications for stress-related diseases," *Peptides*, vol. 28, no. 2, pp. 435–440, 2007.

[19] H. Kim, W. W. Whang, H. T. Kim et al., "Expression of neuropeptide Y and cholecystokinin in the rat brain by chronic mild stress," *Brain Research*, vol. 983, no. 1-2, pp. 201–208, 2003.

[20] T. G. Bedford, C. M. Tipton, N. C. Wilson, R. A. Oppliger, and C. V. Gisolfi, "Maximum oxygen consumption of rats and its changes with various experimental procedures," *Journal of Applied Physiology*, vol. 47, no. 6, pp. 1278–1283, 1979.

[21] T. Suda, F. Tozawa, I. Iwai et al., "Neuropeptide Y increases the corticotropin-releasing factor messenger ribonucleic acid level in the rat hypothalamus," *Molecular Brain Research*, vol. 18, no. 4, pp. 311–315, 1993.

[22] G. Moreno, M. Perelló, R. C. Gaillard, and E. Spinedi, "Orexin a stimulates hypothalamic-pituitary-adrenal (HPA) axis function, but not food intake, in the absence of full hypothalamic NPY-ergic activity," *Endocrine*, vol. 26, no. 2, pp. 99–106, 2005.

[23] A. Sainsbury, F. Rohner-Jeanrenaud, E. Grouzmann, and B. Jeanrenaud, "Acute intracerebroventricular administration of neuropeptide Y stimulates corticosterone output and feeding but not insulin output in normal rats," *Neuroendocrinology*, vol. 63, no. 4, pp. 318–326, 1996.

[24] D. R. Gehlert, "Role of hypothalamic neuropeptide Y in feeding and obesity," *Neuropeptides*, vol. 33, no. 5, pp. 329–338, 1999.

[25] L. Guidi, A. Tricerri, M. Vangeli et al., "Neuropeptide Y plasma levels and immunological changes during academic stress," *Neuropsychobiology*, vol. 40, no. 4, pp. 188–195, 1999.

[26] Y. Q. Zhang, M. Han, Z. J. Liu, J. Wang, Q. Y. He, and J. P. Liu, "Chinese herbal formula Xiao Yao San for treatment of depression: a systematic review of randomized controlled trials," *Evidence-Based Complementary and Alternative Medicine*, vol. 2012, Article ID 931636, 13 pages, 2012.

[27] X. K. Qin, P. Li, M. Han, Z. J. Liu, and J. P. Liu, "Systematic review of randomize controlled trials of Xiaoyao powder in treatment of depression," *Journal of Traditional Chinese Medicine*, vol. 51, no. 6, pp. 500–505, 2010.

[28] X. T. Chen and X. D. Shi, "Application of Xiaoyaosan on mental disease and nervous system disease," *Jiangsu Journal of Traditional Chinese Medicine*, vol. 39, no. 6, pp. 66–67, 2007.

[29] B. Ji, J. X. Chen, and Z. L. Lu, "Thinking on Xiaoyaosan powder," *Journal of Beijing University of Traditional Chinese Medicine*, vol. 24, no. 5, pp. 4–7, 2001.

[30] B. Ji, J. X. Chen, Z. L. Lu, L. S. Hu, X. Wan, and S. P. Chang, "Investigation of the scope of macroscopic indications related with the syndrome represented by Xiaoyao powder," *Journal of Beijing University of Traditional Chinese Medicine*, vol. 26, no. 5, pp. 70–73, 2003.

[31] J. X. Chen, Y. T. Tang, and J. X. Yang, "Changes of glucocorticoid receptor and levels of CRF mRNA, POMC mRNA in brain of chronic immobilization stress rats," *Cellular and Molecular Neurobiology*, vol. 28, no. 2, pp. 237–244, 2008.

[32] J. X. Chen, W. Li, X. Zhao, J. X. Yang, and H. Y. Xu, "Effects of Chinese herbs on enkaphalin mRNA and prodynorphin mRNA gene expression in rat hippocampus with chronic immobilization stress," *Chinese Journal of Applied Physiology*, vol. 21, no. 2, pp. 121–125, 2005.

[33] H. G. Luo, J. X. Chen, G. X. Yue, J. Ding, and X. Z. Yan, "Metabonomic study on the regulatory effect of Xiaoyaosan powder on chronic immobilization stressed rats," *Chinese Journal of Integrative Medicine*, vol. 28, no. 12, pp. 1112–1117, 2008.

[34] Y. Dai, Z. Li, L. Xue et al., "Metabolomics study on the anti-depression effect of Xiaoyaosan on rat model of chronic unpredictable mild stress," *Journal of Ethnopharmacology*, vol. 128, no. 2, pp. 482–489, 2010.

[35] X. Gao, X. Zheng, Z. Li et al., "Metabonomic study on chronic unpredictable mild stress and intervention effects of Xiaoyaosan in rats using gas chromatography coupled with mass spectrometry," *Journal of Ethnopharmacology*, vol. 137, no. 1, pp. 690–699, 2011.

[36] H. Z. Guan, Q. C. Li, and Z. Y. Jiang, "Ghrelin acts on rat dorsal vagal complex to stimulate feeding via arcuate neuropeptide Y/agouti-related peptide neurons activation," *Acta Physiologica Sinica*, vol. 62, no. 4, pp. 357–364, 2010.

[37] L. Zhang, T. Liu, M. Wang, L. J. Xing, G. Ji, and P. Y. Zheng, "Effect of Jiangzhi granula on leptin and leptin receptor of hypothalamus in rats with nonalcoholic liver disease," *Chinese Journal of Integrated Traditional and Western Medicine on Liver Diseases*, vol. 19, no. 2, pp. 88–91, 2009.

[38] K. J. Livak and T. D. Schmittgen, "Analysis of relative gene expression data using real-time quantitative PCR and the $2^{-\Delta\Delta C_T}$ method," *Methods*, vol. 25, no. 4, pp. 402–408, 2001.

[39] T. D. Schmittgen and K. J. Livak, "Analyzing real-time PCR data by the comparative C_T method," *Nature Protocols*, vol. 3, no. 6, pp. 1101–1108, 2008.

[40] S. P. Kalra, M. G. Dube, S. Pu, B. Xu, T. L. Horvath, and P. S. Kalra, "Interacting appetite-regulating pathways in the hypothalamic regulation of body weight," *Endocrine Reviews*, vol. 20, no. 1, pp. 68–100, 1999.

[41] M. W. Schwartz, S. C. Woods, D. Porte Jr., R. J. Seeley, and D. G. Baskin, "Central nervous system control of food intake," *Nature*, vol. 404, no. 6778, pp. 661–671, 2000.

[42] N. R. Lenard and H. R. Berthoud, "Central and peripheral regulation of food intake and physical activity: pathways and genes," *Obesity*, vol. 16, supplement 3, pp. S11–S22, 2008.

[43] P. C. Konturek, J. W. Konturek, M. Cześnikiewicz-Guzik, T. Brzozowski, E. Sito, and S. J. Konturek, "Neuro-hormonal control of food intake; basic mechanisms and clinical implications," *Journal of Physiology and Pharmacology*, vol. 56, no. 6, pp. 5–25, 2005.

[44] J. M. Friedman and J. L. Halaas, "Leptin and the regulation of body weight in mammals," *Nature*, vol. 395, no. 6704, pp. 763–770, 1998.

[45] N. Satoh, Y. Ogawa, G. Katsuura et al., "Satiety effect and sympathetic activation of leptin are mediated by hypothalamic melanocortin system," *Neuroscience Letters*, vol. 249, no. 2-3, pp. 107–110, 1998.

[46] N. Wu and H. R. Tan, "Leptin receptor and its relations with obesity," *Chinese Pharmacological Bulletin*, vol. 20, no. 12, pp. 1334–1336, 2004.

[47] J. G. Mercer, N. Hoggard, L. M. Williams, C. B. Lawrence, L. T. Hannah, and P. Trayhurn, "Localization of leptin receptor mRNA and the long form splice variant (*Ob-R*b) in mouse hypothalamus and adjacent brain regions by *in situ* hybridization," *FEBS Letters*, vol. 387, no. 2-3, pp. 113–116, 1996.

[48] V. Emilsson, Y. L. Liu, M. A. Cawthorne, N. M. Morton, and M. Davenport, "Expression of the functional leptin receptor mRNA in pancreatic islets and direct inhibitory action of leptin on insulin secretion," *Diabetes*, vol. 46, no. 2, pp. 313–316, 1997.

[49] B. M. Spiegelman and J. S. Flier, "Obesity and the regulation of energy balance," *Cell*, vol. 104, no. 4, pp. 531–543, 2001.

[50] C. F. Elias, C. Aschkenasi, C. Lee et al., "Leptin differentially regulates NPY and POMC neurons projecting to the lateral hypothalamic area," *Neuron*, vol. 23, no. 4, pp. 775–786, 1999.

[51] C. L. Boguszewski, G. Paz-Filho, and L. A. Velloso, "Neuroendocrine body weight regulation: integration between fat tissue, gastrointestinal tract, and the brain," *Endokrynologia Polska*, vol. 61, no. 2, pp. 194–206, 2010.

[52] H. M. Rao, *Changes on behavior and NPY, CCK in immobilization stress rat and its relations with liver function of smoothing qi flow [M.S. thesis]*, Beijing University of Traditional Chinese Medicine, 2007.

[53] V. Sergeyev, S. Fetissov, A. A. Mathé et al., "Neuropeptide expression in rats exposed to chronic mild stresses," *Psychopharmacology*, vol. 178, no. 2-3, pp. 115–124, 2005.

[54] S. Makino, R. A. Baker, M. A. Smith, and P. W. Gold, "Differential regulation of neuropeptide Y mRNA expression in the arcuate nucleus and locus coeruleus by stress and antidepressants," *Journal of Neuroendocrinology*, vol. 12, no. 5, pp. 387–395, 2000.

[55] A. M. Strack, R. J. Sebastian, M. W. Schwartz, and M. F. Dallman, "Glucocorticoids and insulin: reciprocal signals for energy balance," *American Journal of Physiology*, vol. 268, no. 1, part 2, pp. R142–R149, 1995.

[56] C. Yang, M. Hu, T. Zou, S. Q. Yao, and Y. X. Gong, "Neuropeptide Y: a possible factor enhancing diabetes onset in Chinese Hamster with psychological stress," *Chinese Journal of Psychiatry*, vol. 33, no. 4, pp. 226–228, 2000.

[57] X. Z. Xie, X. L. Chi, W. X. Zhou, Y. Ma, and Y. X. Zhang, "Progress in research of animal stress models," *Chinese Journal of New Drugs*, vol. 17, no. 16, pp. 1375–1380, 2008.

[58] X. M. Qin and X. X. Gao, "Exploring Xiaoyaosan syndromes and anti-depression in perspective of modernization of traditional Chinese medicine and materia medica," *World Science and Technology-Modernization of Traditional Chinese Medicine and Materia Medica*, vol. 12, no. 4, pp. 521–525, 2010.

Hindawi Publishing Corporation
Evidence-Based Complementary and Alternative Medicine
Volume 2012, Article ID 479016, 10 pages
doi:10.1155/2012/479016

Research Article

Red Ginseng Extract Attenuates Kainate-Induced Excitotoxicity by Antioxidative Effects

Jin-Yi Han,[1] Sun-Young Ahn,[2] Eun-Hye Oh,[3] Sang-Yoon Nam,[4] Jin Tae Hong,[2] Ki-Wan Oh,[2] and Mi Kyeong Lee[2]

[1] *Research Institute of Veterinary Medicine, Chungbuk National University, Cheongju 361-763, Republic of Korea*
[2] *College of Pharmacy, Chungbuk National University, Cheongju 361-763, Republic of Korea*
[3] *College of Medicine, Chungbuk National University, Cheongju 361-763, Republic of Korea*
[4] *College of Veterinary Medicine, Chungbuk National University, Cheongju 361-763, Republic of Korea*

Correspondence should be addressed to Ki-Wan Oh, kiwan@chungbuk.ac.kr and Mi Kyeong Lee, mklee@cbnu.ac.kr

Received 17 April 2012; Revised 11 September 2012; Accepted 20 September 2012

Academic Editor: Paul Siu-Po Ip

This study investigated the neuroprotective activity of red ginseng extract (RGE, *Panax ginseng*, C. A. Meyer) against kainic acid- (KA-) induced excitotoxicity *in vitro* and *in vivo*. In hippocampal cells, RGE inhibited KA-induced excitotoxicity in a dose-dependent manner as measured by the MTT assay. To study the possible mechanisms of the RGE-mediated neuroprotective effect against KA-induced cytotoxicity, we examined the levels of intracellular reactive oxygen species (ROS) and $[Ca^{2+}]_i$ in cultured hippocampal neurons and found that RGE treatment dose-dependently inhibited intracellular ROS and $[Ca^{2+}]_i$ elevation. Oral administration of RGE (30 and 200 mg/kg) in mice decreased the malondialdehyde (MDA) level induced by KA injection (30 mg/kg, i.p.). In addition, similar results were obtained after pretreatment with the radical scavengers Trolox and *N*, *N*′-dimethylthiourea (DMTU). Finally, after confirming the protective effect of RGE on hippocampal brain-derived neurotropic factor (BDNF) protein levels, we found that RGE is active compounds mixture in KA-induced hippocampal mossy-fiber function improvement. Furthermore, RGE eliminated 1,1-diphenyl-2-picrylhydrazyl (DPPH) radicals, and the IC_{50} was approximately 10 mg/ml. The reductive activity of RGE, as measured by reaction with hydroxyl radical ($^{\bullet}OH$), was similar to trolox. The second-order rate constant of RGE for $^{\bullet}OH$ was $3.5–4.5 \times 10^9\ M^{-1}\cdot S^{-1}$. Therefore, these results indicate that RGE possesses radical reduction activity and alleviates KA-induced excitotoxicity by quenching ROS in hippocampal neurons.

1. Introduction

Panax ginseng C. A. Meyer (Araliaceae) is one of the most widely used medicinal plants, particularly in traditional oriental medicine, for the treatment of various diseases. It has a wide range of pharmacological and physiological actions [1, 2]. Red ginseng extract (RGE) derives from a ginseng plant that has been cultivated for 4–6 years or more and goes through an extensive cleaning, steaming, and drying process [3]. Heat treatment of ginseng at 98–100°C for 2-3 h under high pressure increases the production of nonpolar or lesspolar saponins such as Rg_3, Rg_5, Rg_6, Rh_2, and RK_1. These improved biologically active ginseng products result from changes in the chemical constituents that occur during steaming treatment [4]. In addition, the content of maltol (3-hydroxy-2-methyl-4-pyrone) is increased by heat processing of ginseng. The antioxidant activity of phenolic compounds is correlated with their chemical structures. The structure-activity relationships of some phenolic compounds (e.g., flavonoids, phenolic acids, and tannins) have previously been studied [5–7]. In general, the free radical scavenging and antioxidant activity of phenolics (e.g., flavonoids and phenolic acids) mainly depends on the number and position of hydrogen-donating hydroxyl groups on the aromatic ring of the phenolic molecules and is affected by factors such as the glycosylation of aglycones and other H-donating groups (–NH, –SH). There have been many reports on antioxidant components that generally focus on phenolic acids [5, 8, 9]. RGE has both stimulatory and inhibitory effects on the

central nervous system (CNS) and may modulate neurotransmission [10]. Some studies have reported that RGE has antioxidant, memory enhancing, antihypertensive, and antistress effects [11, 12]. Red ginseng protected smokers from oxidative damage and reduced cancer risk associated with smoking [13]. RGE has been reported to scavenge hydroxyl radicals (•OH), DPPH, and superoxide radicals [14].

Excitatory amino acids (EEAs) such as glutamate are well known as the primary neurotransmitters that mediate synaptic excitation in the vertebrate CNS [15]. Glutamate has dual actions on CNS neurons, acting as an excitatory neurotransmitter at physiologic concentrations and as a neurotoxic substance when present in excess. Glutamate has also been implicated in the initiation of nerve cell death under conditions of stroke, epilepsy, and other forms of central nervous system insult. Glutamate kills neuronal cells through either a receptor-mediated pathway or the inhibition of cysteine uptake and the oxidative pathway [16]. KA is a glutamate analogue with excitotoxic properties [17, 18]. It is well known that KA induces elevations of intracellular Ca^{2+} and extracellular glutamate levels via coactivation of N-methyl-D-aspartate (NMDA) receptors. Glutamate-evoked Na^{+} influx has also been proposed to contribute to the acute form of neurotoxicity [19, 20]. Hippocampal mossy fiber (MF) sprouting is a potential therapeutic target for epilepsy [21, 22]. The induction of BDNF protein is most evident in the MF pathway [21].

Reactive oxygen species (ROS) are by-products generated by cellular oxidative metabolism. Oxidative stress is a causal, or at least an ancillary, factor in the neuropathology of several adult neurodegenerative disorders [23]. ROS are known to play a role in KA-induced neuronal damage. Accumulating evidence indicates that hippocampal oxidative insults might be involved in KA-induced neurotoxicity *in vivo* [24, 25] and *in vitro*. Direct evidence of free radical generation during KA stimulation of cultured retinal neurons was provided by electron spin resonance (ESR) spectroscopy [26, 27]. ESR is a sophisticated spectroscopic technique that detects free radicals or inorganic complexes in chemical and biological systems [28]. ESR spectroscopy of spin-trapped radicals has become the method of choice for the detection and identification of free radicals formed in biological systems [29, 30]. The spin-trapping technique utilizing nitrones has been applied to the detection of free radicals for over thirty years. Nitrone spin traps are used in ESR studies because they specifically react with free radicals to form a radical adduct with a longer lifetime than the initial free radical. For biological applications, nitrone spin traps such as 5, 5-dimethyl-l-pyrroline-N oxide (DMPO) have been used most frequently [29].

Despite the widespread use of RGE, knowledge of its mechanism of action or protective effects on glutamate-mediated toxicity is limited. In this study, to elucidate these issues, we investigated the protective effect and possible mechanism of RGE on kainate-induced excitotoxicity in hippocampal neurons.

2. Materials and Methods

2.1. Chemicals and Reagents. RGE was kindly provided by the Korea Ginseng Cooperation (Daejeon, Republic of Korea). RGE yielded 4.37% saponins: the main components of ginsenosides were Rb_1 (12.6%), Rb_2 (6.2%), Rc (6.9%), Rd (3.4%), Re (6.4%), Rf (2.1%), Rg_1 (15.8%), and Rg_3 (1,4%). Those constituents are well standardized and qualified by the Korea Ginseng Cooperation. KA ((2S,3S,4S)-carboxy-4-(1-methylethenyl)-3-pyrrolidineacetic acid) was purchased from Tocris (Ellisville, MO, USA). BDNF was purchased from Abcam Inc. (Cambridge, MA, USA). The OXYTEK thiobarbituric acid reacting substances (TBARS) assay kit was purchased from Alexis (Farmindale, NY, USA). 6-Carboxy-2′,7′-dichlorofluorescin diacetate (DCFH-DA) and fura-4/AM were purchased from Molecular Probes Inc. (Eugene, OR, USA). DMPO was purchased from Enzo (Plymouth Meeting, PA, USA). Ferrous sulfate ($Fe_2SO_4 \cdot 7H_2O$), hydrogen peroxide (H_2O_2, 30%), diethylenetriamene pentaacetate (DTPA), DPPH, 6-hydroxy-2,5,7,7-tetramethyl-chromane-2-carboxylic acid (Trolox), DMTU, 3-(4,5-dimethylthiazol-2-yl)-2,5-diphenyl tetrazolium bromide (MTT), and all other chemicals were of high quality and were obtained from Sigma (St. Louis, MO, USA).

2.2. Animals. Male ICR mice (Samtako, Osan, Korea) weighing 30–35 g were used for *in vivo* experiments (n = 7-8). Animals were housed in acrylic cages (45 cm × 60 cm × 25 cm) with water and food available *ad libitum* under an artificial 12 h light/dark cycle (light on at 7 : 00) and constant temperature (22 ± 2°C). Mice were housed in the departmental room for 1 week before testing to ensure adaptation to the new environment. All experiments involving animals were performed in accordance with the National Institutes of Health Guide for the Care and Use of Laboratory Animals (NIH publication no. 85-23, revised 1985). The Institutional Animal Care and Use Committee of Chungbuk National University approved the protocol.

2.3. Primary Hippocampal Neuronal Cell Culture and KA Exposure. Primary cultures of rat hippocampal neurons were prepared from the hippocampi of E18-19 Sprague-Dawley (SD) rat embryos and cultured according to a previously described method [31]. The hippocampi were dissected and incubated with 0.25% papain in Ca^{2+} and Mg^{2+}-free Hank's balanced salt solution at 37°C for 20 min. Cells were then mechanically dissociated with fire-polished Pasteur pipettes by trituration and plated on poly-L-lysine coated coverslips in 35 mm culture dishes. Cells were maintained in Neurobasal/B27 medium containing 0.5 mM L-glutamine, 25 μM glutamate, 25 μM 2-mercaptoethanol, 100 unit/mL penicillin, and 100 μg/mL streptomycin in a humidified atmosphere of 95% air and 5% CO_2 at 37°C, with half of the medium changed every 2 days. Hippocampal neurons were cultured for 12–14 days before KA (100 μM) exposure. RGE (0.01–1.0 mg/mL) was added 0.5–1 h before KA treatment.

2.4. Cell Viability Assay. Cell viability assays were performed as described [32]. After exposure for the indicated times, neurons were assayed for viability using MTT (Sigma, St. Louis, MO, USA), which was added at a final concentration of 5 mg/mL for 4 h. MTT was removed, and neurons were lysed in 200 μL of dimethyl sulfoxide (DMSO). The absorbance was measured at 570 nm on a SpectraMax M2 multimode microplate reader (Sunnyvale, CA, USA). The data are expressed as the percentage of unexposed neurons that remained in the presence of KA.

2.5. Intracellular ROS Measurement. Production of ROS in neurons was determined using DCFH-DA (Molecular Probes, Eugene, OR, USA) as previously described [33]. Cultures were incubated with 10 μM DCFH-DA at 37°C for 30 min. After DCFH-DA was removed, the cells were recorded. DCFH-DA-loaded cells were placed in a SpectraMax M2 multiwell fluorescence microplate reader (Sunnyvale, CA, USA) with excitation at 515 nm and emission 552 nm. The protein concentration was determined by the Bradford assay.

2.6. Intracellular Calcium Measurement. The acetoxymethyl ester form of fura-4 (Molecular probes, Eugene, OR, USA) was used as the fluorescent Ca^{2+} indicator. Hippocampal cells were incubated for 60 min at room temperature with 5 μM fura-4/AM and 0.001% Pluronic F-127 in a HEPES-buffered solution composed of (in mM) 150 NaCl, 5 KCl, 1 $MgCl_2$, 2 $CaCl_2$, 10 HEPES, and 10 glucose. The pH was adjusted to 7.4 with NaOH. The cells were then washed with HEPES-buffered solution and placed on a SpectraMax M2 multiwell fluorescence microplate reader (Sunnyvale, CA, USA). Emitted fluorescence was calculated using a fluorescence analyzer and converted to intracellular free Ca^{2+} concentration $[Ca^{2+}]_i$.

2.7. Lipid Peroxidation Assay. Lipid peroxide formation was analyzed by measuring the TBARS in homogenates, as described by Suematsu et al. [34]. The OXYTEK TBARS assay Kit was used for these measurements. Lipid peroxidation was determined using their protocol by measuring the absorbance at 532 nm and was expressed as nmol of malondialdehyde (MDA)/mg of protein. The protein concentrations of hippocampi were determined using the Bradford assay.

2.8. Western Blotting Assay. Cells were harvested, washed twice with ice-cold PBS, and lysed in a lysis buffer for 30 min on ice, with vortexing every 5 min. Lysates were then centrifuged at 14,000 rpm for 5 min to remove insoluble material. Protein concentrations were determined by the Bradford method (Bio-Rad) using BSA as a standard. For BDNF, protein was separated on 16% SDS-PAGE gels. The gels were subsequently transferred onto PVDF membranes (Amersham Hybond TM-P, GE Healthcare, Buckinghamshire, UK) by electroblotting for 2 h at 60–75 V. Membranes were then blocked with 5% nonfat milk solution in Tris-NaCl buffer (TNT) containing 0.5% Tween-20 and incubated with primary antibodies as indicated. Monoclonal donkey anti-rabbit IgG horseradish peroxidase-conjugated secondary antibodies were used at 1 : 3,000. Proteins were detected by enhanced chemiluminescence using a commercial kit (Amersham).

2.9. 1,1-Dipheny-2-picrylhydrazyl (DPPH) Assay. The scavenging of the stable free radical DPPH by RGE was assayed spectrophotometrically [35]. DPPH in ethanol (0.1 mM) (control) was mixed thoroughly with various concentrations of RGE (0–10 mg/mL), and the absorbance was read at 517 nm. The degree of DPPH radical scavenging activity of RGE was calculated as a percentage of inhibition (% inhibition), where

$$\%\ \text{inhibition} = \left[\frac{\left(A_{\text{control}} - A_{\text{sample}}\right)}{A_{\text{control}}}\right] \times 100. \quad (1)$$

2.10. $^{\bullet}$OH Scavenging Activity by ESR. $^{\bullet}$OH was generated by the Fenton Reaction System, and the generated $^{\bullet}$OH rapidly reacted with the nitrone spin trap DMPO [29]. The resultant DMPO/$^{\bullet}$OH adduct was detected with an ESR spectrometer. RGE (0.2 mL) at various concentrations was mixed with DMPO (0.2 M, 0.2 mL), Fe_2SO_4 (2.0 mM, 0.2 mL), and H_2O_2 (2.0 mM, 0.2 mL) in a phosphate buffer solution (100 mM, pH 7.2), and the mixture was transferred to a quartz flat cell for ESR measurements. The mixture was performed in an ESR cavity at room temperature (24-25°C). After reaction, the ESR spectrum was recorded at room temperature using an ESR (JEOL JESTE-300) spectrometer (JEOL, Inc., Tokyo, Japan) equipped with a TE_{102} cavity. Experimental conditions were as follows: magnetic field, 339.3 ± 10 mT; power, 2.2 mW; modulation frequency, 9.44 GHz; amplitude, 10 × 10; sweep time, 0.5 min. The results were indicated as the time required to produce a 50% inhibition or decrease in signal peak height (IH_{50}) by ESR.

2.11. Statistical Analysis. Data were presented as means ± SEM. For statistical comparisons, the results were analyzed using one-way analysis of variance (ANOVA). A P value < 0.05 was considered statistically significant. In the case of significant variation, the individual values were compared with the Holm-Sidak test.

3. Results

3.1. Protection from Kainate Toxicity by RGE. To evaluate the protective effect of RGE against KA-induced cytotoxicity, we examined cell death in primary hippocampal neurons by the MTT assay. Neurons were exposed to KA at concentrations of 0, 30, 50, 70, and 100 μM for 48 h (Figure 1(a)). Figure 2 shows that cell death is rapid, with growth inhibited to 55.1 ± 1.0% of control levels after 48 h of KA exposure. When cells were exposed to 100 μM KA, cell death was significant after 48 h (Figure 1). Exposure of hippocampal neurons to 100 μM of KA for 48 h elicited a significant decrease in cell survival, whereas KA-induced neuronal loss was inhibited by 63.1 ± 1.8% and 74.4 ± 1.4% by adding 0.01 and 1.0 mg/mL of RGE, respectively (Figure 1). Additionally, 76.8 ± 1.9% and

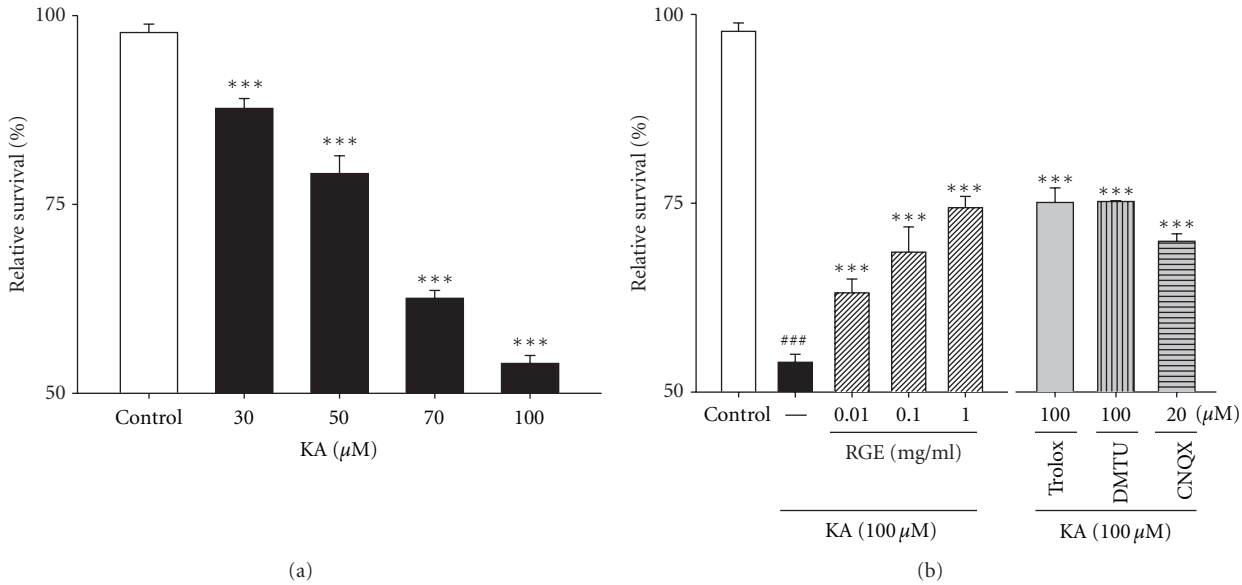

Figure 1: RGE prevents KA-induced neuronal loss in primary cultured hippocampal cells. (a) Concentration data for KA-induced toxicity in primary cultured hippocampal neurons. Examination of the dose effect of KA on neuronal viability by the MTT assay. Neurons were exposed to KA at concentrations of 0, 30, 50, 70, and 100 μM for 48 h. (b) Protection of hippocampal neurons against KA-induced cell loss by RGE. Neurons were exposed to 100 μM KA at 1 h after 0.01–1.0 mg/mL of RGE, Trolox (100 μM), or DMTU (100 μM) treatment. Cell viability at 48 h after KA exposure was measured by the MTT assay. All data are presented as means ± SE. $^{\#\#\#}P < 0.001$ versus the control group. $^{***}P < 0.001$ versus the KA group.

76.9 ± 0.1% inhibition of cell death were achieved by 100 μM trolox and DMTU, respectively. When we explored the role of non-N-methyl-D-aspartate (NMDA) receptors in excitotoxicity, KA-induced cell death was blocked by 20 μM 6-cyano-7-nitroquinoxaline-2,3-dione (CNQX), a non-NMDA receptor antagonist. These results indicate that RGE can protect neurons against KA-induced cytotoxicity.

3.2. Effects of RGE against Oxidative Stress. Because KA induces oxidative damage in cultured murine neurons, we examined whether RGE affected 100 μM KA-induced ROS levels in primary hippocampal neuronal cells by the DCFH-DA assay. Low levels of ROS were found in control (2,582 ± 124 fluorescence intensity), and these values were considered physiological. In contrast, a significant increase in ROS concentration was seen, with an intensity value of 3,424 ± 79, after treatment with 100 μM KA for 48 h. As shown in Figure 2, ROS levels displayed intensity values of 3,056 ± 89 and 2,883 ± 157 at doses of 0.1 and 1.0 mg/mL of RGE, respectively. Trolox and DMTU also exhibited an inhibition in ROS production at the highest KA dose of 100 μM (Figure 2). Taken together, these results indicate that 100 μM KA treatment elevates ROS production and that pretreatment with 0.1 to 1.0 mg/mL of RGE significantly decreases ROS production (Figure 2). These results indicate that RGE can protect neurons against KA-induced excitotoxicity through its antioxidant effects.

3.3. Inhibition of Ca^{2+} Influx. In oxidative glutamate toxicity, a 100-fold increase in intracellular ROS results in the elevation of cytosolic Ca^{2+}, which precedes cell death. To investigate the mechanism of protection of RGE against KA-induced neurotoxicity, we examined whether RGE could inhibit KA-induced intracellular $[Ca^{2+}]_i$ elevation in cultured hippocampal neurons. We measured $[Ca^{2+}]_i$ levels using the Ca^{2+} indicator, fura-4. As shown in Figure 3, 100 μM KA treatment led to a significant elevation of $[Ca^{2+}]_i$ (data not shown). The % inhibition of $[Ca^{2+}]_i$ elevation by RGE in hippocampal neurons was 4.4 ± 0.04%, 10.1 ± 0.02%, and 18.9 ± 0.04%, at doses of 0.01, 0.1, and 1.0 mg/mL, respectively, where $[Ca^{2+}]_i$ levels in normal controls were considered 100% (Figure 3). Treatment with RGE at doses of 0.01, 0.1, and 1.0 mg/mL inhibited KA-induced $[Ca^{2+}]_i$ elevation in a dose-dependent manner. In contrast, treatment with trolox, DMTU, or CNQX made slight effect. These results indicate that 100 μM KA treatment of cultured hippocampal neurons elevates $[Ca^{2+}]_i$ and that this effect is attenuated by treatment with RGE at concentrations of 0.01, 0.1, and 1.0 mg/mL.

3.4. Inhibition of MDA Levels by RGE. Free radicals may be one of the major causes of excitotoxicity lesions. Therefore, we estimated free radical generation using a TBARS assay. TBARS levels, an indicator of lipid peroxidation, were significantly increased in the hippocampi of mice treated with KA dose-dependently when compared to the control group (vehicle) that had not received the stressor agent. However, pretreatment with 30 and 200 mg/kg doses of RGE for 10 days significantly prevented KA-induced increase in TBARS levels. Complete inhibition of lipid peroxidation was observed at 200 mg/mL of RGE (Figure 4). Animals treated

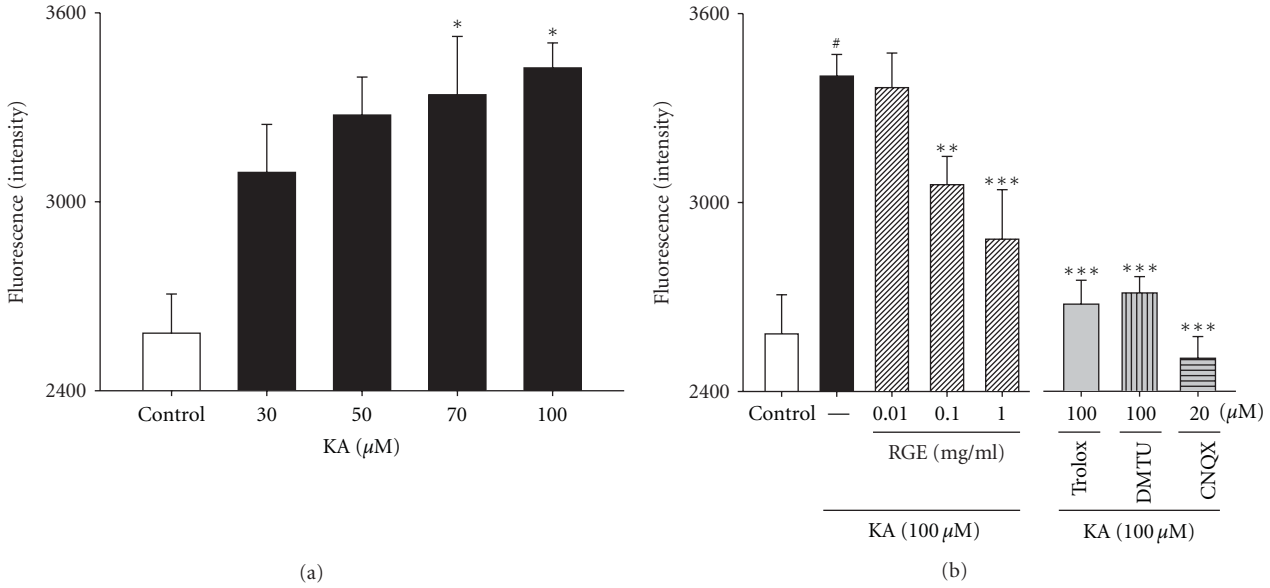

Figure 2: Effects of RGE and scavengers against oxidative stress in primary cultured hippocampal cells. (a) Concentration data for KA-induced ROS levels in primary cultured hippocampal neurons. Examination of the dose effect of KA on neuronal ROS level by the DCFH-DA assay. Neurons were exposed to KA at concentrations of 0, 30, 50, 70, and 100 μM for 48 h. (b) Protection of hippocampal neurons against KA-induced ROS levels by RGE. Neurons were exposed to 100 μM KA at 1 h after 0.01–1 mg/mL of RGE, trolox (100 μM), or DMTU (100 μM) treatment. All data are presented as means ± SE. $^{\#\#\#}P < 0.001$ versus the control group. $^{*}P < 0.05$, $^{**}P < 0.01$, $^{***}P < 0.001$ versus the KA group.

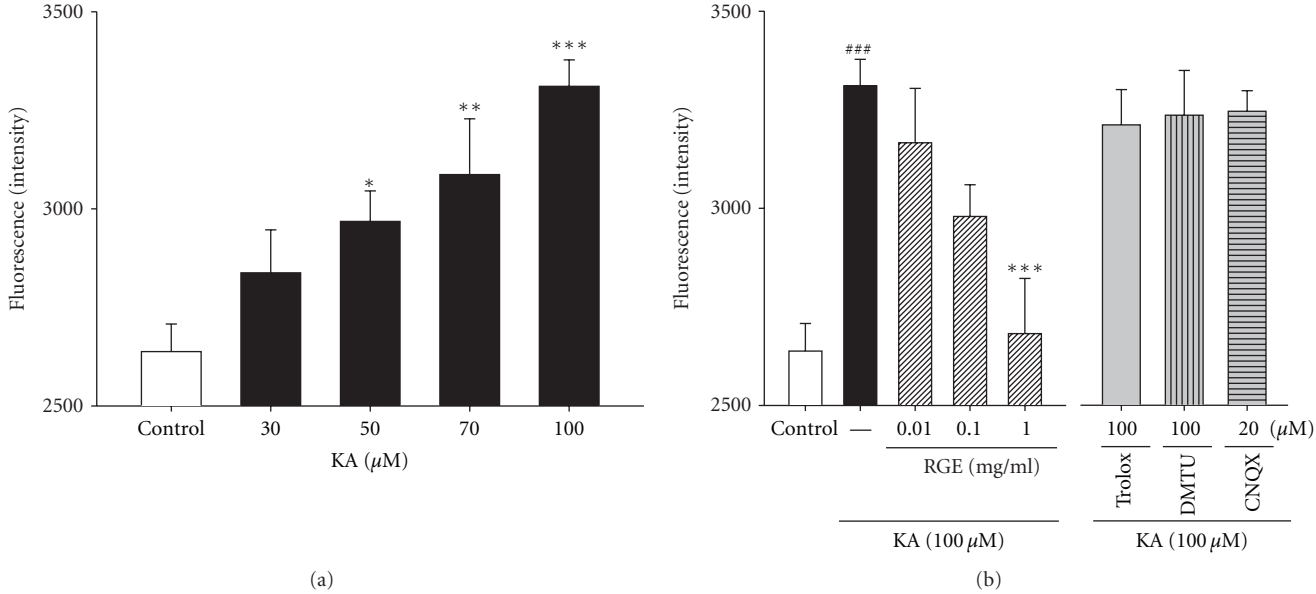

Figure 3: Effect of RGE and scavengers on $[Ca^{2+}]_i$ influx in primary cultured hippocampal cells. (a) Concentration data for KA-induced $[Ca^{2+}]_i$ in primary cultured hippocampal neurons. Examination of the dose effect of KA on neuronal $[Ca^{2+}]_i$ by the Ca^{2+} indicator with fura-4. Neurons were exposed to KA at concentrations of 0, 30, 50, 70, and 100 μM for 48 h. (b) Protection of hippocampal neurons against KA-induced $[Ca^{2+}]_i$ by RGE. Neurons were exposed to 100 μM KA at 1 h after 0.01–1.0 mg/mL of RGE, trolox (100 μM), or DMTU (100 μM) treatment. All data are presented as means ± SE. $^{\#\#\#}P < 0.001$ versus the control group. $^{*}P < 0.05$, and $^{**}P < 0.01$, $^{***}P < 0.001$ versus the KA group.

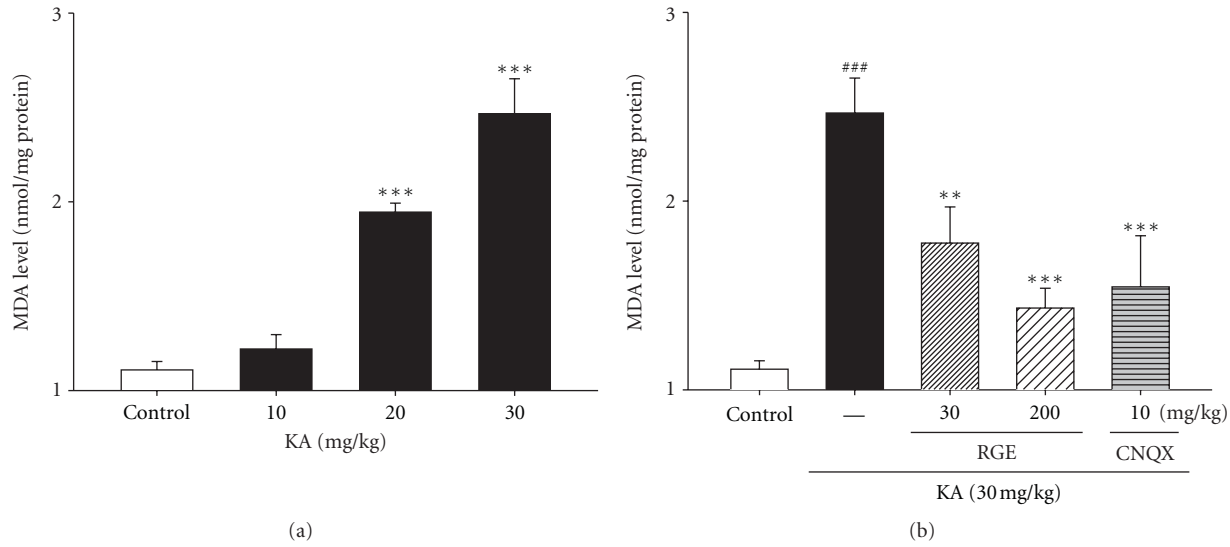

Figure 4: Effect of RGE and scavengers on MDA levels in KA-treated hippocampal tissue homogenates. Male mice were grouped ($n = 5$ or 6/group) and pretreated (i.p. injection) with RGE (30–200 mg/kg) and scavengers such as trolox (50 mg/kg, i.p.) and DMTU (50 mg/kg, i.p.), or NaCl (0.9%). Thirty minutes after the final RGE or saline pretreatment, seizures in the KA, scavengers + KA, and RGE + KA groups were induced by KA injection (30 mg/kg, i.p.); the mice in the saline group received an equal volume of 0.9% NaCl. All data are presented as means ± SE. $^{###}P < 0.001$ versus the control group. $^{**}P < 0.01$, $^{***}P < 0.001$ versus the KA group.

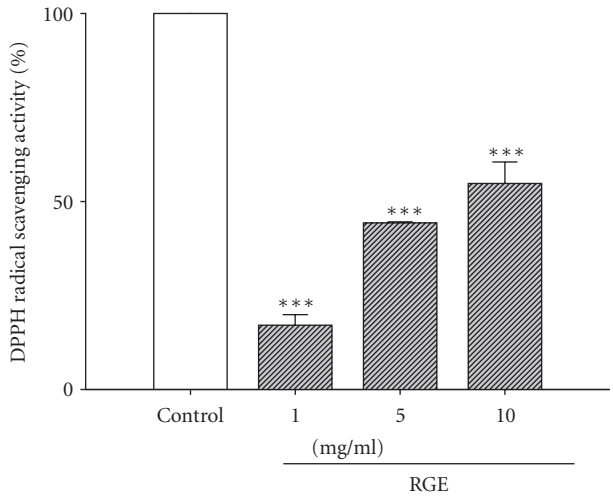

Figure 5: DPPH radical-scavenging activity of RGE. 0.01–1.0 mg/mL of RGE was used. Trolox, as a positive control, scavenged 100% of the DPPH radical at 0.25 mg/mL. All data are presented as means ± SE. $^{***}P < 0.001$ versus the control group.

only with RGE at both doses presented no alteration in TBARS levels (data not shown).

3.5. DPPH Radical Reduction Activity of RGE. The activity of ginseng is generally explained by its antioxidative efficacy. To identify the redox potential of RGE, the reduction of the DPPH radical was analyzed in mixed solutions (RGE+DPPH). Figure 5 shows that RGE scavenged the DPPH radical in a dose-dependent manner, and the IC_{50} of RGE was approximately 10 mg/mL (Figure 5). Trolox used as a positive control scavenged 100% of the DPPH radical at 0.25 mg/mL.

3.6. $^{\bullet}OH$ Reduction Activity of RGE. $^{\bullet}OH$ generated by the Fenton Reaction System was trapped by DMPO, which could be detected by an ESR spectrometer. The typical 1 : 2 : 2 : 1 ESR signal of the DMPO/$^{\bullet}OH$ adduct ($A_N = A_H = 14.4$ G) was observed as shown in Figure 6(a). Each spectrum was obtained 15 min after the start of the Fenton Reaction. RGE inhibits the Fenton Reaction by reaction with $^{\bullet}OH$. In addition, as shown in Figure 6(b), the signal of the DMPO/$^{\bullet}OH$ adduct gradually decreased over time. The decay rate showed approximately a pseudo-first-order kinetics over the period of measurement (10 min), and the half-life of the DMPO/$^{\bullet}OH$ signal was estimated to be 8.15 min. The order of reduction activities in the Fenton Reaction System was DMTU > RGE > trolox. The RGE reduction activity was similar to trolox. The activities of DMTU, RGE, and trolox were 5.76, 7.5–8, and 8.17 min, respectively. The second-order rate constants were estimated to be $3.4 \times 10^9\ M^{-1}\cdot S^{-1}$ for trolox and $4.7 \times 10^9\ M^{-1}\cdot S^{-1}$ for DMTU. From these results, it is possible to estimate the apparent second-order rate constant of RGE for $^{\bullet}OH$. Therefore, we demonstrated that RGE reacts with $^{\bullet}OH$ and has reduction activity and that the second-order rate constant of RGE for $^{\bullet}OH$ is approximately $3.5–4.5 \times 10^9\ M^{-1}\cdot S^{-1}$.

3.7. Alterations in BDNF Protein Levels after KA Injury. In search of endogenous substances having protective action against EAA, we investigated alterations in hippocampal BDNF expression induced by KA (Figure 7). BDNF protein was decreased after KA exposure. Downregulation of hippocampal BDNF protein induced by KA was increased

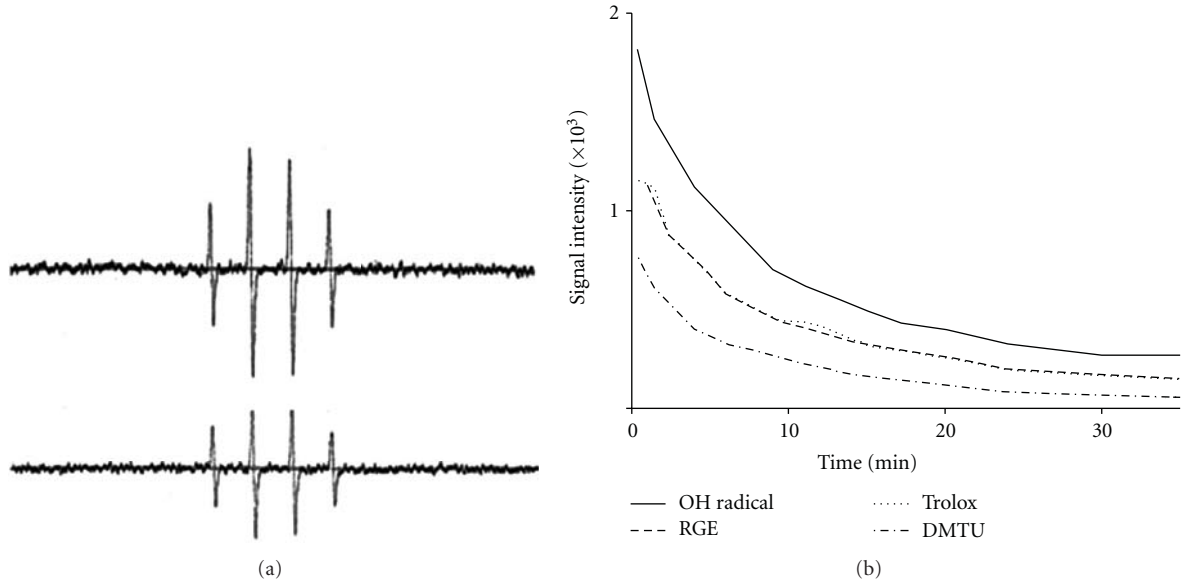

Figure 6: Reduction activity of RGE on •OH. (a) ESR spectra of the DMPO/•OH adduct were generated in a Fenton Reaction System. The solutions with a final volume of 0.1 mL contained 2.0 mM ferrous sulfate, 2.0 mM H_2O_2, and 100 mM phosphate buffer (pH 7.2). Reactions were started by the addition of ferrous ammonium sulfate (2.0 mM final concentration), and the steady-state ESR spectra were recorded at 15 min after the Fenton Reaction. Upper line, DMPO/•OH adduct; lower line, RGE (1.0 mg/mL). (b) Time course of •OH degradation induced by the Fenton Reaction System. DMPO/•OH adduct, RGE (1.0 mg/mL), trolox (1.0 mM), and DMTU (1 mM).

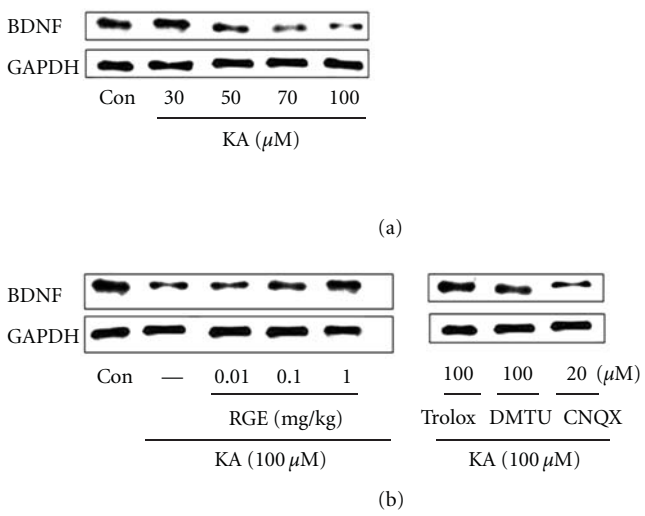

Figure 7: Effect of RGE and scavengers on BDNF levels in KA-treated hippocampal neurons. Immunoblots of lysed embryonic rat hippocampi 2 days following administration of RGE or KA are shown. Neurons were exposed to KA at concentrations of 0, 30, 50, 70, and 100 μM for 48 h. Neurons were exposed to 100 μM KA at 1 h after 0.01–1.0 mg/mL of RGE, trolox (100 μM), and DMTU (100 μM) treatment. GAPDH levels were measured to confirm equal protein loading.

above control levels by RGE treatment. Decrease in BDNF expression in response to KA was antagonized by CNQX. Moreover, slight changes in BDNF expression were noted in trolox and DMTU treatment. Collectively, these data suggest that RGE is an active compound in KA-induced hippocampal mossy-fiber function improvement.

4. Discussion

Our results clearly demonstrate that RGE, one of the most widely used medicinal plants, has significant antioxidant/neuroprotective effects against kainic acid- (KA-) induced excitotoxicity *in vitro* and *in vivo*. We found that RGE reduced *in vitro* toxicity induced by KA, a potent neurotoxin. KA inhibited cell death and the generation of $[Ca^{2+}]_i$ and ROS in hippocampal neurons and increased MDA and BDNF levels in hippocampal tissue. In addition, RGE possesses •OH reduction activity in the Fenton Reaction System as measured using the ESR spectrometer.

KA is a specific agonist of the KA receptor and a selective ionotropic glutamate agonist. Glutamate toxicity is the major contributor to pathological cell death within the nervous system and appears to be mediated by ROS [36]. Oxidative glutamate toxicity has also been implicated in the initiation of nerve cell death under conditions of stroke, epilepsy, and other forms of central nervous system insult. •OH is a strong oxidant. ESR is the preferred tool for detecting and identifying free radicals and is widely used. The ESR spin-trapping technique is the only viable spectroscopic technique for detecting •OH under physiologically relevant conditions [29, 30, 37]. For •OH signal detection, we used the Fenton Reaction System, as shown in Figure 6. RGE inhibits the Fenton Reaction by reaction with •OH because of its fast initial velocity and high second-order rate constant. DPPH and ESR spin-trapping data are good pieces of evidence that indicate the radical reduction activity of RGE (Figures 5 and 6)

[38, 39]. Additionally, we estimated the second-order rate constant of RGE/$^{\bullet}$OH to be 3.5–4.5 $\times$ 10^9 $M^{-1}\cdot S^{-1}$.

The mammalian hippocampus plays a pivotal role in a diverse set of cognitive functions, including memory. Glutamatergic signaling in the hippocampus changes during oxidative stress. Cultured rat hippocampal neurons are a useful model for studying the glutamate system. In the toxicity experiments shown in Figure 1, RGE exerted neuroprotective effects against glutamate-induced neurotoxicity. These effects may be explained by the redox antioxidant system, although we cannot rule out the involvement of other mechanisms. Antioxidants in foods and medicinal plants (or herbs) have attracted interest in recent years. Ginsenosides, the main pharmacologically active constituents of ginseng, consist of four hydrophobic ring steroid-like structures with hydrophilic sugar moieties. Free, monomeric, dimeric, or trimeric sugars are bound to hydroxyl groups ($^{\bullet}$OH) on carbon-3, -6, and -20 of ginsenosides. They also exist as stereoisomers. This epimerization is known to occur by the selective attack of $^{\bullet}$OH after the elimination of the glycosyl residue at C-20 during the steaming process. In addition, less-polar ginsenosides such as RGE are known to be easily produced by the elimination of H_2O at C-20 of the RG species under high pressure and temperature conditions as in autoclaving. Phenolic compounds are commonly found in plants and have been reported to have multiple biological effects, including antioxidant activity [8, 40, 41]. Phenolic compounds and maltol have strong free radical scavenging activities [42, 43]. In addition, the chelating activity of the hydroxypyrone structure, like other iron chelators such as desferrioxamine (DFO), is very important. Based on these reasons, it is possible that the activity of the phenol extract of RGE is due to its hydrogen-donating ability or chelating ability.

Intracellular calcium levels are usually very low ($\sim 10^{-7}$ M). Excessive accumulation of intracellular calcium is the key process leading to neuronal death or injury. NMDA receptors activate channels that allow the influx of extracellular calcium (and sodium) [44]. Overstimulation of this type of glutamate receptor leads to neuronal calcium overload. Both AMPA and KA receptors are linked to Na^+ permeable channels. Depolarization is initiated primarily by activation of AMPA receptors and subsequently by activation of voltage-dependent sodium channels. This leads to sodium entry and further depolarization. Na^+ influx can be involved in the toxic process by causing osmotic stress [20] and via depolarization by opening voltage-operated calcium channels. In addition, Ca^{2+} influx can damage neurons by activating various enzymes. If the cell becomes chronically depolarized, the NMDA receptor will relinquish its magnesium block and become available for activation by synaptic glutamate. Its activation is a major source of calcium entry into the cell. Sustained increase in intracellular Ca^{2+} concentration $[Ca^{2+}]_i$ initiates the excitotoxic processes culminating in delayed neuronal death.

KA is toxic mainly in the hippocampus, which has high-affinity KA binding sites. To search for endogenous substances having a protective effect against EAA, we investigated the alterations in hippocampal BDNF expression. The protein family of neurotrophins consisting of nerve growth factor (NGF), BDNF, NT-3, NT-4/5, NT-6, and NT-7 is known to regulate the survival and differentiation of peripheral nervous system (PNS) and CNS neurons [45]. In the recent years, evidence has accumulated that BDNF plays an additional important role in hippocampal synaptic plasticity by either facilitating transmitter release from presynaptic terminals or enhancing postsynaptic NMDA receptor function. Therefore, it is possible that the attenuation of NMDA neurotoxicity is caused by diffusible factors secreted by the striatal cells, such as neurotrophins like BDNF. The substances protecting neurons from stress caused by ROS such as $^{\bullet}$OH may have a role in the promotion of hippocampal mossy-fiber functions in the CNS.

5. Conclusions

RGE protected hippocampal neurons from toxicity due to KA-induced increases in $[Ca^{2+}]_i$, ROS, and MDA levels. The RGE reaction with DPPH and $^{\bullet}$OH possesses radical reduction activity, and the second-order rate constant for $^{\bullet}$OH is 3.5–4.5 $\times$ 10^9 $M^{-1}\cdot S^{-1}$. RGE alleviates KA-induced excitotoxicity by quenching ROS in hippocampal neurons.

Acknowledgments

This work was supported by the Priority Research Centers Program through the National Research Foundation of Korea (NRF) funded by the Ministry of Education, Science and Technology (2011-0031403), by the Medical Research Center program (2010-0029480) and the Regional Core Research program(Chungbuk BIT Research-Oriented University Consortium) through the National Research Foundation of Korea and by the 2011 grant from the Korea Society of Ginseng funded by the Korea Ginseng Corporation.

References

[1] R. J. Ko, "Adulterants in Asian patent medicines," *The New England Journal of Medicine*, vol. 339, no. 12, p. 847, 1998.

[2] N. R. Slifman, W. R. Obermeyer, B. K. Aloi et al., "Contamination of botanical dietary supplements by Digitalis lanata," *The New England Journal of Medicine*, vol. 339, no. 12, pp. 806–811, 1998.

[3] T. K. Yun, "Brief introduction of Panax ginseng C.A. Meyer," *Journal of Korean Medical Science*, vol. 16, supplement, pp. S3–S5, 2001.

[4] K. S. Kang, H. Y. Kim, S. H. Baek, H. H. Yoo, J. H. Park, and T. Yokozawa, "Study on the hydroxyl radical scavenging activity changes of ginseng and ginsenoside-Rb2 by heat processing," *Biological and Pharmaceutical Bulletin*, vol. 30, no. 4, pp. 724–728, 2007.

[5] C. A. Rice-Evans, N. J. Miller, and G. Paganga, "Structure-antioxidant activity relationships of flavonoids and phenolic acids," *Free Radical Biology and Medicine*, vol. 20, no. 7, pp. 933–956, 1996.

[6] E. J. Lien, S. Ren, H. H. Bui, and R. Wang, "Quantitative structure-activity relationship analysis of phenolic antioxidants," *Free Radical Biology and Medicine*, vol. 26, no. 3-4, pp. 285–294, 1999.

[7] S. Son and B. A. Lewis, "Free radical scavenging and antioxidative activity of caffeic acid amide and ester analogues: structure-activity relationship," *Journal of Agricultural and Food Chemistry*, vol. 50, no. 3, pp. 468–472, 2002.

[8] W. Zheng and S. Y. Wang, "Antioxidant activity and phenolic compounds in selected herbs," *Journal of Agricultural and Food Chemistry*, vol. 49, no. 11, pp. 5165–5170, 2001.

[9] N. Nakatani, "Phenolic antioxidants from herbs and spices," *BioFactors*, vol. 13, no. 1–4, pp. 141–146, 2000.

[10] A. S. Attele, J. A. Wu, and C. S. Yuan, "Ginseng pharmacology: multiple constituents and multiple actions," *Biochemical Pharmacology*, vol. 58, no. 11, pp. 1685–1693, 1999.

[11] H. Kaneko and K. Nakanishi, "Proof of the mysterious efficacy of ginseng: basic and clinical trials: clinical effects of medical ginseng, Korean red ginseng: specifically its anti-stress action for prevention of disease," *Journal of Pharmacological Sciences*, vol. 95, no. 2, pp. 158–162, 2004.

[12] H. Nishijo, T. Uwano, Y. M. Zhong, and T. Ono, "Proof of the mysterious efficacy of ginseng: basic and clinical trials: effects of red ginseng of learning and memory deficits in an animal model of amnesia," *Journal of Pharmacological Sciences*, vol. 95, no. 2, pp. 145–152, 2004.

[13] B. M. Lee, S. K. Lee, and H. S. Kim, "Inhibition of oxidative DNA damage, 8-OHdG, and carbonyl contents in smokers treated with antioxidants (vitamin E, vitamin C, beta-carotene and red ginseng)," *Cancer Letters*, vol. 132, no. 1-2, pp. 219–227, 1998.

[14] R. Zhao and W. F. McDaniel, "Ginseng improves strategic learning by normal and brain-damaged rats," *NeuroReport*, vol. 9, no. 7, pp. 1619–1624, 1998.

[15] A. Akaike, H. Katsuki, T. Kume, and T. Maeda, "Reactive oxygen species in NMDA receptor-mediated glutamate neurotoxicity," *Parkinsonism and Related Disorders*, vol. 5, no. 4, pp. 203–207, 1999.

[16] D. W. Choi, "Glutamate neurotoxicity and diseases of the nervous system," *Neuron*, vol. 1, no. 8, pp. 623–634, 1988.

[17] J. W. Ferkany, R. Zaczek, and J. T. Coyle, "Kainic acid stimulates excitatory amino acid neurotransmitter release at presynaptic receptors," *Nature*, vol. 298, no. 5876, pp. 757–759, 1982.

[18] W. Liu, R. Liu, J. T. Chun et al., "Kainate excitotoxicity in organotypic hippocampal slice cultures: evidence for multiple apoptotic pathways," *Brain Research*, vol. 916, no. 1-2, pp. 239–248, 2001.

[19] S. M. Rothman, "The neurotoxicity of excitatory amino acids is produced by passive chloride influx," *Journal of Neuroscience*, vol. 5, no. 6, pp. 1483–1489, 1985.

[20] J. W. Olney, M. T. Price, L. Samson, and J. Labruyere, "The role of specific ions in glutamate neurotoxicity," *Neuroscience Letters*, vol. 65, no. 1, pp. 65–71, 1986.

[21] M. Hartmann, R. Heumann, and V. Lessmann, "Synaptic secretion of BDNF after high-frequency stimulation of glutamatergic synapses," *The EMBO Journal*, vol. 20, no. 21, pp. 5887–5897, 2001.

[22] R. Koyama and Y. Ikegaya, "Mossy fiber sprouting as a potential therapeutic target for epilepsy," *Current Neurovascular Research*, vol. 1, no. 1, pp. 3–10, 2004.

[23] P. Jenner, "Oxidative damage in neurodegenerative disease," *The Lancet*, vol. 344, no. 8925, pp. 796–798, 1994.

[24] L. P. Liang, M. E. Beaudoin, M. J. Fritz, R. Fulton, and M. Patel, "Kainate-induced seizures, oxidative stress and neuronal loss in aging rats," *Neuroscience*, vol. 147, no. 4, pp. 1114–1118, 2007.

[25] K. Xu and J. L. Stringer, "Antioxidants and free radical scavengers do not consistently delay seizure onset in animal models of acute seizures," *Epilepsy and Behavior*, vol. 13, no. 1, pp. 77–82, 2008.

[26] A. Y. Sun, Y. Cheng, Q. Bu, and F. Oldfield, "The biochemical mechanisms of the excitotoxicity of kainic acid: free radical formation," *Molecular and Chemical Neuropathology*, vol. 17, no. 1, pp. 51–63, 1992.

[27] T. Masumizu, Y. Noda, A. Mori, and L. Packer, "Electron spin resonance assay of ascorbyl radical generation in mouse hippocampal slices during and after kainate-induced seizures," *Brain Research Protocols*, vol. 16, no. 1–3, pp. 65–69, 2005.

[28] J. Y. Han, K. Takeshita, and H. Utsumi, "Noninvasive detection of hydroxyl radical generation in lung by diesel exhaust particles," *Free Radical Biology and Medicine*, vol. 30, no. 5, pp. 516–525, 2001.

[29] G. M. Rosen and E. J. Rauckman, "Spin trapping of superoxide and hydroxyl radicals," *Methods in Enzymology*, vol. 105, pp. 198–209, 1984.

[30] M. J. Turner and G. M. Rosen, "Spin trapping of superoxide and hydroxyl radicals with substituted pyrroline 1-oxides," *Journal of Medicinal Chemistry*, vol. 29, no. 12, pp. 2439–2444, 1986.

[31] C. Lesuisse, D. Qiu, C. M. Böse, K. Nakaso, and F. Rupp, "Regulation of agrin expression in hippocampal neurons by cell contact and electrical activity," *Molecular Brain Research*, vol. 81, no. 1-2, pp. 92–100, 2000.

[32] S. Y. Li, J. H. Ni, D. S. Xu, and H. T. Jia, "Down-regulation of GluR2 is associated with Ca^{2+}-dependent protease activities in kainate-induced apoptotic cell death in culturd rat hippocampal neurons," *Neuroscience Letters*, vol. 352, no. 2, pp. 105–108, 2003.

[33] H. Wang and J. A. Joseph, "Quantifying cellular oxidative stress by dichlorofluorescein assay using microplate reader," *Free Radical Biology and Medicine*, vol. 27, no. 5-6, pp. 612–616, 1999.

[34] T. Suematsu, T. Kamada, and H. Abe, "Serum lipoperoxide level in patients suffering from liver diseases," *Clinica Chimica Acta*, vol. 79, no. 1, pp. 267–270, 1977.

[35] K. Marxen, K. H. Vanselow, S. Lippemeier, R. Hintze, A. Ruser, and U. P. Hansen, "Determination of DPPH radical oxidation caused by methanolic extracts of some microalgal species by linear regression analysis of spectrophotometric measurements," *Sensors*, vol. 7, no. 10, pp. 2080–2095, 2007.

[36] J. T. Coyle and P. Puttfarcken, "Oxidative stress, glutamate, and neurodegenerative disorders," *Science*, vol. 262, no. 5134, pp. 689–695, 1993.

[37] G. R. Buettner and R. P. Mason, "Spin-trapping methods for detecting superoxide and hydroxyl free radicals in vitro and in vivo," *Methods in Enzymology*, vol. 186, pp. 127–133, 1990.

[38] N. Yamabe, J. G. Lee, Y. J. Lee et al., "The chemical and 1, 1-diphenyl-2-picrylhydrazyl radical scavenging activity changes of ginsenosides Rb1 and Rg1 by malliard reaction," *Journal of Ginseng Research*, vol. 35, no. 1, pp. 60–68, 2011.

[39] J. Y. Han, J. T. Hong, S. Y. Nam, and K. W. Oh, "Evaluation of hydroxyl radical reduction activity of red ginseng extract using ESR spectroscopy," *Journal of Biomedical Research*, vol. 13, no. 1, pp. 83–92, 2012.

[40] Y. Cai, Q. Luo, M. Sun, and H. Corke, "Antioxidant activity and phenolic compounds of 112 traditional Chinese medicinal plants associated with anticancer," *Life Sciences*, vol. 74, no. 17, pp. 2157–2184, 2004.

[41] Y. H. Kong, Y. C. Lee, and S. Y. Choi, "Neuroprotecyive and anti-inflammatory effects of phenolic compounds in panax

ginseng C. A. Meyer," *Journal of Ginseng Research*, vol. 23, no. 2, pp. 111–114, 2009.

[42] K. S. Kang, H. Y. Kim, J. S. Pyo, and T. Yokozawa, "Increase in the free radical scavenging activity of ginseng by heat-processing," *Biological and Pharmaceutical Bulletin*, vol. 29, no. 4, pp. 750–754, 2006.

[43] B. H. Han, M. H. Park, and Y. N. Han, "Studies on the antioxidant components of korean ginseng(V): the mechanism of antioxidant activity of maltol and phenolic acid," *Korean Biochemistry Journal*, vol. 18, pp. 337–340, 1985.

[44] B. K. Lee, S. Lee, K. Y. Yi, S. E. Yoo, and Y. S. Jung, "KR-33028, a Novel Na+/H+ exchanger-1 inhibitor, attenuates glutamate-induced apoptotic cell death through Maintaining Mitochondrial Function," *Biomolecules & Therapeutics*, vol. 19, no. 4, pp. 445–450, 2011.

[45] G. R. Lewin and Y. A. Barde, "Physiology of the neurotrophins," *Annual Review of Neuroscience*, vol. 19, pp. 289–317, 1996.

Hindawi Publishing Corporation
Evidence-Based Complementary and Alternative Medicine
Volume 2012, Article ID 940846, 9 pages
doi:10.1155/2012/940846

Research Article

Antidepressant-Like Effects of Shuyusan in Rats Exposed to Chronic Stress: Effects on Hypothalamic-Pituitary-Adrenal Function

Liping Chen,[1] Mengli Chen,[2] Fawei Wang,[1] Zhigao Sun,[3] Huang Quanzhi,[3] Miao Geng,[4] Hongyan Chen,[4] and Dongmei Duan[1]

[1] *Department of Traditional Chinese Medicine, General Hospital of PLA, Beijing 100853, China*
[2] *Department of Chinese Pharmaceutical, General Hospital of PLA, Beijing 100853, China*
[3] *Postgraduate Medical School, General Hospital of PLA, Beijing 100853, China*
[4] *Institute of Gerontology, General Hospital of PLA, Beijing 100853, China*

Correspondence should be addressed to Liping Chen, lipingschen@yahoo.com.cn

Received 10 April 2012; Revised 25 June 2012; Accepted 9 July 2012

Academic Editor: Paul Siu-Po Ip

This study was to investigate antidepressant activities of Shuyusan (a Chinese herb), using a rats model of depression induced by unpredictable chronic mild stress (UCMS). The administration groups were treated with Shuyusan decoction for 3 weeks and compared with fluoxetine treatment. In order to understand the potential antidepressant-like activities of Shuyusan, tail suspension test (TST) and forced swimming test (FST) were used as behavioral despair study. The level of corticotropin-releasing factor (CRH), adrenocorticotropic hormone (ACTH), corticosterone (CORT) and hippocampus glucocorticoid receptor expression were examined. After modeling, there was a significant prolongation of immobility time in administration groups with the TST and FST. High-dose Shuyusan could reduce the immobility time measured with the TST and FST. The immobility time in high-dose herbs group and fluoxetine group was increased significantly compared with the model group. After 3 weeks herbs fed, the serum contents level of CRH, ACTH, and CORT in high-dose herb group was significantly decreased compared to the model group. The result indicated that Shuyusan had antidepressant activity effects on UCMS model rats. The potential antidepressant effect may be related to decreasing glucocorticoid levels activity, regulating the function of HPA axis, and inhibiting glucocorticoid receptor expression in hippocampus.

1. Introduction

In studies of pathogenesis on depression, hypothalamic-pituitary-adrenal axis (HPA) hyperactivity, and neuroendocrine disorders are more recognized; in addition to monoamine neurotransmitters [1–3]. Hippocampus, as an important role of brain for cognition, emotion, and memory function, is the center of motional for learning and memory consolidation [4]. Studies have proposed that long-term chronic stress could cause hyperthyroidism of the HPA, that increased level of corticotropin-releasing factor (CRH), adrenocorticotropic hormone (ACTH), and corticosterone (CORT), which led to excessive expression of glucocorticoid receptor (GR) of HPA [5]. This long-term overexpression and increased levels of glucocorticoid caused by chronic stress could lead to hippocampus neuronal cell damage and lead to depressive symptoms, such as depressed mood, feeling of worthlessness, insomnia, forgetfulness, sexual dysfunction, and other symptoms of depression [6, 7].

Traditional Chinese medicine has a good effect in treatment of depression. An increasing use of traditional Chinese medicine for depression treatment showed that traditional prescription drugs exhibited certain clinical efficacy, enhanced efficacy, and reduced dosages and side effects of common medicines, in combination with other antidepressants [8]. In Chinese medicine theory, liver plays an important role in the pathology of depression. Depression is commonly caused by emotional stress and injury as well as

failure of liver catharsis function and stagnation of liver Qi, (Qi is an energy flow, a vital energy, that circulates the body to regulate body functions) or life source [9–11]. Shuyusan has been effective herbs prescription against depression in our hospital for many years, which shows the effect of purifying the heart heat and regulating Qi and Blood. Our previous clinical study showed that Shuyusan could improve the clinical symptoms of depression, and laboratory study indicated that Shuyusan could increase 5-hydroxytryptamine (5-HT) and improve the 5-HT expression of hippocampus neurons on rats caused by chronic mild unpredictable stress-induced depression [12–14]. The main component of Shuyusan was Geniposide, Deoxyschizandrin, and Spinosae flavonoid glycosides. The Geniposide has a protective effect for SH-SY5Y cells, which injured by the high-dose corticosterone injury model using SH-SY5Y cells [15]. Therefore, protecting neurotransmitters from injury is one of the most important neuroprotective roles of Shuyusan whether the antidepressant activity effect of Shuyusan is dependent on its interaction with GR receptors in the hippocampus and could regulate the serum level of CRH, ACTH, and CORT in the rat of chronic stress-induced depression. In the present study, we aimed to investigate the effect of Shuyusan on the behavioral despair tasks, serum level of CRH, ACTH, and CORT, and expression of glucocorticoid receptor of HPA in current study.

2. Materials and Methods

2.1. Animals. We used 70 adult male Sprague-Dawley (SD) rats weighed 180–220 g (license no. SLXK 2009-0007) for quantitative analysis. SD rats were supplied by the medical experimental animal center of the Chinese People Liberation Army (PLA) General Hospital. The 70 SD rats were equally and randomly assigned into one of six groups, namely, normal control, model, high-dose treatments, medium-dose treatments, low-dose treatments with Shuyusan decoction, and fluoxetine treatment group ($N = 10$). In addition, traditional Chinese medicine and Western medicine treatment groups were administered by Shuyusan herbs decoction and fluoxetine, respectively. Model and control groups were treated with saline. One rat in the traditional Chinese medicine treatment group died at 24 days and hence was excluded from analysis, but all remaining rats were included in the final analysis. Protocols were conducted in accordance with the Guidance Suggestions for the Care and Use of Laboratory Animals, formulated by the Ministry of Science and Technology of the People's Republic of China.

2.2. Drugs, Reagents, and Drug Administration. Shuyusan (10 g *Bupleurum*, 15 g Radix Curcumae, 6 g mint, 10 g cape jasmine fruit, 10 g *Poria cocos*, 10 g radix polygalae, 10 g calamus, 15 g spine date seed, and 10 g flower of silk tree *Albizzia* in Table 1) was provided by the pharmacy of the PLA General Hospital. Its main active compounds are spine date seed, magnoliavine fruit, and cape jasmine fruit. Shuyusan was boiled, filtrated and concentrated to 5 g/mL liquided at 80°C water bath, and stored at 4°C refrigerator. When used, it was diluted with distilled water gavages to rats. Prozac (fluoxetine hydrochloride dispersible tablets, pantheons France company, France, Lot: 9711B, 20 mg/tablet), was used in concentration to 2 mg/mL liquid by distilled water. The control group was normally fed without any treatment. The rats in the model, Shuyusan groups, and fluoxetine group were subjected to a model of unpredictable chronic mild stress and fed isolation. The model group was fed normally after 21-day stress stimulation; high-dose Shuyusan group was administered with Shuyusan contained the herds of 25 g/kg by gastric perfusion one time per day; medium-dose Shuyusan group was with the herds of 7.5 g/kg; low-dose Shuyusan group was with herds of 2.5 g/kg; fluoxetine was dissolved into 2 mL normal saline and was administered 10 mg/kg through gastric perfusion for the fluoxetine group. The fed dosage of Shuyusan: according to clinical experience, the effective dosage of normal 60 kilogram adult was to take 96 gram per day of Shuyusan, so the rat of 200 gram would take Shuyusan 0.32 gram per day. The rats started accepting the above treatments in the 21 days and the rats in treatment groups were continuously administered with the drugs through gastric perfusion for 21 days. All rats were included in the final analysis. Rat CRH, ACTH, and CORT ELISA kit (R&D, United States), GR primary antibody kit (Santa Cruz), low temperature for high-speed centrifuge (Sigma, USA), inverted microscope (OLYMPUS Japan), microplate reader (TECAN, Switzerland), homemade open boxes, and so forth.

Table 1: The table of components and ratio of Shuyusan.

Plant species	Family	Plant part	Pinyin
Bupleurum	Umbelliferae	Root	Chaihu
Radix curcumae	Zingiberaceae	Root	Yujin
Mint	Labiatae	Leaf	Bohe
Cape jasmine fruit	Rubiaceae	Fruit	Zhizi
Poria cocos	Polyporaceae	Sclerotium	Fuling
Radix polygalae	Polygalaceae	Root	Yuanzhi
Calamus	Araceae	Rootstock	Shichangpu
Spine date seed	Rhamnaceae	Seed	Suanzaoren
Flower of silk tree *Albizzia*	Pea family	Inflorescence	Hehuanhua

2.3. Model of Depression for Chronic Unpredictable Mild Stress (CUMS). Adopted model of depression for chronic unpredictable mild stress (CUMS) and improvement for a little. The normal control group was housed five rats per cage and dieted, drunk water, not to any stimulus. The model group was fed one rat for each cage and received 21 days of stress stimulation, that contains water deprivation (24 h), fasting (24 h), clamping the tail (1 min), electric shock foot (20 v, 10 seconds/time, 1 min), forcing swim in ice water (4°C, 4 min), tilting cages (45°C, 12 h), converting the circadian rhythm, braking (2 h), and thermal stimulation (40°C, 5 min), randomly assigned 1-2 kinds of stimulation daily, and each stimulus repeated 2-3 times.

2.4. ELISA Analysis of CRH, ACTH, and CORT. After the end of the experimental period, all rats were intraperitoneally injected for anesthesia by 10% chloral hydrate (3 mL/kg), exposed heart, perfused rinse through the ascending aorta by 0.9% saline (37°C, 250 mL) and perfuse 4% paraformaldehyde solution (4°C, PH = 7.4, 200 mL) until limbs stiff of the animals. Finally, the brains were removed and repaired block, stored in 10% polyformaldehyde solution. The organization of the brain tissue was added an appropriate amount of saline and mashed, centrifuged for 10 min (3000 rpm), and extracted the supernatant. Then we removed the ELISA kit (CRH, ACTH, and CORT) from 4°C refrigerator and coordinated to room temperature, removed the reaction plate, and set blank wells separately (blank comparison wells did not add sample and HRP-conjugate reagent, other each step operation is same). The sample test well: we added sample dilution 40 μL to testing sample well, then added testing sample 10 μL (sample final dilution is 5-fold), added sample to wells, did not touch the well wall as far as possible, and gently mix. After closed plate with closure plate membrane, we incubate for 30 min at 37°C, then uncovered closure plate membrane, discarded liquid, dried by swing, add washed buffer to every well, still for 30 s then drained, repeated 5 times, and dried by pat. Then added HRP-conjugate reagent 50 μL to each well, except blank well; added chromogen solution A 50 μL and chromogen solution B to each well, evaded the light preservation for 15 min at 37°C; added stop solution 50 μL to each well; stop the reaction. We took blank well as zero, read absorbance at 450 nm after added stop solution and within 15 min. In the end, we detected the concentration in the standard curve according to OD values of samples.

2.5. Behavior Despair Study. Open-field test: an open-field method was used to conduct praxeological scoring in all group rats. The open-field device was made of opaque materials with 76 cm × 76 cm square, located on the bottom, which was equally divided into 25 equilateral squares. Around, there was a wall with the height of 45 cm. The rat was put in the central square and then measured the square numbers the rat crossed in 3 minutes (only the squares the rat entered on four feet could be numbered as the score of horizontal activity) and the times of standing on hind limbs were observed. Each rat was measured once for three minutes, which would be scored by two observers and the average value was taken. The percentage time spent in this central zone is considered indicative of exploratory behavior and may reflect a decrease in anxiety, although this OF parameter is not sensitive to all anxiolytics and may not model certain features of anxiety disorders [16, 17].

Forced-Swimming Test (FST). A forced-swimming test was used to all groups, according to the method of Porsolt [18]. Rats were placed in an open cylindrical container (diameter 10 cm, height 25 cm), containing 15 cm of water at 25 ± 1°C. The duration of observed immobility was recorded during the last 4 min of the 6 min testing period [19, 20]. Rats are forced to swim in the restricted space from which they cannot escape and are induced to the characteristic behavior of immobility. The duration of observed immobility was recorded during the last 4 min of the 6 min testing period. When rats ceased struggling and remained floating motionless in the water, they were judged to be immobile. Decrease in the duration of immobility during the FST was taken as a measure of antidepressant activity.

Tail Suspension Test (TST). The duration of immobility time induced by tail suspension was measured according to the method of Steru [21]. Rats both acoustically and visually isolated were suspended above the floor by adhesive tape placed approximately 1 cm from the tip of the tail. The remained immobile time of TST was quantified for 6 min. Rats were considered immobile only when they hung passively and completely motionless.

2.6. GR-Receptor Determination. Endogenous peroxidase was inactivated with 3% H_2O_2. Sections were blocked in 10% normal goat serum at 37°C for 30 minutes, added primary antibody at 4°C overnight, and washed with PBS. The average optical density of positively stained cells of the slices obtained above was analyzed using Image-Image Pro software (Media Cybernetic, Bethesda, Maryland, USA) to analyse the immunohistochemical positive cells and integrated optical density (integral optical density, IOD). Three slices from each group were chosen for the analysis. For each slice, three images from three different areas, the layer four to layer five of frontal cortex, region CA1 of hippocampus (located about 600 um away from the starting point of middle line of A1 area) and region CA3 of hippocampus (the top point of hippocampus turning area), were evaluated under 200x objective lens.

2.7. Statistical Analysis. All results are calculated with means ± SEM. The variance analysis was used to compare among groups. If P value is less than 0.05, the difference was considered statistically significant. We use test for homogeneity to examine the data: if the data is homogeneous, we conduct analysis of variance (one-way ANOVA) directly on the data. Between the two groups, we used the LSD method to compare any difference. Otherwise, we changed parameters first and then used test for homogeneity again. We only conduct ANOVA on data which becomes homogeneous after change of parameters. All statistical analyses were carried out by using SPSS for Windows (SPSS Inc.).

3. Results

3.1. The Open-Field Test. The results of the open-field test are reported in Figure 1. It shows observation of rats on activity (horizontal, vertical). There was no significant difference before modeling in among groups ($F = 1.307$, $P > 0.05$). After modeling, it was observed that there was significant changes in the open-field test in these groups. After 3 weeks herbs fed treatment with high-dose herbs and fluoxetine, the immobility time was increased significantly, compared with the model group (high-dose group versus the model group

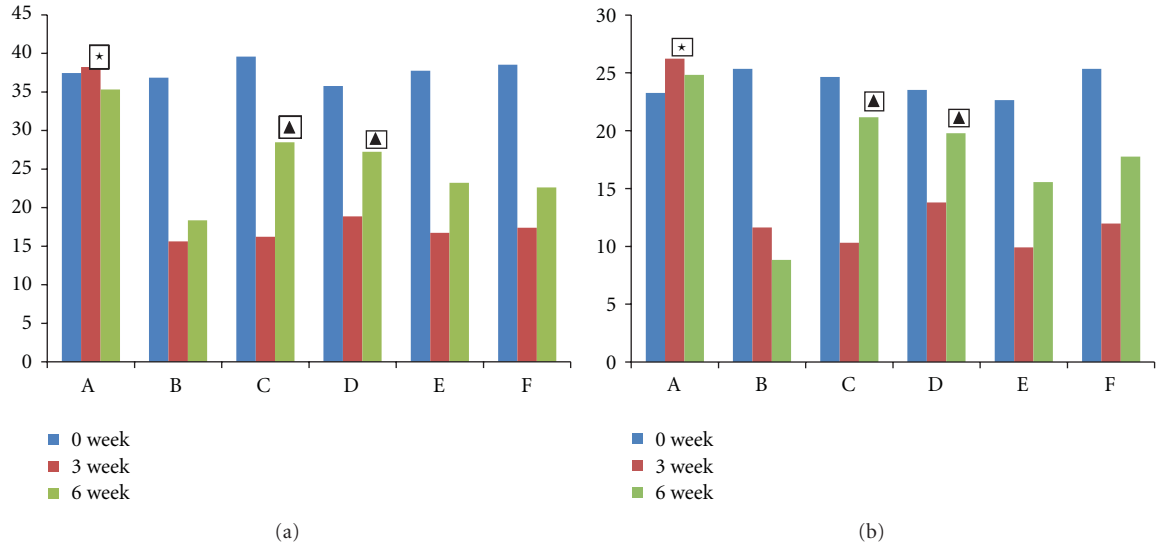

Figure 1: Observation of rats on open-field activities (horizontal, vertical). Horizontal movement scores reflect range of motion; vertical movement scores reflect exploratory behaviors. High scores represent high degree of activity. A: normal group, B: model group, C: fluoxetine group, D: high-dose Shuyu group, E: medium-dose Shuyu group, and F: low-dose Shuyu group. All data are expressed as the $\bar{x} \pm s$, ($n = 10$). $\star P < 0.05$ versus other groups; $\blacktriangle P < 0.05$ versus model group.

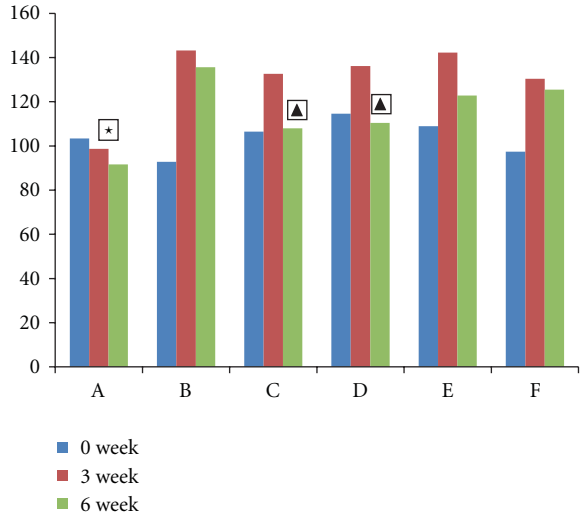

Figure 2: The FST in each group. Effects of immobility time during the forced swimming test. The vertical axis shows the immobility time (sec). High scores represent high degree of depression. A: normal group, B: model group, C: fluoxetine group, D: high-dose Shuyusan group, and E: medium-dose Shuyusan group. F: low-dose Shuyusan group. All data are expressed as the $\bar{x} \pm s$, ($n = 10$). $\star P < 0.05$ versus other groups; $\blacktriangle P < 0.05$ versus model group.

$t = 2.273$, $P < 0.05$; fluoxetine group versus the model group $t = 3.461$, $P < 0.01$).

3.2. The FST in Each Group. The results of FST are reported in Figure 2. There was no significant difference before modeling in among groups ($F = 1.77$, $P > 0.05$). After modeling, it was observed that there was a significant prolongation of immobility time in these groups. After 3 weeks herbs fed treatment with high-dose herbs and fluoxetine, the immobility time was increased significantly, compared with the model group (high-dose group versus the model group $t = 2.575$, $P < 0.05$; fluoxetine group versus the model group $t = 3.061$, $P < 0.01$).

3.3. The TST in Each Group. The results of pooling all the tests performed with TST are reported in Figure 3. There was no significant difference before modeling among groups ($F = 1.05$, $P > 0.05$). After modeling, it was observed that there was a significant prolongation of immobility time in these groups. High-dose Shuyusan herbs also could reduce the immobility time in TST. After high-dose herbs and fluoxetine treatment for 3 weeks, the immobility time was increased significantly, compared with the model group (high-dose group versus the model group $t = 2.763$, $P < 0.05$; fluoxetine group versus the model group $t = 3.182$, $P < 0.01$).

3.4. Determination of Serum Contents Level of CRH, ACTH, and CORT. Figure 4 shows the serum contents level change of CRH, ACTH, and CORT in each group after treatment. The serum contents level in mode group was significantly increased for CRH, ACTH, and CORT (CRH: the model group versus the normal group $t = 2.893$, $P < 0.01$; ACTH: the model group versus the normal group $t = 2.904$, $P < 0.01$; CORT: the model group versus the normal group $t = 3.646$, $P < 0.01$). After 3 weeks herbs fed treatment, the serum contents level of CRH, ACTH, and CORT in high-dose group was significantly decreased, compared to the model group (CRH: high-dose group versus the model

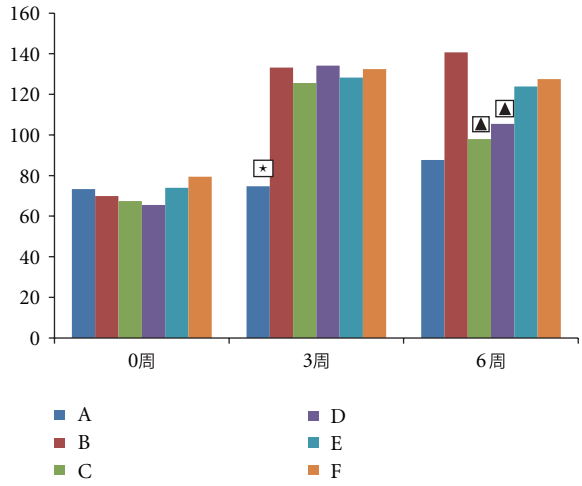

Figure 3: The TST in each group. Effects of immobility time during the tail suspension test. The vertical axis shows the immobility time (sec). High scores represent high degree of depression. A means normal group, B means model group, C means fluoxetine group, D means high-dose Shuyusan group, E means medium-dose Shuyusan group, and F means low-dose Shuyusan group. All data are expressed as the $\bar{x} \pm s$, $(n = 10)$. $\star P < 0.05$ versus other groups; $\blacktriangle P < 0.05$ versus model group.

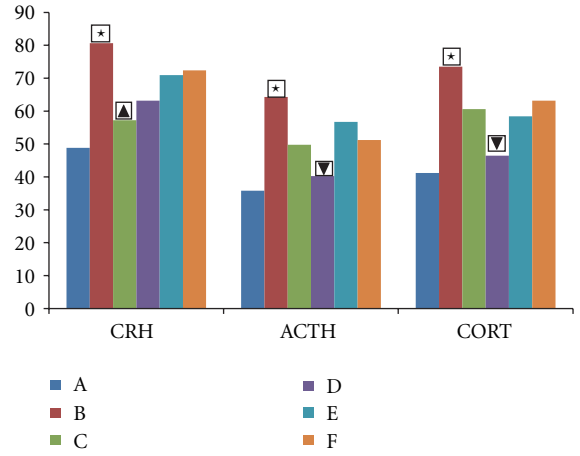

Figure 4: The serum contents level of CRH, ACTH, and CORT. The serum contents level of CRH, ACTH, and CORT in rats. The vertical axis shows the value. High scores represent high degree of depression. A: normal group, B: model group, C: fluoxetine group, D: high-dose Shuyu group, E: medium-dose Shuyu group, and F: low-dose Shuyu group. All data are expressed as the $\bar{x} \pm s$, $(n = 10)$. $\star P < 0.05$ versus normal groups; $\blacktriangledown P < 0.05$ versus model group.

group $t = 2.261$, $P < 0.05$; ACTH: high-dose group versus the model group $t = 2.387$, $P < 0.05$; CORT: High-dose group versus the model group $t = 2.478$, $P < 0.05$). Although the serum contents level of CRH, ACTH, and CORT was decreased in the low-dose group and the fluoxetine group, there was no significant difference compared to the model group.

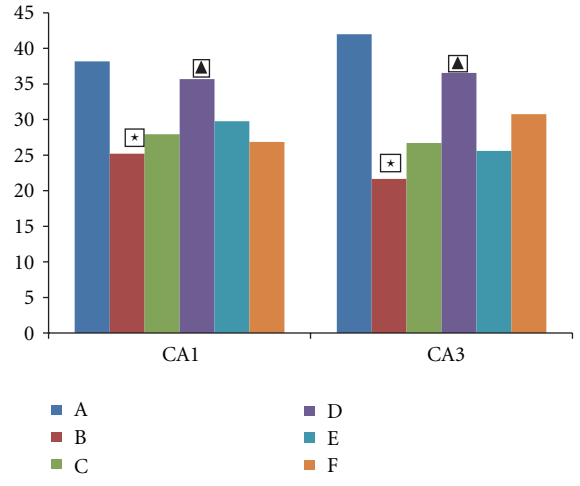

Figure 5: Expression of GR-receptor-positive cells in rat hippocampus. Comparison of GR-positive cells in rat hippocampus. The vertical axis shows the value (n). Low value represent high degree of depression. A: normal group, B: model group, C: fluoxetine group, D: high-dose Shuyu group, E: medium-dose Shuyu group, and F: low-dose Shuyu group. All data are expressed as the $\bar{x} \pm s$, $(n = 10)$. $\star P < 0.05$ versus normal groups. $\blacktriangle P < 0.05$ versus model group. $\blacktriangledown P < 0.01$ versus model group.

3.5. Expression of GR Receptor in the Rat Hippocampus. Figures 5, 6, and 7 show the number of GR-receptor-positive cells in the hippocampus of rats in each group. The GR-receptor positive cells in the hippocampus of rats in each group change of GR for chronic unpredictable mild stress mainly manifested in the areas of CA1 and CA3 of the hippocampus (CA3 region is more prominent). GR-positive-cells in the hippocampus of normal group arranged in dense, structured, and distributed in normal. The immune response in hippocampus of model rats was significantly decreased, GR-positive cells arranged loose, and less structured. The number of GR-receptor-positive cells was significantly decreased compared to the mode group (CA1 region: the model group versus the normal group $t = 2.713$, $P < 0.05$; CA3 region: the model group versus the normal group $t = 5.275$, $P < 0.01$). The number of GR-receptor-positive cells was significantly increased compared to the model group in the CA1 region and CA3 region (CA1 region: high-dose group versus the model group $t = 2.157$, $P < 0.05$; CA3 region: high-dose group versus the model group $t = 3.257$, $P < 0.01$). The medium-dose group, low-dose group, and the fluoxetine group all have increased trend for the contents of the number of positive cells and IOD, but there was no significant difference.

4. Discussion

Behavioral studies play an important role in the evaluation of antidepressant activity effect [22]. The forced swimming and tail suspension tests are behavioral despair tests, and it is useful for probing the pathological mechanism of depression

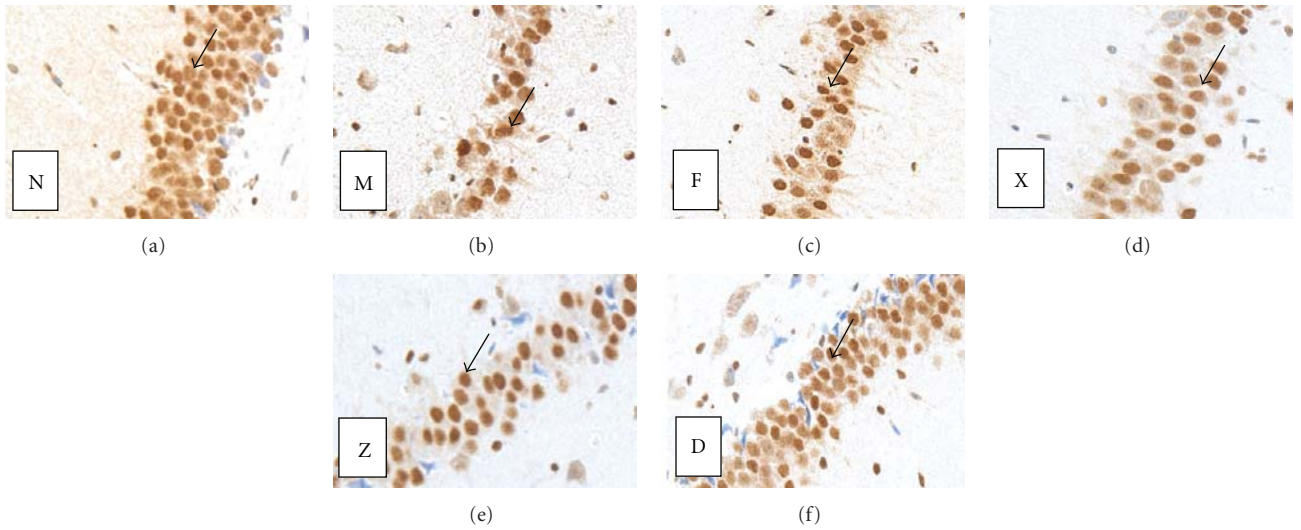

Figure 6: Expression of GR receptor in the rat hippocampus in the CA1 region. Changes in GR expression in the rat hippocampal CA1 region (immunohistochemistry, ×400). (N) GR expression was normal in the control group. (M) GR expression was subdued in the model group. (F) GR expression was enhanced in the fluoxetine group. Arrows indicate GR positive neurons. (D) GR expression was enhanced in the high-dose Shuyusan group. Arrows indicate GR positive neurons. (Z) GR expression was enhanced in the medium-dose Shuyusan group. Arrows indicate GR positive neurons. (X) GR expression was enhanced in the low-dose Shuyusan group. Arrows indicate GR positive neurons.

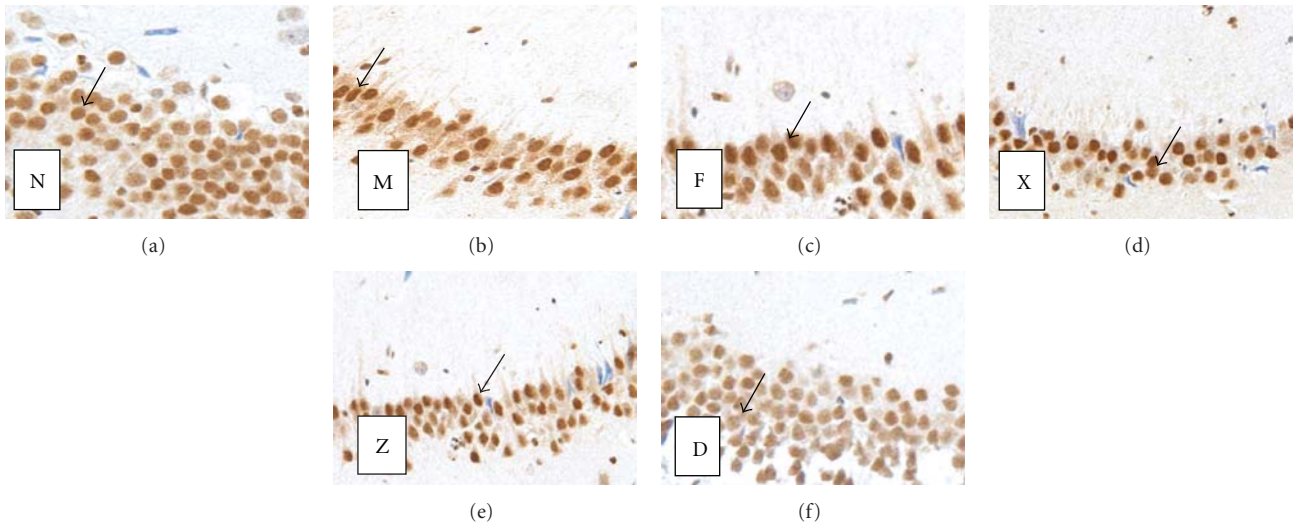

Figure 7: Expression of GR receptor in the rat hippocampus in the CA3 region. Morphology Changes in GR expression positive cells in the hippocampus of chronically stressed rat following treatment with Shuyusan in the rat hippocampal CA3 region (immunohistochemistry, ×400). The area of GR-positive cells in the hippocampus was decreased in the model group, and most of the cells were shrunk or lightly stained. The area of GR-positive cells in the hippocampus was increased in the M- and H-Shuyusan groups. (N) GR expression was normal in the control group. (M) GR expression was subdued in the model group. (F) GR expression was enhanced in the fluoxetine group. Arrows indicate GR positive neurons. (D) GR expression was enhanced in the high-dose Shuyusan group. Arrows indicate GR positive neurons. (Z) GR expression was enhanced in the medium-dose Shuyusan group. Arrows indicate GR positive neurons. (X) GR expression was enhanced in the low-dose Shuyusan group. Arrows indicate GR positive neurons.

and for the evaluation of antidepressant drugs [23]. FST and TST had been widely used as preclinical screening tool of antidepressant drugs [24, 25]. Characteristic of rat behaviors scored in both tests is termed immobility, which reflects behavioral despair as seen in human depression [26]. The duration of immobility time in rats that are trapped and forced to swim is closely related to helplessness. It was observed from our results that there was a significant prolongation of immobility time in these groups after modeling; with high-dose herbs of Shuyusan administer,

the immobility time increased significantly. It suggests that Shuyusan has effect in producing significant antidepressant-like activity, when assessed in FST and TST. Based on the traditional Chinese medicine theories, as well as achievements from modern scientific studies and clinical trials, Shuyusan exhibits therapeutic effects on depression by purifying the heart heat, resolving phlegm, and regulating Qi and blood. Previous animal studies have revealed the antidepressant effects of Shuyusan based on behavioral improvement in rat models of depression [11, 13].

Many studies suggested that depression is related to psychological, neuron-endocrine disorders, imbalances of monoamine neurotransmitter, dysfunction of hippocampus neurogenesis, and many other factors [27–30]. Long-time stress and elevated glucocorticoid levels leaded to the emergence of mood disorders [31]. Steroid hormones can modulate neuronal transmission by a variety of mechanisms. Hippocampus is rich in glucocorticoid receptors, the neurons of this area can be damaged by the high level of glucocorticoid; in the pathogenesis of depression studies, HPA axis response stress becomes the focus [32, 33]. Beside monoamine neurotransmitters, the serum level of CRH, CORT, and ACTH and changes in levels of GR were being used to evaluate depression [24–26]. Stress is under the influence of external environmental stimuli and could awaken the internal psychological corresponding; this response occurs through the nervous system and hormonal system [34, 35]. HPA hyperactivity is a major pathology-physiological factor for the depression, the continuous increased CORT in combined with GR overexpressions which in the hippocampus damage the hippocampus and locus coeruleus, so leads to atrophy and apoptosis of hippocampus neurons [36, 37]. In addition, hyperactivity of the HPA axis during stress is inhibited by GR, so that it returned to baseline levels. The effect of the GR reduced after it damaged so that HPA axis is more hyperactive and form a vicious cycle [38]. On the other hand, as hyperactivity of HPA axis, the 5-HT content is inhibited. As high concentration of CORT could induce the liver to produce tryptophan pyrrole enzyme, it could degradate the tryptophan in the blood. Tryptophan is the precursor of 5-TH, its reduction could lead to synthesis of 5-TH, so led to 5-HT content decrease in the brain, thus causing depressive symptoms [39, 40]. In physiological conditions, the secretion of CRH and ACTH regulated by the 5-TH system. In a stress state, HPA axis function becomes hyperactive and 5-HT synthesis significantly decreases as a result of insufficient tryptophan transported into the central nervous system [41–43]. Results from the present study demonstrated that Shuyusan could decrease the serum contents of CRH, ACTH, and CORT. It also could increase the expression of hippocampus GR receptor in the rat model of depression. Our results suggested that the mechanisms of action of Shuyusan were due to decreasing the serum contents level of CRH, ACTH, and CORT and increasing the expression of hippocampus GR receptor. Fluoxetine is selective serotonin reuptake inhibitors' (SSRIs) medications, it could increase the levels of NE, 5-HT, and DA in the brain of rat and was related to downregulation of 5-HT receptor, but not decreased the serum contents level of CRH, ACTH, and CORT and increased the expression of hippocampus GR receptor.

The chronic stress-induced depression model is an effective model for studying depression and has been widely utilized in basic research and drug screening for depression [44, 45]. The model can simulate the core symptoms of depression, that is, loss of interest, anhedonia, and decrease of exploring ability and sexual behavior. In fact, helplessness and anhedonia is the core symptom of depression and most of the current models only mimic anhedonia. The currently available chronic mild stress model is probably the most valid and the most widely used animal model of depression. Presently, the FST is the most widely used tool in depression research [45]. The experiment shows that the immobility time in forced swimming extends. That proved the replication model of depression in rats were succeed.

In conclusion, our data indicated that high-dose herbs Shuyusan had antidepressant activity effect on chronic stress-induced depression model rats. The behavioral indicators improved compared with model group. We found that CRH, ACTH, and level of CORT in serum and GR expression in hippocampus of the high-dose herbs Shuyusan group were significantly improved, compared with the model group by ELISA and immunohistochemical methods. Thus, we confirmed that Shuyusan has antidepressant activity effect, its mechanism may be related to decreasing glucocorticoid levels activity, regulating the function of HPA axis, and inhibiting glucocorticoid receptor expression in hippocampus.

Authors' Contribution

The study was conceived and designed under the guidance of L. Chen, in charge of funds from L. Chen, and provided data support by Z. Sun, and Q. Zhi. M. Chen, F. Wang, M. Geng, H. Chen, and D. Duan participated in the study concept and design, data analysis, and paper draft.

Conflict of Interests

The authors declare that they have no conflict of interests.

Ethical Approval

The experiment was approved by Animal Ethics Committee, Chinese PLA General Hospital China.

Acknowledgment

Military Science and Technology Research fund during the Twelfths Five-Year Plan, PLA China, no. CWS11J067.

References

[1] X. Li, L. Li, L. L. Shen, Y. Qian, Y. X. Cao, and D. N. Zhu, "Changes of adrenomedullin and its receptor components mRNAs expression in the brain stem and hypothalamus-pituitary-adrenal axis of stress-induced hypertensive rats," *Sheng Li Xue Bao*, vol. 56, no. 6, pp. 723–729, 2004.

[2] S. B. Sartori, N. Whittle, A. Hetzenauer, and N. Singewald, "Magnesium deficiency induces anxiety and HPA axis dysregulation: modulation by therapeutic drug treatment," *Neuropharmacology*, vol. 62, no. 1, pp. 304–312, 2012.

[3] C. M. Pariante, "Risk factors for development of depression and psychosis: glucocorticoid receptors and pituitary implications for treatment with antidepressant and glucocorticoids," *Annals of the New York Academy of Sciences*, vol. 1179, pp. 144–152, 2009.

[4] U. Ehlert, J. Gaab, and M. Heinrichs, "Psychoneuroendocrinological contributions to the etiology of depression, posttraumatic stress disorder, and stress-related bodily disorders: the role of the hypothalamus-pituitary-adrenal axis," *Biological Psychology*, vol. 57, no. 1–3, pp. 141–152, 2001.

[5] W. Pitchot, C. Herrera, and M. Ansseau, "HPA axis dysfunction in major depression: relationship to 5-HT1A receptor activity," *Neuropsychobiology*, vol. 44, no. 2, pp. 74–77, 2001.

[6] G. Naert, T. Maurice, L. Tapia-Arancibia, and L. Givalois, "Neuroactive steroids modulate HPA axis activity and cerebral brain-derived neurotrophic factor (BDNF) protein levels in adult male rats," *Psychoneuroendocrinology*, vol. 32, no. 8–10, pp. 1062–1078, 2007.

[7] M. Iijima, A. Ito, S. Kurosu, and S. Chaki, "Pharmacological characterization of repeated corticosterone injection-induced depression model in rats," *Brain Research*, vol. 1359, pp. 75–80, 2010.

[8] P. Liu, "Development and basic research overview of antidepressant drugs," *Zhongguo Yaowu Yingyong yu Jiance*, vol. 3, pp. 1–3, 2004.

[9] Y. Li, D. Xu, and Q. Li, "Shugan Jieyu Yin for treatment of senile depression—a clinical report of 84 cases," *Journal of Traditional Chinese Medicine*, vol. 26, no. 1, pp. 39–41, 2006.

[10] Y. H. Li, C. H. Zhang, S. E. Wang, J. Qiu, S. Y. Hu, and G. L. Xiao, "Effects of Chaihu Shugan San on behavior and plasma levels of corticotropin releasing hormone and adrenocorticotropic hormone of rats with chronic mild unpredicted stress depression," *Zhong Xi Yi Jie He Xue*, vol. 7, no. 11, pp. 1073–1077, 2009.

[11] L. P. Chen, Y. Sun, F. W. Wang, D. M. Duan, and Y. Z. Hu, "Effect of Shuyusan on neuropeptide Y and serotonin expression in the hippocampal neurons of rats with chronic mild unpredictable stress-induced depression," *Nan Fang Yi Ke Da Xue Xue Bao*, vol. 31, no. 1, pp. 113–116, 2011.

[12] L. P. Chen, F. W. Wang, and W. Herbert, "Effect of the combination of acupuncture and shuyusan in the treatment of depression," *Zhongguo Linchuang Kangfu*, vol. 8, no. 21, pp. 4250–4251, 2004.

[13] I. P. Chen, W. Li, M. X. Lin et al., "The eftect of suyu decoction on rat behavior in stress induced depressive model," *Zhongguo Yaowu Yingyong yu Jiance*, vol. 4, pp. 19–20, 2007.

[14] Y. Zhang, J. Jia, L. Chen et al., "Effects of Shuyusan on monoamine neurotransmitters expression in a rat model of chronic stress-induced depression," *Neural Regeneration Research*, vol. 6, pp. 2582–2588, 2011.

[15] L. Chen, F. Wang, M. Geng, H. Chen, and D. Duan, "Geniposide protects human neuroblastoma SH-SY5Y cells against corticosterone-induced injury," *Neural Regeneration Research*, vol. 6, pp. 1618–1622, 2011.

[16] P. Simon, R. Dupuis, and J. Costentin, "Thigmotaxis as an index of anxiety in mice. influence of dopaminergic transmissions," *Behavioural Brain Research*, vol. 61, no. 1, pp. 59–64, 1994.

[17] L. Prut and C. Belzung, "The open field as a paradigm to measure the effects of drugs on anxiety-like behaviors: a review," *European Journal of Pharmacology*, vol. 463, no. 1–3, pp. 3–33, 2003.

[18] R. D. Porsolt, A. Bertin, and M. Jalfre, "Behavioral despair in mice: a primary screening test for antidepressants," *Archives Internationales de Pharmacodynamie et de Therapie*, vol. 229, no. 2, pp. 327–336, 1977.

[19] A. Dias Elpo Zomkowski, A. Oscar Rosa, J. Lin, A. R. S. Santos, J. Batista Calixto, and A. Lúcia Severo Rodrigues, "Evidence for serotonin receptor subtypes involvement in agmatine antidepressant like-effect in the mouse forced swimming test," *Brain Research*, vol. 1023, no. 2, pp. 253–263, 2004.

[20] A. D. E. Zomkowski, A. R. S. Santos, and A. L. S. Rodrigues, "Evidence for the involvement of the opioid system in the agmatine antidepressant-like effect in the forced swimming test," *Neuroscience Letters*, vol. 381, no. 3, pp. 279–283, 2005.

[21] L. Steru, R. Chermat, B. Thierry, and P. Simon, "The tail suspension test: a new method for screening antidepressants in mice," *Psychopharmacology*, vol. 85, no. 3, pp. 367–370, 1985.

[22] B. Karolewicz and I. A. Paul, "Group housing of mice increases immobility and antidepressant sensitivity in the forced swim and tail suspension tests," *European Journal of Pharmacology*, vol. 415, no. 2-3, pp. 197–201, 2001.

[23] X. Q. Li and J. Xu, "Progresses on animal models of depression study," *Chinese Journal of Psychiatry*, vol. 35, pp. 184–186, 2002.

[24] M. J. Detke, M. Rickels, and I. Lucki, "Active behaviors in the rat forced swimming test differentially produced by serotonergic and noradrenergic antidepressants," *Psychopharmacology*, vol. 121, no. 1, pp. 66–72, 1995.

[25] J. Nirmal, C. S. Babu, T. Harisudhan, and M. Ramanathan, "Evaluation of behavioural and antioxidant activity of cytisus scoparius link in rats exposed to chronic unpredictable mild stress," *BMC Complementary and Alternative Medicine*, vol. 24, pp. 8–15, 2008.

[26] P. Willner, "Validity, reliability and utility of the chronic mild stress model of depression: a 10-year review and evaluation," *Psychopharmacology*, vol. 134, no. 4, pp. 319–329, 1997.

[27] L. Du, G. Faludi, M. Palkovits, P. Sotonyi, D. Bakish, and P. D. Hrdina, "High activity-related allele of MAO-A gene associated with depressed suicide in males," *NeuroReport*, vol. 13, no. 9, pp. 1195–1198, 2002.

[28] A. Raone, A. Cassanelli, S. Scheggi, R. Rauggi, B. Danielli, and M. G. De Montis, "Hypothalamus-pituitary-adrenal modifications consequent to chronic stress exposure in an experimental model of depression in rats," *Neuroscience*, vol. 146, no. 4, pp. 1734–1742, 2007.

[29] L. Yu, S. C. An, and T. Lian, "Involvement of hippocampal NMDA receptor and neuropeptide Y in depression induced by chronic unpredictable mild stress," *Sheng Li Xue Bao*, vol. 62, no. 1, pp. 14–22, 2010.

[30] C. Girish, V. Raj, J. Arya, and S. Balakrishnan, "Evidence for the involvement of the monoaminergic system, but not the opioid system in the antidepressant-like activity of ellagic acid in mice," *European Journal of Pharmacology*, vol. 682, pp. 118–125, 2012.

[31] Z. Xu, Y. Zhang, B. Hou, Y. Gao, Y. Wu, and C. Zhang, "Chronic corticosterone administration from adolescence through early adulthood attenuates depression-like behaviors in mice," *Journal of Affective Disorders*, vol. 131, no. 1–3, pp. 128–135, 2011.

[32] R. L. Hauger, S. G. Helat, and E. E. Edei, "Decreased corticotrophin-releasingfactor receptor espression and adrenocorticotropic hormone responsiveness in anterior pituitarys

cells ofW istar-Kyoto rats," *Journal of Neuroendocrinology*, vol. 14, pp. 126–134, 2002.

[33] M. Szymańska, B. Budziszewska, L. Jaworska-Feil et al., "The effect of antidepressant drugs on the HPA axis activity, glucocorticoid receptor level and FKBP51 concentration in prenatally stressed rats," *Psychoneuroendocrinology*, vol. 34, no. 6, pp. 822–832, 2009.

[34] Y. F. Li and Z. P. Luo, "Depression: damage of neurons and down-regulation of neurogenesis," *Yaoxue Xuebao*, vol. 39, no. 11, pp. 949–953, 2004.

[35] Y. Liu, S. Ma, and R. Qu, "SCLM, total saponins extracted from Chaihu-jia-longgu-muli-tang, reduces chronic mild stress-induced apoptosis in the hippocampus in mice," *Pharmaceutical Biology*, vol. 48, no. 8, pp. 840–848, 2010.

[36] A. Urbach, C. Redecker, and O. W. Witte, "Induction of neurogenesis in the adult dentate gyrus by cortical spreading depression," *Stroke*, vol. 39, no. 11, pp. 3064–3072, 2008.

[37] L. J. Xiu, Y. X. Yang, S. Yu, D. Z. Sun, and P. K. Wei, "Research of depression in traditional Chinese medicine: review and prospect," *Zhong Xi Yi Jie He Xue Bao*, vol. 6, no. 4, pp. 416–421, 2008.

[38] M. Otczyk, K. Mulik, B. Budziszewska et al., "Effect of some antidepressants on the low corticosterone concentration-induced gene transcription in LMCAT fibroblast cells," *Journal of Physiology and Pharmacology*, vol. 59, no. 1, pp. 153–162, 2008.

[39] X. Z. Jiang, Y. F. Li, Y. Z. Zhang, H. X. Chen, J. Li, and N. P. Wang, "5-HT1A/1B receptors, α2 -adrenoceptors and the post-receptor adenylate cyclase activation in the mice brain are involved in the antidepressant-like action of agmatine," *Yaoxue Xuebao*, vol. 43, no. 5, pp. 467–473, 2008.

[40] N. Barden, "Implication of the hypothalamic-pituitary-adrenal axis in the physiopathology of depression," *Journal of Psychiatry and Neuroscience*, vol. 29, no. 3, pp. 185–193, 2004.

[41] T. Lian and S. C. An, "Antidepressant effect of microinjection of neuropeptide Y into the hippocampus is mediated by decreased expression of nitric oxide synthase," *Sheng Li Xue Bao*, vol. 62, no. 3, pp. 237–246, 2010.

[42] C. H. Lai and Y. T. Wu, "Duloxetine's modest short-term influences in subcortical structures of first episode drug-naïve patients with major depressive disorder and panic disorder," *Psychiatry Research*, vol. 194, no. 2, pp. 157–162, 2011.

[43] X. Q. Li and J. Xu, "Progresses on animal models of depression study," *Chinese Society of Psychiatry*, vol. 35, pp. 184–186, 2002.

[44] Y. Xu, P. A. Barish, J. Pan, W. O. Ogle, and J. M. O'Donnell, "Animal models of depression and neuroplasticity: assessing drug action in relation to behavior and neurogenesis," *Methods in Molecular Biology*, vol. 829, pp. 103–124, 2012.

[45] H. C. Yan, X. Cao, M. Das, X. H. Zhu, and T. M. Gao, "Behavioral animal models of depression," *Neuroscience Bulletin*, vol. 26, no. 4, pp. 327–337, 2010.

Hindawi Publishing Corporation
Evidence-Based Complementary and Alternative Medicine
Volume 2012, Article ID 840247, 10 pages
doi:10.1155/2012/840247

Research Article

The Antiparkinsonian and Antidyskinetic Mechanisms of *Mucuna pruriens* in the MPTP-Treated Nonhuman Primate

Christopher A. Lieu,[1] Kala Venkiteswaran,[2,3] Timothy P. Gilmour,[2,3] Anand N. Rao,[2,3] Andrew C. Petticoffer,[2,3] Erin V. Gilbert,[4] Milind Deogaonkar,[4] Bala V. Manyam,[2] and Thyagarajan Subramanian[2,3]

[1] *Buck Institute for Research on Aging, Novato, CA 94945, USA*
[2] *Department of Neurology, The Pennsylvania State University College of Medicine, Hershey, PA 17033, USA*
[3] *Department of Neural and Behavioral Sciences, The Pennsylvania State University College of Medicine, Hershey, PA 17033, USA*
[4] *Center for Neurological Restoration, The Cleveland Clinic Foundation, Cleveland, OH 44195, USA*

Correspondence should be addressed to Thyagarajan Subramanian, tsubram@yahoo.com

Received 26 May 2012; Accepted 27 July 2012

Academic Editor: Paul Siu-Po Ip

Chronic treatment with levodopa (LD) in Parkinson's disease (PD) can cause drug induced dyskinesias. *Mucuna pruriens* endocarp powder (MPEP) contains several compounds including natural LD and has been reported to not cause drug-induced dyskinesias. We evaluated the effects of *Mucuna pruriens* to determine if its underlying mechanistic actions are exclusively due to LD. We first compared MPEP with and without carbidopa (CD), and LD+CD in hemiparkinsonian (HP) monkeys. Each treatment ameliorated parkinsonism. We then compared the neuronal firing properties of the substantia nigra reticulata (SNR) and subthalamic nucleus (STN) in HP monkeys with MPEP+CD and LD+CD to evaluate basal ganglia circuitry alterations. Both treatments decreased SNR firing rate compared to HP state. However, LD+CD treatments significantly increased SNR bursting firing patterns that were not seen with MPEP+CD treatments. No significant changes were seen in STN firing properties. We then evaluated the effects of a water extract of MPEP. Oral MPWE ameliorated parkinsonism without causing drug-induced dyskinesias. The distinctive neurophysiological findings in the basal ganglia and the ability to ameliorate parkinsonism without causing dyskinesias strongly suggest that *Mucuna pruriens* acts through a novel mechanism that is different from that of LD.

1. Introduction

Dopamine replacement therapy with LD+DDCI (dopa decarboxylase inhibitor) is the most effective pharmacological treatment for PD. However, LD+DDCI remains expensive and out of reach of many PD patients in developing countries [1] and causes disabling drug-induced dyskinesias, motor fluctuations, and neuropsychiatric complications in most PD patients [2–4]. Development of an oral treatment with the same or higher efficacy of LD+DDCI that does not cause drug-induced complications is an unmet need.

MPEP in Ayurvedic medicine provides alleviation of parkinsonism but has been reported to not cause drug-induced dyskinesias [5–7]. MPEP contains 4-5% natural LD, which had been implicated as its main mechanism of action and the reason for not causing drug-induced dyskinesias (i.e., did not contain enough LD). Despite MPEP being well-tolerated in clinical trials [8–10], PD patients complain of inability to consume a large volume (30 g) of this leguminous protein as it often causes adverse gastrointestinal side effects. Therefore, despite wide availability of MPEP as a nutraceutical via Internet marketing and in Ayurvedic pharmacies, MPEP is rarely utilized as allopathic treatment for PD even in India [1, 11]. This lack of popularity of MPEP is related to its gastrointestinal side effects and the erroneous notion that MPEP simply represents a natural form of low-dose LD. However, MPEP is ubiquitously used by Ayurvedic physicians worldwide as an ingredient in medications for the treatment of PD.

We recently reported that a newly formulated, simple MPEP water extract (MPWE) given parenterally significantly ameliorates parkinsonism with reduced drug-induced dyskinesias in the HP rat [12]. This suggested that its anti-PD and antidyskinetic effects could not be explained by the presence of small quantities of natural LD alone and that MPWE is more effective when used alone without the addition of a DDCI. These surprising findings led us to further investigate the unique anti-PD and anti-dyskinetic properties of MPEP and MPWE in the 1-methyl-4-phenyl-1,2,3,6-tetrahydropyridine-(MPTP-) treated parkinsonian monkey. Further evaluation of the mechanistic actions of MPEP and MPWE may increase its potential as an alternative therapy for PD.

2. Materials and Methods

2.1. Animals. Fourteen adult (6–9 kg) rhesus (*Macaca mulatta*) and two cynomolgus (*Macaca fascicularis*) monkeys received either intracarotid (ICA) MPTP to induce an HP state, ICA+systemic (IV) MPTP to induce an overlesioned HP (OHP) model, or systemic (IM or IV) injections of MPTP to induce bilateral parkinsonism [13–16]. Each animal was operant-conditioned behaviorally trained [17] to accept medications to ensure proper consumption and clinical oral simulation. Clinical assessments were taken after MPTP to ensure stability of parkinsonism and at subsequent treatment exposure using the modified version of the Unified Parkinson's Disease Rating scale for primates (mUPDRS) [15]. Electrophysiological recordings before and after treatments were done in awake, behaving parkinsonian animals. Standard extracellular single-cell recording techniques were used as described in detail elsewhere [16]. All procedures were in compliance with the "Principles of Laboratory Animal Care" (NIH no. 86–23, revised 1985) and approved by the institutional animal care and use committee.

2.1.1. Administration of MPTP to Induce Parkinsonism. For ICA administration of MPTP to create an HP state, animals were placed under deep general anesthesia, the left common carotid artery was exposed, and the internal carotid artery was isolated followed by manual retrograde injection of MPTP solution (0.5 mg/kg body weight at a concentration of 1 mg/mL) over a period of 15 minutes. The animal was allowed to recover and assessed for stability of HP. Depending on stability of HP state (see below for behavioral testing details), exposure to ICA MPTP was performed up to 4 times in each animal. Repeat surgeries were not performed before 2 weeks of observation had been completed and surgical scar from the previous surgery had healed. The cumulative ICA MPTP dose ranged from 0.5 to 2.5 mg/kg. A subset of animals was rendered overlesioned HP (OHP). To achieve an OHP state, animals were initially treated with ICA MPTP. Once HP state was stable, the animal received subsequent injections of IV MPTP (0.2 mg/kg), inducing mild parkinsonism in the previously unaffected side. Another set of animals was rendered bilaterally parkinsonian with systemic IV or IM injections of MPTP (0.2 mg/kg). Cumulative doses of systemic MPTP ranged from 0.2 mg/kg to 1.0 mg/kg. Drug treatments were then given only when animals were stable parkinsonian for >3 months as determined by no changes in the mUPDRS ratings (see below) performed twice each month separated by a minimum of 15 days and operant-conditioned for a minimum of 6 months such that they were compliant with oral dosing of medications (see the section below).

2.1.2. Operant Conditioning for Oral Medication Compliance without Compromising Enrichment Protocols in Parkinsonian Primates. The following protocol was used for operant conditioning and behavioral training in each animal to ensure compliance and complete consumption of antiparkinsonian medications. Each animal was individually housed such that visual and olfactory contact with conspecifics was maintained at all times. Various types of toys were placed in each cage and rotated every other week. At any one time, every cage contained a hanging toy, such as a ball or a mirror and at least one (usually two) chewing toy, such as a Hercules dental chew toy, Dental ball, Kong toys, nylabones, or pieces of wood (Bio-Serv). In some instances, certain animals showed adverse stress reactions to certain types of toys. In this case, that toy was removed from the animal's cage and replaced with another toy. In addition to the regular feed, monkey diet was supplemented with fruits, vegetables, nuts, or other types of "treats" every day. The size, quantity, and time of day that these "treats" were given (always in the late afternoon after training) were monitored carefully so as not to interfere with our behavioral training. Also, each day, Monday–Friday, the animals were presented with an enrichment activity. These activities included watching cartoons, "novel" food day, foraging devices, and special activities such as air-popped popcorn or bowls of water to play with. On weekends, the animals were given extra food treats. Cages were checked for any remaining monkey biscuits or treats each evening; any remaining food was removed in order to maintain the appropriate level of food scheduling necessary for operant training of a food-picking task or voluntary consumption of medications. All animals were observed for stereotypical (pacing, rocking, digit-sucking) and self-injurious behaviors (self-biting, head banging). If any such behaviors were seen, enrichment for those animals was increased. Oral LD and MPEP were successfully administered twice daily (AM and PM) by hiding powdered drug in food treats. MPWE was typically given orally without the need of hiding it in any additional foods or liquids. Animals appeared to enjoy MPWE and voluntarily consumed it completely at each dose. Improvement in parkinsonism was then assessed by using the mUPDRS and confirmed through analysis of blood plasma levels in representative animals at the same time as the mUPDRS exams. Animals were continuously monitored to ensure complete consumption and drug compliance during treatments by investigators. Depending on the desired task (consumption of treatment or interaction with investigator to evaluate mUPDRS), any of the enrichment protocols in Table 1 could be detrimental to operant conditioning. Similarly, any of the training conditions could cause behavioral

Table 1: Conditions for operant conditioning in parkinsonian primates.

Ideal conditions for training	Ideal conditions for enrichment
Single-housed animals	Group-housed animals
Supplemental toys without food (mirrors, chew toys)	Supplemental toys containing food (foraging devices)
No visual contact with conspecifics	Visual contact with conspecifics
No sound	Sound (movies, radio, wildlife sounds)

problems in monkeys due to lack of appropriate enrichment. To overcome these barriers to operant conditioning, we limited the time when enrichment was given (all enrichment was given after training session to maintain food scheduling), scheduled enrichment only in the afternoon or following the end of a testing session, and maintained visual, sound, and olfactory stimuli without interfering with operant conditioning. The same individuals were involved in the enrichment, operant conditioning, and husbandry to limit distress and to reinforce the operant conditioning. Veterinary care interaction with these monkeys with individuals other than the persons involved in operant conditioning and enrichment was limited to yearly physicals and twice a year TB testing and any other USDA mandated veterinary checkups.

2.1.3. Clinical Assessment. Behavioral ratings were performed using the mUPDRS in a blinded fashion. A more detailed description can be found in our previous publications [15, 16]. Briefly, the mUPDRS consists of subjective-rater-dependent but validated and reliable blinded evaluations of vocalization/hooting, facial expression, tremor (rest or action), muscle tone/rigidity, hypokinesia, finger dexterity, foot agility, balance/postural instability, spontaneous gait, dystonia, and circling/dyskinesia. Each item on the mUPDRS has a range from 0 (no motor deficits) to 4 (very severe impairment) for each limb or body part and is modeled after the UPDRS was used to rate PD patients in clinical trials. Animals were also further assessed for drug-induced dyskinesias using a modified Abnormal Involuntary Movements Scale (AIMS) previously described for primates [18, 19]. AIMS scores are represented as the total sum of dystonic posturing and choreiform movements in the face, trunk, and each limb. Severity was evaluated using the following scale: 0 = none; occasional, mild = 1; intermittent, moderate = 2; continuous, severe = 3. The entire clinical rating session was videotaped for minimum of 4 hours after each dose of medication for a minimum of 8 hours of video in representative animals. mUPDRS and AIMS scores were taken at stable parkinsonian baseline state, placebo, and at an average time of 75 minutes after drug treatments. We established the optimal LD/CD dose for each animal using blinded testing every 2 weeks at monthly intervals starting at a dose of 50 mg LD/12.5 mg CD b.i.d. (i.e., LD 100 mg/CD 25 mg/day) and escalated by 100 mg LD every 2 weeks to achieve no further improvements in mUPDRS scores despite dose escalation. Thereafter, the lowest dose of LD that produced the largest improvement in mUPDRS scores was chosen as the optimal dose of LD in each animal. Thus, animals were tested on LD treatment for a minimum of 3-4 months to determine their optimal LD dose. All animals were washed out of LD treatments for 1 month before initiating MPEP or MPWE treatments. In a similar fashion, optimal dose of MPEP, and MPWE was also determined and optimal behavioral plateau that coincided for LD, LD+DDCI, MPEP, and MPWE was identified. This plateau phase was used for all the experiments described in this paper to make comparisons with equipoise and validity.

2.1.4. Electrophysiology. After recordings were taken during placebo and on drug treatments, the recordings were sorted by offline principal component analysis, and interspike intervals (ISIs) were generated. Acceptable records were comprised of at least 400 spikes and had duration between 60 and 120 sec. Firing rates and seven measures of the firing patterns were employed: the coefficient of variation (CV) of the ISIs, the burst index (mean of the ISI distribution divided by the mode [20]), the percent of spikes in bursts and percentage of time in bursts calculated by the Poisson surprise method [21], the density discharge histogram (DDH) compared to the DDH of a random Poisson spike train [22], the range of the DDH, and the sample entropy [23]. The seven numeric firing pattern metrics were compared using the Wilcoxon-Mann-Whitney rank-sum test, and the categorical DDH classification was compared using Fisher's 2×2 exact test (grouping together "Poisson" and "bursty" categories).

2.2. Drug Treatments

2.2.1. Preliminary Dose-Finding and Toxicity Studies of MPEP: Experimental Design and Results. We first completed a preliminary dose-finding study to determine optimal doses and toxicity adverse effects of MPEP and MPEP+CD. HP monkeys were tested on MPEP and MPEP+CD (25 mg) to find optimal dosing after attaining stable HP state ($N = 3$). Each treatment epoch was followed by 2 weeks of washout. Two separate mUPDRS scores 14 days apart were obtained on placebo and for each treatment epoch. MPEP was titrated in these studies from 6 g/day to the highest dose of 18 g/day ($N = 11$) to evaluate gastrointestinal effects, drug-induced dyskinesias, or behavioral correlates of psychiatric symptoms. Blood draw was performed 90 minutes after administration and consumption of medications (placebo, LD+CD (250 mg/62.5 mg) and MPEP+CD (4.5 g/25 mg)) to test the bioavailability of orally administered LD and MPEP at approximately equivalent doses for pharmacological estimation of dopamine levels. See Table 2 for representative drug-dosing block design.

In these initial studies, mean mUPDRS scores improved by 4% (change from 35 to 33.5), 24.2% (35 to 26.5), and 27.1% (35 to 25.5), respectively, with 3 g, 6 g, and 9 g (total daily dose) of MPEP alone. Optimal dose for MPEP+CD was determined to be 9 g of MPEP + 50 mg of CD/day.

Table 2: Dosing regimen for non-human primates. A block design was devised for each testing session. Each behavioral testing cohort was varied to maintain blind and to prevent the behavioral rater from guessing the treatments. Each such block design was repeated twice for each experiment and videos are independently rated. Representative animals were videotaped continuously in the room $24 \times 5 \times 365$ days. The postdrug treatment videos were culled from these videos by the person who administered the drug who was unblinded. These culled video segments were used for the scoring along with the rater executed direct observational scoring of mUPDRS and AIMS. These culled segments began as soon as the person administering the drug confirmed successful consumption of the drug and lasted 8 hours from that time. The notion of the average time of 75 minutes refers to the average time at which behavioral ratings using mUPDRS and AIMS were scored for the study. The validity of this time frame for the detection of optimal effects of LD and LD/DDCI oral treatments has been published previously. To make meaningful valid comparisons MPEP and MPWE treatments were also performed at the same time schedule. The remainder of the video was rated, but it does not have the observer interaction and it only shows routine animal activity in its home cage. As expected, LD and LD/DDCI treatments had behavioral benefits that lasted 180 minutes and then ameliorated. Effects of MPEP and MPWE lasted longer and appeared to dissipate only after 6 hours.

	Monkey 1	Monkey 2	Monkey 3	Monkey 4	Monkey 5
Block 1	LD	Placebo	Placebo	MPEP	MPEP
Block 2	LD	Placebo	Placebo	MPEP	MPEP
Block 3	Placebo	LD	LD	Placebo	Placebo
Block 4	Placebo	LD	LD	Placebo	Placebo
Block 5	MPEP	Placebo	Placebo	LD	LD
Block 6	MPEP	Placebo	Placebo	LD	LD
Block 7	Placebo	MPEP	MPEP	Placebo	Placebo
Block 8	Placebo	MPEP	MPEP	Placebo	Placebo

In this experiment, mean mUPDRS score showed no improvements for the placebo treatments (mean mUPDRS score of 35 to 35.2) compared to a 49.1% improvement (mean mUPDRS score changed from 35 to 17.8) at this optimal MPEP+CD dose. No observable adverse events were evident at these doses of MPEP alone or MPEP+CD. Doses at 12 g/day and 18 g/day caused compliance issues and severe adverse effects with successful consumption. These included nausea, retching, vomiting, behavior that mimicked hallucinations, and increased aggression. Serum peak dose estimation of dopamine levels was 180 pg/mL after placebo treatment, 27,600 pg/mL after MPEP+CD treatment (4.5 g MPEP+25 mg CD; ~225 mg of LD), and 22,220 pg/mL after LD+CD administration (250/62.5).

2.2.2. Experiment 1: Effects of MPEP, MPEP+CD, and LD+CD. After finding preliminary optimal doses of MPEP, we examined the effects of 4.5 g MPEP alone (~225 mg LD) ($N = 5$), 4.5 g MPEP (~225 mg LD) + 25 mg CD ($N = 6$) and 100–200 mg LD + 25–50 mg CD (i.e., daily doses were 9 g MPEP alone ($N = 5$), 9 g MPEP+50 mg CD ($N = 6$), and 200–400 mg levodopa + 50–100 mg CD ($N = 6$)) in HP and OHP primates. In a subset of animals, cranial recording chambers were surgically implanted to permit chronic single-cell extracellular neuronal recording from the left STN and SNR in the stable HP state ($N = 3$), with LD+CD treatment ($N = 2$) and with MPEP+CD treatment ($N = 1$) (a portion of this study has been presented elsewhere [16]).

2.2.3. Expriment 2: Effects of MPWE and LD. MPEP was dissolved in sterile water and thoroughly mixed for 30–45 mins. The mixture was then centrifuged at 14,000–15,000 RPM for 15–20 mins, and the supernatant was extracted and filtered. The MPWE solution was then stored in sterile containers at 4°C. Prior to administration, the MPWE solution was briefly agitated and dispensed orally. The dosage concentration of MPWE was based on 4-5% of natural occurring LD in MPEP such that the MPWE solution had approximately 24 mg LD per mL.

HP, OHP, and bilateral parkinsonian animals ($N = 5$) were treated with placebo, LD+CD or MPWE b.i.d. for 3–11 days. mUPDRS scores were obtained on placebo, oral LD (1 to 3.5 tablets LD/CD–100/25), and escalating doses of 4 mL–36 mL MPWE orally (~96 mg–864 mg LD, resp.) until optimal doses were found using a blinded, randomized design with 2 weeks of washout between treatments. When compliance was an issue with oral LD+CD, animals received systemic injections of LD at the equivalent optimal doses of oral LD (LD methyl ester with benserazide (BZ)). Drug-induced dyskinesias were assessed using the abnormal involuntary movements (AIMS) rating scale in animals that displayed clear LD-induced dyskinesias similar in advanced PD [15, 18, 19]. Data was analyzed using ANOVA with Tukey posttest or Chi-square test (mean ± SEM).

3. Results

3.1. MPEP and LD Effects on Parkinsonism and Basal Ganglia Electrophysiology. mUPDRS scores on placebo were 15.6 ± 2.6 and decreased to 8.0 ± 1.6 with MPEP alone, 7.7 ± 1.5 with MPEP+CD, and 4.5 ± 1.1 with LD+CD, optimal doses (Figure 1). These doses caused no observable adverse effects.

A portion of this electrophysiological data has been presented in a previously published report [16]. SNR firing rate showed significant reduction in SNR on both LD+CD and MPEP+CD. STN firing rate showed no significant difference, but a trend toward reduction on MPEP+CD (Figure 2(a)). SNR firing pattern became more bursty on LD+CD, measured by Poisson DDH comparison. SNR patterns changes on MPEP+CD did not reach statistical significance, but showed a trend toward increased burstiness, but not as pronounced as LD+CD. STN patterns did not show a statistical change, although both LD+CD and MPEP+CD showed a trend toward reduction of the number of bursty neurons (Figure 2(b)). Median SNR normalized coefficient of variation was higher on LD+CD than baseline HP state. On MPEP, the SNR showed a trend toward increased normalized CV, but it was not significant. There were no significant changes in the STN (Figure 2(c)). The proportion of spikes in bursts and proportion of time in bursts (measured from the Poisson-surprise method) did

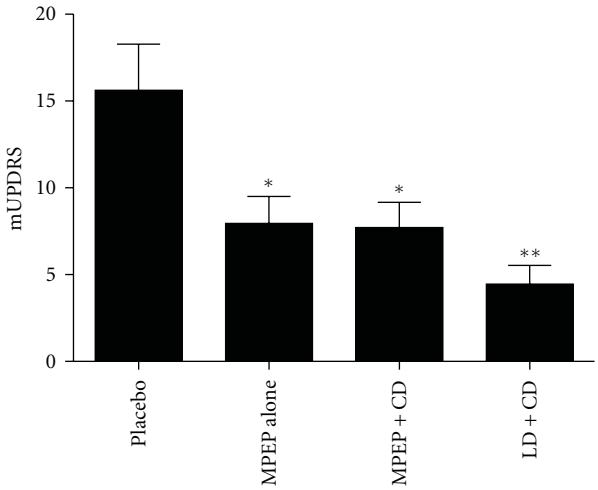

Figure 1: Comparison of mUPDRS scores in parkinsonian primates with placebo, MPEP alone, MPEP+CD, and LD+CD demonstrates significant amelioration of parkinsonism after treatments. $^{*}P < 0.05$, $^{**}P < 0.01$.

not show any statistically significant changes. However, there was a trend for both LD+CD and MPEP+CD to make the SNR more bursty, with MPEP+CD showing a smaller effect than LD+CD. There was a trend for LD+CD to make the STN less bursty, and MPEP+CD showed the same trend to an even larger degree (Figures 2(d) and 2(e)). DDH range counts were not statistically different in the different conditions. However, there was a trend for LD+CD to make the SNR more bursty. MPEP+CD showed a trend toward making the SNR more bursty but it was not significant (Figure 2(f)). The burst index was not statistically significant between groups. However, there was a trend for LD+CD to make the SNR more bursty, which was not replicated on MPEP+CD. In fact, there was a trend for MPEP+CD to reduce the burstiness of SNR. In the STN, the trends were reversed, but again neither were significant (Figure 2(g)). Sample entropy did not show any significant differences, although the MPEP+CD treatment slightly reduced the SNR sample entropy and slightly increased the STN sample entropy (Figure 2(h)).

3.2. MPWE Ameliorates Parkinsonism without Causing Drug-Induced Dyskinesias. mUPDRS scores on placebo were 18.0 ± 5.6, which significantly decreased with optimal doses of MPWE treatments (5.4 ± 0.4) and LD+CD treatments (5.3 ± 1.9) (Figure 3(a)). Average optimal dose of LD was 250 mg and optimal dose of MPWE was 20 mL (~480 mg LD) b.i.d. in this experiment that included HP, OHP, and bilateral parkinsonian animals. MPWE caused no apparent GI problems or drug-induced hallucinations. However, LD+CD treatments produced significant drug-induced dyskinesias (AIMS score = 7.3 ± 1.3) in two bilaterally parkinsonian animals, whereas no apparent drug-induced dyskinesias were observed with MPWE treatments (AIMS score = 0) (Figure 3(b)).

4. Discussion

In the present study, we demonstrate that *Mucuna pruriens* in powder and water extract form can significantly ameliorate behavioral deficits in primate models of PD. We also demonstrate that the mechanistic actions of *Mucuna pruriens* cannot be attributed to LD alone and that *Mucuna pruriens* has a unique mechanism of action on the basal ganglia electrophysiology that is different from that of LD when tested at equivalent doses. This is a confirmation of earlier suggestions that the anti-PD effects of *Mucuna pruriens* were not simply due to natural LD. Indigenous medicines based on natural products like *Mucuna pruriens* are often unique in that they contain several constituents in combination. *Mucuna pruriens* has over 50 known constituents that have been identified to date (Table 3) and perhaps others yet to be discovered [24–26]. Identifying the single component or combination of components in *Mucuna pruriens* responsible for its anti-parkinsonian/anti-dyskinetic effects is daunting. Although identification of each individual component and its exact quantity required to reproduce these effects is theoretically possible, such a task is time consuming and expensive. *Mucuna pruriens* is widely farmed in many countries as an intercrop and is exceedingly inexpensive to produce as a standardized natural product with uniform efficacy. Thus, this renewable, natural product may represent a new treatment that is different from contemporary drug discovery methods where identification of active ingredients, synthetic manufacture, safety, and efficacy testing followed by mass marketing of the synthesized compounds is replaced by a strategy that focuses on identification of safety and efficacy of a standardized natural product and its mechanism of action when used as a whole. While such an approach may sound counterintuitive, archaic, and confrontational to the current wisdom of scientific advancement, it is pragmatic and has the potential to advance the therapy of PD with the possibility of worldwide availability of inexpensive *Mucuna pruriens* formulations.

4.1. Effects of Mucuna pruriens Endocarp Powder. In experiment 1, we found that MPEP had to be dosed at higher quantities to get maximal effect when compared to LD (100–200 mg synthetic LD versus 225 mg natural LD in MPEP). The large volume of MPEP powder (6 g to 18 g/day) in preliminary studies and in experiment 1 was very difficult to successfully administer in monkeys due to gastrointestinal side effects, similar to those of earlier reports [1, 8–10]. These gastrointestinal effects could be in part due to the large protein content in this leguminous cotyledon powder, a well-known cause of abdominal bloating, flatulence, and gastrointestinal irritability. Serum dopamine measurements demonstrate that bioavailability and peak plasma pharmacokinetics of natural LD contained in MPEP and synthetic LD are quite similar. This finding further strengthens the notion that MPEP contains additional anti-PD and anti-dyskinetic agents beyond the 4-5% natural LD content.

Previous reports have demonstrated that LD and other dopamine replacement therapies can significantly alter firing

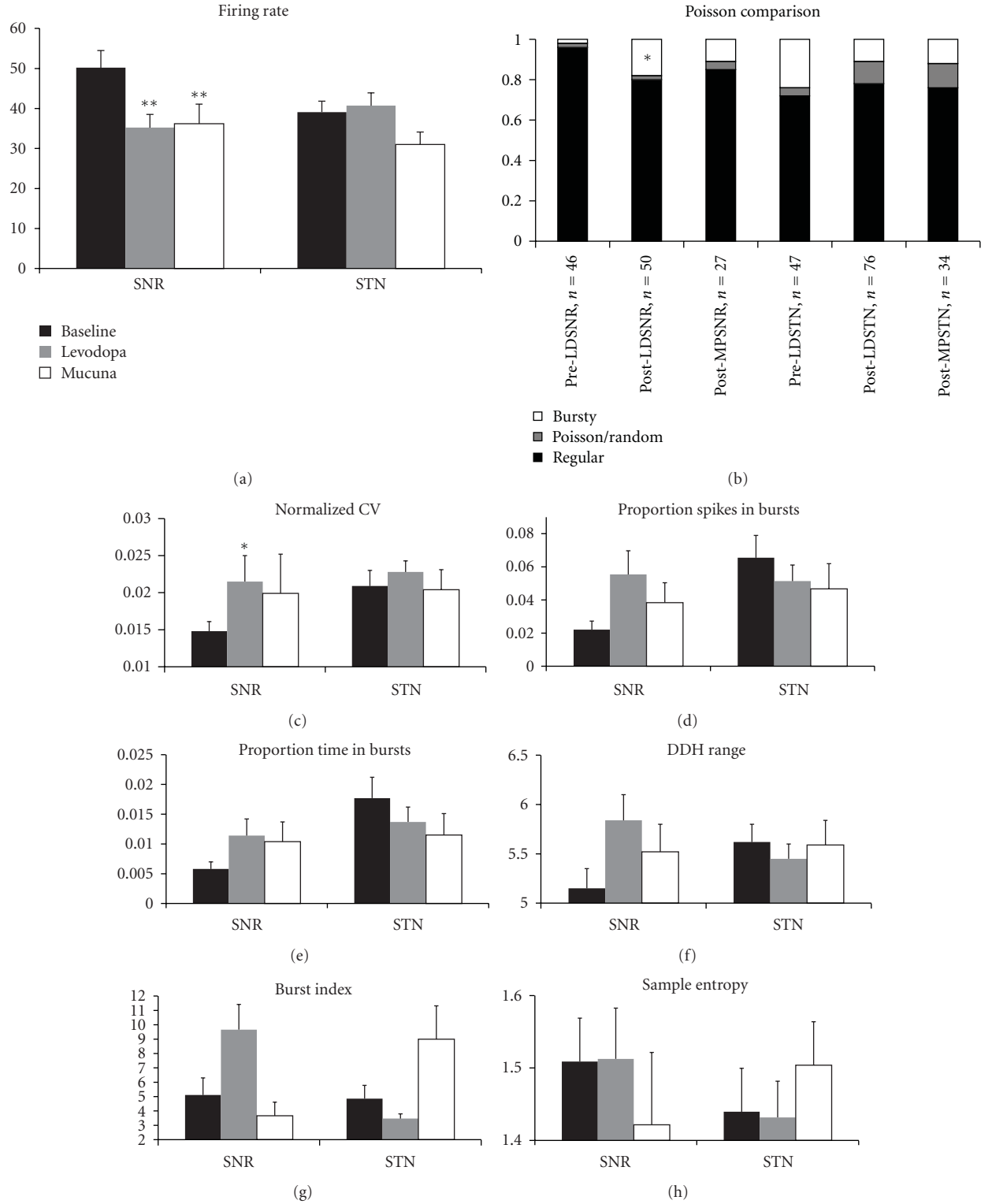

Figure 2: (a) Firing rates of SNR and STN in the HP monkey in stable HP state (baseline) and on LD+CD (Levodopa) and MPEP+CD (Mucuna) (Kruskal-Wallis $P < 0.01$, $^{**}P < 0.01$ rank-sum using Tukey's HSD correction, compared to baseline HP state). (b) Poisson comparison of SNR and STN neurons Pre-LD (stable baseline HP state) (Fisher's 2×2 two-sided exact test grouping "Poisson" category together with "regular," $^{*}P = 0.0164$), Post-LD (LD treatments), and Post-MP (MPEP+CD). (c) Coefficient of variation at HP state and with treatments (Kruskal-Wallis $P < 0.05$, $^{*}P < 0.05$ rank-sum using Tukey's HSD correction, compared to baseline HP) (d–g) Measures of firing patterns in the SNR and STN in HP state and on treatments. (h) Sample entropy of SNR and STN.

Table 3: Known components of *Mucuna pruriens*.

Arachidic acid	Lysine
Arginine	Methionine
Ash	6-Methoxyharman
Aspartic acid	1-Methyl-3-carboxyl-6,7-dihydroxy-1,2,3,4-tetrahydroisoquinoline
Behenic acid	Mucunadine
Beta carboline	Mucunain
Beta sitosterol	Mucunine
Bufotenine	Myristic acid
Calcium	Niacin
Carbohydrates	Nicotine
Choline	Nicotinamide adenine dinucleotide
Cystine	Oleic acid
Coenzyme Q-10	5-Oxyindole-3-alkylamine
N,N-Dimethyltryptamine	Palmitic acid
N,N-Dimethyltryptamine-N-oxide	Palmitoleic acid
L-Dopa	Phenylalanine
Cis-12,13-epoxyoctadec-trans-9-cis-acid	Phosphorus
Cis-12,13-epoxyoctadec-trans-9-enoic-acid 5-Methoxy-N,N-dimethyltrytamine-N-Oxide	Proline
Fat	Protein
Fiber	Prurienidine
Gallic acid	Prurienine
Glutamic acid	Riboflavin
Glutathione	Saponins
Glycine	SD
Histidine	Serine
5-Hydroxytryptamine	Serotonin
Indole-3-alkylamine	Stearic acid
Iron	Thiamin
Isoleucine	Threonine
Lecithin	Tryptamine
Leucine	Tyrosine
Linoleic acid	Valine
Linolenic acid	Vernolic acid

properties of basal ganglia nuclei. This has been discussed in our recently published paper in detail [16, 20, 27–34]. We demonstrate that SNr firing rate is significantly decreased after treatment with both LD and MPEP. However, LD treatment did not decrease STN firing rate. Interestingly, MPEP did cause a trend in decreasing STN firing rate. We also found differential firing patterns between the two treatments. LD caused a significant increase in SNr bursting activity but this increase was not seen with MPEP. We also found slight differences between LD and MPEP in the other measures of burstiness. Various pharmacological agents are known to alter basal ganglia firing patterns, which include serotonin, N-methyl-D-aspartate modulators, and dopamine agonists [29, 35–37]; the presence of similar compounds in MPEP may account for the differential bursting firing patterns of MPEP.

4.2. Effects of Mucuna Pruriens Endocarp Powder Water Extract. The ameliorative effects of oral MPWE treatments are similar to the anti-PD effects of LD+CD treatment, a gold standard for pharmacological therapeutic efficacy in PD, sans its deleterious side effects in the parkinsonian primate. As shown in experiment 2, MPWE provides a simple and inexpensive solution to these problems with gastrointestinal intolerance of MPEP and demonstrates that the anti-PD and anti-dyskinetic compounds contained in *Mucuna pruriens* are water soluble and effective without the need for concomitant DDCI. This suggests that even monkeys "primed" to develop drug-induced dyskinesias from repeated exposure to LD+CD treatments can be successfully treated with MPWE without causing dyskinesias. Furthermore, the anti-PD and anti-dyskinetic effects of MPWE were not diminished by chronic exposure, drug washout, and reexposure. We have

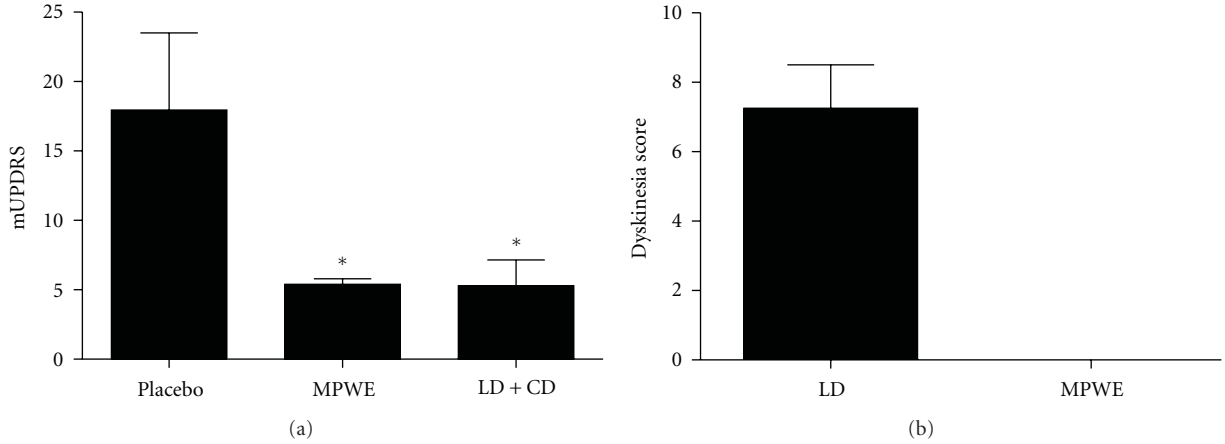

Figure 3: (a) A water extract of MPEP (MPWE) significantly reduces parkinsonism in the parkinsonian primate at optimal doses similar to LD+CD ($^*P < 0.05$) (b) and does not cause dyskinesias ($P = 0.045$, Chi-square test).

recently shown that LD does not cause dyskinesias in HP rhesus monkeys [15]. In this context, we demonstrate the anti-PD properties of MPWE in HP and OHP primates, models that represent restricted nigrostriatal dopaminergic loss, and the anti-PD and anti-dyskinetic effects in the bilateral parkinsonian monkey, a model that represents more severe PD and readily exhibits drug-induced dyskinesias. These findings in the MPTP-treated monkey models are similar to what we have reported in the HP rat [12]. Some investigators have argued that drug-induced abnormal involuntary movements displayed by the parkinsonian rat are not equivalent of drug-induced dyskinesias seen in PD and believe that the phenomenology of drug-induced dyskinesias in the primate model more closely resembles clinical drug-induced dyskinesias [38]. We address this in the current study, confirming the preclinical relevance of the anti-PD and anti-dyskinetic effects of MPWE without a DDCI in parkinsonian primates. Taken together, these studies in the rodent and primate models of PD provide compelling preclinical evidence of the efficacy and safety for MPWE. Biochemical measurements previously mentioned provide proof that LD+CD treatments were appropriately dosed in animals that developed drug-induced dyskinesias in the MPWE experiments. We hypothesize that the improved safety profile of MPWE may be due to additional beneficial compounds as speculated in previous studies [8, 25, 26].

We escalated the dose of MPWE more than what was needed to match the optimal anti-PD effects obtained from LD+CD treatments (MPWE doses up to >1600 mg LD equivalent dose per day). Nonetheless, these animals tolerated these large doses without adverse effects. MPWE contains 4-5% LD that is identical to the 4-5% LD content reported for MPEP powder. Since MPWE was administered without a DDCI, we hypothesize that the effects cannot be entirely due to LD content in MPWE because LD would be metabolized via peripheral DDC, suggesting that MPWE may have DDCI-like activities or other mechanisms to protect LD degradation via the action of peripheral DDCI. However, our previous rodent studies suggest that MPWE action cannot be accounted for just on the basis of its purported DDCI-like activity [12]. Thus, our rodent studies [12] and the current experiment collectively provide behavioral evidence that the anti-PD effects of MPWE cannot be explained by the presence of 4-5% natural LD alone or the combination of natural LD and a yet-to-be identified DDCI constituent. Other water-soluble compounds that remain unidentified contained in MPWE have to be implicated for the anti-PD and anti-dyskinetic effects observed in these studies.

4.3. Oral Administration of Antiparkinsonian Treatments to Parkinsonian Monkeys. This is the first report of any phytomedicine that has been tested in primates using operant conditioned methods for oral voluntary consumption to simulate clinical PD pharmacotherapy, using placebo controls and a blinded prospective study design. This study design could represent an ideal method to perform future preclinical studies of phytomedicines in PD. We found compliance with oral consumption easier with MPWE compared to MPEP, MPEP+CD, or LD+CD. Previous studies with various MPEP formulations [8–10, 39, 40] have a number of disadvantages that include variable behavioral assessments, use of concomitant medications, inadequate washout, lack of LD dose controls, and excess variability in study populations (see detailed discussion in our recent report [12]). In the present study, we overcame these disadvantages by (1) using well-established primate models of PD that exhibit motor fluctuations and drug-induced dyskinesias that closely resemble its phenomenology to patients with PD, (2) ensuring drug compliance to replicate the clinical experience of PD patients, (3) utilizing the same behavioral rater for all mUPDRS assessments to eliminate interrater variability, and (4) ensuring that animals received no concomitant medications.

5. Conclusion

We demonstrate that *Mucuna pruriens* and MPWE have unique mechanistic properties that are differential from LD

and that the unique combination of constituents within *Mucuna pruriens* contributes to both its anti-PD and anti-dyskinetic effects. This will be advantageous to PD patients who currently take LD-containing formulations and have to experience its long-term side effects that often require invasive surgical intervention. This study also shows that MPWE contains a yet-to-be investigated portfolio of anti-PD and anti-dyskinetic agents that could open up new therapeutic avenues for PD, yet constitute a daunting and expensive conventional drug discovery approach. While additional scientific studies to identify these individual anti-PD and anti-dyskinetic components contained in MPWE may be warranted, parallel studies to evaluate the clinical use of MPWE as a safe and effective alternative to LD therapy in PD is also immediately indicated with our demonstration of its unique beneficial mechanisms of action.

Acknowledgments

The authors thank Samar Shah, Swetha Suresh, Stasha Rezak, and Shalini Garg for their technical assistance in placebo-controlled studies, Allen Kunselman for statistical analysis, and Mark Hallett, M.D., and Mark Nolt, Ph.D., for their valuable critique of this manuscript. The authors thank Merck & Co., Inc./Dupont Co. for the donation of carbidopa/levodopa. They also thank Zandu Pharmaceuticals, Mumbai, India, for providing them with standardized formulation of MPEP that meet the NIH natural products standards and the NCCAM policy on natural product integrity. This work was supported in part by research grants from the National Institutes of Health National Center for Complementary and Alternative Medicine (NCCAM) R21AT001607 and National Institute of Neurological Disorders and Stroke (NINDS) R01NS42402, Health Resources and Services Administration DIBTH0632, and the Pennsylvania Tobacco Settlement Funds Biomedical Research Grant to T. Subramanian The Pennsylvania Department of Health specifically disclaims responsibility for any analyses, interpretations, or conclusions. Additional funding was provided by Penn State University Brain Repair Research Fund.

References

[1] M. Behari, S. P. Bhatnagar, U. Muthane, and D. Deo, "Experiences of Parkinson's disease in India," *The Lancet Neurology*, vol. 1, no. 4, pp. 258–262, 2002.

[2] M. Deogaonkar and T. Subramanian, "Pathophysiological basis of drug-induced dyskinesias in Parkinson's disease," *Brain Research Reviews*, vol. 50, no. 1, pp. 156–168, 2005.

[3] S. Kuzuhara, "Drug-induced psychotic symptoms in Parkinson's disease. Problems, management and dilemma," *Journal of Neurology*, vol. 248, supplement 3, pp. III28–III31, 2001.

[4] V. Voon, P. O. Fernagut, J. Wickens et al., "Chronic dopaminergic stimulation in Parkinson's disease: from dyskinesias to impulse control disorders," *The Lancet Neurology*, vol. 8, no. 12, pp. 1140–1149, 2009.

[5] B. V. Manyam, "Paralysis agitans and levodopa in "Ayurveda": ancient Indian medical treatise," *Movement Disorders*, vol. 5, no. 1, pp. 47–48, 1990.

[6] B. V. Manyam and J. R. Sánchez-Ramos, "Traditional and complementary therapies in Parkinson's disease," *Advances in Neurology*, vol. 80, pp. 565–574, 1999.

[7] B. Singhal, J. Lalkaka, and C. Sankhla, "Epidemiology and treatment of Parkinson's disease in India," *Parkinsonism and Related Disorders*, vol. 9, supplement 2, pp. S105–S109, 2003.

[8] HP-200 in Parkinson's Disease Study Group, "An alternative medicine treatment for Parkinson's disease: results of a multicenter clinical trial," *Journal of Alternative and Complementary Medicine*, vol. 1, pp. 249–255, 1995.

[9] R. Katzenshlager, A. Evans, A. Manson et al., "*Mucuna pruriens* in Parkinson's disease: a double blind clinical and pharmacological study," *Journal of Neurology, Neurosurgery and Psychiatry*, vol. 75, no. 12, pp. 1672–1677, 2004.

[10] A. B. Vaidya, T. G. Rajagopalan, and N. A. Mankodi, "Treatment of Parkinson's disease with the cowhage plant—*Mucuna pruriens* Bak," *Neurology India*, vol. 26, no. 4, pp. 171–176, 1978.

[11] O. Suchowersky, G. Gronseth, J. Perlmutter, S. Reich, T. Zesiewicz, and W. J. Weiner, "Practice parameter: neuroprotective strategies and alternative therapies for Parkinson disease (an evidence-based review): report of the quality standards subcommittee of the American Academy of Neurology," *Neurology*, vol. 66, no. 7, pp. 976–982, 2006.

[12] C. A. Lieu, A. R. Kunselman, B. V. Manyam, K. Venkiteswaran, and T. Subramanian, "A water extract of *Mucuna pruriens* provides long-term amelioration of parkinsonism with reduced risk for dyskinesias," *Parkinsonism and Related Disorders*, vol. 16, no. 7, pp. 458–465, 2010.

[13] Y. Oiwa, J. L. Eberling, D. Nagy, P. Pivirotto, M. E. Emborg, and K. S. Bankiewicz, "Overlesioned hemiparkinsonian non human primate model: correlation between clinical, neurochemical and histochemical changes," *Frontiers in Bioscience*, vol. 8, pp. a155–a166, 2003.

[14] T. Subramanian, C. A. Lieu, K. Guttalu, and D. Berg, "Detection of MPTP-induced substantia nigra hyperechogenicity in rhesus monkeys by transcranial ultrasound," *Ultrasound in Medicine and Biology*, vol. 36, no. 4, pp. 604–609, 2010.

[15] C. A. Lieu, M. Deogaonkar, R. A. E. Bakay, and T. Subramanian, "Dyskinesias do not develop after chronic intermittent levodopa therapy in clinically hemiparkinsonian rhesus monkeys," *Parkinsonism and Related Disorders*, vol. 17, no. 1, pp. 34–39, 2011.

[16] T. P. Gilmour, C. A. Lieu, M. J. Nolt, B. Piallat, M. Deogaonkar, and T. Subramanian, "The effects of chronic levodopa treatments on the neuronal firing properties of the subthalamic nucleus and substantia nigra reticulata in hemiparkinsonian rhesus monkeys," *Experimental Neurology*, vol. 228, no. 1, pp. 53–58, 2011.

[17] E. V. Gilbert, J. K. Leszczynski, T. Subramanian, and J. Zhang, "Methods to provide enrichment to MPTP-treated hemiparkinsonian (HP) monkeys without interfering with operant conditioned behavioral testing," Program 67616, Neuroscience Meeting Planner, Society for Neuroscience, San Diego, Calif, USA, 2004.

[18] S. Konitsiotis, P. J. Blanchet, L. Verhagen, E. Lamers, and T. N. Chase, "AMPA receptor blockade improves levodopa-induced dyskinesia in MPTP monkeys," *Neurology*, vol. 54, no. 8, pp. 1589–1595, 2000.

[19] P. J. Blanchet, S. Konitsiotis, and T. N. Chase, "Amantadine reduces levodopa-induced dyskinesias in parkinsonian monkeys," *Movement Disorders*, vol. 13, no. 5, pp. 798–802, 1998.

[20] W. D. Hutchison, R. Levy, J. O. Dostrovsky, A. M. Lozano, and A. E. Lang, "Effects of apomorphine on globus pallidus

neurons in parkinsonian patients," *Annals of Neurology*, vol. 42, no. 5, pp. 767–775, 1997.

[21] C. R. Legendy and M. Salcman, "Bursts and recurrences of bursts in the spike trains of spontaneously active striate cortex neurons," *Journal of Neurophysiology*, vol. 53, no. 4, pp. 926–939, 1985.

[22] Y. Kaneoke and J. L. Vitek, "Burst and oscillation as disparate neuronal properties," *Journal of Neuroscience Methods*, vol. 68, no. 2, pp. 211–223, 1996.

[23] J. S. Richman and J. R. Moorman, "Physiological time-series analysis using approximate and sample entropy," *American Journal of Physiology*, vol. 278, no. 6, pp. H2039–H2049, 2000.

[24] S. Burgess, A. Hemmer, and R. Myhrman, "Examination of raw and roasted *Mucuna pruriens* for tumerogenic substances," *Tropical and Subtropical Agroecosystems*, vol. 1, pp. 287–293, 2003.

[25] B. V. Manyam, M. Dhanasekaran, and T. A. Hare, "Neuroprotective effects of the antiparkinson drug *Mucuna pruriens*," *Phytotherapy Research*, vol. 18, no. 9, pp. 706–712, 2004.

[26] B. V. Manyam, M. Dhanasekaran, and T. A. Hare, "Effect of antiparkinson drug HP-200 (*Mucuna pruriens*) on the central monoaminergic neurotransmitters," *Phytotherapy Research*, vol. 18, no. 2, pp. 97–101, 2004.

[27] M. Lafreniere-Roula, O. Darbin, W. D. Hutchison, T. Wichmann, A. M. Lozano, and J. O. Dostrovsky, "Apomorphine reduces subthalamic neuronal entropy in parkinsonian patients," *Experimental Neurology*, vol. 225, no. 2, pp. 455–458, 2010.

[28] A. M. Lozano, A. E. Lang, R. Levy, W. Hutchison, and J. Dostrovsky, "Neuronal recordings in Parkinson's disease patients with dyskinesias induced by apomorphine," *Annals of Neurology*, vol. 47, no. 4, supplement 1, pp. S141–S146, 2000.

[29] R. Levy, J. O. Dostrovsky, A. E. Lang, E. Sime, W. D. Hutchison, and A. M. Lozano, "Effects of apomorphine on subthalamic nucleus and globus pallidus internus neurons in patients with Parkinson's disease," *Journal of Neurophysiology*, vol. 86, no. 1, pp. 249–260, 2001.

[30] T. Boraud, E. Bezard, D. Guehl, B. Bioulac, and C. Gross, "Effects of L-DOPA on neuronal activity of the globus pallidus externalis (GPe) and globus pallidus internalis (GPi) in the MPTP-treated monkey," *Brain Research*, vol. 787, no. 1, pp. 157–160, 1998.

[31] G. Giannicola, S. Marceglia, L. Rossi et al., "The effects of levodopa and ongoing deep brain stimulation on subthalamic beta oscillations in Parkinson's disease," *Experimental Neurology*, vol. 226, no. 1, pp. 120–127, 2010.

[32] G. Heimer, M. Rivlin-Etzion, I. Bar-Gad, J. A. Goldberg, S. N. Haber, and H. Bergman, "Dopamine replacement therapy does not restore the full spectrum of normal pallidal activity in the 1-methyl-4-phenyl-1,2,3,6-tetra-hydropyridine primate model of Parkinsonism," *Journal of Neuroscience*, vol. 26, no. 31, pp. 8101–8114, 2006.

[33] R. L. Albin, A. B. Young, and J. B. Penney, "The functional anatomy of basal ganglia disorders," *Trends in Neurosciences*, vol. 12, no. 10, pp. 366–375, 1989.

[34] M. R. DeLong, "Primate models of movement disorders of basal ganglia origin," *Trends in Neurosciences*, vol. 13, no. 7, pp. 281–285, 1990.

[35] J. I. Lee, H. J. Shin, D. H. Nam et al., "Increased burst firing in substantia nigra pars reticulata neurons and enhanced response to selective D2 agonist in hemiparkinsonian rats after repeated administration of apomorphine," *Journal of Korean Medical Science*, vol. 16, no. 5, pp. 636–642, 2001.

[36] K. Y. Tseng, L. A. Riquelme, J. E. Belforte, J. H. Pazo, and M. G. Murer, "Substantia nigra pars reticulata units in 6-hydroxydopamine-lesioned rats: responses to striatal D2 dopamine receptor stimulation and subthalamic lesions," *European Journal of Neuroscience*, vol. 12, no. 1, pp. 247–256, 2000.

[37] K. Z. Shen, L. B. Kozell, and S. W. Johnson, "Multiple conductances are modulated by 5-HT receptor subtypes in rat subthalamic nucleus neurons," *Neuroscience*, vol. 148, no. 4, pp. 996–1003, 2007.

[38] J. W. Langston, M. Quik, G. Petzinger, M. Jakowec, and D. A. Di Monte, "Investigating levodopa-induced dyskinesias in the Parkinsonian primate," *Annals of Neurology*, vol. 47, no. 4, pp. S79–S89, 2000.

[39] S. Kasture, S. Pontis, A. Pinna et al., "Assessment of symptomatic and neuroprotective efficacy of *Mucuna pruriens* seed extract in rodent model of Parkinson's disease," *Neurotoxicity Research*, vol. 15, no. 2, pp. 111–122, 2009.

[40] G. Hussian and B. V. Manyam, "*Mucuna pruriens* proves more effective than L-DOPA in Parkinson's disease animal model," *Phytotherapy Research*, vol. 11, pp. 419–423, 1997.

Hindawi Publishing Corporation
Evidence-Based Complementary and Alternative Medicine
Volume 2012, Article ID 149256, 13 pages
doi:10.1155/2012/149256

Research Article

A Standardized Chinese Herbal Decoction, Kai-Xin-San, Restores Decreased Levels of Neurotransmitters and Neurotrophic Factors in the Brain of Chronic Stress-Induced Depressive Rats

Kevin Yue Zhu,[1] Qing-Qiu Mao,[2] Siu-Po Ip,[2] Roy Chi-Yan Choi,[1] Tina Ting-Xia Dong,[1] David Tai-Wai Lau,[1] and Karl Wah-Keung Tsim[1]

[1] *Division of Life Science, Center for Chinese Medicine and State Key Laboratory of Molecular Neuroscience, The Hong Kong University of Science and Technology, Clear Water Bay Road, Hong Kong*
[2] *School of Chinese Medicine, The Chinese University of Hong Kong, Shatin, N.T., Hong Kong*

Correspondence should be addressed to Karl Wah-Keung Tsim, botsim@ust.hk

Received 20 April 2012; Revised 16 June 2012; Accepted 10 July 2012

Academic Editor: Kelvin Chan

Kai-xin-san (KXS), a Chinese herbal decoction being prescribed by Sun Simiao in *Beiji Qianjin Yaofang* about 1400 years ago, contains Ginseng Radix et Rhizoma, Polygalae Radix, Acori tatarinowii Rhizoma, and Poria. KXS has been used to treat stress-related psychiatric disease with the symptoms of depression and forgetfulness in ancient China until today. However, the mechanism of its antidepression action is still unknown. Here, the chronic mild-stress-(CMS-) induced depressive rats were applied in exploring the action mechanisms of KXS treatment. Daily intragastric administration of KXS for four weeks significantly alleviated the CMS-induced depressive symptoms displayed by enhanced sucrose consumption. In addition, the expressions of those molecular bio-markers relating to depression in rat brains were altered by the treatment of KXS. These KXS-regulated brain biomarkers included: (i) the levels of dopamine, norepinephrine, and serotonin (ii) the transcript levels of proteins relating to neurotransmitter metabolism; (iii) the transcript levels of neurotrophic factors and their receptors. The results suggested that the anti-depressant-like action of KXS might be mediated by an increase of neurotransmitters and expression of neurotrophic factors and its corresponding receptors in the brain. Thus, KXS could serve as alternative medicine, or health food supplement, for patients suffering from depression.

1. Introduction

Today, a lot of people are suffering from a depressive episode. If a person encounters these symptoms, for example, anhedonia (loss of interest and pleasure), persistent depression, difficulty in sleeping, suicidal tendency, occuring together and lasting for more than two weeks without significant improvement, thus major depression disorder is being diagnosed [1]. The major depression disorder (depression) today is a common psychiatric disorder having an incidence up to 15% and perhaps higher for women at 25% [2], which is estimated to be a major burden on mental health service by the year of 2020 according to WHO's prediction.

Currently, several therapies are used for the treatment of depression, which can be categorized into two parts, psychotherapy and pharmacotherapy, supplemented with other therapies, for example, electroconvulsive seizures, deep brain stimulation, and exercises [3]. The modulation of neurotransmitters, especially restoring the decreased level in the brain of depressive patients, had become the target for development of anti-depression drugs. At least three categories of antidepression drugs have been developed: (i) the tricyclic anti-depressants, such as imipramine, dothiepin, and clomipramine, (ii) the selective neurotransmitters reuptake inhibitors, such as selective serotonin reuptake inhibitors, and norepinephrine reuptake inhibitors, norepinephrine-dopamine reuptake inhibitors, and (iii) monoamine oxidase inhibitors. However, about 30%–40% of patients are not responding to an initial 4–6-week treatment with these drugs. About 10–15% of patients fail to improve sufficiently,

even after several attempts of different treatments, while 12–15% of depressive patients show no response at all, not to mention the possible side effects [4]. Therefore, other theories of the etiology of depression have been proposed, and the deficiency of neurotrophic factors in the brain is an important one [5].

Traditional Chinese medicine (TCM) has offered a possible therapy for the treatment of depression. The records of treating mental disorders could be found in ancient medicinal books, and a herbal decoction kai-xin-san (KXS) is the most popular one. The first description of KXS is recorded in *Beiji Qianjin Yaofang* <*Thousand Formulae for Emergency*> written by Sun Simiao in Tang Dynasty (i.e., 652 AD). This herbal formula composes of four herbs: Ginseng Radix et Rhizoma (root and rhizome of *Panax ginseng* C. A. Mey.), Polygalae Radix (root of *Polygala tenuifolia* Wild.), Acori Tatarinowii Rhizoma (rhizome of *Acorus tatarinowii* Schott), and Poria (sclerotium of *Poria cocos* (Schw.) Wolf). KXS has been used to treat the diseases having symptoms of depressed mood and morbid forgetfulness [6]. Although this decoction has been used frequently, the mechanism of KXS for anti-depression is still unknown, which therefore hinders the further clinical application of this herbal formula. Here, we applied chronic mild-stress-(CMS-) induced depressive rat models to search the mechanism of KXS on anti-depression. The long-term treatment of a chemical standardized herbal extract of KXS suppressed the CMS-induced depression in rats. In the brains of KXS-treated rats, the levels of neurotransmitters, the mRNA expressions of crucial enzymes in regulating those neurotransmitters, and the mRNA expressions of neurotrophic factors and its receptors were significantly altered.

2. Materials and Methods

2.1. Chemicals. Dopamine hydrochloride, 5-hydroxyindoleacetic acid, serotonin hydrochloride, and norepinepherine were purchased from Sigma-Aldrich (St. Louis, MO, USA). Internal standards with isotope labeling were 2-(3,4-dihydroxyphenyl)ethyl-1,1,2,2-d_4-amine HCl (dopamine-d_4, 98 atom % D); 5-hydroxyindole-4,6,7-d_3-3-acetic-d_2-acid (5-hydroxyindole-3-acetic acid-d_5, 98 atom % D); L-glutamic-2,3,3,4,4-d_5-acid (glutamate-d_5, 98 atom % D); serotonin-$\alpha,\alpha,\beta,\beta$-$d_4$ creatinine sulfate complex (serotonin-d_4, 98 atom % D); norepinepherine-2,5,6,α,β,β-d_6 HCl (norepinepherine-d_6, 98 atom % D). The internal standards were purchased from CDN Isotopes (Quebec, Canada). LC-MS-grade acetonitrile and water were purchased from Capitol Scientific (Austin, TX, USA). Formic acid was purchased from Riedel-de Haën Inc. (Hannover, Germany). Imipramine was purchased from Sigma-Aldrich. RNAzol reagent was purchased from Molecular Research Center (Cincinnati, OH, USA). High-Capacity cDNA Reverse Transcription Kit was purchased from Applied Biosystems (Foster City, CA, USA). KAPA SYBR FAST qPCR Kit was purchased from Kapa Biosystems (Woburn, MA, USA).

2.2. Preparation of Extract of KXS Decoction. KXS decoction composed of the following dried raw materials: 4 g Ginseng Radix et Rhizome (root and rhizome of *P. ginseng*), 4 g Polygalae Radix (root of *P. tenuifolia*), 100 g Acori Tatarinowii Rhizoma (rhizome of *A. tatarinowii*), and 200 g Poria (sclerotium of *P. cocos*). The herbs were purchased from Qingping Market of Chinese herbs in Guangzhou, China, which were authenticated by one of the authors, Dr. Tina T.X. Dong, according to their morphological characteristics. The voucher specimens were deposited in the Centre for Chinese Medicine at Hong Kong University of Science and Technology. The herb materials were combined and boiled in 2,500 mL of water for 2 hours, and the herbs were extracted twice. For the second extraction of KXS, the residue from the first extraction was filtered: the same extraction condition was applied on the filtered residue. Then, the extracts were combined and concentrated to the powder and stored at −80°C. Before the KXS treatment, the powder was re-dissolved and vortexed in room temperature. The herbal extract was chemically standardized as reported previously [7].

2.3. Animals and Drug Treatment. Male Sprague-Dawley rats weighing 200–220 g were obtained from the Laboratory Animal Services Center, Chinese University of Hong Kong. Animals were maintained on a 12-hour light/dark cycle (lights on at 6 : 00 a.m., lights off at 6 : 00 p.m.) under controlled temperature (22 ± 2°C) and humidity (50 ± 10%), and they were given standard diet and water. They were allowed to acclimatize for 7 days before use. The experiments on animals have been approved by the Animal Experimentation Ethics Committee of the Chinese University of Hong Kong and conformed to the guidelines of "Principles of Laboratory Animal Care" (NIH publication no. 80-23, revised 1996). The efforts were made to minimize the number and suffering of animals. Rats were randomly divided into five groups of eight individuals. The control animals were given with saline. For another four groups, the animals were treated simultaneously with chronic mild stress (CMS). The drugs (KXS at 0.9 and 2.7 g/kg/day and imipramine at 20 mg/kg) were intragastrically given daily at 30 min before the stress exposure for the entire 4-week treatment.

2.4. Chronic Mild Stress Procedure. The procedure of CMS was performed as described previously [8]. In brief, the CMS protocol consisted of the sequential application of a variety of mild stressors: (1) food deprivation for 24 hours, (2) water deprivation for 24 hours, (3) exposure to a empty bottle for 1 hours, (4) cage tilt (45°) for 7 hours, (5) overnight illumination, (6) soiled cage (200 mL water in 100 g sawdust bedding) for 24 hours, (7) forced swimming at 8°C for 6 minutes, (8) physically restraint for 2 hours, and (9) exposure to a foreign object (e.g., a piece of plastic) for 24 hours. These stressors were randomly scheduled over a one-week period and repeated throughout the 4 weeks of experiment (see Figure 1). Nonstressed animals were left undisturbed in their home cages except during housekeeping procedures such as cage cleaning.

2.5. Rat Sucrose Preference Test. Sucrose preference test was carried out at the end of 4-week CMS exposure. The test was performed as described previously with minor

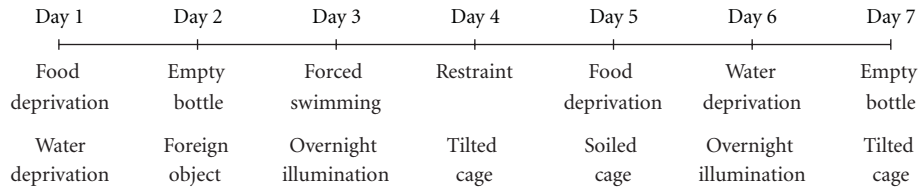

Figure 1: Schedule of chronic mild stress (CMS) procedure. The CMS protocol consisted of the sequential application of a variety of mild stressors. These stressors were randomly scheduled over a one-week period from Day 1 to Day 7 and repeated for 4 weeks during the entire experiment.

modifications. Briefly, 72 hours before the test, the rats were trained to adapt to 1% sucrose solution (w/v): two bottles of 1% sucrose solution were placed in each cage, and 24 hours later 1% sucrose in one bottle was replaced with tap water for 24 hours. After the adaptation, rats were deprived of water and food for 24 hours. Sucrose preference test was conducted at 9 : 00 a.m. in which rats were housed in individual cages and were free to access to two bottles containing 100 mL of sucrose solution (1%, w/v) and 100 mL of water, respectively. After 3 hours, the volumes of consumed sucrose solution and water were measured, and the sucrose preference was calculated by the following formula: sucrose preference = sucrose consumption/(water consumption + sucrose consumption) ×100% [8].

2.6. Analysis of Neurotransmitters. The rats were sacrificed by decapitation, and the whole brain tissues were dissected. Brain tissues were rapidly frozen in liquid nitrogen and kept in −80°C for storage. For lysate preparation, the brain tissues were homogenized in ice-cold 0.5 M formic acid with the concentration of 5 mL/g tissue, in the presence of the internal standard at 500 ng/g tissue. The lysates were centrifuged 15,000 ×g for 30 min at 4°C. The supernatant was separated and stored at −20°C until the LC-MS analysis. The detection of neurotransmitters analysis was performed as described [9]. The chromatographic separation was performed on an Agilent UHPLC 1290 series system (Agilent, Waldbronn, Germany), which was equipped with a degasser, a binary pump, an autosampler, and a thermostated column compartment. The brain sample was separated on an ACE C18 column (3.0 μm i.d., 100 mm × 2.1 mm). The mobile phase was composed of 0.1% formic acid in water (A) and 0.1% formic acid in acetonitrile (B) using the following gradient program: 0–2 min, isocratic gradient 1.0% (B); 2–6 min, linear gradient 1.0–90.0% (B); 6–10 min, isocratic gradient 90.0% (B). A preequilibration period of 4 min was used between each run. The flow rate was 0.2 mL/min, the column temperature was 25°C, and the injection volume was 5 μL. An Agilent QQQ-MS/MS (6410A) equipped with an ESI ion source was operated in positive ion mode. The following conditions were optimized: drying gas, nitrogen (10 L/min, 325°C); capillary voltage, 1950 V; scan mode, SRM. The detected ion pairs, the acquired fragmentor, and the collision energy were tuned with the aids of Agilent optimization software (B02.01). The mass spectrometry calibration was performed with the autofeature of Agilent Mass Hunter Chemstation software (version B01.03) using the ESI-L low-concentration tuning mix supplied with the apparatus. Agilent Mass Hunter workstation software version B.01.00 was used for data acquisition and processing.

2.7. Total RNA Extraction. Total RNA from brain tissue was isolated with RNAzol reagent according to the manufacturer's protocol. In details, total brain tissues were added with RNAzol reagent (1.5 mL/g) and homogenized. The homogenate was centrifuged at 16,100 ×g for 5 min at 4°C. The supernatants were removed, added with diethylpyrocarbonate-(DEPC-) treated water (prepared by autoclaving water with DEPC in a 1000 : 1 ratio), and vortexed vigorously for 15 sec, followed by centrifugation at 13,500 rpm (16,100 ×g) for 10 min at 4°C. The aqueous layer was collected and added with half volume of 70% ethanol in DEPC-treated water for RNA precipitation. The RNA pallet was collected by centrifugation at 16,100 ×g for 10 min at 4°C and washed with 70% ethanol in DEPC-treated water twice. After air dry, the RNA was re-suspended in 200 μL of DEPC-treated water. Concentrations of extracted RNA were calculated from the UV absorbance at 260 nm. The quality of RNA was assessed by absorbance at 260 nm and 280 nm, with the ratio of 260/280 nm ranging from 1.90 to 2.10 being acceptable.

2.8. Real-Time Quantitative PCR. Isolated RNAs were reverse transcribed by the moloney murine leukemia virus (MMLV) reverse transcriptase with oligo-d(T) primer in a 20 μL reaction by using High-Capacity cDNA Reverse Transcription Kit. In details, three μg of total RNA was mixed with 1 μL of 0.5 μg/mL oligo-d(T) primer, 1 μL of 10 mM dNTP mix, and RNAase/DNAase-free water in a 12 μL reaction. The mixture was incubated in 65°C for 5 min. Two μL of 0.1 M dithiothreitol (DTT), 1 μL of 40 U/μL RNase out, and 4 μL of 5 × first strand buffer (250 mM Tris-HCl, pH 8.3, 375 mM KCl, 15 mM $MgCl_2$) were added into the reaction mix and incubated at 37°C for 5 min. One μL MMLV was added into the reaction and incubated at 37°C for 50 min. Then, the reaction was incubated at 70°C for 15 min. Quantification of the cDNA was determined by UV absorbance at 260 nm and 280 nm by NanoDrop. Applications were performed in an Applied Biosystems PCR system for 40 cycles. Ten μL aliquots of the PCR products were size-separated by electrophoresis on a 2% agarose gel. Real-time quantitative PCR was performed by using SYBR Green Master mix and ROX reference dye, according to the manufacturer's instructions of KAPA SYBR FAST qPCR Kit. In brief, cDNAs were obtained from the reverse

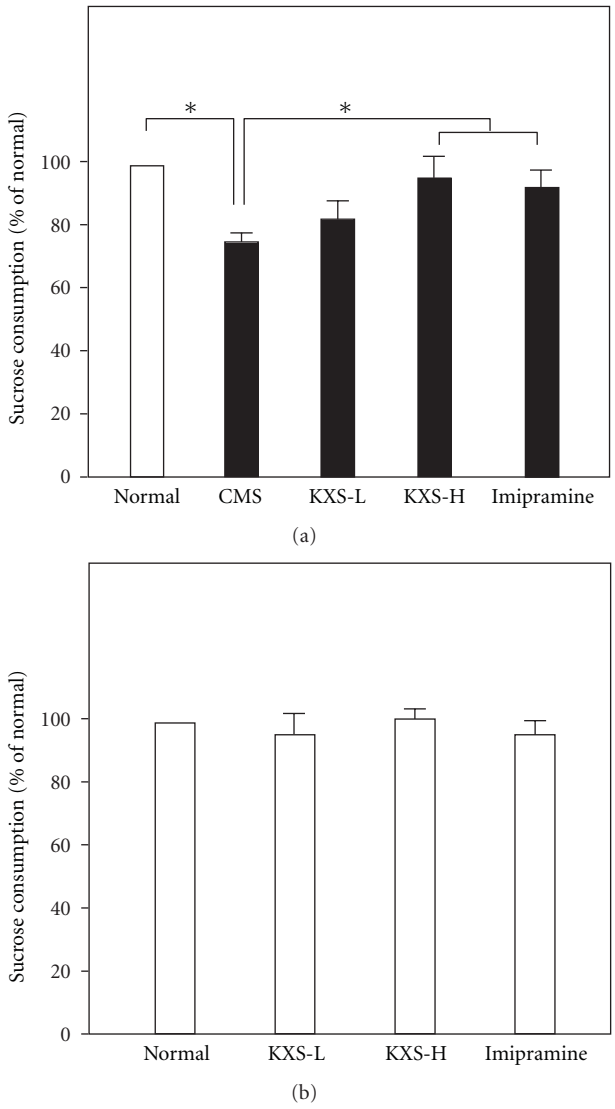

Figure 2: KXS increases the sucrose consumption in CMS-treated rats. (a) Five groups of rats were employed for the sucrose preference test, as stated in Figure 1. KXS treatment, intra-gastrically, was administrated daily at 30 min before the stress exposure for 4 weeks of experimental period. Two doses of KXS were applied including low dosage at 0.9 g/kg (KXS-L) and high dosage at 2.7 g/kg (KXS-H). Imipramine at daily dosage of 20 mg/kg was set as a positive control. (b) Treatment of KXS and imipramine as in (a) but these were all in normal rats. Values are expressed in the percentage of normal (unstressed, or no drug, control), as mean ± SEM ($n = 8$). $^*P < 0.05$.

transcription of the RNA from rat brain. SYBR green signal was detected by M × 3000 ptm multiplex quantitative PCR machine. Transcript levels were quantified by using the Ct value method [11], where values were normalized by the internal-control GAPDH in the same sample. PCR products were analyzed by gel electrophoresis on a 1.5% agarose gel, and the specificity of amplification was confirmed by the melting curves. Primers employed in RT-PCR and real-time quantitative PCR analyses were listed in Table 1.

3. Results

3.1. KXS Alleviates the Depressive-Like Symptoms Induced by Chronic Mild Stress. A chemically standardized herbal extract was prepared according to the ancient recipe: this was an important prerequisite criterion to ensure the repeatability of KXS treatment. KXS was prepared by having Ginseng Radix et Rhizoma, Polygalae Radix, Acori Tatarinowii Rhizoma, and Poria in a ratio of 1 : 1 : 25 : 50. A standardized extraction method of herbal extraction and a quantification of KXS chemically by HPLC-DAD-MS/MS method were developed previously [7]. In addition, an HPLC-MS/MS fingerprint of KXS was shown in Supplementary Figure avalible online at doi:10.1155/2012/149256: this was to ensure the quality of the herbal decoction. By determining the amounts of marker chemicals from each herb, we recommended that a standardized KXS extract should contain no less than 20.4 ± 1.7 mg of ginsenoside Rb_1, 8.0 ± 0.6 mg of ginsenoside Rd, 19.0 ± 1.3 mg of ginsenoside Re, 24.6 ± 2.2 mg of ginsenoside Rg_1, 33.6 ± 0.3 mg of 3, 6′-disinapoyl sucrose, 51.4 ± 0.2 mg of α-asarone, 1112.4 ± 1.9 mg of β-asarone, 21.1 e^{-3} ± 0.4e^{-3} mg of pachymic acid, in 100 g of KXS extract, and the yield of KXS was 14.3 ± 6% (mean ± SD, $n = 3$). These parameters established the chemical standards of KXS for subsequent studies on animals.

To evaluate the anti-depression efficacy of KXS on animal model, the depressive rats induced by CMS were employed for this exploration. The CMS paradigm involved the exposure of animals to a series of mild and unpredictable stressors for 4 weeks (Figure 1). The effect of KXS treatment on the percentage of sucrose consumption in CMS-treated rats was shown in Figure 2(a). Five groups of rats were employed for the sucrose preference test. Imipramine at daily dosage of 20 mg/kg was set as a positive control. KXS treatment was set for two dosages: low dosage (KXS-L) at 0.9 g/kg and high dosage (KXS-H) at 2.7 g/kg. The applied KXS dosage here was estimated according to the current clinical usage in human. A 4-week CMS exposure significantly reduced the percentage of sucrose consumption by ∼21% in the animals as compared to the nonstressed control. The long-term treatment of KXS-H increased the sucrose consumption in CMS-treated rats (∼20%), as compared to the CMS-treated control, that is, an improved behavior. The treatment of imipramine increased the percentage of sucrose consumption in CMS-treated rats (∼18%). The long-term treatment with KXS-L also showed an increase in tendency (∼15%), but without statistical significance. Both treatments almost restored the sucrose consumption back to the normal condition. The treatment of KXS, or imipramine, in normal rats however did not show any significant effect on the sucrose consumption (Figure 2(b)). Thus, KXS exerted a profound anti-depression effect in alleviating the depressive-like symptom on CMS-induced depressive rats.

3.2. KXS Restores the Decreased Level of Neurotransmitters in Brain of the Depressive Rats. The developed HPLC-MS/MS method was employed to determine the total levels of neurotransmitters in the brain of CMS-treated rats [9]. The effects of KXS and imipramine on the amount of

Table 1: Primer sequences, length of PCR products and optimal annealing temperature for each gene used in real-time quantitative PCR.

Primer	Sequence (5′-3′)	Source	bp	Ta (°C)
TH-S	CCA GTT CTC CCA GGA CAT TGG AC	NM_012740.3	312	59
TH-AS	GAG GCA TAG TTC CTG AGC TTG TCC			
DBH-S	GAA GAA TGC TGT GAC TGT CCA CCA G	NM_013158.2	387	59
DBH-AS	CAG AGG CTG CAG GTT CCA GTT AC			
AADC-S	GTT GTC ACC CTA GGA ACC ACA TCT TG	NM_012545.3	444	59
AADC-AS	CTC ATG AGA CAG CTT CAC GTG CTT TC			
MAO_A-S	GCC AAA GTT CTG GGA TCT CAA GAA GC	NM_033653.1	204	59
MAO_A-AS	CAC CAG TGA TCT TGA GCA GAC CAG			
MAO_B-S	GAG AAG AAC TGG TGT GAG GAG CAG	NM_013198.1	342	59
MAO_B-AS	AGC TGT TGC TGA CAA GAT GGT GGT			
COMT-S	GGT GAC GCG AAA GGC CAA ATC ATG	NM_012531.2	351	59
COMT-AS	CAG GCC ACA TTT CTC CAG GAG AAG			
DAT-S	GGT TCT ACG GCG TCC AGC AAT TC	M80570.1	291	59
DAT-AS	CAT AGG CCA GTT TCT CCC GGA AG			
VMAT2-S	GGT GGA CTC CTC TAT GAT GCC TAT C	NM_013031.3	351	59
VMAT2-AS	CTC CTT AGC AGG TGG ACT TCG AAG			
NET-S	CAG GTT CAG CAA TGA CAT CCA GCA G	NM_031343.1	282	59
NET-AS	GTG ATT CCG TAG GCC ACT CTC TC			
DrD2-S	AAC TGT ACC CAC CCT GAG GAC ATG	NM_012547.1	236	59
DrD2-AS	CTG TCA GGG TTG CTA TGT AGG CC			
Adra1A-S	TGG TGG GTT GCT TCG TCC TCT G	NM_017191.2	211	59
Adra1A-AS	CGA AGA CAC TGG ATT CGC AGG AC			
TPH-S	CAC CCA GGA TTC AAG GAC AAC GTC	NM_173839.2	421	59
TPH-AS	CAC TGT GAA GCC AGA TCG CTC TTT C			
SERT-S	ATG GTT CGT GCT CAT CGT GGT CAT C	NM_013034.3	268	59
SERT-AS	GAT GAA CAG GAG AAA CAG AGG GCT G			
Htr1A-S	CAT CAG CAA GGA CCA CGG CTA C	NM_012585.1	353	59
Htr1A-AS	GGA AGG TGC TCT TTG GAG TTG CC			
NGF-S	CAC TCT GAG GTG CAT AGC GTA ATG TC	XP_001067130.2	374	59
NGF-AS	CTG TGA GTC CTG TTG AAG GAG ATT GTA C			
BDNF-S	GAG CTG AGC GTG TGT GAC AGT ATT AG	BC087634	229	59
BDNF-AS	ATT GGG TAGT TCG GCA TTG CGA GTT C			
GDNF-S	GCG CTG ACC AGT GAC TCC AAT ATG	AF497634	318	59
GDNF-AS	CGC TTC ACA GGA ACC GCT ACA ATAT C			
NT3-S	ACA AGC TCT CCA AGC AGA TGG TAG ATG	M61179.1	310	59
NT3-AS	TCT CCT CGG TGA CTC TTA TGC TCT G			
NT4-S	TCA GTA CTT CTT CGA GAC GCG CTG	NM_013184.3	135	59
NT4-AS	GGC ACA TAG GAC TGT TTA GCC TTG CAT			
NT5-S	ATG CAG TGA GTG GCT GGG TGA C	S69323.1	229	59
NT5-AS	GTT TAG CCT TGC ATT CTG AGA GCC AG			
TrkA-S	ACC TCA ACC GTT TCC TCC GGT C	M85214.	330	57
TrkA-AS	CTC GAT CGC CTC AGT GTT GGA GA			
TrkB-S	CGG GAG CAT CTC TCG GTC TAT G	M55291.1	221	57
TrkB-AS	CAA ATG TGT CCG GCT TGA GCT GG			
TrkC-S	CAC TGT CTA CTA CCC TCC ACG TG	L03813.1	253	57
TrkC-AS	CTC TCT GGA AAG GGC TCC TTA AGG			
GAPDH-S	AAC GGA TTT GGC CGT ATT GG	Lee et al., 2009 [10]	516	57
GAPDH-AS	CTT CCC GTT CAG CTC TGG G			

Abbreviations: S: sense primer; AS: antisense primer; TH: tyrosine hydroxylase; DBH: dopamine β-hydroxylase; AADC: aromatic acid decarboxylase; MAO_A: monoamine oxidase A; MAO_B: monoamine oxidase B; COMT: catechol-O-methyltransferase; DAT: dopamine transporter; VMAT2: vesicular monoamine transporter 2; NET: norepinepherine transporter; DrD2: dopamine receptor D2; Adra1A: adrenergic receptor α1A; Htr 1A: serotonin receptor 1A; TPH: tryptophan hydroxylase; SERT: serotonin transporter; Htr1a: serotonin receptor 1A; NGF: nerve growth factor; BDNF: brain derived neurotrophic factor; GDNF: glial-cell-line-derived neurotrophic factor; NT3: neurotrophin 3; NT4: neurotrophin 4; NT5: neurotrophin 5; Trk A: tyrosine kinase receptor A; Trk B: tyrosine kinase receptor B; Trk C: tyrosine kinase receptor C; GAPDH: glyceraldehyde-3-phosphate dehydrogenase.

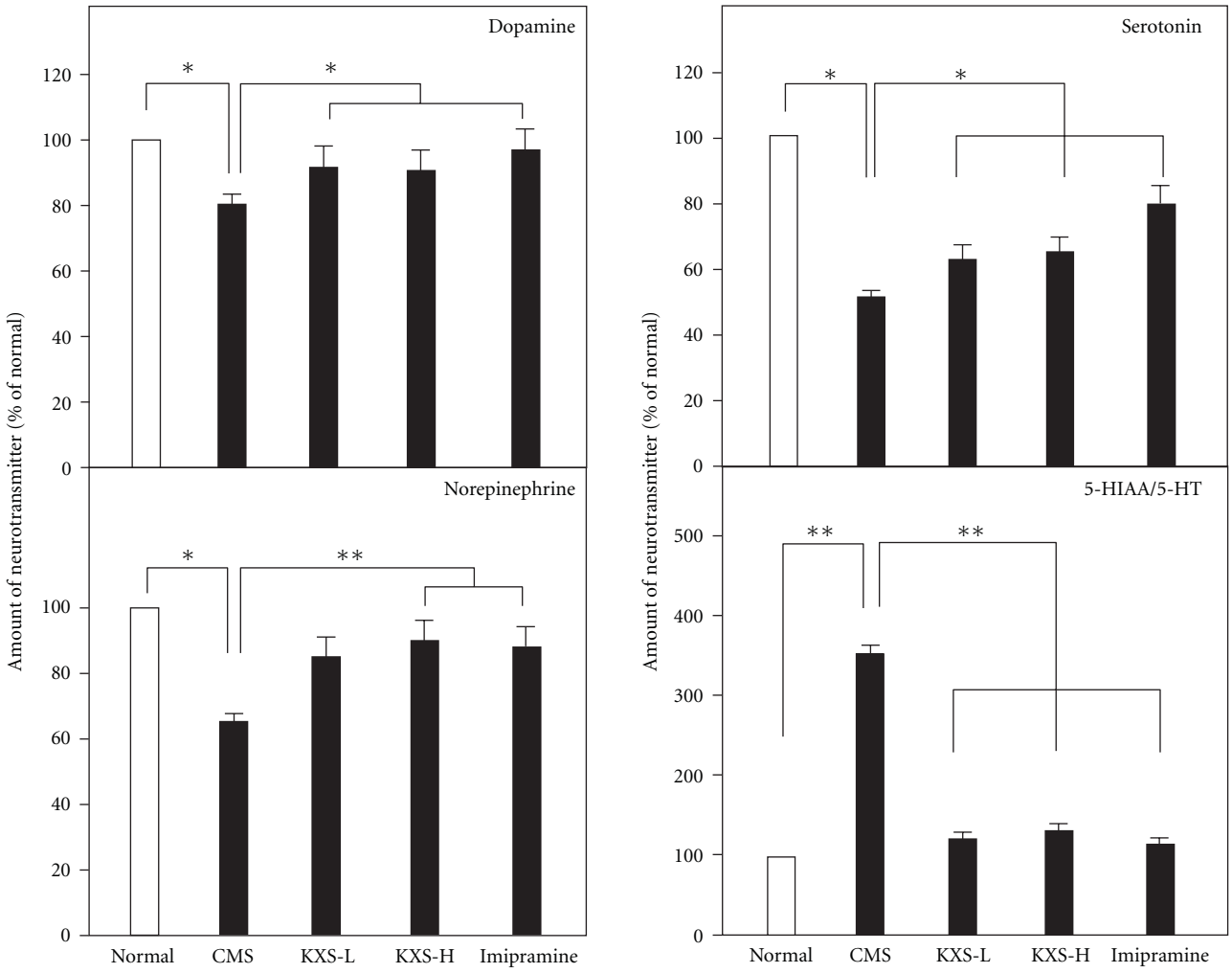

FIGURE 3: KXS restores the decreased level of neurotransmitters in depressive rats. The treatment of KXS in the rats was as that in Figure 2. The total brain was collected after the treatment. The amounts of dopamine, norepinepherine, serotonin, and 5-HIAA in rat brains were analyzed by LC-MS. Two doses of KXS were applied including low dosage at 0.9 g/kg (KXS-L) and high dosage at 2.7 g/kg (KXS-H). The imipramine at dose of 20 mg/kg was set as the positive control. Values are showed as the mean ± SEM ($n = 8$). $^{*}P < 0.05$ $^{**}P < 0.01$.

neurotransmitters in the brains were summarized in Figure 3. In the CMS-treated rat brains, the reductions of norepinepherine, dopamine, and serotonin were significantly revealed: the decrease was from 20 to 50%. Imipramine treatment was able to fully reverse the effects of CMS on the amounts of norepinepherine, dopamine, and serotonin in the brain. The treatment with KXS, both low and high doses, was effective in reversing the effect of CMS on norepinepherine and dopamine; that is, the levels returned to normal control (Figure 3).

Here, the amounts of serotonin and 5-hydroxyindoleacetic acid (5-HIAA), a metabolite of serotonin, were analyzed in the KXS-treated rat brains. The ratio of 5-HIAA to serotonin could be used as an index for the turnover of serotonin [12, 13]. The amount of serotonin was markedly reduced in the CMS-treated rat brains (Figure 3). In parallel, the amount of 5-HIAA was markedly increased, that is, an increase of serotonin breakdown. This CMS-induced phenomenon could be significantly reversed by the treatment of KXS, as well as the control treatment of imipramine (Figure 3). The reduced 5-HIAA/5-HT ratio suggested that the turnover of serotonin was decreased by the treatment of KXS.

3.3. KXS Regulates the mRNA Expression of Proteins Relating to the Regulation of Neurotransmitters. The mRNA levels of proteins relating to the regulation of dopamine and norepinephrine (see Table 1) were determined by quantitative PCR: these proteins included tyrosine hydroxylase, dopamine β-hydroxylase, monoamine oxidase B, catechol-O-methyltransferase, dopamine transporter, norepinepherine transporter, dopamine receptor 2, and norepinepherine receptor. The mRNAs encoding enzymes accounting for the metabolism of dopamine and norepinepherine were significantly altered, except tyrosine hydroxylase and monoamine oxidase B, in the CMS-treated rat brains (Figure 4). As compared to CMS control, the KXS treatment could significantly increase the mRNA levels of tyrosine hydroxylase at ~3-fold under KXS-H, dopamine β-hydroxylase at ~2-fold under both KXS-L and KXS-H, and monoamine oxidase B from

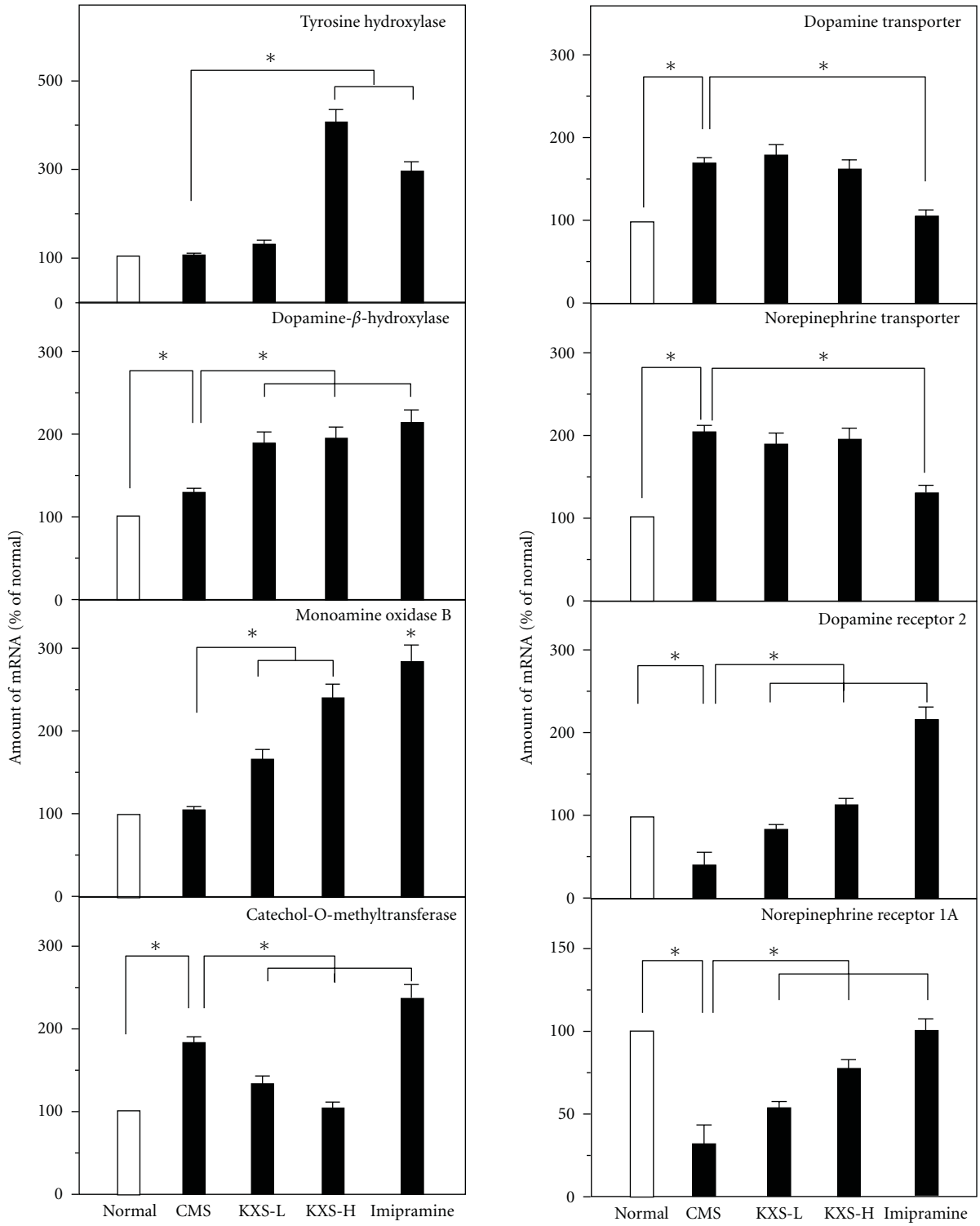

FIGURE 4: KXS regulates the mRNA expression of proteins relating to catecholamine metabolism in depressive rats. The treatment of KXS in the rats was as that in Figure 2. The total RNA was isolated from the rat brains. The mRNA expression was analyzed by real-time quantitative PCR. Two doses of KXS were applied including low dosage at 0.9 g/kg (KXS-L) and high dosage at 2.7 g/kg (KXS-H). The imipramine at dose of 20 mg/kg was set as the positive control. Values are showed as the mean ± SEM ($n = 8$). $^*P < 0.05$.

1.8-fold to 2.5-fold under KXS-L and KXS-H, respectively (Figure 4). In contrast, the level of mRNA encoding catechol-O-methyltransferase was markedly reduced in the KXS-treated depressive rats. Increase of synthesizing enzymes and decrease of degrading enzymes could account for the restoration of dopamine and norepinepherine back to the normal concentration. For the transporters of dopamine and norepinepherine, the mRNA levels of dopamine transporter and norepinepherine transporter were significantly increased in the CMS-treated rat brains (Figure 4). This tendency could be reversed by the imipramine treatment, while the KXS treatment had no effect. For dopamine receptor D2 and norepinepherine receptor 1A (adrenergic receptor α1A), CMS could significantly downregulate the mRNA level of the receptors in rat brains (Figure 4). Here, both KXS and imipramine treatments could restore the decreased levels back to the normal condition.

The mRNA levels of regulating proteins relating to serotonin metabolism (see Table 1) were also determined. The mRNAs encoding tryptophan hydroxylase, aromatic acid decarboxylase and monoamine oxidase A were determined. These mRNAs were significantly reduced under the CMS treatment (Figure 5). The KXS treatment in both dosages restored the mRNA levels of tryptophan hydroxylase, aromatic acid decarboxylase, and monoamine oxidase A. Imipramine could only restored the levels of mRNAs encoding aromatic acid decarboxylase, and monoamine oxidase A (Figure 5). The mRNA expressions of transporter and receptor for serotonin were also determined under the herbal treatment. The CMS-suppressed mRNA levels of these proteins were restore by the treatment of KXS significantly, except serotonin receptor 1A (Figure 5).

3.4. Effect of KXS on mRNA Expression Levels of Proteins Related to the Regulation of Neurotrophic Factors. The deficiency of neurotrophic factors in the brain was one of the theories in accounting for depression. Here, the expression levels of mRNA encoding NGF, BDNF, GDNF, NT3, NT4, and NT5 and their related receptors were explored. In the CMS-treated rat brains, the mRNA expressions of neurotropic factors were significantly reduced in all cases (Figure 6). The treatment of KXS in CMS-treated rats could increase the expressions of NGF, BDNF, GDNF, NT3, and NT5 mRNAs but not the mRNA of NT4. In contrast, the treatment of imipramine did not show any effect on the CMS-reduced mRNA expression of those neurotropic factors, except GDNF (Figure 6). In addition, the mRNA expressions of Trk A, Trk B, and Trk C receptors were determined: these expressions showed a reduction in the CMS-treated rat brains (Figure 7). In parallel, the levels of Trk A, Trk B and Trk C receptors in the CMS-treated rat brains were restored under the treatment of KXS. Imipramine treatment could only restore the CMS-suppressed Trk A and Trk B receptors (Figure 7).

4. Discussions

KXS, an ancient Chinese herbal decoction, has been used in Chinese medicinal herbal mixture in treating anti-depression; however, the action mechanism of which in brain functions has not been revealed. Here, we provided different lines of evidence to support the anti-depression role of KXS in CMS rat model system. The intake of KXS in the CMS-treated rats could result in the following: (i) the sucrose consumption was increased; (ii) the amounts of dopamine, norepinephrine, and serotonin, as well as its metabolic proteins including the transporters and receptors, were regulated; (iii) the amounts of NGF, BDNF, GDNF, NT3, NT4, and NT5, as well as their receptors including Trk A and Trk B, were increased. Under this scenario, the regulation of neurotransmitters and neurotropic factors could lead to a result of the improved behavior of those CMS-treated rats. However, the molecular targets of KXS in the brains have not been revealed, in particular this herbal mixture is containing numerical amount of chemicals [7].

The four individual herbs of KXS are known to affect our nervous system and frequently applied in the treatment, or the prevention, of anti-depression, no matter in a form of single herb or in an herbal mixed formula [14]. In KXS, the four herbs could be separated into two herb pairs. The pair of Ginseng Radix et Rhizoma and Polygalae Radix is to invigorate the Xin-qi, while that of Acori Tatarinowii Rhizoma and Poria is to eliminate the dampness. The pharmacological effects of active chemicals deriving from these four herbs on anti-depression have been reported. The total saponins derived from Ginseng Radix et Rhizoma, especially ginsenosides, are the main chemicals with strong neurotrophic and neuroprotective effects [15]. Indeed, the saponins of Ginseng Radix et Rhizoma were shown to reverse the reduction in sucrose preference index in CMS-treated rats through enhancing the amount of monoamine neurotransmitter [16] and the expression of BDNF mRNA in hippocampus and frontal cortex of the brain [17]. In CMS-treated rats, the oligosaccharide ester of Polygalae Radix increased sucrose consumption, reduced the levels of cortistatin, adrenocorticotropic hormone, and corticotropin-releasing factor in serum, and also enhanced the expression of glucocorticoid receptor mRNA [18, 19]. The water extract of Acori Tatarinowii Rhizoma could significantly shortened the motionless time of forced swimming and the despair time of tail suspension in mouse animal models of depression [20]. Compared to other herbs, the studies of neuronal function of Poria are very limited, in spite of its widely application in treating mental disorder by herbalists. In line to its clinical usages, the water extract of Poria protected cultured PC12 cells through suppressing the oxidative stress and the apoptosis induced by Aβ [21]. The triterpenoids from Poria could regulate the expressed 5-HT3A receptors in *Xenopus* oocytes [10]. Although each herb showed the potent effect in anti-depression, a herbal mixed formula of four herbs was frequently applied clinically instead of a single form, according to the usages of Chinese medicine.

The first catecholamine theory of depression was proposed in 1965 [22]. Thus, the aim of the drug development was to restore the decreased levels of neurotransmitters in the synaptic cleft or in the depressive brain. Dopamine, norepinepherine, and serotonin were regarded as the crucial neurotransmitters in the etiology of depression. Indeed, many

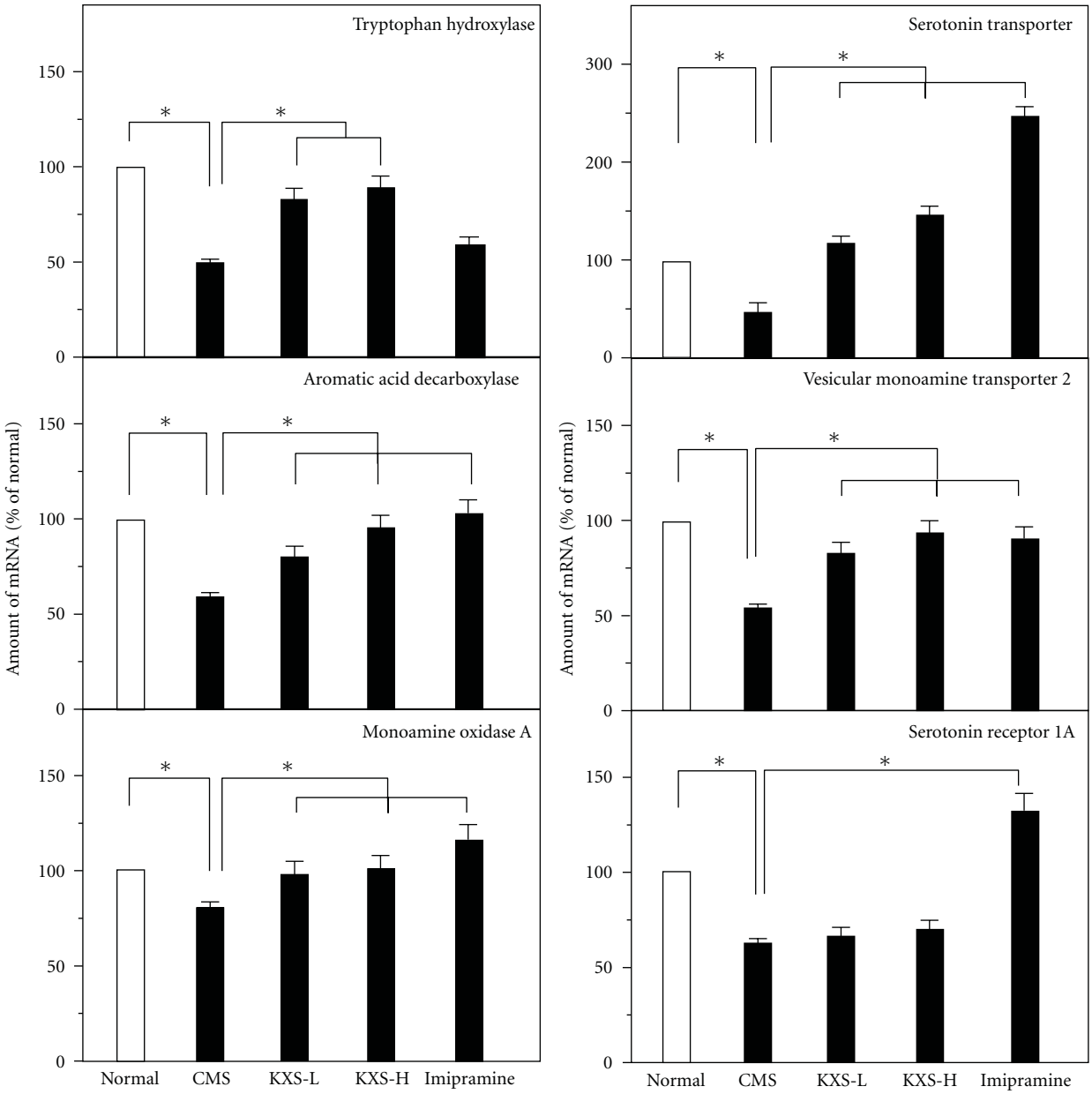

Figure 5: KXS regulates the mRNA expression of proteins relating to serotonin in depressive rats. The treatment of KXS in the rats was as that in Figure 2. The total RNA was isolated from the rat brains. The mRNA expression was analyzed by real-time quantitative PCR. Two doses of KXS were applied including low dosage at 0.9 g/kg (KXS-L) and high dosage at 2.7 g/kg (KXS-H). The imipramine at dose of 20 mg/kg was set as the positive control. Values are showed as the mean ± SEM ($n = 8$). $^*P < 0.05$.

drugs targeting to the neurotransmitter metabolism have been developed, for example, reserpine, tetrabenazine, iproniazid, and imipramine [4]. In the present studies, KXS treatment tended to restore the levels of dopamine, norepinepherine and serotonin in the CMS-treated rat brains: the restored levels were similar to that in the nonstressed group. Compared to the positive control imipramine, one of the first-generation tricyclic anti-depression drug and norepinepherine and serotonin reuptake inhibitors, KXS showed similar effects, which implied that it might exert anti-depression actions by modulating dopaminergic, noradrenalinergic, and serotoninergic neuronal systems.

In order to explore the mechanism of neurotransmitter regulation, the mRNA expression levels of related proteins were evaluated. For dopamine and norepinepherine, they share the same biosynthesis pathway at the start point, while that of serotonin has a distinct pathway (Figure 8). In the treatment of KXS in those CMS-treated rats, the enzymes responding for synthesis of dopamine/norepinephrine, and serotonin were increased, for example, tyrosine hydroxylase, dopamine β-hydroxylase, and aromatic acid decarboxylase. Under the CMS treatment, the brain receptors for dopamine and norepinepherine, and the transporter of serotonin were increased. Based on the results, KXS might regulate the

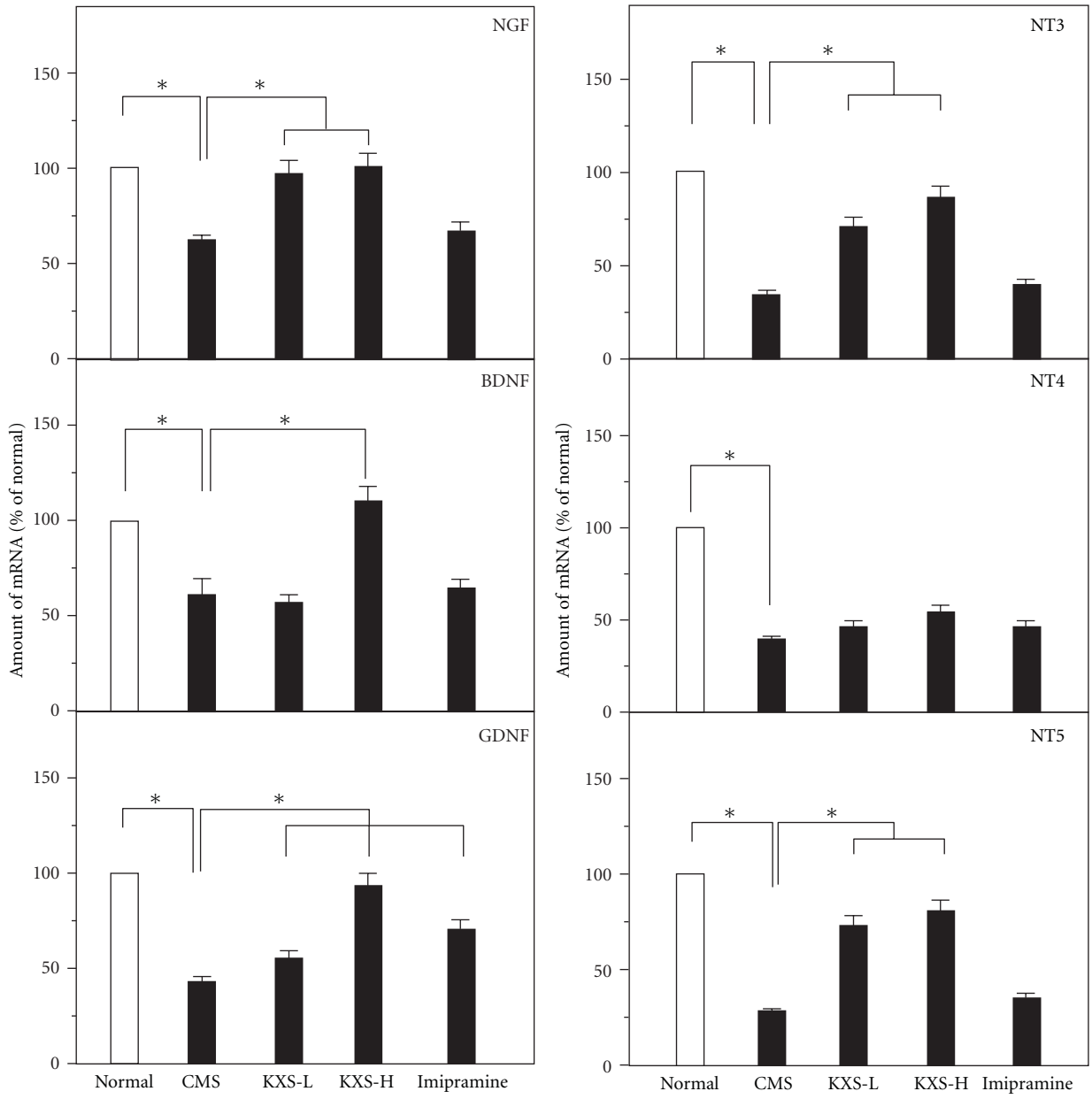

Figure 6: KXS increases the mRNA expression of neurotrophic factors in depressive rats. The treatment of KXS in the rats was as that in Figure 2. The total RNA was isolated from the rat brains. The mRNA expression was analyzed by real-time quantitative PCR. Two doses of KXS were applied including low dosage at 0.9 g/kg (KXS-L) and high dosage at 2.7 g/kg (KXS-H). The imipramine at dose of 20 mg/kg was set as the positive control. Values are showed as the mean ± SEM ($n = 8$). $^*P < 0.05$.

neurotransmitter systems by acting on synthesis, storage, and upregulating the receptors in order to compensate for the deficient availability of neurotransmitters caused by the depressive state. Although imipramine could upregulate the levels of neurotransmitters, the regulations on those aforementioned proteins are very different to that of KXS treatment.

The theory of neurotrophic factors in the etiology of depression has attracted much attention. The theory holds that the normal physiology of neuron is supported and maintained with the help of a series of neurotrophic factors, including NGF, BDNF, GDNF, NT-3, NT-4, and NT-5. If the deficiency of neurotrophic factors occurred, the neuron cannot survive and/or grow healthy, which will subsequently lead to neurodegenerative disorders, for example, depression. Postmortem analyses of brain tissues from patients with major depression showed a reduction in brain BDNF [23] and in serum BDNF [24, 25], whereas brain infusion of BDNF produced anti-depressant-like action in animals [26]. In addition, NGF was also found to have novel anti-depressant-like action in rats, but did not appear to have biochemical actions similar to that of other anti-depressants [27]. In the present study, the CMS-treated rat showed a decrease in the expression of neurotrophic factors and its

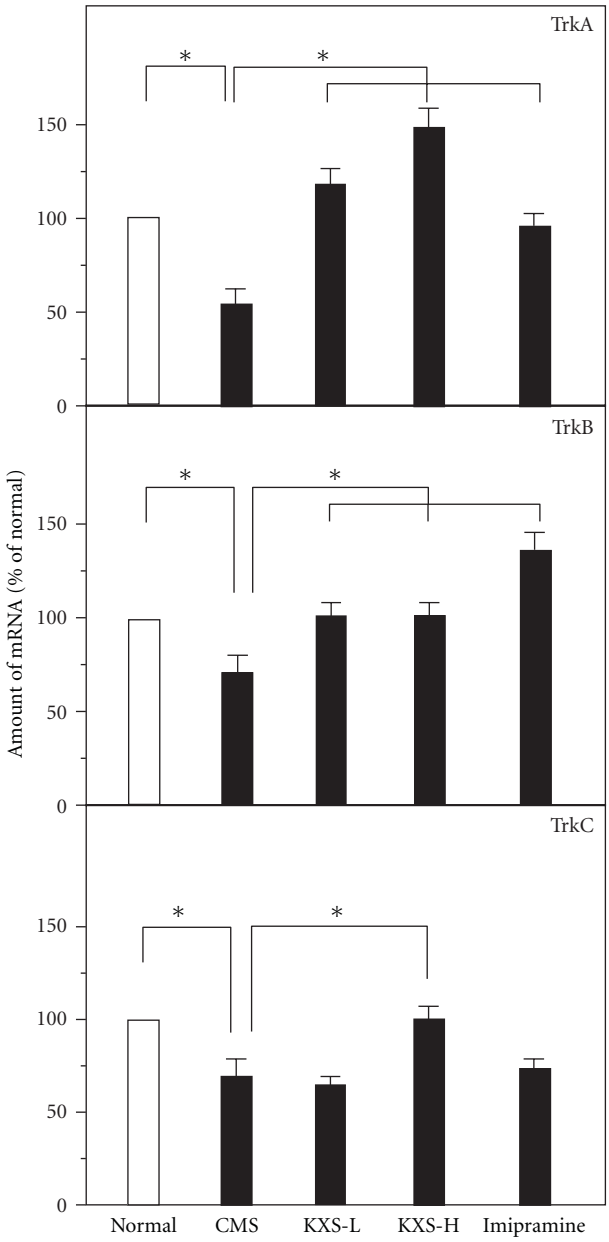

Figure 7: KXS increases the mRNA expression of neurotrophic receptors in depressive rats. The treatment of KXS in the rats was as that in Figure 2. The total RNA was isolated from the rat brains. The mRNA expression was analyzed by real-time quantitative PCR. Two doses of KXS were applied including low dosage at 0.9 g/kg (KXS-L) and high dosage at 2.7 g/kg (KXS-H). The imipramine at dose of 20 mg/kg was set as the positive control. Values are showed as the mean ± SEM ($n = 8$). $^*P < 0.05$.

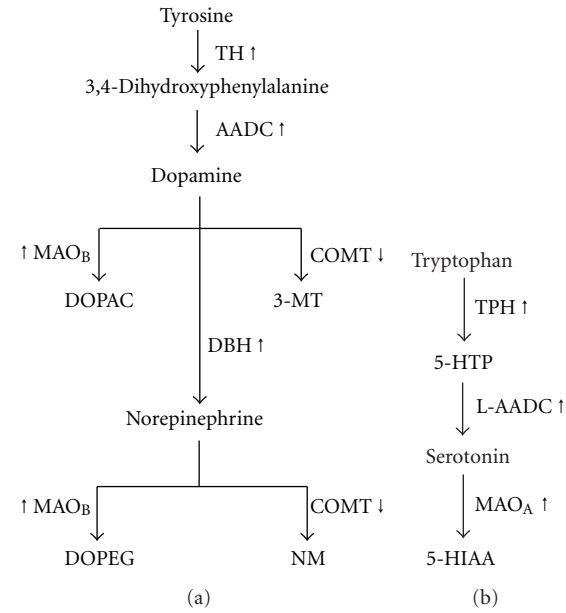

Figure 8: Synthesis and degradation of dopamine, norepinephrine, and serotonin. The detailed pathway of the synthesis and degradation of dopamine, norepinepherine (a) and serotonin (b) were shown. The arrows indicate the up- and downregulation of the corresponding mRNA level by the treatment of KXS. TH: tyrosine hydroxylase; AADC: aromatic acid decarboxylase; MAO$_B$: monoamine oxidase B; COMT: catechol-O-methyl-transferase; DOPAC: dihydroxyphenylacetic acid; 3-MT: 3-methoxytyramine; DBH: dopamine β-hydroxylase; DOPEG: dihydroxyphenylglycol; NM: normetanephrine; TPH: tryptophan hydroxylase; 5-HTP: 5-hydroxytryptophan; MAO$_A$: monoamine oxidase A; 5-HIAA: 5-hydroxyindole-3-acetic acid.

corresponding receptors. However, KXS could increase the expression levels of neurotrophic factors and its receptors in restoring abnormal growth state of neuron under depression. Indeed, our preliminary results suggested that the application of KXS onto cultured astrocytes could induce the expression of neurotrophic factors (Zhu et al., unpublished results). For imipramine in CMS-treated rats, only the expression of GDNF level was elevated, which was also consistent with a previous report [28].

Based on our current study, KXS might have multitargets in the brain for anti-depression. These findings are in line with previous studies. KXS treatment in rats has been shown to enhance the learning and memory abilities [29]. In parallel, KXS, in different ratio of the four herbs, was found to exert profound effects in anti-depression [16]. Thus, KXS could be a valuable herbal formula for the treatment of anti-depression, either as a form of health food supplement or a prescribed drug. More importantly, the toxicity of long-term intake of KXS has been very minimal, which has made it be used over a thousand of years in human [30].

5. Conclusions

The treatment of KXS could alleviate the depression-like symptoms in CMS-induced rats. The anti-depressive action of KXS might be accounted by modulating the neurotransmitters system and increasing the expression of neurotrophic factors in the brain. This herbal extract is being chemically standardized and therefore could serve as alternative medicine or health food supplement for patients suffering from depression. Since KXS is a mixture of compounds,

the identification of active ingredients here will be further evaluated.

Acknowledgments

This research was supported by grants from the University Grants Committee (AoE/B-15/01), the Research Grants Council of Hong Kong (HKUST 6419/06 M, 662608, 662911, N_HKUST629/07), and The Croucher Foundation (CAS-CF07/08.SC03) awarded to K. Tsim.

References

[1] G. Parker, "Beyond major depression," *Psychological Medicine*, vol. 35, no. 4, pp. 467–474, 2005.

[2] C. Lanni, S. Govoni, A. Lucchelli, and C. Boselli, "Depression and antidepressants: molecular and cellular aspects," *Cellular and Molecular Life Sciences*, vol. 66, no. 18, pp. 2985–3008, 2009.

[3] M. D. Binder, N. Hirokawa, and U. Windhorst, *Encyclopedia of Neuroscience*, Springer, Berlin, Germany, 2009.

[4] S. M. Stahl, *Stahl's Essential Psychopharmacology: Neuroscientific Basis and Practical Applications*, Cambridge University Press, Cambridge, UK.

[5] V. Krishnan and E. J. Nestler, "The molecular neurobiology of depression," *Nature*, vol. 455, no. 7215, pp. 894–902, 2008.

[6] S. M. Sun, *Beiji QIanjin Yaofang JIaoshi*, People Medicinal Publishing House, Beijing, China, 1998.

[7] K. Y. Zhu, Q. Fu, H. Q. Xie et al., "Quality assessment of a formulated Chinese herbal decoction, Kaixinsan, by using rapid resolution liquid chromatography coupled with mass spectrometry: a chemical evaluation of different historical formulae," *Journal of Separation Science*, vol. 33, no. 23-24, pp. 3666–3674, 2010.

[8] Q. Q. Mao, S. P. Ip, K. M. Ko, S. H. Tsai, and C. T. Che, "Peony glycosides produce antidepressant-like action in mice exposed to chronic unpredictable mild stress: effects on hypothalamic-pituitary-adrenal function and brain-derived neurotrophic factor," *Progress in Neuro-Psychopharmacology and Biological Psychiatry*, vol. 33, no. 7, pp. 1211–1216, 2009.

[9] K. Y. Zhu, Q. Fu, K. W. Leung, Z. C. F. Wong, R. C. Y. Choi, and K. W. K. Tsim, "The establishment of a sensitive method in determining different neurotransmitters simultaneously in rat brains by using liquid chromatography-electrospray tandem mass spectrometry," *Journal of Chromatography B*, vol. 879, no. 11-12, pp. 737–742, 2011.

[10] J. H. Lee, Y. J. Lee, J. K. Shin et al., "Effects of triterpenoids from *Poria cocos* Wolf on the serotonin type 3A receptor-mediated ion current in Xenopus oocytes," *European Journal of Pharmacology*, vol. 615, no. 1–3, pp. 27–32, 2009.

[11] J. Winer, C. K. S. Jung, I. Shackel, and P. M. Williams, "Development and validation of real-time quantitative reverse transcriptase-polymerase chain reaction for monitoring gene expression in cardiac myocytes in vitro," *Analytical Biochemistry*, vol. 270, no. 1, pp. 41–49, 1999.

[12] J. W. Commissiong, "Monoamine metabolites: their relationship and lack of relationship to monoaminergic neuronal activity," *Biochemical Pharmacology*, vol. 34, no. 8, pp. 1127–1131, 1985.

[13] R. K. W. Schwarting and J. P. Huston, "Behavioral concomitants of regional changes in the brain's biogenic amines after apomorphine and amphetamine," *Pharmacology Biochemistry and Behavior*, vol. 41, no. 4, pp. 675–682, 1992.

[14] T. H. H. Pang, F. C. F. Ip, and N. Y. Ip, "Recent development in the search for effective antidepressants using traditional Chinese medicine," *Central Nervous System Agents in Medicinal Chemistry*, vol. 8, no. 1, pp. 64–71, 2008.

[15] H. Dang, Y. Chen, X. Liu et al., "Antidepressant effects of ginseng total saponins in the forced swimming test and chronic mild stress models of depression," *Progress in Neuro-Psychopharmacology and Biological Psychiatry*, vol. 33, no. 8, pp. 1417–1424, 2009.

[16] H. Dang, L. Sun, X. Liu et al., "Preventive action of Kai Xin San aqueous extract on depressive-like symptoms and cognition deficit induced by chronic mild stress," *Experimental Biology and Medicine*, vol. 234, no. 7, pp. 785–793, 2009.

[17] L. Liu, Y. Luo, R. Zhang, and J. Guo, "Effects of ginsenosides on hypothalamic-pituitary-adrenal function and brain-derived neurotrophic factor in rats exposed to chronic unpredictable mild stress," *Zhongguo Zhongyao Zazhi*, vol. 36, no. 10, pp. 1342–1347, 2011.

[18] Y. Hu, H. B. Liao, G. Dai-Hong, P. Liu, Y. Y. Wang, and K. Rahman, "Antidepressant-like effects of 3,6′-disinapoyl sucrose on hippocampal neuronal plasticity and neurotrophic signal pathway in chronically mild stressed rats," *Neurochemistry International*, vol. 56, no. 3, pp. 461–465, 2010.

[19] P. Liu, D. X. Wang, D. H. Guo et al., "Antidepressant effect of 3′, 6-disinapoyl sucrose from *Polygala tenuifolia* willd in pharmacological depression model," *Chinese Pharmaceutical Journal*, vol. 43, no. 18, pp. 1391–1394, 2008.

[20] M. Li and H. Chen, "Antidepressant effect of water decoction of Rhizoma acori tatarinowii in the behavioural despair animal models of depression," *Journal of Chinese Medicinal Materials*, vol. 24, no. 1, pp. 40–41, 2001.

[21] Y. H. Park, I. H. Son, B. Kim, Y. S. Lyu, H. I. Moon, and H. W. Kang, "*Poria cocos* water extract (PCW) protects PC12 neuronal cells from beta-amyloid-induced cell death through antioxidant and antiapoptotic functions," *Pharmazie*, vol. 64, no. 11, pp. 760–764, 2009.

[22] J. J. Schildkraut, "The catecholamine hypothesis of affective disorders: a review of supporting evidence," *The American journal of psychiatry*, vol. 122, no. 5, pp. 509–522, 1965.

[23] E. Castrén, V. Võikar, and T. Rantamäki, "Role of neurotrophic factors in depression," *Current Opinion in Pharmacology*, vol. 7, no. 1, pp. 18–21, 2007.

[24] F. Karege, G. Perret, G. Bondolfi, M. Schwald, G. Bertschy, and J. M. Aubry, "Decreased serum brain-derived neurotrophic factor levels in major depressed patients," *Psychiatry Research*, vol. 109, no. 2, pp. 143–148, 2002.

[25] C. Aydemir, E. S. Yalcin, S. Aksaray et al., "Brain-derived neurotrophic factor (BDNF) changes in the serum of depressed women," *Progress in Neuro-Psychopharmacology and Biological Psychiatry*, vol. 30, no. 7, pp. 1256–1260, 2006.

[26] J. A. Siuciak, D. R. Lewis, S. J. Wiegand, and R. M. Lindsay, "Antidepressant-like effect of brain-derived neurotrophic factor (BDNF)," *Pharmacology Biochemistry and Behavior*, vol. 56, no. 1, pp. 131–137, 1996.

[27] D. H. Overstreet, K. Fredericks, D. Knapp, G. Breese, and J. McMichael, "Nerve growth factor (NGF) has novel antidepressant-like properties in rats," *Pharmacology Biochemistry and Behavior*, vol. 94, no. 4, pp. 553–560, 2010.

[28] Y. Kim, S. H. Kim, Y. S. Kim, Y. H. Lee, K. Ha, and S. Y. Shin, "Imipramine activates glial cell line-derived neurotrophic factor via early growth response gene 1 in astrocytes," *Progress in Neuro-Psychopharmacology and Biological Psychiatry*, vol. 35, no. 4, pp. 1026–1032, 2011.

[29] N. Nishiyama, Y. Zhou, and H. Saito, "Beneficial effects of DX-9386, a traditional Chinese prescription, on memory disorder produced by lesioning the amygdala in mice," *Biological and Pharmaceutical Bulletin*, vol. 17, no. 12, pp. 1679–1681, 1994.

[30] L. H. Mu, Z. X. Huang, P. Liu, Y. Hu, and Y. Gao, "Acute and subchronic oral toxicity assessment of the herbal formula Kai-Xin-San," *Journal of Ethnopharmacology*, vol. 138, no. 2, pp. 351–357, 2011.

Hindawi Publishing Corporation
Evidence-Based Complementary and Alternative Medicine
Volume 2012, Article ID 419257, 6 pages
doi:10.1155/2012/419257

Research Article

Involvement of the Cerebral Monoamine Neurotransmitters System in Antidepressant-Like Effects of a Chinese Herbal Decoction, Baihe Dihuang Tang, in Mice Model

Meng-Li Chen,[1] Jie Gao,[2] Xin-Rong He,[3] and Qian Chen[1]

[1] *Department of Clinical Pharmacology, General Hospital of Peoples Liberation Army, Beijing 100853, China*
[2] *Department of Pathology, General Hospital of Peoples Liberation Army, Beijing 100853, China*
[3] *Traditional Chinese Medicine Dispensary, General Hospital of Peoples Liberation Army, Beijing 100853, China*

Correspondence should be addressed to Qian Chen, chenqian@301hospital.com.cn

Received 26 April 2012; Accepted 8 June 2012

Academic Editor: Paul Siu-Po Ip

Baihe Dihuang Tang (BDT) is a renowned Chinese herbal formula which is commonly used for treating patients with mental instability, absentmindedness, insomnia, deficient dysphoria, and other psychological diseases. These major symptoms closely associated with the depressive disorders. BDT was widely popular use for treating emotion-thought disorders for many years in China. In the present study, the antidepressant-like effect of BDT in mice was investigated by using the forced swim test (FST) and the tail suspension test (TST). The underlying mechanism was explored by determining the effect of BDT on the level of cerebral monoamine neurotransmitters. BDT (9 and 18 g/kg, p.o. for 14 days) administration significantly reduced the immobility time in both the FST and the TST without changing locomotion in the open field-test (OFT). Moreover, BDT treatment at the dose of 18 g/kg inhibited reserpine-induced ptosis. Meanwhile, BDT enhanced 5-HT and NA levels in mouse cerebrum as well as decreased the ratio of 5-HT compared to its metabolite, 5-HIAA, (turnover, 5-HIAA/5-HT) after TST. The results demonstrated that the antidepressant-like effect of BDT is mediated, at least partially, via the central monoaminergic neurotransmitter system.

1. Introduction

Depression is a mental illness that significantly affect a person's thoughts, behavior, feelings, and physical well-being and has become a major global psychiatric problem. In whole globe, approximately 450 million people suffer from depression or behavioral disorder. According to prediction, depression will become the second common disease by the year 2020 [1]. The classical antidepressants include the tricyclic antidepressant (TCA), monoamine oxidase inhibitor (MAOI), selective serotonin reuptake inhibitor (SSRI), noradrenergic reuptake inhibitor (NARI), and serotonin and noradrenaline reuptake inhibitor (SNRI) [2, 3]. Although these drugs show excellent efficacy, most of them frequently produce undesirable adverse effects. So it is urgent to explore more promising antidepressants for clinical needs of depressed patients.

Traditional herbal formulae have been clinically used for thousands of years in China. Nowadays, the use of traditional herbal formulae has provided us a prospective alternative in the treatment of depression [4, 5]. Baihe Dihuang Tang (BDT) is a renowned Chinese herbal formula and firstly described in "synopsis of the Golden Chamber" (Jinkui Yaolue) written by Zhang Zhong Jing in the early 3th century. It is composed of two component herbs: lily bulb (Bulbus Lilii) and rehmannia root (Radix Rehmanniae). BDT is commonly used in folk for the therapeutic treatment of mental instability, absentmindedness, insomnia, deficient dysphoria, and other psychological diseases [6]. These major symptoms closely associated with the depressive disorders.

BDT is widely popular use for treating emotion-thought disorders for many years in China. Some clinical studies have demonstrated antidepressant-like effects of BDT[7, 8]. Recently, pharmacological studies also have authenticated that plants of the BDT and some of their chemical constituents, including saponins, iridoids, and polysaccharides, displaying nervous system activities. Prepared *Rehmannia*, steamed roots of *Rehmannia glutinosa*, have effects on depression-like disorders, and antioxidation may be one of the mechanisms underlying its antidepressant action [9]. Catalpol, an iridoid glycoside, contained richly in *Rehmannia*, is found to be neuroprotective effect antioxidative ability, reduces cognitive impairment significantly [10–12] and therapeutic potential against inflammation-related neurodegenerative diseases [13]. As the component herbal drug, lily bulb or saponins from lily bulb also have depressant-like effects involved in the serotonergic system [14, 15] and the hypothalamic-pituitary-adrenal (HPA) axis in animal [16].

In the present study, we aim to investigate the antidepressant-like effects of BDT by using the forced swim and tail suspension tests in mice. The underlying mechanism of antidepression is explored by measuring the levels of monoamine neurotransmitters in mouse cerebrum.

2. Materials and Methods

2.1. Chemicals and Reagents. Desipramine, norepinephrine (NE), dopamine (DA), serotonin (5-HT), 8-O-acetylharpagide, and 5-hydroxyindoleacetic acid (5-HIAA) were obtained from Sigma-Aldrich (St. Louis, MO, USA). Reserpine injection (1 mg/mL) was produced by Guangdong Bangmin Pharmaceutical Co., Ltd. Ginsenoside Re, quercetin, was supplied by the State Drug Analysis Institute (Beijing, China). All other reagents and solvents used in the study were of analytical grade.

2.2. Plant Materials and Preparation of BDT. Bulbus Lilii (BL) and Radix Rehmanniae (RR) were purchased from Tongrentang Chinese Pharmaceutical Co. Ltd. (Beijing, China). The two herbs were ground into a coarse powder, respectively. BDT was formulated by mixing the two herbal powders in relative proportions according to a ratio of 2 : 1 (BL : RR). The herbal powder mixture was boiled in 8 volumes of water (v/w) in reflux for 60 minutes. The extraction procedure was repeated twice for 45 minutes. The pooled extract was filtered to remove debris. The concentrated extract was then dried by lyophilization to obtain the extract at a yield of 32.84% (w/w). The extract was stored in the desiccator at 4°C until use. Contents of total saponins [17], total flavonoids [18], total iridoids [19], and total polysaccharides [20] in BDT extract were measured by modified methods, using ginsenoside Re, quercetin, 8-acetylharpagide, and dextran as standards, respectively. The results indicated that BDT contained saponins, flavonoids, total iridoids, and total polysaccharides at concentrations of 0.91%, 0.52%, 0.66%, and 4.36% (w/w), respectively.

2.3. Animal and Treatment. Male ICR mice weighting 20–25 g were obtained from the Laboratory Animal Centre, General Hospital of PLA, Beijing, China. The animals were maintained on a 12 h light/dark cycle under regulated temperature (22 ± 2°C) and humidity (50 ± 10%) and fed with standard diet and water ad libitum. They were allowed to acclimate three days before use. The experimental protocols for the present study have been approved by the Ethics Committee of the PLA General Hospital and were conducted in accordance with the Guide for the Care and Use of Laboratory Animals (China Ministry of Health). All experiments were performed between 09:30–14:00, and each animal was used only once.

The animals were randomly assigned into groups of 50 individuals. Distilled water was given to animals in group 1 (Vehicle group). Animals in group 2 were administered with positive compounds (Desipramine 20 mg/kg). Animals in groups 3, 4, and 5 received intragastric doses of BDT extract powder at 4.5 g, 9 g and 18 g/kg, respectively. The drugs were given daily between 9:30 and 10:30 AM for 14 days. The test was conducted 2 h after the last treatment. The mice, after performing TST behavioral tests, were sacrificed for the determination of monoamine neurotransmitters.

2.4. Forced Swim Test (FST). The forced swim test was performed according to the method described by Porsolt et al. [21] with modifications. Briefly, mice were forced to swim in a transparent glass vessel (25 cm in high 14 cm in diameter) filled with 10 cm of water at 24 ± 2°C. The total duration of immobility (seconds) was measured as described previously [22] during the last 4 minutes of a single 6-minute test session. Mice were considered immobile when they ceased struggling and remained floating motionless in the water except the movements necessary to keep their heads above the water.

2.5. Tail Suspension Test (TST). Tail suspension test was carried out according to the method of Steru et al. [23]. Briefly, mice were suspended 5 cm above the floor by means of an adhesive tape placed approximately 1 cm from the tip of the tail. The total duration of immobility (s) was quantified during a test period of 6 minutes. Mice were considered immobile only when they hung passively.

2.6. Open-Field Test (OFT). The ambulatory behaviour was assessed in an open-field test as described previously [24, 25]. The open-field apparatus consisted of a square wooden arena (40 cm × 60 cm × 50 cm) with black surface covering the inside walls. The floor of the wooden arena was divided equally into 12 equal squares marked by black lines. Each mouse was placed individually into the center of the arena and allowed to explore freely. The number of squares crossed by the mouse and the number of rearings on the hind paws were recorded during a test period of 5 minutes. The arena floor was cleaned between the trials with a detergent, and the test was carried out in a temperature-, noise-, and light-controlled room.

2.7. Reversal of Reserpine-Induced Ptosis in Mice. The reserpine test was performed according to the method

described by Bourin et al. [26] with modifications. Reserpine (2.5 mg/kg) was given intraperitoneally to the animals, and ptosis was evaluated 120 minutes after reserpine treatment. Animals were placed on a shelf (20 cm above the tabletop) and the score of eyes ptosis was calculated as described previously [27], eyes open = 0; one-quarter closed = 1; half closed = 2; three-quarters closed = 3; completely closed = 4.

2.8. Measurement of Monoamine Neurotransmitter Levels. To explore the detailed neurochemical mechanisms involved in the antidepressant-like effect of BDT, mice receiving BDT for 14 days were used for the determinations of NE, DA, 5-HT, and 5-HIAA (The metabolite of 5-HT) levels in the brain after TST. Mice were sacrificed by decapitation. Whole brains were rapidly removed from mice, weighted and frozen in liquid nitrogen immediately. The tissue samples were stored at −80°C until assay. Samples were homogenized in 10 volumes of tissue lysis buffer (0.6 mmol/L Perchloric acid, 0.5 mmol/L Na2EDTA and 0.1 g/L L-Cysteine) centrifuged at 15,000 g for 15 minutes. The supernatant was mixed with equal volume of buffer (1.2 mol/L K2HPO4, 2.0 mmol/L Na2EDTA) and centrifuged at 15,000 g for 15 minutes. The resulting supernatant was used for assay. The contents of 5-HT, NA, DA, and 5-HIAA were measured as described previously using high-performance liquid chromatography (HPLC) with fluorescence detection with minor modifications [28]. The supernatant was analyzed by HPLC using an Alltech Alltima C18 column (particle size 5 mm, 4.6 mm × 250 mm). HPLC separation was achieved by an isocratic elution (1 mL/min) with a mobile phase consisting of 87% buffer solution (50 mmol/L citric acid, 50 mmol/L sodium acetate, 0.5 mmol 1-sodium heptanesulfonate, 5 mmol/L triethylamine, and 0.5 mmol/L Na2EDTA, PH = 3.8) and 13% methanol (v/v). The eluate was monitored by fluorescence detector set at emission wavelength 280 nm and excitation wavelength 315 nm. Calibration curve and limit of quantitation were listed (Table 2, Supplementary Material available online at doi:10.1155/2012/419257). The concentration of 5-HT, NE, DA, and 5-HIAA was estimated using a calibration curve of standard solution. The monoamine neurotransmitter levels was expressed as μg/g wet weight of tissue.

2.9. Statistical Analysis. The results were expressed as mean ± SEM. Multiple group comparisons were performed using one-way analysis of variance (ANOVA) followed by Dunnett's test in order to detect intergroup differences. A significant difference was determined when $P < 0.05$.

3. Results

The FST and TST are the most widely used as behavioural tools for assessing antidepressant activity [29, 30]. The results of BDT on the immobility duration in FST are demonstrated in Figure 1. Compared with the vehicle group, only BDT administration for 14 successive days at dose 18 g/kg decreased the immobility time by 33.8% ($P < 0.05$). The same treatment regimen with BDT at doses of 9 and 18 g/kg also significantly decreased the immobility time in TST. The duration of immobility was reduced respectively by 37.3% and 42.2% when compared with the vehicle (Figure 2). Under the same experimental conditions, the similar effects were observed in mice treated with desipramine at a dose of 20 mg/kg, which served as a positive control of the experiment. The reduction in the duration of immobility for mice given with desipramine was 55.9% and 46.1% in FST and TST, respectively (Figures 1 and 2).

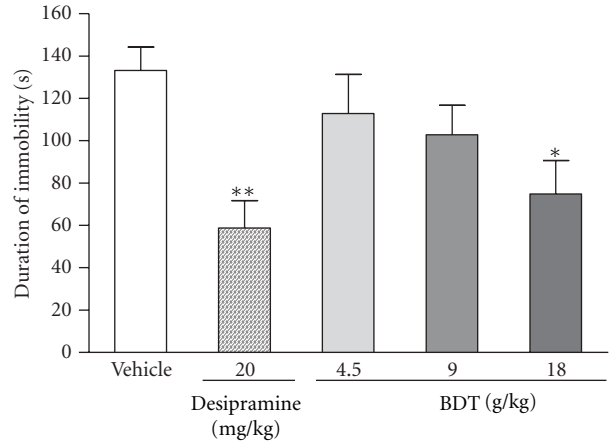

Figure 1: The effect of Baihe Dihuang Tang (BDT, 4.5, 9, 18 g/kg, p.o.) or desipramine (20 mg/kg, p.o.) on the immobility duration of in the forced swimming test. Values given are the mean ± SEM ($n = 10$). $^*P < 0.05$ and $^{**}P < 0.01$ as compared with vehicle group.

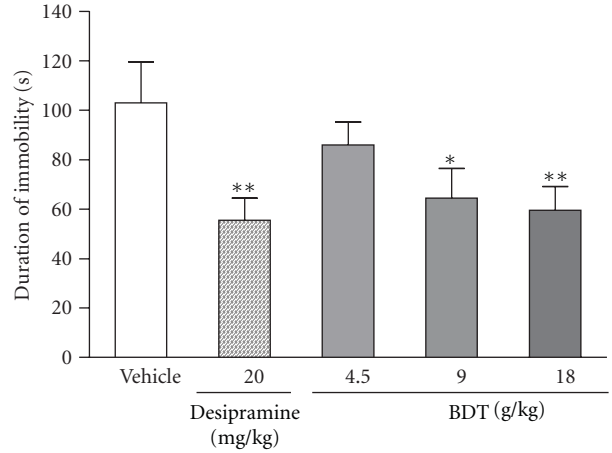

Figure 2: The effect of Baihe Dihuang Tang (BDT, 4.5, 9, 18 g/kg, p.o.) or desipramine (20 mg/kg, p.o.) on the immobility duration of mice in tail suspension test. Values given are the mean ± SEM ($n = 10$). $^*P < 0.05$ and $^{**}P < 0.01$ as compared with vehicle group.

As shown in Figure 3, BDT or desipramine administered for 14 successive days did not significantly affect the number of crossings and rearings in the open-field test (OFT) when compared with the vehicle group. It was an indication that the locomotor activity in mice OFT was not affected by the treatment of BDT or desipramine.

As shown in Figure 4, treating with BDT only at daily doses of 18 g/kg for 14 days significantly antagonized

Table 1: The effect of BDT on the monoamine neurotransmitter levels and 5-HIAA/5-HT turnover ratio in brain after mouse TST.

Group	Dose	Ratio of brain/body (%)	Monoamine neurotransmitter level (μg/g wet tissue)				5-HIAA/5-HT
			NA	DA	5-HT	5-HIAA	
Normal	—	1.16 ± 0.024	1.08 ± 0.04	1.21 ± 0.05	1.49 ± 0.04	0.48 ± 0.05	0.32 ± 0.03
Vehicle	—	1.19 ± 0.031	0.77 ± 0.07$^{\#\#}$	0.97 ± 0.09	1.07 ± 0.15$^{\#\#}$	0.35 ± 0.07	0.32 ± 0.02
Desipramine (mg/kg)	20	1.25 ± 0.056	1.15 ± 0.03**	1.01 ± 0.03	1.87 ± 0.05**	0.55 ± 0.03	0.29 ± 0.01
BDT (g/kg)	4.5	1.18 ± 0.025	0.78 ± 0.08	1.04 ± 0.02	1.23 ± 0.13	0.39 ± 0.09	0.31 ± 0.05
	9.0	1.26 ± 0.071	0.79 ± 0.07	1.01 ± 0.05	1.48 ± 0.11*	0.42 ± 0.05	0.28 ± 0.06
	18.0	1.21 ± 0.053	0.91 ± 0.06*	1.02 ± 0.07	1.74 ± 0.06**	0.51 ± 0.04*	0.25 ± 0.02*

Values were expressed as mean ± SEM ($n = 10$). $^{\#\#}P < 0.01$ as compared with the normal group. $^{*}P < 0.05$ and $^{**}P < 0.01$ as compared with the vehicle group.

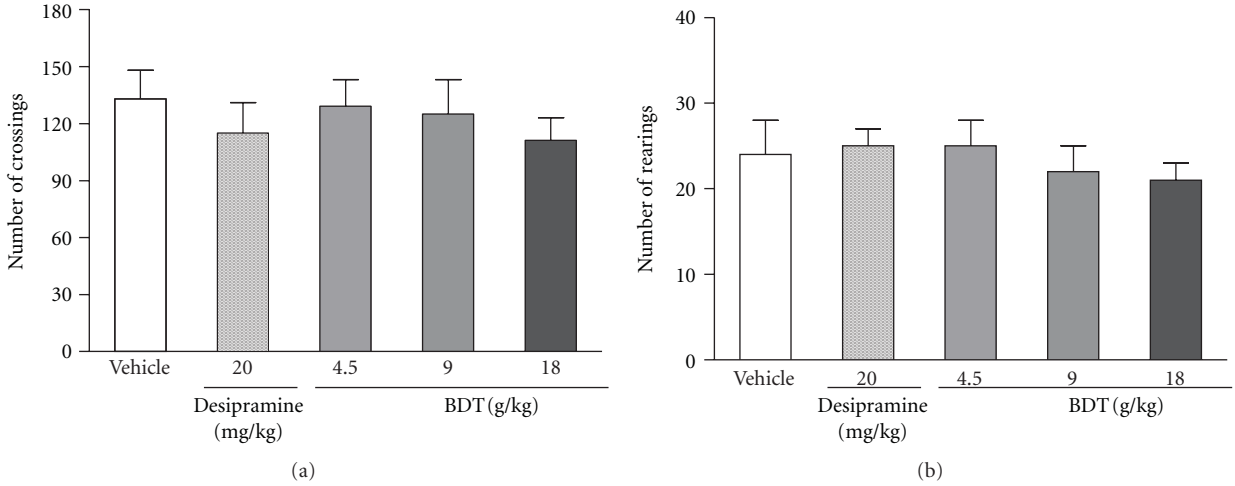

Figure 3: The effect of Baihe Dihuang Tang (BDT, 4.5, 9, 18 g/kg, p.o.) or desipramine (20 mg/kg, p.o.) on the crossings (a) and rearings (b) in the open-field test in mice. Values given are the mean ± SEM ($n = 10$). $^{*}P < 0.05$ and $^{**}P < 0.01$ as compared with vehicle group.

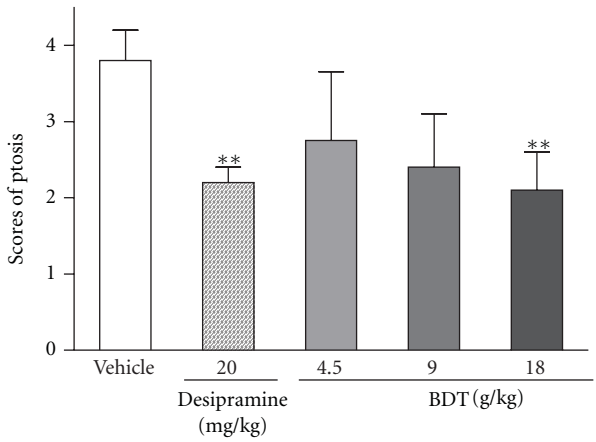

Figure 4: The effect of Baihe Dihuang Tang (BDT, 4.5, 9, 18 g/kg, p.o.) or desipramine (20 mg/kg, p.o.) on reserpine-induced palpebral ptosis in mice. Values given are the mean ± SEM ($n = 10$). $^{*}P < 0.05$ and $^{**}P < 0.01$ as compared with vehicle group.

ptosis induced by reserpine. The same treatment protocol using desipramine at 20 mg/kg also significantly antagonized reserpine-induced ptosis.

The data shows BDT has no effect on brain/body of mice (Table 1). The levels of NA, DA, 5-HT, and 5-HIAA in the brain of mice after TST were measured and recorded as shown in Table 1. Compared with normal group, the significantly decreased responses to the TST exposure on 5-HT and NA levels were revealed in mice brain. BDT at 9 and 18 g/kg significantly increased 5-HT levels ($P < 0.05$, $P < 0.01$, resp.), while BDT at 18 g/kg significantly elevated 5-HT metabolite, 5-HIAA, level ($P < 0.05$). NA level was significantly increased after treatment with the higher dose of BDT (18 g/kg). As positive control, desipramine (20 mg/kg) produced an increase in the levels of monoamines 5-HT and NE. No significant changes in DA were observed in any treatment regimen after mice TST. The 5-HT turnover, as represented by the ratio of 5-HIAA/5-HT, was calculated. The significant difference in the 5-HT turnover were observed in group 5 received oral dose at 18 g/kg of BDT ($P < 0.05$) (Table 1).

4. Discussion

Forced swim test and tail suspension test are the widely used animal models of depression for the screening of antidepressive activity [21, 23]. In these tests, animals are under stress from which they cannot escape in the confined

space. After an initial period of struggling, they would become immobile. Such immobility represented a hopeless state similar to human mental depression and amenable to reversal by antidepressant drugs [21, 23]. In the present study, the antidepressive effects of BDT were assessed by using the two classical animal models. In addition, the effect of BDT on locomotion was evaluated by the OFT for excluding false-positive effects attributable to any psychostimulant effect of BDT. After treated with BDT at 9 and 18 g/kg for 14 days, the mice showed a significant reduction of immobility time in both forced swim (Figure 1) and tail suspension tests (Figure 2). Moreover, BDT treatment did not increase the number of crossings and rearings (Figure 3). Our finding suggested that the reduction of immobility time elicited by BDT treatment in FST and TST was not related to a psychostimulant effect, but rather an antidepressant-like effect of BDT.

Depression has been associated with disturbances of brain monoamine neurotransmitters [31, 32]. As inhibitor, reserpine can irreversibly inhibit the vesicular uptake of monoamines, including noradrenaline, dopamine and 5-hydroxytrytamine and its metabolites. Therefore, we explored the underlying antidepressive mechanism of BDT on the reserpine-induced animal depression model which is based on the monoamine hypothesis of depression [33]. Ptosis is observed as depletion of monoamines reserves or stimulation of monoamines reuptake [34, 35]. In the reserpine-induced ptosis test, the results indicated that antidepressant-like effect of BDT may be involved in the preservation of monoamine neurotransmitters.

The dysfunction of the central nervous system involving the neurotransmitter 5-HT, NA, and DA has been suggested to play an important role in the pathogenesis of depression. For further evidence for antidepressant-like effect of BDT related to monoamine neurotransmitters, the contents of NE, DA, 5-HT, and 5-HIAA in brain were measured in TST. the TST is commonly used to detect and characterize the efficacy of antidepressant drugs and possesses greater sensitivity than the FST [36]. Our results show that BDT (9 and 18 mg/kg) increased the 5-HT levels in a dose-dependent manner in mice brain. These effects were similar to those observed with the positive drug desipramine. As the ratio of neurotransmitter compared to its metabolites (turnover) can be used as an index of neurotransmitter metabolism, the reduction of turnover indicates a slowdown in the metabolism of neurotransmitters [37]. In present study, the decreased turnover (5-HIAA/5-HT) was observed, indicating a reduction in 5-HT metabolism. Our results suggest that BDT can cause serotonergic activation in the brain, which is consistent with the behavioral changes exhibited in TST. In parallel with the serotonergic system, the noradrenergic system is also important in depression and in mediating behavioral effects of antidepressant drugs [38]. NE level in brain of mice with BDT treatment also showed an increase after TST. The increase is consistent with the effect on reserpine-induced ptosis. Thus, the current study confirmed that the serotonergic system and noradrenergic system might be implicated in the antidepressant-like effect of BDT.

In conclusion, BDT possess antidepressant-like effect in the FST and TST in mice. The results demonstrated that the antidepressant-like effect of BDT is mediated, at least partially, via the central monoaminergic neurotransmitter system.

Acknowledgments

M. L. Chen and J. Gao contributed equally to this work. This study is supported in part by the National Natural Science foundation of China (no. 30973599).

References

[1] J. H. Kim, S. Y. Kim, S. Y. Lee, and C. G. Jang, "Antidepressant-like effects of Albizzia julibrissin in mice: Involvement of the 5-HT_{1A} receptor system," *Pharmacology Biochemistry & Behavior*, vol. 87, no. 1, pp. 41–47, 2007.

[2] N. Bouvier, T. Trenque, and H. Millart, "Development of antidepressants drugs: experience and prospects," *Presse Medicale*, vol. 32, no. 11, pp. 519–522, 2003.

[3] C. B. Nemeroff, "Stress, menopause and vulnerability for psychiatric illness," *Expert Review of Neurotherapeutics*, vol. 7, supplement 1–3, no. 11, pp. S11–S13, 2007.

[4] Y. Z. Zhang, N. J. Yu, L. Yuan et al., "Antipressant effect of total flavonoids extracted from Xiaobuxing Tang in forced swimming test and learned helpness in rats and mice," *Chinese Journal of Pharmcology and Toxicology*, vol. 22, no. 1, pp. 1–8, 2008.

[5] G. K. Singh, D. Garabadu, A. V. Muruganandam, V. K. Joshi, and S. Krishnamurthy, "Antidepressant activity of Asparagus racemosus in rodent models," *Pharmacology Biochemistry and Behavior*, vol. 91, no. 3, pp. 283–290, 2009.

[6] H. W. Chen and S. F. Yin, "The progress on treatment of depression in TCM," *Heilongjiang Journal of Traditional Chinese Medicine*, vol. 40, no. 2, pp. 53–55, 2011.

[7] S. J. Quan, "Therapeutic effect of Baihe Dihuang Tang on the depressive patients," *New Journal of Traditional Chinese Medicine*, vol. 31, no. 2, pp. 16–17, 1999.

[8] W. Chen, S. H. Zhao, S. F. Xu et al., "Therapeutic effect of Baihe Dihuang Tang on the patients with post-stroke depression," *Chinese Journal of Gerontology*, vol. 24, no. 5, pp. 417–418, 2004.

[9] D. Zhang, X. S. Wen, X. Y. Wang, M. Shi, and Y. Zhao, "Antidepressant effect of Shudihuang on mice exposed to unpredictable chronic mild stress," *Journal of Ethnopharmacology*, vol. 123, no. 1, pp. 55–60, 2009.

[10] B. Jiang, J. H. Liu, Y. M. Bao, and L. J. An, "Catalpol inhibits apoptosis in hydrogen peroxide-induced PC12 cells by preventing cytochrome c release and inactivating of caspase cascade," *Toxicon*, vol. 43, no. 1, pp. 53–59, 2004.

[11] D. Q. Li, Y. L. Duan, Y. M. Bao, C. P. Liu, Y. Liu, and L. J. An, "Neuroprotection of catalpol in transient global ischemia in gerbils," *Neuroscience Research*, vol. 50, no. 2, pp. 169–177, 2004.

[12] D. Q. Li, Y. Li, Y. X. Liu, Y. M. Bao, B. Hu, and L. J. An, "Catalpol prevents the loss of CA1 hippocampal neurons and reduces working errors in gerbils after ischemia-reperfusion injury," *Toxicon*, vol. 46, no. 8, pp. 845–851, 2005.

[13] Y. Y. Tian, L. J. An, L. Jiang, Y. L. Duan, J. Chen, and B. Jiang, "Catalpol protects dopaminergic neurons from LPS-induced neurotoxicity in mesencephalic neuron-glia cultures," *Life Sciences*, vol. 80, no. 3, pp. 193–199, 2006.

[14] L. L. Yin, C. A. Peng, Y. Zhang et al., "The expression of 5-HT in brian treated with the Longshan lily, the famous-region drug, in chronic depression mice model," *Lishizhen Medicine and Materia Medica Research*, vol. 23, no. 2, pp. 357–358, 2012.

[15] Q. P. Guo, Y. Gao, and W. M. Li, "The depressive effect of active parts from lily on monoamine neurotransmitters in rat brian," *Chinese Traditional Patent Medicine*, vol. 31, no. 11, pp. 1669–1672, 2009.

[16] Q. P. Guo, Y. Gao, and W. M. Li, "Influence of the lilium saponins on HPA axis of the depression model rats," *Chinese Pharmacological Bulletin*, vol. 26, no. 5, pp. 699–700, 2010.

[17] S. Hiai, H. Oura, H. Hamanaka, and Y. Odaka, "A color reaction of panaxadiol with vanillin and sulfuric acid," *Planta Medica*, vol. 28, no. 2, pp. 131–138, 1975.

[18] C. C. Chang, M. H. Yang, H. M. Wen, and J. C. Chern, "Estimation of total flavonoid content in propolis by two complementary colometric methods," *Journal of Food and Drug Analysis*, vol. 10, no. 3, pp. 178–182, 2002.

[19] L. D. Kotenko, M. Y. Yakubova, N. A. Tselishcheva, M. T. Turakhozhaev, and T. A. Badalbaeva, "Quantitative determination of the total iridoids in plants of the genus *Lagochilus*," *Chemistry of Natural Compounds*, vol. 30, no. 6, pp. 669–672, 1994.

[20] X. G. Xi, X. L. Wei, Y. F. Wang, Q. Chu, and J. Xiao, "Determination of tea polysaccharides in Camellia sinensis by a modified phenol-sulfuric acid method," *Archives of Biological Sciences*, vol. 62, no. 3, pp. 669–676, 2010.

[21] R. D. Porsolt, A. Bertin, and M. Jalfre, "Behavioral despair in mice: a primary screening test for antidepressants," *Archives Internationales de Pharmacodynamie et de Thérapie*, vol. 229, no. 2, pp. 327–336, 1977.

[22] A. D. E. Zomkowski, A. O. Rosa, J. Lin, A. R. S. Santos, J. B. Calixto, and A. L. S. Rodrigues, "Evidence for serotonin receptor subtypes involvement in agmatine antidepressant like-effect in the mouse forced swimming test," *Brain Research*, vol. 1023, no. 2, pp. 253–263, 2004.

[23] L. Steru, R. Chermat, B. Thierry, and P. Simon, "The tail suspension test: a new method for screening antidepressants in mice," *Psychopharmacology*, vol. 85, no. 3, pp. 367–370, 1985.

[24] J. R. Royce, "On the construct validity of open-field measures," *Psychological Bulletin*, vol. 84, no. 6, pp. 1098–1106, 1977.

[25] A. D. E. Zomkowski, D. Engel, N. H. Gabilan, and A. L. S. Rodrigues, "Involvement of NMDA receptors and l-arginine-nitric oxide-cyclic guanosine monophosphate pathway in the antidepressant-like effects of escitalopram in the forced swimming test," *European Neuropsychopharmacology*, vol. 20, no. 11, pp. 793–801, 2010.

[26] M. Bourin, M. Poncelet, R. Chermat, and P. Simon, "The value of the reserpine test in psychopharmacology," *Arzneimittel-Forschung*, vol. 33, no. 8, pp. 1173–1176, 1983.

[27] C. C. Sánchez-Mateo, C. X. Bonkanka, B. Prado, and R. M. Rabanal, "Antidepressant activity of some Hypericum reflexum L. fil. extracts in the forced swimming test in mice," *Journal of Ethnopharmacology*, vol. 112, no. 1, pp. 115–121, 2007.

[28] M. K. Lakshmana and T. R. Raju, "An isocratic assay for norepinephrine, dopamine, and 5- hydroxytryptamine using their native fluorescence by high-performance liquid chromatography with fluorescence detection in discrete brain areas of rat," *Analytical Biochemistry*, vol. 246, no. 2, pp. 166–170, 1997.

[29] J. F. Cryan, A. Markou, and I. Lucki, "Assessing antidepressant activity in rodents: recent developments and future needs," *Trends in Pharmacological Sciences*, vol. 23, no. 5, pp. 238–245, 2002.

[30] J. F. Cryan, C. Mombereau, and A. Vassout, "The tail suspension test as a model for assessing antidepressant activity: review of pharmacological and genetic studies in mice," *Neuroscience and Biobehavioral Reviews*, vol. 29, no. 4-5, pp. 571–625, 2005.

[31] D. J. Nutt, "Relationship of neurotransmitters to the symptoms of major depressive disorder," *The Journal of Clinical Psychiatry*, vol. 69, pp. 4–7, 2008.

[32] A. S. Elhwuegi, "Central monoamines and their role in major depression," *Progress in Neuro-Psychopharmacology & Biological Psychiatry*, vol. 28, no. 3, pp. 435–451, 2004.

[33] Q. Q. Mao and Z. Huang, "Antidepressant drugs and animal models of depression," *Foreign MedicalSciences*, vol. 32, pp. 216–220, 2005.

[34] D. Dhingra and A. Sharma, "Antidepressant-like activity of Glycyrrhiza glabra L. in mouse models of immobility tests," *Progress in Neuro-Psychopharmacology & Biological Psychiatry*, vol. 30, no. 3, pp. 449–454, 2006.

[35] M. Bourin, M. Poncelet, R. Chermat, and P. Simon, "The value of the reserpine test in psychopharmacology," *Arzneimittel-Forschung*, vol. 33, no. 8, pp. 1173–1176, 1983.

[36] J. Steru, R. Chermat, B. Thierry et al., "The automated tail suspension test: a computerized device which differentiates psychotropic drugs," *Progress in Neuro-Psychopharmacology & Biological Psychiatry*, vol. 11, no. 6, pp. 659–671, 1987.

[37] M. Maes and H. Y. Meltzer, "The serotonin hypothesis of major depression," in *Psychopharmacology: the 4th Generation of Progress*, F. E. Bloom and D. J. Kupfer, Eds., pp. 933–944, Raven Press, New York, NY, USA.

[38] S. A. Montgomery, "Is there a role for a pure noradrenergic drug in the treatment of depression?" *European Neuropsychopharmacology*, vol. 7, no. 1, pp. S3–S9, 1997.

Hindawi Publishing Corporation
Evidence-Based Complementary and Alternative Medicine
Volume 2012, Article ID 902413, 9 pages
doi:10.1155/2012/902413

Research Article

Effects of Electroacupuncture at Head Points on the Function of Cerebral Motor Areas in Stroke Patients: A PET Study

Zuo Fang,[1] Jia Ning,[2] Chang Xiong,[3] and Yao Shulin[4]

[1] *TCM and Acupuncture & Moxibustion Department of Nanlou, Chinese PLA General Hospital, Beijing 100853, China*
[2] *Department of Nosocomial Infection and Disease Control, Chinese PLA General Hospital, Beijing 100853, China*
[3] *Chinamed USA, Charlottesville, VA 22901, USA*
[4] *Department of Nucleus Medicine, Chinese PLA General Hospital, Beijing 100853, China*

Correspondence should be addressed to Jia Ning, jianing@263.net

Received 26 April 2012; Accepted 18 June 2012

Academic Editor: Paul Siu-Po Ip

Positron emission tomography (PET) is used to observe the cerebral function widely and is a good method to explore the mechanism of acupuncture treatment on the central nervous system. By using this method, we observed the cerebral function of 6 patients suffering from ischemic stroke after receiving EA treatment at Baihui(GV20) and right Qubin(GB7). The results were: (1) the glucose metabolism changed significantly on primary motor area (M1), premotor cortex (PMC), and superior parietal louble (LPs) bilaterally, as well as the Supplementary Motor Area (SMA) on the unaffected hemisphere right after the first EA treatment. (2) The glucose metabolism on bilateral M1 and LPs changed significantly after three weeks of daily EA treatments. (3) The glucose metabolism on other areas such as insula, putamen, and cerebellum changed significantly. It demonstrated that EA at Qubin and Baihui couldactivate the cerebral structures related to motor function on the bilateral hemispheres.We concluded that EA was very helpful for the cerebral motor plasticity after the ischemic stroke. Also based on this study we assumed that the brain plasticity should be a network and that acupuncture participated in some sections of this course.

1. Introduction

Acupuncture has been used in stroke rehabilitation in China for over 3000 years. However, its mechanisms are still under discussion. Most researchers used biochemical or anatomical tests to observe the animals or electrophysiological tests to observe human beings and tried to explain the mechanisms [1–3]. Unfortunately what they got was just indirect evidence. PET (positron emission tomography), a vivo functional examination technology can be done without invasive procedures. Its image reflects not only the structure of the organs and tissues, but also their physiological and biochemical changes. It can clearly reflect the change of corresponding functional areas of brain after stimulus. Therefore PET is called "vivo molecular biological imaging" [4]. Since the functional changes can be detected visually, it has been widely used in the study of the brain function [5–7] and the central nervous mechanism of acupuncture effect [8, 9]. However, no research was done with involving movements. We believed that the study on the changes of glucose metabolism after EA with movements which could activate the cerebral motor functional areas could reflect impact of EA on motor function more accurately, compared with the study in the resting state after accepting the EA.

EA has a nearly 200-year history. French physician Louis Berlioz was the first to apply the electricity on acupuncture needles in his clinical work in 1810. He believed that the current generated by the battery might enhance the therapeutic effect of the acupuncture needles [10]. In China, EA appeared for the first time in the Journal of Acupuncture and Moxibustion 1934 and Tang Shicheng proposed that EA with pulsed current generated by the electronic tube could be used clinically. It was probably Zhu longyu in Shaanxi Province, China who brought about the therapeutic EA officially in

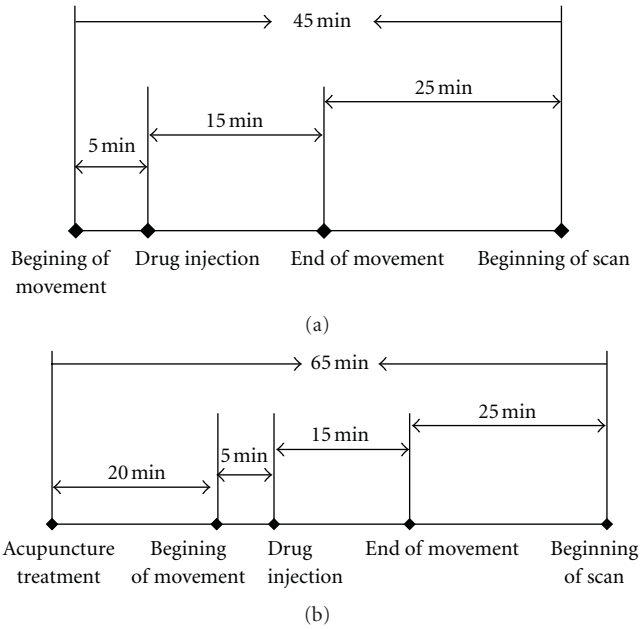

Figure 1: (a) First test chart flow diagram. (b) Second test chart flow diagram.

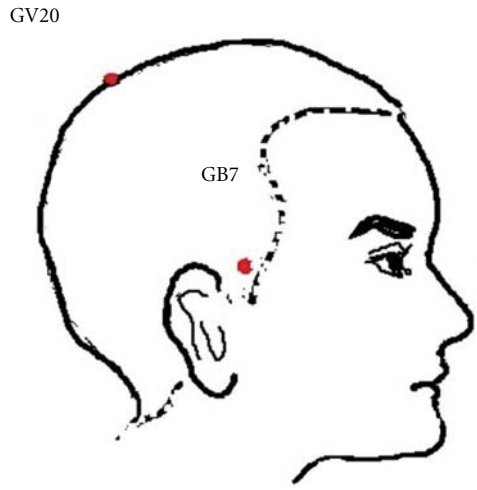

Figure 2: Schematic diagram of GV20 and GB7.

1950s. He invented the EA stimulator successfully in 1953 and found that EA has a significant analgesic effect in 1956 [11]. Since then EA has been widely used in acupuncture anesthesia and other diseases treatment. After nearly 60 years of clinical and experimental applications, EA has become one of the most widely used medical therapeutic methods. It promoted the development of clinical and scientific research on acupuncture somehow. The amount of stimulation of EA is more objective than the traditional manual acupuncture, so it has been used in acupuncture clinical or experimental studies for control studies. A large number of studies have shown that EA has a significant treatment effect on stroke [12, 13], and in the department where I worked, EA was a routine clinic treatment for stroke. So we used EA in this study.

So far the researches on stroke recovery mechanisms have found (1) the recovery of an animal experimental focal cerebral ischemia (sensory or motor cortex) was related to the reorganization in the adjacent unaffected cortex around the lesion [14, 15]; (2) the activation of the supplementary motor area (SMA) is considered with the recovery of motor function [16]; (3) during the recovery process, a certain number of cells and tissues of the unaffected hemisphere change [17].

Therefore, we observed cerebral glucose metabolism in stroke patients before and after EA treatments with patients' fist-clenching movement, in order to explore the effect of head acupoints on multiple cerebral areas above mentioned and to interpret the mechanism of acupuncture on stroke patients' motor function recovery.

2. Patients and Methods

2.1. Patients. Six right-handed stroke patients (3 males, 3 females) were recruited for the study. Each patient received an explanation of the study protocol and signed an informed consent prior to participating in the study. Patients accepted short-term movement task training before the experiment.

Inclusion criteria were (i) first-ever ischemic stroke (confirmed by computerized tomography (CT) scan or magnetic resonance imaging (MRI)) involving the right basal ganglion region; (ii) age 50–75 years; (iii) admission within 1–3 months of onset; (iv) upper extremity motor function of patients was damaged, but patients could finish the movements that the study required (muscle strength was 3-4); (v) for the diabetic patients with the controlled blood sugar, the blood sugar was tested on the dates of the scan for the correction.

Patients were excluded if they: (i) had severe diabetes and severe heart disease and (ii) were taking any central nervous system depressants or stimulant drugs in the previous month.

2.2. Instrument and Methods

2.2.1. Instrument: Positron Emission Tomography (PET). PET scanner (ECAT EXACT HR$^+$, Siemens Co. Germany) was used with the scanning mode of three dimensions (3D), and the thickness of each slice was 3 mm with septa retracted and scatters correction. The EXACT HR$^+$ had a 15.2-cm axial FOV, sufficient to image the whole brain in a single scan.

2.2.2. Methods. The temperature of the examination room was 22–24°C. The tracer was 18 fluoride-deoxyglucose (18F-FDG, produced by accelerator CTIRDS111, and its purity >95%, 148–185 MBq), which was administered by intravenous injection at 110 mCi/kg (bodyweight). The patients had the earplugs and eye patches on to block auditory and visual stimuli until the end of the scan. Before each scan the patient's head was placed into a supporting device, localized by laser, and fixed in a position where superior and inferior

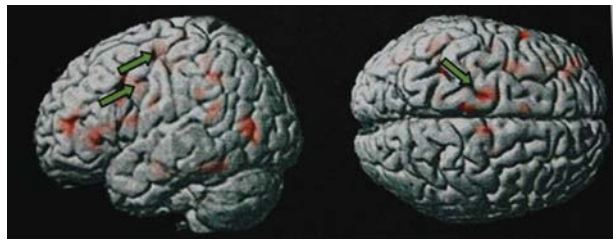

(a)

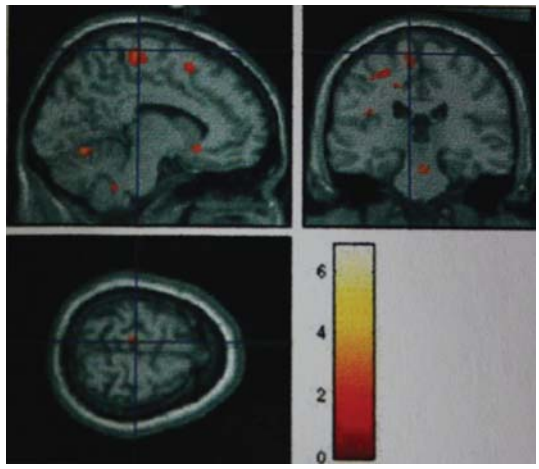

Coordinate (−8 −26 70) $t = 3.1$

(b)

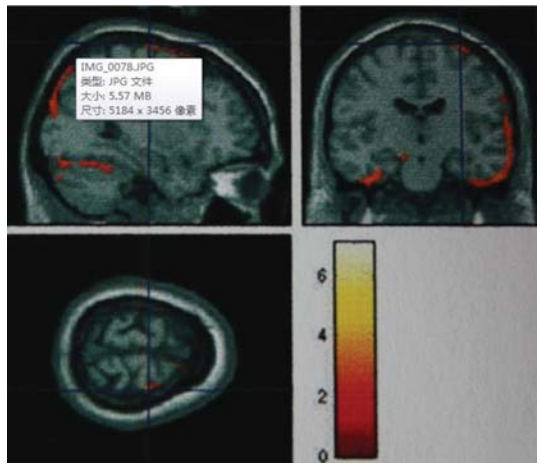

Coordinate (32 −16 76) $t = 3.89$

(c)

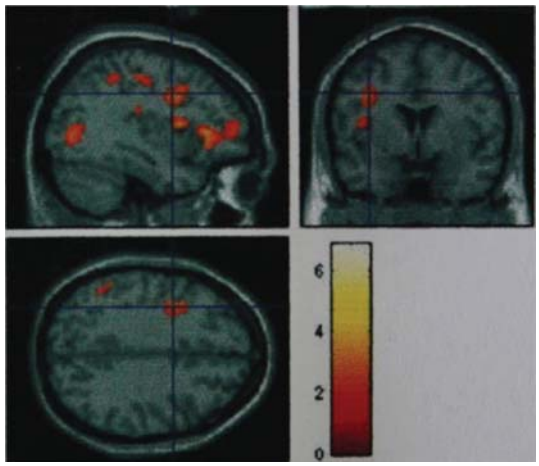

Coordinate (−36 2 36) $t = 3.2$

(d)

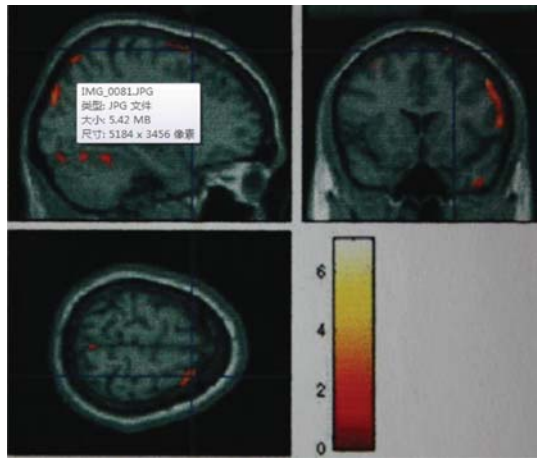

Coordinate (26 16 68) $t = 3.36$

(e)

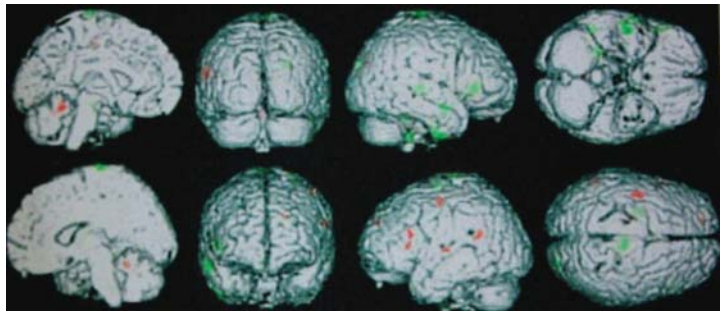

(f)

(a)

Figure 3: Continued.

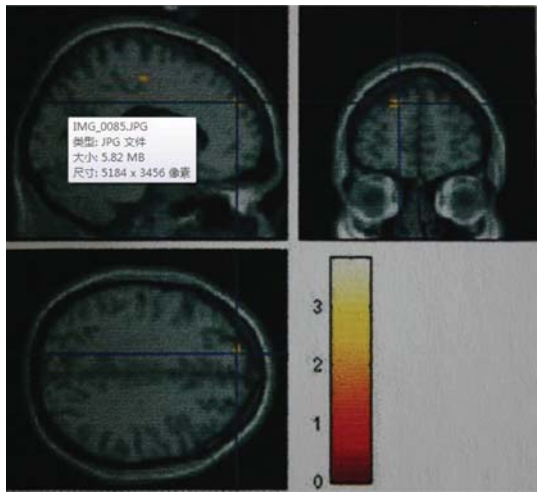

Coordinate (−14 54 34) $t = 2.25$

(g)

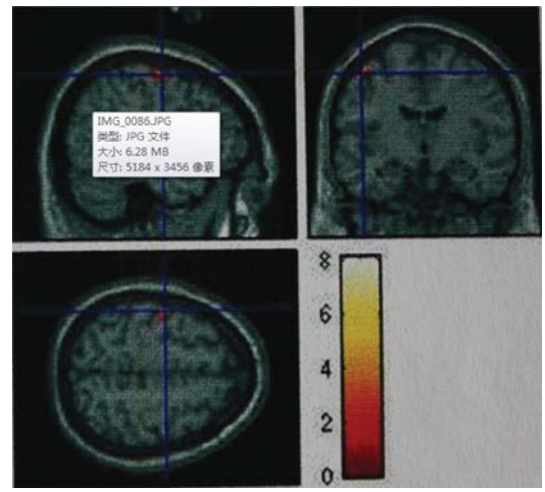

Coordinate (−46 −10 56) $t = 4.59$

(h)

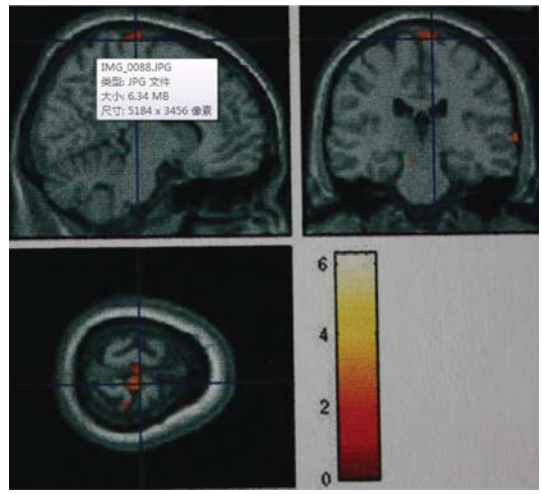

Coordinate (10 −24 78) $t = 3.39$

(i)

(b)

Figure 3: (a) EA instant effect: brain glucose metabolism of the stroke patients increases. The red represented the areas with increased glucose metabolism, and the green arrow referred to M1. (b) The glucose metabolism on the left precentral gyrus increased. (c) The glucose metabolism on the right precentral gyrus decreased. (d) The glucose metabolism on the left midfrontal gyrus increased. (e) The glucose metabolism on the right midfrontal gyrus decreased. (f) Three weeks of EA treatment effect: brain glucose metabolism alteration. The red represented the areas with increased glucose metabolism, and the green represented the areas with decreased glucose metabolism. The glucose metabolism alteration areas included bilateral M1, temporal lobe, and so forth. (g) Left superior frontal gyrus glucose metabolism increased. (h) Left precentral gyrus glucose metabolism increased. (i) Right precentral gyrus glucose metabolism decreased.

laser lines were parallel to the orbit mastoid (OM) line and the cerebrum and the cerebellum were covered.

2.2.3. Procedure Details. The observation was conducted as the followed steps. (1) The patient laid flat on the examination table and made fist-clenching movements regularly (the affected hand) at a frequency of about 0.5 Hz (metronome interrupter, Nikko, P1440, Japan) continuously for 20 minutes. Five minutes after the movements started, 18 fluorine deoxyglucose (18F-FDG) (4mci) was injected into the vein of the unaffected hand. 40 minutes after the injection, the patients had the PET scans (Figure 1(a)). (2) On the following day, the patient accepted acupuncture treatment at Baihui (GV20) and right Qubin (GB7, on the affected hemisphere) (Figure 2) for 20 minutes. The needles were connected to an electroacupuncture (EA) therapeutic apparatus. Then the same procedure as the first step was repeated, the images of the second time were collected (Figure 1(b)). (3) After three weeks of EA daily treatment the patients got the same PET scan as the first step.

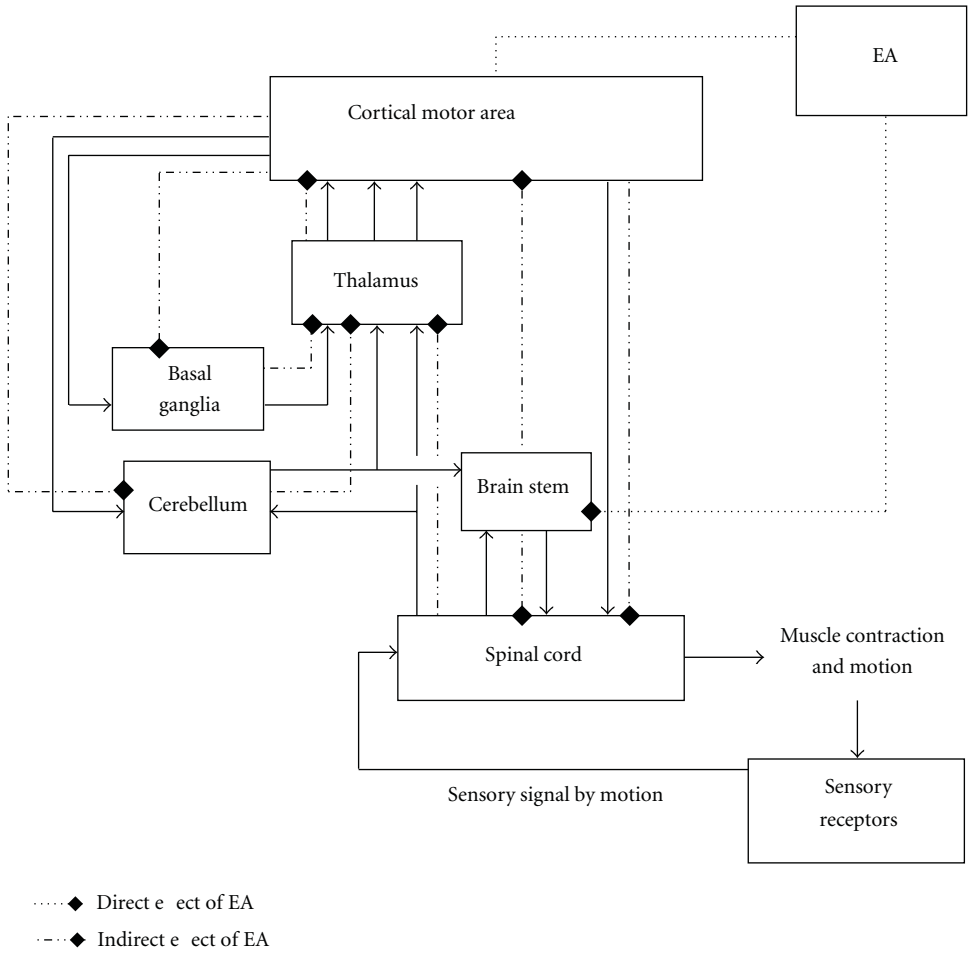

Figure 4: Schematic diagram of the relationship between the structures of the motor system.

Needling process: the acupuncture pointes were cleaned with 75 percent alcohol. The needles were the single-use, disposable stainless steel acupuncture needles (Huatuo, Suzhou Medical Supplies Co. Ltd; Suzhou, China), with a diameter of 0.25 mm and a length of 25 mm. The needles were inserted horizontally into both acupuncture points, forming a less than 30 angle with the skin surface. Depth of needle insertion was approximately 10 mm. Then two needles were connected to a commercial electro-acupuncture device (model SDZ-V, Suzhou Medical Supplies Co. Ltd; Suzhou, China). The frequency was 2 Hz with continuous waves. The intensity of the stimulation was increased to the point where the patient reported the needling reaction and then it was adjusted gradually to a comfortable intensity and remained at that level for 20 minutes.

2.2.4. Image Analysis. PET data were processed and analyzed by statistical parametric mapping (SPM99) (Institute of Neurology, University of London, London, UK) and the Matlab 6.1 program (Mathworks Inc., Sherborn, MA, USA) was used. Brain images were anatomically normalized to a standard brain template (FDG-PET version adapted to the MNI-MRI template by Montreal Neurological Institute) by linear (affine) and nonlinear transformations to minimize intersubject anatomical variations by using an SPM routine. To identify brain regions in which the perfusion and glucose metabolism had changed following EA, linear contrasts were used to test for regionally specific differences between groups, producing paired t-statistic maps in Talairach standard space. These t-statistics were transformed to corresponding Z maps, which constituted the statistical map (SPM-Z). The peak voxel-based significance of statistics was set at uncorrected $P < 0.05$.

3. Results

(1) EA instant effects: the significant increase of glucose metabolism was found on the unaffected side: the Primary motor area (M1), the precentral gyrus (the 4th Area), the supplementary motor area (SMA), the medial frontal gyrus (the 6th area), premotor cortex (PMC), the central frontal gyrus (the 6th Area), and the superior parietal lobule (LPs, the 7th Area) (Table 1(a), Figures 3(a), 3(b), and 3(d)). The decrease of glucose metabolism was found on M1, PMC, and LPs in the affected side (Table 1(b), Figures 3(c) and 3(e)).

Table 1: (a) Talairach coordinates and t value of peak activation of activated fields that showed increased cerebral glucose metabolism of the patients after electro-acupuncture, (b) Talairach coordinates and t value of peak activation of activated fields that showed decreased cerebral glucose metabolism of the patients after electro-acupuncture.

(a)

	Peak	Corrected	Coordinates		
	t value	P value	x	y	z
GPrC (Area4) L	3.10	0.0087	−8	−26	70
GFd (Area6) L	2.99	0.0101	−16	−12	58
LPs (Area7) L	2.79	0.0134	−32	−42	50
GFm (Area6) L	3.20	0.0075	−36	2	36
GFd (Area6) R	3.05	0.0092	10	−14	56
GTm (Area37) L	5.91	$<10^{-4}$	−44	−68	8
GTs (Area22) L	3.75	0.0036	−54	−48	18
Cerebellum L	3.51	0.0049	−8	−66	−10
Putamen L	3.01	0.0097	−12	16	−4

$P < 0.05$, and the coordinates indicated the location of maximally significant activity.

(b)

	Peak	Corrected	Coordinates		
	t value	P value	x	y	z
GPrC (Area4) R	3.89	0.0030	32	−16	76
GFm (Area6) R	3.36	0.0060	26	16	68
LPs (Area7) R	2.23	0.0302	2	−60	68
GFd (Area9) R	4.17	0.0021	6	62	26
GFm (Area10) R	2. 51	0.0200	48	54	4
GTm (Area21) R	5.38	$<10^{-4}$	60	0	−26
GFm (Area6) L	2.39	0.0236	−34	10	60

$P < 0.05$, and the coordinates indicated the location of maximally significant activity.

(2) After three weeks daily EA treatments, the increase of glucose metabolism (Table 2(a), Figures 3(f), 3(g), and 3(h)) was found on the unaffected hemisphere (left side); and the decrease of glucose metabolism (Table 2(b), Figures 3(f) and 3(i)) was found in the affected hemisphere. Among these areas, M1 and LPs were related to motor function.

(3) Besides these areas related to motion directly, the other areas where glucose metabolism had changed included middle temporal gyrus, superior temporal gyrus, putamen, and cerebellum.

4. Discussion

(1) *Huang Di nei jing su wen* pointed out that the *Head is the Smart House*. It means that the human's meridian Qi concentrates in the head and face through meridians and branched channels. It also pointed out that *Qi goes out of the brain*. It means that the driving force comes from the brain. Therefore, the limbs are controlled by the brain. Motor dysfunction, hemiplegia, is the main symptom of stroke. And the location of this disease is in the brain.

In this study, head acupoints took the role of local treatments. Furthermore, it is very important to select the points on Governor and Foot Gallbladder meridians to treat stroke. Since the Governor meridian goes through the spine upto the neck and brain and is the governor of the Yang of the body; and the Foot Gallbladder meridian goes through the body side up to the top of the head and its meridian sinew intercrosses the musculature of meridians on two sides of the body, and goes along with the Yang Heel Vessel. Their main function is to treat paralysis after stroke and all other kinds of symptoms in the head. Previous research showed that the acupuncture treatments at those points alleviated brain damage after ischemic stroke in the monkeys and rats [18, 19]. And some studies demonstrated that the GV20 is located in the area of the frontal lobe of the anterior precentral sulcus [20]. So we selected these two points. Based on traditional Chinese medical theories, acupuncture on these two points can activate Qi of the Governor and Gallbladder meridians, regulate the channels' function, and balance Yin and Yang of the body, thus contribute to the improvement of motor function of limbs. Other previous clinical studies have shown that: stimulating Baihui could well regulate central bioelectrical activity in cerebral cortex of stroke patients and was conducive to the resurrection of the nerve cells of the penumbra or awakening dormant brain cells. So the link between the functional areas of cerebral cortex and compensatory function were strengthened [21, 22].

(2) It helped us realize that noninvasive functional examination in vivo could clearly reflect the changes of biological

Table 2: (a) Talairach coordinates and t value of peak activation of activated fields that showed increased cerebral glucose metabolism of the patients after three weeks of daily electro-acupuncture treatments, (b) Talairach coordinates and t value of peak activation of activated fields that showed the decreased cerebral glucose metabolism of the patients after three weeks of daily electro-acupuncture treatments.

(a)

	Peak	Corrected	Coordinates		
	t value	P value	x	y	z
GPrC (Area4) L	4.59	0.0029	−46	−10	56
GFm (Area6) L	2.68	0.0217	−68	18	20
LPs (Area7) L	2.25	0.0291	−14	54	34
GFd (Area9) L	3.75	0.0036	−54	−50	22
Cerebellum R	3.14	0.0082	28	−40	−50

$P < 0.05$, and the coordinates indicated the location of maximally significant activity.

(b)

	Peak	Corrected	Coordinates		
	t value	P value	x	y	z
GPrC (Area4) R	3.39	0.0058	10	−24	78
GFd (Area45) R	2.72	0.0147	50	28	4
thalamus R	3.11	0.0085	20	−10	12
GTs (Area22) R	2.95	0.0107	74	−26	4
GTm (Area21) R	2.80	0.0131	60	−2	−20
Cuneus (Area19) R	2.61	0.0173	24	−90	30
GTs (Area38) R	1.96	0.0441	50	16	−10
GFs (Area6) L	2.39	0.0238	−26	−8	70

$P < 0.05$, and the coordinates indicated the location of maximally significant activity.

metabolism of cerebral nervous tissue after acupuncture by using PET. Asking the patients to move their hands to activate or deactivate the glucose metabolism was helpful in identifying which cerebral motor areas were engaged and we could obtain the direct evidence from spatial and time aspects, which could reflect the effect of acupuncture on the motor recovery of stroke patients more objectively than in the resting condition.

(a) Instant effect of EA: the results of the study showed that after EA, the bilateral M1, PMC, and LPs, as well as SMA of the unaffected hemisphere had significant changes in glucose metabolism, with remarkable increase in these regions of the unaffected hemisphere and decrease in the affected hemisphere. Acupuncture activated not only the cerebral tissues of the affected hemisphere, but also the related regions of the unaffected hemisphere, particularly SMA. The results confirmed the previous research: the activation of the SMA was considered to be related to the recovery of the motor function [23, 24]. In humans with unilateral stroke, previous studies have found increased excitability [25] and, sometimes, increased cerebral blood flow in the contralateral cortex [26, 27]. Some of these contralesional changes are related to enhanced ipsilesional function. It demonstrated that acupuncture could activate bilateral motor areas of the brain and initiate excitement of the nerve tissue related to the motor activity and it played a role of compensation, which is important for the recovery of neural tissue of the semidark band and the activation of potential functional regions.

(b) Effect of three weeks of EA treatments: after three weeks of daily acupuncture treatments, the changes in the region related to the motor ability directly was only the M1, but still showed the same trend as the instant effects: bilateral changes with increased glucose metabolism on the unaffected hemisphere and decreased metabolism on the ipsilesional hemisphere. It showed that the contralateral hemisphere played an important role in the stroke recovery process [28, 29] and that EA treatment for stroke patients had played a good role in the recovery of motor function.

(3) We adopted a functional description to describe the experimental results since different cerebral structures often have the same function. M1 is in the precentral gyrus and paracentral lobule, equivalent to Brodmann area 4 and controls voluntary movements. PMC is located in Area 6 in the front of the precentral gyrus. SMA mainly is located in area 6 in the internal and upper dorsolateral hemisphere. They are related to the state of readiness before exercises. This function division indicated that the region of programming the movement preparation and controlling the movement implementation cannot be limited to a special area and may involve a lot of "modules" in a dynamic network. After EA treatment, these areas had the metabolic changes. It

demonstrated that the EA on head acupoints may improve the recovery of motor function through the regulation of "module" of this network.

(4) After EA at Qubin (GB7) and Baihui (GV20), the changes took place not only in the motor areas but also in the insular cortex, temporal lobe, occipital lobe, putamen, and cerebellum. These changes may be related to the specificity of the acupoints. However, some literatures also mentioned that metabolic changes on the areas such as the insular cortex, parietal lobe, thalamus, putamen, and cerebellum were relevant to the movement [30, 31]. In the central nervous system, no functional areas are simple and independent. Only motor function is involving multiple areas (Figure 4 [32]). These areas connected closely with ipsilateral and contralateral cortex or nuclei and interacted with each other by both excitatory and inhibitory mechanisms. It is a complex network. So the metabolic function changes in these areas were most likely indirect evidence of the changes of motor function. We believed that EA at head acupoints may activate all levels of the structures related to the motor function (Figure 4): EA at Baihui (GV20) and Qubin (GB7) may affect the structure of motion system in two ways directly or indirectly at all levels. One way was that the stimuli went up through the brain stem, cornuposterius medullae—trigeminal lemniscus, spinothalamic tract—thalamus—cerebral cortex, and interacted between the cerebral cortices and influenced on subcortical structures. The other possible way was that EA at head acupoints may produce weaker bioelectrical signals in local neuromuscular tissue, thereby creating a weaker biological magnetic field and penetrating the skull, directly to influence the cerebral cortex and its associated areas [33] and then to adjust movement structure at all levels through the neural network. This presumption needed further experimental study.

(5) The increased or decreased changes of glucose metabolism after acupuncture reflected the degrees of the excitement and inhibition of the related cerebral areas. Those excitement and inhibition had the important role. Because the neurons have an extensive mutual connection, they may excite or inhibit each other and serve to conduct sequential processing and transmission of the complicated information. The inhibition of some neurons may be the aftereffect of excitement of some other neurons or the initiation of the excitement in other sites. The metabolic decrease in some cerebral areas was likely a compensative mode of other areas. Hence, we should pay more attention to which cerebral areas were involved and how much changes happened. When acupuncture activated some areas, it also induced changes in relative areas. It can be thought that the regulation of acupuncture should be a relatively specific network effect and a multiple regulation course.

In conclusion, EA at head points might activate the cerebral motor areas bilaterally and induce the excitation of nerve tissue related to motion, and the activation of other regions demonstrated that the reorganization of the injured motor function was a neural network behavior, and that acupuncture may act on multiple aspects of the neural network, thus further contributing to the recovery of motor function.

Acknowledgment

This work was supported by the National Natural Science Foundation of China (30972523).

References

[1] F. Zhang, Y. Wu, and J. Jia, "Electro-acupuncture can alleviate the cerebral oedema of rat after ischemia," *Brain Injury*, vol. 25, no. 9, pp. 895–900, 2011.

[2] E. H. Kim, Y. J. Kim, H. J. Lee et al., "Acupuncture increases cell proliferation in dentate gyrus after transient global ischemia in gerbils," *Neuroscience Letters*, vol. 297, no. 1, pp. 21–24, 2001.

[3] J. D. Lee, J. S. Chon, H. K. Jeong et al., "The cerebrovascular response to traditional acupuncture after stroke," *Neuroradiology*, vol. 45, no. 11, pp. 780–784, 2003.

[4] F. Conchou, I. Loubinoux, E. Castel-Lacanal et al., "Neural substrates of low-frequency repetitive transcranial magnetic stimulation during movement in healthy subjects and acute stroke patients. A PET study," *Human Brain Mapping*, vol. 30, no. 8, pp. 2542–2557, 2009.

[5] S. T. Grafton, "PET: activation of cerebral blood flow and glucose metabolism," *Advances in Neurology*, vol. 83, pp. 87–103, 2000.

[6] D. H. S. Silverman and A. Alavi, "PET imaging in the assessment of normal and impaired cognitive function," *Radiologic Clinics of North America*, vol. 43, no. 1, pp. 67–77, 2005.

[7] S. Chinchure, C. Kesavadas, and B. Thomas, "Structural and functional neuroimaging in intractable epilepsy," *Neurology India*, vol. 58, no. 3, pp. 361–370, 2010.

[8] L. Yin, X. Jin, W. Qiao et al., "PET imaging of brain function while puncturing the acupoint ST36," *Chinese Medical Journal*, vol. 116, no. 12, pp. 1836–1839, 2003.

[9] M. S. Park, Y. Y. Sunwoo, K. S. Jang et al., "Changes in brain FDG metabolism induced by acupuncture in healthy volunteers," *Acta Radiologica*, vol. 51, no. 8, pp. 947–952, 2010.

[10] D. M. Chen and X. L. Cai, "A preliminary research on electro-acupuncture therapy," *Jiangxi Zhong Yi Xue Bao*, no. 1, pp. 95–105, 1959.

[11] L. Y. Zhu, *Electroacupuncture Therapeutics*, Shanxi People's, Xi'an, China, 1956.

[12] Q.-M. Si, G.-C. Wu, and X.-D. Cao, "Effects of electroacupuncture on acute cerebral infarction," *Acupuncture and Electro-Therapeutics Research*, vol. 23, no. 2, pp. 117–124, 1998.

[13] J. Pei, L. Sun, R. Chen, T. Zhu, Y. Qian, and D. Yuan, "The effect of electro-acupuncture on motor function recovery in patients with acute cerebral infarction: a randomly controlled trial," *Journal of Traditional Chinese Medicine*, vol. 21, no. 4, pp. 270–272, 2001.

[14] W. M. Jenkins and M. M. Merzenich, "Chapter 21 Reorganization of neocortical representations after brain injury: a neurophysiological model of the bases of recovery from stroke," *Progress in Brain Research*, vol. 71, pp. 249–266, 1987.

[15] R. J. Nudo, B. M. Wise, F. SiFuentes, and G. W. Milliken, "Neural substrates for the effects of rehabilitative training on motor recovery after ischemic infarct," *Science*, vol. 272, no. 5269, pp. 1791–1794, 1996.

[16] H. Aizawa, M. Inase, H. Mushiake, K. Shima, and J. Tanji, "Reorganization of activity in the supplementary motor area associated with motor learning and functional recovery," *Experimental Brain Research*, vol. 84, no. 3, pp. 668–671, 1991.

[17] T. A. Jones and T. Schallert, "Use-dependent growth of pyramidal neurons after neocortical damage," *Journal of Neuroscience*, vol. 14, no. 4, pp. 2140–2152, 1994.
[18] H. Gao, J. Guo, P. Zhao, and J. Cheng, "The neuroprotective effects of electroacupuncture on focal cerebral ischemia in monkey," *Acupuncture and Electro-Therapeutics Research*, vol. 27, no. 1, pp. 45–57, 2002.
[19] C. M. Chuang, C. L. Hsieh, T. C. Li, and J. G. Lin, "Acupuncture stimulation at Baihui acupoint reduced cerebral infarct and increased dopamine levels in chronic cerebral hypoperfusion and ischemia-reperfusion injured Sprague-Dawley rats," *American Journal of Chinese Medicine*, vol. 35, no. 5, pp. 779–791, 2007.
[20] E. Y. Shen, F. J. Chen, Y. Y. Chen, and M. F. Lin, "Locating the acupoint Baihui (GV20) beneath the cerebral cortex with MRI reconstructed 3D neuroimages," *Evidence-Based Complementary and Alternative Medicine*, vol. 2011, Article ID 362494, 6 pages, 2011.
[21] N. Hui, "Dynamic observation of electro-acupunctureon stroke patients with hemiplegiawith somatosensory evoked potentials," *Chinese Acupuncture & Moxibustionvol*, vol. 19, no. 6, pp. 369–370, 1999.
[22] W. Z. Zhu, J. X. Ni, Q. Tang, G. R. Dong, and H. Y. Li, "Study on the effect of cluster needling of scalp acupuncture on the plasticity protein MAP-2 in rats with focal cerebral infarction," *Chinese Acupuncture & Moxibustion*, vol. 30, no. 1, pp. 46–50, 2010.
[23] L. M. Carey, D. F. Abbott, G. F. Egan, J. Bernhardt, and G. A. Donnan, "Motor impairment and recovery in the upper limb after stroke: behavioral and neuroanatomical correlates," *Stroke*, vol. 36, no. 3, pp. 625–629, 2005.
[24] L. M. Carey, D. F. Abbott, G. F. Egan et al., "Evolution of brain activation with good and poor motor recovery after stroke," *Neurorehabilitation and Neural Repair*, vol. 20, no. 1, pp. 24–41, 2006.
[25] J. Liepert, F. Hamzei, and C. Weiller, "Motor cortex disinhibition of the unaffected hemisphere after acute stroke," *Muscle and Nerve*, vol. 23, no. 11, pp. 1761–1763, 2000.
[26] S. C. Cramer, G. Nelles, R. R. Benson et al., "A functional MRI study of subjects recovered from hemiparetic stroke," *Stroke*, vol. 28, no. 12, pp. 2518–2527, 1997.
[27] R. S. Marshall, G. M. Perera, R. M. Lazar, J. W. Krakauer, R. C. Constantine, and R. L. DeLaPaz, "Evolution of cortical activation during recovery from corticospinal tract infarction," *Stroke*, vol. 31, no. 3, pp. 656–661, 2000.
[28] P. Pantano, R. Formisano, M. Ricci et al., "Motor recovery after stroke Morphological and functional brain alterations," *Brain*, vol. 119, no. 6, pp. 1849–1857, 1996.
[29] C. Weiller, S. C. Ramsay, R. J. S. Wise, K. J. Friston, and R. S. J. Frackowiak, "Individual patterns of functional reorganization in the human cerebral cortex after capsular infarction," *Annals of Neurology*, vol. 33, no. 2, pp. 181–189, 1993.
[30] R. J. Seitz and N. P. Azari, "Cerebral reorganization in man after acquired lesions," *Advances in Neurology*, vol. 81, pp. 37–47, 1999.
[31] F. Binkofski, R. J. Seitz, S. Arnold, J. Classen, R. Benecke, and H. J. Freund, "Thalamic metabolism and corticospinal tract integrity determine motor recovery in stroke," *Annals of Neurology*, vol. 39, no. 4, pp. 460–470, 1996.
[32] E. R. Kandel, J. H. Schwartz, and T. M. Jessel, *Principle of Neural Science*, Elesvier, 3rd edition, 1991.
[33] O. Gang and W. Dongyan, "Preliminary exploration of pathway of scalp acupuncture therapy," *Hebei Journal of Traditional Chinese Medicine*, vol. 22, no. 11, p. 848, 2000.

Hindawi Publishing Corporation
Evidence-Based Complementary and Alternative Medicine
Volume 2012, Article ID 173565, 7 pages
doi:10.1155/2012/173565

Research Article

Mechanistic Study on the Antidepressant-Like Effect of Danggui-Shaoyao-San, a Chinese Herbal Formula

Zhen Huang,[1] Qing-Qiu Mao,[2] Xiao-Ming Zhong,[1] Zhao-Yi Li,[1] Feng-Mei Qiu,[1] and Siu-Po Ip[2]

[1] *College of Pharmaceutical Sciences, Zhejiang Chinese Medicine University, Hangzhou 310053, China*
[2] *School of Chinese Medicine, The Chinese University of Hong Kong, Hong Kong*

Correspondence should be addressed to Zhen Huang, zhen626@yahoo.com.cn and Siu-Po Ip, paulip@cuhk.edu.hk

Received 24 April 2012; Revised 27 June 2012; Accepted 4 July 2012

Academic Editor: Karl Wah-Keung Tsim

Danggui-Shaoyao-San (DSS), a famous Chinese herbal formula, has been widely used in the treatment of various diseases. Previous studies have shown that DSS produces antidepressant-like effect in rodents. This study aims to investigate the mechanism(s) underlying the antidepressant-like action of DDS. The results showed that DSS treatment significantly antagonized reserpine-induced ptosis in mice. In addition, DSS treatment significantly increased sucrose consumption in chronic unpredictable stress- (CUS-) treated mice. DSS treatment also markedly attenuated CUS-induced decreases in noradrenaline and dopamine concentrations in mouse brain. Furthermore, DSS treatment significantly reversed CUS-induced increase in serum malondialdehyde (MDA) content and decrease in serum superoxide dismutase (SOD) activity in mice. The results suggest that the antidepressant-like activity of DSS is probably mediated by the modulation of central monoamine neurotransmitter systems and the reduction of oxidative stress.

1. Introduction

Depression is a prevalent psychiatric disease affecting the quality of life of many people. Based on latest available data from the World Health Organization, depression is expected to become the second leading cause of disease-related disability by the year 2020. It is generally believed that monoamine neurotransmitters including serotonin (5-HT), noradrenaline (NA), and dopamine (DA) are involved in the pathogenesis of depression, and most antidepressant drugs exert their action by elevating monoamine neurotransmitters concentrations [1, 2]. Oxidative stress, which is defined as a disturbance in the balance between the production of reactive oxygen species (ROS) and antioxidant defense systems, has also been shown to play a role in the pathogenesis of neuropsychiatric disorders [3, 4]. Furthermore, preclinical studies have demonstrated that the inhibition of oxidative stress may contribute to the therapeutic effects of some antidepressant drugs [5–8].

Danggui-Shaoyao-San (DSS) is a traditional herbal medicine which is widely used in China, Japan, and Korea. DSS, the herbal formula, is first recorded in "JinKuiYaoLue" and it consists of six medicinal herbs (Table 1). The herbal drug was traditionally used to relieve menorrhalgia and other abdominal pains of women [9]. Recently, a clinical study has showed that DSS is effective in treating insomnia [10], which is a symptom and predictor of depression [11]. Preclinical studies have showed that DSS possesses antioxidative, antithrombotic, cognitive enhancing, and neuroprotective effects [9, 12, 13]. Moreover, a previous report suggested that DSS treatment could significantly decrease immobility time in the forced swim test in mice [14]. The herbal preparation was also effective in improving chronic stress-induced behavioral alterations in rats, which were related to the central arginine vasopressin system [14]. However, the action mechanism for the antidepressant-like effect of DSS is still not fully elucidated. In this study, we aim to explore different antidepression mechanisms of DSS by investigating its effect on the monoamine neurotransmitter systems. In addition, the effects of DSS on brain monoaminergic neurotransmitter and serum antioxidant status were examined in an animal model of depression [15, 16].

Table 1: Composition of Danggui-shaoyao-san (DSS).

Components	Ratio
(1) Dang gui (*Angelica sinensis* (Oliv.) Diels., root)	3
(2) Bai Shao (*Paeonia lactiflora* Pall., root)	16
(3) Fu Ling (*Poria cocos* (Schw.) Wolf., fungus nucleus)	4
(4) Bai Zhu (*Astractylodes macrocephala* Koidz., root and rhizome)	4
(5) Chuan Xiong (*Ligusticum chuanxiong* Hort., rhizome)	8
(6) Ze Xie (*Alisma orientale* (Sam.) Juzep., rhizome)	8

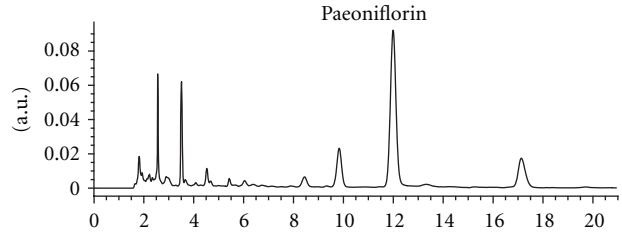

Figure 1: High-performance liquid chromatography analysis of DSS.

2. Materials and Methods

2.1. DSS Preparation. All the crude drugs of DSS were purchased from Zhejiang Provincial Hospital of Traditional Chinese Medicine (Zhejiang Province, China). They were identified and authenticated by Associate Professor KR. Chen, College of Pharmacy, Zhejiang Chinese Medicine University, where voucher specimens (number 100925) had been kept. Aqueous extract of DSS was prepared as following procedure of Kou et al. [12]. In brief, six medicinal materials were mixed in proportion and were macerated for 1 h with eight volumes of distilled water and then decocted for 1.5 h. Next, the cooled extract was filtered. The extraction procedure was repeated twice. The extracted fractions were pooled and concentrated using a rotary evaporator. The yield of the extract was 29.32% on dry weight basis. DSS extract contained 1.43% of paeoniflorin as analyzed by high-performance liquid chromatography (Figure 1). HPLC analytical conditions were as follows: a Waters Nova-Pak C18 HPLC column (4.6 × 250 mm) was used for the separation. Separation was achieved by an isocratic elution with a mobile phase consisted of acetonitrile and 0.04% phosphoric acid (16 : 84, v/v) at a flow rate of 1.0 mL/min. The eluate was monitored by a diode array detector at wavelength of 230 nm.

2.2. Chemical Reagents. 5-Hydroxytryptamine (5-HT), noradrenaline (NA), and dopamine (DA) were purchased from Sigma-Aldrich (St. Louis, MO). Paeoniflorin was purchased from National Institute for the Control of Pharmaceutical and Biological Products (Beijing, China). Other reagents were analytical grades made in PR China.

2.3. Animals. Male ICR mice weighing 20–25 g were obtained from the Laboratory Animal Services Center, Zhejiang Chinese Medicine University, Hangzhou, Zhejiang. The animals were individually maintained on a 12 h light/dark cycle (lights on at 6:00 a.m., lights off at 6:00 p.m.) under controlled temperature conditions (22 ± 2°C) and given standard food and water *ad libitum*. They were allowed to acclimatize for seven days before use. All experiments conformed to the guidelines of the "Principles of Laboratory Animal Care" (NIH publication number 80-23, revised 1996) and the legislation of the People's Republic of China for the use and care of laboratory animals. The experimental protocols were approved by the Animal Experimentation Ethics Committee of Zhejiang Chinese Medicine University. Effort was made to minimize the number and suffering of the animals.

2.4. Reversal of Reserpine-Induced Ptosis in Mice. The animals were randomly assigned into five groups of eight individuals: control group (physiological saline), control plus DSS-H group (3 g/kg), reserpine plus vehicle group (physiological saline), reserpine plus DSS-L group (1.5 g/kg), and reserpine plus DSS-H group (3 g/kg). DSS and physiological saline were given intragastrically daily between 9:30 to 10:30 a.m. for seven days. The doses used in the present study were selected on the basis of Xu et al. [14] and our preliminary tests. Sixty minutes after the last dose, mice in reserpine groups were injected intraperitoneally with 2.5 mg/kg of reserpine. The degree of ptosis of each animal was recorded at 60 min after the injection of reserpine. For the evaluation of ptosis, mice were placed on a shelf (20 cm above the bench top). The degree of ptosis was rated according to the following rating scale: 0, eyes open; 1, one-quarter closed; 2, half closed; 3, three-quarters closed; 4, completely closed [17].

2.5. Chronic Unpredictable Stress (CUS). Mice were randomly assigned into four groups of eight individuals: control group, CUS plus vehicle group (physiological saline), CUS plus DSS-L group (1.5 g/kg), and CUS plus DSS-H group (3 g/kg). The CUS procedure was performed as described by Mao et al. [6], with a slight modification. Briefly, mice in stressed groups were individually housed and exposed to the following stressors once daily for 21 days: 24 h food deprivation, 24-h water deprivation, 7 h cage tilt (45°), 24 h exposure to a foreign object (e.g., a piece of plastic), 1 min tail pinch (1 cm from the end of the tail), 21 h soiled cage (200 mL water in 100 g sawdust bedding), and overnight illumination. DSS and physiological saline were given intragastrically 30 min before each stressor once every day for 21 days. Control (unstressed) animals were undisturbed except for necessary procedures such as routine cage cleaning.

2.6. Sucrose Preference Test. Sucrose preference test was carried out 1 day after CUS starting at 09:30 am. The test was performed as described previously [18] with minor modifications. Briefly, 72 h before the test, mice were trained to adapt 1% sucrose solution (w/v): two bottles of 1% sucrose solution were placed in each cage, and 24 h later 1% sucrose

in one bottle was replaced with tap water for 24 h. After adaptation, mice were deprived of water and food for 12 h, followed by the sucrose preference test, in which mice were free to access to two bottles containing 100 mL of 1% sucrose and 100 mL of tap water, respectively. After 1 h, the volumes of consumed sucrose solution and water were recorded, and sucrose preference was calculated as calculated using the following formula:

$$\text{Sucrose preference} = \frac{\text{Sucrose consumption}}{\text{Water consumption} + \text{sucrose consumption}} \times 100\%. \quad (1)$$

2.7. Blood and Tissue Collection. Twenty-four hours after the behavioral test (2 days after CUS), between 09:30 am to 11:30 am, mice were sacrificed by decapitation to obtain venous blood samples on ice. Different groups of mice were used for each time point. Serum was separated by centrifugation at 4000 g for 10 min at 4°C and stored at −80°C until assay. Following blood collection, their whole brains were quickly removed, frozen in liquid nitrogen and stored at −80°C until assayed.

2.8. Measurement of Monoamine Neurotransmitter Levels. Brain 5-HT, NA, and DA levels were measured by HPLC coupled with electrochemical detection method as described previously [19]. Briefly, each frozen tissue sample was homogenized by ultrasonication in 200 Al of 0.4 M perchloric acid (solution A). The homogenate was kept on ice for 1 h and then centrifuged at 12,000 g (4°C) for 20 min. The pellet was discarded. An aliquot of 160 μL of supernatant was added to 80 μL of solution B (containing 0.2 M potassium citrate, 0.3 M dipotassium hydrogen phosphate, and 0.2 M EDTA). The mixture was kept on ice for 1 h and then centrifuged at 12,000 g (4°C) for 20 min again. Twenty μL of the resultant supernatant was directly injected into an ESA liquid chromatography system equipped with a reversed-phase C18 column (150 4.6 mm I.D., 5 μm) and an electrochemical detector (ESA CoulArray, Chelmstord, MA, USA.). The detector potential was set at 50, 100, 200, 300, 400, and 500 mV, respectively. The mobile phase consisted of 125 mM citric acid-sodium citrate (pH 4.3), 0.1 mM EDTA, 1.2 mM sodium octanesulfonate, and 16% methanol. The flow rate was 1.0 mL/min. 5-HT, NA, and DA were identified and quantified by comparing their retention times and peak areas to those of standard solutions. The contents of 5-HT, NA, and DA were expressed as ng/g wet weight tissue.

2.9. Measurement of MDA Level and SOD Activity. Serum MDA level was determined by measuring thiobarbituric-acid reacting substances [20]. Serum SOD was determined based on its ability to inhibit the oxidation of oxymine by O^{2-} produced from the xanthine/xanthine oxidase system [21]. Protein concentration was determined by the Coomassie blue protein binding [22] using bovine serum albumin (BSA) as a standard. The detailed procedures of measurements followed the manufacture instruction in different reagent kits (Nanjing Jiancheng Institute of Biological Engineering, China).

Table 2: Effect of DSS on reserpine-induced ptosis in mice.

Treatment	Ptosis mean score
Control	0.0
Control + DSS-H	0.0
Reserpine + vehicle	$2.2 \pm 0.4^{\#\#}$
Reserpine + DSS-L	$0.4 \pm 0.3^{**}$
Reserpine + DSS-H	$0.5 \pm 0.3^{**}$

Values given are the mean ± SEMs ($n = 8$).
$^{\#\#}P < 0.01$ as compared with the control; $^{**}P < 0.01$ as compared with the reserpine-treated control.

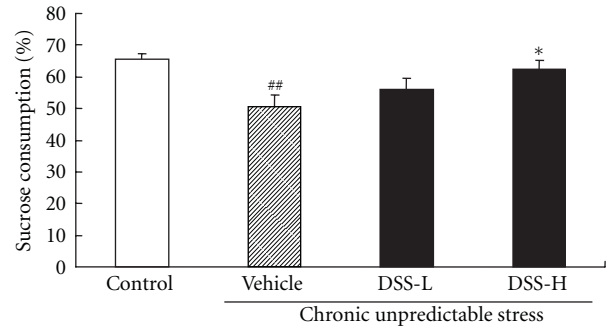

Figure 2: Effect of DSS treatment on the percentage of sucrose consumption in CUS-treated mice. Values given are the mean ± SEMs ($n = 8$). $^{\#\#}P < 0.01$ as compared with the nonstressed control; $^{*}P < 0.05$ as compared with the CUS-treated control.

2.10. Statistical Analysis. Data are expressed as means ± SEM. Significant differences between means were performed using one-way analysis of variance (ANOVA) followed by Dunnett's test. A difference was considered statistically significant when $P < 0.05$.

3. Results

The effect of DSS on reserpine-induced ptosis in mice was given in Table 2. One-way ANOVA showed a significant difference on the mean score of ptosis among groups ($F(4, 35) = 97.9$, $P < 0.01$). Treating the animals with DSS-H did not provide any significant change on the mean score of ptosis when compared with the controls. The reserpine injections resulted in a significant increase in the mean score of ptosis in the animals ($P < 0.01$) compared with the controls. Treating the animals with DSS-L or DSS-H significantly decreased the mean score of ptosis in the reserpine-treated mice ($P < 0.01$ and $P < 0.01$, resp.) compared with the reserpine-treated control.

The effect of DSS on the percentage of sucrose consumption in CUS-treated mice was given in Figure 2. One-way ANOVA showed a significant difference on the percentage of sucrose consumption among groups ($F(3, 28) = 6.3$, $P < 0.01$). A 21-day CUS exposure significantly reduced

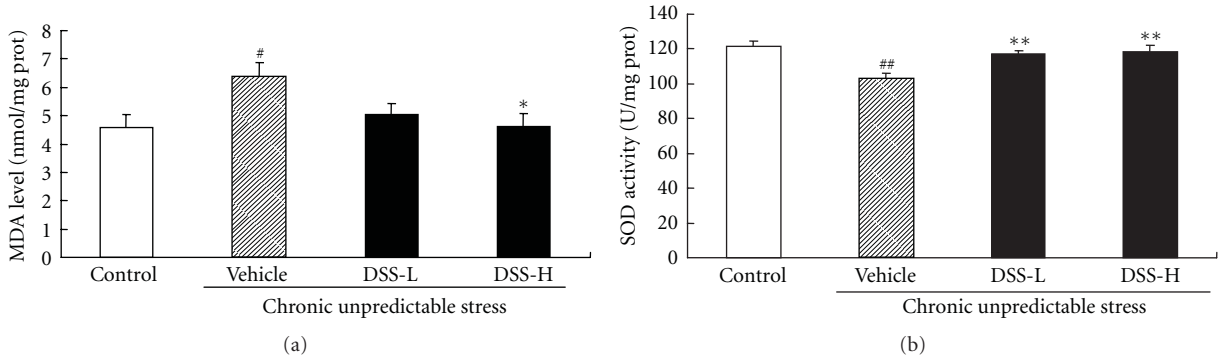

Figure 3: Effect of DSS treatment on serum antioxidant status in CUS-treated mice. The antioxidant status was assessed by measuring MDA level (a) and SOD activity (b). Values given are the mean ± SEMs ($n = 8$). $^{\#}P < 0.05$; $^{\#\#}P < 0.01$ as compared with the nonstressed control; $^{*}P < 0.05$; $^{**}P < 0.01$ as compared with the CUS-treated control.

the percentage of sucrose consumption in the animals ($P < 0.01$) compared with the control (i.e., non-CUS-treated mice). Long-term treatment with DSS-H significantly increased the percentage of sucrose consumption in CUS-treated mice ($P < 0.05$) compared with the CUS-treated control.

The effect of DSS on brain monoamine neurotransmitter levels in CUS-treated mice was given in Table 3. One-way ANOVA showed a significant difference on the concentrations of 5-HT, NA, and DA in mouse brain among groups ($F(3, 28) = 12.9$, $P < 0.01$, $F(3, 28) = 21.6$, $P < 0.01$, and $F(3, 28) = 3.7$, $P < 0.05$, resp.). A 21-day CUS exposure significantly decreased the concentrations of 5-HT, NA, and DA in mouse brain ($P < 0.01$, $P < 0.01$, and $P < 0.05$, resp.) compared with those of the controls. DSS-H treatment significantly increased the concentrations of NA and DA in brain of CUS-treated mice ($P < 0.01$ and $P < 0.01$, resp.) compared with the CUS-treated control, while DSS treatment did not produce a significant influence on brain 5-HT concentrations.

The effect of DSS on serum antioxidant status in CUS-treated mice was given in Figure 3. The antioxidant status was assessed by measuring MDA level (Figure 3(a)) and SOD activity (Figure 3(b)). One-way ANOVA showed a significant difference on MDA level and SOD activity among groups ($F(3, 28) = 4.1$, $P < 0.05$, and $F(3, 28) = 7.6$, $P < 0.05$, resp.). A 21-day CUS exposure significantly increased MDA level ($P < 0.05$) and reduced SOD activity ($P < 0.01$) when compared with those of the controls. DSS-L or DSS-H treatment significantly increased SOD activity in CUS-treated mice ($P < 0.05$ and $P < 0.01$, resp.) compared with the CUS-treated control. DSS-H treatment also significantly decreased MDA level in CUS-treated mice ($P < 0.05$) compared with the CUS-treated control.

Table 3: Effect of DSS treatment on brain monoamine neurotransmitter levels in CUS-treated mice.

Treatment	5-HT (ng/g)	NA (ng/g)	DA (ng/g)
Control	1016.2 ± 43.1	1433.5 ± 66.7	1444.4 ± 59.8
CUS + vehicle	713.2 ± 18.4$^{\#\#}$	1012.2 ± 34.6$^{\#\#}$	1254.8 ± 38.6$^{\#}$
CUS + DSS-L	779.0 ± 47.9	1002.7 ± 33.4	1369.8 ± 19.1
CUS + DSS-H	831.0 ± 27.4	1181.8 ± 27.2*	1445.1 ± 56.6*

Brain monoamine neurotransmitter levels were obtained by using HPLC coupled with electrochemical detection method. Values given are the mean ± SEMs ($n = 8$).
$^{\#}P < 0.05$; $^{\#\#}P < 0.01$ as compared with the nonstressed control; $^{*}P < 0.05$ as compared with the CUS-treated control.

4. Discussion

Several hypotheses have been suggested for the pathological mechanism of depression. The early hypothesis of depression, namely the monoamine hypothesis, supposed that the main symptoms of depression were due to the functional deficiency of brain monoamine neurotransmitters such as 5-HT, NA, and/or DA [23]. Consistent with this view, drugs that are acted by increasing the bioavailability of brain monoamine neurotransmitters, such as tricyclic antidepressants, selective serotonin reuptake inhibitors, and monoamine oxidase inhibitors, are widely used in clinical depression treatment [24]. The reserpine-induced depression is animal model based on the monoamine hypothesis of depression. Reserpine can irreversibly inhibit the vesicular uptake of monoamines, including noradrenaline, dopamine, and 5-hydroxytrytamine. As a consequence, ptosis and hypothermia are observed as the depletion of monoamines stores [25, 26]. These syndromes can be antagonized by major classes of antidepressant drugs. In this study, pretreating mice with DSS for 7 days significantly antagonized reserpine-induced ptosis, suggesting that the antidepressant effect of DSS may be mediated via central monoaminergic neurotransmitter system.

Several studies suggest that CUS can induce behavioral and physiological changes resembling symptoms of clinical depression [8, 15, 16, 27–29] and that CUS-induced depression model can be used for evaluating the efficacy of antidepressants through the sucrose preference test [8, 16, 19, 27–29]. The sucrose preference test is an indicator

of anhedonia-like behavioral change [16]. Anhedonia, a core symptom of major depression, is modeled by inducing a decrease in responsiveness to rewards reflected by reduced consumption of and/or preference for sweetened solutions [16]. The results of the present study showed that mice subjected to a 21-day period of CUS consumed less sucrose solution when compared to nonstressed mice, while long-term treatment with DSS significantly suppressed this behavioral change. Although we did not use a conventional antidepressant as positive control in this study, the CUS-induced depression model is generally thought to be the most valuable and steady depressive model in animals and has been successfully established in our previous studies [6, 18].

To further investigate the antidepression mechanisms of DSS, the effects of DSS on the monoamine neurotransmitter systems in CUS-treated mice were studied. Our results showed that CUS caused significant decreases of 5-HT, NA, and DA levels in mouse brain which were consistent with other studies [30–34], while DSS treatment significantly increased the concentrations of NA and DA, but not 5-HT, in brain of CUS-treated mice. Moreover, previous reports have shown that DSS increased the levels of brain monoamine neurotransmitters in normal mice as well as in aged mice [12, 35]. These results suggested that the antidepressant-like effect of DSS may be related to the monoamine neurotransmitter systems, particularly NA and DA systems.

Recent studies have shown that reactive oxygen species (ROS) also play a role in the pathogenesis of depression [3, 4]. Previous studies have demonstrated that chronic stress caused a significant increase in the production of ROS [36]. Excessive ROS can cause damages to the major macromolecules in cells, including lipids, proteins, and nucleic acids, culminating in neuronal dysfunction and depression [8, 37]. MDA, a by product of lipid peroxidation, is produced under oxidative stress. It indicates the oxidative damages of the plasma membrane and resultant thiobarbituric acid reactive substances, which are proportional to lipid peroxidation and oxidant stress [38]. It has been reported that brain MDA level was significantly increased in rodents exposed to chronic stress, which could be reversed by antidepressants [6, 7, 36, 39]. There is an intrinsic antioxidant defense system in cells for scavenging ROS to prevent cellular damage. SOD, one of the most important antioxidant enzymes, has been shown to directly catalyze the transformation of peroxides and superoxide to nontoxic species [40]. Previous studies have showed that chronic stress caused a significant decrease in brain SOD activity in rodents, and antidepressant treatment was found to restore the level of SOD [5, 36]. Consistently, the present study showed that 21-day CUS caused a marked increase in oxidative stress as characterized by excessive MDA production and a reduction in SOD activity. However, DSS treatment attenuated these changes in the CUS-treated mice, suggesting that the antidepressant-like effect of DSS may be related to its antioxidant activity.

It has been shown that oxidation of monoamine neurotransmitters by monoamine oxidase might result in increased radical burden [41, 42]. On the other hand, ROS has been shown to modulate the synaptic transmission, resulting in decreasing DA release [39]. The foregoing findings suggest an association between monoamine oxidation and overproduction of ROS in the pathogenesis of depression. It has been suggested that the antidepressant-like effect of antioxidant is mediated via the monoaminergic system [43]. The present study also suggested a correlation between the monoamine system and oxidative stress in CUS-treated mice. This finding was consistent with previous studies [5, 6, 44].

In conclusion, the antidepressant-like effect of DSS may be mediated by the modulation of central monoaminergic neurotransmitter systems and the inhibition of oxidative stress. Further investigation on the interaction among the component herbs of DSS is warranted.

Acknowledgment

This study was supported by the Zhejiang Provincial Program for the Cultivation of High-level Innovative Health talents (awarded to Z. Huang).

References

[1] E. J. Nestler, M. Barrot, R. J. DiLeone, A. J. Eisch, S. J. Gold, and L. M. Monteggia, "Neurobiology of depression," *Neuron*, vol. 34, no. 1, pp. 13–25, 2002.

[2] L. Savegnago, C. R. Jesse, L. G. Pinto, J. B. T. Rocha, C. W. Nogueira, and G. Zeni, "Monoaminergic agents modulate antidepressant-like effect caused by diphenyl diselenide in rats," *Progress in Neuro-Psychopharmacology and Biological Psychiatry*, vol. 31, no. 6, pp. 1261–1269, 2007.

[3] M. Bilici, H. Efe, M. A. Köroğlu, H. A. Uydu, M. Bekaroğlu, and O. Değer, "Antioxidative enzyme activities and lipid peroxidation in major depression: alterations by antidepressant treatments," *Journal of Affective Disorders*, vol. 64, no. 1, pp. 43–51, 2001.

[4] S. D. Khanzode, G. N. Dakhale, S. S. Khanzode, A. Saoji, and R. Palasodkar, "Oxidative damage and major depression: the potential antioxidant action of selective serotonin-re-uptake inhibitors," *Redox Report*, vol. 8, no. 6, pp. 365–370, 2003.

[5] Y. Chen, H. D. Wang, X. Xia, H. F. Kung, Y. Pan, and L. D. Kong, "Behavioral and biochemical studies of total furocoumarins from seeds of Psoralea corylifolia in the chronic mild stress model of depression in mice," *Phytomedicine*, vol. 14, no. 7-8, pp. 523–529, 2007.

[6] Q. Q. Mao, S. P. Ip, K. M. Ko, S. H. Tsai, Y. F. Xian, and C. T. Che, "Effects of peony glycosides on mice exposed to chronic unpredictable stress: further evidence for antidepressant-like activity," *Journal of Ethnopharmacology*, vol. 124, no. 2, pp. 316–320, 2009.

[7] A. Zafir and N. Banu, "Antioxidant potential of fluoxetine in comparison to Curcuma longa in restraint-stressed rats," *European Journal of Pharmacology*, vol. 572, no. 1, pp. 23–31, 2007.

[8] Z. Zhao, W. Wang, H. Guo, and D. Zhou, "Antidepressant-like effect of liquiritin from Glycyrrhiza uralensis in chronic variable stress induced depression model rats," *Behavioural Brain Research*, vol. 194, no. 1, pp. 108–113, 2008.

[9] W. W. Shang and S. Y. Qiao, "Advances on the study of Danggui Shaoyao powder," *Journal of Chinese Materia Medica*, vol. 31, no. 8, pp. 630–633, 2006.

[10] D. Y. Li, "Clinical analysis of Danggui Shaoyao San in treatment of 30 patients with insomnia," *China Journal of Modern Medicine*, vol. 20, no. 24, pp. 3787–3789, 2010.

[11] W. R. Pigeon, "Insomnia as a predictor of depression: do insomnia subtypes matter?" *Sleep*, vol. 33, no. 12, pp. 1585–1586, 2010.

[12] J. Kou, D. Zhu, and Y. Yan, "Neuroprotective effects of the aqueous extract of the Chinese medicine Danggui-Shaoyao-san on aged mice," *Journal of Ethnopharmacology*, vol. 97, no. 2, pp. 313–318, 2005.

[13] Z. Y. Hu, G. Liu, H. Yuan et al., "Danggui-Shaoyao-San and its active fraction JD-30 improve Aβ-induced spatial recognition deficits in mice," *Journal of Ethnopharmacology*, vol. 128, no. 2, pp. 365–372, 2010.

[14] F. Xu, D. Peng, C. Tao et al., "Anti-depression effects of Danggui-Shaoyao-San, a fixed combination of Traditional Chinese Medicine, on depression model in mice and rats," *Phytomedicine*, vol. 18, no. 13, pp. 1130–1136, 2011.

[15] R. J. Katz, K. A. Roth, and K. Schmaltz, "Amphetamine and tranylcypromine in an animal model of depression: pharmacological specificity of the reversal effect," *Neuroscience and Biobehavioral Reviews*, vol. 5, no. 2, pp. 259–264, 1981.

[16] P. Willner, "Validity, reliability and utility of the chronic mild stress model of depression: a 10-year review and evaluation," *Psychopharmacology*, vol. 134, no. 4, pp. 319–329, 1997.

[17] Q. Mao, Z. Huang, S. Ip, and C. Che, "Antidepressant-like effect of ethanol extract from paeonia lactiflora in mice," *Phytotherapy Research*, vol. 22, no. 11, pp. 1496–1499, 2008.

[18] Q. Q. Mao, S. P. Ip, K. M. Ko, S. H. Tsai, and C. T. Che, "Peony glycosides produce antidepressant-like action in mice exposed to chronic unpredictable mild stress: effects on hypothalamic-pituitary-adrenal function and brain-derived neurotrophic factor," *Progress in Neuro-Psychopharmacology and Biological Psychiatry*, vol. 33, no. 7, pp. 1211–1216, 2009.

[19] X. Xia, G. Cheng, Y. Pan, Z. H. Xia, and L. D. Kong, "Behavioral, neurochemical and neuroendocrine effects of the ethanolic extract from Curcuma longa L. in the mouse forced swimming test," *Journal of Ethnopharmacology*, vol. 110, no. 2, pp. 356–363, 2007.

[20] H. Ohkawa, N. Ohishi, and K. Yagi, "Assay for lipid peroxides in animal tissues by thiobarbituric acid reaction," *Analytical Biochemistry*, vol. 95, no. 2, pp. 351–358, 1979.

[21] J. M. McCord and I. Fridovich, "Superoxide dismutase: the first twenty years (1968–1988)," *Free Radical Biology and Medicine*, vol. 5, no. 5-6, pp. 363–369, 1988.

[22] M. M. Bradford, "A rapid and sensitive method for the quantitation of microgram quantities of protein utilizing the principle of protein dye binding," *Analytical Biochemistry*, vol. 72, no. 1-2, pp. 248–254, 1976.

[23] J. J. Schildkraut, "The catecholamine hypothesis of affective disorders: a review of supporting evidence," *The American Journal of Psychiatry*, vol. 122, no. 5, pp. 509–522, 1965.

[24] N. Bouvier, T. Trenque, and H. Millart, "The development of antidepressants: experience and prospects," *Presse Medicale*, vol. 32, no. 11, pp. 519–522, 2003.

[25] M. Bourin, M. Poncelet, R. Chermat, and P. Simon, "The value of the reserpine test in psychopharmacology," *Arzneimittel-Forschung/Drug Research*, vol. 33, no. 8, pp. 1173–1176, 1983.

[26] B. Yan, D. Y. Wang, D. M. Xing et al., "The antidepressant effect of ethanol extract of radix puerariae in mice exposed to cerebral ischemia reperfusion," *Pharmacology Biochemistry and Behavior*, vol. 78, no. 2, pp. 319–325, 2004.

[27] S. Li, C. Wang, M. Wang, W. Li, K. Matsumoto, and Y. Tang, "Antidepressant like effects of piperine in chronic mild stress treated mice and its possible mechanisms," *Life Sciences*, vol. 80, no. 15, pp. 1373–1381, 2007.

[28] J. Y. Guo, C. Y. Li, Y. P. Ruan et al., "Chronic treatment with celecoxib reverses chronic unpredictable stress-induced depressive-like behavior via reducing cyclooxygenase-2 expression in rat brain," *European Journal of Pharmacology*, vol. 612, no. 1-3, pp. 54–60, 2009.

[29] J. Y. Guo, H. R. Huo, L. F. Li, S. Y. Guo, and T. L. Jiang, "Sini Tang prevents depression-like behavior in rats exposed to chronic unpredictable stress," *American Journal of Chinese Medicine*, vol. 37, no. 2, pp. 261–272, 2009.

[30] L. An, Y. Z. Zhang, N. J. Yu et al., "Role for serotonin in the antidepressant-like effect of a flavonoid extract of Xiaobuxin-Tang," *Pharmacology Biochemistry and Behavior*, vol. 89, no. 4, pp. 572–580, 2008.

[31] S. Bekris, K. Antoniou, S. Daskas, and Z. Papadopoulou-Daifoti, "Behavioural and neurochemical effects induced by chronic mild stress applied to two different rat strains," *Behavioural Brain Research*, vol. 161, no. 1, pp. 45–59, 2005.

[32] H. Dang, Y. Chen, X. Liu et al., "Antidepressant effects of ginseng total saponins in the forced swimming test and chronic mild stress models of depression," *Progress in Neuro-Psychopharmacology and Biological Psychiatry*, vol. 33, no. 8, pp. 1417–1424, 2009.

[33] M. Konstandi, E. Johnson, M. A. Lang, M. Malamas, and M. Marselos, "Noradrenaline, dopamine, serotonin: different effects of psychological stress on brain biogenic amines in mice and rats," *Pharmacological Research*, vol. 41, no. 3, pp. 341–346, 2000.

[34] N. Sheikh, A. Ahmad, K. B. Siripurapu, V. K. Kuchibhotla, S. Singh, and G. Palit, "Effect of Bacopa monniera on stress induced changes in plasma corticosterone and brain monoamines in rats," *Journal of Ethnopharmacology*, vol. 111, no. 3, pp. 671–676, 2007.

[35] T. Itoh, S. Murai, H. Saito, and Y. Masuda, "Effects of single and repeated administrations of Toki-shakuyaku-san on the concentrations of brain neurotransmitters in mice," *Methods and Findings in Experimental and Clinical Pharmacology*, vol. 20, no. 1, pp. 11–17, 1998.

[36] G. Lucca, C. M. Comim, S. S. Valvassori et al., "Effects of chronic mild stress on the oxidative parameters in the rat brain," *Neurochemistry International*, vol. 54, no. 5-6, pp. 358–362, 2009.

[37] I. Niebrój-Dobosz, D. Dziewulska, and H. Kwieciński, "Oxidative damage to proteins in the spinal cord in amyotrophic lateral sclerosis (ALS)," *Folia Neuropathologica*, vol. 42, no. 3, pp. 151–156, 2004.

[38] X. Xiao, J. Liu, J. Hu et al., "Protective effects of protopine on hydrogen peroxide-induced oxidative injury of PC12 cells via Ca^{2+} antagonism and antioxidant mechanisms," *European Journal of Pharmacology*, vol. 591, no. 1-3, pp. 21–27, 2008.

[39] B. T. Chen, M. V. Avshalumov, and M. E. Rice, "H_2O_2 is a novel, endogenous modulator of synaptic dopamine release," *Journal of Neurophysiology*, vol. 85, no. 6, pp. 2468–2476, 2001.

[40] K. K. Griendling and M. Ushio-Fukai, "Reactive oxygen species as mediators of angiotensin II signaling," *Regulatory Peptides*, vol. 91, no. 1-3, pp. 21–27, 2000.

[41] J. M. C. Gutteridge, "Lipid peroxidation and antioxidants as biomarkers of tissue damage," *Clinical Chemistry*, vol. 41, no. 12, pp. 1819–1828, 1995.

[42] H. Herken, A. Gurel, S. Selek et al., "Adenosine deaminase, nitric oxide, superoxide dismutase, and xanthine oxidase in patients with major depression: impact of antidepressant

treatment," *Archives of Medical Research*, vol. 38, no. 2, pp. 247–252, 2007.

[43] T. Posser, M. P. Kaster, S. C. Baraúna, J. B. T. Rocha, A. L. S. Rodrigues, and R. B. Leal, "Antidepressant-like effect of the organoselenium compound ebselen in mice: evidence for the involvement of the monoaminergic system," *European Journal of Pharmacology*, vol. 602, no. 1, pp. 85–91, 2009.

[44] J. M. Li, L. D. Kong, Y. M. Wang, C. H. K. Cheng, W. Y. Zhang, and W. Z. Tan, "Behavioral and biochemical studies on chronic mild stress models in rats treated with a Chinese traditional prescription Banxia-houpu decoction," *Life Sciences*, vol. 74, no. 1, pp. 55–73, 2003.

Hindawi Publishing Corporation
Evidence-Based Complementary and Alternative Medicine
Volume 2012, Article ID 605303, 20 pages
doi:10.1155/2012/605303

Review Article

From Omics to Drug Metabolism and High Content Screen of Natural Product in Zebrafish: A New Model for Discovery of Neuroactive Compound

Ming Wai Hung,[1,2] Zai Jun Zhang,[1,2] Shang Li,[1,2] Benson Lei,[2] Shuai Yuan,[1,2] Guo Zhen Cui,[1,2] Pui Man Hoi,[1,2] Kelvin Chan,[3,4] and Simon Ming Yuen Lee[1,2]

[1] *State Key Laboratory of Quality Research in Chinese Medicine, University of Macau, Avenue Padre Tomás Pereira S.J., Taipa, Macau, China*
[2] *Institute of Chinese Medical Sciences, University of Macau, Avenue Padre Tomás Pereira S.J., Taipa, Macau, China*
[3] *Faculty of Pharmacy, The University of Sydney, NSW 2006, Australia*
[4] *Centre for Complementary Medicine Research, University of Western Sydney, NSW 2560, Australia*

Correspondence should be addressed to Pui Man Hoi, maghoi@umac.mo and Simon Ming Yuen Lee, simonlee@umac.mo

Received 3 February 2012; Accepted 16 April 2012

Academic Editor: Karl Wah-Keung Tsim

The zebrafish (*Danio rerio*) has recently become a common model in the fields of genetics, environmental science, toxicology, and especially drug screening. Zebrafish has emerged as a biomedically relevant model for *in vivo* high content drug screening and the simultaneous determination of multiple efficacy parameters, including behaviour, selectivity, and toxicity in the content of the whole organism. A zebrafish behavioural assay has been demonstrated as a novel, rapid, and high-throughput approach to the discovery of neuroactive, psychoactive, and memory-modulating compounds. Recent studies found a functional similarity of drug metabolism systems in zebrafish and mammals, providing a clue with why some compounds are active in zebrafish *in vivo* but not *in vitro*, as well as providing grounds for the rationales supporting the use of a zebrafish screen to identify prodrugs. Here, we discuss the advantages of the zebrafish model for evaluating drug metabolism and the mode of pharmacological action with the emerging omics approaches. Why this model is suitable for identifying lead compounds from natural products for therapy of disorders with multifactorial etiopathogenesis and imbalance of angiogenesis, such as Parkinson's disease, epilepsy, cardiotoxicity, cerebral hemorrhage, dyslipidemia, and hyperlipidemia, is addressed.

1. Introduction

The zebrafish (*Danio rerio*) is a tropical freshwater fish that has become one of the most popular vertebrate model organisms in biological research. The zebrafish has traditionally been used as a model for studying developmental biology and embryology. Recently, zebrafish has become famous in the fields of genetics, environmental science, toxicological studies, and especially drug screening [1, 2].

Zebrafish are small, even adults are only 3-4 cm long, and are suitable, therefore, for animal studies in laboratories with limited space. Their high fecundity enables each adult female to produce hundreds of eggs per mating at intervals of only a few days. The embryos grow and develop rapidly. By 120 h after fertilization (hpf), the heart, liver, brain, pancreas, kidney, and other organs are completely developed. Zebrafish cardiovascular, nervous systems and metabolic pathways are highly similar to those of mammals at the anatomical, physiological, and molecular levels. The zebrafish genome is highly similar to the human genome, with approximately 87% similarity [2]. Their pharmacological response is comparable with that of human, suggesting applications in identifying test compounds with therapeutic potential. The larvae are only 1–4 mm long and can survive in a single well of a standard 384-well plate for several days by using the nutrients stored in the yolk sac. Assay studies require only

Table 1: Discrepancies and similarities of the effect of drugs in human and zebrafish.

Area of evaluation in zebrafish	Test compounds	Proportion of drugs with expected effects (%)	Reference
Inhibition of hERG or QTc prolongation	Study 1: Amiodarone, bepridil, cisapride, haloperidol, pimozide, procainamide, D,L-sotalol, terfenadine, thioridazine	All compounds, except for procainamide	[3]
	Study 2: Negative controls: amoxicillin, aspirin Positive controls: chlorpromazine, cisapride, cromakalim, isoprenaline, moxifloxacin, nicotine, verapamil	7 out of 9 compounds, including negative controls	[1]
Visual safety or optomotor response	Study 1: 27 compounds, including 19 with positive and 8 with negative effects on inhibition of optomotor response	About 70% in overall showed the predicted drug effects.	[4]
	Study 2: Negative control: aspirin Positive controls: chloroquine, chlorpromazine, diazepam, nicotine, ouabain, phenytoin, atropine, lithium	7 out of 9 compounds including negative control	[1]
Seizure liability	25 drugs including 17 positive and 8 negative controls	72% in overall	[5]
Gut contraction	Negative controls: aspirin and moxifloxacin Positive controls: amoxicillin, chlorpromazine, cisapride, cromakalim, isoprenaline, nicotine, nitrendipine, and verapamil	5 out of 10 compounds including negative controls	[1]

a small quantity (10–100 ng) of test compounds, such as small molecules, which are easily absorbed through the skin and gills, or directly by swallowing after 72 hpf. Early zebrafish embryos and larvae are optically transparent, which allows real-time imaging *in vivo*. These advantageous features combine and make zebrafish an ideal model for studying the biological activity profiling of natural products containing complex chemical components.

2. Relevance and Predictability of Drug Response between Zebrafish and Human

Using zebrafish as a model for drug screening will always raise the question of whether the beneficial effect of a drug lead compound observed in zebrafish would have clinical relevance. Although it has been shown that the zebrafish and human genomes are highly similar, a study should be done to compare the physiological response of human and zebrafish after exposure to a series of drugs. Mittelstadt has tested the effect of nine drugs with QT prolongation in zebrafish and found eight of these compounds (except procainamide) induced dissociation between the atrium and ventricular rates (Table 1) [3]. A similar study was done by Berghmans, who measured the atrial and ventricular rates of zebrafish in response to seven known QT-induced drugs and 2 negative controls and found that 7 of the 9 compounds, including the negative controls, showed the expected effects (Table 1) [1]. Two studies focused on the optomotor response were followed independently by Berghmans and Richards They both found zebrafish showed a high percentage of predictability (~78% and ~70%) of drug response (Table 1) [1, 4]. The zebrafish is also a good model for screening drugs with potential seizure liability. Winter reported the animal model offered 72% overall predictability as 13 out of 17 positive controls and 5 out of 8 negative controls showed their predicted effects (Table 1) [5]. Orally active anti-VEGF agents including sunitinib malate and ZM323881 effectively blocked hypoxia-induced retinal neovascularization in zebrafish. [6]. Two known antiangiogenic compounds, SU5416 and TNP470, which has shown antiangiogenic activity in mammalian system, have also demonstrated reduced vessel formation in zebrafish [7]. A range of known sedative compounds such as clozapine, fluoxetine, melatonin, diazepam, and pentobarbital have comparable response in zebrafish and all of these compounds resulted in reduced locomotor activity. [8–10]. Also, zebrafish also showed comparable responses to toxins for inducing pathologic consequences mimicking Parkinson's disease and epilepsy which will be addressed in later chapters. These evidences suggested that zebrafish demonstrate a good correlation with clinical relevance and support its potential as a model for pharmacological assessment [1, 3–5].

3. Similarity of Drug Metabolism between Zebrafish and Mammals: Omics Approach Provides a Clue

It is a common phenomenon that many compounds that occur naturally in metabolic tissues, such as liver and gastrointestinal tract, are inactive *in vitro* but are bioactivated *in vivo* into an active metabolite. One pioneer study with a zebrafish screen searched for cell-cycle modulators and identified 14 active candidates from a library of 2000 compounds (0.7% positive hits). The cell cycle-modulating activities of the active compounds identified from the zebrafish screen were validated in cell lines derived from both zebrafish and mammals [11]. Interestingly, only half of the active compounds were shown to be active in both embryos and either one of the cell lines, showing that some compounds are active in *in vivo* but inactive *in vitro*. The use of zebrafish for drug screening as well as for various pharmacological studies has received increasing attention

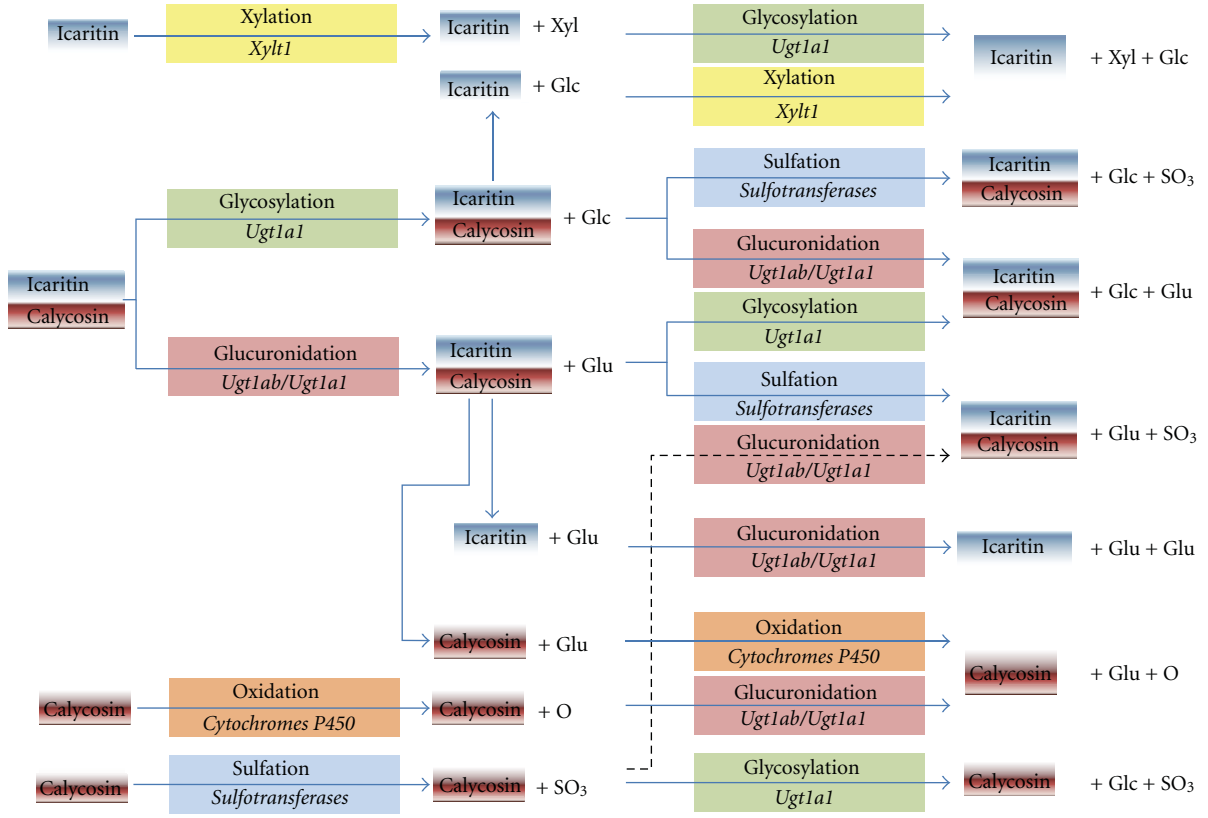

Figure 1: The metabolism of icaritin and calycosin in zebrafish embryos and larvae. The proposed routes of how icaritin and calycosin are metabolized in zebrafish embryos and larvae are summarized and some drug metabolism enzymes are identified by omics approach. The process and the corresponding gene are shown in each colored box. Glc: glycosylated group; Glu: glucuronidated group; Xyl: xylated group; SO_3: sulfonated group; *Xylt1*: Xylosyltransferase 1; *Ugt1a1*, *Ugt1ab*: UDP-glucuronosyltransferase.

in the fields of drug absorption, metabolism, distribution, and excretion [12]. However, there are few reports in the literature of detailed systematic studies investigating the fate of drugs after absorption as well as identification of the enzymes involved in drug metabolism in zebrafish larvae.

Our recent study addressed drug absorption and metabolism in zebrafish embryos and larvae. We used LC-MS/MS to identify and profile the metabolites of icaritin and its glycoside derivatives in zebrafish larvae [13]. Icaritin is a prenylated flavonoid compound that is regarded as an active ingredient of *Herba Epimedii*, which has been widely used in China as a medicinal herb for the treatment of infertility, osteoporosis, and weakness of the limbs. The result showed clearly that the metabolic pathway involving icaritin and its glycoside derivatives in zebrafish larvae is similar to that reported in mammals (Figure 1). The first step in the pathway is the enzymatic removal of the sugar moiety of these compounds after consumption in the cells of the gastrointestinal mucosa or by enzymes secreted by the colon flora [14]. Hydrolysis of the flavonoid derivative produces the free aglycone, which is conjugated by sulfation, glucuronidation, or methylation or in different combinations with steps that are controlled by phase II metabolism enzymes.

In order to investigate whether zebrafish larvae express the essential drug-metabolizing enzymes that are involved in the proposed metabolic pathways for the production of icaritin and its glycoside derivatives, combined transcriptomic and proteomic approaches were used to identify these enzymes [13]. In fact, transcriptomic profiling procedures identified 51 unique mRNA transcripts (out of a total of 13,310 nonredundant mRNA transcripts) that belong to three categories of key enzymes involved in phase I drug metabolism [15], including the cytochrome P450 family, flavin-containing monooxygenases, and epoxide hydrolases in zebrafish larvae. Moreover, mRNA transcripts of several key phase II drug metabolism enzymes [16], including UDP-glucuronosyltransferase, sulfotransferases, catechol-*O*-methyltransferase, and glutathione-*S*-transferases, were identified. However, the proteomic approach identified only three proteins (out of 2998 distinct proteins) that belong to the glutathione-*S*-transferases, a major type of phase II detoxification enzymes. The result illustrates that the metabolism of icaritin and its derivatives in both zebrafish larvae and mammalian models are highly conserved.

In addition, calycosin, an active constituent in Radix Astragali, was found to promote angiogenesis in zebrafish and human endothelial cells involving activation of the estrogen receptor and mitogen-activated protein kinase (MAPK) signaling pathway [17]. Our recently accepted paper characterizes drug absorption and metabolism using calycosin

as a probe in zebrafish larvae [18]. Ten metabolites of calycosin produced by glucuronidation, glycosylation, sulfation, oxidation, or combinations of any two of these metabolisms in zebrafish larvae were identified by LC-MS/MS (Figure 1). The results showed the kinetic changes of calycosin and its metabolites in zebrafish larvae. This study identified drug metabolites previously identified in mammals, reconfirming the conservation of drug metabolism systems in zebrafish and identified novel metabolites, providing insight into the possibility of the discovery of novel drug metabolite diversity in zebrafish. In addition, the abundance of calycosin and its metabolites were increased steadily during 24 h after treatment [18], which reflects the difference of common drug administration between zebrafish and mammals. Unlike the common drug administration routes, such as gastric irrigation and oral administration, used in rodents, the drug treatment for zebrafish was usually performed by keeping the whole fish in a drug-containing incubation medium. This method keeps the zebrafish in an environment of constant drug concentration and drug compounds are continuously taken into the body through both the GI tract and the respiratory systems. Future in-depth systematic investigation of absorption, distribution, metabolism, and excretion (ADME) in zebrafish is warranted.

The high similarity of phase I and phase II metabolisms in zebrafish may be attributed to the highly conserved genetic expression profiles in liver as well as gut microbiota with human and mice counterparts, respectively [19, 20]. Drug screening in other small invertebrate model organisms, such as the fruit fly *Drosophila melanogaster*, has identified some very promising lead compounds, particularly for antiaging [21]. Nonetheless, the proof of concept of the highly conserved drug metabolism between zebrafish and mammals strongly supports the usefulness of zebrafish as a vertebrate model rather than other invertebrate model organisms for drug discovery as well as drug metabolism studies.

4. Presence of Blood-Brain Barrier (BBB) in Zebrafish

The BBB is crucial for the maintenance of a stable environment with the regulation of ionic balance and nutrient transport and the blockage of potentially toxic molecules. The intrinsic complexity of the cell-matrix-cell interactions of the neural-vascular unit has made analysis of gene function difficult in cell culture, tissue explants, and even animal models. The zebrafish has emerged as a premier vertebrate model for analyzing the complex cellular interactions *in vivo* and the genetic mechanisms of embryonic development [22]. Brain endothelial cells show immunoreactivity to Claudin-5 and Zonula Occludens-1 (ZO-1), implying the presence of tight junctions in these cells. The expression of Claudin-5 and ZO-1 was detected in cerebral microvessels starting from 3 dpf, concomitant with maturation of the BBB [23]. Zhang et al. observed that zebrafish embryos develop BBB functions by 3 dpf, with earlier expression of Claudin-5 in the central arteries at 2 dpf [24].

Our recent study of the neuroprotective effect of quercetin shed light on the presence of functional BBB in zebrafish larvae at 3 dpf and the role of BBB permeability in determining the beneficial effect of a neuroprotective drug in Parkinson's disease (PD) in *in vivo*. Quercetin is one of the commonest naturally occurring flavonoids. Although it and structurally related flavonoids have been shown to have a neuroprotective capacity in various *in vitro* and *in vivo* experimental models [25–27], the neuroprotective effect of quercetin remains controversial. Nevertheless, quercetin did not protect substantia nigra neurons from an oxidative insult *in vivo*, probably due to inefficiency in passing through the BBB in *in vivo* conditions [28]. There is an urgent need for appropriate *in vivo* studies in order to confirm the neuroprotective effect of quercetin and to identify the reason for the discrepancy between findings *in vitro* and *in vivo*. In order to address this controversy, we administered quercetin at different maturation stages of the BBB in zebrafish and we found it can prevent but not rescue the DA neuronal injury induced by 6-OHDA [28]. When quercetin was administered to zebrafish larvae before 3 dpf when BBB is not well established, it could spread rapidly throughout the brain and exert a protective effect against 6-OHDA toxicity. However, when quercetin was administered to zebrafish after 3 dpf, the matured BBB posed an obstacle to quercetin entering the brain, preventing it from rescuing 6-OHDA insult in dopaminergic (DA) neurons. This result supports earlier findings of the presence of BBB in zebrafish by 72 hpf [23, 24].

5. Behaviour Screen in Zebrafish

Zebrafish displays learning, sleeping, drug addiction, and neurobehavioral phenotypes that are quantifiable and comparable with those in human [10, 29]. A zebrafish behavioural assay has been demonstrated as a novel, rapid, and high-throughput approach to the discovery of neuroactive, psychoactive, and memory-modulating compounds [30–32]. In the past, a major obstacle to the discovery of psychoactive drugs was the inability to predict how small molecules will alter complex behaviours. Recently, Rihel et al. reported that the multidimensional nature of zebrafish phenotypes enabled the hierarchical clustering of molecules with comparable effects. This behavioural profiling revealed conserved functions of psychotropic molecules and predicted the mechanism of action of poorly characterized compounds [30]. In addition, Kokel and his colleagues used automated screening assays to evaluate thousands of chemical compounds and found that diverse classes of neuroactive molecules led to distinct patterns of locomotor behaviour. They concluded that a zebrafish behaviour assay can rapidly identify novel psychotropic chemicals and predict their molecular targets [31].

6. Zebrafish Bioassay Screening for Selectivity

Toxicity is now the first obstacle to drug development. From 2003–2010, the overall success rate for drugs passing from Phase I to FDA approval was only 9% [33]. A high percentage of drug developments failed at different stages, including animal testing or clinical trial, owing to nontolerated side

effects and toxicity. As *in vitro* studies, which are usually cell based or molecular based, such as enzymatic or ligand-binding assays, drug screening with these assays predict the potential therapeutic action toward a specific molecular target and/or cell type; however, hidden toxicity and side effects due to interactions of the drug or its metabolites with other molecular targets, are not fully known.

Recently, a number of drugs were withdrawn from the market due to their human ether-a-gogo-related (hERG) cardiac toxicity [34]. The hERG potassium ion channel has a major role during the repolarization of the cardiac action potential, and the blockade of this ion channel can lead to prolongation of the QT interval, which is closely associated with torsade de pointes, a potentially lethal heart arrhythmia [35]. As a result, hERG (I_{Kr}) preclinical safety data are an essential part of any investigation of new drug submissions recommended in the FDA ICH guideline [36]. Zebrafish may present a good alternative model for large-scale screening of drug toxicity on QT prolongation through the ERG channel. hERG and its zebrafish homolog (zERG) have a high degree of similarity as zERG shows 99% conserved amino acid sequence in drug-binding and pore domains with the human ortholog [37]. Inhibition or knockdown of the zERG gene resulted in characteristic arrhythmia with 2 : 1 atrioventricular blockage (2 atrial beats coupled to 1 ventricular beat) [37]. The pharmaceutical industry has changed strategy by prescreening compound libraries for hERG cardiac toxicity before screening for therapeutic targets. According to the ICH S7A guidelines, CNS studies including behavior, learning and memory, neurochemistry, optomotor, and/or electrophysiology examinations are recommended before product approval [38]. Zebrafish may be a good model for the CNS assessment, since the animal possesses matched defined area in brain including hypothalamus and olfactory bulb [39]. The hippocampus was proposed to be located in the lateral zone of the pallium in zebrafish [39, 40]. In addition, important neurotransmitter systems such as the cholinergic, 5-hydroxytryptaminergic, dopaminergic, and noradrenergic pathways are also present in zebrafish brain [41, 42]. Zebrafish also has comparable neurological pharmacological response including locomotor activity [10], circadian pacemaking [43], and drug addiction [44] to human counterpart. These evidences support that zebrafish may be physiologically relevant model for screening out neurotoxic compounds.

Assessment of gastrointestinal complications may also be important during drug development, since the adverse reactions may result in death caused by gastrointestinal bleeding [45]. The zebrafish displayed similar physiology in gastrointestinal system with human. For example, the small intestine is lined with most of the cell types except Paneth cells [46, 47]; the peristalsis is controlled by a pair of smooth muscles and regulated by enteric nervous system [48]. However, it did not have a stomach [49] and a submucosa layer containing connective tissue to separate the epithelium from smooth muscle layer [46]. Moreover, in the study of the effect of 10 known compounds on gastrointestinal contraction in zebrafish, 5 out of 10 compounds showed expected effect [1] (Table 1). The relatively low predictability was due to the low reproducibility of cromakalim, nicotine, and nitrendipine in duplicated experiments [1] (Table 1). Nevertheless, zebrafish still has the potential for predicting adverse effects in gastrointestinal system [1]. There is increasing research on predicting the toxicity of a compound and excluding those compounds predicted to be toxic early in the drug discovery process [50].

Efficacy and toxicity are two important criteria for a drug to be marketed and the zebrafish model allows simultaneous measurement of these two parameters. The survival rate and/or mortality are/is a common and direct parameter used to indicate the toxicity of a compound. The beating heart of the embryo is the golden parameter used to indicate the living status of drug-treated zebrafish embryos. Thus, the lethal toxicity of a compound to zebrafish embryos reflected by the heartbeat rate could be monitored simultaneously with observation of the activity, such as antiangiogenesis, associated with the compound of interest. Moreover, other signs of toxicity, such as delayed development of zebrafish embryos, can be observed from the lower level of pigmentation in body and eyes, larger yolk sac, and shorter trunk in response to drug treatment. For instance, in our ongoing screening of antiangiogenesis activities of a series of methoxyflavone derivatives, we identified structural modification in a single chemical group of the same scaffold, which exhibited higher potency of antiangiogenic activity and lower toxicity to zebrafish embryos [51]. This pilot study serves as proof of concept, suggesting the advantage of zebrafish over HUVEC cells as an angiogenic assay is that the zebrafish allows content screening of both activity and *in vivo* toxicity.

Along with studying an antiangiogenic compound in zebrafish, we could evaluate the selectivity of molecular action, such as cell-cycle arrest, to blood vessel cells in a live organism. Zebrafish embryos were trypsinized into a live cell suspension which was stained with the DNA-staining dye DRAQ5 (Biostatus Ltd., UK) for subsequent cell-cycle analysis (Figure 2). The differential effect of the compound on the cell cycle of endothelial GFP-expressing cells and the non-GFP-expressing cells could be determined by flow cytometry. Using this technique, the resveratrol derivative *trans*-3,5,4′-trimethoxystilbene (TMS) was found to induce cell-cycle arrest more significantly in endothelial cells (in about 20–30% of GFP-positive cells and in only 5–10% of GFP-negative cells) in zebrafish embryos (Figure 3), confirming that TMS exerted a more specific cytotoxic effect on endothelial cells than on other cell types *in vitro* and, more importantly, *in vivo* [52]. However, there was still an overall increase in G2/M phase cells in the whole cell population, indicating that TMS caused cell-cycle arrest in some other cell types (Figure 3). This finding provides a solution to the controversial issue regarding whether resveratrol and related compounds cause cell-cycle arrest through the G1 or G2/M phase in cell culture *in vitro* [53]. This study in zebrafish embryos, which showed the induction of G2/M cell-cycle arrest in GFP-positive endothelial cells by TMS in a whole live organism, provides insight into the physiological relevance of the compound. The concept of determining selectivity of antiangiogenic action on zebrafish endothelial cells was supported by the results of a similar study, in which

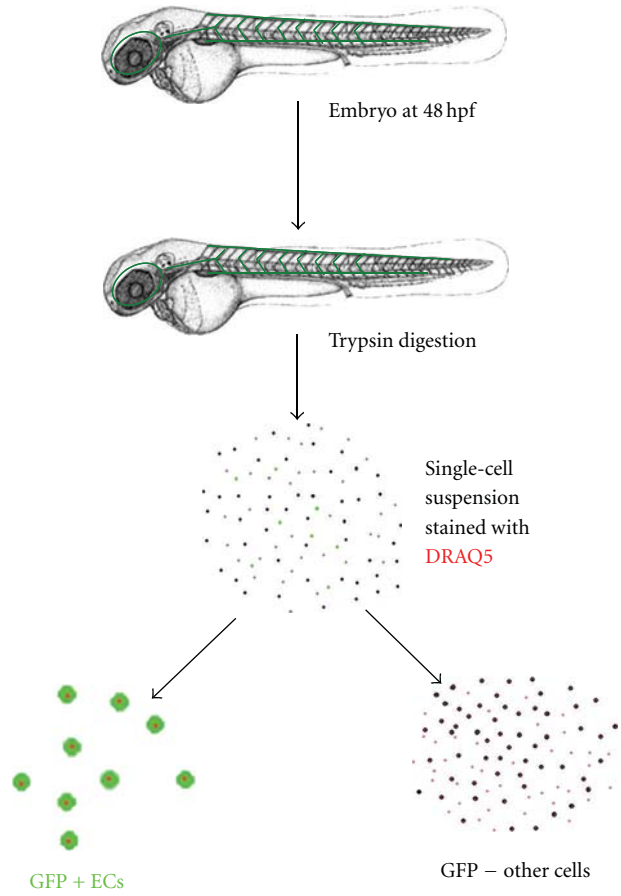

Figure 2: A diagram showing the processing of zebrafish embryos for isolating endothelial cells followed by staining with DRAQ5. Tg(fli-1:EGFP) zebrafish embryos are firstly trypsinized into a cell suspension, stained with DRAQ5, and separated into GFP expressing endothelial cells and others.

nobiletin (5,6,7,8,3′,4′-hexamethoxyflavone) exhibited an effect on cell-cycle arrest differently via inducing G0/G1 phase accumulation in GFP-positive endothelial cells [54]. Besides analysis of the cell cycle, a similar approach could probably be adopted to probe cells for different cellular physiological parameters, such as oxidative stress and mitochondrial function, by different stains. This approach allows examination of how a candidate selective drug may act on specific cell types in a live organism.

7. Phenomics and Biological Activity Profiling

Phenomics was originally an area of biology that involved studies of phenotype as a whole organism. Image-based bioassays reflecting changes of locomotor behaviour in the phenotype of different cell types, organs, and physiological systems in wildtype or transgenic zebrafish offer the opportunity to assess multiple pharmacological activities of a chemical compound (Figure 4). Pharmacological action of a compound could be decoded by a system biology approach through data mining of the multidimensional phenotypic data of an organism [55] together with measurement of the relative levels of mRNA transcripts (transcriptome), proteins (proteome), and metabolite components (metabolome). Recently, this omics approach has been incorporated increasingly into drug discovery and toxicology. Omics data provide much more information than typical phenotypic assay, including observable changes of morphology in the embryo as well as behaviour and mortality. By coupling omics data with an existing phenotypic end-point assay, more details of the mechanism and the toxicity of a chemical could be used to explain the cause-and-effect relationship. Even though the phenotypic changes are the same, such as vitellogenin, which indicate the estrogenic exposure in fish was upregulated by 17b-estradiol, bisphenol A, and genistein [56], the modes of action may differ. This possibility can be shown by differential gene expression induced by these chemicals based on transcriptome analysis [56].

8. Integrative Transcriptomic and Proteomic Analysis of Zebrafish

Because the therapeutic action of a drug on normalizing pathological change can originate from different cellular pathways in the complex regulatory network, an *in vivo* study could provide considerably more information than *in vitro* assays using purified targets. mRNA transcripts and proteins are the primary molecules responsible for biological

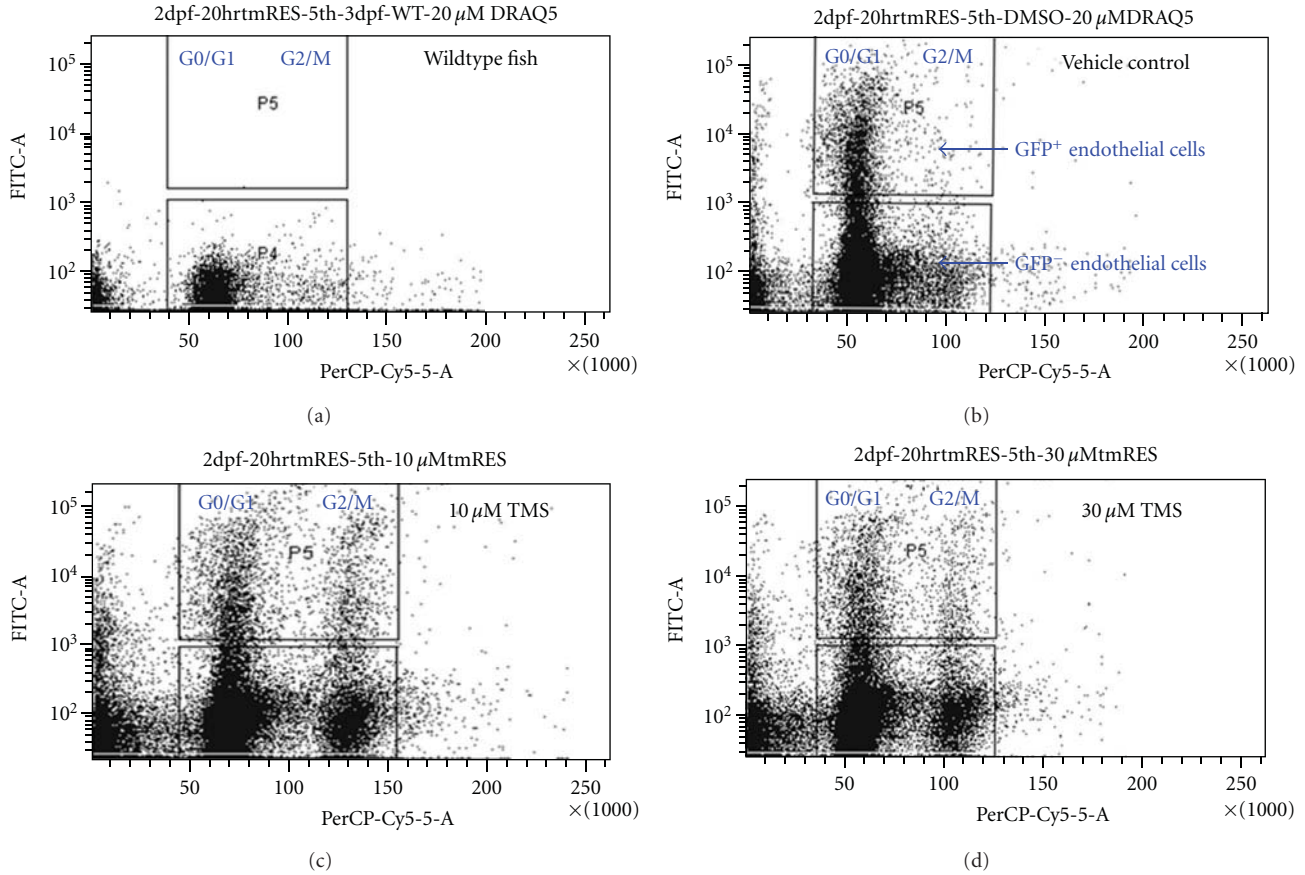

Figure 3: Cell-cycle analysis of zebrafish embryos after treatment with different concentration of an antiangiogenesis compound named trans-3,5,4′-trimethoxystilbene (TMS). Tg(fli-1:EGFP) zebrafish embryos treated with TMS for 20 h were then trypsinized and DRAQ5-stained for cell-cycle studies by flow cytometry. (a) Wildtype embryos did not show GFP-expressing-cells. (b) Tg(fli-1:EGFP) showed GFP expressing and non-GFP expressing cells. (c) 10 μM TMS and (d) 30 μM TMS exerted G2/M cell-cycle arrest preferentially in endothelial cells.

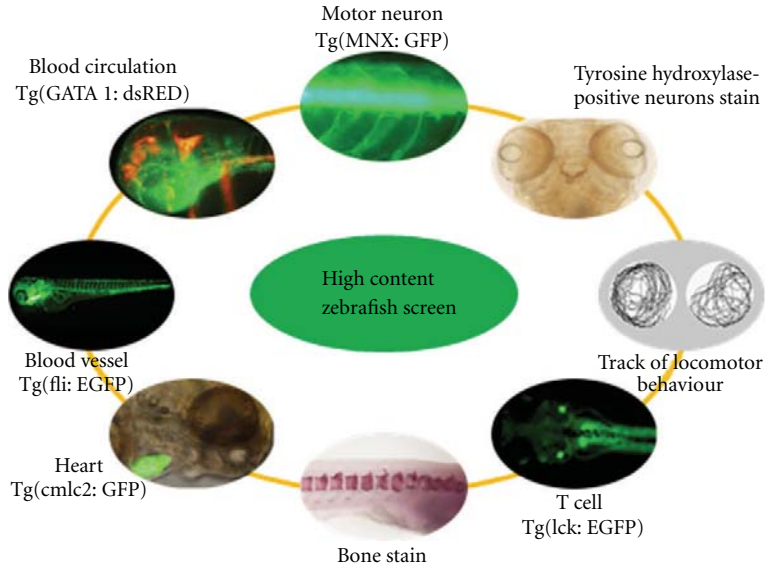

Figure 4: The examples of zebrafish model for high content drug screening. Image-based bioassays reflecting the physiological changes in either wildtype or transgenic zebrafish enable the assessment of multiple pharmacological activities of a chemical compound.

functions in cells and the ability to examine the transcriptome and the proteome of an organism provides a robust overview of the physiological changes taking place and could greatly augment target-oriented biological data. Therefore, we recently used an RNA-seq technology for transcriptome profiling and a fully automatable RP-RP 2DLC system for shotgun proteomics to address the drug metabolism system of zebrafish and the downstream transcriptional effect of a drug. The recent advancement of deep sequencing and 2D RP-RP LC-MS/MS technology identified a total of 12,560 mRNA transcripts (obtained from about 5 million reads per RNA sample) with matched annotated genes [13, 57] and 1752 unique proteins from the zebrafish lysate, respectively, in a single analysis [58].

The current transcriptome profiling tools used in zebrafish are microarray and RNA-seq. RNA-seq or deep sequencing of RNA samples using the next generation of sequencing technology is becoming a popular transcriptome profiling tool because it is an open platform that does not require predefined probes. In principle, RNA-seq profiles known and novel transcripts and it yields data with higher resolution, wider dynamic range, and lower background noise, while it only requires smaller amounts of RNA sample than microarrays [59].

By contrast, proteomic studies have used mainly integrated technologies, including separation of proteins by 2D polyacrylamide gel electrophoresis (2D-PAGE) and identification of proteins by matrix-assisted, laser desorption/ionization time-of-flight mass spectrometry (MALDI-TOF MS). Another major advantage of LC-MS/MS over conventional 2D PAGE is that the high sensitivity of LC allows for faster detection and direct identification of wider range of proteins, including high molecular weight proteins and very acidic or basic proteins, all of which are problematic when using methods such as 2D PAGE [58].

After transcriptomics, proteomics is often considered the next step in the study of biological systems. The integrated study of the two approaches is often considered as a study of causality. The focus is especially on identifying some biological response that initiates at the transcriptional level and exhibits functional information at the protein level. Transcriptomics has advantages over proteomics by allowing larger scale and higher throughput of analysis and about 10 times more coverage of detected gene targets in a single run of a zebrafish sample, while proteomics has advantages over transcriptomics in terms of potentially observing functional change in protein expression and posttranslational levels.

The methodology of conventional immunology depends on the availability of antibodies and *a priori* knowledge of the targets and, in general, is not amenable to global monitoring. Moreover, it is now known that the transcript level is often not correlated with the protein expression level, and the proteomic approach defines responses at the protein level that are probably not regulated at the transcription level, thus providing additional information [60]. Therefore, utilization of integrated transcriptomics and proteomics could provide more confirmatory evidence for the identification of molecular targets involved in the biological response of zebrafish to drug treatment. One of the advantages of integrating transcriptomics and proteomics lies in its neutrality to *a priori* knowledge and targets. The observation-driven result could lead to insights into previously unsuspected targets. The recent advancement of deep sequencing technology and the 2D LC-MS/MS system provides an unprecedented opportunity to formulate a system biology approach to unravel the resulting effect of holistic action of a drug or natural product containing multiple components through either interacting with a specific or multiple targets in a whole organism.

9. Zebrafish Disease Models

A highly relevant disease model should be developed when exploring the pathophysiological mechanism and the biological activity of any drug compound. Zebrafish models have been developed in several therapeutic areas for investigating human diseases. Disease models are created by mutation or inactivation of genes, treatment with chemicals, or even modification of a diet.

10. Neurodegenerative Disease Models

10.1. Parkinson's Disease. PD is the second most common neurodegenerative disease characterized by progressive loss of DA neurons in the substantia nigra pars compacta. The etiology of PD is not completely understood but increasing evidence suggests that oxidative damage induced by reactive oxygen species (ROS) and reactive nitric species (RNS) neuroinflammation, excitotoxicity, and apoptosis are involved in the progression of DA neurodegeneration [61].

Recently, the zebrafish has been demonstrated to be an appropriate model for PD [62]. The DA system in the posterior tuberculum of the ventral diencephalon is comparable with the nigrostriatal system in human [63]. PD-related neurotoxins cause the loss of DA neurons, reduced expression of tyrosine hydroxylase (TH) (Table 2) and the impairment of motor behaviour in zebrafish that are comparable with the pathophysiological features observed in other animal models [64]. In addition, clinical and experimental neuroprotective agents (nomifensine, a DAT inhibitor; L-deprenyl, an MAO-B inhibitor) (Table 2) have been demonstrated to be active in protecting zebrafish from neuronal insult [65]. Either knockdown or mutation of important genes, including PARKIN and LRRK2, contributes to a significant decrease in the number DA neurons (Table 2). Taken together, the results of earlier studies suggest that the zebrafish is a good alternative species for a PD model and offers great opportunity for screening and discovery of novel PD therapeutic agents.

The brain structure and function of the zebrafish are very similar to those of other vertebrates [70]. The anatomy of the zebrafish brain DA system was studied recently, and a region anatomically similar to the striatum was identified in the forebrain [71]. Neurotoxins, such as MPTP, 6-OHDA, and rotenone, are known to induce DA neuron loss in animal models. Among those neurotoxins, MPTP/MPP^+ is the best characterized toxin to generate model of PD and has proved useful for studying the striatal circuitry involved in PD pathophysiology [72]. Exposure of zebrafish to

Table 2: Potential marker genes for PD.

Gene	Function	Assessment method	Reference
Tyrosine hydroxylase (TH)	Catalytic conversion of the amino acid L-tyrosine to dihydroxyphenylalanine	Immunostaining, locomotion behaviour test	[28, 64, 66]
Dopamine transporter (DAT)	Membrane-spanning protein for pumping neurotransmitter DA back into cytosol from the synaptic region	Whole mount *in situ* hybridization (WISH), swimming behaviour	[65]
Vesicular monoamine transporter 2 (VMAT2)	Integral membrane protein for transporting neurotransmitter carrying monoamine structure, for example, dopamine and norepinephrine from cellular cytosol into synaptic vesicles	Visualization in VMAT2: GFP transgenic fish	[67]
MAO-B	Catalytic oxidation of monoamines	Monoamine oxidase enzyme histochemistry	[66]
PARKIN (PARK2)	Gene knockdown leads to complex I deficiency and dopaminergic neuronal cell loss	WISH, whole-mount antibody immunofluorescence, behaviour analysis	[68]
LRRK2	Genetic mutant caused loss of DA neuron and locomotive defect	WISH, swimming behaviour	[69]

MPTP caused profound loss of tyrosine hydroxylase-positive (TH^+) neurons and downregulated *TH* mRNA expression in contrast to vehicle-treated healthy zebrafish (Figure 5) leading to a deficit in locomotor behaviour (Figure 6). Earlier studies revealed that 6-OHDA is taken up selectively by the plasma membrane dopamine transporter and subsequently accumulates in the mitochondria, resulting in the formation of ROS and RNS [73]. In addition, neuroinflammation plays a key role in 6-OHDA-induced DA neuron damage *in vivo* [74]. We measured the gene expression of proinflammatory mediators in 6-OHDA-treated zebrafish by quantitative real-time PCR and showed that 6-OHDA caused overexpression of *IL-1β*, *TNF-α*, and *COX-2*, several-fold higher than that of untreated control fish [75]. These proinflammatory genes play important roles in the etiology of PD [76]. It has been shown that the level of the COX-2 protein is upregulated in substantia nigra DA neurons in PD patients and in animal models [77]. The inhibition of COX-2 and TNF-*α* has provided neuroprotection in rats [76]. Our current iTRAQ-based shotgun proteomics study in a zebrafish model for PD suggested the potential involvement of both TNF-*α*/NF-*κ*B and oxidative phosphorylation pathways in 6-OHDA-induced neurodegeneration in zebrafish (unpublished data). However, given that, all reported promising studies on this chemical induced PD experimental zebrafish model, more researches need to be done to differentiate systemic toxicity and selective neuronal toxicity of the neurotoxins. In addition, generation of transgenic zebrafish expressing fluorescent protein specifically in DA neuron, that allows tracking the kinetic change of living DA neurons *in vivo*, is a viable strategy to replace the postimmunochemical staining of TH-positive neurons.

10.2. Epilepsy. Epilepsy is a common neurological disorder characterized by the recurrent appearance of spontaneous seizures due to neuronal hyperactivity, and the disease afflicts nearly 50 million people worldwide [78]. Recent studies showed that the pathogenesis of epilepsy involves altered distribution of GABA receptors (Table 3), enhanced activity of excitatory circuits, neuronal loss, and synaptic reorganization [79–82]. A number of genes encoding transcription factors, synaptic receptors, ion channels, and glucose transporters have shown altered mRNA expression in rodent models of epilepsy (Table 3). These findings suggest potential gene markers other than *c-fos*. Although some antiepileptic drugs (AEDs) are marketed, there is no drug capable of reversing the cause of pathological changes in the brain [83] and some disease subtypes, such as temporal lobe epilepsy, are even resistant to current pharmacotherapies [84]. This problem calls for large-scale screening of new candidates of AED, but this is difficult to achieve in a rodent model.

A PTZ-induced epilepsy model of zebrafish was established by Baraban in 2005 [85], who reported the upregulation of *c-fos* in the CNS region of zebrafish exposed to PTZ. After exposure to PTZ, the larval zebrafish shows three stages of seizure: a dramatic increase in total distance travelled at Stage I, rapid whirlpool-like circling swimming behaviour at Stage II, and culmination in clonus-like convulsions leading to loss of posture at Stage III. Current AEDs can stop the seizure at Stages I and II and, therefore, epileptic zebrafish at both stages are suitable for drug screening [92].

10.3. Heart Disease and Cardiotoxicity. Mutations found in cardiac troponin T type 2 (TNNT2) [93] and T-box-5 (Tbx5) are implicated in cardiomyopathy. Severe heart defect was observed in zebrafish carrying the mutated TNNT2. Mutation in Tbx5 leads to the maldevelopment of heart and upper limbs known as Holt-Oram syndrome [94]. Zebrafish carrying the same mutation have comparable deformed heart and pectoral fins [95]. In fact, troponin T was considered as a biomarker in congenital heart failure from dilated cardiomyopathy [96, 97]. Other biomarkers, such as myosin light chain-I [96, 97], cardiotrophin [98], and endothelin-1 [99], are proposed to have diagnostic value in congestive heart failure and hypertension (Table 4).

The zebrafish is a good model for studying cardiotoxicity. The cardiac function can be studied in zebrafish embryos

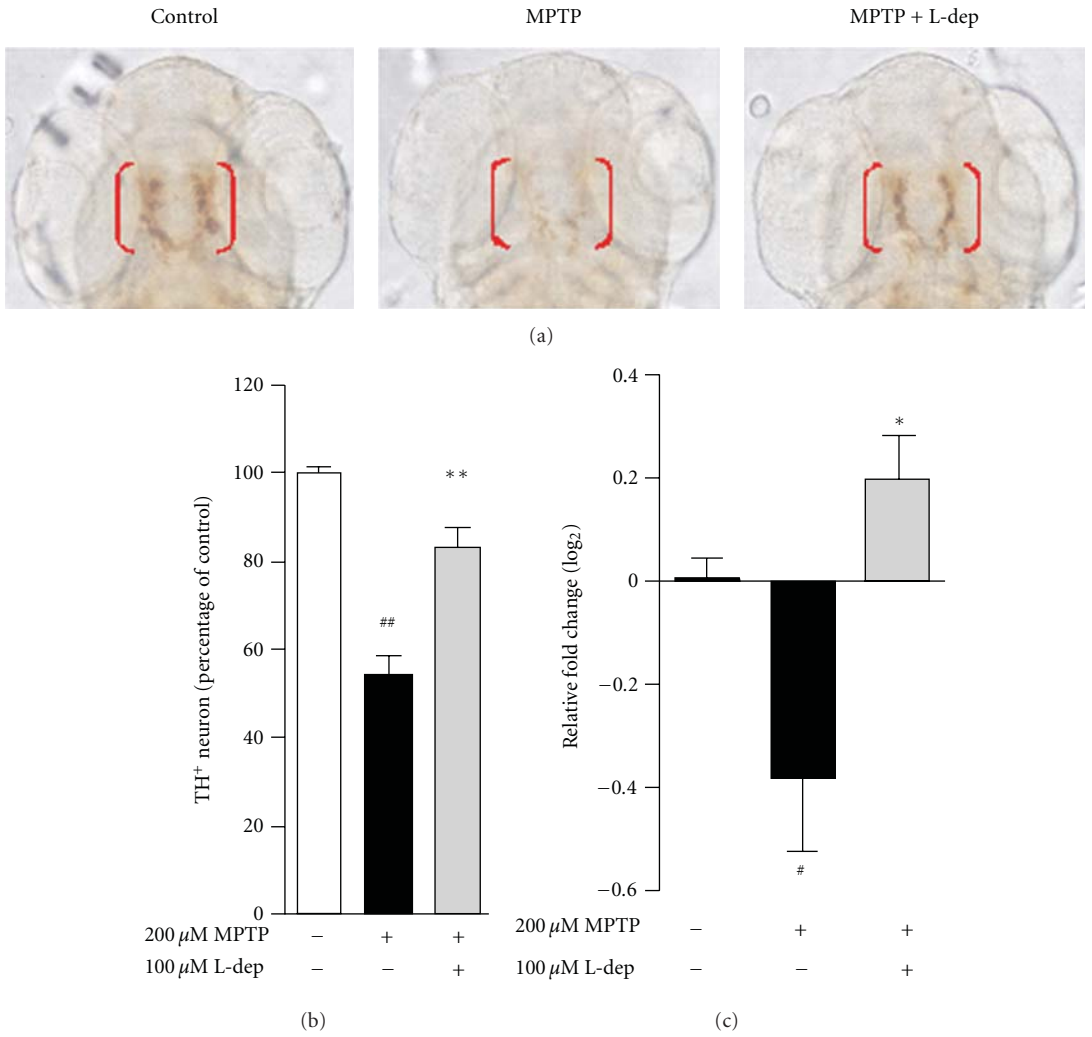

FIGURE 5: MPTP induces DA neuron loss in zebrafish. (a) Representative picture of anti-TH whole mount immunostaining. TH^+ neurons in diencephalic region were indicated by bracket, dorsal view. L-dep, L-deprenyl (selegiline), a selective MAO-B inhibitor, was used as positive control. (b) Counting of TH^+ neuron. (c) Relative fold change of *th* gene expression as compared to control, MPTP downregulated *th* gene expression. $^{\#}P < 0.05$ and $^{\#\#}P < 0.01$ compared with untreated control. $^{*}P < 0.05$ and $^{**}P < 0.01$ compared with MPTP treated alone.

TABLE 3: Potential marker genes for epilepsy.

Function	Gene	Assessment method	References
Transcription factor	c-Fos	Immunohistochemistry, *In situ* hybridization, real-time PCR	[85]
	c-Jun	Electrophoretic mobility-shift assay	[86]
	CREB	Real-time PCR, northern blot	[87]
	Zac 1	Immunohistochemistry, *In situ* hybridization	[88]
Receptor	NMDAR1	Immunohistochemistry, Western blot	[89]
	GABA(A)-receptor delta	Immunohistochemistry	[81]
Ion channel	Kv1.2 and Kv4.2	*In situ* hybridization	[90]
Transporter	GLUT1 and GLUT3	*In situ* hybridization, Western blot	[91]

through assessment of heart rate, heart morphology, cardiac myocytes number, and heart size [101]. Recently, we explored the cardiotoxicity of chemotherapeutic agents such as sunitinib malate (Sutent; SU11248; Pfizer). Sutent is a multitargeted tyrosine kinase inhibitor with antiangiogenic activity. It has been approved for first-line and adjuvant treatment of renal cell carcinoma. However, long-term angiogenesis inhibition would involve unwanted side effects, including cardiac and renal toxicity in patients with cancer [102]. Our study showed that Sutent deteriorates heart function through

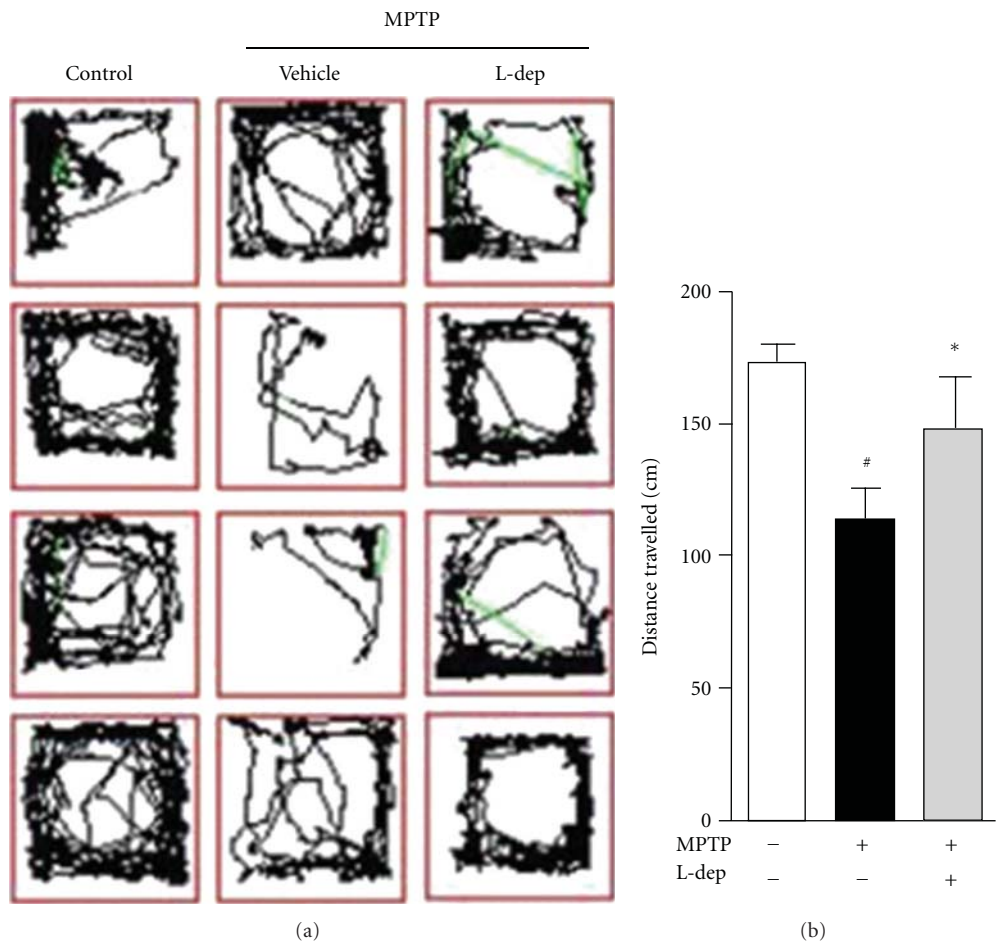

Figure 6: MPTP induces deficit of swimming behavior in zebrafish. (a) Typical swimming patterns of control and MPTP-treated zebrafish. Lines show the track of zebrafish movement. Zebrafish treated with MPTP was less active as compared to the control. (b) Quantitative analysis of total distance travelled. $^{\#}P < 0.05$ compared with untreated control. $^{*}P < 0.05$ compared with MPTP treated alone.

induction of pericardial edema and decrease in heart rate in zebrafish embryos (Figure 7).

11. Cerebral Hemorrhage Model

Cerebral hemorrhage, also known as hemorrhagic stroke, occurs when a blood vessel in the brain becomes weak and bursts, allowing blood to leak into the brain. Atorvastatin, a 3-hydroxy-3-methylglutaryl coenzyme-A (HMG-CoA) reductase inhibitor, reduces cholesterol, ameliorates, and vascular atherosclerosis and improves cardiovascular morbidity and mortality [103]. Pretreatment with atorvastatin significantly reduced infarct volume induced by permanent middle cerebral artery occlusion in animal studies [104]. Clinical studies showed patients with postischemic-stroke treatment with atorvastatin showed improving neurological recovery [105]. However, this beneficial effect is partly counteracted by an increased risk of hemorrhagic stroke [106]. Moreover, atorvastatin induced intracranial hemorrhages in wildtype fish [107] and induced cerebral hemorrhage in a zebrafish model (Figure 8), which offers an opportunity to screen cerebrovascular-protective compounds.

12. Dyslipidemia and Hyperlipidemia

The zebrafish model can be used in the study of lipid metabolism. The quenched fluorescent phospholipid substrate *N*-((6-(2,4-dinitrophenyl)amino)hexanoyl)-1-palmitoyl-2-BODIPY-FL-pentanoyl-*sn*-glycero-3-phosphoethanolamine (PED6) taken up by zebrafish larvae can fluoresce after cleavage by phospholipases in the intestine. It has been reported that this assay can be used to detect the fat-free (*ffr*) mutation, which likely results in disturbed lipid processing through impaired intestinal phospholipase activity [108] and reduced protease activity [109]. A research team led by Stoletov has developed a hypercholesterolemic (HCD) model in zebrafish utilizing a fluorescent cholesteryl ester to observe vascular lipid accumulation and fluorescent dextran in the endothelial cell layer disorganization after an HCD diet [110]. The reliability of the model was further supported by accumulation of macrophages, increased phospholipase A_2 activity, and elevated levels of oxidized phosphatidylcholines in zebrafish fed an HCD diet compared to those fed a normal diet [110, 111]. Another research group led by Jin has demonstrated the antiatherosclerotic effect of turmeric

Table 4: Potential biomarkers for human heart disease.

Gene	Function	Assessment method	Associated cardiovascular disease
Troponin T	Myocardial contraction	ELISA	Congestive heart failure [96, 97]
Heart fatty acid binding protein	Carrier proteins for fatty acids and other lipophilic substances, such as eicosanoids and retinoids	ELISA	Congestive heart failure [96, 97]
Myosin light chain-I	Myocardial contraction	ELISA	Congestive heart failure [96, 100]
Creatine kinase MB	Energy metabolism	ELISA	Congestive heart failure [96]
Cardiotrophin-1	Response to stress and humoral factors such as angiotensin II	ELISA	Hypertension [98]
Endothelin-1	Potent endothelium-derived vasoconstrictor peptide	Radioimmunoassay	Heart failure [99]

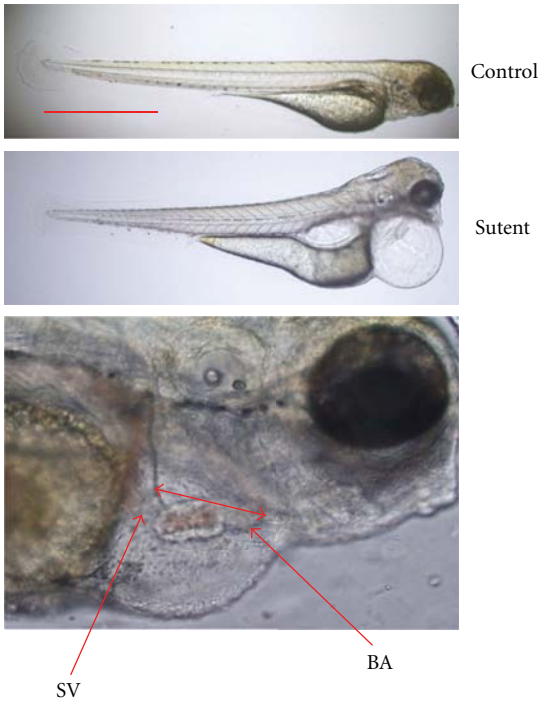

Figure 7: Sutent-induced cardiotoxicity in zebrafish embryos. Embryos at 5 dpf were treated with Sutent for 72 h followed by assessment of cardiac function. (a) Pericardial edema was observed after administration of Sutent compared to the control. The severity of pericardial edema was quantified by measuring the distance between sinus venosus (SV) and bulbus arteriosus (BA). (b) Embryo heart rate was decreased by treatment with Sutent in dose-dependent manner.

and laurel aqueous extracts using this HCD model [112]. These disease models have proved to be highly relevant to human diseases and showed a number of conserved phenotype between zebrafish and human. Moreover, the difficulty of studying the atherogenic events in a temporal manner has been overcome due to its optical transparency.

13. Searching for Active Compounds from Natural Products

Many natural products exhibit a range of biological activity that is probably due to interaction of their complex chemical constituents with multiple targets in the body, which opens new avenues for therapy of disorders, with multifactorial etiopathogenesis such as neurodegeneration. The physiological complexity of zebrafish is similar to that of mammals, providing a suitable model for the study of human diseases as well as throughput drug screens. Using a whole organism as a model allows a more comprehensive and simultaneous analysis of the range of biological activity and toxicity of a chemical or multiple chemicals compared to an *in vitro* assay. Zebrafish embryos and early larvae are optically transparent, allowing screens with a measurable phenotypic readout using imaging microscopy for assessing pathological changes in Parkinson's disease, epilepsy, heart disease or cardiotoxicity, cerebral hemorrhage, and hyperlipidemia. This approach allows live and continuous observation on individuals which are often inapplicable in other *in vivo* models. More importantly, invasive approaches are often applied in these animal models, so reassessment of individuals may not be possible. For example, cerebral hemorrhage in rodent models was commonly done by intraparenchymal infusion of either autologous blood or bacterial collagenase. The hematoma size and location were evaluated with histologic analysis [113, 114]; hyperlipidemia in rodent models was achieved by feeding ApoE deficient mice with high fat diet for eight weeks and the atherosclerotic lesion was also observed by histology [115, 116]. Also, visual observation with imaging microscopy may require less technical skills and also far more convenient. For example, the evaluation of cardiotoxicity in zebrafish was determined by heart rate, heart morphology, cardiac myocyte number, and heart size. However, in rodent models, the heart function was often assessed by electrocardiogram or echocardiogram which requires intensive technical and labor input. Using rodent disease models for early stage drug screening may sound inapplicable since high-throughput studies are usually required. In addition, zebrafish model

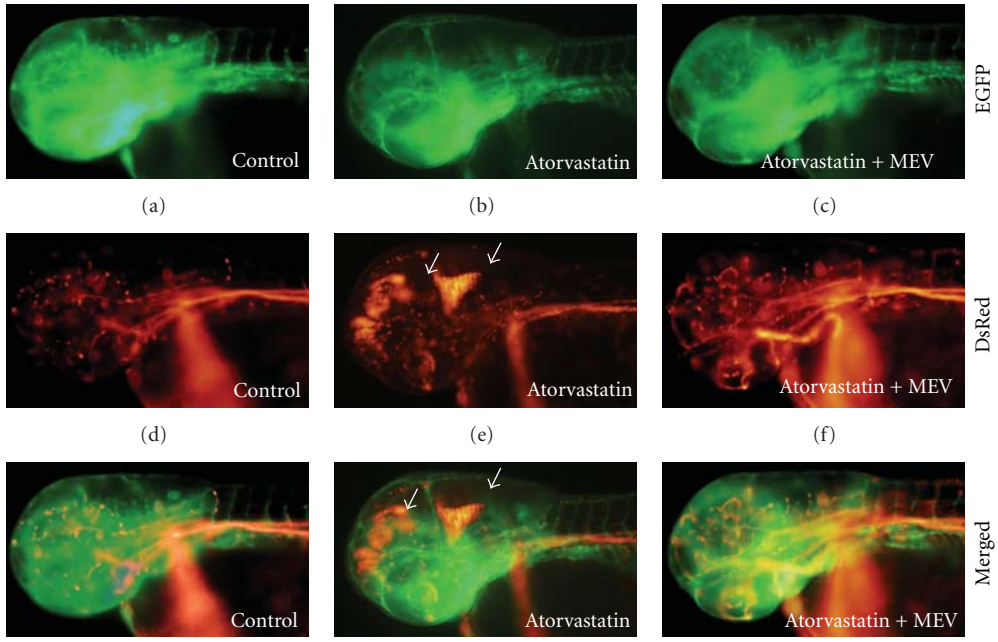

Figure 8: Atorvastatin-induced cerebral hemorrhage in zebrafish embryos. Tg(fli1:EGFP); Tg(gata1:dsred) homozygous double transgenic zebrafish embryos at 24 hpf were treated with atorvastatin alone or with atorvastatin and mevalonate (MEV) in combination for 24 h. Images showing blood vessels (EGFP, green) were superimposed on images showing blood flow (DsRed, red). Hemorrhage observed in the atorvastatin treatment group was prevented by cotreatment with MEV. Fluorescent microscopic images are at magnification 100x.

enables the observation of any pharmacological effect(s) on multiple targets underlying the pathway of a disease or a normal physiological process can be observed. The zebrafish model is, therefore, very suitable for identifying the off-target effects or multiple targets due to the holistic action of natural products.

14. Identifying Angiogenic Compounds from Natural Products

Angiogenesis is the establishment of the mature blood vessel network through expansion and remodeling of the vascular primordium. Blood vessel formation through angiogenesis involves the induction of new sprouts, coordinated and directed endothelial cell migration, proliferation, sprout fusion (anastomosis), and lumen formation [117]. Under normal conditions, tiny vessels do not increase in size or number, except in wound healing, embryonic development, and development of the corpus luteum. In fact, many diseases are associated with an imbalance in the regulation of angiogenesis, in which either excessive or insufficient blood vessel formation occurs.

To evaluate the angiogenic response in zebrafish, transgenic fish expressing green fluorescent protein (GFP) specifically in endothelial cells, for example, Tg(fli-1:EGFP) and Tg(fli-1:nEGFP), are recently used for rapid analysis of changed vasculature in live embryos in response to drugs [118]. In fact, zebrafish is an excellent animal model for the study of angiogenesis, with many antiangiogenic drugs eliciting responses similar to those in mammalian systems [119]. During the vasculature development, subintestinal vein vessels (SIVs) originate from the duct of Cuvier at 48 hpf and form a vascular basket in the yolk sac during the next 24 h. The angiogenic response was evaluated visually with respect to the following criteria: (1) the appearance of spikes or sprouts projecting from the subintestinal vessel basket or the lengthening of such spikes; (2) the extension of the basket into the yolk region with more than seven vertical branches within the basket [120]; (3) statistical increases in diameter compared to the medium control; (4) the ectopic growth of newly formed blood vessels from SIVs and increased numbers of SIVs in the endothelial cells [121]. Sprout formation was seen as the main characteristic in proangiogenesis [17, 120, 121]. Recently, we demonstrated the feasibility of drug screening in a zebrafish model and found the antiangiogenesis effect of a resveratrol derivative [52], indirubin [122], nobiletin [54], and sinensetin [51] as well as proangiogenesis effects of *Angelica sinensis* extract [123, 124], *Panax notoginseng* extract [125], and *Radix Astragali* extract [17].

Angiogenesis plays an important role in the development of human chronic inflammatory diseases, including cancer, psoriasis, rheumatoid arthritis, macular degeneration, and diabetes retinopathy [126, 127]. There is growing evidence that chronic inflammation and angiogenesis are codependent, involving increased cellular infiltration and proliferation as well as overlapping roles of regulatory growth factors and cytokines [126]. Persistent inflammation is linked with the progression of cancer, as proinflammatory cytokines are detected frequently in tumor tissue[128]. In rheumatoid

arthritis, the formation of pannus [129], which is an inflammatory connective tissue mass rich in blood vessels, is apparently because angiogenic factors, such as VEGF, stimulate encephalitogenic T cells and induce more severe and prolonged encephalomyelitis [130]. Besides angiogenic factors, transcription factors such as NF-κB plays a central role in the signaling of apoptosis and inflammation [131]. NF-κB expression is associated with VEGF in the development and progression of tumorigenesis [132]. Signaling by the cyclooxygenase-2 (COX-2) downstream of NF-κB may play a key role in the tumorigenesis of a variety of human malignancies by stimulating cell proliferation and angiogenesis [133]. Moreover, a recent study showed that chronic inflammation in benign prostatic hyperplasia causes an overexpression of COX-2, which induces the increased expression of Bcl-2 and VEGF [134].

Pharmacology of many anti-inflammatory drugs revealed at least some part of their efficacy is due to their antiangiogenic effect [126]. Tocotrienol, a member of the vitamin E family, possesses anticancer properties acting through regulating multiple signaling pathways, including anti-inflammation and antiangiogenesis [135]. The extract of *Physalis angulate* shows antimetastatic and antiangiogenic activity in human oral squamous carcinoma and human umbilical vein endothelial cells, probably due to its anti-inflammatory properties [136]. Indirubin inhibits inflammatory reactions by suppressing the production of interferon-γ and interleukin-6, which is a well-known inflammatory cytokine [137]. Interestingly, it also displays antiangiogenic activity by inducing HUVEC apoptosis and cell-cycle arrest at the G0/G1 phase [122]. Resveratrol and its derivative exert antiangiogenic and vascular-disrupting effects in zebrafish through downregulation of VEGFR2 and cell-cycle modulation [52]. The anti-inflammatory property of resveratrol is reported to prevent an increase in the levels of serum amyloid A, tumor necrosis factor-α, interleukin (IL-6), IL-1β, and nuclear transcription factor-κB in colitis-associated disease [138].

Angiogenesis deficiencies are associated with numerous human cardiovascular and cerebrovascular diseases (e.g., ischemic cardiac and cerebral problems). Our previous discovery of a pro-angiogenic herb called *Angelica sinensis* by zebrafish assay leading to development of a wound healing formulation for diabetic foot ulcer patients [124, 139]. Our recent work presented, for the first time, that a chemical-induced blood vessel loss in zebrafish *in vivo* could mimic angiogenesis deficiencies associated with human disease conditions and be used to identify pro-angiogenic agents. VEGFR tyrosine kinase inhibitor II (VRI), a pyridinyl-anthranilamide compound that displays antiangiogenic properties, strongly inhibits the kinase activities of both VEGF receptor 1 and 2. Treatment of the zebrafish with VRI induces significant blood vessel loss in ISV (intersegmental vessels) and DLAV (dorsal longitudinal anastomotic vessels). For instance, we identified a polysaccharide fraction (50000 D < MW and DM < 0.1 μm) isolated from Astragali Radix partially restores the chemical-induced blood vessel loss in the zebrafish model [140]. This is also the first study to prove the concept of screening the bioactivity of polysaccharides in live zebrafish, whose drug metabolism systems were shown recently to have a high degree of functional similarity to that of mammals. Since polysaccharides isolated from natural products usually undergo the enzymatic breakdown of the sugar moiety in the cells of the gastrointestinal mucosa, or by enzymes secreted by the colon flora, to become active metabolites after oral consumption by humans, the study of the bioactivity of the polysaccharides required the development of an *in vivo* assay equipped with mammalian-equivalent drug metabolism systems. Our findings provide insight into a new angiogenesis deficiency zebrafish model for screening vascular regenerative agents as well as the important roles of various substances from Chinese medicines for the treatment of various pathological conditions associated with deficient angiogenesis, such as ageing, stroke, ulcers, and cardiovascular diseases [140, 141].

15. Identifying Anti-Parkinson's Disease Compounds from Natural Products

PD patients usually suffer primarily from the death of dopaminergic (DA) neurons in the substantia nigra. Recent research in the pharmacotherapy of PD has identified numerous agents for the symptomatic control of motor impairments, but none is able to prevent, slow, or halt the progression of the disease [142]. The main obstacle to developing neuroprotective therapies is our limited understanding of the key molecular events that provoke neurodegeneration. Earlier studies highlighted the pathological involvement of oxidative stress, neuroinflammation, excitotoxicity, and apoptosis in neurodegenerative diseases [143]. Because PD, as well as other neurodegenerative disorders, usually has multifactorial etiopathogenesis, multiple drug therapy is required to address the varied pathological aspects [144]. Multiple drug strategy has been the essence of the rationales used for formulating traditional Chinese medicines (TCMs) for thousands of years. TCMs contain a mixture of chemical components from a single herb or a combination of several herbs and thus versatile functions and possess great potential in the multitarget approach for improved treatment of complicated diseases, such as PD.

By combining whole mount immunostaining and a behavioural screen, we have identified the neuroprotective activity of a few TCMs, including Fructus *Alpinia oxyphylla* extract (AOE) and *Eriocaulon buergerianum* extract (EBE) [75, 145]. Recently, increasing evidence suggests the beneficial effects of Fructus AOE on various neurodegenerative diseases. Treatment with aqueous AOE attenuated the death of cortical astrocytes induced by amyloid-β (Aβ) *in vitro*, prevented ischemia-induced learning disability, and rescued hippocampal CA1 neurons from lethal ischemic damage in mice [146]. Treatment with the ethanolic AOE in the presence of glutamate significantly enhanced viability and reduced apoptosis in a cortical neuron culture [147]. We found that ethanolic AOE prevented and restored 6-OHDA-induced DA neurodegeneration and attenuated the deficit of locomotor activity in zebrafish [75]. In addition, the aquatic plant EB (Gujingcao) is a TCM with anti-inflammatory and antimicrobial properties [148]. In the

Chinese Pharmacopoeia (2005), the capitulum of EB is one of the most frequently used Chinese medicinal herbs, with flavonoids, volatile oils, anthraquinone, naphthopyranones, protocatechuic acid, and c-tocopheryl acetate being the bioactive constituents [149]. Flavonoids such as patuletin hispidulin, quercetin, quercetagetin, and quercetagetin derivatives and volatile oil such as palmitic acid, (Z,Z)-9,12-octacosane-dienoic acid are the two major classes of chemicals in EB [148]. EB demonstrates significant therapeutic effects on headache, toothache, nasosinusitis, night blindness, glaucoma, retinochoroiditis, conjunctivitis, and other eye diseases [150]. The results of our study suggested that EBE has profound neuroprotective activity in zebrafish, including the dose-dependent recovery of DA neuron loss caused by 6-OHDA *in vivo* and inhibition of the 6-OHDA-induced decrease of total movement distance in zebrafish [145]. We found that quercetin was one of the active neuroprotective constituents in EBE [28]. All these groundwork warrants further study of how the interaction of multiple components in these natural products elicits neuroprotection.

16. Conclusions

Zebrafish offers interesting possibilities for the simultaneous assessment of efficacy and toxicity of target compounds, which is not easily addressed with current rodent models. With its physiological similarities to human, many disease models could be established for identifying the off-target and the targeted effects of target compounds. More importantly, it allows integrative studies of transcriptomics and proteomics for identifying drug metabolic pathways and known or novel molecular targets involved in the biological response of zebrafish to drug treatment.

Acknowledgments

This study was supported by grants from the Science and Technology Development Fund of Macau SAR (Ref. nos. 045/2007, 058/2009, 014/2011 and 078/2011/A3) and the Research Committee, University of Macau (Ref. no. UL017).

References

[1] S. Berghmans, P. Butler, P. Goldsmith et al., "Zebrafish based assays for the assessment of cardiac, visual and gut function—potential safety screens for early drug discovery," *Journal of Pharmacological and Toxicological Methods*, vol. 58, no. 1, pp. 59–68, 2008.

[2] G. J. Lieschke and P. D. Currie, "Animal models of human disease: zebrafish swim into view," *Nature Reviews Genetics*, vol. 8, no. 5, pp. 353–367, 2007.

[3] S. W. Mittelstadt, C. L. Hemenway, M. P. Craig, and J. R. Hove, "Evaluation of zebrafish embryos as a model for assessing inhibition of hERG," *Journal of Pharmacological and Toxicological Methods*, vol. 57, no. 2, pp. 100–105, 2008.

[4] F. M. Richards, W. K. Alderton, G. M. Kimber et al., "Validation of the use of zebrafish larvae in visual safety assessment," *Journal of Pharmacological and Toxicological Methods*, vol. 58, no. 1, pp. 50–58, 2008.

[5] M. J. Winter, W. S. Redfern, A. J. Hayfield, S. F. Owen, J. P. Valentin, and T. H. Hutchinson, "Validation of a larval zebrafish locomotor assay for assessing the seizure liability of early-stage development drugs," *Journal of Pharmacological and Toxicological Methods*, vol. 57, no. 3, pp. 176–187, 2008.

[6] R. Cao, L. D. E. Jensen, I. Söll, G. Hauptmann, and Y. Cao, "Hypoxia-induced retinal angiogenesis in zebrafish as a model to study retinopathy," *PLoS ONE*, vol. 3, no. 7, Article ID e2748, 2008.

[7] G. N. Serbedzija, E. Flynn, and C. E. Willett, "Zebrafish angiogenesis: a new model for drug screening," *Angiogenesis*, vol. 3, no. 4, pp. 353–359, 1999.

[8] M. J. Airhart, D. H. Lee, T. D. Wilson, B. E. Miller, M. N. Miller, and R. G. Skalko, "Movement disorders and neurochemical changes in zebrafish larvae after bath exposure to fluoxetine (PROZAC)," *Neurotoxicology and Teratology*, vol. 29, no. 6, pp. 652–664, 2007.

[9] W. Boehmler, T. Carr, C. Thisse, B. Thisse, V. A. Canfield, and R. Levenson, "D4 Dopamine receptor genes of zebrafish and effects of the antipsychotic clozapine on larval swimming behaviour," *Genes, Brain and Behavior*, vol. 6, no. 2, pp. 155–166, 2007.

[10] I. V. Zhdanova, S. Y. Wang, O. U. Leclair, and N. P. Danilova, "Melatonin promotes sleep-like state in zebrafish," *Brain Research*, vol. 903, no. 1-2, pp. 263–268, 2001.

[11] R. D. Murphey, H. M. Stern, C. T. Straub, and L. I. Zon, "A chemical genetic screen for cell cycle inhibitors in zebrafish embryos," *Chemical Biology and Drug Design*, vol. 68, no. 4, pp. 213–219, 2006.

[12] J. F. Rawls, B. S. Samuel, and J. I. Gordon, "Gnotobiotic zebrafish reveal evolutionarily conserved responses to the gut microbiota," *Proceedings of the National Academy of Sciences of the United States of America*, vol. 101, no. 13, pp. 4596–4601, 2004.

[13] Z. H. Li, D. Alex, S. O. Siu et al., "Combined *in vivo* imaging and omics approaches reveal metabolism of icaritin and its glycosides in zebrafish larvae," *Molecular BioSystems*, vol. 7, no. 7, pp. 2128–2138, 2011.

[14] T. Walle, "Absorption and metabolism of flavonoids," *Free Radical Biology and Medicine*, vol. 36, no. 7, pp. 829–837, 2004.

[15] L. L. Brunton, L. S. Goodman, D. Blumenthal et al., *Goodman and Gilman's Manual of Pharmacology and Therapeutics*, McGraw-Hill Professional, New York, NY, USA, 2007.

[16] P. Jancova, P. Anzenbacher, and E. Anzenbacherova, "Phase II drug metabolizing enzymes," *Biomedical papers of the Medical Faculty of the University Palacký*, vol. 154, no. 2, pp. 103–116, 2010.

[17] J. Y. Tang, S. Li, Z. H. Li et al., "Calycosin promotes angiogenesis involving estrogen receptor and mitogen-activated protein kinase (MAPK) signaling pathway in zebrafish and HUVEC," *PLoS ONE*, vol. 5, no. 7, Article ID e11822, 2010.

[18] G. Hu, S. O. Siu, S. Li et al., "Metabolism of calycosin, an isoflavone from astragali radix, in zebrafish larvae," *Xenobiotica*, vol. 42, no. 3, pp. 294–303, 2012.

[19] H. L. Siew, L. W. Yi, V. B. Vega et al., "Conservation of gene expression signatures between zebrafish and human liver tumors and tumor progression," *Nature Biotechnology*, vol. 24, no. 1, pp. 73–75, 2006.

[20] J. F. Rawls, M. A. Mahowald, R. E. Ley, and J. I. Gordon, "Reciprocal gut microbiota transplants from zebrafish and mice to germ-free recipients reveal host habitat selection," *Cell*, vol. 127, no. 2, pp. 423–433, 2006.

[21] J. H. Bauer, S. Goupil, G. B. Garber, and S. L. Helfand, "An accelerated assay for the identification of lifespan-extending interventions in Drosophila melanogaster," *Proceedings of the National Academy of Sciences of the United States of America*, vol. 101, no. 35, pp. 12980–12985, 2004.

[22] K. Watanabe, Y. Nishimura, T. Oka et al., "*In vivo* imaging of zebrafish retinal cells using fluorescent coumarin derivatives," *BMC Neuroscience*, vol. 11, article 116, 2010.

[23] J. Y. Jeong, H. B. Kwon, J. C. Ahn et al., "Functional and developmental analysis of the blood-brain barrier in zebrafish," *Brain Research Bulletin*, vol. 75, no. 5, pp. 619–628, 2008.

[24] J. Zhang, J. Piontek, H. Wolburg et al., "Establishment of a neuroepithelial barrier by Claudin5a is essential for zebrafish brain ventricular lumen expansion," *Proceedings of the National Academy of Sciences of the United States of America*, vol. 107, no. 4, pp. 1425–1430, 2010.

[25] A. Woodgate, G. MacGibbon, M. Walton, and M. Dragunow, "The toxicity of 6-hydroxydopamine on PC12 and P19 cells," *Molecular Brain Research*, vol. 69, no. 1, pp. 84–92, 1999.

[26] S. Singh, T. Das, A. Ravindran et al., "Involvement of nitric oxide in neurodegeneration: a study on the experimental models of Parkinson's disease," *Redox Report*, vol. 10, no. 2, pp. 103–109, 2005.

[27] Y. C. Lin, H. W. Uang, R. J. Lin, I. J. Chen, and Y. C. Lo, "Neuroprotective effects of glyceryl nonivamide against microglia-like cells and 6-hydroxydopamine-induced neurotoxicity in SH-SY5Y human dopaminergic neuroblastoma cells," *Journal of Pharmacology and Experimental Therapeutics*, vol. 323, no. 3, pp. 877–887, 2007.

[28] Z. J. Zhang, L. C. V. Cheang, M. W. Wang, and S. M. Y. Lee, "Quercetin exerts a neuroprotective effect through inhibition of the iNOS/NO system and pro-inflammation gene expression in PC12 cells and in zebrafish," *International Journal of Molecular Medicine*, vol. 27, no. 2, pp. 195–203, 2011.

[29] P. Panula, V. Sallinen, M. Sundvik et al., "Modulatory neurotransmitter systems and behavior: towards zebrafish models of neurodegenerative diseases," *Zebrafish*, vol. 3, no. 2, pp. 235–247, 2006.

[30] J. Rihel, D. A. Prober, A. Arvanites et al., "Zebrafish behavioral profiling links drugs to biological targets and rest/wake regulation," *Science*, vol. 327, no. 5963, pp. 348–351, 2010.

[31] D. Kokel, J. Bryan, C. Laggner et al., "Rapid behavior-based identification of neuroactive small molecules in the zebrafish," *Nature Chemical Biology*, vol. 6, no. 3, pp. 231–237, 2010.

[32] M. A. Wolman, R. A. Jain, L. Liss et al., "Chemical modulation of memory formation in larval zebrafish," *Proceedings of the National Academy of Sciences the United States of America*, vol. 108, no. 37, pp. 15468–15473, 2011.

[33] S. Chatrchyan, V. Khachatryan, A. M. Sirunyan et al., "Search for neutral minimal supersymmetric standard model Higgs bosons decaying to tau pairs in pp collisions at radicals = 7 TeV," *Physical Review Letters*, vol. 106, no. 23, Article ID 231801, 15 pages, 2011.

[34] R. R. Shah, "Pharmacogenetic aspects of drug-induced torsade de pointes: potential tool for improving clinical drug development and prescribing," *Drug Safety*, vol. 27, no. 3, pp. 145–172, 2004.

[35] D. M. Roden, "Drug-induced prolongation of the QT interval," *The New England Journal of Medicine*, vol. 350, no. 10, pp. 1013–1022, 2004.

[36] FDA, "ICH Guidance for Industry: S7B Nonclinical Evaluation of the Potential for Delayed Ventricular Repolarization (QT Interval Prolongation) by Human Pharmaceuticals," U.S. Department of Health and Human Services, 2005.

[37] U. Langheinrich, G. Vacun, and T. Wagner, "Zebrafish embryos express an orthologue of HERG and are sensitive toward a range of QT-prolonging drugs inducing severe arrhythmia," *Toxicology and Applied Pharmacology*, vol. 193, no. 3, pp. 370–382, 2003.

[38] FDA, "ICH Guidance for Industry: S7A Safety Pharmacology Studies for Human Pharmaceutical," U.S. Department of Health and Human Services, 2001.

[39] V. Tropepe and H. L. Sive, "Can zebrafish be used as a model to study the neurodevelopmental causes of autism?" *Genes, Brain and Behavior*, vol. 2, no. 5, pp. 268–281, 2003.

[40] M. Portavella, B. Torres, and C. Salas, "Avoidance response in goldfish: emotional and temporal involvement of medial and lateral telencephalic pallium," *Journal of Neuroscience*, vol. 24, no. 9, pp. 2335–2342, 2004.

[41] E. Rink and M. F. Wullimann, "Connections of the ventral telencephalon (subpallium) in the zebrafish (*Danio rerio*)," *Brain Research*, vol. 1011, no. 2, pp. 206–220, 2004.

[42] M. F. Wullimann and T. Mueller, "Teleostean and mammalian forebrains contrasted: evidence from genes to behavior," *Journal of Comparative Neurology*, vol. 475, no. 2, pp. 143–162, 2004.

[43] G. M. Cahill, "Clock mechanisms in zebrafish," *Cell and Tissue Research*, vol. 309, no. 1, pp. 27–34, 2002.

[44] S. Guo, "Linking genes to brain, behavior and neurological diseases: what can we learn from zebrafish?" *Genes, Brain and Behavior*, vol. 3, no. 2, pp. 63–74, 2004.

[45] M. Pirmohamed, S. James, S. Meakin et al., "Adverse drug reactions as cause of admission to hospital: prospective analysis of 18 820 patients," *British Medical Journal*, vol. 329, no. 7456, pp. 15–19, 2004.

[46] K. N. Wallace, S. Akhter, E. M. Smith, K. Lorent, and M. Pack, "Intestinal growth and differentiation in zebrafish," *Mechanisms of Development*, vol. 122, no. 2, pp. 157–173, 2005.

[47] A. Rich, S. A. Leddon, S. L. Hess et al., "Kit-like immunoreactivity in the zebrafish gastrointestinal tract reveals putative ICC," *Developmental Dynamics*, vol. 236, no. 3, pp. 903–911, 2007.

[48] A. Holmberg, T. Schwerte, B. Pelster, and S. Holmgren, "Ontogeny of the gut motility control system in zebrafish *Danio rerio* embryos and larvae," *Journal of Experimental Biology*, vol. 207, no. 23, pp. 4085–4094, 2004.

[49] K. N. Wallace and M. Pack, "Unique and conserved aspects of gut development in zebrafish," *Developmental Biology*, vol. 255, no. 1, pp. 12–29, 2003.

[50] L. Guo and H. Guthrie, "Automated electrophysiology in the preclinical evaluation of drugs for potential QT prolongation," *Journal of Pharmacological and Toxicological Methods*, vol. 52, no. 1, pp. 123–135, 2005.

[51] I. K. Lam, D. Alex, Y. H. Wang et al., "*In vitro* and *in vivo* structure and activity relationship analysis of polymethoxylated flavonoids: identifying sinensetin as a novel antiangiogenesis agent," *Molecular Nutrition and Food Research*, vol. 56, no. 6, pp. 945–956, 2012.

[52] D. Alex, E. C. Leong, Z. J. Zhang et al., "Resveratrol derivative, trans-3,5,4′-trimethoxystilbene, exerts antiangiogenic and vascular-disrupting effects in zebrafish through the downregulation of VEGFR2 and cell-cycle modulation," *Journal of Cellular Biochemistry*, vol. 109, no. 2, pp. 339–346, 2010.

[53] G. Notas, A. P. Nifli, M. Kampa, J. Vercauteren, E. Kouroumalis, and E. Castanas, "Resveratrol exerts its anti-proliferative effect on HepG2 hepatocellular carcinoma cells, by inducing cell cycle arrest, and NOS activation," *Biochimica et Biophysica Acta*, vol. 1760, no. 11, pp. 1657–1666, 2006.

[54] K. H. Lam, D. Alex, I. K. Lam et al., "Nobiletin, a polymethoxylated flavonoid from citrus, shows anti-angiogenic activity in a zebrafish *in vivo* model and HUVEC *in vitro* model," *Journal of Cellular Biochemistry*, vol. 112, no. 11, pp. 3313–3321, 2011.

[55] D. Houle, D. R. Govindaraju, and S. Omholt, "Phenomics: the next challenge," *Nature Reviews Genetics*, vol. 11, no. 12, pp. 855–866, 2010.

[56] U. Kausch, M. Alberti, S. Haindl, J. Budczies, and B. Hock, "Biomarkers for exposure to estrogenic compounds: gene expression analysis in zebrafish (*Danio rerio*)," *Environmental Toxicology*, vol. 23, no. 1, pp. 15–24, 2008.

[57] S. Li, S. Lou, B. U. Lei et al., "Transcriptional profiling of angiogenesis activities of calycosin in zebrafish," *Molecular BioSystems*, vol. 7, no. 11, pp. 3112–3121, 2011.

[58] S. O. Siu, M. P. Y. Lam, E. Lau, R. P. W. Kong, S. M. Y. Lee, and I. K. Chu, "Fully automatable two-dimensional reversed-phase capillary liquid chromatography with online tandem mass spectrometry for shotgun proteomics," *Proteomics*, vol. 11, no. 11, pp. 2308–2319, 2011.

[59] Z. Wang, M. Gerstein, and M. Snyder, "RNA-Seq: A revolutionary tool for transcriptomics," *Nature Reviews Genetics*, vol. 10, no. 1, pp. 57–63, 2009.

[60] M. D. Wit, D. Keil, K. van der Ven, S. Vandamme, E. Witters, and W. D. Coen, "An integrated transcriptomic and proteomic approach characterizing estrogenic and metabolic effects of 17 α-ethinylestradiol in zebrafish (*Danio rerio*)," *General and Comparative Endocrinology*, vol. 167, no. 2, pp. 190–201, 2010.

[61] K. J. Barnham, F. Haeffner, G. D. Ciccotosto et al., "Tyrosine gated electron transfer is key to the toxic mechanism of Alzheimer's disease β-amyloid," *The FASEB Journal*, vol. 18, no. 12, pp. 1427–1429, 2004.

[62] L. Flinn, S. Bretaud, C. Lo, P. W. Ingham, and O. Bandmann, "Zebrafish as a new animal model for movement disorders," *Journal of Neurochemistry*, vol. 106, no. 5, pp. 1991–1997, 2008.

[63] J. Holzschuh, S. Ryu, F. Aberger, and W. Driever, "Dopamine transporter expression distinguishes dopaminergic neurons from other catecholaminergic neurons in the developing zebrafish embryo," *Mechanisms of Development*, vol. 101, no. 1-2, pp. 237–243, 2001.

[64] O. V. Anichtchik, J. Kaslin, N. Peitsaro, M. Scheinin, and P. Panula, "Neurochemical and behavioural changes in zebrafish *Danio rerio* after systemic administration of 6-hydroxydopamine and 1-methyl-4-phenyl-1,2,3,6-tetrahydropyridine," *Journal of Neurochemistry*, vol. 88, no. 2, pp. 443–453, 2004.

[65] E. T. McKinley, T. C. Baranowski, D. O. Blavo, C. Cato, T. N. Doan, and A. L. Rubinstein, "Neuroprotection of MPTP-induced toxicity in zebrafish dopaminergic neurons," *Molecular Brain Research*, vol. 141, no. 2, pp. 128–137, 2005.

[66] V. Sallinen, V. Torkko, M. Sundvik et al., "MPTP and MPP+ target specific aminergic cell populations in larval zebrafish," *Journal of Neurochemistry*, vol. 108, no. 3, pp. 719–731, 2009.

[67] L. Wen, W. Wei, W. Gu et al., "Visualization of monoaminergic neurons and neurotoxicity of MPTP in live transgenic zebrafish," *Developmental Biology*, vol. 314, no. 1, pp. 84–92, 2008.

[68] L. Flinn, H. Mortiboys, K. Volkmann, R. W. Kster, P. W. Ingham, and O. Bandmann, "Complex I deficiency and dopaminergic neuronal cell loss in parkin-deficient zebrafish (*Danio rerio*)," *Brain*, vol. 132, no. 6, pp. 1613–1623, 2009.

[69] D. Sheng, D. Qu, K. H. H. Kwok et al., "Deletion of the WD40 domain of LRRK2 in zebrafish causes parkinsonism-like loss of neurons and locomotive defect," *PLoS Genetics*, vol. 6, no. 4, 2010.

[70] C. Parng, C. Ton, Y. X. Lin, N. M. Roy, and P. McGrath, "A zebrafish assay for identifying neuroprotectants *in vivo*," *Neurotoxicology and Teratology*, vol. 28, no. 4, pp. 509–516, 2006.

[71] E. Rink and M. F. Wullimann, "The teleostean (zebrafish) dopaminergic system ascending to the subpallium (striatum) is located in the basal diencephalon (posterior tuberculum)," *Brain Research*, vol. 889, no. 1-2, pp. 316–330, 2001.

[72] D. Blum, S. Torch, N. Lambeng et al., "Molecular pathways involved in the neurotoxicity of 6-OHDA, dopamine and MPTP: contribution to the apoptotic theory in Parkinson's disease," *Progress in Neurobiology*, vol. 65, no. 2, pp. 135–172, 2001.

[73] R. Sharma, C. R. McMillan, C. C. Tenn, and L. P. Niles, "Physiological neuroprotection by melatonin in a 6-hydroxydopamine model of Parkinson's disease," *Brain Research*, vol. 1068, no. 1, pp. 230–236, 2006.

[74] F. Cicchetti, A. L. Brownell, K. Williams, Y. I. Chen, E. Livni, and O. Isacson, "Neuroinflammation of the nigrostriatal pathway during progressive 6-OHDA dopamine degeneration in rats monitored by immunohistochemistry and PET imaging," *European Journal of Neuroscience*, vol. 15, no. 6, pp. 991–998, 2002.

[75] Z. J. Zhang, L. C. V. Cheang, M. W. Wang et al., "Ethanolic extract of fructus *Alpinia oxyphylla* protects against 6-hydroxydopamine-induced damage of PC12 cells *in vitro* and dopaminergic neurons in zebrafish," *Cellular and Molecular Neurobiology*, pp. 1–14, 2011.

[76] R. L. Hunter, N. Dragicevic, K. Seifert et al., "Inflammation induces mitochondrial dysfunction and dopaminergic neurodegeneration in the nigrostriatal system," *Journal of Neurochemistry*, vol. 100, no. 5, pp. 1375–1386, 2007.

[77] E. Esposito, V. Di Matteo, A. Benigno, M. Pierucci, G. Crescimanno, and G. Di Giovanni, "Non-steroidal anti-inflammatory drugs in Parkinson's disease," *Experimental Neurology*, vol. 205, no. 2, pp. 295–312, 2007.

[78] S. C. Baraban, "Emerging epilepsy models: insights from mice, flies, worms and fish," *Current Opinion in Neurology*, vol. 20, no. 2, pp. 164–168, 2007.

[79] T. Dugladze, I. Vida, A. B. Tort et al., "Impaired hippocampal rhythmogenesis in a mouse model of mesial temporal lobe epilepsy," *Proceedings of the National Academy of Sciences of the United States of America*, vol. 104, no. 44, pp. 17530–17535, 2007.

[80] C. R. Houser, N. H. Zhang, and Z. C. Peng, "Alterations in the distribution of GABAA receptorsin epilepsy," *Epilepsia*, vol. 51, no. 5, article 47, 2010.

[81] S. Penschuck, B. Lüscher, J. M. Fritschy, and F. Crestani, "Activation of the GABA(A)-receptor δ-subunit gene promoter following pentylenetetrazole-induced seizures in transgenic mice," *Molecular Brain Research*, vol. 51, no. 1-2, pp. 212–219, 1997.

[82] A. A. Prinz, "Understanding epilepsy through network modeling," *Proceedings of the National Academy of Sciences of the United States of America*, vol. 105, no. 16, pp. 5953–5954, 2008.

[83] W. Löscher, "Animal models of epilepsy for the development of antiepileptogenic and disease-modifying drugs. A comparison of the pharmacology of kindling and post-status epilepticus models of temporal lobe epilepsy," *Epilepsy Research*, vol. 50, no. 1-2, pp. 105–123, 2002.

[84] K. Morimoto, M. Fahnestock, and R. J. Racine, "Kindling and status epilepticus models of epilepsy: rewiring the brain," *Progress in Neurobiology*, vol. 73, no. 1, pp. 1–60, 2004.

[85] S. C. Baraban, M. R. Taylor, P. A. Castro, and H. Baier, "Pentylenetetrazole induced changes in zebrafish behavior, neural activity and c-fos expression," *Neuroscience*, vol. 131, no. 3, pp. 759–768, 2005.

[86] K. Lukasiuk and L. Kaczmarek, "AP-1 and CRE DNA binding activities in rat brain following pentylenetetrazole induced seizures," *Brain Research*, vol. 643, no. 1-2, pp. 227–233, 1994.

[87] P. Wang, W. P. Wang, S. Zhang, H. X. Wang, Y. Lou, and Y. H. Fan, "Impaired spatial learning related with decreased expression of calcium/calmodulin-dependent protein kinase II_{α} and cAMP-response element binding protein in the pentylenetetrazol-kindled rats," *Brain Research*, vol. 1238, pp. 108–117, 2008.

[88] T. Valente, M. I. Domínguez, A. Bellmann, L. Journot, I. Ferrer, and C. Auladell, "Zac1 is up-regulated in neural cells of the limbic system of mouse brain following seizures that provoke strong cell activation," *Neuroscience*, vol. 128, no. 2, pp. 323–336, 2004.

[89] W. F. Chen, H. Chang, L. T. Huang et al., "Alterations in long-term seizure susceptibility and the complex of PSD-95 with NMDA receptor from animals previously exposed to perinatal hypoxia," *Epilepsia*, vol. 47, no. 2, pp. 288–296, 2006.

[90] M. L. Tsaur, M. Sheng, D. H. Lowenstein, Y. N. Jan, and L. Y. Jan, "Differential expression of K^+ channel mRNAs in the rat brain and down-regulation in the hippocampus following seizures," *Neuron*, vol. 8, no. 6, pp. 1055–1067, 1992.

[91] A. Nehlig, G. Rudolf, C. Leroy, M. A. Rigoulot, I. A. Simpson, and S. J. Vannucci, "Pentylenetetrazol-induced status epilepticus up-regulates the expression of glucose transporter mRNAs but not proteins in the immature rat brain," *Brain Research*, vol. 1082, no. 1, pp. 32–42, 2006.

[92] A. M. Siebel, E. P. Rico, K. M. Capiotti et al., "*In vitro* effects of antiepileptic drugs on acetylcholinesterase and ectonucleotidase activities in zebrafish (*Danio rerio*) brain," *Toxicology In Vitro*, vol. 24, no. 4, pp. 1279–1284, 2010.

[93] A. J. Sehnert, A. Huq, B. M. Weinstein, C. Walker, M. Fishman, and D. Y. R. Stainier, "Cardiac troponin T is essential in sarcomere assembly and cardiac contractility," *Nature Genetics*, vol. 31, no. 1, pp. 106–110, 2002.

[94] C. T. Basson, D. R. Bachinsky, R. C. Lin et al., "Mutations in human TBX5 cause limb and cardiac malformation in Holt-Oram syndrome," *Nature Genetics*, vol. 15, no. 1, pp. 30–35, 1997.

[95] D. M. Garrity, S. Childs, and M. C. Fishman, "The heartstrings mutation in zebrafish causes heart/fin Tbx5 deficiency syndrome," *Development*, vol. 129, no. 19, pp. 4635–4645, 2002.

[96] T. Goto, H. Takase, T. Toriyama et al., "Circulating concentrations of cardiac proteins indicate the severity of congestive heart failure," *Heart*, vol. 89, no. 11, pp. 1303–1307, 2003.

[97] K. Setsuta, Y. Seino, T. Ogawa, M. Arao, Y. Miyatake, and T. Takano, "Use of cytosolic and myofibril markers in the detection of ongoing myocardial damage in patients with chronic heart failure," *American Journal of Medicine*, vol. 113, no. 9, pp. 717–722, 2002.

[98] C. J. Pemberton, S. D. Raudsepp, T. G. Yandle, V. A. Cameron, and A. M. Richards, "Plasma cardiotrophin-1 is elevated in human hypertension and stimulated by ventricular stretch," *Cardiovascular Research*, vol. 68, no. 1, pp. 109–117, 2005.

[99] D. J. Stewart, P. Cernacek, K. B. Costello, and J. L. Rouleau, "Elevated endothelin-1 in heart failure and loss of normal response to postural change," *Circulation*, vol. 85, no. 2, pp. 510–517, 1992.

[100] M. S. Hansen, E. B. Stanton, Y. Gawad et al., "Relation of circulating cardiac myosin light chain 1 isoform in stable severe congestive heart failure to survival and treatment with flosequinan," *American Journal of Cardiology*, vol. 90, no. 9, pp. 969–973, 2002.

[101] C. G. Burns, D. J. Milan, E. J. Grande, W. Rottbauer, C. A. MacRae, and M. C. Fishman, "High-throughput assay for small molecules that modulate zebrafish embryonic heart rate," *Nature Chemical Biology*, vol. 1, no. 5, pp. 263–264, 2005.

[102] M. H. W. Kappers, J. H. M. van Esch, S. Sleijfer, A. J. Danser, and A. H. van den Meiracker, "Cardiovascular and renal toxicity during angiogenesis inhibition: clinical and mechanistic aspects," *Journal of Hypertension*, vol. 27, no. 12, pp. 2297–2309, 2009.

[103] S. J. Nicholls, G. Brandrup-Wognsen, M. Palmer, and P. J. Barter, "Meta-analysis of comparative efficacy of increasing dose of Atorvastatin versus Rosuvastatin versus Simvastatin on lowering levels of atherogenic lipids (from VOYAGER)," *American Journal of Cardiology*, vol. 105, no. 1, pp. 69–76, 2010.

[104] J. Yrjänheikki, J. Koistinaho, M. Kettunen et al., "Long-term protective effect of atorvastatin in permanent focal cerebral ischemia," *Brain Research*, vol. 1052, no. 2, pp. 174–179, 2005.

[105] Y. Lampl, M. Lorberboym, R. Gilad et al., "Early outcome of acute ischemic stroke in hyperlipidemic patients under atorvastatin versus simvastatin," *Clinical Neuropharmacology*, vol. 33, no. 3, pp. 129–134, 2010.

[106] B. N. Huisa, A. B. Stemer, and J. A. Zivin, "Atorvastatin in stroke: a review of SPARCL and subgroup analysis," *Vascular Health and Risk Management*, vol. 6, no. 1, pp. 229–236, 2010.

[107] E. Gjini, L. H. Hekking, A. Küchler et al., "Zebrafish Tie-2 shares a redundant role with Tie-1 in heart development and regulates vessel integrity," *Disease Models and Mechanisms*, vol. 4, no. 1, pp. 57–66, 2011.

[108] S. A. Farber, M. Pack, S. Y. Ho et al., "Genetic analysis of digestive physiology using fluorescent phospholipid reporters," *Science*, vol. 292, no. 5520, pp. 1385–1388, 2001.

[109] K. Hama, E. Provost, T. C. Baranowski et al., "*In vivo* imaging of zebrafish digestive organ function using multiple quenched fluorescent reporters," *American Journal of Physiology*, vol. 296, no. 2, pp. G445–G453, 2009.

[110] K. Stoletov, L. Fang, S. H. Choi et al., "Vascular lipid accumulation, lipoprotein oxidation, and macrophage lipid uptake in hypercholesterolemic zebrafish," *Circulation Research*, vol. 104, no. 8, pp. 952–960, 2009.

[111] L. Fang, R. Harkewicz, K. Hartvigsen et al., "Oxidized cholesteryl esters and phospholipids in zebrafish larvae fed a high cholesterol diet: macrophage binding and activation," *The Journal of Biological Chemistry*, vol. 285, no. 42, pp. 32343–32351, 2010.

[112] S. Jin, J. H. Hong, S. H. Jung, and K. H. Cho, "Turmeric and laurel aqueous extracts exhibit *in vitro* anti-atherosclerotic activity and *in vivo* hypolipidemic effects in a zebrafish model," *Journal of Medicinal Food*, vol. 14, no. 3, pp. 247–256, 2011.

[113] G. A. Rosenberg, S. Mun-Bryce, M. Wesley, and M. Kornfeld, "Collagenase-induced intracerebral hemorrhage in rats," *Stroke*, vol. 21, no. 5, pp. 801–807, 1990.

[114] R. Bullock, A. D. Mendelow, G. M. Teasdale, and D. I. Graham, "Intracranial haemorrhage induced at arterial pressure in the rat. Part 1: description of technique, ICP changes and neuropathological findings," *Neurological Research*, vol. 6, no. 4, pp. 184–188, 1984.

[115] K. M. Wilson, R. B. McCaw, L. Leo et al., "Prothrombotic effects of hyperhomocysteinemia and hypercholesterolemia in ApoE-deficient mice," *Arteriosclerosis, Thrombosis, and Vascular Biology*, vol. 27, no. 1, pp. 233–240, 2007.

[116] A. S. Plump, J. D. Smith, T. Hayek et al., "Severe hypercholesterolemia and atherosclerosis in apolipoprotein E-deficient mice created by homologous recombination in ES cells," *Cell*, vol. 71, no. 2, pp. 343–353, 1992.

[117] C. A. Franco, S. Liebner, and H. Gerhardt, "Vascular morphogenesis: a Wnt for every vessel?" *Current Opinion in Genetics and Development*, vol. 19, no. 5, pp. 476–483, 2009.

[118] N. D. Lawson and B. M. Weinstein, "*In vivo* imaging of embryonic vascular development using transgenic zebrafish," *Developmental Biology*, vol. 248, no. 2, pp. 307–318, 2002.

[119] U. Langheinrich, "Zebrafish: a new model on the pharmaceutical catwalk," *BioEssays*, vol. 25, no. 9, pp. 904–912, 2003.

[120] M. Raghunath, Y. Sy Wong, M. Farooq, and R. Ge, "Pharmacologically induced angiogenesis in transgenic zebrafish," *Biochemical and Biophysical Research Communications*, vol. 378, no. 4, pp. 766–771, 2009.

[121] S. Nicoli, G. De Sena, and M. Presta, "Fibroblast growth factor 2-induced angiogenesis in zebrafish: the zebrafish yolk membrane (ZFYM) angiogenesis assay," *Journal of Cellular and Molecular Medicine*, vol. 13, no. 8, pp. 2061–2068, 2009.

[122] D. Alex, I. K. Lam, Z. Lin, and S. M. Y. Lee, "Indirubin shows anti-angiogenic activity in an *in vivo* zebrafish model and an *in vitro* HUVEC model," *Journal of Ethnopharmacology*, vol. 131, no. 2, pp. 242–247, 2010.

[123] X. L. Lu, D. Luo, X. L. Yao et al., "Dl-3n-butylphthalide promotes angiogenesis via the extracellular signal-regulated kinase 1/2 and phosphatidylinositol 3-kinase/Akt-endothelial nitric oxide synthase signaling pathways," *Journal of Cardiovascular Pharmacology*, vol. 59, no. 4, pp. 352–362, 2012.

[124] H. W. Lam, H. C. Lin, S. C. Lao et al., "The angiogenic effects of *Angelica sinensis* extract on HUVEC *in vitro* and zebrafish *in vivo*," *Journal of Cellular Biochemistry*, vol. 103, no. 1, pp. 195–211, 2008.

[125] S. J. Hong, J. B. Wan, Y. Zhang et al., "Angiogenic effect of saponin extract from *Panax notoginseng* on HUVECs *in vitro* and zebrafish *in vivo*," *Phytotherapy Research*, vol. 23, no. 5, pp. 677–686, 2009.

[126] J. R. Jackson, M. P. Seed, C. H. Kircher, D. A. Willoughby, and J. D. Winkler, "The codependence of angiogenesis and chronic inflammation," *The FASEB Journal*, vol. 11, no. 6, pp. 457–465, 1997.

[127] P. Carmeliet and R. K. Jain, "Angiogenesis in cancer and other diseases," *Nature*, vol. 407, no. 6801, pp. 249–257, 2000.

[128] F. Balkwill and A. Mantovani, "Inflammation and cancer: back to Virchow?" *The Lancet*, vol. 357, no. 9255, pp. 539–545, 2001.

[129] M. Hau, C. Kneitz, H. P. Tony, M. Keberle, R. Jahns, and M. Jenett, "High resolution ultrasound detects a decrease in pannus vascularisation of small finger joints in patients with rheumatoid arthritis receiving treatment with soluble tumour necrosis factor α receptor (etanercept)," *Annals of the Rheumatic Diseases*, vol. 61, no. 1, pp. 55–58, 2002.

[130] F. Mor, F. J. Quintana, and I. R. Cohen, "Angiogenesis-inflammation cross-talk: vascular endothelial growth factor is secreted by activated T cells and induces Th1 polarization," *Journal of Immunology*, vol. 172, no. 7, pp. 4618–4623, 2004.

[131] G. Bonizzi and M. Karin, "The two NF-κB activation pathways and their role in innate and adaptive immunity," *Trends in Immunology*, vol. 25, no. 6, pp. 280–288, 2004.

[132] I. Meteoglu, I. H. Erdogdu, N. Meydan, M. Erkus, and S. Barutca, "NF-κB expression correlates with apoptosis and angiogenesis in clear cell renal cell carcinoma tissues," *Journal of Experimental and Clinical Cancer Research*, vol. 27, no. 1, article 53, 2008.

[133] W. K. Leung, K. F. To, M. Y. Go et al., "Cyclooxygenase-2 upregulates vascular endothelial growth factor expression and angiogenesis in human gastric carcinoma," *International Journal of Oncology*, vol. 23, no. 5, pp. 1317–1322, 2003.

[134] B. H. Kim, C. I. Kim, H. S. Chang et al., "Cyclooxygenase-2 overexpression in chronic inflammation associated with benign prostatic hyperplasia: Is it related to apoptosis and angiogenesis of prostate cancer?" *Korean Journal of Urology*, vol. 52, no. 4, pp. 253–259, 2011.

[135] R. Kannappan, S. C. Gupta, J. H. Kim, and B. B. Aggarwal, "Tocotrienols fight cancer by targeting multiple cell signaling pathways," *Genes and Nutrition*, vol. 7, no. 1, pp. 43–52, 2012.

[136] Y. C. Hseu, C. R. Wu, H. W. Chang et al., "Inhibitory effects of *Physalis angulata* on tumor metastasis and angiogenesis," *Journal of Ethnopharmacology*, vol. 135, no. 3, pp. 762–771, 2011.

[137] T. Kunikata, T. Tatefuji, H. Aga, K. Iwaki, M. Ikeda, and M. Kurimoto, "Indirubin inhibits inflammatory reactions in delayed-type hypersensitivity," *European Journal of Pharmacology*, vol. 410, no. 1, pp. 93–100, 2000.

[138] U. P. Singh, N. P. Singh, B. Singh et al., "Resveratrol (Trans-3,5,4′-trihydroxystilbene) induces silent mating type information regulation-1 and down-regulates nuclear transcription factor-κB activation to abrogate dextran sulfate sodium-induced colitis," *Journal of Pharmacology and Experimental Therapeutics*, vol. 332, no. 3, pp. 829–839, 2010.

[139] H. Zhao, J. Deneau, G. O. Che et al., "*Angelica sinensis* isolate SBD.4: composition, gene expression profiling, mechanism of action and effect on wounds, in rats and humans," *European Journal of Dermatology*, vol. 22, no. 1, pp. 58–67, 2012.

[140] G. Hu, G. B. Mahady, S. Li et al., "Polysaccharides from astragali radix restore chemical-induced blood vessel loss in zebrafish," *Vascular Cell*, vol. 4, no. 1, article 2, 2012.

[141] H. Y. Tse, M. N. Hui, L. Li et al., "Angiogenic efficacy of simplified 2-herb formula (NF3) in zebrafish embryos *in vivo* and rat aortic ring *in vitro*," *Journal of Ethnopharmacology*, vol. 139, no. 2, pp. 447–453, 2012.

[142] S. B. Dunnett and A. Björklund, "Prospects for new restorative and neuroprotective treatments in Parkinson's disease," *Nature*, vol. 399, no. 6738, supplement, pp. A32–A39, 1999.

[143] K. J. Barnham, C. L. Masters, and A. I. Bush, "Neurodegenerative diseases and oxidatives stress," *Nature Reviews Drug Discovery*, vol. 3, no. 3, pp. 205–214, 2004.

[144] O. Weinreb, T. Amit, O. Bar-Am, and M. B. H. Youdim, "Rasagiline: a novel anti-Parkinsonian monoamine oxidase-B inhibitor with neuroprotective activity," *Progress in Neurobiology*, vol. 92, no. 3, pp. 330–344, 2010.

[145] M. Wang, Z. Zhang, L. C. Cheang, Z. Lin, and S. M. Lee, "Eriocaulon buergerianum extract protects PC12 cells and neurons in zebrafish against 6-hydroxydopamine-induced damage," *Chinese Medicine*, vol. 6, article 16, 2011.

[146] B. S. Koo, W. C. Lee, Y. C. Chang, and C. H. Kim, "Protective effects of alpinae oxyphyllae fructus (*Alpinia oxyphylla* MIQ) water-extracts on neurons from ischemic damage and neuronal cell toxicity," *Phytotherapy Research*, vol. 18, no. 2, pp. 142–148, 2004.

[147] X. Yu, L. An, Y. Wang, H. Zhao, and C. Gao, "Neuroprotective effect of *Alpinia oxyphylla* Miq. fruits against glutamate-induced apoptosis in cortical neurons," *Toxicology Letters*, vol. 144, no. 2, pp. 205–212, 2003.

[148] J. C. Ho and C. M. Chen, "Flavonoids from the aquatic plant *Eriocaulon buergerianum*," *Phytochemistry*, vol. 61, no. 4, pp. 405–408, 2002.

[149] L. X. Yang, K. X. Huang, H. B. Li et al., "Design, synthesis, and examination of neuron protective properties of alkenylated and amidated dehydro-silybin derivatives," *Journal of Medicinal Chemistry*, vol. 52, no. 23, pp. 7732–7752, 2009.

[150] Y. C. Lo, Y. T. Shih, I. J. Chen, and Y. C. Wu, "San-Huang-Xie-Xin-Tang protects against activated microglia- and 6-OHDA-induced toxicity in neuronal SH-SY5Y cells," *Evidence-Based Complementary and Alternative Medicine*, vol. 2011, Article ID 429384, 11 pages, 2011.

Hindawi Publishing Corporation
Evidence-Based Complementary and Alternative Medicine
Volume 2012, Article ID 426757, 8 pages
doi:10.1155/2012/426757

Research Article

Behavioral, Neurochemical and Neuroendocrine Effects of Abnormal Savda Munziq in the Chronic Stress Mice

Nurmuhammat Amat,[1] Parida Hoxur,[2] Dang Ming,[1] Aynur Matsidik,[1] Anake Kijjoa,[3] and Halmurat Upur[1]

[1] *Traditional Uighur Medicine Department, Xinjiang Medical University, 393 Medical University Road, Urumqi, Xinjiang 830011, China*
[2] *Neurology Department, Xinjiang Medical University Affiliation of Traditional Chinese Medicine Hospital, 116 Huanghe Road, Urumqi, Xinjiang 83000, China*
[3] *Instituto de Ciências Biomédicas de Abel Salazar (ICBAS), Universidade do Porto, Rua de Jorge Viterbo Ferreira 228, 40-50-313 Porto, Portugal*

Correspondence should be addressed to Halmurat Upur, halmurat@263.net

Received 6 April 2012; Revised 1 June 2012; Accepted 18 June 2012

Academic Editor: Paul Siu-Po Ip

Oral administration of Abnormal Savda Munsiq (ASMq), a herbal preparation used in Traditional Uighur Medicine, was found to exert a memory-enhancing effect in the chronic stressed mice, induced by electric foot-shock. The memory improvement of the stressed mice was shown by an increase of the latency time in the step-through test and the decrease of the latency time in the Y-maze test. Treatment with ASMq was found to significantly decrease the serum levels of adrenocorticotropic hormone (ACTH), corticosterone (CORT) and β-endorphin (β-EP) as well as the brain and serum level of norepinephrine (NE). Furthermore, ASMq was able to significantly reverse the chronic stress by decreasing the brain and serum levels of the monoamine neurotransmitters dopamine (DA), 5-hydroxytryptamine (5-HT) and 3,4-dihydroxyphenylalanine (DOPAC). The results obtained from this study suggested that the memory-enhancing effect of ASMq was mediated through regulations of neurochemical and neuroendocrine systems.

1. Introduction

According to the Traditional Uighur Medicine (TUM), the abnormal Savda syndrome can be caused by exogenous (environmental, psychological, and emotional) as well as endogenous stimuli or stressors [1]. We thus hypothesized, in terms of modern medicine, the etiology and pathogenesis of abnormal Savda syndrome as the state under stress conditions whose symptoms, manifested in the clinical conditions of chronic diseases, include mental stress, tantrum, hypomnesis, dry skin, polydipsia, polyphagia, and memory dysfunction [2].

Abnormal Savda Munsiq (ASMq) is a well-known complex prescription of Traditional Uighur Medicine for abnormal Savda which consists of crude drugs of ten medicinal herbs: *Adiantum capillus-veneris* L. *Alhagi pseudalhagi* (Bieb.) Desv., *Anchusa italica* Retz., *Cordia dichotoma* G. Forst., *Euphorbia maculata* L., *Foeniculum vulgare* Mill., *Glycyrrhiza glabra* L., *Lavandula angustifolia* Mill., *Melissa officinalis* L., and *Ziziphus jujuba* Mill. ASMq is widely used in the prevention and treatment of many chronic diseases such as cancer, hypertension, diabetes mellitus, and memory dysfunction, the diseases which are associated with abnormal Savda Hilit and whose symptomatic expression is known as abnormal Savda Syndrome [3].

It is well established that the disruption of the hypothalamus-pituitary-adrenal (HPA) axis, a central pathway to the entire endocrine system, is often central to most health problems, syndromes, diseases, and even aging itself [4–6]. Hyperactive status of the HPA axis can result in increasing levels of corticotropin-releasing hormone (CRH), adrenocorticotropic hormone (ACTH), and glucocorticoids

in the hypothalamus, pituitary, and adrenal cortex, respectively [7, 8]. On the one hand, stress can also alter the physiological homeostasis which can result in various neuronal, endocrine, and visceral dysfunctions [9]. Furthermore, stress is also known to alter cognitive functions, such as memory, and it has been linked to the pathophysiology of mood and anxiety disorders [7, 10]. A central feature of the stress response is the activation of the HPA axis which can result in an increase in plasma levels of glucocorticoids [11]. As a consequence of their profound effects on neurons, glucocorticoids can influence behavior, mood, and memory process [12, 13]. Neurotransmitter systems are also involved in learning and memory processes, and a substantial part of learning and memory impairments is due to changes in neurotransmission [14]. It is well established that neurotransmitters can interfere with learning acquisition and memory [15]. In this context, the memory dysfunction described in abnormal Savda syndrome could involve an excessive production of corticotropin-releasing hormone (CRH), adrenocorticotropic hormone (ACTH), and glucocorticoids in the hypothalamus, pituitary, and adrenal cortex, respectively, under the stress condition.

Although ASMq has been previously investigated pharmacologically and clinically for its antioxidant [2], immunomodulatory [3], and anticancer activities [16] as well as for its protective effects against radiation-induced and oxidative stress-induced damages [17–20], its potential protective effects against neurological hormone imbalance have never been systematically evaluated. Therefore, in our continuing effort to support the therapeutic values of Traditional Uighur Medicine (TUM), we have further evaluated the effects of ASMq on memory capability and concomitant biochemical parameters, such as neurotransmitters (ACTH, CORT, and β-EP), as pathophysiological indicators involved in the chronic stress mice model. The selected model is based on the fact that psychological chronic stress-induced (electric foot-shock) pathophysiology is similar to the conditions of abnormal Savda syndrome described in the ancient theory of TUM.

2. Materials and Methods

2.1. Reagents. Mice adrenocorticotropin (ACTH), corticosterone (CORT), and β-endorphin (β-EP) kits were obtained from R&D Systems, USA. Norepinephrine (NE, purity ≥ 97%), dopamine (DA, purity ≥ 99%), 5-hydroxytryptamine (5-HT, purity ≥ 99%), 3,4–dihydroxyphenylamine (DOPAC, purity ≥ 99%),and 3,4-dihydroxybenzylamine (DHBA, purity ≥ 98%) were obtained from Sigma Co., Ltd., USA. All other reagents were of analytical grade.

2.2. Preparation of the Aqueous Extract of ASMq. Plant materials for ASMq (Table 1) were purchased from Xinjiang Uighur Autonomous Region Traditional Uighur Medicine Hospital in Urumqi (China) and authenticated by Pharmacist Abuduwar of the Uighur Medicine Preparation Center of Xinjiang Autonomous Region Traditional Uighur Medicine Hospital. The voucher specimens (070818) were deposited at the herbarium of this Preparation Center. Briefly, all the herbs were chopped into small pieces and ground. The powdered material (1 kg) was macerated in warm distilled water (10 L) at 80°C for 12 h. The solution was then boiled for 30 min and left to stand for 1 h before filtration. The filtrate was then concentrated to semisolid mass under reduced pressure and dried at 60°C under vacuum condition. The yield of the extract was 29.4% (w/w) of the dried plant materials. The extract was dissolved in 0.5% sodium carboxymethyl cellulose (CMC-Na) solution and administered to the mice according to the experimental dosages.

2.3. Animal. The pathogen-free ICR male mice weighing 18–20 g (Xinjiang Medical University Animal Center, Urumqi, China) were kept under condition of controlled temperature (24°C) and illumination (12 h light cycle) and were maintained on laboratory standard diet and water freely. The animals were divided randomly into five groups of 10 mice. The mice were kept under laboratory condition for 3 days before drug administration. The mice of normal group (Gr. I) were housed and fed in the normal condition. The chronic stress was induced in mice by application of the electric-foot shock. The stress model group (Gr. II) received the repeated electric foot-shock (volume 20–30 V, interval 0.2–0.5 s during 20 min/day) in the electric foot-shock instrument before being housed in the climatic cabinet from 8:30 am–10:30 pm (at 6°C and 25–32.8% of relative humidity). The experimental procedures were approved by the guidelines of the Animal Care and Use Committee of Xinjiang Uighur Autonomous Region.

2.4. Drug Administration. 0.5% Sodium carboxyl methyl cellulose (CMC-Na) solution (20 mL/kg, b.w.) was administered orally to the normal (Gr. I) and the stress model (Gr. II) mice once a day during 14 days. Another groups of mice received ASMq solution orally at the dose of 2.53 g/kg (Gr. IIIa), 5.06 g/kg (Gr. IIIb), and 10.12 g/kg (Gr. IIIc), respectively, between 7:30 am–9:30 am daily during 14 days. These doses were calculated according to the conversion table of equivalent effective dose ratios from human to animals based on the body surface area. Food was withdrawn from the animals 2 h prior to drug administration but water was allowed freely. The ASMq pretreatment groups (Gr. IIIa, IIIb, and IIIc) received the same electric foot-shock one hour after drug administration (8:30 am–10:30 am).

2.5. Determination of Memory Capacity by the Y-Maze Task and the Passive Avoidance Task

2.5.1. Y-Maze Task. The Y-maze task test was performed as previously described by Munck et al. [21]. The Y-maze apparatus with a conductive grid floor consisted of three identical arms (40 L × 10 w × 20 h cm) made of dark opaque Plexiglas and positioned at equal angles. Arms 1 and 3 were in the non-safety zone (where shocks were administered) while arm 2 was in a safety zone (on top of which there was an insulated grid floor of 10 × 15 cm). The test was conducted in two consecutive days at the same time of the day

Table 1: Plants for the Uighur herbal formula of Abnormal Savda Munsiq (ASMq).

Latin name	Family	Part used	Uighur name	Chinese name
Adiantumcapillus-veneris L.	Adiantaceae	whole plant	Pirsiyavxan	Tiexianjue
Alhagi pseudalhagi (Bieb.) Desv.	Fabaceae	branch secretion	Kök tantak	Citang
Anchusa italica Retz.	Boraginaceae	whole plant	Gavziban	Niushecao
Cordia dichotoma G.Forst.	Boraginaceae	fruit	Serbistan	Pobumuguo
Euphorbia maculata L.	Euphorbiaceae	whole plant	—	—
Foeniculum vulgare Mill.	Apiaceae	fruit	Arpabidiyan	Xiaohuixiang
Glycyrrhiza glabra L.	Fabaceae	radix or rhizoma	—	—
Lavandula angustifolia Mill.	Lamiaceae	aerial parts	Üstihuddus	Xunyicao
Melissa officinalis L.	Lamiaceae	whole plant	Badrenjiboye hindi	Mifenghua
Ziziphus jujuba Mill.	Rhamnaceae	fruit	Qilan	Dazao

(after 14 days of oral administration with ASMq for Gr. IIIa, IIIb, and IIIc). On the first day, each mouse was placed on the top of arm 1, and a fixed resistance shock source was connected to an automatically operated switch, and electric shocks (36 V) were applied. After shocking, the mice escaped from foot-shocks by accidentally entering the top of arm 2 and this was counted as one practice and the mice were repeatedly trained for this procedure for ten more times. After a 24 h interval, the mice were successively tested ten times and their latency time to enter the safety zone (i.e., insulated grid floor) from non-safety zone for the first time and the number of errors displayed by entering the non-safety zone within ten repetitions were recorded as learning performances.

2.5.2. Passive Avoidance Task: Step-Through Test. A passive avoidance reflex apparatus was provided by Xinjiang Medical University (Urumqi, China), which was separated into a lightened chamber (11 cm × 3.2 cm) and a dark chamber (17 cm × 3.2 cm), with a connecting tunnel and copper grids on the floor. The test was conducted in two consecutive days at the same time of the day (after 14 days of oral administration with different doses of ASMq for Gr. IIIa, IIIb, and IIIc). On the first day, each mouse was placed in the illuminated compartment. Each mouse received a learning trial 24 h before the test. Mice were placed into the lightened chamber and on stepping through the tunnel into the dark chamber; they would suffer a 40 V electric stimulation (in order to condition them to stay in the lightened chamber) and escape out of the dark chamber. 24 h later, mice were placed into the lightened chamber again and the latency time of mice staying in the lightened chamber and the number of times they entered the dark chamber within 5 min were recorded to evaluate their memory capacity.

2.6. Measurements of Adrenocorticotropin (ACTH), Corticosterone (CORT), and β-Endorphin (β-EP). On the last day of drug administration, the blood was collected and centrifuged at 4°C; the serum was stored at −80°C before assay. Serum levels of ACTH, CORT, and β-EP were determined using ELISA kit (obtained from R&D Systems). The sensitivity of the assay was 1.0 ng/mL. Intra-assay and inter-assay coefficients of variation were less than 4.85% and 6.08%, respectively. The test was performed according to the manufacturer's specification.

2.7. Measurements of Monoamine Neurotransmitters by HPLC-FCD. Levels of monoamine neurotransmitters (NE, DA, 5-HT, and DOPAC) in serum and brain were measured by HPLC coupled with a fluorescence detector (FCD). Mice were sacrificed immediately after exposure to the stress. Blood was sampled into EDTA-containing tubes at 10:00 am, and separated in a refrigerated centrifuge at 10,000 ×g for 10 min at 4°C. The serum was stored at −80°C until assayed. After blood collection, the brains were quickly removed, frozen in liquid nitrogen, and stored at −80°C until assayed. To determine serum monoamine neurotransmitter levels, an equal volume of 0.1 M HCl was added to the serum samples containing 200 μg/mL of DHBA as an internal standard. The samples were then shaken and mixed for 1.5 min in ice water. One drop of concentrated HCl was then added to the solution and mixed in ice water for another 1.5 min and then centrifuged at 3000 rpm, 4°C for 10 min. The samples of brain tissue were homogenized in ice water solution of 0.1 M HCl. Then, 0.1 M HCl solution was added to the samples (1 μL/1 mg tissue) containing 200 μg/mL of DHBA as an internal standard and centrifuged at 18000 rpm, 4°C for 10 min. The samples were filtered through 0.45 μm microfilters (MFS Inc., USA). Aliquots (10 μL) of supernatant were injected into a reverse phase HPLC column (condition: Agilent 110180 high-voltage pump coupled to a fluorescence detector, chromatographic column ZORBAX ODB C18 4.6 mm × 150 mm × 5 mm, voltage 121 V, and wavelength 360 nm). All the brain samples were weighed on an electronic scale prior to HPLC analysis, and the results were expressed as ng of monoamine/mg of wet weight tissue.

2.8. Statistical Analysis. Data were expressed as the mean ± standard error of the mean (SEM). The statistical significance of the differences between the groups was analyzed by one-way analysis of variance (ANOVA) following by least significant difference (LSD) tests. All statistical calculations were performed using SPSS v13.0. Value of $P < 0.05$ was considered to be significant.

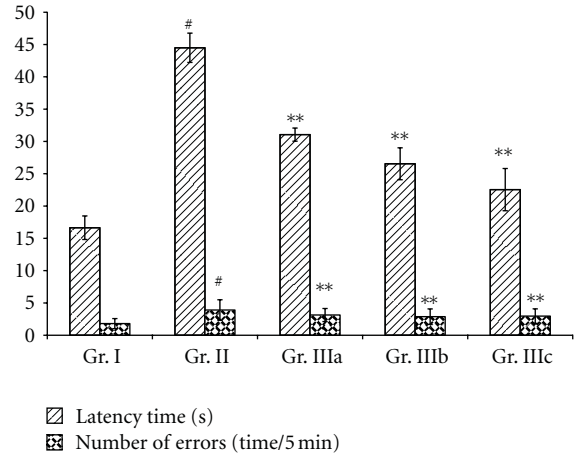

Figure 1: The effect of ASMq on chronic stress-induced spatial working memory deficit in the Y-maze test. According to protocol, the animals received daily administration of 2.53, 5.06, and 10.12 g/kg of ASMq for 14 days. Two weeks after the drug administration period, the Y-maze test was conducted. Each data column represents the mean ± SEM ($n = 10$). $^{\#}P < 0.05$ compared with vehicle-treated group (Gr. I). $^{**}P < 0.05$ compared with vehicle-treated model group (Gr. II).

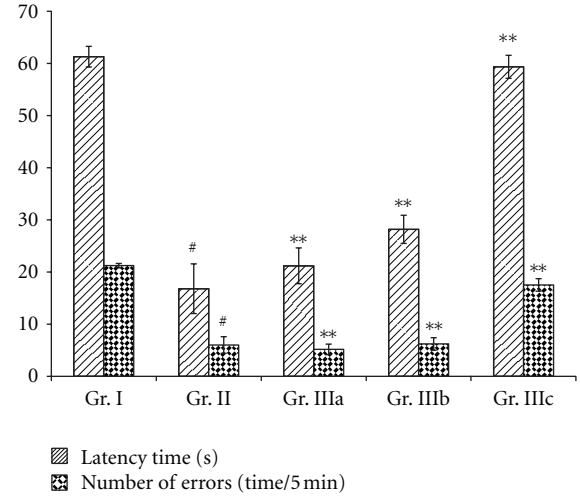

Figure 2: Behavioral effect of ASMq in the passive avoidance task. ASMq or vehicle was orally administered once a day for 14 days (2.53, 5.06, and 10.12 g/kg/day). The last treatment with ASMq or vehicle was administered 120 min before an acquisition trial. Twenty four hours after the acquisition trial, a 5 min retention trial was carried out. Data are expressed as means ± SEM ($n = 10$/group). $^{\#}P < 0.05$ compared with the vehicle-treated group (Gr. I). $^{**}P < 0.05$ compared with the vehicle-treated model group (Gr. II).

3. Results

3.1. Effects of ASMq on Memory Capability in Stress Mice. In the Y-maze task test, the latency time and number of errors of the chronic stress mice (Gr. II) were found to be markedly increased when compared to the normal group (Gr. I). In contrast, mice treated with ASMq, by oral administration, at doses of 2.53 g/kg, 5.06 g/kg, and 10.12 g/kg (Gr. IIIa, IIIb, and IIIc) for 14 days showed an improvement of a memory as evidenced by a decrease of the latency time and the number of errors (Figure 1). On the other hand, in the passive avoidance task, the chronic stress mice (Gr. II) showed a significant decrease of the latency time and an increase in the number of errors when compared to the normal group (Gr. I). Oral administration with ASMq at doses of 2.53 g/kg, 5.06 g/kg, and 10.12 g/kg (Gr. IIIa, IIIb, and IIIc) for 14 days has boosted the memory capability as indicated by an increase of latency time and a decrease of the number of errors (Figure 2).

3.2. Effects of ASMq on the Serum Levels of ACTH, CORT, and β-EP in the Chronic Stress Mice. Table 2 showed that the serum levels of ACTH, CORT, and β-EP were markedly increased ($P < 0.01$) in the chronic stress mice (Gr. II) when compared to the normal group (Gr. I). Oral administration of ASMq at doses of 2.53 g/kg, 5.06 g/kg, and 10.12 g/kg (Gr. IIIa, IIIb, and IIIc) for 14 days caused a decrease of the levels of ACTH, CORT, and β-EP in the serum when compared to the model group (Gr. II).

3.3. Effects of ASMq on the Contents of Monoamine Neurotransmitters of Brain and Serum in the Chronic Stress Mice. Figures 3 and 4 showed an increase ($P < 0.05$) of NE level in the serum of the chronic stress mice (Gr. II) and a decrease of the serum levels of DA, 5-HT, and DOPAC ($P < 0.01$), when compared to the normal group (Gr. I). Oral administration of ASMq during 14 days at doses of 2.53 g/kg, 5.06 g/kg, and 10.12 g/kg (Gr. IIIa, Gr. IIIb, and Gr. IIIc) was able to decrease the NE levels ($P < 0.01$), while the levels of DA, 5-HT, and DOPAC were increased ($P < 0.05$).

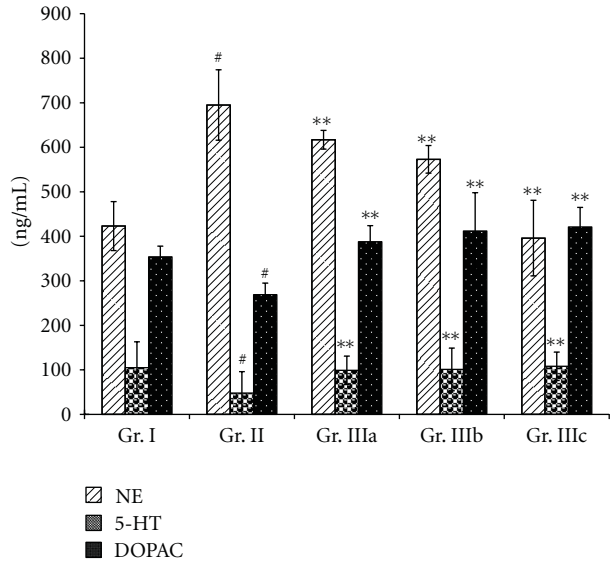

Figure 3: Effect of ASMq (2.53, 5.06, and 10.12 g/kg) on the concentration of NE, 5-HT, and DOPAC.

Figures 5 and 6 showed similar results with an increase of the NE level ($P < 0.01$) but a decrease in the levels of DA and

Table 2: Effects of ASMq on the serum level of ACTH, CORT, and β-EP in the stress mice.

	ACTH (pg/mL)	CORT (pg/mL)	β-EP (pg/mL)
Gr. I	16.01 ± 3.12	12.10 ± 4.9	154.17 ± 27.19
Gr. II	32.16 ± 4.14*	29.23 ± 4.5*	256.21 ± 23.12*
Gr. IIIa	22.31 ± 3.89**	19.98 ± 5.6**	201.32 ± 34.25**
Gr. IIIb	19.64 ± 4.21**	21.51 ± 3.34**	193.11 ± 19.65**
Gr. IIIc	17.56 ± 2.84**	21.46 ± 2.1**	176.01 ± 20.56**

* Results are given as means ± SEM, when compared to the normal group (Gr. I), $P < 0.01$.
** Results are given as means ± SEM, when compared to the model group (Gr. II), $P < 0.05$.

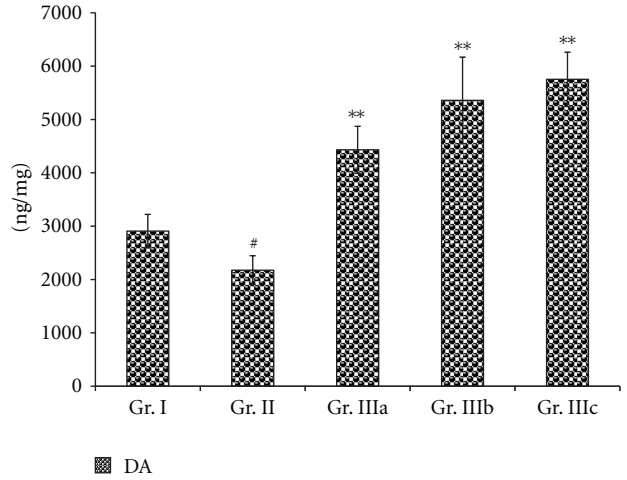

Figure 4: Effect of of ASMq (2.53, 5.06 and 10.12 g/kg) on the serum concentration of DA in the chronic stress. Values given are means ± SEM ($n = 10$).

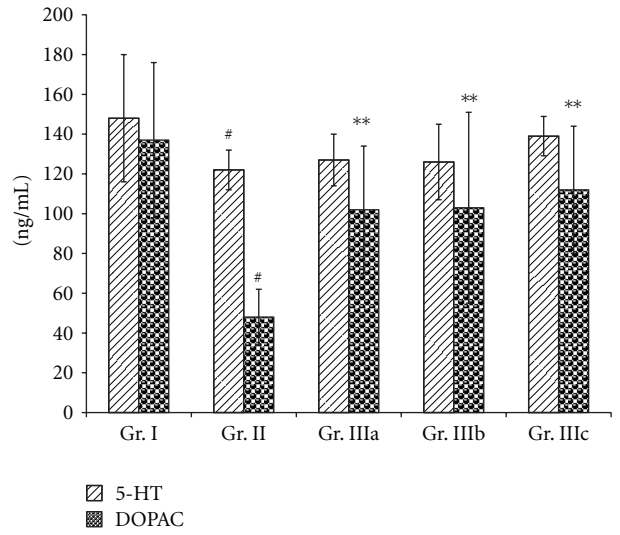

Figure 5: Effect of ASMq (2.53, 5.06, and 10.12 g/kg) on the concentration of 5-HT and DOPAC in the brain of the chronic stress mice. Values given are means ± SEM ($n = 10$).

DOPAC ($P < 0.01$) in the brain of the chronic stress mice (Gr. II), when compared to the normal group (Gr. I). However, there were no statistically significant differences in the levels of 5-HT between the stress mice (Gr. II) and the normal group (Gr. I). All doses of ASMq (2.53 g/kg, 5.06 g/kg, and 10.12 g/kg) were found to reduce the concentration of NE in the brain ($P < 0.01$) when compared to the stress mice (Gr. II). In contrast, only the dosages of 5.06 g/kg and 10.12 g/kg of ASMq (Gr. IIIb and IIIc) could raise the levels of DA in the brain ($P < 0.05$) of the stress mice (Gr. II) while the concentrations of DOPAC in the brain were increased with all doses of ASMq ($P < 0.05$).

4. Discussion

It is generally accepted today that there is a strong link between stressful experiences and altered neurochemistry, endocrinology, and immunology [22], and it is also well established that unpredictable and uncontrollable stressful events can affect cognitive processes. However, only hippocampus-mediated memory processes are thought to be sensitive to the effects of chronic stress.

Many studies of nootropic (memory-enhancing) drugs use step-down, step-through, maze test, and so forth, which

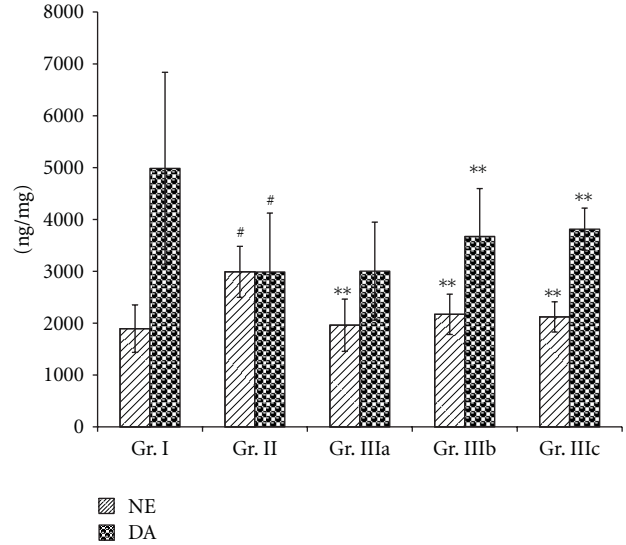

Figure 6: Effect of ASMq (2.53, 5.06, and 10.12 g/kg) on the concentration of NE and DA in the brain of the chronic mice. Values given are means ± SEM ($n = 10$).

are often applied to the determination of capabilities of passive avoidance and spatial memory in animals to investigate their behavior changes. For this reason, we used the Y-maze task and the passive avoidance task tests to evaluate of the effects of ASMq on the memory capability of the stress mice model. Figures 1 and 2 show an improvement in learning performances of aged mice receiving ASMq by an increased latency and a decreased number of errors in the step-through test, as well as by a shortened latency and a decreased number of errors in the Y-maze test.

In contrast, the hippocampus-independent memory processes have been shown to be resistant to chronic stressful experiences [23]. Generally, two systems are being considered in the pathogenesis of memory dysfunction—the hormones of the sympathetic nervous system (adrenalin and noradrenalin) and the hormones of the HPA axis (CRH, ACTH, and CORT). These stress-responsive systems interact at multiple levels in the periphery and in the brain, and together, they influence memory in a complex manner. Many neurotransmitters, including acetylcholine, dopamine (DA), norepinephrine (NE), and serotonin (5-HT), are found to play an important role in the learning and memory processes, and some monoamines are also known to be potent activators of the HPA axis [24]. NE is considered to be relevant to learning and memory consolidation, possibly by acting as a coordinator of signals [25]. It can also control the release of CRH in the hypothalamus and hence an ACTH mediator of the acute stress response and HPA axis, respectively. The catecholamine system, especially DA, has been also implicated in learning and memory process; however, excessive or insufficient levels of DA can lead to impairment [26]. It has been shown that DA has a beneficial impact on spatial working memory [27] and motivational processes [28] while serotonin (5-HT) may be seen also as a crucial "fine tuner" of normal and pathological processes in addition to having a role as a conventional neurotransmitter [29]. Clinical and experimental evidences have suggested that 5-HT is involved in the regulation of mood, sleep, memory, learning, and behavior, all of which are deranged to varying extents in patients with severe depression [30]. Furthermore, 5-HT has been linked to emotional processes [31], and it was found to play a particular role in emotionally related tasks. Despite the lack of functional specialization, the serotonergic system can play a significant role in learning and memory [32]. The function of HPA axis and 5-HT is intimately linked, and 5-HT is found to participate in modulating the HPA axis [33]. The results of our study have corroborated this proposal. Table 2 showed that the levels of ACTH, CORT, and β-EP were dramatically increased in the electric foot-shock-induced chronic stress mice and oral administration of ASMq at doses of 2.53 g/kg, 5.06 g/kg, and 10.12 g/kg for 14 days was able to reverse the levels of these hormones. Our finding is particularly relevant since it is also well known that cognitive deficits induced by various lesions to the locus are reversible by administration of drugs that enhance noradrenergic neurotransmission.

Our results showed also that oral administration of ASMq at doses of 2.53 g/kg, 5.06 g/kg, and 10.12 g/kg clearly regulated the serum and brain monoamine neurotransmitter levels after alteration induced by chronic electric foot-shock. These findings demonstrate that the brain and serum levels of NE were decreased whereas those of DA and DOPAC were markedly increased (Figures 3, 4, 5, and 6). Although the serum levels of 5-HT were found to be markedly increased, the levels of 5-HT in the brain were not statistically different ($P > 0.05$) between the model (Gr. II) and the normal groups (Gr. I).

Considering the composition of ASMq, it is pertinent to mention also that the chemical constituents of the ten herbal drugs used in the preparation could contribute to its capacity to restore memory and cognitive function of the stress mice. For example, flavonoids have been reported as constituents of *Adiantum capillus-veneris* [34], *Euphorbia maculata* [35], and *Zizyphus jujuba* [36], and emerging evidence suggested that they may exert beneficial effects on the central nervous system by protecting neurons against stress-induced injury, by suppressing neuroinflammation, and by improving cognitive function. It is likely that flavonoids exert such effects, through selective actions on different components of a number of protein kinases and lipid kinase signaling cascades, such as the phosphatidylinositol-3 kinase (PI3 K)/Akt, protein kinase C, and mitogen-activated protein kinase (MAPK) pathways rather than via their potential to act as classical antioxidants [37]. It was also reported that daily oral administration of flavonoids (35 mg/kg, for 19-20 days), isolated from aerial parts of *Scutellaria baicalensis* Georgi, could reduce memory dysfunction and neuronal injury caused by permanent global ischemia in rats [38]. Another group of phytochemicals is saponins which are constituents of *Anchusa italica* [39] and *Glycyrrhiza glabra* [40, 41]. Previous reports have demonstrated that they could be responsible for improvement of the learning impairment [42]. Zhang et al. [42] have found that tenuifolin, extracted from *radix polygalae*, was able to significantly enhance learning performances in aged mice by the step-down and Y-maze tasks. They have suggested that the improvement of learning and memory of aged mice was mediated by the effects of tenuifolin on the three stages of memory process, that is, acquisition, consolidation, and retrieval by relatively increasing the levels of NE, DA in the hippocampus and by decreasing the activity of acetylcholine esterase in the cortex. Interestingly, essential oil, which is a major constituent of *Melissa officinalis* and *Lavandula angustifolia* [43], can also exert its function on learning and memory processes. Zhang et al. [44] have reported the ameliorating effects of essential oil from *Acori graminei rhizoma* on learning and memory in aged rat and mice. By investigating the levels of cerebral neurotransmitters, they have suggested that essential oil improved cognitive function in aged rats possibly by increasing NE, DA, and 5-HT relative levels, as well as by decreasing the activity of acetylcholine esterase in the cerebra. Not surprisingly, *Melissa officinalis,* a herbal drug of the traditional medicine in many cultures, has been attributed with memory-enhancing properties. Interestingly, the ethanol crude extract of *Melissa officinalis* leaves was shown to be able to modulate mood and cognitive performance during acute administration in healthy young volunteers [44]. Finally, the aqueous extract of *Lavandula angustifolia* flowers was

found to significantly block glutamate-induced neurotoxicity [45] while the methanolic extract of the whole plant of *Foeniculum vulgare* could ameliorate the amnesic effect of scopolamine and aging-induced memory deficit in mice [46], and administration of *Foeniculum vulgare* extract was able to increase step-down latency and inhibit significantly acetylcholine esterase.

5. Conclusion

The results of this study have demonstrated that the effects of ASMq on the HPA axis dysfunction and memory deficits, induced by chronic stress, may be related to its modulating effects on neuroendocrine and monoamine neurotransmitters. In addition to supporting traditional claims and the previously reported antichronic disease properties, this study also suggests that ASMq may prevent HPA hyperactivity induced by chronic stress. Oral administration of ASMq to the chronic stress mice was found to significantly enhance their learning performance by the step-through and Y-maze tasks. Interestingly, these effects were found to be concomitant with the regulation of monoamine neurotransmitter levels in their serum and brain. The capacity of ASMq in regulating neurochemicals and neuroendocrine system could be attributed to the presence of particular types of phytochemicals belonging to the herbal drugs constituting the ASMq preparation.

Acknowledgments

Work in China was supported by the National Natural Science Foundation of China (no: 30260128). Amat thanks the Eurasia-Pacific Uninet (EPU) for a postdoctoral scholarship.

References

[1] H. Upur and A. Yusup, *The Theory of Mizaj and Hilit of Traditional Uighur Medicine Modern Study on Mizaj and Its Modern Study*, Xinjiang Science and Technology Publishing House, Xinjiang, China, 2003.

[2] H. Upur, A. Yusup, A. Umar, and N. Moore, "Uighur traditional medicine syndrome of abnormal savda in men is associated with oxidative stress, which can be improved by Munziq and Mushil of abnormal savda," *Therapie*, vol. 59, no. 4, pp. 483–484, 2004.

[3] N. Amat, H. Upur, A. Ablimit, A. Matsidik, A. Yusup, and A. Kijjoa, "Immunomodulatory effects of abnormal savda Munsiq, a traditional Uighur medicine, on the combined stress mice," *Journal of Ethnopharmacology*, vol. 122, no. 1, pp. 42–47, 2009.

[4] R. M. Reynolds, K. E. Chapman, J. R. Seckl, B. R. Walker, P. M. McKeigue, and H. O. Lithell, "Skeletal muscle glucocorticoid receptor density and insulin resistance," *Journal of the American Medical Association*, vol. 287, no. 19, pp. 2505–2506, 2002.

[5] A. M. V. Ward, C. H. D. Fall, C. E. Stein et al., "Cortisol and the metabolic syndrome in South Asians," *Clinical Endocrinology*, vol. 58, no. 4, pp. 500–505, 2003.

[6] J. P. Girod and D. J. Brotman, "Does altered glucocorticoid homeostasis increase cardiovascular risk?" *Cardiovascular Research*, vol. 64, no. 2, pp. 217–226, 2004.

[7] G. Gerra, A. Zaimovic, G. G. Mascetti et al., "Neuroendocrine responses to experimentally-induced psychological stress in healthy humans," *Psychoneuroendocrinology*, vol. 26, no. 1, pp. 91–107, 2001.

[8] J. K. Sluiter, M. H. W. Frings-Dresen, A. J. van der Beek, and T. F. Meijman, "The relation between work-induced neuroendocrine reactivity and recovery, subjective need for recovery, and health status," *Journal of Psychosomatic Research*, vol. 50, no. 1, pp. 29–37, 2001.

[9] H. Shivakumar, T. Javed, T. Prakash, R. Nagendra Rao, B. H. M. J. Swamy, and A. V. Goud, "Adaptogenic activity of ethanolic extract of *Tribulus terrestris* L," *Journal of Natural Remedies*, vol. 6, no. 1, pp. 87–95, 2006.

[10] L. Song, W. Che, W. Min-Wei, Y. Murakami, and K. Matsumoto, "Impairment of the spatial learning and memory induced by learned helplessness and chronic mild stress," *Pharmacology Biochemistry and Behavior*, vol. 83, no. 2, pp. 186–193, 2006.

[11] B. Adinoff, K. Junghanns, F. Kiefer, and S. Krishnan-Sarin, "Suppression of the HPA axis stress-response: implications for relapse," *Alcoholism, Clinical and Experimental Research*, vol. 29, no. 7, pp. 1351–1355, 2005.

[12] L. E. Carlson and B. B. Sherwin, "Steroid hormones, memory and mood in a healthy elderly population," *Psychoneuroendocrinology*, vol. 23, no. 6, pp. 583–603, 1998.

[13] O. M. Wolkowitz, "Prospective controlled studies of the behavioral and biological effects of exogenous corticosteroids," *Psychoneuroendocrinology*, vol. 19, no. 3, pp. 233–255, 1994.

[14] G. Wenk, D. Hughey, V. Boundy, A. Kim, L. Walker, and D. Olton, "Neurotransmitters and memory: role of cholinergic, serotonergic, and noradrenergic systems," *Behavioral Neuroscience*, vol. 101, no. 3, pp. 325–332, 1987.

[15] E. Nowakowska, A. Chodera, K. Kus, P. Nowak, and R. Szkilnik, "Reversal of stress-induced memory changes by moclobemide: the role of neurotransmitters," *Polish Journal of Pharmacology*, vol. 53, no. 3, pp. 227–233, 2001.

[16] A. Yusup, H. Upur, I. Baudrimont et al., "Cytotoxicity of abnormal savda Munziq aqueous extract in human hepatoma (HepG2) cells," *Fundamental and Clinical Pharmacology*, vol. 19, no. 4, pp. 465–472, 2005.

[17] A. Yusup, H. Upur, A. Umar, and N. Moore, "Protective effects of Munziq and Mushil of abnormal savda to mitochondrial oxidative damage," *Fundamental and Clinical Pharmacology*, vol. 18, no. 4, pp. 471–476, 2004.

[18] A. Yusup and H. Upur, "Antioxidant effects of Munziq and Mushil of abnormal savda by electron paramagnetic resonance," *Traditional Chinese Drug Research & Clinical Pharmacology*, vol. 6, pp. 420–422, 2001.

[19] L. Zhang, U. Hamurat, and L. Zhang, "Protective effect of abnormal savda munzip on radiation-induced damage in mice," *Zhong Nan Da Xue Xue Bao*, vol. 32, no. 1, pp. 69–73, 2007.

[20] S. Y. Xu, R. L. Bian, and X. Chen, *Experimental Methodology of Pharmacology (Third Version)*, Peoples' Medical Publishing House, Beijing, China, 2002.

[21] A. Munck, P. M. Guyre, and N. J. Holbrook, "Physiological functions of glucocorticoids in stress and their relation to pharmacological actions," *Endocrine Reviews*, vol. 5, no. 1, pp. 25–44, 1984.

[22] F. Ohl and E. Fuchs, "Differential effects of chronic stress on memory processes in the tree shrew," *Cognitive Brain Research*, vol. 7, no. 3, pp. 379–387, 1999.

[23] T. Myhrer, "Neurotransmitter systems involved in learning and memory in the rat: a meta-analysis based on studies of

four behavioral tasks," *Brain Research Reviews*, vol. 41, no. 2-3, pp. 268–287, 2003.

[24] T. J. Crow, "Cortical synapses and reinforcement: a hypothesis," *Nature*, vol. 219, no. 5155, pp. 736–737, 1968.

[25] J. Zahrt, J. R. Taylor, R. G. Mathew, and A. F. T. Arnsten, "Supranormal stimulation of D1 dopamine receptors in the rodent prefrontal cortex impairs spatial working memory performance," *Journal of Neuroscience*, vol. 17, no. 21, pp. 8528–8535, 1997.

[26] M. Bubser and W. J. Schmidt, "6-Hydroxydopamine lesion of the rat prefrontal cortex increases locomotor activity, impairs acquisition of delayed alternation tasks, but does not affect uninterrupted tasks in the radial maze," *Behavioural Brain Research*, vol. 37, no. 2, pp. 157–168, 1990.

[27] C. Wilson, G. G. Nomikos, M. Collu, and H. C. Fibiger, "Dopaminergic correlates of motivated behavior: importance of drive," *Journal of Neuroscience*, vol. 15, no. 7, pp. 5169–5178, 1995.

[28] Y. Xu, B. S. Ku, H. Y. Yao et al., "The effects of curcumin on depressive-like behaviors in mice," *European Journal of Pharmacology*, vol. 518, no. 1, pp. 40–46, 2005.

[29] J. Szelényi and Z. Selmeczy, "Immunomodulatory effect of antidepressants," *Current Opinion in Pharmacology*, vol. 2, no. 4, pp. 428–432, 2002.

[30] S. Hashimoto, T. Inoue, and T. Koyama, "Effects of conditioned fear stress on serotonin neurotransmission and freezing behavior in rats," *European Journal of Pharmacology*, vol. 378, no. 1, pp. 23–30, 1999.

[31] M. C. Buhot, S. Martin, and L. Segu, "Role of serotonin in memory impairment," *Annals of Medicine*, vol. 32, no. 3, pp. 210–221, 2000.

[32] M. Naughton, J. B. Mulrooney, and B. E. Leonard, "A review of the role of serotonin receptors in psychiatric disorders," *Human Psychopharmacology*, vol. 15, no. 6, pp. 397–415, 2000.

[33] F. Pourmorad, S. J. Hosseinimehr, and N. Shahabimajd, "Antioxidant activity, phenol and flavonoid contents of some selected Iranian medicinal plants," *African Journal of Biotechnology*, vol. 5, no. 11, pp. 1142–1145, 2006.

[34] Y. Amakura, K. Kawada, T. Hatano et al., "Four new hydrolyzable tannins and an acylated flavonol glycoside from *Euphorbia maculata*," *Canadian Journal of Chemistry*, vol. 75, no. 6, pp. 727–733, 1997.

[35] A. M. Pawlowska, F. Camangi, A. Bader, and A. Braca, "Flavonoids of *Zizyphus jujuba* L. and *Zizyphus spina-christi* (L.) Willd (Rhamnaceae) fruits," *Food Chemistry*, vol. 112, no. 4, pp. 858–862, 2009.

[36] J. P. E. Spencer, "Flavonoids: modulators of brain function?" *British Journal of Nutrition*, vol. 99, no. 1, pp. ES60–ES77, 2008.

[37] Y. Shang, J. Cheng, J. Qi, and H. Miao, "Scutellaria flavonoid reduced memory dysfunction and neuronal injury caused by permanent global ischemia in rats," *Pharmacology Biochemistry and Behavior*, vol. 82, no. 1, pp. 67–73, 2005.

[38] F. Mojab, M. Kamalinejad, N. Ghaderi, and H. R. Vahidipour, "Phytochemical screening of some species of Iranian plants," *Iranian Journal of Pharmaceutical Research*, vol. 2, no. 2, pp. 77–82, 2003.

[39] I. P. Varshney, D. C. Jain, and H. C. Srivastava, "Study of saponins from *Glycyrrhiza glabra* root," *International Journal of Crude Drug Research*, vol. 21, no. 4, pp. 169–172, 1983.

[40] S. H. Jin, J. K. Park, K. Y. Nam, S. N. Park, and N. P. Jung, "Korean red ginseng saponins with low ratios of protopanaxadiol and protopanaxatriol saponin improve scopolamine-induced learning disability and spatial working memory in mice," *Journal of Ethnopharmacology*, vol. 66, no. 2, pp. 123–129, 1999.

[41] H. Wagner, S. Bladt, and E. M. Zgainski, *Plant Drug Analysis*, Springer, Berlin, Germany, 1984.

[42] H. Zhang, T. Han, L. Zhang et al., "Effects of tenuifolin extracted from *radix polygalae* on learning and memory: a behavioral and biochemical study on aged and amnesic mice," *Phytomedicine*, vol. 15, no. 8, pp. 587–594, 2008.

[43] D. O. Kennedy, G. Wake, S. Savelev et al., "Modulation of mood and cognitive performance following acute administration of single doses of *Melissa officinalis* (Lemon balm) with human CNS nicotinic and muscarinic receptor-binding properties," *Neuropsychopharmacology*, vol. 28, no. 10, pp. 1871–1881, 2003.

[44] H. Zhang, T. Han, C. H. Yu, K. Rahman, L. P. Qin, and C. Peng, "Ameliorating effects of essential oil from Acori graminei rhizoma on learning and memory in aged rats and mice," *Journal of Pharmacy and Pharmacology*, vol. 59, no. 2, pp. 301–309, 2007.

[45] M. E. Büyükokuroğlu, A. Gepdiremen, A. Hacimüftüoğlu, and M. Oktay, "The effects of aqueous extract of *Lavandula angustifolia* flowers in glutamate-induced neurotoxicity of cerebellar granular cell culture of rat pups," *Journal of Ethnopharmacology*, vol. 84, no. 1, pp. 91–94, 2003.

[46] H. Joshi and M. Parle, "Cholinergic basis of memory-strengthening effect of *Foeniculum vulgare* Linn.," *Journal of Medicinal Food*, vol. 9, no. 3, pp. 413–417, 2006.

Hindawi Publishing Corporation
Evidence-Based Complementary and Alternative Medicine
Volume 2012, Article ID 163106, 11 pages
doi:10.1155/2012/163106

Research Article

Green Tea Extract Ameliorates Learning and Memory Deficits in Ischemic Rats via Its Active Component Polyphenol Epigallocatechin-3-gallate by Modulation of Oxidative Stress and Neuroinflammation

Kuo-Jen Wu,[1] Ming-Tsuen Hsieh,[1] Chi-Rei Wu,[1] W. Gibson Wood,[2] and Yuh-Fung Chen[3,4]

[1] *School of Chinese Pharmaceutical Sciences and Chinese Medicine Resources, College of Pharmacy, China Medical University, 91 Hsueh-Shih Road, Taichung 40402, Taiwan*
[2] *Department of Pharmacology, University of Minnesota and Geriatric Research, Education and Clinical Center, VA Medical Center, Minneapolis, MN 55455, USA*
[3] *Department of Pharmacology, College of Medicine, China Medical University, 91 Hsueh-Shih Road, Taichung 40402, Taiwan*
[4] *Department of Pharmacy, China Medical University Hospital, Taichung 40421, Taiwan*

Correspondence should be addressed to Yuh-Fung Chen, yfchen@mail.cmu.edu.tw

Received 22 March 2012; Revised 6 June 2012; Accepted 8 June 2012

Academic Editor: Paul Siu-Po Ip

Ischemic stroke results in brain damage and behavioral deficits including memory impairment. Protective effects of green tea extract (GTex) and its major functional polyphenol (−)-epigallocatechin gallate (EGCG) on memory were examined in cerebral ischemic rats. GTex and EGCG were administered 1 hr before middle cerebral artery ligation in rats. GTex, EGCG, and pentoxifylline (PTX) significantly improved ishemic-induced memory impairment in a Morris water maze test. Malondialdehyde (MDA) levels, glutathione (GSH), and superoxide dismutase (SOD) activity in the cerebral cortex and hippocampus were increased by long-term treatment with GTex and EGCG. Both compounds were also associated with reduced cerebral infraction breakdown of MDA and GSH in the hippocampus. In *in vitro* experiments, EGCG had anti-inflammatory effects in BV-2 microglia cells. EGCG inhibited lipopolysaccharide- (LPS-) induced nitric oxide production and reduced cyclooxygenase-2 and inducible nitric oxide synthase expression in BV-2 cells. GTex and its active polyphenol EGCG improved learning and memory deficits in a cerebral ischemia animal model and such protection may be due to the reduction of oxidative stress and neuroinflammation.

1. Introduction

Ischemic stroke results from a temporary or permanent reduction of cerebral blood flow that leads to functional and structural damage in different brain regions. Cellular damage occurs during ischemia [1, 2] and reperfusion [3, 4]. Deleterious effects include ATP depletion, intracellular calcium changes, loss of ion homeostasis, excitotoxicity, activation of enzymes, arachidonic acid release, and mitochondrial dysfunction [5, 6].

These changes are associated with increased production of reactive oxygen species (ROS) which can cause severe oxidative damage to brain tissue [7]. Superoxide dismutase (SOD), glutathione peroxidase (GSH-Px), and catalase (CAT) are involved in the intracellular defense against ROS [8]. ROS are usually scavenged by antioxidant enzymes, such as SOD. SODs catalyze the production of O_2 and H_2O_2 from superoxide (O_2^-) followed by catalase and glutathione-peroxidase-catalyzed decomposition of hydrogen peroxide into water [9]. Subsequently, reperfusion can trigger inflammation mediated by phospholipases, COX-2, and nitric oxide synthases (NOSs) [5, 6].

Some brain regions, such as the striatum and hippocampus, are more vulnerable to ischemic damage [10]. CA1

hippocampal pyramidal neurons exhibit cell death several days after ischemic injury [11]. Spatial memory in rats and humans is largely dependent on the hippocampus [12] and hippocampal neuronal damage induced by ischemia is associated with spatial memory impairment. Microglia is widely distributed throughout large nonoverlapping regions of the central nervous system [13, 14]. Microglia is sensitive to even small pathological changes and is traveling within the brain [15, 16] and will be stimulated to proliferate when the brain or tissues are damaged. They are constantly cleaning damaging neurons, plaques, and infectious pathogens, to stop potentially fatal injuries [17]. Over the past decade, they are considered as a modulator of neurotransmission, although the mechanisms are not yet fully understood [18, 19]. Murine BV-2 microglia cells were consciously used to study the bioactivities of neuroprotection, synthases, and cytokine of microglia cells [20–22].

Green tea was neuroprotective in ischemia-reperfusion brain injury in rats and gerbils [23–25]. The main catechins in green tea are (−)-epicatechin; (−)-epicatechin gallate (ECG); (−)-epigallocatechin (EGC); (−)-epigallocatechin gallate (EGCG). EGCG is the most active polyphenol in green tea [26]. EGCG has antioxidative [27], anticancer [28], and anti-inflammatory effects [29, 30]. Many studies have reported that EGCG had neuroprotective effects in animal models of cerebral ischemia [31–34] which may be attributed to its antioxidant and free radical scavenging actions. There have been few studies reporting on the effects of green tea and its main component, EGCG on memory in an animal model of cerebral ischemia. Therefore, we determined if green tea extract and EGCG would reduce memory impairment in a rat model of cerebral ischemia. Effects of green tea extract and EGCG on neuroinflammation in LPS-induced BV-2 microglia cells were also examined.

2. Materials and Methods

2.1. Preparation of Green Tea Extracts. Green tea (*Camellia sinensis (*L.*) O. Kuntze*) was provided by Mr. Tsung-Chih Wu of the Kuo-Ming Tea Factory, Nantou, Taiwan. Fresh tea leaves (3000 g) were immersed in 10 L distilled water and were extracted using 85°C water for 12 hr and repeated twice. The extracts were filtered and freeze-dried. The yield percentage of green tea extract (GTex) was 217 g and 7.23% of the total.

2.2. Reagents and Chemicals. (−)-Epicatechin, (−)-epicatechin gallate (ECG), (−)-epigallocatechin (EGC), (−)-epigallocatechin gallate (EGCG), caffeine, *tert*-butylhydroquinone(BHQ), acetic acid, pentoxifylline (PTX), N-methyl-2-phenylindole (NMPI), tetramethoxy propane (TMP), lipopolysaccharide (LPS), and Griess reagent were purchased from Sigma-Aldrich (St. Louis, MO, USA). Zoletil was purchased from Virbac Laboratories (Carros, France). BCA Protein assay kit was purchased from Thermo Fisher Scientific (Lafayette, CO, USA). MDA-586 assay Kit and Glutathione (GSH) assay kit were purchased from Cayman Chemical (Ann Arbor, MI, USA). Anti-iNOS antibody (rabbit polyclonal to iNOS, sc-651) and anti-COX-2 antibody (rabbit polyclonal to COX-2, sc-7951) were purchased from Santa Cruz Biotechnology (Santa Cruz, CA, USA).

2.3. Determination of Polyphenol Compounds by HPLC. The quantification of polyphenol compounds was using a HPLC procedure following the previous report [35]. GTex was dissolved in methanol and then filtered with a 0.22 μm membrane filter (Millipore, MA, USA). Stock solutions of the standards were prepared in methanol to final concentrations of 1 mg/mL. All standard and sample solutions were injected into 20 μL in triplicate. The Shimadzu VP series HPLC system and Shimadzu Class-VP chromatography data system were used. All chromatographic operations were carried out at 25°C. The chromatographic peaks of polyphenol compounds were confirmed by comparing their retention times and UV spectra. A LiChrospher RP-18e (250 × 4 mm, 5 μm) column (Merck KGaA, Darmstadt, Germany) was used. Chromatographic separations of polyphenol compounds, including (−)-epicatechin, (−)-ECG, (−)-EGC, (−)-EGCG, and caffeine, were carried out using a two-solvent system: solvent A 100% methanol and solvent B 0.2% acetic acid at pH = 3.23. The analyses were performed using a gradient program. The conditions were as follows: initial condition of 90% solvent B, 0–5 min changed to 80% solvent B, 5–30 min unchanged, 30–50 min changed to 50% solvent B, 50–55 min changed to 40% solvent B, and 55–60 min unchanged. Signals were detected at 280 nm. *tert*-butylhydroquinone (BHQ, 25 μg/mL) was used as an internal standard. Quantification was carried out using standard calibration curves. The concentrations used for the calibration of reference polyphenol compounds were between 10 and 150 μg/mL.

2.4. Animals and Drug Administration. Male Sprague–Dawley (SD) rats, 8-9 wks of age, weighing 250–300 g, were purchased from BioLASCO Taiwan Co., Ltd. Rats were fed normal rat chow and housed in standard cages at a constant room temperature of 22 ± 1°C, with humidity 55 ± 5% and a 12 hr inverted light-dark cycle for at least 1 week before the experiment. The experimental protocol was approved by the Institutional Animal Care and Use Committee (IACUC), China Medical University, protocol 100–220-C. The minimum number of animals and duration of observations required to obtain reliable data were used. For infarct size evaluation studies, the animals were divided into seven groups of six animals each: the ischemia/reperfusion induction group (I/R; as a control group), treatment with GTex (30, 100, and 300 mg/kg) groups, and EGCG (10 mg/kg) group. GTex and EGCG were dissolved in distilled water and administered orally 1 hr before cerebral artery ligation.

For behavioral studies, the animals were divided into seven groups of six animals each: the sham operation group (sham; as a normal group), the ischemia/reperfusion induction group (I/R; as a control group), treatment with GTex (30, 100, and 300 mg/kg) groups, EGCG (10 mg/kg) group, and PTX (100 mg/kg) group. Drugs were dissolved in

distilled water and administered orally 1 hr before ischemia occlusion and once daily during the duration of the experiment. Four days after ischemia/reperfusion surgery, the rats were given behavioral training in a Morris water maze. The schedule for drug treatment, surgery, and behavioral testing is shown in Figure 1.

2.5. Transient Focal Cerebral Ischemia-Reperfusion Model. Focal ischemia was induced by occlusion of the right middle cerebral artery (MCA) and both common carotid arteries (CCAs) as previously described [36]. Briefly, all rats were fasted overnight with free access to water and then anesthetized with zoletil (25 mg/kg, i.p.) and the skull exposed and a small burr hole was made over the MCA. A 10–0 nylon monofilament (Davis & Geck, Wayne, NJ, USA) was placed underneath the right MCA rostral to the rhinal fissure, proximal to the major bifurcation of the right MCA, and distal to the lenticulostriate arteries. The artery then was lifted, and the wire rotated clockwise. Both CCAs were then occluded using a microvascular clip (FE691; Aesculap, Tuttlingen, Germany). Reperfusion was established after 90 minutes of occlusion by first removing the microvascular clips from the CCA, then rotating the wire counterclockwise, and removing it from beneath the MCA.

2.6. Infarct Volume Measurement. The rats were deeply anesthetized by intraperitoneal dose of 50 mg/kg of zoletil; intracardiac perfusion with 200 mL of freezing PBS was performed before animals were decapitated. The brain was removed and sliced in 2 mm sections using a rodent brain matrix slicer (RBM-4000C; ASI Instruments, Warren, MI, USA). The sections were stained with 2% 2,3,5-triphenyltetrazolium chloride (TTC) for 10 min at room temperature and fixed in 10% formalin. The image of each section was digitized and the infarct volumes were determined morphometrically using Image-Pro Plus 6.0 (Media Cybernetics, MD, USA).

2.7. Morris Water Maze Test. Behavioral testing was performed in water maze. The apparatus consisted of a round water tank with a transparent platform stand inside. The transparent platform was submerged 1 cm below the water level and located in a constant position in the middle of one quadrant, equidistant from the center and edge of the pool. For each training session, the rats were put into the water at one of four starting positions, the sequence of the positions being selected randomly. In each training session, the latency to escape onto the hidden platform was recorded with a camera fixed on the ceiling of the room and images stored in a computer. In the hidden-platform test, the rats were given four trials per day [37, 38]. Training was conducted for 3 consecutive days (Morris Water Maze spatial memory test on treatment day 4–6). During each trial, the rats were released from four pseudorandomly assigned starting points and allowed to swim for 120 s. After mounting the platform, the rat was allowed to remain on the platform for 30 s. The rat was then placed in the home cage until the start of the next trial. The rat would be guided to the platform and would be allowed to rest on the platform for 30 s, if the rat was unable to find the platform within 120 s. In the probe trial, the hidden platform was removed, and the animal was allowed to float freely for 60 s. The parameters measured during the probe trial were the time spent in the quadrant of the target platform (Morris Water Maze reference memory study on treatment day 7).

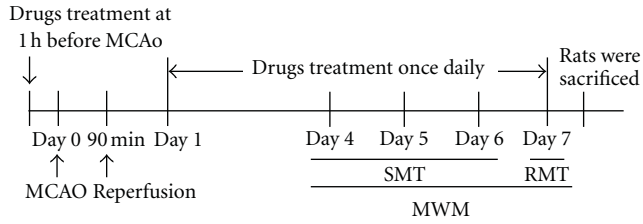

Figure 1: Schedule of drug treatment and experiment orders. Green tea extract (GTex), EGCG, and PTX were administrated orally 1 h before the surgery. The oral administration to rat continued once daily for 7 days and 1 h prior to training or testing. Four to seven days after surgery, the spatial memory test (SMT) of the Morris water maze (MWM) was performed 4 trials a day for 3 consecutive days, followed 24 h later (day 7) by the reference memory test (RMT). Rats were sacrificed immediately after the behavioral test.

2.8. Biochemical Assays

2.8.1. Biochemical Examinations. At the end of the behavioral test, rats were sacrificed using zoletil (50 mg/kg, i.p.) for biochemical studies. Brains were quickly removed and the cerebral cortex and hippocampus were separated on ice. To prepare a homogenate, brain tissue was mixed with 0.1 M phosphate buffer saline (PBS, pH = 7.4) and centrifuged at a 10,000(g) at 4°C for 15 min to remove cellular debris. The supernatant was used for the estimation of the following malonyldialdehyde (MDA) levels, SOD activity, and GSH levels. Protein concentration of samples was determined by BCA Protein assay kit with BSA used as a standard.

2.8.2. Measurement of Malonyldialdehyde (MDA) Level. Malonyldialdehyde (MDA) was determined spectrophotometrically using the *N*-methyl-2-phenylindole (NMPI) method of Bergman [39]. Fifty μL sample or standard was added and followed by 160 μL of 10 mM solution of NMPI. A similar approach was used for the standard; TTMP (tetramethoxy propane) was used at concentrations from 0.8 to 8 μM. The plate was incubated for 48 min at 45°C. The chromophore absorbs at 586 nm.

2.8.3. Measurement of Superoxide Dismutase (SOD) Activity. Superoxide dismutase (SOD) activity was based on the inhibitory effect of SOD on the reduction of nitroblue tetrazolium (NBT) by the superoxide anion generated by the system xanthine/xanthine oxidase, measuring the absorption at 560 nm [40].

2.8.4. Measurement of Glutathione (GSH) Level. Glutathione (GSH) levels were determined spectrophotometrically using

the DTNB-GSH reductase recycling method, measuring the absorption at 405 nm [41].

2.9. Cell Culture

2.9.1. BV-2 Cell Culture. The murine microglial BV-2 cell line was provided by Professor Jau-Shyong Hong from the Neuropharmacology Section Lab of Pharmacology and Chemistry, NIEHS/NIH, Bethesda, USA. The BV-2 cells were maintained in DMEM supplemented with 10% FBS. One hundred U/mL of penicillin and 100 μg/mL streptomycin were added to DMEM, and the cells were kept at 37°C in a humidified incubator under 5% CO_2 and 95% air.

2.9.2. Nitrite Assay. Nitrite, the stable metabolite of NO, was assayed as the production of NO in the culture medium, and the accumulation of nitrite in the medium was determined by colorimetric assay with Griess reagent. 1×10^4 BV-2 cells were seeded in each well of 96-well plates and kept overnight. Cells were then changed to phenol-red free DMEM. The BV-2 cells were pretreated with EGCG for 1 hr and then stimulated with 0.5 μg/mL LPS. After further 24 h of incubation, 100 μL of culture supernatant reacted with an equal amount of Griess reagent (1% sulfanilamide in 5% H_3PO_4 and 0.1% N-1-naphthylethylenediamide dihydrochloride) in 96-well culture plates for 10 min at room temperature in the dark. Nitrite concentrations were determined by using standard solutions of sodium nitrite prepared in cell-culture medium. The absorbance at 550 nm was determined using an ELISA reader [42]. Each experiment was performed in triplicate.

2.9.3. Preparation of Cell Extracts. The test medium was removed from culture dishes, and cells were washed with ice-cold PBS. The cells were scraped, resuspended in lysis buffer, then centrifuged at 12,000 (rpm) for 30 min at 4°C. Protein concentrations of samples were determined by the BCA Protein assay kit with BSA as a standard.

2.9.4. Western Blotting. Samples containing 70 μg of protein were separated on 10% SDS-PAGE (sodium dodecyl sulfate-polyacrylamide gel electrophoresis) and transferred to PVDF (polyvinylidene difluoride) membranes. The membranes were incubated for 1 hr with 5% dry skim milk in TBST buffer at room temperature to prevent nonspecific binding. The membranes were then incubated with rabbit anti-iNOS (1 : 1000) and rabbit anti-COX-2 (1 : 1000). Subsequently, the membranes were incubated with goat anti-rabbit alkaline-phosphatase-conjugated secondary antibody (1 : 1000) for 1 hr at room temperature. Bands were visualized using the chromogenic substrate 5-bromo-4-chloro-3-indolyl phosphate in the presence of nitroblue tetrazolium.

2.10. Statistical Analysis.

All data were expressed as the mean ± standard error. Data were analyzed using either Student's t-test or one-way ANOVA followed by Dunnett's test. $P < 0.05$ was considered significant.

3. Results

3.1. Composition and Stability of Polyphenol Compounds in GTex. Analysis of GTex by HPLC indicated that the total green tea solids in the extract contained (−)-epigallocatechin gallate (3.21%), (−)-epigallocatechin (4.59%), (−)-epicatechin gallate (1.06%), (−)-epicatechin (1.31%), and caffeine (4.46%) as shown in Figure 2 and Table 1.

3.2. Effects of GTex and EGCG on Cerebral Infarct Volume. It can be seen in Figure 3 that visible boundaries were clearly observable between normal brain tissue and untreated cerebral infarct tissue. GTex treatment (100 and 300 mg/kg) markedly reduced cerebral infarction at 24 hr after reperfusion as compared with the ischemia/reperfusion (I/R) group (Figure 3(a)). The percent infarct size was 11.9 ± 0.54% in the untreated group and 6.0 ± 0.76% and 4.3 ± 0.99% in the 100 and 300 mg/kg GTex treatments, respectively (Figure 3(b)). EGCG also significantly reduced infarct size ($P < 0.001$) (Figure 3(b)) as compared with the I/R group but no EGCG. The sizes of the cerebral infarction in the GTex and EGCG groups were similar.

3.3. Effects of GTex, EGCG, and PTX on Spatial Performance Memory in Ischemic Rats. The sham group quickly learned the location of the platform as demonstrated by a reduction in escape latencies on days 1 and 2 and by reaching stable latencies on day 3 (Figure 4). Furthermore, we found the swimming pathway required to reach the submerged platform was simplified in the sham group. By contrast, in the I/R group, a typical swimming behavior consisted of circling around the pool and the escape latencies in trials 1 and 2 remained essentially unchanged throughout the 3-day testing period. GTex (100 and 300 mg/kg) treatment significantly improved performance (i.e., reduced escape latency) of ischemic/reperfusion rats on the escape latency on day 2 ($P < 0.01$) and day 3 ($P < 0.001$) testing periods. EGCG (10 mg/kg) and PTX (100 mg/kg) treatment reduced the escape latency in the day 2 ($P < 0.05$) and day 3 ($P < 0.001$) testing periods.

3.4. Effects of GTex, EGCG, and PTX on Time in the Target Quadrant. It can be seen in Figure 5 that the time in the target quadrant in the I/R group was significantly reduced compared to that of the sham group ($P < 0.05$). GTex (100 and 300 mg/kg) significantly reduced ischemia/reperfusion-induced time in the target quadrant when administered before the training trial ($P < 0.05$–0.01) as compared with the I/R group. EGCG (10 mg/kg) had similar effects as GTex but PTX did not improve performance (Figure 5).

3.5. MDA Levels in Cortex and Hippocampus. MDA levels in the cortex and hippocampus of the different groups are shown in Table 2. MDA levels were significantly increased in the I/R group ($P < 0.001$) as compared with the sham group. In contrast, MDA levels were decreased significantly after treatment with GTex (300 mg/kg) ($P < 0.001$) and EGCG (10 mg/kg) ($P < 0.05$–0.001, Table 1). GTex at lower dosage

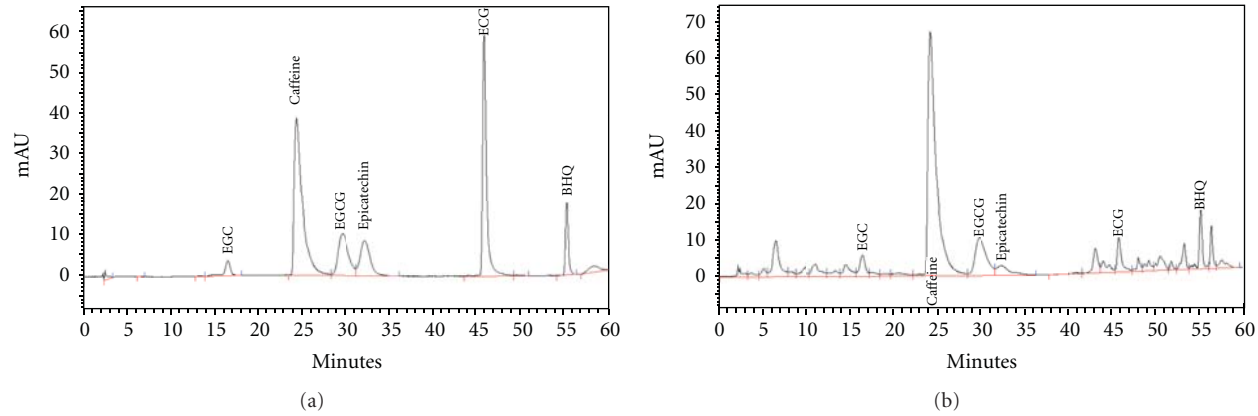

Figure 2: HPLC chromatograms of the GTex at 280 nm. Trace: (a) standard, (b) GTex. BHQ: *tert*-butylhydroquinone as an internal standard. (EGCG: (−)-epigallocatechin gallate, ECG: (−)-epigallocatechin, EGC: (−)-epicatechin gallate).

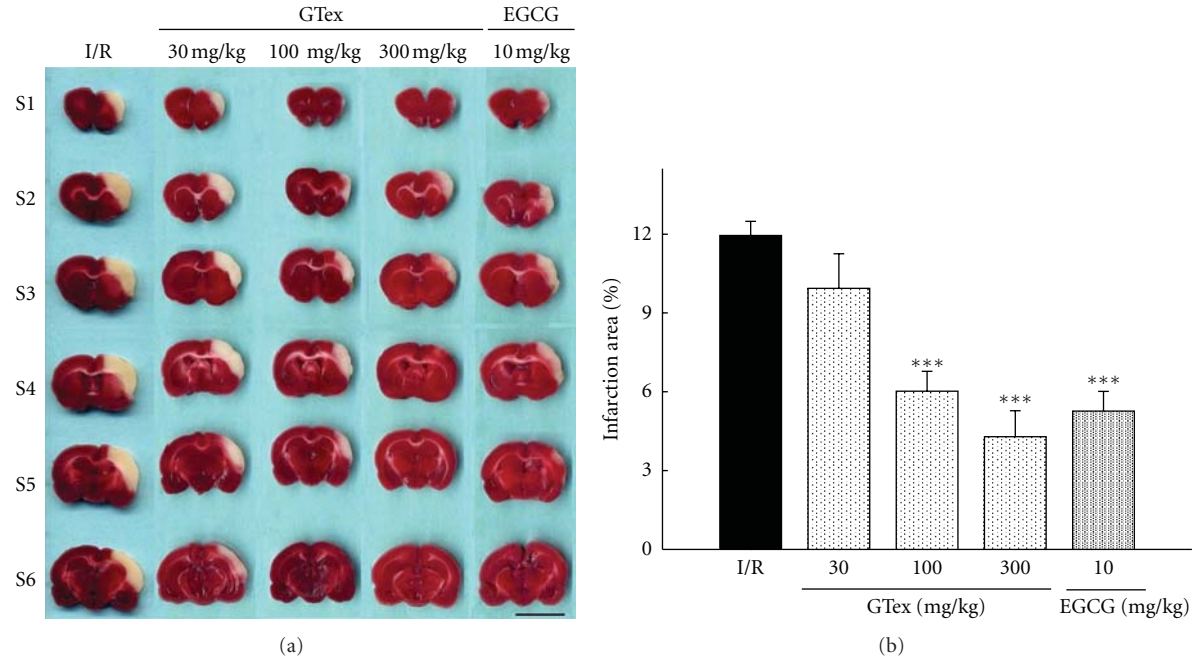

Figure 3: Effects of GTex and EGCG on cerebral infarction. (a) Effect of GTex (30~300 mg/kg, p.o.) groups and EGCG (10 mg/kg, p.o.) on cerebral infarct area at 24 h after reperfusion. The pale area represents infarct tissue and the red area normal tissue. (b) Infarction area by TTC staining ($n = 6$ in each group). I/R: ischemia/reperfusion control group. Each vertical bar represented mean ± S.E. $^{*}P < 0.05$, $^{***}P < 0.001$ compared to I/R group. Scale bar = 1 cm.

(30 and 100 mg/kg) and PTX (100 mg/kg) did not alter MDA levels in the cortex and hippocampus of the rats as compared with the I/R group with an exception that GTex 100 mg/kg significantly reduced MDA levels in the hippocampus ($P < 0.01$).

3.6. SOD Activity in Cortex and Hippocampus. There were no significant differences in SOD activity in brain tissue of I/R and sham animals. However, SOD activity was significantly decreased after treatment with GTex (300 mg/kg) and EGCG (10 mg/kg) in the cortex ($P < 0.05$) and hippocampus ($P < 0.01$) when compared with the I/R group. The lower GTex concentrations (30 and 100 mg/kg) and PTX (100 mg/kg) did not significantly change SOD activity as compared with the I/R group (Table 3).

3.7. GSH Levels in Cortex and Hippocampus. GSH levels were significantly decreased in the cortex and hippocampus (Table 4) of the I/R group ($P < 0.001$). After treatment with GTex (100 and 300 mg/kg) and EGCG (10 mg/kg), GSH levels were significantly increased in the cortex ($P < 0.01$) and hippocampus ($P < 0.001$). GTex at the lowest concentration tested (30 mg/kg) and PTX (100 mg/kg) did not significantly change GSH levels in the rat cortex and hippocampus.

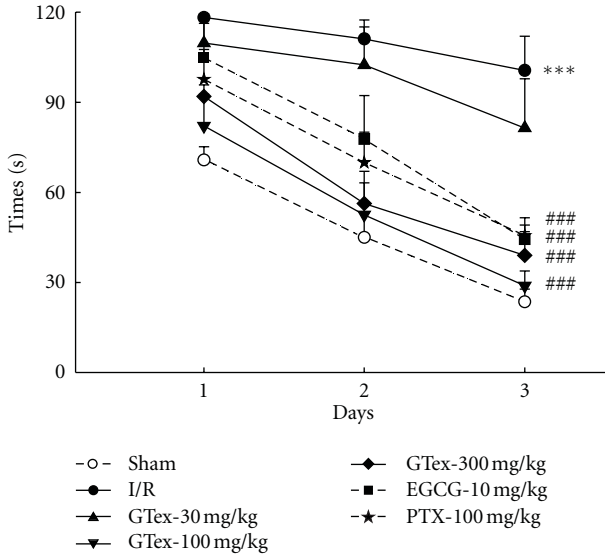

Figure 4: Effect of GTex (30~300 mg/kg, p.o.), EGCG (10 mg/kg, p.o.), and pentoxifylline (PTX, 100 mg/kg, p.o.), on the swimming time took to reach the hidden platform of the Morris water maze in the ischemia/reperfusion (I/R) rats. $^{**}P < 0.01$, $^{***}P < 0.001$ compared to the sham group. $^{\#}P < 0.05$, $^{\#\#}P < 0.01$, $^{\#\#\#}P < 0.001$ compared to I/R group ($n = 6$ in each group).

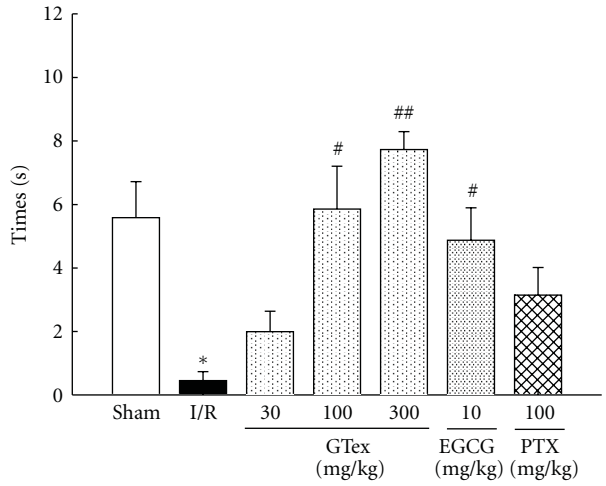

Figure 5: Effect of GTex (30~300 mg/kg, p.o.), EGCG (10 mg/kg, p.o.), and pentoxifylline (PTX, 100 mg/kg, p.o.), on the time spent in the target quadrant in ischemia/reperfusion (I/R) rats. The performance of each rat was tested 24 hours after the final training day in a probe trial (60 sec) during which the platform was removed. $^{*}P < 0.05$ compared to the sham group. $^{\#}P < 0.05$, $^{\#\#}P < 0.01$ compared to I/R group ($n = 6$ in each group).

3.8. Effects of EGCG on LPS-Induced NO Production in BV-2 Cells. BV-2 cells incubated with 0.5 μg/mL LPS displayed a significant increase in nitrite production as compared with sham controls (Figure 6). EGCG in a concentration-dependent manner significantly reduced LPS-induced nitrite production (Figure 6). The IC_{50} for ECGC on inhibition of LPS-induced nitrite production was 5.91 μM in BV-2 cells (Figure 6).

3.9. Effects of EGCG on Expression of COX-2 and iNOS in BV-2 Cells. Changes in protein abundance of COX-2 and iNOS induced by LPS were measured at by Western blot analysis. Elevated COX-2 and iNOS protein production were detected at 24 hr following LPS treatment. LPS-induced iNOS and COX-2 expression were significantly suppressed by EGCG pretreatment at concentrations of 10 and 25 μM but not at a lower concentration of 2 μM (Figure 7).

Table 1: Composition of GTex.

Component	μg/mg	% of GTex
Total polyphenols	101.80 ± 4.55	10.18%
Polyphenols		
(−)-Epigallocatechin gallate	32.10 ± 0.44	3.21%
(−)-Epigallocatechin	45.96 ± 3.01	4.59%
(−)-Epicatechin gallate	10.62 ± 0.57	1.06%
(−)-Epicatechin	13.11 ± 1.08	1.31%
Caffeine	44.60 ± 0.29	4.46%

Table 2: Effect of GTex (p.o.) and EGCG (p.o.) on MDA levels in cortex and hippocampus of ischemia/reperfusion (I/R) rats.

	MDA levels (nmole/mg Protein)	
	Cortex	Hippocampus
Sham	0.73 ± 0.04	0.31 ± 0.03
I/R	1.60 ± 0.19***	1.03 ± 0.07***
GTex (30 mg/kg)	1.23 ± 0.19	0.89 ± 0.09
GTex (100 mg/kg)	1.16 ± 0.13	0.54 ± 0.06##
GTex (300 mg/kg)	0.65 ± 0.08###	0.30 ± 0.03###
EGCG (10 mg/kg)	0.96 ± 0.09##	0.56 ± 0.11#
PTX (100 mg/kg)	1.24 ± 0.06	1.02 ± 0.06

$^{***}P < 0.001$ compared to the sham group, $^{\#}P < 0.05$, $^{\#\#}P < 0.01$, $^{\#\#\#}P < 0.001$ compared to I/R group ($N = 6$).

Table 3: Effect of GTex (p.o.) and EGCG (p.o.) on SOD activities in cortex and hippocampus of ischemia/reperfusion (I/R) rats.

	SOD activity (U/mg Protein)	
	Cortex	Hippocampus
Sham	1.05 ± 0.08	2.06 ± 0.12
I/R	1.08 ± 0.06	2.02 ± 0.08
GTex (30 mg/kg)	1.02 ± 0.15	2.04 ± 0.15
GTex (100 mg/kg)	0.89 ± 0.10	1.90 ± 0.14
GTex (300 mg/kg)	0.69 ± 0.09#	1.48 ± 0.10##
EGCG (10 mg/kg)	0.72 ± 0.03#	1.47 ± 0.08##
PTX (100 mg/kg)	1.04 ± 0.1	2.19 ± 0.06

$^{\#}P < 0.05$, $^{\#\#}P < 0.01$ compared to I/R group ($N = 6$).

4. Discussion

Cerebral ischemia causes cognitive deficits, including memory impairment [43, 44]. The Morris water maze is a

Table 4: Effect of GTex (p.o.) and EGCG (p.o.) on GSH levels in cortex and hippocampus of ischemia/reperfusion (I/R) rats.

	GSH levels (pmole/mg Protein)	
	Cortex	Hippocampus
Sham	20.29 ± 1.12	103.72 ± 5.73
I/R	10.61 ± 1.22***	63.71 ± 4.83***
GTex (30 mg/kg)	13.78 ± 1.09	66.88 ± 7.17
GTex (100 mg/kg)	17.80 ± 1.92##	96.43 ± 6.74###
GTex (300 mg/kg)	18.95 ± 0.88###	104.73 ± 7.83###
EGCG (10 mg/kg)	17.80 ± 0.98##	139.01 ± 8.26###
PTX (100 mg/kg)	14.06 ± 1.43	76.09 ± 6.25

***$P < 0.001$ compared to the sham group, ##$P < 0.01$, ###$P < 0.001$ compared to I/R group ($N = 6$).

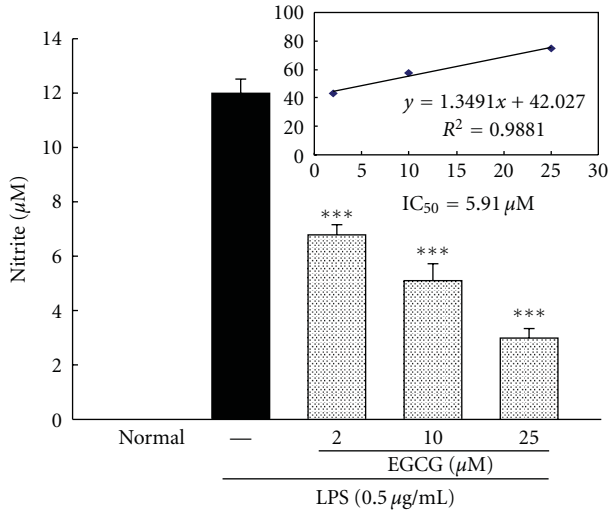

Figure 6: Inhibitory effect of EGCG on LPS-induced NO production in BV-2 cells incubated with LPS (0.5 μg/mL) in the presence or absence of indicated concentration of EGCG. Accumulated nitrite in the culture medium was determined by the Griess reaction. Each vertical bars represented mean ± S.E. ***$P < 0.001$ compared to LPS only group.

widely used test in behavioral neuroscience for studying the neural mechanisms of spatial learning and memory. Cerebral ischemia has been reported to produce deficits in memory performance in the Morris water maze [37]. Our results showed that cerebral ischemia induced impairment in both spatial memory and reference memory in a Morris water maze and is in agreement with previous studies [43, 44]. GTex (100 and 300 mg/kg) markedly improved deficits in spatial memory induced by cerebral ischemia. In addition, cerebral ischemia-induced reference memory deficits were also blocked by treatment with GTex. We also found that oral administration of EGCG for 7 days could reduce deficits in spatial and reference memory in rats of the ischemic group. EGCG is a major component of GTex and our results suggest that improved memory observed in GTex rats may be attributable to EGCG, although other GTex active compounds cannot be ruled out. There are reports that EGCG improved learning and memory in animal models of Alzheimer's disease and diabetes [45, 46]. EGCG did not reduce deficits in learning and memory deficits induced by cerebral ischemia in another study report [47]. There are several differences between the present study and the earlier report. In the earlier study, a 4-VO (four-vessel occlusion) model was used to restrict the cerebral circulation for ten minutes, two times within 60 min. Also, 50 mg/kg of EGCG was given intraperitoneally 30 min before the first occlusion. We used a 3-VO (three-vessel occlusion) model to induce ischemia/reperfusion damage and 10 mg/kg of EGCG was orally administered once daily for 7 days. In the current study, repeated administration of EGCG (10 mg/kg) improved both spatial memory and reference memory in a water-maze test. Results from the present experiments indicated that EGCG improved learning and memory in an animal model of ischemia rodents and required long-term treatment.

The present study evaluated the neuroprotective effects of GTex and EGCG in an ischemic stroke animal model and the anti-inflammatory effects of EGCG in BV-2 cells. GTex administered *in vivo* was effective in reducing damage in a stroke model. Treatment with GTex (100 and 300 mg/kg) significantly reduced cerebral infraction at 90 min ischemic occlusion and 24 hr reperfusion. The present studies showed that green tea had a neuroprotective effect in a transient focal ischemia model in agreement with previous studies [23–25]. EGCG also had similar effects and those results are consistent with previous reports [31, 48].

It has been reported that oxygen free radical-induced lipid peroxidation plays an important role in the neurological damage occurring after cerebral ischemia [49]. We found that 7 days following cerebral ischemia MDA levels were significantly increased as compared with levels in sham-operated rats. Administration of GTex and EGCG reversed the spike in MDA levels seen in the cerebral ischemic rats. GTex and EGCG may act by scavenging oxygen free radicals. Reactive oxygen species (ROS) are produced continuously *in vivo* under aerobic conditions. GSH-Px, CAT, and SOD, along with GSH and other nonenzymatic antioxidants act in concert to protect brain cells against oxidative damage. ROS are contributors to ischemic brain damage [49]. SOD is involved in the regulation of antioxidant defenses by catalyzing the dismutation of superoxide anion into H_2O_2 and O_2. Candelario-Jalil et al. [50] showed that SOD activity was increased at 24~72 hr after cerebral ischemia then returned to normal after 96 hr. We found that SOD activity 7 days after cerebral ischemia did not differ from control animals and this finding was similar with a previous study [50]. In contrast, ischemic rats treated with GTex or EGCG once daily for 7 days lowered SOD activity in comparison with cerebral ischemic rats without treatment. Most studies focused on the changes of oxidation markers 24 h after ischemia [8, 51, 52]. The present study determined oxidation marker activities 7 days after cerebral ischemia and found that GTex and EGCG showed significant inhibition. The protective effects of GTex and EGCG are largely due to their inhibition of some enzymes and antioxidative activities by scavenging free radicals. However, EGCG could be converted to an anthocyaninlike compound followed by cleavage of the

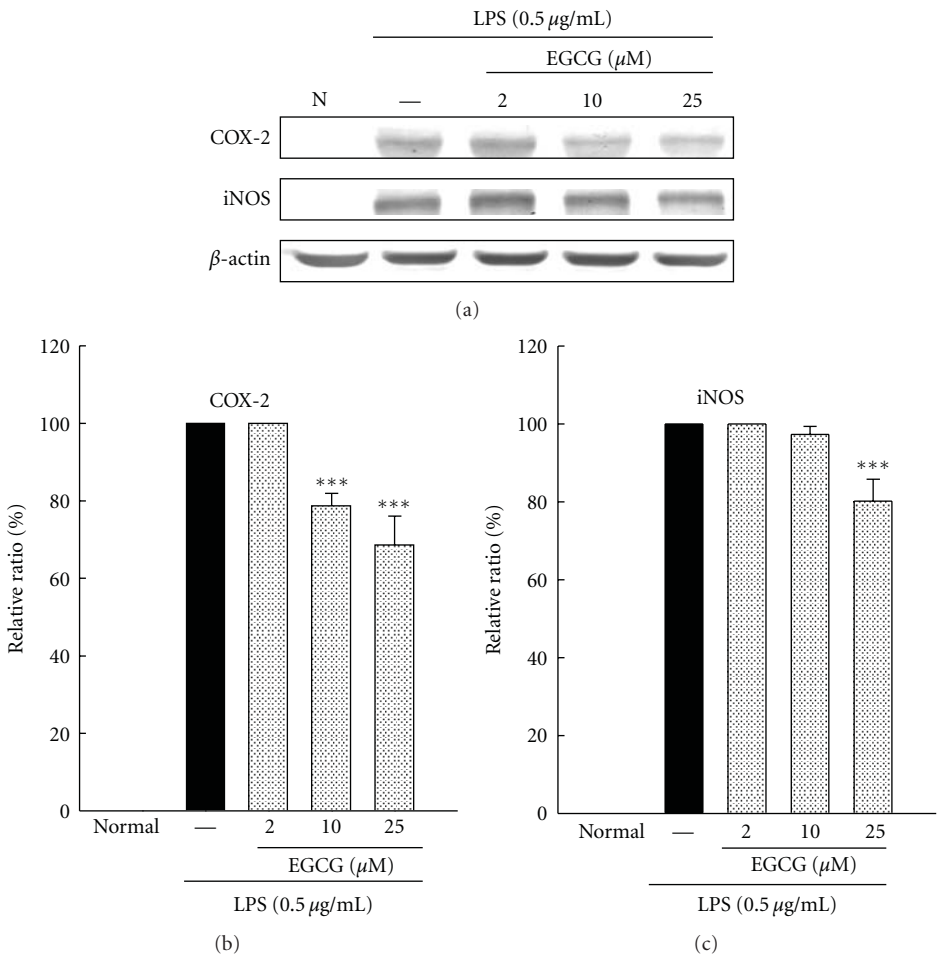

Figure 7: Effects of EGCG (2, 10, and 25 μM) on expression of COX-2 and iNOS in BV-2 cells treated with lipopolysaccharide (LPS, 0.5 μg/mL) for 24 h. Cultures were pretreated with EGCG for 1 h before the addition of LPS treatment. Bars represent the mean ± SE from three independent experiments. Densitometry analyses are presented as the relative ratio of protein/β-actin protein and are represented as percentages of the LPS only group. $^{***}P < 0.001$ compared to LPS only.

gallate moiety by oxidation. Active oxygen including superoxide (O_2^-) was produced by EGCG, which could decrease SOD activity by peroxyl radicals formation of superoxide during the inhibitory action [53]. That could be explaining the cause decreased SOD activity in administration of GTex and EGCG once daily for 7 days in the present study.

GSH is an endogenous antioxidant protecting cells against damage produced by oxygen free radicals. There was a significant decrease in GSH levels 7 days after cerebral ischemia as compared with GSH levels in the sham-operated rats. Treatment with GTex and EGCG once daily for 7 days increased GSH levels in ischemic rats, which may be indicative of neuroprotection. The lower dose of GTex 30 mg/kg was ineffective as there was an insignificant difference between the GTex-treated and I/R (control) rats on the MDA and GSH levels. This result was well correlated with the smaller infarction volume and better functional recovery for higher dose (100, 300 mg/kg) GTex-treated rats than for lower dose (30 mg/kg) GTex-treated or I/R (control) rats.

PTX has been used to treat vascular dementia and multiinfarct dementia in clinical medicine [54, 55] and also proved to slow the progression of dementia [56]. In the present study, PTX was used as a positive control and ameliorated the spatial performance impairment, but did not ameliorate reference memory deficit in cerebral ischemia rats. PTX found to be no antioxidant and anti-lipid peroxidation effects in this study, which is consistent with a previous study [57].

Brain inflammation occurs following ischemia-reperfusion [58]. Previous studies showed that activation of BV-2 cells during LPS stimulation could be used to survey the neuroinflammatory effects [59]. Excessive NO and ROS production in the brain contribute to neuronal cell injury processes [60]. Recent studies showed that inhibiting LPS-induced NO production may be neuroprotective [61]. Microglia activation by LPS releases proinflammatory factors, tumor necrosis factor-alpha (TNF-α), interleukin 1-beta (IL-1β), NO, and superoxide, thus leading to neuronal

injury and death [62]. We investigated NO production and iNOS protein expression in BV2 cells treated with EGCG and found that EGCG inhibited LPS-induced NO production and iNOS protein expression in BV-2 cells. Li et al. [30] showed that EGCG inhibited NO production and iNOS protein expression in primary microglia induced by LPS. EGCG could potently inhibit NO and TNF-α generation in microglia. Many inflammatory diseases are associated with increased levels of COX-2, another inflammatory factor [59]. In the present study, EGCG inhibited COX-2 protein expression in BV-2 cells. Activated microglia are the primary donor of free radicals and inflammatory factors.

In summary, GTex and EGCG reduced cerebral infarction and improved learning and memory deficits induced by cerebral ischemia. These effects may involve a reduction in oxidative stress and neuroinflammation induced by ischemia. GTex and EGCG may be efficacious in treating ischemia-induced learning and memory deficits.

Acknowledgments

The authors would like to thank Mr. Tsung-Chih Wu of the Kuo-Ming Tea Factory, Nantou, Taiwan for provide the tea leaves and Professor Jau-Shyong Hong from the Neuropharmacology Section Lab of Pharmacology and Chemistry, NIEHS/NIH, Bethesda, USA for providing the BV-2 microglia cells. The authors would also like to thank the National Science Council (Taipei, Taiwan) and China Medical University (Taichung, Taiwan) for supporting this work (NSC-98-2320-B039-025-MY3 and CMU 09551AR*).

References

[1] E. H. Lo, T. Dalkara, and M. A. Moskowitz, "Mechanisms, challenges and opportunities in stroke," *Nature Reviews Neuroscience*, vol. 4, no. 5, pp. 399–415, 2003.

[2] J. Xiang, Y. P. Tang, P. Wu, J. P. Gao, and D. F. Cai, "Chinese medicine Nao-Shuan-Tong attenuates cerebral ischemic injury by inhibiting apoptosis in a rat model of stroke," *Journal of Ethnopharmacology*, vol. 131, no. 1, pp. 174–181, 2010.

[3] S. U. Yanpallewar, D. Hota, S. Rai, M. Kumar, and S. B. Acharya, "Nimodipine attenuates biochemical, behavioral and histopathological alterations induced by acute transient and long-term bilateral common carotid occlusion in rats," *Pharmacological Research*, vol. 49, no. 2, pp. 143–150, 2004.

[4] J. M. McCord, "Oxygen-derived free radicals in postischemic tissue injury," *The New England Journal of Medicine*, vol. 312, no. 3, pp. 159–163, 1985.

[5] R. L. Macdonald and M. Stoodley, "Pathophysiology of cerebral ischemia," *Neurologia Medico-Chirurgica*, vol. 38, no. 1, pp. 1–11, 1998.

[6] J. M. Lee, G. J. Zipfel, and D. W. Choi, "The changing landscape of ischaemic brain injury mechanisms," *Nature*, vol. 399, no. 6738, supplement, pp. A7–14, 1999.

[7] P. H. Chan, "Role of oxidants in ischemic brain damage," *Stroke*, vol. 27, no. 6, pp. 1124–1129, 1996.

[8] M. K. Reddy and V. Labhasetwar, "Nanoparticle-mediated delivery of superoxide dismutase to the brain: an effective strategy to reduce ischemia-reperfusion injury," *The FASEB Journal*, vol. 23, no. 5, pp. 1384–1395, 2009.

[9] J. Pan, A. A. Konstas, B. Bateman, G. A. Ortolano, and J. Pile-Spellman, "Reperfusion injury following cerebral ischemia: pathophysiology, MR imaging, and potential therapies," *Neuroradiology*, vol. 49, no. 2, pp. 93–102, 2007.

[10] M. S. Kindy, A. N. Bhat, and N. R. Bhat, "Transient ischemia stimulates glial fibrillary acid protein and vimentin gene expression in the gerbil neocortex, striatum and hippocampus," *Molecular Brain Research*, vol. 13, no. 3, pp. 199–206, 1992.

[11] V. L. Raghavendra Rao, A. M. Rao, A. Dogan et al., "Glial glutamate transporter GLT-1 down-regulation precedes delayed neuronal death in gerbil hippocampus following transient global cerebral ischemia," *Neurochemistry International*, vol. 36, no. 6, pp. 531–537, 2000.

[12] R. G. M. Morris, P. Garrud, J. N. P. Rawlins, and J. O'Keefe, "Place navigation impaired in rats with hippocampal lesions," *Nature*, vol. 297, no. 5868, pp. 681–683, 1982.

[13] G. W. Kreutzberg, "Microglia, the first line of defence in brain pathologies," *Arzneimittel-Forschung*, vol. 45, no. 3, pp. 357–360, 1995.

[14] E. A. Bushong, M. E. Martone, Y. Z. Jones, and M. H. Ellisman, "Protoplasmic astrocytes in CA1 stratum radiatum occupy separate anatomical domains," *Journal of Neuroscience*, vol. 22, no. 1, pp. 183–192, 2002.

[15] L. Dissing-Olesen, R. Ladeby, H. H. Nielsen, H. Toft-Hansen, I. Dalmau, and B. Finsen, "Axonal lesion-induced microglial proliferation and microglial cluster formation in the mouse," *Neuroscience*, vol. 149, no. 1, pp. 112–122, 2007.

[16] L. Walter and H. Neumann, "Role of microglia in neuronal degeneration and regeneration," *Seminars in Immunopathology*, vol. 31, no. 4, pp. 513–525, 2009.

[17] J. Gehrmann, Y. Matsumoto, and G. W. Kreutzberg, "Microglia: intrinsic immuneffector cell of the brain," *Brain Research Reviews*, vol. 20, no. 3, pp. 269–287, 1995.

[18] H. Wolosker, E. Dumin, L. Balan, and V. N. Foltyn, "D-amino acids in the brain: D-serine in neurotransmission and neurodegeneration," *The FEBS Journal*, vol. 275, no. 14, pp. 3514–3526, 2008.

[19] A. V. Gourine, V. Kasymov, N. Marina et al., "Astrocytes control breathing through pH-dependent release of ATP," *Science*, vol. 329, no. 5991, pp. 571–575, 2010.

[20] E. Blasi, R. Barluzzi, R. Mazzolla et al., "Role of nitric oxide and melanogenesis in the accomplishment of anticryptococcal activity by the BV-2 microglial cell line," *Journal of Neuroimmunology*, vol. 58, no. 1, pp. 111–116, 1995.

[21] G. Kang, P. J. Kong, Y. J. Yuh et al., "Curcumin suppresses lipopolysaccharide-induced cyclooxygenase-2 expression by inhibiting activator protein 1 and nuclear factor κb bindings in BV2 microglial cells," *Journal of Pharmacological Sciences*, vol. 94, no. 3, pp. 325–328, 2004.

[22] J. Neumann, M. Gunzer, H. O. Gutzeit, O. Ullrich, K. G. Reymann, and K. Dinkel, "Microglia provide neuroprotection after ischemia," *The FASEB Journal*, vol. 20, no. 6, pp. 714–716, 2006.

[23] J. T. Hong, S. R. Ryu, H. J. Kim et al., "Neuroprotective effect of green tea extract in experimental ischemia-reperfusion brain injury," *Brain Research Bulletin*, vol. 53, no. 6, pp. 743–749, 2000.

[24] M. Suzuki, M. Tabuchi, M. Ikeda, K. Umegaki, and T. Tomita, "Protective effects of green tea catechins on cerebral ischemic damage," *Medical Science Monitor*, vol. 10, no. 6, pp. BR166–BR174, 2004.

[25] J. T. Hong, S. R. Ryu, H. J. Kim et al., "Protective effect of green tea extract on ischemia/reperfusion-induced brain injury in

Mongolian gerbils," *Brain Research*, vol. 888, no. 1, pp. 11–18, 2001.

[26] Q. Guo, B. Zhao, M. Li, S. Shen, and X. Wenjuan, "Studies on protective mechanisms of four components of green tea polyphenols against lipid peroxidation in synaptosomes," *Biochimica et Biophysica Acta*, vol. 1304, no. 3, pp. 210–222, 1996.

[27] B. Zhao, Q. Guo, and W. Xin, "Free radical scavenging by green tea polyphenols," *Methods in Enzymology*, vol. 335, pp. 217–231, 2001.

[28] R. L. Thangapazham, A. K. Singh, A. Sharma, J. Warren, J. P. Gaddipati, and R. K. Maheshwari, "Green tea polyphenols and its constituent epigallocatechin gallate inhibits proliferation of human breast cancer cells *in vitro* and *in vivo*," *Cancer Letters*, vol. 245, no. 1-2, pp. 232–241, 2007.

[29] H. P. Kim, K. H. Son, H. W. Chang, and S. S. Kang, "Anti-inflammatory plant flavonoids and cellular action mechanisms," *Journal of Pharmacological Sciences*, vol. 96, no. 3, pp. 229–245, 2004.

[30] R. Li, Y. G. Huang, D. Fang, and W. D. Le, "(-)-Epigallocatechin gallate inhibits lipopolysaccharide-induced microglial activation and protects against inflammation-mediated dopaminergic neuronal injury," *Journal of Neuroscience Research*, vol. 78, no. 5, pp. 723–731, 2004.

[31] R. M. A. Rahman, S. M. Nair, S. C. Helps et al., "(-)-Epigallocatechin gallate as an intervention for the acute treatment of cerebral ischemia," *Neuroscience Letters*, vol. 382, no. 3, pp. 227–230, 2005.

[32] Y. B. Choi, Y. I. Kim, K. S. Lee, B. S. Kim, and D. J. Kim, "Protective effect of epigallocatechin gallate on brain damage after transient middle cerebral artery occlusion in rats," *Brain Research*, vol. 1019, no. 1-2, pp. 47–54, 2004.

[33] S. R. Lee, S. I. Suh, and S. P. Kim, "Protective effects of the green tea polyphenol (-)-epigallocatechin gallate against hippocampal neuronal damage after transient global ischemia in gerbils," *Neuroscience Letters*, vol. 287, no. 3, pp. 191–194, 2000.

[34] H. Lee, J. H. Bae, and S. R. Lee, "Protective effect of green tea polyphenol EGCG against neuronal damage and brain edema after unilateral cerebral ischemia in gerbils," *Journal of Neuroscience Research*, vol. 77, no. 6, pp. 892–900, 2004.

[35] H. Y. Ju, S. C. Chen, K. J. Wu et al., "Antioxidant phenolic profile from ethyl acetate fraction of Fructus Ligustri Lucidi with protection against hydrogen peroxide-induced oxidative damage in SH-SY5Y cells," *Food and Chemical Toxicology*, vol. 50, no. 3-4, pp. 492–502, 2012.

[36] H. Yanamoto, I. Nagata, Y. Niitsu, J. H. Xue, Z. Zhang, and H. Kikuchi, "Evaluation of MCAO stroke models in normotensive rats: standardized neocortical infarction by the 3VO technique," *Experimental Neurology*, vol. 182, no. 2, pp. 261–274, 2003.

[37] R. Morris, "Developments of a water-maze procedure for studying spatial learning in the rat," *Journal of Neuroscience Methods*, vol. 11, no. 1, pp. 47–60, 1984.

[38] C. R. Wu, L. W. Lin, C. L. Hsieh, W. H. Wang, Y. T. Lin, and M. T. Hsieh, "Petroleum ether extract of Cnidium monnieri ameliorated scopolamine-induced amnesia through adrenal gland-mediated mechanism in male rats," *Journal of Ethnopharmacology*, vol. 117, no. 3, pp. 403–407, 2008.

[39] M. Bergman, A. Perelman, Z. Dubinsky, and S. Grossman, "Scavenging of reactive oxygen species by a novel glucurinated flavonoid antioxidant isolated and purified from spinach," *Phytochemistry*, vol. 62, no. 5, pp. 753–762, 2003.

[40] T. Kasemsri and W. M. Armstead, "Endothelin production links superoxide generation to altered opioid-induced pial artery vasodilation after brain injury in pigs," *Stroke*, vol. 28, no. 1, pp. 190–197, 1997.

[41] M. E. Anderson, "Determination of glutathione and glutathione disulfide in biological samples," *Methods in Enzymology*, vol. 113, pp. 548–555, 1985.

[42] Y. F. Chen, P. C. Kuo, H. H. Chan et al., "β-Carboline alkaloids from *Stellaria dichotoma* var. *lanceolata* and their anti-inflammatory activity," *Journal of Natural Products*, vol. 73, no. 12, pp. 1993–1998, 2010.

[43] J. T. Hong, S. R. Ryu, H. J. Kim, S. H. Lee, B. M. Lee, and P. Y. Kim, "Involvement of cortical damage in the ischemia/reperfusion-induced memory impairment of Wistar rats," *Archives of Pharmacal Research*, vol. 23, no. 4, pp. 413–417, 2000.

[44] H. P. Davis, J. Tribuna, W. A. Pulsinelli, and B. T. Volpe, "Reference and working memory of rats following hippocampal damage induced by transient forebrain ischemia," *Physiology and Behavior*, vol. 37, no. 3, pp. 387–392, 1986.

[45] K. Rezai-Zadeh, G. W. Arendash, H. Hou et al., "Green tea epigallocatechin-3-gallate (EGCG) reduces β-amyloid mediated cognitive impairment and modulates tau pathology in Alzheimer transgenic mice," *Brain Research*, vol. 1214, pp. 177–187, 2008.

[46] T. Baluchnejadmojarad and M. Roghani, "Chronic epigallocatechin-3-gallate ameliorates learning and memory deficits in diabetic rats via modulation of nitric oxide and oxidative stress," *Behavioural Brain Research*, vol. 224, no. 2, pp. 305–310, 2011.

[47] F. Pu, K. Mishima, K. Irie et al., "Neuroprotective effects of quercetin and rutin on spatial memory impairment in an 8-arm radial maze task and neuronal death induced by repeated cerebral ischemia in rats," *Journal of Pharmacological Sciences*, vol. 104, no. 4, pp. 329–334, 2007.

[48] K. Cui, X. Luo, K. Xu, and M. R. Ven Murthy, "Role of oxidative stress in neurodegeneration: recent developments in assay methods for oxidative stress and nutraceutical antioxidants," *Progress in Neuro-Psychopharmacology and Biological Psychiatry*, vol. 28, no. 5, pp. 771–799, 2004.

[49] M. Kawase, K. Murakami, M. Fujimura et al., "Exacerbation of delayed cell injury after transient global ischemia in mutant mice with CuZn superoxide dismutase deficiency," *Stroke*, vol. 30, no. 9, pp. 1962–1968, 1999.

[50] E. Candelario-Jalil, N. H. Mhadu, S. M. Al-Dalain, G. Martínez, and O. S. León, "Time course of oxidative damage in different brain regions following transient cerebral ischemia in gerbils," *Neuroscience Research*, vol. 41, no. 3, pp. 233–241, 2001.

[51] J. Wattanathorn, J. Jittiwat, T. Tongun, S. Muchimapura, and K. Ingkaninan, "*Zingiber officinale* mitigates brain damage and improves memory impairment in focal cerebral ischemic rat," *Evidence-Based Complementary and Alternative Medicine*, vol. 2011, Article ID 429505, 8 pages, 2011.

[52] M. Kiray, H. A. Bagriyanik, C. Pekcetin, B. U. Ergur, and N. Uysal, "Protective effects of deprenyl in transient cerebral ischemia in rats," *The Chinese Journal of Physiology*, vol. 51, no. 5, pp. 275–281, 2008.

[53] K. Kondo, M. Kurihara, N. Miyata, T. Suzuki, and M. Toyoda, "Scavenging mechanisms of (-)-epigallocatechin gallate and (-)-epicatechin gallate on peroxyl radicals and formation of superoxide during the inhibitory action," *Free Radical Biology and Medicine*, vol. 27, no. 7-8, pp. 855–863, 1999.

[54] Y. W. Chan and C. S. Kay, "Pentoxifylline in the treatment of acute ischaemic stroke–a reappraisal in Chinese stroke patients," *Clinical and Experimental Neurology*, vol. 30, pp. 110–116, 1993.

[55] P. M. Bath and F. J. Bath-Hextall, "Pentoxifylline, propentofylline and pentifylline for acute ischaemic stroke," *Cochrane Database of Systematic Reviews*, no. 3, Article ID CD000162, 2004.

[56] R. S. Black, L. L. Barclay, K. A. Nolan, H. T. Thaler, S. T. Hardiman, and J. P. Blass, "Pentoxifylline in cerebrovascular dementia," *Journal of the American Geriatrics Society*, vol. 40, no. 3, pp. 237–244, 1992.

[57] B. Horvath, Z. Marton, R. Halmosi et al., "*In vitro* antioxidant properties of pentoxifylline, piracetam, and vinpocetine," *Clinical Neuropharmacology*, vol. 25, no. 1, pp. 37–42, 2002.

[58] A. Chamorro and J. Hallenbeck, "The harms and benefits of inflammatory and immune responses in vascular disease," *Stroke*, vol. 37, no. 2, pp. 291–293, 2006.

[59] D. Y. Lu, C. H. Tang, Y. H. Chen, and I. H. Wei, "Berberine suppresses neuroinflammatory responses through AMP-activated protein kinase activation in BV-2 microglia," *Journal of Cellular Biochemistry*, vol. 110, no. 3, pp. 697–705, 2010.

[60] C. C. Chao, S. Hu, T. W. Molitor, E. G. Shaskan, and P. K. Peterson, "Activated microglia mediate neuronal cell injury via a nitric oxide mechanism," *Journal of Immunology*, vol. 149, no. 8, pp. 2736–2741, 1992.

[61] A. Y. Sun and Y. M. Chen, "Oxidative stress and neurodegenerative disorders," *Journal of Biomedical Science*, vol. 5, no. 6, pp. 401–414, 1998.

[62] B. Liu, L. Du, and J. S. Hong, "Naloxone protects rat dopaminergic neurons against inflammatory damage through inhibition of microglia activation and superoxide generation," *Journal of Pharmacology and Experimental Therapeutics*, vol. 293, no. 2, pp. 607–617, 2000.

Hindawi Publishing Corporation
Evidence-Based Complementary and Alternative Medicine
Volume 2012, Article ID 429124, 9 pages
doi:10.1155/2012/429124

Research Article

A Longitudinal Follow-Up Study of Saffron Supplementation in Early Age-Related Macular Degeneration: Sustained Benefits to Central Retinal Function

M. Piccardi,[1,2] D. Marangoni,[1] A. M. Minnella,[1] M. C. Savastano,[1] P. Valentini,[1] L. Ambrosio,[3] E. Capoluongo,[2] R. Maccarone,[4] S. Bisti,[5,6,7] and B. Falsini[1,8]

[1] *Dipartimento di Scienze Otorinolaringoiatriche e Oftalmologiche, Universita' Cattolica del Sacro Cuore, 00168 Roma, Italy*
[2] *Istituto di Biochimica Clinica, Universita' Cattolica del Sacro Cuore, 00168 Roma, Italy*
[3] *Dipartimento di Scienze Oftalmologiche, Universita' degli Studi di Napoli Federico II, 580131 Napoli, Italy*
[4] *Dipartimento di Scienze e Tecnologie Biomediche, Università degli Studi dell'Aquila, 67100 L' Aquila, Italy*
[5] *Scienze Cliniche ed Applicate Biotecnologiche, DISCAB, Universita' degli Studi dell'Aquila, 67100 L' Aquila, Italy*
[6] *ARC Centre of Excellence in Vision Science, The Australian National University Canberra, ACT 0200, Australia*
[7] *Istituto Nazionale Biostrutture e Biosistemi, 00136 Roma, Italy*
[8] *Istituto di Oftalmologia, Universita' Cattolica del Sacro Cuore, Lgo F. Vito 1, 00168 Roma, Italy*

Correspondence should be addressed to B. Falsini, bfalsini@rm.unicatt.it

Received 21 March 2012; Revised 20 May 2012; Accepted 28 May 2012

Academic Editor: Karl Wah-Keung Tsim

Objectives. In a previous randomized clinical trial (Falsini et al. (2010)), it was shown that short-term Saffron supplementation improves retinal flicker sensitivity in early age-related macular degeneration (AMD). The aim of this study was to evaluate whether the observed functional benefits from Saffron supplementation may extend over a longer follow-up duration. *Design*. Longitudinal, interventional open-label study. *Setting*. Outpatient ophthalmology setting. *Participants*. Twenty-nine early AMD patients (age range: 55–85 years) with a baseline visual acuity >0.3. *Intervention*. Saffron oral supplementation (20 mg/day) over an average period of treatment of 14 (±2) months. *Measurements*. Clinical examination and focal-electroretinogram-(fERG-) derived macular (18°) flicker sensitivity estimate (Falsini et al. (2010)) every three months over a followup of 14 (±2) months. Retinal sensitivity, the reciprocal value of the estimated fERG amplitude threshold, was the main outcome measure. *Results*. After three months of supplementation, mean fERG sensitivity improved by 0.3 log units compared to baseline values ($P < 0.01$), and mean visual acuity improved by two Snellen lines compared to baseline values (0.75 to 0.9, $P < 0.01$). These changes remained stable over the follow-up period. *Conclusion*. These results indicate that in early AMD Saffron supplementation induces macular function improvements from baseline that are extended over a long-term followup.

1. Introduction

Age-related macular degeneration (AMD) is a retinal neurodegenerative disease whose distinctive features in the early stage are large soft drusen and hyper/hypopigmentation of the retinal pigment epithelium (RPE), with a moderate loss of central vision (age-related maculopathy, following the International Classification, [1]). In its late stage, the disease is characterized by the geographic atrophy of the RPE or the subretinal neovascular membranes, leading to a more severe central visual impairment which is a major cause of severe, irreversible low-vision in elderly people of developed world.

Changes of the RPE and photoreceptor cells are early events in AMD and may significantly impact on visual function. Epidemiologic and molecular genetic data indicate that several factors may protect against or increase the individual risk of photoreceptor degeneration/dysfunction in AMD. Many risk factors appear to be oxidative and/or proinflammatory [2–4], while many protective factors are known to act as antioxidants and/or anti-inflammatory [5–7]. Recent clinical studies using focal, psychophysical, or

multifocal electroretinograms (ERGs) techniques as assays of the outer retinal function (cone photoreceptors/bipolar cells) have shown that dietary antioxidant supplementation might influence macular cone-mediated function early in the disease process [8–10]. The large-scale, AREDS investigation results [5] indicate that antioxidant supplementation might prevent the development of the most advanced stage of AMD.

Among various antioxidants, the neuroprotective potential of the ancient spice Saffron was explored [11, 12]. The results showed that Saffron may protect photoreceptors from retinal stress, maintaining both morphology and function and probably acting as a regulator of programmed cell death, in addition to its antioxidant and anti-inflammatory properties [12]. Falsini et al., [13], in a randomized, double-blind, placebo-controlled study showed that three months of dietary Saffron supplementation significantly improved the focal-ERG-(fERG-) estimated retinal flicker sensitivity in early AMD patients. Daily supplementation of 20 mg/d Saffron for 90 days resulted in statistically significant improvements, compared to a placebo control, in the macular fERG parameters (amplitude and modulation threshold) of patients with early AMD. These postsupplementation changes in the macular fERG reflected a beneficial effect of macular function as they were associated with a small, but significant increase in the average Snellen visual acuity. These properties, together with preclinical evidence, provide a strong rationale for testing the effect of prolonged Saffron supplementation in early AMD. The aim of the present longitudinal, open-label study was to evaluate whether the observed functional benefits from Saffron supplementation may be reproducible over a longer follow-up duration.

2. Materials and Methods

2.1. Patients. Twenty-nine consecutive patients (mean age, 69.3 ± 7 years; range, 55–85; 16 men and 13 women) with a diagnosis of bilateral early AMD were recruited prospectively over an interval of 8 months from the outpatient service of the institution. Each patient underwent standard general and ophthalmic examinations. Best-corrected visual acuity was determined with a retroilluminated, standardized Snellen chart, whose luminance and contrast were periodically calibrated. Clinical diagnosis of early AMD was established by direct and indirect ophthalmoscopy, as well as retinal biomicroscopy, when any of the following primary lesions in the macular area (i.e., the area within an eccentricity of approximately 2 disc diameters from the fovea) of one or both eyes was identified: soft distinct or indistinct drusen, areas of hyperpigmentation associated with drusen, or areas of hypopigmentation of the RPE associated with drusen, without any visibility of choroidal vessels. Clinical and demographic data of the patients are summarized in Table 1. All patients met the following inclusion criteria: best-corrected visual acuity of 0.5 or better in the study eye, central fixation (assessed by direct ophthalmoscopy), normal color vision with Farnsworth D-15 testing, no signs of other retinal or optic nerve disease and clear optical media. Eight patients had moderate systemic hypertension. No other systemic diseases were present. None of the patients was taking medications (e.g., chloroquine) that are known to affect macular function or to interfere with carotenoid absorption. AMD lesions of the study eyes were graded on stereoscopic fundus photographs, as previously described [14]. A macular grading scale, based on the international classification and grading system [1], was used by a single grader who evaluated the photographs while masked to subject characteristics and fERG results. The presence of basic AMD lesions was noted within each of the nine subfields delimited by a scoring grid. Fluorescein angiography and macular optical coherence tomography (OCT, Cirrus spectral domain, Zeiss) assessment were also performed in all study eyes at the time of the diagnosis, to confirm the presence of early AMD lesions, to exclude geographic atrophy or RPE detachment, and to determine at baseline the average retinal thickness in the macular region. According to the results of grading, intermediate AMD was diagnosed in all eyes, [5] with one or more drusen, ($\geq 63\,\mu$m) and/or focal hypo/hyperpigmentation within the macular region. The research adhered to the tenets of the Declaration of Helsinki. The study was approved by the Ethics Committee/Institutional Review Board of the University. Written informed consent was obtained from each study participant after the purpose and procedures of the study were fully explained.

2.2. Treatment and Testing Schedule. The patients underwent clinical examination and a focal-ERG- (fERG-)-derived macular (18°) flicker sensitivity estimate [13] at baseline and every three months over a 15-month period of treatment (Saffron 20 mg/day, Zaffit, Hortus Novus, L'Aquila, Italy) and followup. fERG sensitivity, derived from the estimated response amplitude thresholds, was the main outcome measure. Visual acuity was a secondary outcome measure.

In all patients, a clinical examination, including Snellen visual acuity testing, fundus examination by direct and indirect ophthalmoscopy, and fERG testing, was performed at study entry (baseline) and every 90 days of treatment. Clinical and fERG examinations were conducted on the same day, with ophthalmoscopy always performed after fERG recordings. During the entire period of supplementation, no other systemic pharmacologic treatments were given. In all cases, compliance was judged to be satisfactory, since none of the treated subjects refrained, for any reason, from taking the daily dose of supplement during the treatment period. No adverse systemic side effects were recorded.

2.3. Electrophysiological Methods. fERG testing was performed according to a previously published technique [13, 14]. Briefly, ERGs were elicited by the LED-generated sinusoidal luminance modulation of a circular uniform field (diameter, 18°; mean luminance, 80 cd/m^2; dominant wavelength, 630 nm), presented at the frequency of 41 Hz on the rear of a Ganzfeld bowl, illuminated at the same mean luminance as the stimulus. This technique was developed

Table 1: Demographic and clinical findings at baseline in patients with early AMD.

Patient no.	Age (yr), sex	Acuity	Follow-up duration	Fundus*	Macular thickness (microm)	fERG§ (no. of responses at B, 3, 6, 9, 12, 15)¶
1	77, F	0.8	15	Soft drusen, middle subfield	304	4(B), 5(3), 5(6), 5(9), 5(12), 5(15)
2	62, F	0.6	15	Soft drusen, middle subfield	272	6(B), 6(3), 6(6), 6(9), 6(12), 6(15)
3	61, F	0.5	12	Soft drusen, middle subfield	250	5(B), 6(3), 6(6), 6(9), 6(12)
4	63, F	0.7	12	Soft drusen, central and middle subfield	288	5(B), 6(3), 6(6), 6(9), 5(12)
5	75, M	0.7	15	Soft drusen, middle subfield	279	4(B), 5(3), 5(6), 6(9), 6(12), 6(15)
6	85, M	0.8	12	Soft drusen, central and middle subfield	260	5(B), 5(3), 5(6), 5(9), 5(12), 5(15)
7	70, M	0.7	15	Soft drusen, central subfield	280	4(B), 4(3), 4(6), 5(9), 5(12), 5(15)
8	71, M	1.0	12	Soft confluent drusen, middle subfield	254	5(B), 6(3), 6(6), 5(9), 5(12)
9	73, M	1.0	15	Soft drusen, central subfield	294	4(B), 5(3), 5(6), 6(9), 6(12), 6(15)
10	81, F	0.5	6	Soft drusen, middle subfield	251	4(B), 4(3), 4(6)
11	73, M	0.7	15	Soft drusen, central and middle subfield	275	1(B), 5(3), 6(6), 6(9), 6(12)
12	62, F	0.6	15	Soft drusen, middle subfield	297	6(B), 6(3), 6(6), 6(9), 6(12), 6(15)
13	73, M	1.0	15	Soft drusen, hyperpigm., middle subfield	221	4(B), 4(3), 5(6), 5(9), 5(12), 4(15)
14	68, M	0.8	15	Soft confluent drusen, central and middle subfield	242	2(B), 4(3), 4(6), 6(9), 6(12), 5(15)
15	58, M	1.0	6	Soft drusen, middle subfield	280	1(B), 5(3), 5(6)
16	63, M	0.8	15	Soft confluent drusen, hypopigm., middle subfield	278	4(B), 5(3), 5(6), 4(9), 5(12), 5(15)
17	64, F	1.0	15	Soft drusen and hypopigm., middle subfield	264	2(B), 6(3), 6(6), 5(9), 6(12), 6(15)
18	55, M	1.0	15	Soft drusen and hyperpigm., central subfield	295	5(B), 5(3), 6(6), 6(9), 6(12), 5(15)
19	70, F	0.7	15	Soft drusen and hyperpigm., middle subfield	237	2(B), 2(3), 1(6), 3(9), 3(12), 4(15)
20	79, M	0.4	15	Soft drusen and hyperpigm., middle subfield	255	1(B), 1(3), 4(6), 6(9), 6(12), 6(15)
21	70, M	1.0	12	Soft drusen and hyperpigm., central subfield	279	4(B), 5(3), 5(6), 4(9), 4(12)
22	70, M	0.7	15	Soft confluent drusen, central subfield	290	5(B), 5(3), 5(6), 5(9), 5(12), 5(15)
23	85, M	0.3	12	Soft drusen, middle subfield	255	1(B), 2(3), 2(6)
24	71, F	1.0	15	Soft drusen, central and middle subfield	280	4(B), 5(3), 5(6), 6(9), 5(12), 5(15)
25	73, F	1.0	15	Soft drusen and hyperpigm., middle subfield	266	3(B), 5(3), 5(6), 5(9), 5(12), 5(15)
26	71, F	0.6	15	Soft confluent drusen, hypopigm., central subfield	270	6(B), 6(3), 5(6), 5(9), 6(12), 5(15)
27	61, M	0.5	15	Soft confluent drusen, hypopigm., middle subfield	265	2(B), 6(3), 5(6), 6(9), 6(12), 5(15)
28	68, F	0.6	15	Soft confluent drusen., central subfield	293	6(B), 5(3), 5(6), 5(9), 5(12), 5(15)
29	56, F	0.6	12	Soft confluent drusen, middle subfield	277	6(B), 6(3), 6(6), 5(9), 6(12)

*Macular appearance with reference to drusen type, confluence, and location; RPE abnormalities type and main location[1]. Follow-up duration (months). §Number of FERG responses that were above noise level (i.e., S/N ratio ≥ 3) at the different modulation depths of the recording protocol; (6) = S/N ratio ≥ 3 at all modulation depths, (5) = S/N ratio < 3 at the lowest modulation depth, (4) = S/N ratio < 3 at the two lowest modulation depths, etc., B: baseline 3, 6, 9, 12, 15 months of supplementation. ¶Months of follow-up.

according to the indications of published clinical studies, in which the fERG response to sinusoidal flicker stimulation was used to test retinal flicker sensitivity in comparison to psychophysical flicker sensitivity in normal and pathologic conditions [14–16]. In the recording protocol, a series of fERG responses was collected at different modulation depths, quantified by the Michelson luminance contrast formula: $100\% \times (L\text{max} - L\text{min})/(L\text{max} + L\text{min})$, where Lmax and Lmin are maximum and minimum luminance, respectively, between 16.5% and 93.8% in 0.1- to 0.3-log-unit steps (16.5%, 33.1%, 44.8%, 63.6%, 77.2%, and 93.8%). In some patients, the signal-to-noise ratio (S/N) at the modulation of 93.5% was not large enough to allow recording of the whole response family. In those cases, response collection was limited to the highest or the two highest modulation depths. In Table 1, the number of responses that were significantly different from the noise level, collected at every visit, is reported for each patient.

fERGs were recorded monocularly by means of Ag-AgCl superficial cup electrodes taped over the skin of the lower eyelid. A similar electrode, placed over the eyelid of the contralateral, patched eye, was used as the reference (interocular ERG, [17]). fERG signals were amplified, bandpass filtered between 1 and 250 Hz (−6 dB/octave), sampled with 12-bit resolution, (2-kHz sampling rate), and averaged. A total of 1600 events (in eight blocks of 200 events each) were averaged for each stimulus condition. The sweep duration was kept equal to the stimulus period. Single sweeps exceeding the threshold voltage (25 μV) were rejected, to minimize noise coming from blinking or eye movements.

A discrete Fourier analysis was performed off line to isolate the fERG fundamental harmonic and estimate its amplitude (in μV) and phase (in degrees). Component amplitude and phase were also calculated separately for partial blocks (200-event packets) of the total average, from which the standard error of amplitude and phase estimates were derived to test response reliability. Averaging and Fourier analysis were also performed on signals sampled asynchronously at 1.1 times the temporal frequency of the stimulus, to give an estimate of the background noise at the fundamental component. An additional noise estimate at the fundamental harmonic was obtained by recording responses to a blank, unmodulated field kept at the same mean luminance as the stimulus. In all records, the noise amplitudes recorded with both methods were $\leq 0.053\,\mu$V.

In all subjects, the fERG testing protocol was started after a 20-minute period of preadaptation to the stimulus mean illuminance. Pupils were pharmacologically (tropicamide 1%) dilated to 8 to 9 mm. Subjects fixated (from a distance of 30 cm) on the center of the stimulation field with the aid of a small (15 minutes of arc) fixation mark. An fERG response was first collected at the maximum modulation depth (93.5%) included in the protocol and was evaluated with respect to reliability and S/N ratio. In all patients, the responses at 93.5% modulation satisfied the following criteria: standard deviation estimates of <20% (variation coefficient) and 15° for the amplitude and phase, respectively, and an S/N ratio ≥ 4. In AMD patients having a response S/N ≥ 8, fERG signals were also acquired in sequence for six values of modulation depth between 16.5% and 93.5%, presented in an increasing order. For each stimulus modulation depth, fERG responses were accepted only if their S/N ratio was ≥ 2. As described elsewhere [14], fERG log amplitudes were plotted for each patient as a function of log modulation depth. The resulting function slope was determined by linear regression. From the same regression line, fERG threshold was estimated from the value of log modulation depth yielding a criterion amplitude, corresponding to an S/N ratio of 3.28. fERG sensitivity was defined as the reciprocal of this value.

2.4. Statistical Analysis. From each patient included in the study, one eye, typically the eye with the best visual acuity, was selected and designated as the study eye. The data from the study eyes were included in the statistical analysis. Outcome variables were fERG amplitude and fERG function threshold and slope. fERG amplitude data underwent logarithmic transformation to better approximate normal distribution. fERG thresholds and slopes are reported as log10 values. In all statistical analyses, standard error and 95% confidence interval (CI) of the means were used for within-group comparisons.

Sample size estimates were based on those reported in previous investigations [8, 13, 14], in which the between- and within-subjects variability (expressed as the standard deviation) of fERG parameters was determined in patients with early AMD. Assuming between-and within-subject SDs in fERG amplitude and phase of 0.1 log μV and 20°, respectively, the sample size of study patients provided a power of 80%, at an $\alpha = 0.05$, for detecting test-retest differences of 0.1 (SD 0.1) log μV in threshold. Given the absolute mean amplitude and phase values of the patients' fERGs, these differences were considered to be clinically meaningful, since they corresponded approximately to a 25% to 30% change in fERG threshold. A study [8] in patients with early AMD showed that test-retest variability in fERG amplitude and threshold is significantly smaller than this change. Electrophysiological results were analyzed by analysis of variance for repeated measures (ANOVA). Dependent variables in the ANOVA design were fERG log threshold and slope and visual acuity. Repeated-measures ANOVA on log threshold and slope as dependent variables was used to compare the fERG results recorded across the different recording sessions. Visual acuity changes across treatments were analyzed, either individually for every patient or as group means by repeated-measures ANOVA, assuming normal distribution. In all the analyses, results with a $P < 0.05$ were considered as statistically significant.

3. Results

Typical fERG functions (response amplitude versus modulation depth of the stimulus) observed in an early AMD patient after Saffron supplementation across the different recording sessions over a fifteen-month followup are reported in Figure 1(a). fERG amplitude increased from baseline after three months of supplementation, resulting in a reduction of response threshold, as shown by the decrease of the minimum modulation depth yielding a response significantly above the noise level (S/N ratio > 3). Figure 1(b) shows, for comparison, the fERG test-retest results obtained from a normal control subject at baseline and after three months. It can be noted that the test-retest variability of fERG data was considerably smaller than that observed after Saffron supplementation in the AMD patient.

Figure 2 shows the mean fERG functions (±SEM) recorded at baseline and every three months after starting Saffron supplementation. There was an overall increase in fERG amplitude soon after the first three months of supplementation followed by a stabilisation over the subsequent follow-up period. The average fERG functions were uniformly and consistently shifted to the left on the x-axis indicating a decrease in response threshold and an increase in sensitivity, which were reproducible in the various recording sessions. The arrows in the plot highlight the change in the average modulation threshold comparing the baseline with the follow-up recordings (averaged across the different time points).

This point is illustrated in further detail in Figure 3, which shows the fERG threshold and slope results (mean ± SEM) recorded at every follow-up session over the period of follow-up examination. Mean fERG threshold decreased (and consequently the reciprocal sensitivity value increased) by 0.3 log units compared to the baseline value (repeated measures ANOVA, $F = 4.6$; df: 6,168; $P < 0.01$). These changes remained stable over the followup period, since

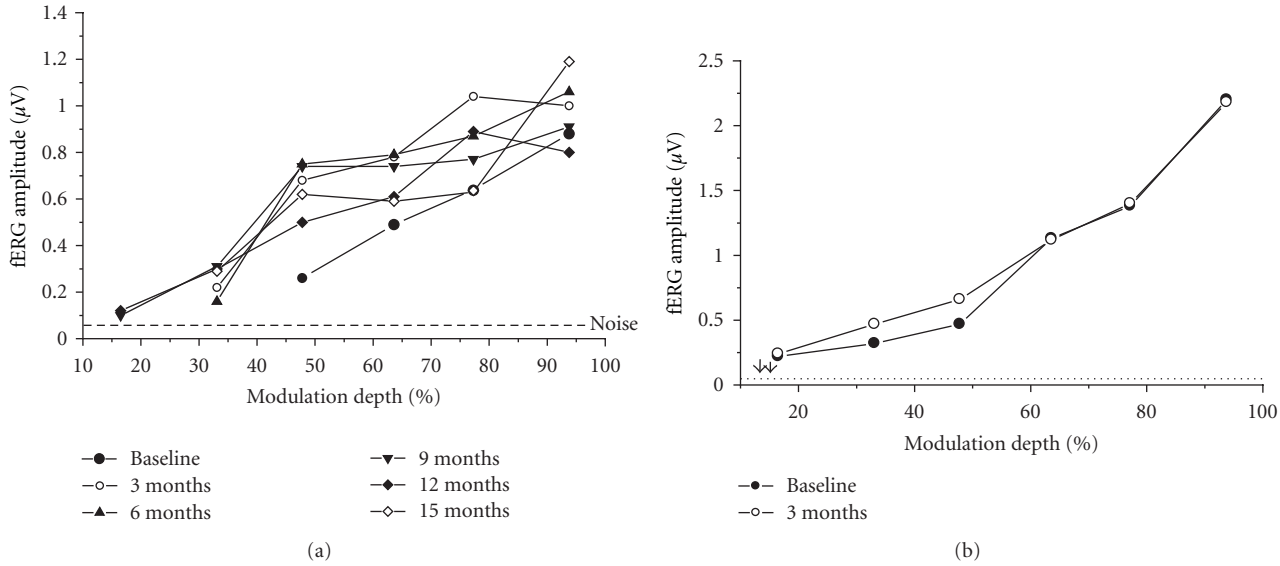

Figure 1: (a) fERG results recorded at baseline and every three months, over a 15 month followup, in an early AMD patient taking saffron supplement (20 mg/day) (b) Plot showing, for comparison, fERG test-retest results obtained from a normal control subject at baseline and after three months.

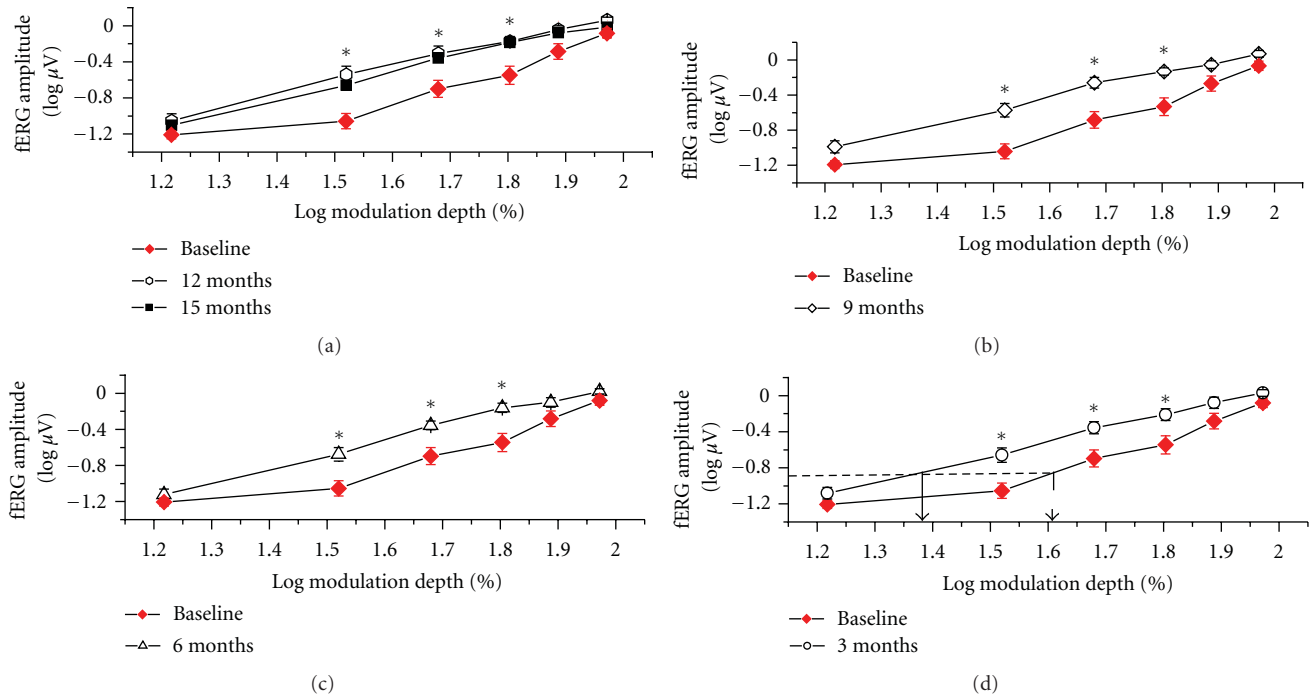

Figure 2: Mean (±SEM) fERG functions, plotting log amplitude versus log modulation depth of the flicker stimulus, recorded from all 29 patients at baseline and at the various time points of the study. Note that mean fERG function was shifted uniformly to the left on the x-axis after the first three months of supplementation and then remained stable. Arrows in the plot indicate the mean shift in fERG sensitivity observed by comparing the baseline with the follow-up fERG recordings (averaged across the different times). Asterisks indicate data points that were significantly ($P < 0.05$) different from baseline.

comparisons at various times of follow-up did not show any significant change. The mean fERG slopes did not change significantly throughout the followup.

In most patients at the various times after starting supplementation, fERG thresholds decreased by a variable amount compared to the corresponding baseline value. Figure 4 provides examples of the observed changes in response thresholds observed at 3, 9, and 15 months. The results found at 6 and 12 months are substantially similar. In the scatterplots of the figure, the values recorded at the

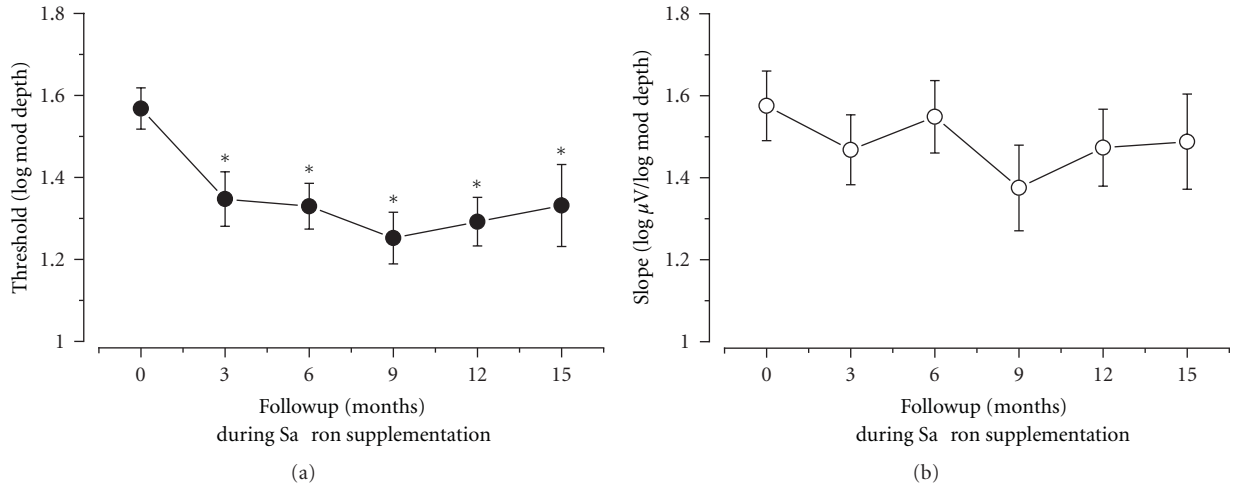

Figure 3: Mean fERG thresholds and slopes (± standard error) recorded at baseline and over the follow-up period in all patients. Note that mean decreased (i.e., sensitivity increased) from baseline already after three months of supplementation and then tended to stabilize. Mean fERG slope did not change significantly over time.

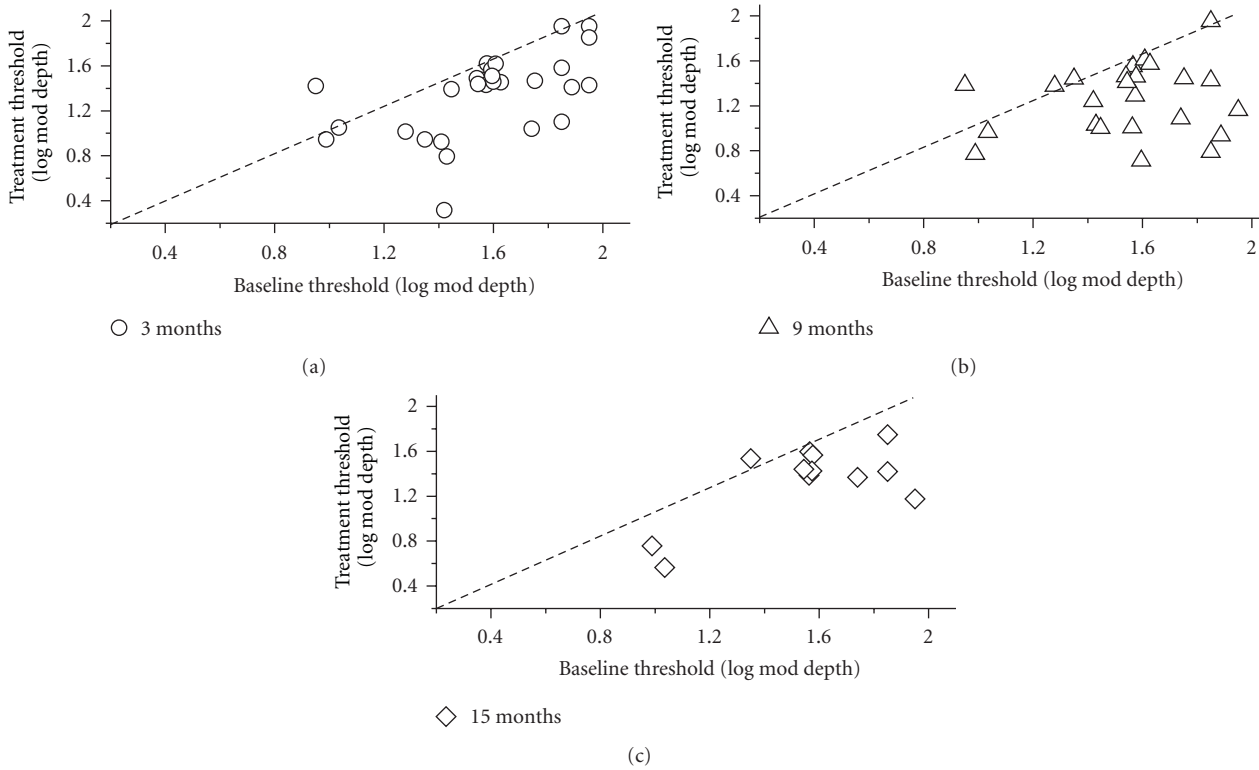

Figure 4: Scatterplots showing the fERG threshold values recorded at different follow-up times (3, 9, and 15 months) plotted as a function of the corresponding baseline values. Diagonal lines in the plots indicate the equivalence between the values recorded at baseline and at a given followup. It can be noted that, at every followup, most values fall on the right of the diagonal line, indicating a decrease in threshold for the majority of patients.

different follow-up times are plotted as a function of the corresponding baseline values. Diagonal lines in the plots indicate the equivalence between the values recorded at baseline and at a given followup. It can be noted that, at every followup, most values fall on the right of the diagonal line, indicating a decrease in threshold for the majority of patients.

Right after three months of supplementation, mean visual acuity improved by two Snellen lines compared to baseline values (0.75 to 0.9, repeated measures ANOVA, $F = 4.3$; df: 6,168; $P < 0.01$). The visual acuity results over the follow-up period are reported in Figure 5 as a plot of mean (± SEM) acuity as a function of follow-up time. It can be

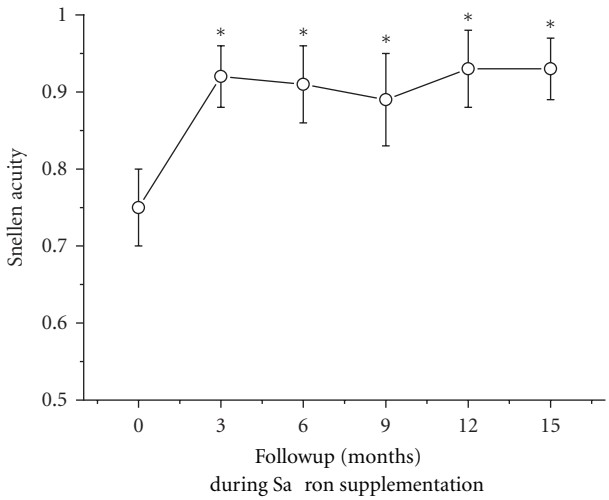

Figure 5: Mean (± standard error) Snellen visual acuity recorded at baseline and every three months throughout the follow-up period.

noted that, similar to fERG sensitivity, the gain in visual acuity remained stable over the study period.

In parallel with the electrophysiological and visual acuity improvement, all patients reported an improvement in their quality of vision. The most commonly reported symptoms of the beneficial effects of supplementation were the improvement in contrast and color perception, reading ability, and vision at low luminances, all ultimately leading to a substantial improvement in the patients' quality of life.

Funduscopic examination, periodically performed in all patients, did not show any significant change in drusen number and size, as well as in the extension of RPE abnormalities. Figure 6 shows fundus pictures of one study patient taken at baseline and at the end of clinical followup. It can be seen that both funduscopic images appeared to be very similar to each other.

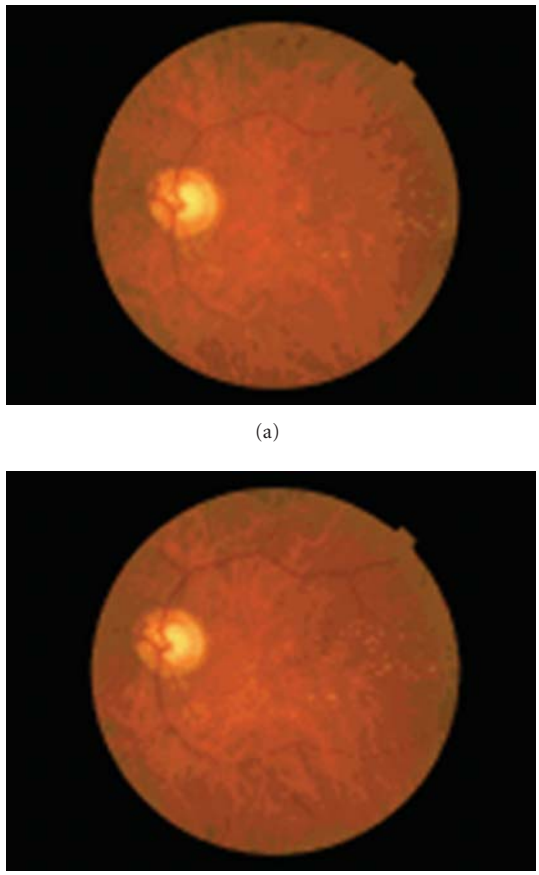

(a)

(b)

Figure 6: Fundus pictures of a representative early AMD patient taken at baseline and at the end of follow-up. No significant changes in fundus features can be found.

4. Discussion

The present data extend the results of a previous, randomized study [13] on the potential efficacy of Saffron supplementation in AMD, showing that such supplementation may induce a long-term, stable improvement in retinal function, as measured by fERG sensitivity. To our knowledge, this is the first longitudinal study, based on an objective electrophysiological technique, documenting the long-term effects of Saffron antioxidant on retinal function in AMD. While several other studies have already shown significant effects of antioxidant supplementation on retinal function [8, 10, 13], all these previous studies were more limited either in their follow-up duration or in the number of testing sessions. The current data show that changes in fERG threshold (and consequently its reciprocal value sensitivity) after supplementation were within-session consistent, reproducible, and durable over a 15-month follow-up period. The sensitivity improvements were observed in association with a constant slope of the fERG functions, further indicating the reproducibility of the fERG function shapes recorded during followup. All patients reported a subjective improvement in their quality of vision and ultimately in their quality of life, supporting the impact of the fERG findings on psychophysical visual function of patients.

Limitations of this study include its open label nature, which may affect mainly the subjective patients' results, and the assumed stability of the main outcome measure, the fERG, without treatment. As far as the first issue is concerned, the efficacy of Saffron supplementation was already demonstrated in a previous double-blind, randomized, placebo-controlled study [13], strongly supporting the hypothesis that the long-term fERG improvement found in our patients similarly results from Saffron supplementation, and not from other unknown and unpredictable factors. Regarding the second issue, previous studies of our group [8, 14], performed in normal subjects and early AMD patients without treatment, have shown an fERG test-retest variability that is small enough to allow macular function to be reliably monitored during treatment. Taking into account the previous limitations, the current findings point at the use of macular fERG sensitivity as a candidate protocol to track changes in central retinal function over the course of AMD.

It may be presumed that the observed improvement in macular function is an effect of integrated activities of Saffron's chemical compounds, mainly of crocin, and crocetin, antioxidant derivatives of carotenoids, which may act through a protective mechanism similar to that seen with carotenoid supplementation [18–21], resulting in a beneficial effect on retinal function. In addition, crocins are able to activate metabolic pathways to protect cells from apoptosis and to reduce light-induced death in isolated photoreceptors, while crocetin increases oxygen diffusivity through liquids, such as plasma [18].

In the original study by Maccarone et al. [11], to test whether the Saffron extract (Crocus sativus L.) given as a dietary supplement counteracts the effects of continuous light exposure in the albino rat retina, Sprague-Dawley rats were prefed either Saffron or beta-carotene before they were exposed to bright continuous light for 24 hours. Flash electroretinograms (ERGs) amplitudes, the thickness of the outer nuclear layer (ONL), and the amount of apoptotic figures in the ONL were the main outcome variables. The photoreceptor layer was largely preserved in Saffron-treated animals as it was the flash ERG response. In addition, the rate of photoreceptor death induced by bright continuous light appeared drastically reduced in treated animals. In beta-carotene prefeeding experiments, morphologic analysis showed preservation of the ONL similar to that obtained with Saffron prefeeding, whereas the ERG response was unrecordable. Western blot analysis showed that exposure to light induced a strong upregulation of fibroblastic growth factor (FGF2) in control and beta-carotene-treated rats, but no change was noted in Saffron-treated rats. These results showed that Saffron may protect photoreceptors against retinal stress, maintaining both morphology and function and probably acting as a regulator of programmed cell death. To identify the genes and noncoding RNAs (ncRNAs) involved in the neuroprotective actions of Saffron, Natoli et al. [12] used continuous bright light as a standardized assay of photoreceptor damage in albino Sprague Dawley rats. RNA from the eye of exposed and unexposed animals was hybridized to Affymetrix rat genome ST arrays. Light damage caused the regulation of 175 entities (genes and ncRNAs) beyond criterion levels. Saffron treatment before light damage exposure reduced the expression of 53 entities and regulated 122 entities not regulated by light damage. This analysis provides a basis for more focused basic studies on Saffron protective mechanism(s).

The peculiar characteristics of Saffron components support our hypothesis of an involvement of very different ways of action going from antioxidant activity to direct control of gene expression. It should be noted that the current results can only be applied to the early/moderate stage of AMD. It is currently unknown whether Saffron supplementation may exert a beneficial protective effect in patients with more advanced stages of disease. In addition, it is unclear how the Saffron efficacy compares with that of other antioxidant supplements currently available, such as the AREDS preparation [5]. While further studies are needed to define the upper beneficial limit of Saffron supplementation, the present approach seems to be promising for a long-term treatment of early retinal dysfunction associated with AMD.

Acknowledgments

We thank the company Hortus Novus for kindly providing the saffron pills and giving support to this study.

References

[1] A. C. Bird, N. M. Bressler, S. B. Bressler et al., "An international classification and grading system for age-related maculopathy and age-related macular degeneration: the International ARM Epidemiological Study group," *Survey of Ophthalmology*, vol. 39, no. 5, pp. 367–374, 1995.

[2] G. S. Hageman, D. H. Anderson, L. V. Johnson et al., "A common haplotype in the complement regulatory gene factor H (HF1/CFH) predisposes individuals to age-related macular degeneration," *Proceedings of the National Academy of Sciences of the United States of America*, vol. 102, no. 20, pp. 7227–7232, 2005.

[3] A. Rivera, S. A. Fisher, L. G. Fritsche et al., "Hypothetical LOC387715 is a second major susceptibility gene for age-related macular degeneration, contributing independently of complement factor H to disease risk," *Human Molecular Genetics*, vol. 14, no. 21, pp. 3227–3236, 2005.

[4] J. G. Hollyfield, V. L. Bonilha, M. E. Rayborn et al., "Oxidative damage-induced inflammation initiates age-related macular degeneration," *Nature Medicine*, vol. 14, no. 2, pp. 194–198, 2008.

[5] Age-Related Eye Disease Study Research Group, "A randomized, placebo-controlled, clinical trial of high-dose supplementation with vitamins C and E, beta carotene, and zinc for age-related macular degeneration and vision loss: AREDS report no. 8," *Archives of Ophthalmology*, vol. 119, pp. 1417–1436, 2001.

[6] W. T. Wong, W. Kam, D. Cunningham et al., "Treatment of geographic atrophy by the topical administration of OT-551: results of a phase ii clinical trial," *Investigative Ophthalmology and Visual Science*, vol. 51, no. 12, pp. 6131–6139, 2010.

[7] D. Weismann, K. Hartvigsen, N. Lauer et al., "Complement factor H binds malondialdehyde epitopes and protects from oxidative stress," *Nature*, vol. 478, pp. 76–81, 2011.

[8] B. Falsini, M. Piccardi, G. Iarossi, A. Fadda, E. Merendino, and P. Valentini, "Influence of short-term antioxidant supplementation on macular function in age-related maculopathy: a pilot study including electrophysiologic assessment," *Ophthalmology*, vol. 110, no. 1, pp. 51–60, 2003.

[9] S. Richer, W. Stiles, L. Statkute et al., "Double-masked, placebo-controlled, randomized trial of lutein and antioxidant supplementation in the intervention of atrophic age-related macular degeneration: the Veterans LAST study (Lutein Antioxidant Supplementation Trial)," *Optometry*, vol. 75, no. 4, pp. 216–230, 2004.

[10] V. Parisi, M. Tedeschi, G. Gallinaro, M. Varano, S. Saviano, and S. Piermarocchi, "Carotenoids and antioxidants in age-related maculopathy italian study. Multifocal electroretinogram modifications after 1 year," *Ophthalmology*, vol. 115, no. 2, pp. 324–333, 2008.

[11] R. Maccarone, S. Di Marco, and S. Bisti, "Saffron supplement maintains morphology and function after exposure to damaging light in mammalian retina," *Investigative Ophthalmology and Visual Science*, vol. 49, no. 3, pp. 1254–1261, 2008.

[12] R. Natoli, Y. Zhu, K. Valter, S. Bisti, J. Eells, and J. Stone, "Gene and noncoding RNA regulation underlying photoreceptor protection: microarray study of dietary antioxidant saffron

and photobiomodulation in rat retina," *Molecular Vision*, vol. 16, pp. 1801–1822, 2010.

[13] B. Falsini, M. Piccardi, A. Minnella et al., "Influence of saffron supplementation on retinal flicker sensitivity in early age-related macular degeneration," *Investigative Ophthalmology and Visual Science*, vol. 51, no. 12, pp. 6118–6124, 2010.

[14] B. Falsini, A. Fadda, G. Iarossi et al., "Retinal sensitivity to flicker modulation: reduced by early age-related maculopathy," *Investigative Ophthalmology and Visual Science*, vol. 41, no. 6, pp. 1498–1506, 2000.

[15] W. Seiple, K. Holopigian, V. Greenstein, and D. C. Hood, "Temporal frequency dependent adaptation at the level of the outer retina in humans," *Vision Research*, vol. 32, no. 11, pp. 2043–2048, 1992.

[16] W. H. Seiple, K. Holopigian, V. C. Greenstein, and D. C. Hood, "Sites of cone system sensitivity loss in retinitis pigmentosa," *Investigative Ophthalmology and Visual Science*, vol. 34, no. 9, pp. 2638–2645, 1993.

[17] A. Fiorentini, L. Maffei, M. Pirchio, D. Spinelli, and V. Porciatti, "The ERG in response to alternating gratings in patients with diseases of the peripheral visual pathway," *Investigative Ophthalmology & Visual Science*, vol. 21, pp. 490–493, 1981.

[18] M. Giaccio, "Crocetin from saffron: an active component of an ancient spice," *Critical Reviews in Food Science and Nutrition*, vol. 44, no. 3, pp. 155–172, 2004.

[19] T. Ochiai, H. Shimeno, K. I. Mishima et al., "Protective effects of carotenoids from saffron on neuronal injury in vitro and in vivo," *Biochimica et Biophysica Acta*, vol. 1770, no. 4, pp. 578–584, 2007.

[20] A. Laabich, G. P. Vissvesvaran, K. L. Lieu et al., "Protective effect of crocin against blue light- and white light-mediated photoreceptor cell death in bovine and primate retinal primary cell culture," *Investigative Ophthalmology and Visual Science*, vol. 47, no. 7, pp. 3156–3163, 2006.

[21] C. D. Kanakis, P. A. Tarantilis, M. G. Polissiou, S. Diamantoglou, and H. A. Tajmir-Riahi, "An overview of DNA and RNA bindings to antioxidant flavonoids," *Cell Biochemistry and Biophysics*, vol. 49, no. 1, pp. 29–36, 2007.

Hindawi Publishing Corporation
Evidence-Based Complementary and Alternative Medicine
Volume 2012, Article ID 701205, 9 pages
doi:10.1155/2012/701205

Research Article

Acute and Chronic Administrations of *Rheum palmatum* Reduced the Bioavailability of Phenytoin in Rats: A New Herb-Drug Interaction

Ying-Chang Chi,[1] Shin-Hun Juang,[1] Wai Keung Chui,[2] Yu-Chi Hou,[3,4] and Pei-Dawn Lee Chao[3]

[1] *Institute of Pharmaceutical Chemistry, China Medical University, Taichung 40402, Taiwan*
[2] *Department of Pharmacy, Faculty of Science, National University of Singapore, 18 Science Drive 4, Singapore 117543*
[3] *School of Pharmacy, China Medical University, Taichung 40402, Taiwan*
[4] *Department of Medical Research, China Medical University Hospital, Taichung 40402, Taiwan*

Correspondence should be addressed to Yu-Chi Hou, hou5133@gmail.com and Pei-Dawn Lee Chao, p22340069@gmail.com

Received 16 March 2012; Revised 23 April 2012; Accepted 27 April 2012

Academic Editor: Paul Siu-Po Ip

The rhizome of *Rheum palmatum* (RP) is a commonly used herb in clinical Chinese medicine. Phenytoin (PHT) is an antiepileptic with narrow therapeutic window. This study investigated the acute and chronic effects of RP on the pharmacokinetics of PHT in rat. Rats were orally administered with PHT (200 mg/kg) with and without RP decoction (single dose and seven doses of 2 g/kg) in a crossover design. The serum concentrations of PHT, PHT glucuronide (PHT-G), 4-hydroxyphenytoin (HPPH), and HPPH glucuronide (HPPH-G) were determined by HPLC method. Cell line models were used to identify the underlying mechanisms. The results showed that coadministration of single dose or multiple doses of RP significantly decreased the C_{max} and AUC_{0-t} as well as the K_{10} of PHT, PHT-G, HPPH, and HPPH-G. Cell line studies revealed that RP significantly induced the P-gp-mediated efflux of PHT and inhibited the MRP-2-medicated transport of PHT and HPPH. In conclusion, acute and chronic coadministrations of RP markedly decreased the oral bioavailability of PHT via activation of P-gp, although the MRP-2-mediated excretion of PHT was inhibited. It is recommended that caution should be exercised during concurrent use of RP and PHT.

1. Introduction

The rhizome of *Rheum palmatum* (RP, Dahuang) is one of the important herbs widely used in China, Russia, and Arabia [1]. The major constituents of RP include a variety of anthraquinones such as aloe-emodin, rhein, emodin, chrysophanol and physcion [2, 3], which have been reported to show various beneficial effects, including neuroprotective, antioxidant, anti-inflammatory, and anticancer activities [4–8]. Recent pharmacokinetic studies of RP have revealed that the anthraquinones were all predominantly present as glucuronides and sulfates in the blood [3, 8] and they are also putative substrates of multidrug resistance proteins (MRPs), namely, the anion transporters.

Phenytoin (PHT), a widely used antiepileptic with narrow therapeutic window, follows nonlinear pharmacokinetics, and thus therapeutic drug monitoring is usually recommended during its use [9]. The adverse reactions of PHT include drowsiness, dysarthria, tremor, and cognitive difficulties [10, 11]. PHT has been reported as a substrate of P-glycoprotein (P-gp) and MRP 2, whose expressions determined the PHT level in brain [12, 13]. PHT is metabolized to its main metabolite 4-hydroxyphenytoin (HPPH) by cytochrome P450 (CYP) 2C9 and to a minor extent by CYP 2C19 [14, 15]. Both PHT and HPPH are metabolized by glucuronidation to form PHT glucuronide (PHT-G) and HPPH glucuronide (HPPH-G), respectively [16, 17].

Based on our understanding on the metabolic fates and pharmacokinetics of PHT and anthraquinones in RP, we hypothesized that the metabolites of anthraquinones might compete with PHT, HPPH, PHT-G, or HPPH-G for anion transporters such as MRP 2. Patients suffering from epilepsy are generally dependent on life-long antiepileptic treatment. On other hand, using RP for constipation is an excellent home remedy in oriental countries. Therefore, it is probable that epileptic patients combined the use of PHT and RP. As such coadministration of RP and PHT may give rise to adverse effects, therefore, this study was set up to investigate the acute and chronic effects of coadministration of RP on the pharmacokinetics of PHT in rats. In addition, cell line models would be used to explore the underlying mechanism of this herb-drug interaction.

2. Materials and Methods

2.1. Chemicals and Reagents. PHT (purity 99%), HPPH (purity 98%), aloe-emodin (purity 95%), rhein (purity 95%), emodin (purity 95%), chrysophanol (purity 98%), physcion (purity 98%), verapamil (purity 99%), indomethacin (purity 98%), propylparaben (purity 99%), 2-methylanthraquinone (purity 95%), rhodamine 123 (purity 99%), and 3-(4,5-dimethylthiazol-2-yl)-2,5-diphenyl tetrazolium bromide (MTT) were purchased from Sigma Chemical Co. (St. Louis, MO, USA). L(+)-Ascorbic acid was obtained from Riedel-de Haën Laborchemikalien GmbH & Co. KG (Seelze, Germany). Fetal bovine serum was supplied by Biological Industries Ltd., Kibbutz Beit Haemek, Israel). L-Glutamine, penicillin, streptomycin, nonessential amino acid, trypsin-EDTA, and Hank's balanced salt solution (HBSS) were purchased from Invitrogen Inc. (Carlsbad, CA, USA). Total protein assay kit was purchased from Bio-Rad Inc. (Mississauga, ON, Canada). Other reagents were HPLC grade or analytical grade. Milli-Q plus water (Millipore, Bedford, MA, USA) was used throughout this study.

2.2. Preparation and Characterization of RP Decoction. The crude drug of RP was purchased from a Chinese drugstore in Taichung, Taiwan. The origin was identified by Dr. Yu-Chi Ho via microscopic examination. A voucher specimen (CMU-P-1905-9) was deposited in the College of Pharmacy, China Medical University. Water (5 L) was added to 250 g of the crude drug. After maceration for 1 h, the mixture was heated to boiling and gentle heating was continued for about 2 h until the volume was reduced to less than 2.5 L. The mixture was filtered while hot and the filtrate was concentrated further by gentle boiling until the volume was reduced to below 500 mL, after which sufficient water was added to make 500 mL (0.5 g/mL of RP). The resultant concentrate was divided into aliquots of 40 mL and stored at −20°C for later use.

The concentrations of aloe-emodin, rhein, emodin, chrysophanol, and physcion in RP decoction and its hydrolysate were determined by an HPLC method. For acid hydrolysis, a portion of the decoction (1.0 mL) was added 1.2 N HCl (1 mL), 25 mg of ascorbic acid and incubated at 80°C for 30 min. This method was determined by a previous preliminary study. The mixture was then added with 4.0 mL of methanol. After vortexing and centrifugation, the supernatant (100 μL) was mixed with 100 μL of internal standard in the form of 2-methylanthraquinone solution (50 μg/mL in methanol) and 20 μL of this solution was subjected to HPLC analysis. A gradient elution was carried out using a mobile phase consisting of 0.1% phosphoric acid (A) and acetonitrile (B) that were mixed in the following program: A/B = 50/50 (0–10 min), 15/85 (15–22 min), 50/50 (27–30 min). The detection wavelength was set at 280 nm and the flow rate was maintained at 1.0 mL/min. The concentration of anthraquinone glycoside was estimated from the difference of aglycone concentrations between RP decoction and its acid hydrolysate.

2.3. Animals and Drug Administration. Male Sprague-Dawley rats were supplied by National Laboratory Animal Center (Taipei, Taiwan) and kept in the animal center of the China Medical University (Taichung, Taiwan). The animal protocol was approved by the Institutional Animal Care and Use Committee of the China Medical University. The animal study was conducted with adherence to "The Guidebook for the Care and Use of Laboratory Animals" published by the Chinese Society of Animal Science, Taiwan. The rats (300–400 g) were fasted for 12 h before drug administration. PHT was dissolved in dil. NaOH to afford a solution of 20.0 mg/mL [18]. PHT was given via gastric gavage to six rats at 200.0 mg/kg with and without a concomitant oral dose of RP decoction (single dose and seven doses of 2 g/kg) in a crossover design. The RP decoction was administered right before PHT.

2.4. Blood Collection. Blood samples (0.5 mL) were withdrawn via cardiac puncture at time points of 0, 15, 30, 60, 120, 240, 480, and 720 min after oral administration of PHT. The blood samples were collected in microtubes and centrifuged at 10,000 g for 15 min to obtain the serum, which was stored at −70°C before analysis.

2.5. Determination of PHT and Its Metabolites in Serum. For the determination of free forms of PHT and HPPH, 100 μL of serum sample was mixed with 50 μL of pH 5 acetate buffer and 50 μL of ascorbic acid (100 mg/mL). The mixture was extracted with 200 μL of ethyl acetate (containing propylparaben as internal standard, 5 μg/mL). The ethyl acetate layer was evaporated under N_2 to dryness and reconstituted with an appropriate volume of acetonitrile and then subjected to HPLC analysis.

For the assay of PHT-G and HPPH-G in serum, indirect determination was carried out through hydrolysis with β-glucuronidase in pH 5 acetate buffer. Serum sample (100 μL) was mixed with 50 μL of β-glucuronidase (1000 units/mL) and 50 μL of ascorbic acid (100 mg/mL) and incubated at 37°C for 60 min under anaerobic condition. After hydrolysis, the analytical procedures followed that for the assay of the free forms as described above.

2.6. Cell Lines and Cell Culture. LS 180, the human colon adenocarcinoma cell line, was obtained from the Food Industry Research and Development Institute (Hsinchu, Taiwan). The nontransfected and MRP-2-overexpressing MDCK II cell lines were kindly provided by Professor Piet Borst (Dutch Cancer Institute, Amsterdam, The Netherlands). The cell lines were cultured in DMEM medium supplemented with 10% fetal bovine serum, 0.1 mM nonessential amino acid (LS 180 cell line only), 100 units/mL of penicillin, 100 μg/mL of streptomycin, and 292 μg/mL of glutamine. Cells were grown at 37°C in a humidified incubator containing 5% CO_2. The medium was changed every other day, and the cells were subcultured until 80–90% confluency was reached.

2.7. Cytotoxicity Assay. Verapamil hydrochloride was dissolved in water. PHT and HPPH were dissolved in dil. NaOH (pH 9.0). Indomethacin (Indo) was dissolved in MeOH and the final concentration of MeOH in medium was below 0.1% (v/v). LS 180, MDCK II, and MDCK II-MRP 2 cells (1×10^5 cells/well) were seeded into 96-well plates. After overnight incubation, the test agents were added into the wells and incubated for 72 h and then 15 μL of MTT (5 mg/mL) was added into each well and incubated for additional 4 h. During this period, MTT was reduced to formazan crystal by live cells. An acidic SDS (10%) solution was added to solubilize the purple crystal formed at the end of incubation and the optical density was measured at 570 nm by a microplate reader (Nunc, Denmark).

2.8. Transport Study of PHT in LS 180. LS 180 cells (passage 50 to 60) were seeded on 12-well plates at a density of 5×10^5 cells/well. Before the experiment, the medium was removed and the cells were quickly rinsed with ice-cold HBSS transport buffer consisting of HEPES (10 mM, pH 7.4.). PHT (10 μM) was coincubated with and without RP (2.0, 1.0 and 0.5 mg/mL) and verapamil (100 μM) with LS 180 for 90 min. After incubation, the cells were rapidly washed twice with ice-cold HBSS buffer and lysed with 200 μL of 0.1% Triton X-100 for 30 min.

Total protein content in the lysate (5 μL) was determined by Bradford method [19], and bovine serum albumin was used as the standard. The protein contents in each well were used for data correction.

2.9. Preparation and Characterization of Serum Metabolites of RP (RPMs). In order to mimic the molecules interacting with MRP 2 in the kidney, RPMs was prepared using rats. After overnight fasting, rats were given RP decoction at 2 g/kg. Blood was collected at 30 min after dosing. The serum was added with 3-fold methanol. After vortex and centrifugation at 10,000 g for 15 min, the supernatant was dried in a rotatory evaporator under vacuum. To the residue, an appropriate volume of water was added to afford a solution with a 10-fold serum concentration, which was divided into aliquots and stored at −80°C for later use. The procedures for the characterization of RPMs followed that of a previous study [2, 3]. Briefly, 100 μL of serum sample were mixed with 50 μL of sulfatase solution (containing 1000 units/mL of sulfatase and 35,600 units/mL of β-glucuronidase) and 50 μL of ascorbic acid (100 mg/mL) and incubated at 37°C for 10 min under anaerobic condition. After hydrolysis, the serum was acidified with 50 μL of 0.1 N HCl and extracted with 250 μL of ethyl acetate (containing 2-methylanthraquinone as internal standard, 1 μg/mL). The ethyl acetate layer was evaporated under N_2 to dryness and reconstituted with an appropriate volume of methanol prior to HPLC analysis. In addition, the serum of rats given water only was collected to prepare the blank control. The blank serum was processed as described above and diluted to various folds of serum concentration for the comparison with correspondent concentration of RPMs.

2.10. Transport Study of PHT and HPPH in MDCK II and MDCK II-MRP 2. MDCK II and MDCK II-MRP 2 cells within 10 passages were seeded on 12-well plates at a density of 3×10^5 cells/well. Before experiment, the medium was removed and the cells were quickly rinsed with ice-cold HBSS transport buffer. To determine whether PHT and HPPH are substrates of MRP 2, PHT (10 μM), HPPH (10 μM) and Indo (50, 100 and 200 μM, as a positive control of MRP 2 inhibitor) were incubated with MDCK II and MDCK II-MRP 2 for 60 min.

In another study, RPMs and Indo (100 μM) in HBSS were preincubated with MDCK II-MRP 2 for 30 min. The supernatants were removed and cells were washed three times with ice-cold PBS. Then, PHT (10 μM) and HPPH (10 μM) were coincubated with and without RPMs (1.0-, 0.5-, and 0.25-fold of serum concentrations) and Indo (200 μM) with MDCK II-MRP 2 for another 30 min. After incubation, the cells were rapidly washed twice with ice-cold HBSS buffer and lysed with 200 μL of 0.1% Triton X-100 for 30 min.

Total protein content in the lysate (5 μL) was determined by Bradford method [19], and bovine serum albumin was used as the standard. The protein contents in each well were used for data correction.

2.11. Determination of PHT and HPPH Concentrations in Cell Lysate. For the assay of PHT and HPPH, 200 μL of cell lysate was extracted with 200 μL of ethyl acetate (containing propylparaben as internal standard, 5 μg/mL). The ethyl acetate layer was evaporated under N_2 to dryness and reconstituted with an appropriate volume of acetonitrile, then subjected to HPLC analysis.

2.12. Assay and Method Validation of PHT and HPPH in Serum and Cell Lysate. An HPLC method using a mixture of methanol and 0.05% phosphoric acid (48 : 52) as mobile phase was developed and validated for the assay of PHT and HPPH in serum and cell lysate. The detection wavelength was set at 214 nm and the flow rate was 1.0 mL/min. The calibration ranges of PHT and HPPH were 0.2–50.0 μg/mL for serum and cell lysate. The precision and accuracy of the analytical method was evaluated by intraday and interday analysis of triplicate standards within one day and over a period of three days. Recoveries from serum were calculated based on the detected concentrations in serum compared

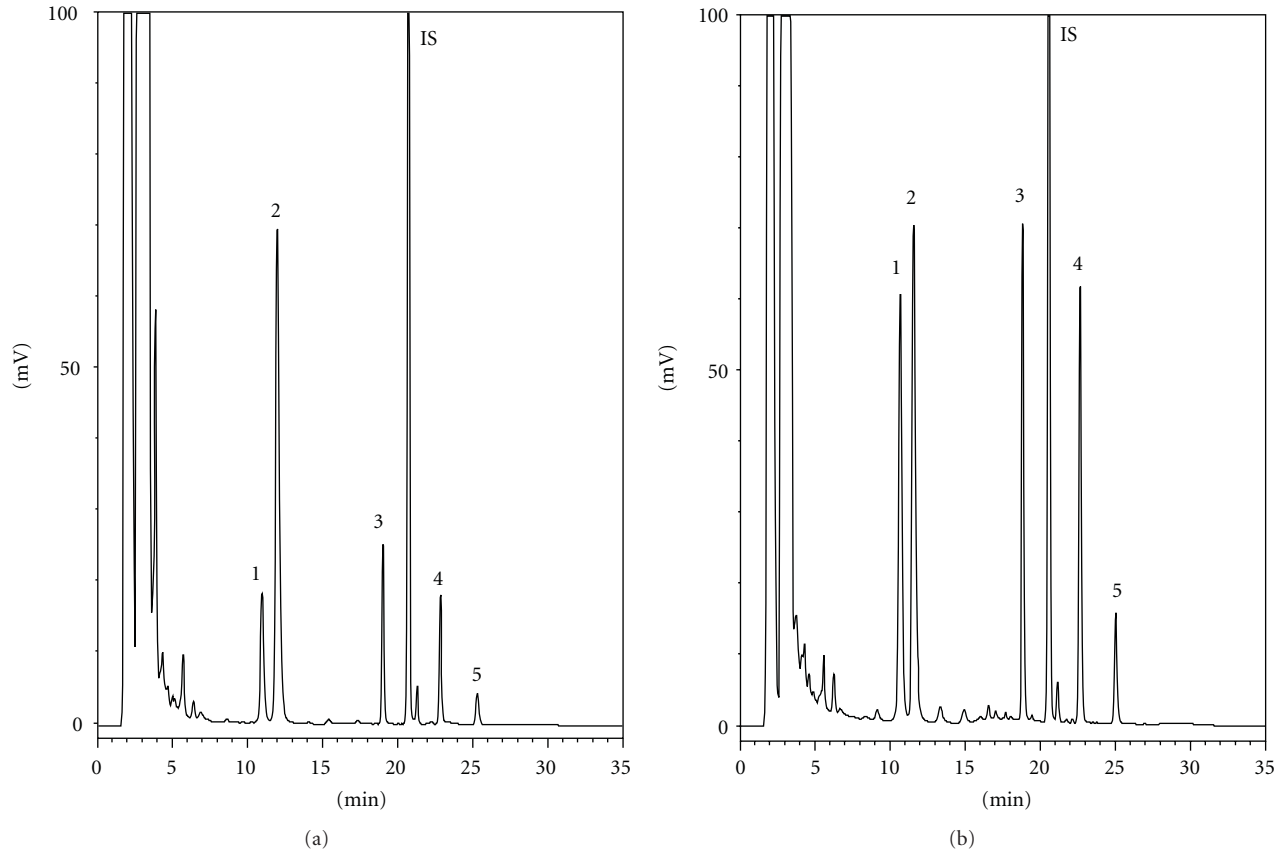

Figure 1: HPLC chromatograms of RP decoction before (a) and after (b) acid hydrolysis. 1: aloe-emodin, 2: rhein, 3: emodin, 4: chrysophanol, 5: physcion, IS: 2-methylanthraquinone.

with those in water. The mixture was extracted with 200 μL of ethyl acetate containing 5 μg/mL of propylparaben as internal standard. The ethyl acetate layer was evaporated under N_2 to dryness and reconstituted with an appropriate volume of acetonitrile and then subjected to HPLC analysis. LOQ (Limit of Quantitation) represents the lowest concentration of analyte that can be determined with acceptable precision and accuracy with coefficients of variation and relative errors below 15% and 20%, respectively. LOD (Limit of Detection) represents the lowest concentration of analyte that can be detected with S/N > 3.

2.13. Data Analysis. The areas under the serum concentration-time curves (AUC_{0-t}) of PHT, PHT-G, HPPH, and HPPH-G were calculated using noncompartment model (version 1.1, SCI software, Statistical Consulting, Inc., Apex, NC, USA). The peak serum concentrations (C_{max}) were from experimental data. One-way ANOVA with Scheffe's test was used for statistical comparison taking $P < 0.05$ as significant.

3. Results

3.1. Characterization of RP Decoction. Figure 1 shows the chromatograms of the RP decoction before and after acid hydrolysis. Quantitation results showed that the concentrations of aloe-emodin, rhein, emodin, chrysophanol, and physcion were 0.9, 2.0, 0.5, 0.4, and 0.1 nmol/mL in the decoction and 2.3, 3.8, 2.0, 1.8, and 0.7 nmol/mL in the acid hydrolysate of decoction, respectively. Accordingly, a dose of 2 g/4 mL/kg RP was found to contain 9.2, 15.2, 8.0, 7.2, and 2.8 nmol/kg of aloe emodin, rhein, emodin, and chrysophanol with the relevant glycosides, respectively.

3.2. Assay of PHT and HPPH in Serum and Method Validation. In serum assay, the calibration curves of PHT and HPPH showed good linearity in the concentration range of 0.2–50 μg/mL. The precision evaluation revealed that all coefficients of variation were below 15% and the accuracy analysis showed that the relative errors to the true concentrations were below 10%. The recoveries of PHT and HPPH from serum were 95.1–100.8% and 94.1–99.0%, respectively. The LLOQ of PHT and HPPH was 0.4 μg/mL and the LOD was 0.01 and 0.02 μg/mL, respectively.

3.3. Effect of RP on PHT Pharmacokinetics in Rats. Figure 2 depicts the mean serum concentration-time profiles of PHT, PHT-G, HPPH, and HPPH-G after oral administration of PHT alone and oral coadministration with single dose and pretreatment with seven doses of 2 g/kg of RP. The pharmacokinetic parameters of PHT, PHT-G, HPPH, and HPPH-G are listed in Table 1. Coadministration of RP with single dose of 2 g/kg significantly decreased the C_{max} of

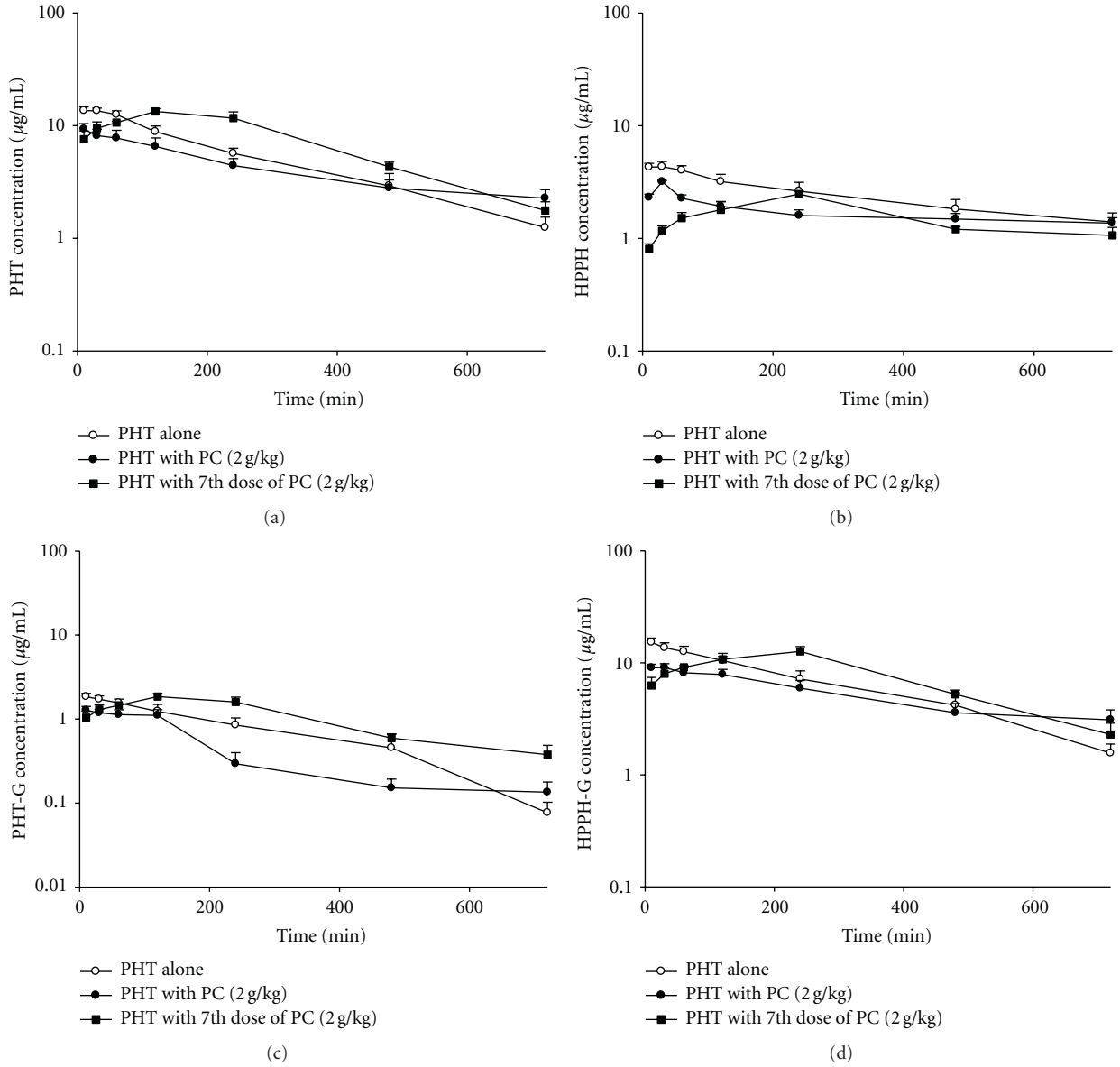

Figure 2: Mean (±S.E.) serum concentration-time profiles of PHT (a), HPPH (b), PHT-G (c), and HPPH-G (d) after oral administration of PHT alone (200 mg/kg) (∘), coadministration with single dose (•), and 7th dose of 2 g/kg (■) of RP decoction in six rats.

PHT, PHT-G, HPPH and HPPH-G by 51.0, 51.7, 43.9, and 42.5% and reduced the AUC_{0-720} by 36.9, 51.7, 30.3, and 22.8%, respectively. Pretreatment with seven doses of RP significantly decreased the C_{max} of PHT, PHT-G, HPPH, and HPPH-G by 53.1%, 65.1%, 46.3%, and 44.3% and reduced their AUC_{0-720} by 51.9%, 64.8%, 37.5% and 30.6%, respectively. In addition, the K_{10} of PHT, PHT-G HPPH, and HPPH-G were significantly decreased upon acute and chronic coadministrations of RP.

3.4. Cytotoxicity Assay. More than 90% of cells were viable at the concentrations of PHT, HPPH and RP up to 10 μM, 10 μM, and 2 mg/mL in LS 180, respectively. In addition, PHT, HPPH, and RPM at 10 μM, 10 μM, and 1.0-fold serum concentration, respectively, did not possess any noticeable cytotoxicity against MDCK II and MDCK II-MRP 2.

3.5. Transport Studies of PHT and HPPH. The effects of RP and verapamil on the intracellular accumulation of PHT in LS 180 cells are shown in Figure 3. RP at 2.0, 1.0 and 0.5 mg/mL significantly decreased the intracellular accumulation of PHT by 43.6, 37.3, and 22.9%, indicating RP concentration-dependently activated the efflux function of P-gp.

Figure 4 shows the differences of intracellular accumulation of PHT and HPPH in presence and absence of Indo in MDCK II and MDCKII-MRP 2. The results showed that the accumulations of PHT and HPPH in MDCKII

Table 1: Pharmacokinetic parameters of PHT, PHT-G, HPPH, and HPPH-G in six rats receiving oral PHT (200 mg/kg) alone and coadministration with single dose and seven doses of RP decoction (2 g/kg).

Parameters	Treatments		
	PHT alone	PHT + RP (2 g/kg)	PHT + RP (7th dose of 2 g/kg)
PHT			
C_{max}	15.7 ± 0.7[a]	7.5 ± 0.6[b]	7.3 ± 0.6[b]
		(−51.0 ± 5.1%)	(−53.1 ± 3.7%)
$AUC_{0–720}$	4261.3 ± 146.8[a]	2650.0 ± 211.1[b]	2024.9 ± 209.0[b]
		(−36.9 ± 6.6%)	(−51.9 ± 5.3%)
K_{10}	0.0039 ± 0.0002[a]	0.0028 ± 0.0003[b]	0.0025 ± 0.0002[b]
		(−27.9 ± 7.9%)	(−30.4 ± 6.2%)
PHT-G			
C_{max}	1.7 ± 0.2[a]	0.8 ± 0.1[b]	0.5 ± 0.1[b]
		(−51.7 ± 4.2%)	(−65.1 ± 10.4%)
$AUC_{0–720}$	557.2 ± 59.9[a]	232.5 ± 37.9[b]	172.5 ± 22.1[b]
		(−51.7 ± 12.1%)	(−64.8 ± 8.5%)
K_{10}	0.0033 ± 0.0003[a]	0.0019 ± 0.0002[b]	0.0023 ± 0.0003[b]
		(−51.5 ± 4.9%)	(−39.9 ± 7.3%)
HPPH			
C_{max}	4.5 ± 0.3[a]	2.5 ± 0.1[b]	2.3 ± 0.1[b]
		(−43.9 ± 4.6%)	(−46.3 ± 6.9%)
$AUC_{0–720}$	1556.0 ± 81.5[a]	1058.3 ± 45.1[b]	954.0 ± 49.8[b]
		(−30.3 ± 5.7%)	(−37.5 ± 5.0%)
K_{10}	0.0013 ± 0.0002[a]	0.0008 ± 0.0003[b]	0.0003 ± 0.0001[b]
		(−67.9 ± 13.8%)	(−76.6 ± 7.0%)
HPPH-G			
C_{max}	14.8 ± 0.7[a]	8.4 ± 0.5[b]	8.1 ± 0.5[b]
		(−42.5 ± 4.0%)	(−44.3 ± 4.2%)
$AUC_{0–720}$	4482.9 ± 114.7[a]	3430.8 ± 208.5[b]	3099.9 ± 155.0[b]
		(−22.8 ± 6.3%)	(−30.6 ± 3.7%)
K_{10}	0.0039 ± 0.0002[a]	0.0018 ± 0.0002[b]	0.0016 ± 0.0002[b]
		(−53.6 ± 3.9%)	(−59.3 ± 4.7%)

[a,b]Significant difference at $P < 0.05$ denoted by different letters.
C_{max} (μg/mL): peak serum concentration.
$AUC_{0–720}$ (μg·min/mL): areas under the curves from time zero to the last point.
K_{10}: the elimination rate (min^{-1}).
Values are means ± SE.

were higher than those in MDCK II-MRP 2. In addition, the intracellular accumulations of PHT and HPPH were significantly increased by Indo in both cell lines.

In order to mimic the molecules interacting with MRP 2 in kidney, the RPMs of rats were prepared and characterized. HPLC analysis of RPMs showed that it contained 2.3, 13.0, 4.1, and 2.0 μM of glucuronides/sulfates of aloe-emodin, rhein, emodin, chrysophanol, respectively, and 6.4 μM of rhein free form in the serum.

The effects of RPMs and Indo on the intracellular accumulation of PHT and HPPH in MDCK II-MRP 2 are shown in Figure 5. RPMs at 1-fold serum concentrations significantly increased the intracellular accumulation of PHT and HPPH by 51.7% and 46.7%. As a positive control, Indo at 200 μM significantly increased the intracellular accumulation of PHT and HPPH by 54.2% and 44.1%, respectively.

4. Discussions

Owing to the general abundance of polyphenol glycosides in plants, characterization of the RP decoction used in this study was carried out to measure the concentrations of aloe-emodin, rhein, emodin, chrysophanol, and physicon before and after acid hydrolysis. Quantitation results showed that upon acid hydrolysis the concentrations of aloe-emodin,

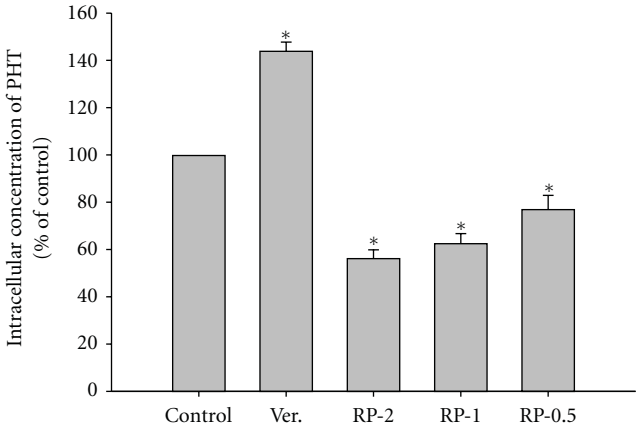

Figure 3: Effects of RP (2.0, 1.0 and 0.5 mg/mL) and verapamil (Ver, 100 μM as a positive control of P-gp inhibitor) on the accumulation of PHT in LS 180 cells. Data expressed as mean ± S.D. of four determinations. $^*P < 0.05$.

rhein, emodin, chrysophanol, and physicon increased by 416%, 85%, 345%, 402% and 367%, respectively, implying that the RP decoction contained aloe-emodin, emodin, chrysophanol, and physicon mainly in their glycoside form, whereas rhein was an exception existing more in the free form.

The assay methods of PHT and HPPH in serum and cell lysate were similar to a previously reported study but with some modifications made and they were validated in this study [17, 20]. The determination of PHT-G and HPPH-G was performed indirectly through hydrolysis with β-glucuronidase [21]. Coadministration of single dose and pretreatment with the seven doses of RP all significantly decreased the AUC and C_{max} of PHT, PHT-G, HPPH, and HPPH-G, suggesting that RP decreased the oral bioavailability of PHT. The serum profiles revealed that the early exposure of PHT was markedly decreased, inferring that the absorption of PHT was hampered. This fact suggested that acute and chronic coadministrations of RP would result in diminished efficacy of PHT.

Based on previous studies which claimed that PHT was a substrate of P-gp and CYP 2C [12, 14], it is reasonable to assume that RP may induce P-gp or CYP 2C thus resulting in the decreased absorption of PHT. However, the unaffected ratio of the AUC of HPPH plus HPPH-G to that of PHT plus PHT-G (data not shown) can be inferred that the decreased absorption of PHT cannot be attributed to the enhanced metabolism mediated by CYP 2C. Subsequently, the possible involvement of P-gp in this interaction was investigated by using LS 180 cells to measure the effect of RP on the efflux transport of PHT. The result showed a decrease in intracellular accumulation of PHT in the presence of RP which indicated that the activity of P-gp could have been induced, which might explain the decreased absorption of PHT in rats. These results could also echo previous studies reporting that overexpression of P-gp could cause a decrease in PHT levels in the rats [18, 22].

While the rats were coadministered with RP in single dose or pretreated with seven doses, the significantly decreased K_{10} of PHT, PHT-G, HPPH, and HPPH-G indicated that eliminations of both the parent form and the metabolites were inhibited in rats. It has been reported that majority of the dose of PHT was excreted as HPPH-G and only small amount was excreted as PHT-G in human urine [23, 24], thus it could be assumed that renal excretion of HPPH-G and PHT-G might also involve renal MRP 2 like PHT [25, 26]. Therefore, it was suspected that RP might decrease the renal elimination of PHT, PHT-G, HPPH, and HPPH-G through the inhibition of MRP 2.

To explore the possible involvement of MRP 2 in this interaction, transport assays of PHT and HPPH in the presence and absence of Indo, an inhibitor of MRP 2, were conducted in MDCK II and MDCK II-MRP 2. The results showed that intracellular accumulation of PHT and HPPH was lower in MDCK II-MRP 2 than the MDCK II, thus suggesting that both PHT and HPPH were substrates of MRP 2. Moreover, the intracellular accumulations of PHT and HPPH in MDCK II-MRP 2 and MDCK II significantly increased by Indo had led to the confirmation that PHT and HPPH were substrates for MRP 2. To our knowledge, this is the first study reporting that HPPH is a substrate of MRP 2. Owing to the unavailability of PHT-G and HPPH-G, whether MRP 2 was involved in the efflux of PHT-G and HPPH-G could not be determined.

Our previous pharmacokinetic study of RP indicated that glucuronides/sulfates of aloe-emodin, rhein, emodin, and chrysophanol were the major molecules in the circulation, and rhein existed in part as free form [3, 8] which were putative substrates of MRPs. Therefore, the serum metabolites of RP (RPMs) were prepared and characterized for mimicking the molecules that interacted with MRP 2 in the kidney. A transport study was subsequently carried out using RPMs to measure the effect on the transport of PHT and HPPH in MDCK II-MRP 2. The increased accumulation of PHT and HPPH in MDCK II-MRP 2 indicated that the efflux activity of MRP 2 was inhibited by RPMs. It can be proposed that the G/S of various anthraquinones and rhein free form in RPMs, existing as anions under pH 7.4 and being putative substrates of MRP 2, are the causative agents that decreased the elimination rates of PHT, PHT-G, HPPH, and HPPH-G following coadministration of RP.

Although the elimination of PHT was inhibited by RPMs, the effect of decreasing the absorption of PHT caused by RP is much stronger than that on the elimination of PHT upon observing the serum profiles in Figure 2. Therefore, an overall effect of decreased systemic exposures to PHT, PHT-G, HPPH, and HPPH-G can be mainly attributable to a significant activation of P-gp by RP. Therefore, it is predicted that the combined therapy of RP with any western medicines which are P-gp substrates, such as digoxin and cyclosporine, can result in diminished efficacy. On the contrary, if RP is coadministered with any western medicines which are MRP 2 substrates rather than P-gp substrates, the efficacy or toxicity might be increased.

In conclusion, acute and chronic coadministration of RP can significantly decrease the systemic exposure of PHT,

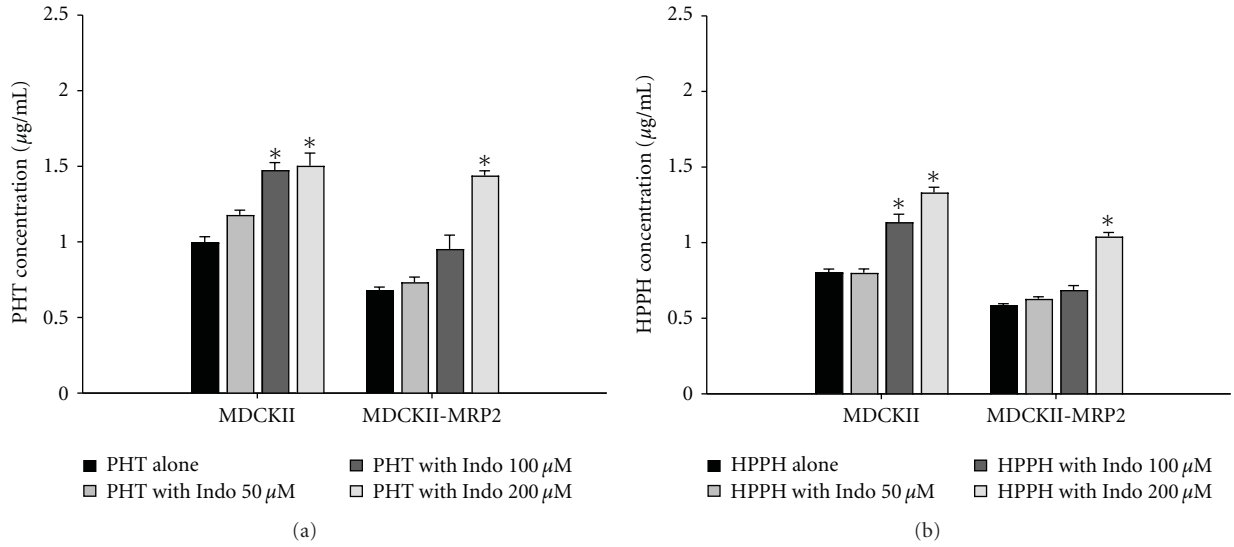

Figure 4: Effects of indomethacin (Indo) on the intracellular accumulation of PHT ((a), 10 μM) and HPPH ((b), 10 μM) in MDCKII and MDCKII-MRP 2 cells. Data expressed as mean ± S.D. of four determinations. $^*P < 0.05$.

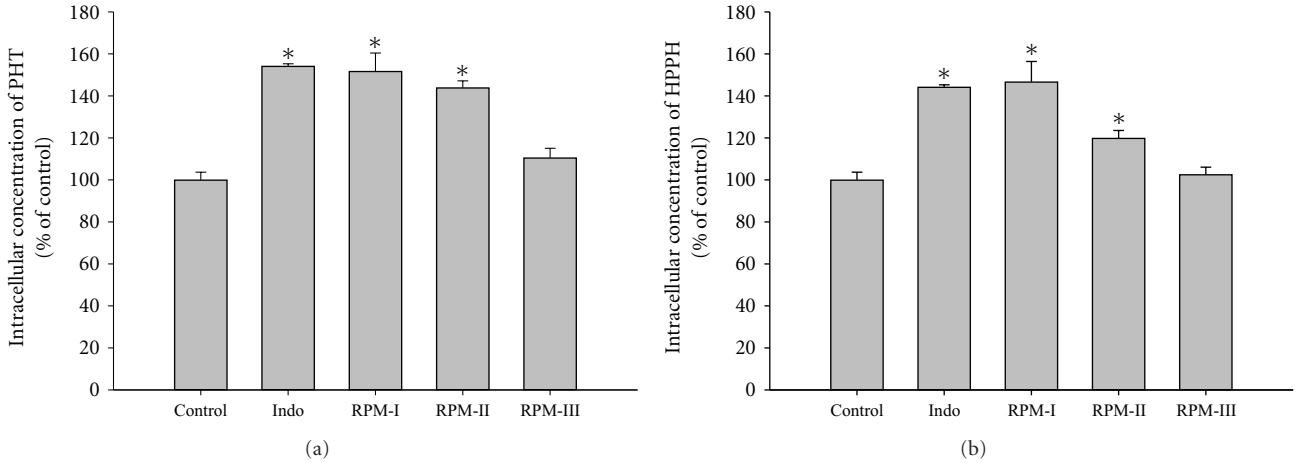

Figure 5: Effects of RP metabolites (RPMs) and indomethacin (Indo, 200 μM as a positive control of MRP 2 inhibitor) on the accumulation of PHT (a) and HPPH (b) in MDCKII-MRP2 cells. Data expressed as mean ± S.D. of five determinations. $^*P < 0.05$. RPMs-I, II, III: 1.0-, 0.5-, and 0.25-fold serum concentration, respectively (1.0-fold: containing 2.3 μM of aloe emodin G/S, 6.4 μM of rhein, 13.0 μM of rhein G/S, 4.1 μM of emodin G/S, and 2.0 μM of chrysophanol G/S).

PHT-G, HPPH, and HPPH-G in rats mainly through activation of P-gp. Therefore, the results from this investigation conclude that caution will need to be exercised when RP and PHT are used concurrently.

Acknowledgments

The work was in part supported by National Science Council, Taiwan, (NSC 99-2320-B-039-017-MY3, NSC99-2628-B-039-005-MY3) and China Medical University, Taichung, Taiwan, (CMU100-S-17, CMU100-S-05).

References

[1] M. F. Clifford, Ed., *Rhubarb: The Wondrous Drug*, Princeton University Press, Princeton, NJ, USA, 1992.

[2] J. Han, M. Ye, M. Xu et al., "Comparison of phenolic compounds of rhubarbs in the section deserticola with *Rheum palmatum* by HPLC-DAD-ESI-MSn," *Planta Medica*, vol. 74, no. 8, pp. 873–879, 2008.

[3] C. S. Shia, S. Y. Tsai, J. C. Lin et al., "Steady-state pharmacokinetics and tissue distribution of anthraquinones of Rhei Rhizoma in rats," *Journal of Ethnopharmacology*, vol. 137, no. 3, pp. 1388–1394, 2011.

[4] J. W. Gu, H. Hasuo, M. Takeya, and T. Akasu, "Effects of emodin on synaptic transmission in rat hippocampal CA1 pyramidal neurons *in vitro*," *Neuropharmacology*, vol. 49, no. 1, pp. 103–111, 2005.

[5] C. Y. Li, Y. C. Hou, P. D. Lee Chao, C. S. Shia, I. C. Hsu, and S. H. Fang, "Potential *ex vivo* immunomodulatory effects of San-Huang-Xie-Xin-Tang and its component herbs on mice and humans," *Journal of Ethnopharmacology*, vol. 127, no. 2, pp. 292–298, 2010.

[6] C. Y. Chang, H. L. Chan, H. Y. Lin et al., "Rhein induces apoptosis in human breast cancer cells," *Evidence-Based Complementary and Alternative Medicine*, vol. 2012, Article ID 952504, 8 pages, 2012.

[7] Y. C. Chang, T. Y. Lai, C. S. Yu et al., "Emodin induces apoptotic death in murine myelomonocytic leukemia WEHI-3 cells *in vitro* and enhances phagocytosis in leukemia mice *in vivo*," *Evidence-Based Complementary and Alternative Medicine*, vol. 2011, Article ID 523596, 13 pages, 2011.

[8] C. S. Shia, S. H. Juang, S. Y. Tsai et al., "Metabolism and pharmacokinetics of anthraquinones in rheum palmatum in rats and *ex vivo* antioxidant activity," *Planta Medica*, vol. 75, no. 13, pp. 1386–1392, 2009.

[9] A. Odani, Y. Hashimoto, Y. Otsuki et al., "Genetic polymorphism of the CYP2C subfamily and its effect on the pharmacokinetics of phenytoin in Japanese patients with epilepsy," *Clinical Pharmacology and Therapeutics*, vol. 62, no. 3, pp. 287–292, 1997.

[10] M. A. Falconer and S. Davidson, "Coarse features in epilepsy as a consequence of anticonvulsant therapy. Report of cases in two pairs of identical twins," *The Lancet*, vol. 2, no. 7838, pp. 1112–1114, 1973.

[11] E. B. Lefebvre, R. G. Haining, and R. F. Labbé, "Coarse facies, calvarial thickening and hyperphosphatasia associated with long-term anticonvulsant therapy," *New England Journal of Medicine*, vol. 286, no. 24, pp. 1301–1302, 1972.

[12] H. Potschka and W. Löscher, "*In vivo* evidence for P-glycoprotein-mediated transport of phenytoin at the blood-brain barrier of rats," *Epilepsia*, vol. 42, no. 10, pp. 1231–1240, 2001.

[13] H. Potschka, M. Fedrowitz, and W. Löscher, "Multidrug resistance protein MRP2 contributes to blood-brain barrier function and restricts antiepileptic drug activity," *Journal of Pharmacology and Experimental Therapeutics*, vol. 306, no. 1, pp. 124–131, 2003.

[14] M. Bajpai, L. K. Roskos, D. D. Shen, and R. H. Levy, "Roles of cytochrome P4502C9 and cytochrome P4502C19 in the stereoselective metabolism of phenytoin to its major metabolite," *Drug Metabolism and Disposition*, vol. 24, no. 12, pp. 1401–1403, 1996.

[15] T. Yasumori, L. S. Chen, Q. H. Li et al., "Human CYP2C-mediated stereoselective phenytoin hydroxylation in Japanese: difference in chiral preference of CYP2C9 and CYP2C19," *Biochemical Pharmacology*, vol. 57, no. 11, pp. 1297–1303, 1999.

[16] M. Nakajima, N. Sakata, N. Ohashi, T. Kume, and T. Yokoi, "Involvement of multiple UDP-glucuronosyltransferase 1A isoforms in glucuronidation of 5-(4′-hydroxyphenyl)-5-phenylhydantoin in human liver microsomes," *Drug Metabolism and Disposition*, vol. 30, no. 11, pp. 1250–1256, 2002.

[17] H. Yamanaka, M. Nakajima, Y. Hara et al., "Urinary excretion of phenytoin metabolites, 5-(4′-hydroxyphenyl)-5-phenylhydantoin and its O-glucuronide in humans and analysis of genetic polymorphisms of UDP-glucuronosyltransferases," *Drug Metabolism and Pharmacokinetics*, vol. 20, no. 2, pp. 135–143, 2005.

[18] E. A. van Vliet, R. van Schaik, P. M. Edelbroek et al., "Region-specific overexpression of P-glycoprotein at the blood-brain barrier affects brain uptake of phenytoin in epileptic rats," *Journal of Pharmacology and Experimental Therapeutics*, vol. 322, no. 1, pp. 141–147, 2007.

[19] M. M. Bradford, "A rapid and sensitive method for the quantitation of microgram quantities of protein utilizing the principle of protein dye binding," *Analytical Biochemistry*, vol. 72, no. 1-2, pp. 248–254, 1976.

[20] Y. Caraco, M. Muszkat, and A. J. Wood, "Phenytoin metabolic ratio: a putative marker of CYP2C9 activity *in vivo*," *Pharmacogenetics*, vol. 11, no. 7, pp. 587–596, 2001.

[21] T. Aliwarga, J. C. Cloyd, V. Goel et al., "Excretion of the principal urinary metabolites of phenytoin and absolute oral bioavailability determined by use of a stable isotope in patients with epilepsy," *Therapeutic Drug Monitoring*, vol. 33, no. 1, pp. 56–63, 2011.

[22] J. P. Bankstahl and W. Löscher, "Resistance to antiepileptic drugs and expression of P-glycoprotein in two rat models of status epilepticus," *Epilepsy Research*, vol. 82, no. 1, pp. 70–85, 2008.

[23] E. W. Maynert, "The metabolic fate of diphenylhydantoin in the dog, rat and man," *The Journal of Pharmacology and Experimental Therapeutics*, vol. 130, pp. 275–284, 1960.

[24] R. G. Smith, G. D. Daves Jr., R. K. Lynn, and N. Gerber, "Hydantoin ring glucuronidation: characterization of a new metabolite of 5,5-diphenylhydantoin in man and the rat," *Biomedical Mass Spectrometry*, vol. 4, no. 4, pp. 275–279, 1977.

[25] G. Jedlitschky, U. Hoffmann, and H. K. Kroemer, "Structure and function of the MRP2 (ABCC2) protein and its role in drug disposition," *Expert Opinion on Drug Metabolism and Toxicology*, vol. 2, no. 3, pp. 351–366, 2006.

[26] A. C. Auansakul and M. Vore, "The effect of pregnancy and estradiol-17 β treatment on the biliary transport maximum of dibromosulfophthalein, and the glucuronide conjugates of 5-phenyl-5-p-hydroxyphenyl[14C]hydantoin and [14C]morphine in the isolated perfused rat liver," *Drug Metabolism and Disposition*, vol. 10, no. 4, pp. 344–349, 1982.

Hindawi Publishing Corporation
Evidence-Based Complementary and Alternative Medicine
Volume 2012, Article ID 802625, 8 pages
doi:10.1155/2012/802625

Research Article

Bioassay-Guided Isolation of Neuroprotective Compounds from *Uncaria rhynchophylla* against Beta-Amyloid-Induced Neurotoxicity

Yan-Fang Xian,[1] Zhi-Xiu Lin,[1] Qing-Qiu Mao,[1] Zhen Hu,[1] Ming Zhao,[2] Chun-Tao Che,[2] and Siu-Po Ip[1]

[1] *School of Chinese Medicine, The Chinese University of Hong Kong, Shatin, Hong Kong*
[2] *Department of Medicinal Chemistry and Pharmacognosy, College of Pharmacy, University of Illinois at Chicago, Chicago IL 60607, USA*

Correspondence should be addressed to Zhi-Xiu Lin, linzx@cuhk.edu.hk and Siu-Po Ip, paulip@cuhk.edu.hk

Received 27 March 2012; Accepted 12 May 2012

Academic Editor: Karl Wah-Keung Tsim

Uncaria rhynchophylla is a component herb of many Chinese herbal formulae for the treatment of neurodegenerative diseases. Previous study in our laboratory has demonstrated that an ethanol extract of *Uncaria rhynchophylla* ameliorated cognitive deficits in a mouse model of Alzheimer's disease induced by D-galactose. However, the active ingredients of *Uncaria rhynchophylla* responsible for the anti-Alzheimer's disease activity have not been identified. This study aims to identify the active ingredients of *Uncaria rhynchophylla* by a bioassay-guided fractionation approach and explore the acting mechanism of these active ingredients by using a well-established cellular model of Alzheimer's disease, beta-amyloid- (Aβ-) induced neurotoxicity in PC12 cells. The results showed that six alkaloids, namely, corynoxine, corynoxine B, corynoxeine, isorhynchophylline, isocorynoxeine, and rhynchophylline were isolated from the extract of *Uncaria rhynchophylla*. Among them, rhynchophylline and isorhynchophylline significantly decreased Aβ-induced cell death, intracellular calcium overloading, and tau protein hyperphosphorylation in PC12 cells. These results suggest that rhynchophylline and isorhynchophylline are the major active ingredients responsible for the protective action of *Uncaria rhynchophylla* against Aβ-induced neuronal toxicity, and their neuroprotective effect may be mediated, at least in part, by inhibiting intracellular calcium overloading and tau protein hyperphosphorylation.

1. Introduction

Alzheimer's disease (AD), a neurodegenerative disorder characterized by a progressive loss of learning, memory, and other cognitive functions, is the most common form of dementia in the elderly. The pathological hallmarks of AD are extracellular senile plaques and intracellular neurofibrillary tangles [1]. It is well known that deposition of β-amyloid (Aβ) is a pivotal event in initiating the neuronal degeneration of AD [2]. Aβ aggregates into amyloid fibrils, which have been reported to be neurotoxic *in vitro* [3] and *in vivo* [4]. In this connection, the toxic effect of Aβ on a cultured neuronal cells can be used as a screening tool for identifying potential therapeutic agents for AD.

Current clinical treatments of AD patients use acetylcholinesterase inhibitors (AChEIs) and antagonists of *N*-methyl-D-aspartate receptors (NMDA) to slow down the progress of the deterioration of AD. However, effective approaches for delaying the progression of AD are yet to be found to date. Thus, searching for safer, better-tolerated, and effective drugs for the treatment of AD remains an important area of drug discovery.

Traditional Chinese herbal medicine has been practiced in China for thousands of years, and vast experience has been accumulated for using medicinal herbs for clinical treatment of diseases. Thus, Chinese herbal medicine may be a promising source of effective drugs for treating AD. *Uncaria rhynchophylla* has been extensively used in Chinese

herbal medicine to relieve headache, dizziness, tremors, and hypertension-induced convulsion [5–7]. In recent years, *Uncaria rhynchophylla* has been shown to be effective for inhibiting Aβ fibril formation, disassembling performed Aβ fibrils [8] and antiacetylcholinesterase [9]. Previous study in our laboratory demonstrated that an ethanol extract of *Uncaria rhynchophylla* significantly reversed cognitive deficits induced by D-galactose, a mouse model of AD [10]. Phytochemical study has shown that alkaloids, terpenoids, and flavonoids are the major chemical ingredients of *Uncaria rhynchophylla* [7]. However, the bioactive principles responsible for the protective action of *Uncaria rhynchophylla* have not been identified. The present study aims to identify the active constituents of *Uncaria rhynchophylla* using bioassay-guided fractionation. Furthermore, the acting mechanism of these active ingredients is explored by using a well-established cellular model of Alzheimer's disease, beta-amyloid- (Aβ-) induced neurotoxicity in PC12 cells.

2. Materials and Methods

2.1. Chemicals and Reagents. Nerve growth factor (NGF), 3-(4,5-dimethylthiazol-2-yl)-2,5-diphenyltetrazolium bromide (MTT), and the fragment of β-amyloid peptide ($A\beta_{25-35}$) were purchased from Sigma-Aldrich (St. Louis, MO, USA). Fura 2-AM, Dulbecco's modified Eagle's medium (DMEM), horse serum, fetal bovine serum, and a penicillin/streptomycin mixture were purchased from Gibco-Invitrogen (Grand Island, NY, USA). All other solvents and chemicals used in the study were of analytical grade.

2.2. Plant Material. The dried stem with hooks of *Uncaria rhynchophylla* was purchased from Zhixin Pharmaceutical Co., a GMP-certified supplier of Chinese medicinal herbal materials (Guangzhou, China). It was authenticated to be the dried rhizome of *Uncaria rhynchophylla* (Miq.) Miq. ex Havil. by Ms. Y. Y. Zong, School of Chinese Medicine, The Chinese University of Hong Kong, Hong Kong, where a voucher specimen (no. 091220) has been deposited.

2.3. Preparation of Aggregated $A\beta_{25-35}$. The aggregated $A\beta_{25-35}$ was prepared according to a method described previously [11]. Briefly, $A\beta_{25-35}$ was dissolved in sterile distilled water at a concentration of 1 mM and incubated at 37°C for 4 days to form the aggregation. It was stored at −20°C until use.

2.4. Extraction, Fractionation, Isolation, and Identification. *Uncaria rhynchophylla* (1 kg) was macerated in 6 L of 70% aqueous ethanol for 24 h at room temperature and then refluxed for 30 min. The extraction was repeated twice. The pooled fractions were concentrated using a rotary evaporator at reduced pressure at 40°C to yield 140 g of extract (UR-E). The extract was resuspended in water and then transferred into a separatory funnel. The solution was partitioned with ethyl acetate and 1-butanol successively to obtain the ethyl acetate-soluble fraction (UR-E-EA, 43 g), the 1-butanol-soluble fraction (UR-E-B, 28 g), and the water-soluble fraction (UR-E-W, 67.5 g), respectively. The UR-E-B was further separated by column chromatography on a Diaion HP-20 column eluted with H_2O-MeOH (100 : 0, 80 : 20, 70 : 30, 60 : 40, 40 : 60, 30 : 70, 20 : 80, 10 : 90, and 0 : 100) and acetone, successively, to yield 10 major fractions (UR-E-B-Fr. 1–10). The fraction eluted by H_2O/MeOH (30 : 70) (UR-E-B-Fr. 6) was further separated by a semipreparative HPLC column (Alltima C18 column, 10 × 250 mm, 5 μm) and eluted with 0.01 mmol/L triethylamine in 80% (v/v) aqueous methanol at a flow rate of 3 mL/min to obtain four fractions (UR-E-B-Fr. 6–1 to 4). UR-E-B-Fr. 6–2 was then separated by a semipreparative HPLC column and eluted with 0.01 mmol/L triethylamine in 70% (v/v) aqueous methanol at a flow rate of 2 mL/min to obtain corynoxine (20 mg) and corynoxine B (20 mg). Corynoxeine (63 mg), isorhynchophylline (50 mg), isocorynoxeine (138 mg), and rhynchophylline (100 mg) were purified from UR-E-B-Fr. 6–3 using the semipreparative HPLC column under the following condition: mobile phase, 0.01 mmol/L triethylamine in 70% (v/v) aqueous methanol; flow rate, 3.0 mL/min.

The structures of corynoxine, corynoxine B, corynoxeine, isorhynchophylline, isocorynoxeine, and rhynchophylline were identified by comparing their ^{1}H, ^{13}C NMR spectroscopic data (Bruker NMR spectrometer, 400 MHz) with published data [12–16].

2.5. Cell Culture and Drug Treatment. Rat pheochromocytoma cells (PC12 cells) were obtained from the American Type Culture Collection (Rockville, MD, USA) and cultured in DMEM medium supplemented with penicillin (100 unit/mL), streptomycin (100 μg/mL), 6% fetal bovine serum, and 6% horse serum at 37°C in humidified atmosphere of 95% air and 5% CO_2. PC12 cells were seeded on poly-D-lysine-coated 96 wells (Coring Incorporated, USA) at a density of 2×10^4 cells/well and allowed to adhere for 24 h at 37°C with the culture medium. PC12 cells were differentiated with 50 ng/mL NGF in serum-free DMEM for 3 days [17]. Thereafter, the culture medium was replaced by fresh serum-free DMEM (without NGF) with or without different concentrations of drugs for 2 h. Then 20 μM of $A\beta_{25-35}$ was added to the cells and incubated for another 24 h. The extracts and isolated compounds were reconstituted in DMSO to produce respective stock solutions and then diluted with culture medium to various concentrations for cell culture experiments. The final DMSO concentration in each sample was less than 0.1%.

2.6. Cell Viability Assay. Cell viability was measured by MTT method as described previously [11]. Briefly, after drug treatment, 20 μL of MTT solution (final concentration, 1 mg/mL) was added into each well, and the cells were incubated at 37°C for 4 h. The culture medium was removed, and the formazan crystals were dissolved with 150 μL of DMSO. The optical density of each well was measured using a microplate reader (FLUOstar OPTIMA, BMG Labtech, Germany) at 570 nm. Cell viability was expressed as percentage of nontreated control.

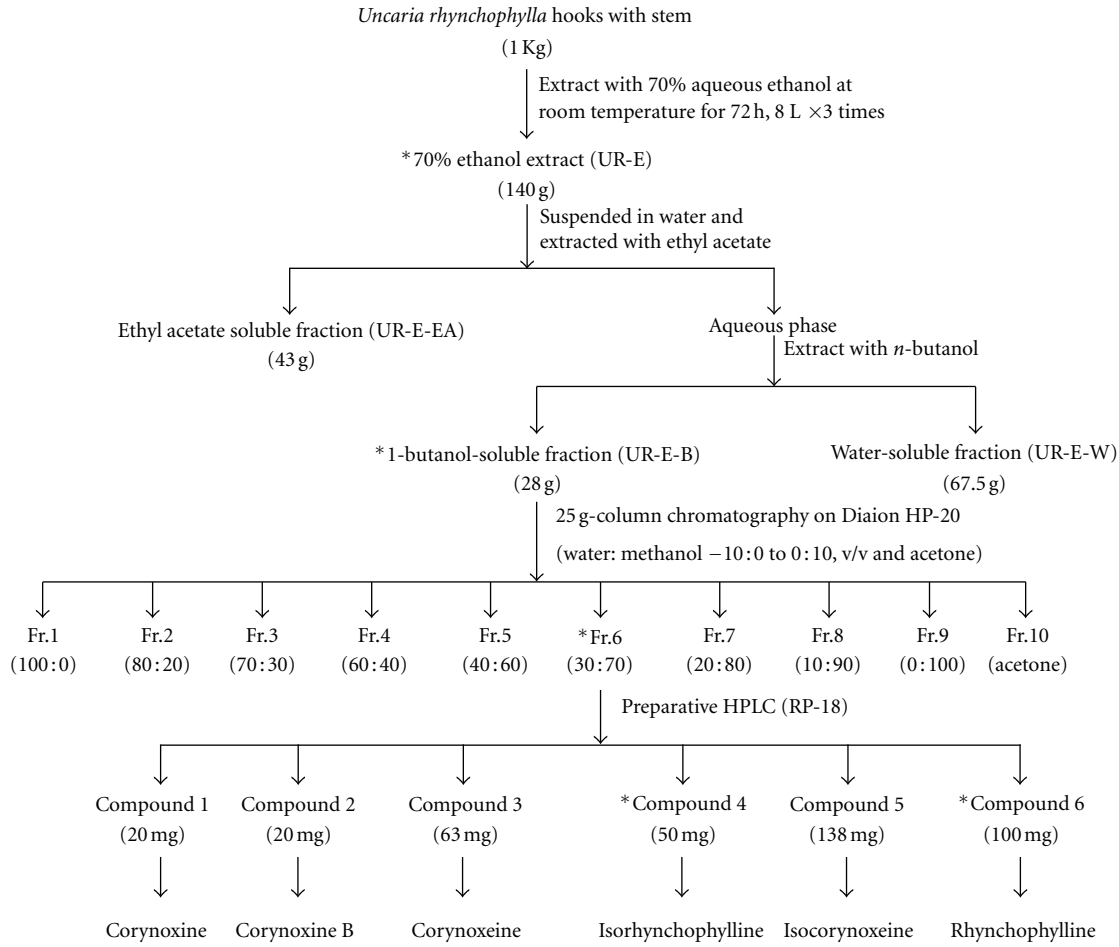

Figure 1: Extraction scheme for the isolation of the six alkaloids from *Uncaria rhynchophylla*. * Biologically active fractions or compounds.

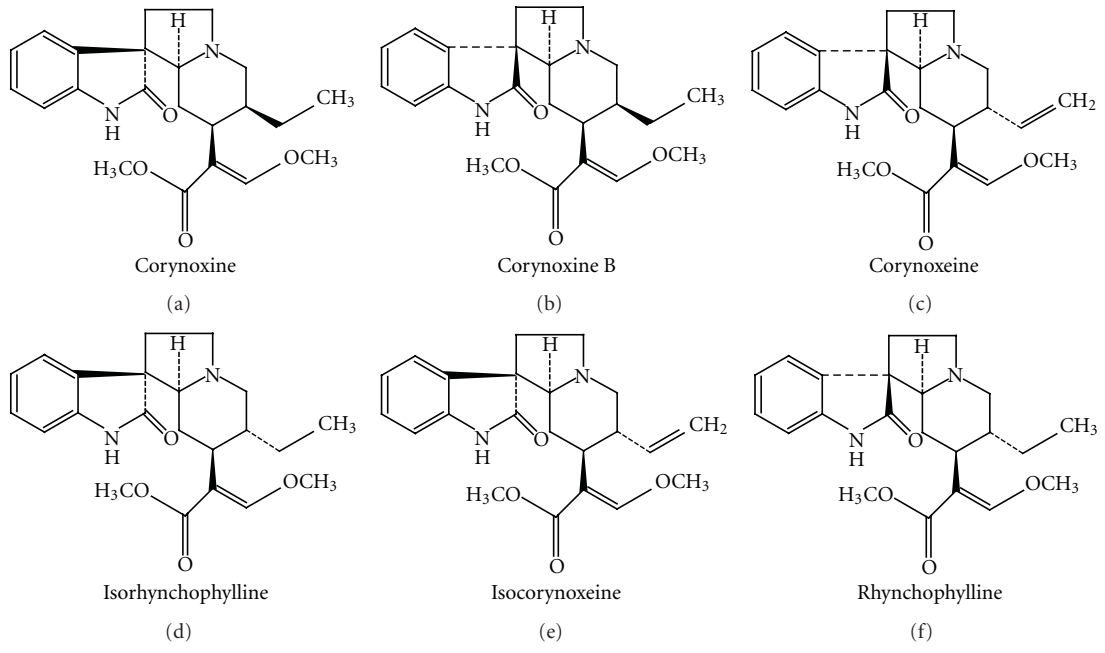

Figure 2: Chemical structures of the six alkaloids isolated from *Uncaria rhynchophylla*.

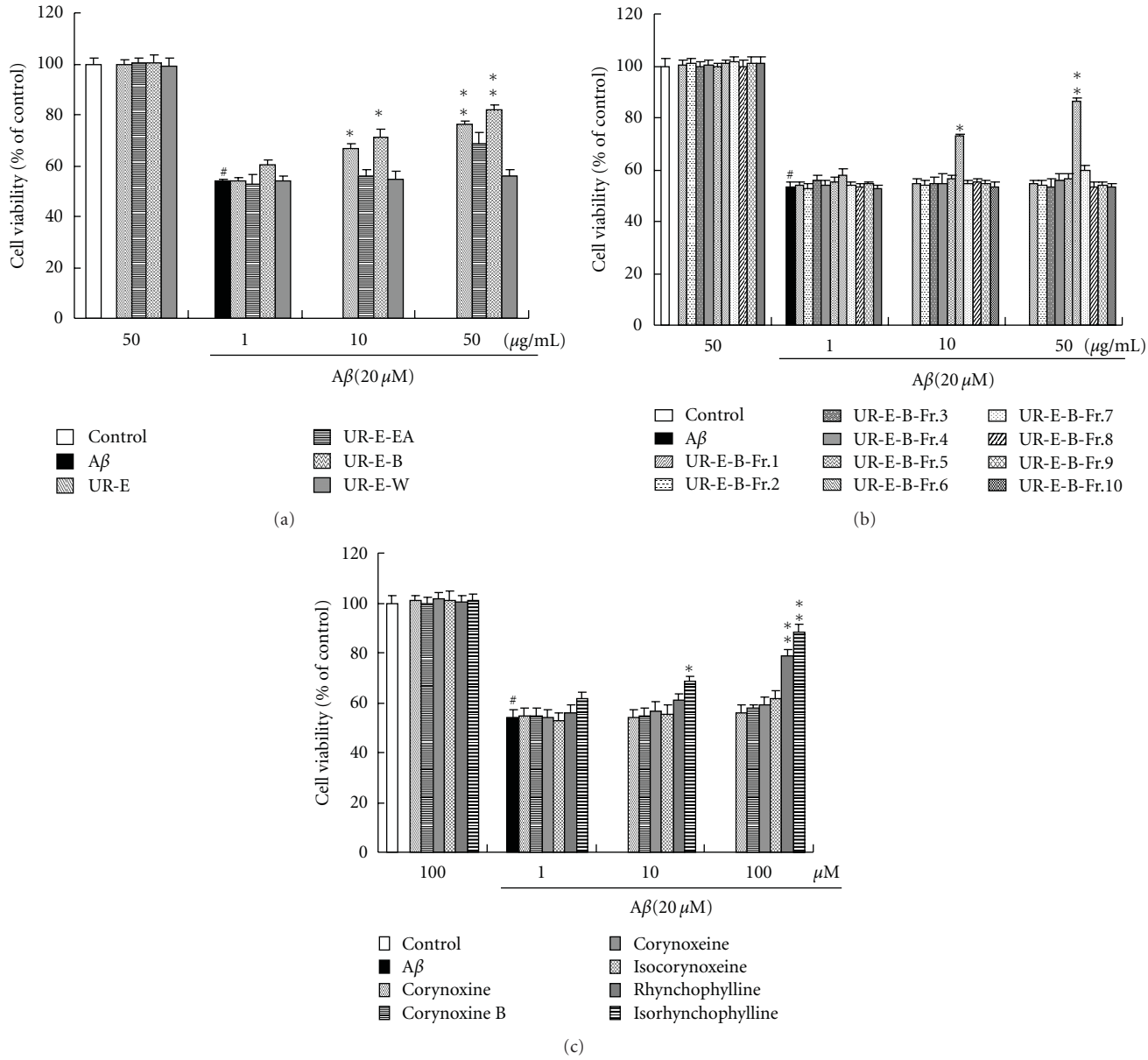

Figure 3: Effect of different extracts (a), fractions (b), and isolated compounds (c) from *Uncaria rhynchophylla* on cell viability in Aβ_{25-35}-treated PC12 cells. Values given are the mean ± SEM ($n = 6$). $^{\#}P < 0.01$ compared with the control group; $^{*}P < 0.05$ and $^{**}P < 0.01$ compared with the Aβ_{25-35}-treated control.

2.7. Measurement of Intracellular Calcium Concentration. The concentration of intracellular calcium was determined by a method described previously [18]. Briefly, PC12 cells were differentiated with NGF for 3 days. The cells were pretreated with rhynchophylline (100 μM) or rhynchophylline (100 μM) for 2 hours and then treated with 20 μM of Aβ_{25-35} for 24 hours. At the end of the treatment, the cells were collected and incubated with the culture medium containing 5 μM Fura-2/AM at 37°C for 50 min. Subsequently, the cells were washed twice with HBSS and resuspended in HBSS solution containing 0.2% bovine serum albumin. The intracellular calcium concentration was determined by setting excitation wavelengths at 340 nm and 380 nm; emission wavelength at 510 nm, using a fluorescence spectrophotometer (Shimadzu, RF-5301, Japan). The concentration of intracellular calcium was expressed as percentage of nontreated control.

2.8. Western Blotting Analysis. The PC12 cells were seeded onto 100 mm^2 dish at 5×1^6 cells/dish. The cells were washed twice with D-Hanks solution after drug treatment. The cells were harvested and lysed with lysis buffer. Protein samples were separated by SDS-PAGE for 2 h at 80 V. The separated proteins were transferred to PVD membranes using a transblotting apparatus (Bio-Rad Laboratories, USA) for 30 min at 15 V. The membranes were blocked with 5% (w/v) nonfat

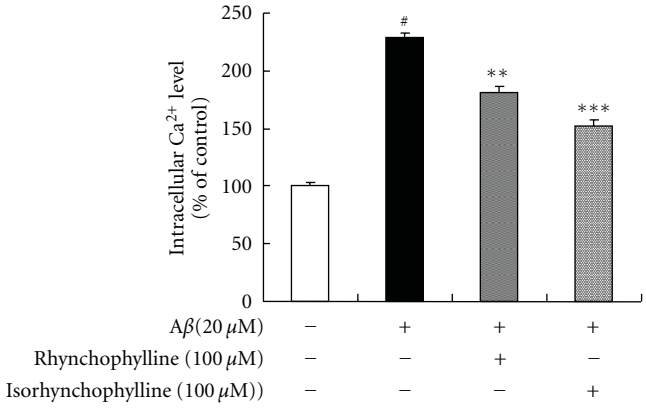

FIGURE 4: Effect of rhynchophylline and isorhynchophylline on intracellular calcium level in Aβ_{25-35}-treated PC12 cells. Values given are the mean ± SEM ($n = 6$). $^{\#}P < 0.01$ compared with the control group; $^{*}P < 0.05$ and $^{**}P < 0.01$ compared with the Aβ_{25-35}-treated control.

milk in TBS-T (Tris-buffer saline containing 0.1% Tween-20) at room temperature for 2 h and subsequently incubated at 4°C overnight with appropriate amount of primary antibody against Tau, p-Tau (Ser 396), p-Tau (Ser 404), p-Tau (Thr 205), and β-actin (Santa Cruz Biotechnology Inc., USA). Then the membrane was washed with TBS-T for three times, and probed with horseradish peroxidase-conjugated secondary antibody at room temperature for 1 h. To verify equal loading of samples, the membranes were incubated with monoclonal antibody β-actin, followed by a horseradish peroxidase-conjugated goat anti-mouse IgG. The membrane again was washed with TBS-T for three times and finally, the protein bands were visualized by the ECL western blotting detection reagents (Amersham Biosciences, Buckinghamshire, UK). The intensity of each band was analyzed using Image J software (NIH Image, Bethesda, MD, USA).

2.9. Statistical Analysis. Data were expressed as mean ± SEM. Multiple group comparisons were performed using one-way analysis of variance (ANOVA) followed by Dunnett's test to detect intergroup differences. GraphPad Prism software was used to perform the statistical analysis (Version 4.0; GraphPad Software Inc., San Diego, CA). A difference was considered statistically significant if the P value was less than 0.05.

3. Results

3.1. Isolation and Structural Determination of the Isolated Compounds. Figure 1 schematically depicted the extraction procedure leading to the isolation of the pure compounds. The structures of these compounds were identified as corynoxine, corynoxine B, corynoxeine, isorhynchophylline, isocorynoxeine, and rhynchophylline, respectively, based on the detailed interpretation of their ^{1}H, ^{13}C NMR spectroscopic data. The chemical structures of these isolated alkaloid compounds were shown in Figure 2.

3.2. Effect of Different Fractions and Isolated Compounds on Aβ_{25-35}-Induced Cells Death in PC12. As shown in Figures 3(a) and 3(b), treating the cells with 20 μM of Aβ_{25-35} for 24 h caused a significant decrease in cell viability (54% of the control). Treating PC12 cells with different fractions (50 μg/mL) or isolated compounds (100 μM) from *Uncaria rhynchophylla* had no effect on cell viability as compared to the control group (Figures 3(a)–3(c)). Pretreatment of the cells with UR-E, UR-E-B, and UR-E-B-Fr.6 (10 and 50 μg/mL) significantly increased cell viability when compared with Aβ_{25-35}-treated control, while other fractions from *Uncaria rhynchophylla* had no effect on cell viability in Aβ_{25-35}-treated PC12 cells. UR-E-B fraction elicited more effective protection against Aβ_{25-35}-induced cell death in PC12 cells when compared with UR-E, UR-E-EA, and UR-E-W fractions. Among these isolated compounds, only rhynchophylline and isorhynchophylline significantly increased the cell viability in Aβ_{25-35}-treated PC12 cells (Figure 3(c)), suggesting that rhynchophylline and isorhynchophylline may be the key active components of *Uncaria rhynchophylla*.

3.3. Effect of Rhynchophylline and Isorhynchophylline on Intracellular Calcium Concentration in Aβ_{25-35}-Treated PC12 Cells. As shown in Figure 4, treating PC12 cells with 20 μM Aβ_{25-35} for 24 h caused a significant increase in the intracellular calcium level (230% of the control), while pretreating the cells with rhynchophylline and isorhynchophylline (100 μM) significantly decreased the intracellular calcium level in Aβ_{25-35}-treated PC12 cells.

3.4. Effect of Rhynchophylline and Isorhynchophylline on Tau Hyperphosphorylation in Aβ_{25-35}-Treated PC12 Cells. As shown in Figure 5, tau protein hyperphosphorylation at Thr 205, Ser 396, and Ser 404 sites was significantly increased (144%, 160%, and 176% of the control, resp.) when treating the cells with 20 μM Aβ_{25-35} for 24 h. However, phosphorylation of tau protein was significantly inhibited by pretreating the cells with rhynchophylline and isorhynchophylline (100 μM) for 2 h. Meanwhile, the total tau protein did not change significantly for all treatments.

4. Discussion

In Chinese herbal medicine, *Uncaria rhynchophylla* is classified as a liver-pacifying and wind-extinguishing herb and is commonly used for treating central nervous system-related symptoms such as tremor, seizure, and epilepsy [19]. Although the neuroprotective effect of *Uncaria rhynchophylla* has been well studied [20–22], this is the first evidence to report for the identification of active anti-AD ingredients from *Uncaria rhynchophylla* by using the bioassay-guided fractionation approach. Six alkaloid compounds including corynoxine, corynoxine B, corynoxeine, isorhynchophylline, isocorynoxeine, and rhynchophylline were isolated and

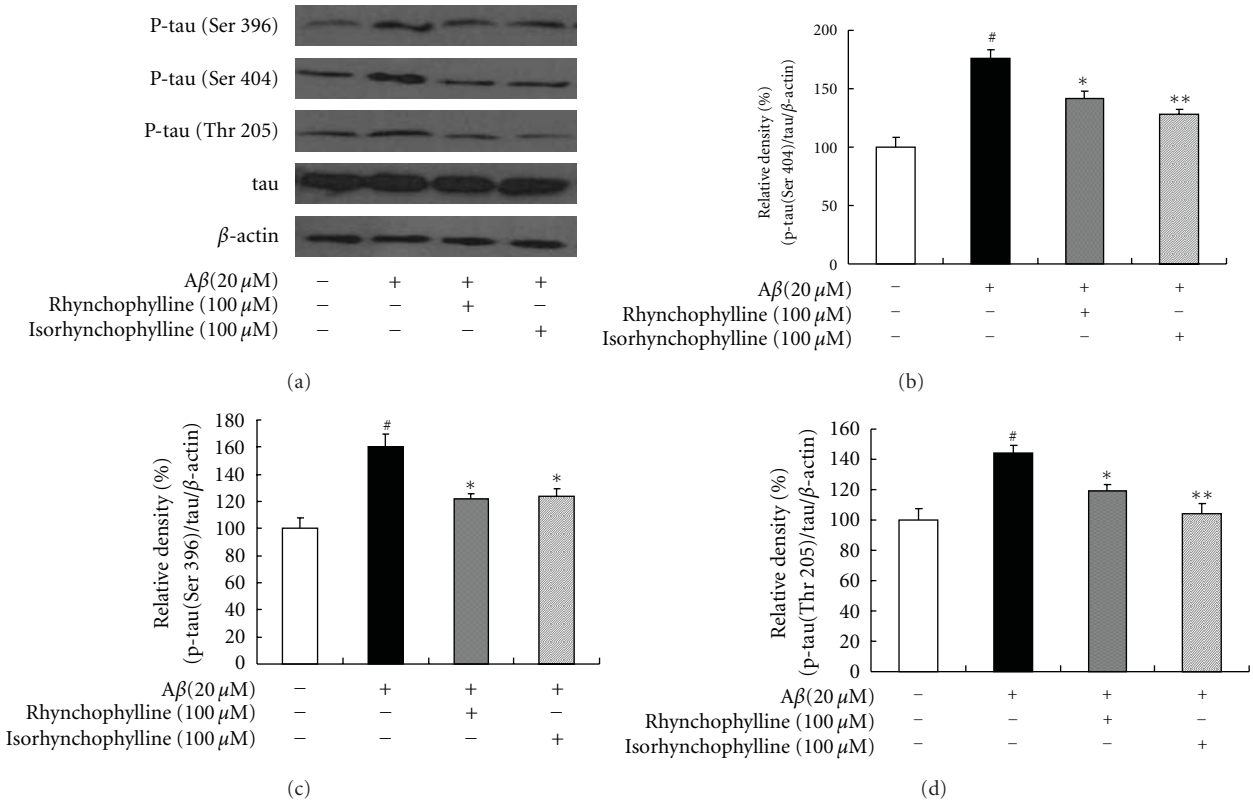

Figure 5: Effect of rhynchophylline and isorhynchophylline on tau protein hyperphosphorylation in Aβ_{25-35}-treated PC12 cells. The tau protein hyperphosphorylation was assessed by measuring the phosphorylated tau protein (at Thr 205, Ser 396, and Ser 404 sites) and total tau. Values given are the mean ± SEM ($n = 3$). $^{\#}P < 0.01$ compared with the control group; $^{*}P < 0.05$ and $^{**}P < 0.01$ compared with the Aβ_{25-35}-treated control.

characterized from the *Uncaria rhynchophylla*. Among these compounds, only rhynchophylline and isorhynchophylline, the major tetracyclic oxindole alkaloids present in *Uncaria rhynchophylla* [23], significantly attenuated Aβ_{25-35}-induced cell death, the intracellular calcium overload, and tau protein hyperphosphorylation in PC12 cell. Recently, the protective effects of rhynchophylline and isorhynchophylline on different models of neurotoxicity have been described [11, 23, 24]. Based on these findings, rhynchophylline and isorhynchophylline may be the major active ingredients of *Uncaria rhynchophylla* for its anti-AD activity.

The intracellular calcium concentration plays a critical role in the neuron development. Recent researches have revealed that the neurotoxicity induced by Aβ is mediated by the overloading of intracellular calcium in primary neurons such as hippocampal neurons [25] and cortical neurons [26]. In addition, the accentuation of the intracellular calcium has been considered as one of the activating pathways for Aβ-induced neurotoxicity [27]. Therefore, the blockage of intracellular calcium overloading might provide neuroprotection against Aβ-induced cell death in PC12 cells. Our finding indicated that treating PC12 cells with Aβ_{25-35} significantly increased intracellular calcium levels, whereas pretreating the cells with rhynchophylline and isorhynchophylline was able to inhibit the intracellular calcium influx which may contribute to the neuroprotective effect of rhynchophylline and isorhynchophylline.

Continuous calcium influx can induce the phosphorylation of tau protein [28]. Neurofibrillary tangles are intracellular aggregates of hyperphosphorylated tau protein which is commonly known as a primary pathological hallmark of AD. It has been reported that hyperphosphorylation of tau protein is an essential element for Aβ-induced neurotoxicity [29]. Upon Aβ stimulation, hyperphosphorylation of tau protein is significantly increased at the AD-related epitope and paired helical filament, resulting in a cytoskeletal destabilization, memory dysfunction, and death of the neurons [30, 31]. It has been suggested that tau phosphorylation is the limiting factor in Aβ-induced cell death [32]. In addition, it has been reported that tau hyperphosphorylations is increased significantly in postmortem brain tissues of AD patients [33]. Thus, pharmaceutical agents that can inhibit Aβ-induced tau phosphorylation are potential candidates for the effective treatment of AD. In this study, Aβ was found to cause a marked elevation of tau protein hyperphosphorylation in PC12 cells, while pretreating the cells with rhynchophylline and isorhynchophylline significantly decreased the level of tau hyperphosphorylation. The results suggest that the inhibition of tau protein hyperphosphorylation rhynchophylline and isorhynchophylline may be

one of the acting mechanisms for the protective effect of rhynchophylline and isorhynchophylline against Aβ-induced neurotoxicity.

5. Conclusions

In summary, our results demonstrated that rhynchophylline and isorhynchophylline significantly decreased $A\beta_{25-35}$-induced cell death, calcium overloading, and tau protein hyperphosphorylation in PC12 cells, suggesting that rhynchophylline and isorhynchophylline may be the major active ingredients of *Uncaria rhynchophylla* for the treatment of AD, and their neuroprotective effect may be mediated, at least in part, by inhibition of intracellular calcium overloading and tau protein hyperphosphorylation. Further investigation on the potential use of rhynchophylline and isorhynchophylline in animal model of AD is warranted.

Acknowledgment

This study was supported by a Direct Grant for Research from The Chinese University of Hong Kong.

References

[1] A. D. Dayan, "Quantitative histological studies on the aged human brain—II. Senile plaques and neurofibrillary tangles in senile dementia (with an appendix on their occurrence in cases of carcinoma)," *Acta Neuropathologica*, vol. 16, no. 2, pp. 95–102, 1970.

[2] J. Hardy and D. J. Selkoe, "The amyloid hypothesis of Alzheimer's disease: progress and problems on the road to therapeutics," *Science*, vol. 297, no. 5580, pp. 353–356, 2002.

[3] W. H. Zheng, S. Bastianetto, F. Mennicken, W. Ma, and S. Kar, "Amyloid β peptide induces tau phosphorylation and loss of cholinergic neurons in rat primary septal cultures," *Neuroscience*, vol. 115, no. 1, pp. 201–211, 2002.

[4] Y. Peng, C. Xing, S. Xu et al., "L-3-n-butylphthalide improves cognitive impairment induced by intracerebroventricular infusion of amyloid-β peptide in rats," *European Journal of Pharmacology*, vol. 621, no. 1–3, pp. 38–45, 2009.

[5] C. L. Hsieh, M. F. Chen, T. C. Li et al., "Anticonvulsant effect of *Uncaria rhynchophylla* (Miq) Jack, in rats with kainic acid-induced epileptic seizure," *American Journal of Chinese Medicine*, vol. 27, no. 2, pp. 257–264, 1999.

[6] C. L. Hsieh, N. Y. Tang, S. Y. Chiang, C. T. Hsieh, and L. Jaung-Geng, "Anticonvulsive and free radical scavenging actions of two herbs, *Uncaria rhynchophylla* (Miq) Jack and Gastrodia elata Bl., in kainic acid-treated rats," *Life Sciences*, vol. 65, no. 20, pp. 2071–2082, 1999.

[7] K. Endo, Y. Oshima, and H. Kikuchi, "Hypotensive principles of Uncaria hooks," *Planta Medica*, vol. 49, no. 3, pp. 188–190, 1983.

[8] H. Fujiwara, K. Iwasaki, K. Furukawa et al., "*Uncaria rhynchophylla*, a Chinese medicinal herb, has potent antiaggregation effects on Alzheimer's β-amyloid proteins," *Journal of Neuroscience Research*, vol. 84, no. 2, pp. 427–433, 2006.

[9] H. Q. Lin, M. T. Ho, L. S. Lau, K. K. Wong, P. C. Shaw, and D. C. C. Wan, "Anti-acetylcholinesterase activities of traditional Chinese medicine for treating Alzheimer's disease," *Chemico-Biological Interactions*, vol. 175, no. 1–3, pp. 352–354, 2008.

[10] Y. F. Xian, Z. X. Lin, M. Zhao, Q. Q. Mao, S. P. Ip, and C. T. Che, "*Uncaria rhynchophylla* ameliorates cognitive deficits induced by D-galactose in mice," *Planta Medica*, vol. 77, no. 18, pp. 1977–1983, 2011.

[11] Y. F. Xian, Z. X. Lin, Q. Q. Mao, S. P. Ip, Z. R. Su, and X. P. Lai, "Protective effect of isorhynchophylline against β-amyloid-induced neurotoxicity in PC12 cells," *Cellular and Molecular Neurobiology*, vol. 32, no. 3, pp. 353–360, 2012.

[12] J. Zhang, C. J. Yang, and D. G. Wu, "Studies on the chemical constituents of *Uncaria rhynchophylla* (Miq) Jack. (II)," *Zhong Cao Yao*, vol. 29, no. 10, pp. 649–651, 1998.

[13] T. Nozoye, Y. Shibanuma, and A. Shigehisa, "Uncaria alkaloids. XXI. Separation of rhynchophylline and corynoxeine (Japanese)," *Yakugaku Zasshi*, vol. 95, no. 6, pp. 758–759, 1975.

[14] J. Haginiwa, S. Sakai, and N. Aimi, "Studies of plants containing indole alkaloids. (II). The alkaloids of *Uncaria rhynchophylla* Miq," *Yakugaku Zasshi*, vol. 93, no. 4, pp. 448–452, 1973.

[15] P. J. Houghton and E. J. Shellard, "The Mitragyna species of Asia. XXVIII. The alkaloidal pattern in Mitragyna rotundifolia from Burma," *Planta Medica*, vol. 26, no. 2, pp. 104–112, 1974.

[16] T. Nozoye, "Studies on uncaria alkaloid. XX. Structure of rhynchophylline. 5. Structure of rhynchophylline and isorhynchophylline," *Chemical & Pharmaceutical Bulletin*, vol. 6, no. 3, pp. 309–312, 1958.

[17] C. P. Hoi, Y. P. Ho, L. Baum, and A. H. L. Chow, "Neuroprotective effect of honokiol and magnolol, compounds from Magnolia officinalis, on beta-amyloid-induced toxicity in PC12 cells," *Phytotherapy Research*, vol. 24, no. 10, pp. 1538–1542, 2010.

[18] A. Berts and K. P. Minneman, "Tyrosine kinase inhibitors and Ca^{2+} signaling: direct interactions with fura-2," *European Journal of Pharmacology*, vol. 389, no. 1, pp. 35–40, 2000.

[19] J. S. Shim, H. G. Kim, M. S. Ju, J. G. Choi, S. Y. Jeong, and M. S. Oh, "Effects of the hook of *Uncaria rhynchophylla* on neurotoxicity in the 6-hydroxydopamine model of Parkinson's disease," *Journal of Ethnopharmacology*, vol. 126, no. 2, pp. 361–365, 2009.

[20] W. Liu, Z. Q. Zhang, X. M. Zhao, and Y. S. Gao, "Protective effect of *Uncaria rhynchophylla* total alkaloids pretreatment on hippocampal neurons after acute hypoxia," *Zhongguo Zhongyao Zazhi*, vol. 31, no. 9, pp. 763–765, 2006.

[21] K. Suk, S. Y. Kim, K. Leem et al., "Neuroprotection by methanol extract of *Uncaria rhynchophylla* against global cerebral ischemia in rats," *Life Sciences*, vol. 70, no. 21, pp. 2467–2480, 2002.

[22] Z. Kawakami, H. Kanno, Y. Ikarashi, and Y. Kase, "Yokukansan, a kampo medicine, protects against glutamate cytotoxicity due to oxidative stress in PC12 cells," *Journal of Ethnopharmacology*, vol. 134, no. 1, pp. 74–81, 2011.

[23] D. Yuan, B. Ma, J. Y. Yang et al., "Anti-inflammatory effects of rhynchophylline and isorhynchophylline in mouse N9 microglial cells and the molecular mechanism," *International Immunopharmacology*, vol. 9, no. 13-14, pp. 1549–1554, 2009.

[24] H. J. Lu, J. Q. Tan, S. S. Durairajan et al., "Isorhynchophylline, a natural alkaloid, promotes the degradation of alpha-synuclein in neuronal cells via inducing autophagy," *Autophagy*, vol. 8, no. 1, pp. 98–108, 2012.

[25] B. L. Kelly and A. Ferreira, "β-amyloid-induced dynamin 1 degradation is mediated by N-methyl-D-aspartate receptors in hippocampal neurons," *Journal of Biological Chemistry*, vol. 281, no. 38, pp. 28079–28089, 2006.

[26] J. T. T. Zhu, R. C. Y. Choi, H. Q. Xie et al., "Hibifolin, a flavonol glycoside, prevents β-amyloid-induced neurotoxicity

in cultured cortical neurons," *Neuroscience Letters*, vol. 461, no. 2, pp. 172–176, 2009.

[27] D. Sul, H. S. Kim, D. Lee, S. S. Joo, K. W. Hwang, and S. Y. Park, "Protective effect of caffeic acid against beta-amyloid-induced neurotoxicity by the inhibition of calcium influx and tau phosphorylation," *Life Sciences*, vol. 84, no. 9-10, pp. 257–262, 2009.

[28] M. J. Berridge, P. Lipp, and M. D. Bootman, "The calcium entry pas de deux," *Science*, vol. 287, no. 5458, pp. 1604–1605, 2000.

[29] M. Rapoport, H. N. Dawson, L. I. Binder, M. P. Vitek, and A. Ferreira, "Tau is essential to β-amyloid-induced neurotoxicity," *Proceedings of the National Academy of Sciences of the United States of America*, vol. 99, no. 9, pp. 6364–6369, 2002.

[30] F. M. LaFerla and S. Oddo, "Alzheimer's disease: Aβ, tau and synaptic dysfunction," *Trends in Molecular Medicine*, vol. 11, no. 4, pp. 170–176, 2005.

[31] M. G. Spillantini and M. Goedert, "Tau protein pathology in neurodegenerative diseases," *Trends in Neurosciences*, vol. 21, no. 10, pp. 428–433, 1998.

[32] J. Leschik, A. Welzel, C. Weissmann, A. Eckert, and R. Brandt, "Inverse and distinct modulation of tau-dependent neurodegeneration by presenilin 1 and amyloid-β in cultured cortical neurons: evidence that tau phosphorylation is the limiting factor in amyloid-β-induced cell death," *Journal of Neurochemistry*, vol. 101, no. 5, pp. 1303–1315, 2007.

[33] X. W. Zhou, X. Li, C. Bjorkdahl et al., "Assessments of the accumulation severities of amyloid β-protein and hyperphosphorylated tau in the medial temporal cortex of control and Alzheimer's brains," *Neurobiology of Disease*, vol. 22, no. 3, pp. 657–668, 2006.

Hindawi Publishing Corporation
Evidence-Based Complementary and Alternative Medicine
Volume 2012, Article ID 278273, 11 pages
doi:10.1155/2012/278273

Research Article

Isorhamnetin, A Flavonol Aglycone from *Ginkgo biloba* L., Induces Neuronal Differentiation of Cultured PC12 Cells: Potentiating the Effect of Nerve Growth Factor

Sherry L. Xu, Roy C. Y. Choi, Kevin Y. Zhu, Ka-Wing Leung, Ava J. Y. Guo, Dan Bi, Hong Xu, David T. W. Lau, Tina T. X. Dong, and Karl W. K. Tsim

Division of Life Science and Center for Chinese Medicine, The Hong Kong University of Science and Technology, Clear Water Bay, Kowloon, Hong Kong

Correspondence should be addressed to Karl W. K. Tsim, botsim@ust.hk

Received 6 March 2012; Accepted 11 April 2012

Academic Editor: Paul Siu-Po Ip

Flavonoids, a group of compounds mainly derived from vegetables and herbal medicines, share a chemical resemblance to estrogen, and indeed some of which have been used as estrogen substitutes. In searching for possible functions of flavonoids, the neuroprotective effect in brain could lead to novel treatment, or prevention, for neurodegenerative diseases. Here, different subclasses of flavonoids were analyzed for its inductive role in neurite outgrowth of cultured PC12 cells. Amongst the tested flavonoids, a flavonol aglycone, isorhamnetin that was isolated mainly from the leaves of *Ginkgo biloba* L. showed robust induction in the expression of neurofilament, a protein marker for neurite outgrowth, of cultured PC12 cells. Although isorhamnetin by itself did not show significant inductive effect on neurite outgrowth of cultured PC12 cells, the application of isorhamnetin potentiated the nerve growth factor- (NGF-)induced neurite outgrowth. In parallel, the expression of neurofilaments was markedly increased in the cotreatment of NGF and isorhamnetin in the cultures. The identification of these neurite-promoting flavonoids could be very useful in finding potential drugs, or food supplements, for treating various neurodegenerative diseases, including Alzheimer's disease and depression.

1. Introduction

Flavonoids belong to a family of polyphenolic compounds and have been considered as substitutes for estrogen [1–3]. They are widely present in our daily diet and also serve as major ingredients of vegetables and herbal supplements. Chemically, flavonoid is dividing into different subclasses including flavanone, flavone, flavonol, flavanonol, isoflavone, chalcone, and others. Recently, attentions have been focused on the neurobeneficial effects of different classes of flavonoids, including neuroprotection against neurotoxin stress, promotion of memory, and learning and cognitive functions. Indeed, the protective functions of flavonoids have been reported in various bioassay systems [3–6]. Interestingly, the beneficial effects of flavonoids are not restricted to mediate the neuroprotection. Different lines of evidence indicated that flavonoids also possessed biological activities in promoting neuronal differentiation. Therefore, flavonoids could serve as one of the resources in developing new drugs, or food supplements, for the prevention of neurodegenerative diseases, for example, Alzheimer's disease and depression. Moreover, the low toxicity of flavonoids in humans has been known [1, 2].

Cultured pheochromocytoma PC12 cell line is commonly being used for the detection of neuronal differentiation in responding to various stimuli, for example, nerve growth factor (NGF) [7–9]. By measuring the length of neurite or the number of cells processing neurites, the status of differentiated PC12 cells could be determined. In addition, the neuronal differentiation could be determined biochemically in analyzing the expression of neurofilaments (NFs) that are the major structural components of the differentiated

neurons [10]. Three mammalian neurofilament subunits, NF68 (M_r at ~68 kDa), NF160 (M_r at ~160 kDa), and NF200 (M_r at ~200 kDa), are believed to form heterodimers in making the structural domain of neurites [11].

Here, the length of neurites and the expression of neurofilaments were determined in cultured PC12 cells under the treatment of different subclasses of common flavonoids. Isorhamnetin, a flavonol aglycone from *Ginkgo biloba* L., was shown to induce the expression of neurofilaments and to potentiate the neurite-inducing activity of NGF. The identification of these neurite-promoting flavonoids could be very useful in finding potential drugs, or food supplements, for treating various neurodegenerative diseases.

2. Materials and Methods

2.1. Chemicals and Flavonoids. Isorhamnetin and other flavonoids were purchased from National Institute for the Control of Pharmaceutical Biology Products (NICPBP; Beijing, China), or Sigma (St. Louis, MO, USA) or Wakojunyaku (Osaka, Japan) or Kunming Institute of Botany, Chinese Academy of Science (Kunming, China) and solubilized in dimethylsulfoxide (DMSO) to give stock solution at a series of concentration from 25–100 mM, stored at −20°C. The MEK1/2 inhibitor U0126 was purchased from Sigma.

2.2. Cell Culture and Flavonoid Treatment. Pheochromocytoma PC12 cells, a cell line derived from rat adrenal medulla, were obtained from American Type Culture Collection (ATCC, Manassas, VA, USA), and which were maintained in Dulbecco's modified Eagle's medium supplemented with 6% fetal calf serum, 6% horse serum, 100 units/mL penicillin, and 100 μg/mL streptomycin in a humidified CO_2 (7.5%) incubator at 37°C. Fresh medium was supplied every other day. All culture reagents were purchased from Invitrogen Technologies (Carlsbad, CA, USA). During the treatment with flavonoids, cultured PC12 cells were serum starved for 3 hours in Dulbecco's modified Eagle's medium supplemented with 1% fetal calf serum, 1% horse serum, and penicillin-streptomycin, and then were treated with the flavonoids and/or other reagents for 72 hours. In analyzing the signaling pathway, the cells were pretreated with the MEK1/2 inhibitor U0126 (20 μM) for 3 hours before the exposure to flavonoid or NGF.

2.3. Cell Viability Test. Cell viability was assessed by MTT [3-(4, 5-dimethyl-2-thiazolyl)-2, 5-diphenyl-2H-tetrazolium bromide] assay [12]. PC12 cells were seeded in the 96-well plate and incubated for 24 hours. After that, cells were treated with the flavonoids, or other chemicals, for another 72 hours. Then, the MTT solution was added to the cell cultures and incubated for 1 hour at 37°C. Absorbance was measured at 570 nm in a microplate reader (Thermo Scientific, Fremont, CA, USA).

2.4. Western Blot Analysis. After the indicated time of treatment, the cells were solubilized in lysis buffer containing 0.125 M Tris-HCl, pH 6.8, 4% SDS, 20% glycerol, 2% 2-mercaptoethanol, and analyzed immediately or stored frozen at −20°C. Proteins were separated on the 8% SDS-polyacrylamide gels and transferred to the nitrocellulose. Transfer and equal loading of the samples was confirmed by staining the Ponceau-S. The nitrocellulose was blocked with 5% fat-free milk in Tris-buffer saline/0.1% Tween 20 (TBS-T), and then incubated in the primary antibody diluted in 2.5% fat-free milk in TBS-T for 2 hours in the room temperature. The primary antibodies used were: anti-NF200 (Sigma), anti-NF160 (Sigma), anti-NF68 (Sigma), anti-glyceraldehyde 3-phosphate dehydrogenase (GAPDH; Abcam Ltd., Cambridge, UK), anti-phospho-TrkA (Cell signaling, Danvers MA, USA), anti-TrkA (Cell Signaling), anti-phospho-Akt (Cell Signaling), anti-Akt (Cell Signaling), anti-phospho-Erk1/2 (Cell Signaling), and anti-Erk1/2 (Cell Signaling). After that, the nitrocellulose was rinsed with TBS-T and incubated for 1 hour at the room temperature in peroxidase- (HRP-)conjugated anti-mouse secondary antibody (Invitrogen), or peroxidase- (HRP-)conjugated anti-rabbit secondary antibody (Invitrogen), diluted in the 2.5% fat-free milk in TBS-T. After intensive washing with TBS-T, the immune complexes were visualized using the enhanced chemiluminescence (ECL) method (GE Healthcare, Piscataway, NJ, USA). The intensities of the bands in the control and different samples, run on the same gel and under strictly standardized ECL conditions, were compared on an image analyzer, using a calibration plot constructed from a parallel gel with serial dilutions of one of the samples.

2.5. Neurite Outgrowth Assay. Cultured PC12 cells were treated with isorhamnetin and/or NGF for 72 hours, with fresh medium and reagents supplied every 24 hours. A light microscope (Diagnostic Instruments, Sterling Heights, MI, USA) equipped with a phase-contrast condenser, 10x objective lens and a digital camera (Diagnostic Instruments) were used to capture the images with the manual setting. For analyzing the number and length of neurite, approximately 100 cells were counted from at least 10 randomly chosen visual fields for each culture. Using the photoshop software, the cells were then analyzed for the number and length of neurite. The cells were scored as differentiated if one or more neurites were longer than the diameter of cell body, and they were also classified to different groups according to the length of neurite that it possessed, that is, <15 μm, 15–30 μm, and >30 μm.

2.6. Statistical Analysis and Other Assays. Statistical analyses were performed using one way ANOVA followed by the Students t-test. Statistically significant changes were classed as * where $P < 0.05$; ** where $P < 0.01$; *** where $P < 0.001$.

3. Results

3.1. Effect of Flavonoids on the Differentiation of PC12 Cells. Sixty-five flavonoids from different subclasses were screened for their differentiating effect on cultured PC12 cells. These flavonoids are mainly derived from health foods and Chinese

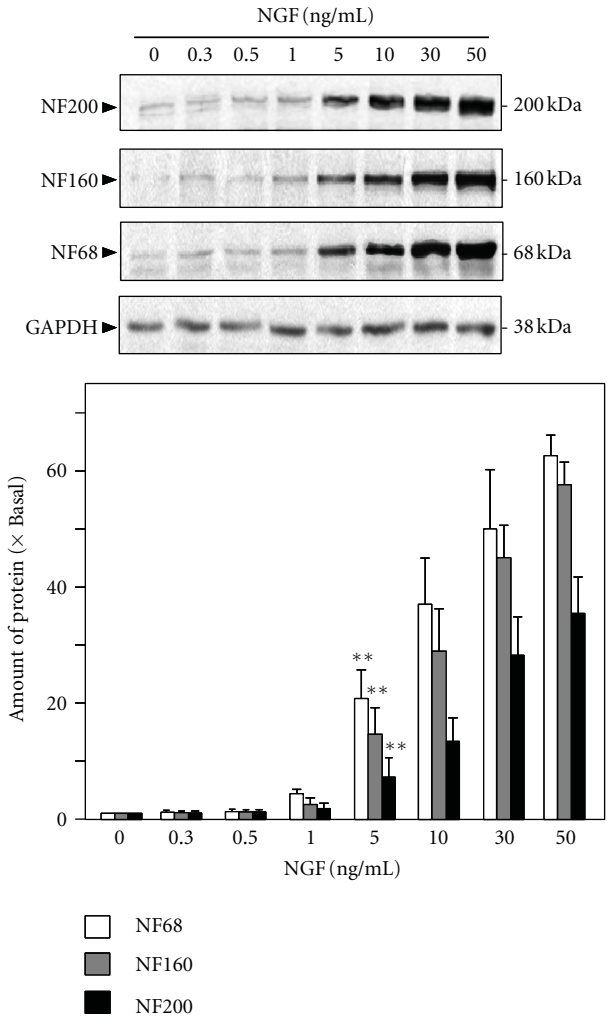

Figure 1: NGF induces the expression of neurofilaments in cultured PC12 cells. Cultured PC12 cells were treated with NGF (0.3 to 50 ng/mL) for 72 hours. The cell lysates were collected to determine the expressions of NF68 (M_r ~ 68 kDa), NF160 (M_r ~ 160 kDa), and NF200 (M_r ~ 200 kDa). GADPH (M_r ~ 38 kDa) served as a loading control (upper panel). Quantification plot was shown in lower panel. Values are expressed as the fold of change (×Basal) against the control (no treatment; set as 1), and in Mean ± SEM, $n = 4$, each with triplicate samples. Representative images were shown. $^{**}P < 0.01$ compared to the control.

herbal medicines. To enhance the efficiency of the screening platform, the first screening test was done on the expression of neurofilaments, including NF68, NF160, and NF200, instead of the extension of neurite. Indeed, application of NGF in cultured PC12 cells induced the expression of neurofilaments in a dose-dependent manner (Figure 1). Up to 5 ng/mL of NGF, the increased expressions of NF68 (at ~68 kDa) and NF160 (at ~160 kDa), and NF200 (at ~ 200 kDa) that could be significant are revealed here. The NGF-induced expression was more robust for NF68 and NF160 induction: the maximal expression at 50 ng/mL NGF was ~50 folds. The maximal induction of NF200 was over 30 folds.

To screen the potential neuronal differentiation effect of flavonoids, different flavonoids were applied onto cultured PC12 cells for 72 hours in different concentrations: these concentrations (e.g., isorhamnetin) had neither cytotoxicity nor proliferating effect, as achieved from the MTT assay (Supplementary figure available online at doi: 10.1155/2012/278273). After the treatment, the cells were collected to perform western blot analysis to determine the expression levels of NF68, NF160, and NF200. Some of the flavonoids increased the expression levels of neurofilaments (Table 1). For those having strong inductive effects (i.e., > ±±) were: hesperidin from *Citrus medica* var. *sarcodactylis* and *Citrus limonum* var. *dulcis*, luteolin from *Flos lonicerae*, sulphuretin from *Cotinus* family, daidzein, genistein and glycitein from *Glycine max* (L.) Merr., tectoridin from *Belamcanda chinensis*, cardamonin from *Alpinia katsumadai*, and kaempferol, quercetin, and isorhamnetin from *G. biloba.* Among these flavonoids, the flavonol aglycone, isorhamnetin, was found to have the most evident effect in inducing the expression of neurofilaments in PC12 cells. Thus, isorhamnetin was chosen for further investigation.

Isorhamnetin is a flavonol aglycone (Figure 2(a)). In the cultures treated with isorhamnetin, the expressions of NF68, NF168, and NF200 were increased: the neurofilament induction was in a dose-dependent manner (Figure 2(b)). The protein induction was significantly revealed at 1 μM of isorhamnetin. Under 10 μM of isorhamnetin in the cultures, the expressions of NF68 and NF160 were increased over 6 folds: while NF200 was significantly altered to over 3 folds. The expression level of control protein GAPDH was unchanged (Figure 2(b)). The outgrowth of neurite was subsequently analyzed in isorhamnetin-treated PC12 cells. The effect of isorhamnetin in inducing neurite outgrowth of cultured PC12 cells was not significant (Figure 2(c)), at lease under the low concentration at 3 μM. At higher concentration of isorhamnetin (10 μM), the differentiated cell was revealed, but the induction was much less than that of NGF at 50 ng/mL (Figure 2(c)). Quantitation was performed on the extent of those neurites. Counting the number of differentiated cells (i.e., having a neurite longer than the cell body), only ~30% of total cell population could be considered as differentiated under the treatment of 10 μM isorhamnetin (Figure 2(d), *upper panel*). Low concentration of isorhamnetin did not show any induction effect. In contrast, NGF at 50 ng/mL induced the cell differentiation almost to 100%. The length of neurite was also measured: the number of cells possessing neurite length at 15–30 μm was significantly increased (~10%) in 10 μM isorhamnetin-treated cells (Figure 2(d), *lower panel*). Thus, the neurite-inducing effect of isorhamnetin in cultured PC12 cells was very little as compared to that of NGF at 50 ng/mL.

3.2. Isorhamnetin Potentiates the NGF-Induced Differentiation of PC12 Cells. Since isorhamnetin did not seem to have a significant effect on neurite outgrowth of PC12 cells, we therefore aimed to search for the collaborative effect of this flavonoid when applied together with NGF. First, a suitable

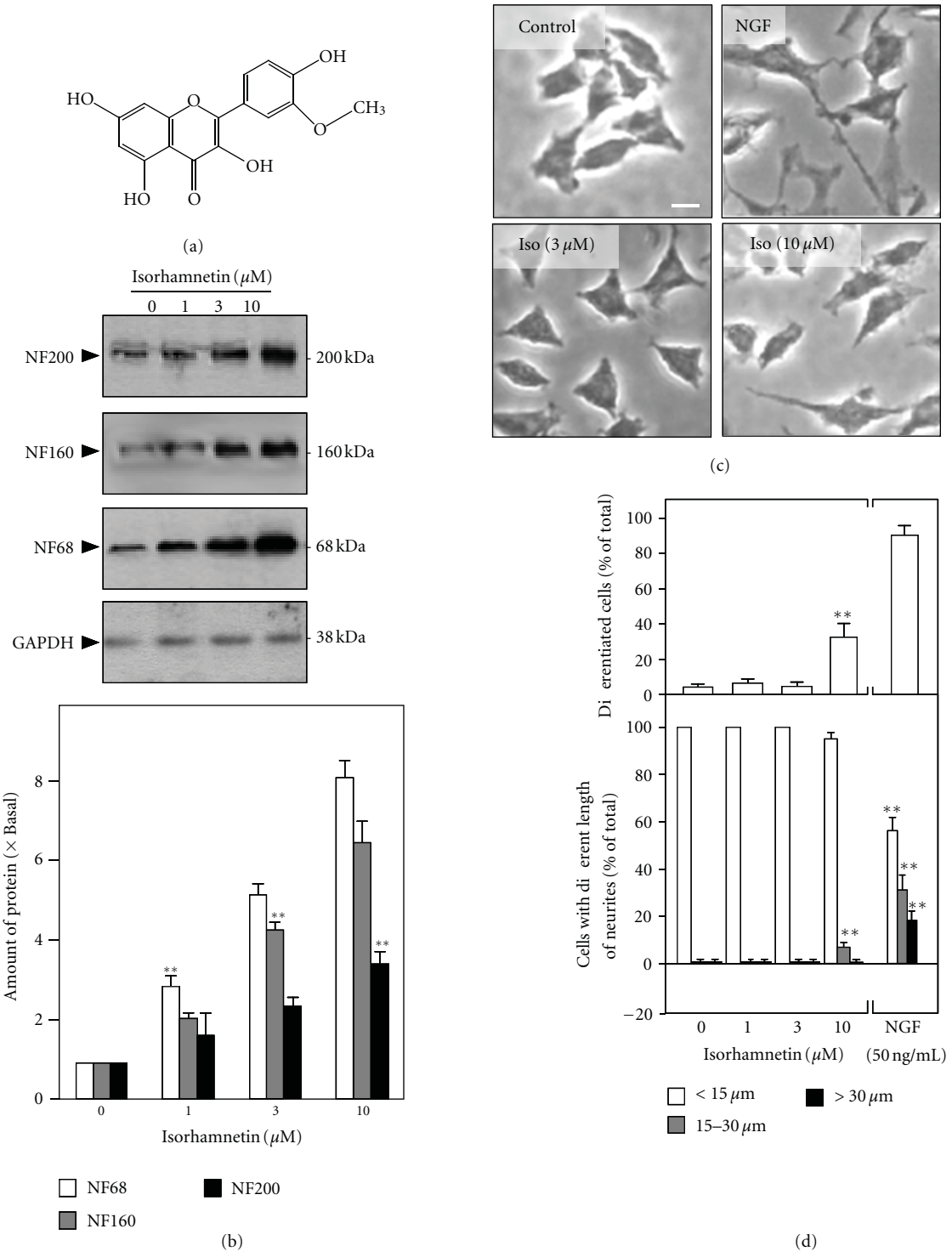

Figure 2: Isorhamnetin induces the neurofilament expression in cultured PC12 cells but not the neurite outgrowth. (a) The chemical structure of isorhamnetin is illustrated. (b) Cultured PC12 cells were treated with isorhamnetin (1 to 10 μM) for 72 hours. The cell lysates were collected to determine the expressions of NF68, NF160, and NF200 (upper panel). GADPH served as a loading control. The lower panel shows the quantitation from the blots by a densitometer. Values are expressed as the fold of change (×Basal) against the control (no treatment; set as 1), and in mean ± SEM, $n = 4$, each with triplicate samples. (c) Cultures were treated with isorhamnetin (3 or 10 μM) and NGF (50 ng/mL), as indicated, for 72 hours. Cells were fixed with ice-cold 4% paraformaldehyde. Bar = 10 μm. Representative images were shown. (d) Cultured PC12 cell was treated as in (c). The % of differentiated cell (upper panel) and length of neurite (lower panel) were counted as described in the Materials and Methods section. Values are expressed as % of total cells in 100 counted cells, mean ± SEM, $n = 4$. $^{**}P < 0.01$ compared to the control.

Table 1: Flavonoids induce the expressions of NF68, NF160, and NF200.

Flavonoid	NF68	NF160	NF200	Flavonoid	NF68	NF160	NF200	Flavonoid	NF68	NF160	NF200
Flavanones				*Biflavones*				*Chalcones*			
Alpinetin	−	−	−	Ginkgetin	+	+	−	Cardamonin	++	+	+
Farrerol	−	−	−	*Dihydrochalcones*				*Flavanes*			
Hesperidin	++	+	−	Phloretin	−	−	−	(−)-Catechin	−	−	−
Liquiritin	−	−	−	Phloridzin	−	−	−	(−)-Epicatechin	−	−	−
Naringenine	+	−	−	*Flavanonols*				*Flavonols*			
Naringin	−	−	−	Dihydromyricetin	−	−	−	Astragalin	−	−	−
Neohesperidin	−	−	−	Silybin	−	−	−	Galangin	+	+	−
Prunin	−	−	−	*Isoflavones*				Hibifolin	−	−	−
Flavones				Calycosin	−	−	−	Hyperin	+	+	−
Apigenin	−	−	−	Calycosin-7-O-glc	−	−	−	Icariin	−	−	−
Apiin	−	−	−	Daidzein	++	+	−	Isoquercitrin	−	−	−
Baicalein	−	−	−	Daidzin	−	−	−	Isorhamnetin	+++	+++	+
Baicalin	−	−	−	Formononetin	−	−	−	Isorhamnetin-3-O-rut	−	−	−
Chrysin	−	−	−	Genistein	++	+	−	Kaempferol	++	+	+
Hebacetin-8-OCH_3	+	−	−	Genistin	−	−	−	Kaempferol-3-O-rut	−	−	−
Isovitexin	−	−	−	Glycitein	++	+	−	Kaempferol-3-O-glc	+	−	−
Luteolin	++	+	+	Glycitin	−	−	−	Quercetin	++	+	−
Lysionotin	−	−	−	Irisflorentin	+	+	−	Quercetin-3′-O-glc	+	−	−
Morusin	−	−	−	Ononin	−	−	−	RNFG	+	+	−
Scutellarin	−	−	−	Pratensein	+	+	−	Rutin	−	−	−
Scoparin	+	−	−	Puerarin	−	−	−	Tiliroside	−	−	−
Tangeretin	+	−	−	4′,7-OCH_3-puerarin	−	−	−	Vitexicarpin	−	−	−
Wogonin	−	−	−	4′,7-$OCOCH_3$-puerarin	−	−	−				
Aurones				Tectoridin	++	+	−				
Sulphuretin	++	+	−	Tectorigenin	−	−	−	NGF	+++	+++	+++

Data are means ± SEM, $n = 3$. Data are based on the means. And the value of SEM is within 5% of the mean, which is not shown for clarity. "+" to "+++" indicate the percentage of increasing of the neurofilaments expression level ("+" indicates 100% to 200% increasing in the tested activities, "++" indicates 200% to 300% increasing, and "+++" indicates >300% increasing). "−" indicates no effect, that is, below 10%. For the tested flavonoids, the maximal testing concentrations distribute from 3 μM to 30 μM, according to the results from cell viability assay. The submaximal doses of these flavonoids were used for comparison. NGF at 50 ng/ml served as a positive control. RNFG is corresponding to Radix Notoginseng flavonol glucoside or quercetin 3-O-β-D-xylopyranosyl-β-D-galactopyranoside.

concentration of NGF was selected: this concentration should have no effect on the neurite outgrowth and/or the neurofilament expression. The concentration of NGF below 1 ng/mL did not show any significant effect on the number of differentiated cell and/or the neurite outgrowth of cultured PC12 cells (Figure 3). Moreover, the expression of neurofilament was not increased under NGF concentration below 1 ng/mL (see Figure 1). Under this scenario, 0.5 ng/mL, a concentration of NGF at which it showed no induction effect at all, was used here to cotreat PC12 cultures together with isorhamnetin.

Isorhamnetin (10 μM) and NGF (0.5 ng/mL) were coapplied in cultured PC12 cells for 72 hours. Then, the cultures were collected to perform Western blot analysis to determine the change of neurofilament expression, including NF68, NF160, and NF200. NGF at 0.5 ng/mL showed no effect on neurofilament expression, while isorhamnetin at 10 μM only showed the induction of NF68 at ~10% (Figure 4). The cotreatment of isorhamnetin and NGF robustly increased the expressions of neurofilaments, that is, NF68, NF160 and NF200. The induction of these neurofilaments was over 30 folds: this magnitude of induction shared a similarity to that of high concentration of NGF at 50 ng/mL (Figure 4). In addition, the outgrowth of neurite in the cultures was analyzed. The cotreatment of isorhamnetin (10 μM) and NGF (0.5 ng/mL) induced the differentiation of cultured PC12 cells, and the outgrowth of neurite was clearly revealed in the cotreatment (Figure 5(a)). In addition, the number of differentiated cells significantly increased by ~60% after this cotreatment (Figure 5(b), *upper panel*), and which also induced the length of neurite (Figure 5(b), *lower panel*). After the cotreatment, those cells having the long neurite, for example, above 15 μm in length, were markedly increased: this induction effect was similar to that of high concentration of NGF at 50 ng/mL (Figure 5(b), *lower panel*). These results therefore suggested the potentiating role of isorhamnetin in the neurite outgrowth activity of NGF.

3.3. The Effect of Isorhamnetin on NGF-Induced Signaling Pathways. To explore the mechanism of isorhamnetin-induced neurofilament expression and its potentiating effect

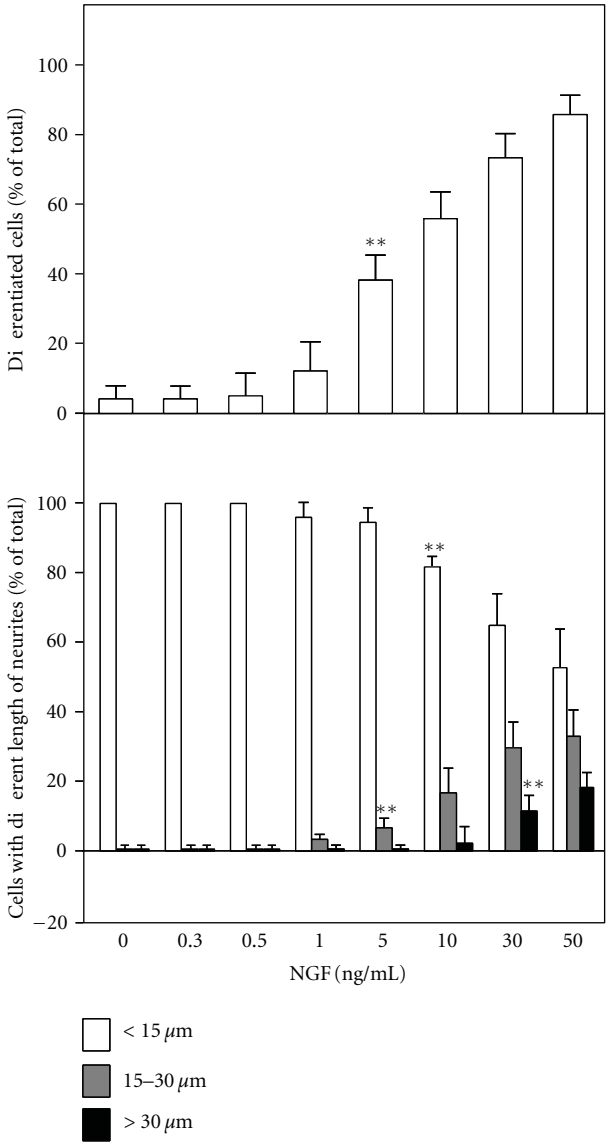

Figure 3: NGF induces the neurite outgrowth in a dose-dependent manner. Cultured PC12 cultures were treated with NGF (0.3 to 50 ng/mL) for 72 hours. Cells were fixed with ice-cold 4% paraformaldehyde. The % of differentiated cell (upper panel) and length of neurite (lower panel) were counted as described in the Method section. Values are expressed as % of total cells in 100 counted cells, Mean ± SEM, $n = 4$. $^{**}P < 0.01$ compared to the control.

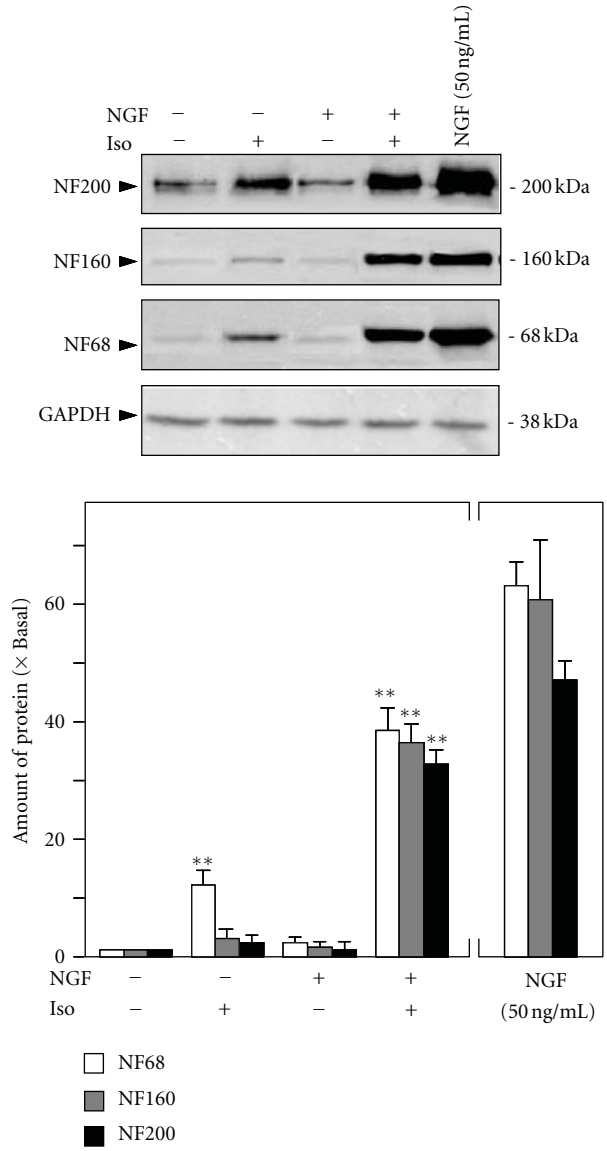

Figure 4: Isorhamnetin potentiates the NGF-induced neurofilament expression. Cultured PC12 cells were treated with NGF (0.5 ng/mL), isorhamnetin (10 μM), and NGF (0.5 ng/mL) + isorhamnetin (10 μM) for 72 hours. NGF at 50 ng/mL was applied as a control. The cell lysates were collected to determine the expressions of NF68, NF160, and NF200 (upper panel). GADPH served as a loading control. Quantification plot was shown in lower panel. Values are expressed as the fold of change (× Basal) against the control (no treatment; set as 1), and in mean ± SEM, $n = 4$. Representative images were shown. ** where $P < 0.01$ compared to the control.

on NGF-induced neurite outgrowth, the effects of isorhamnetin in phosphorylating the NGF-induced signaling molecules was tested. NGF, or isorhamnetin, was applied onto the serum-starved PC12 cell cultures. After treatment at different time periods, the cell lysates were collected to perform western blotting, as to reveal the phosphorylation levels of various signaling molecules. NGF at low level induced the phosphorylations of TrkA (~140 kDA), Erk1/2 (~44/42 kDa), and Akt (~60 kDa) within 5 min (Figure 6). However, isorhamnetin could not induce the phosphorylation of any of these molecules, even up to 30 min of treatment. To test the possible potentiating effect of isorhamnetin in the NGF-activated signaling, we cotreated isorhamnetin with NGF at 5 ng/mL. Here, NGF in 5 ng/mL was the lowest concentration to phosphorylate the molecules (Figure 6); however, the cotreatment with isorhamnetin did not enhance the phosphorylation. To further confirm the role of MEK

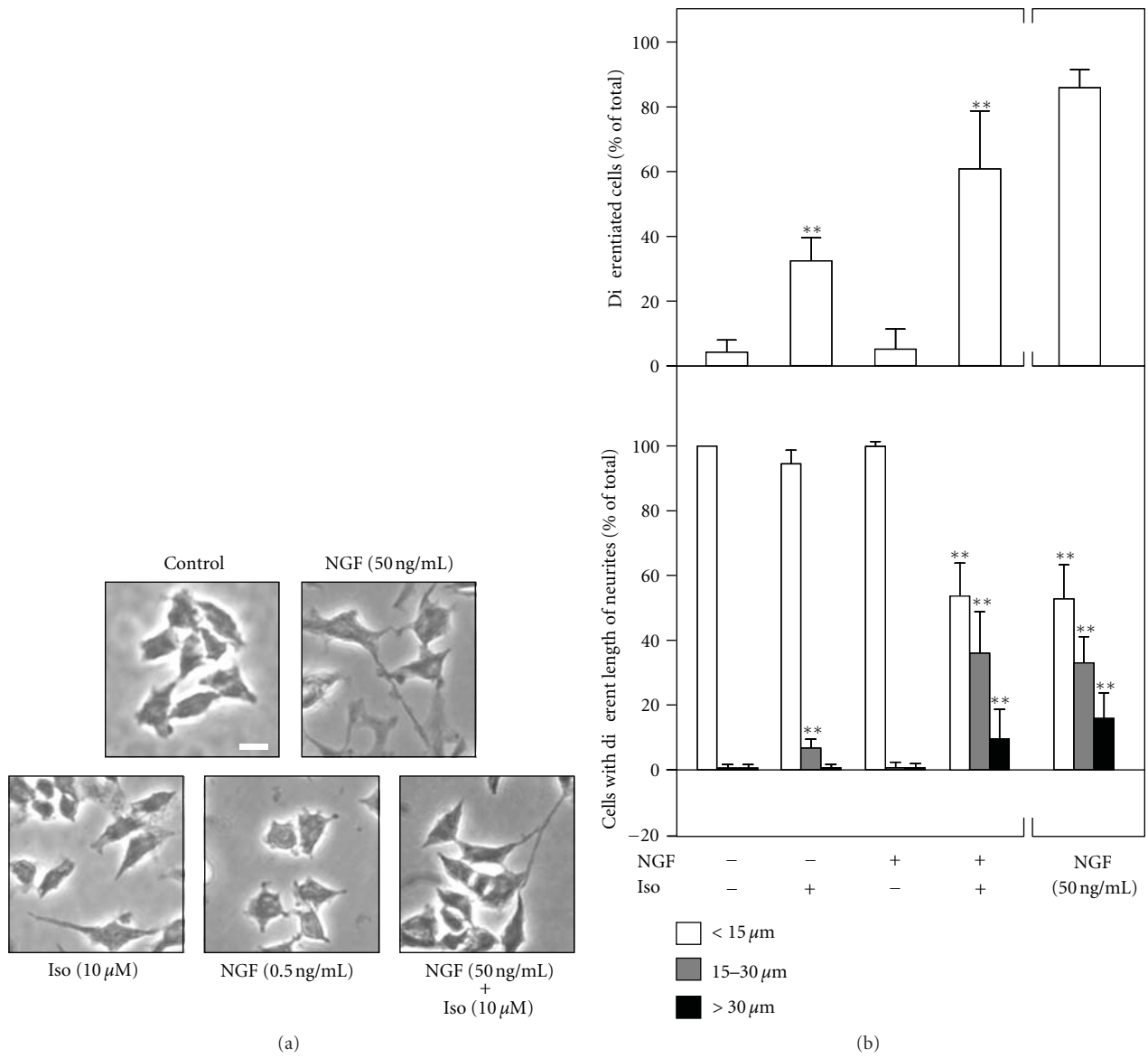

Figure 5: Isorhamnetin potentiates the NGF-induced neurite outgrowth. Cultured PC12 cells were treated with NGF (0.5 ng/mL), isorhamnetin (10 μM), and NGF (0.5 ng/mL) + isorhamnetin (10 μM) for 72 hours, as in Figure 4. (a) Cells were fixed with ice-cold 4% paraformaldehyde and the extension of neurites was revealed. Bar = 10 μm. (b) The % of differentiated cell (upper panel) and length of neurite (lower panel) were counted as described in the Method section. Values are expressed as % of cells in 100 counted cells, mean ± SEM, $n = 4$. $^{**}P < 0.01$ compared to the control.

pathway in the function of isorhamnetin, the pretreatment of U0126 at 20 μM was applied onto the cultures, as to block the mitogen-activated protein kinase signaling. Results showed that U0126 did not block the neurofilament expression induced by isorhamnetin, or the potentiating effect of isorhamnetin, on NGF-induced neurite outgrowth (Figure 7). In contrast, this concentration of U0126 was demonstrated to partially blocked the NGF signaling (data not shown here), and which was in line to previous studies [13, 14]. These results suggested that the response triggered by isorhamnetin could be very different to that of NGF in the cultures.

4. Discussion

Sixty-five flavonoids were screened for their differentiating effect on cultured PC12 cells. Over 20 of them showed inductive effect on the expression of neurofilaments; however, which did not simultaneously induce the neurite out-

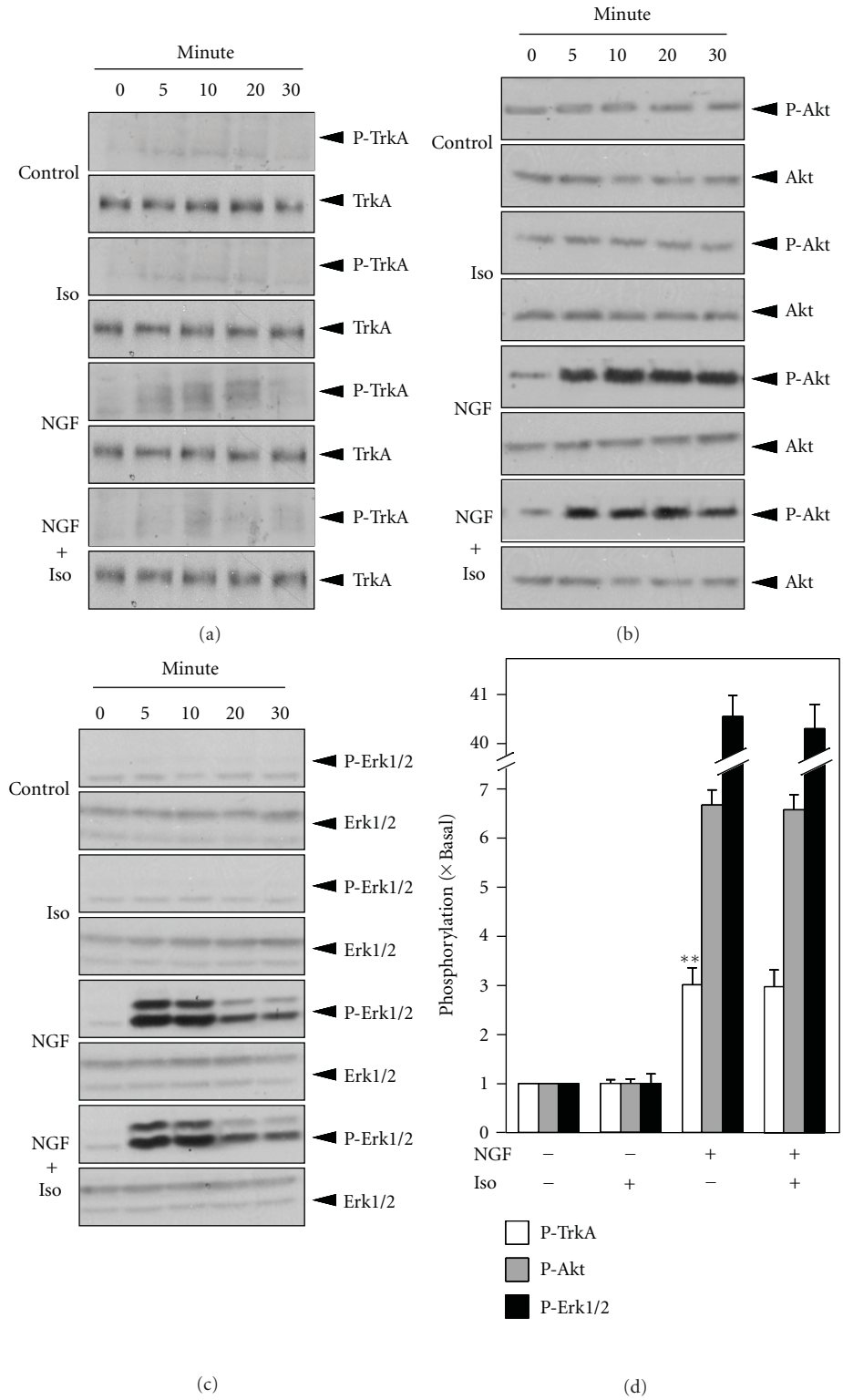

Figure 6: The potentiating effect of isorhamnetin is not mediated by NGF-induced signaling cascade. Cultured PC12 cells, serum starvation for 5 hours, were treated with NGF (5 ng/mL), isorhamnetin (Iso; 10 μM), and NGF (5 ng/mL) + isorhamnetin (Iso; 10 μM) for different time. Total TrkA and phosphorylated TrkA (a) total Akt and phosphorylated Akt (b) total Erk1/2 and phosphorylated Erk1/2 (c) were revealed by using specific antibodies. (d) Quantification plot of the phosphorylation level in treatment of 5 min was shown. Values are expressed as the fold of change (×Basal) against the control (no treatment; set as 1), and in mean ± SEM, $n = 4$. Representative images were shown. ** where $P < 0.01$ compared to the control.

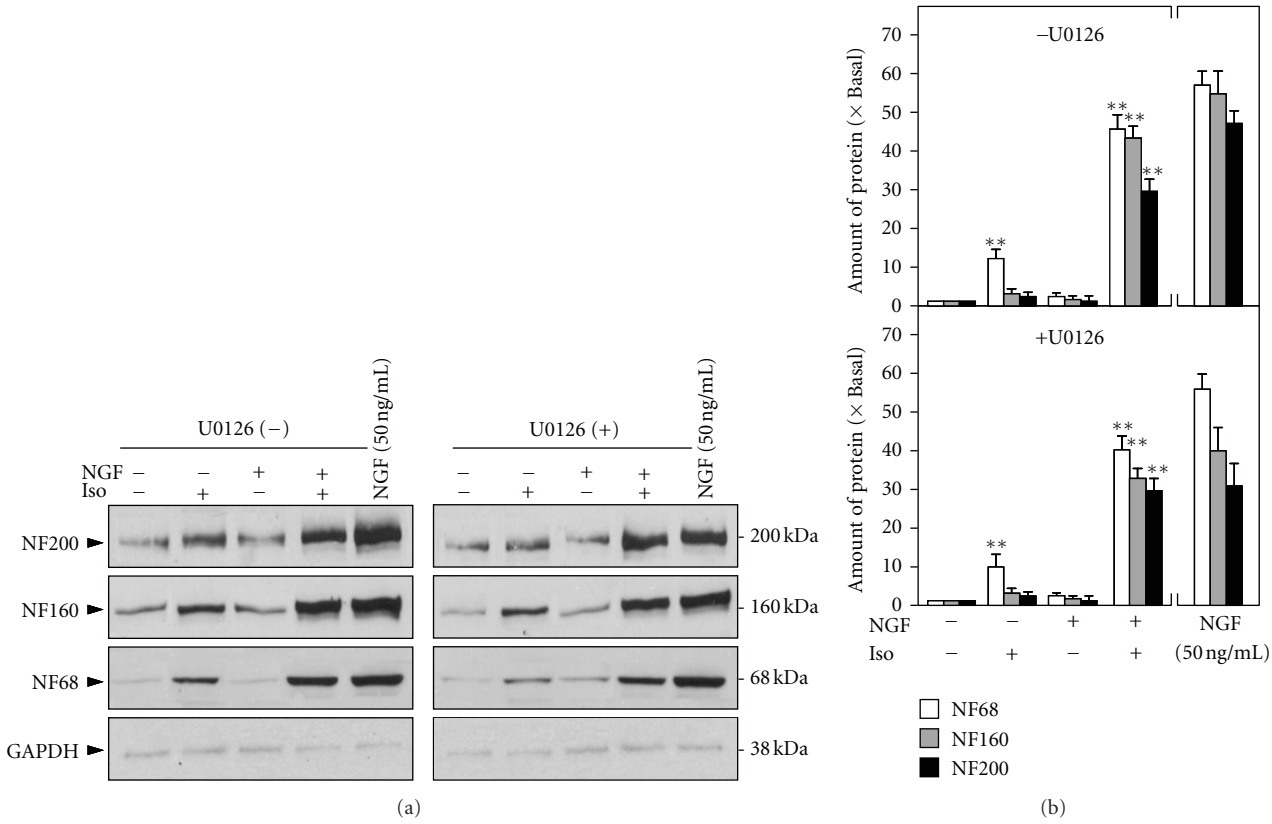

Figure 7: The potentiating effect of isorhamnetin on NGF-induced response could not be blocked by U0126. Cultured PC12 cells, serum starvation for 5 hours, were treated with NGF (0.5 ng/mL), isorhamnetin (Iso; 10 μM), and NGF (0.5 ng/mL) + isorhamnetin (Iso; 10 μM) for 72 hours with or without the pretreatment of U0126 (20 μM) for 3 hours. NGF at 50 ng/mL served as a positive control. (a) The cell lysates were collected to determine the expressions of NF68, NF160, and NF200. GADPH served as a loading control. (b) Quantification plot was shown in lower panel. Values are expressed as the fold of change (×Basal) against the control (no treatment; set as 1), and in mean ± SEM, $n = 4$. Representative images were shown. **where $P < 0.01$ compared to the control.

growth in the cultures. Isorhamnetin, a flavonol aglycone isolated mainly from *G. biloba*, was chosen to do the following studies including the cotreatment with NGF in low concentration. However, the effect of isorhamnetin on neurite outgrowth was very limited. Thus, the expression of neurofilament and neurite outgrowth in cultured PC12 cells could be two independent events. On the other hand, isorhamnetin showed a robust effect in potentiating the neurite-inducing activity of NGF, that is, the coapplication of isorhamnetin with low concentration of NGF (0.5 ng/mL) could achieve the effect as that of high concentration of NGF (50 ng/mL). Therefore, the NGF-potentiating effect of isorhamnetin could be considered as a new direction in developing health food supplements to help the recovery of neurodegenerative diseases relating to NGF insufficient.

Ginkgo leaf extract is the most popular herbal supplement being sold in Europe and the USA, where it is used to treat the symptoms of early-stage Alzheimer's disease, vascular dementia and tinnitus of vascular origin [15]. The most well-known standardized preparation of Ginkgo extract on the current herbal market is Egb 761 that consists of two major groups of substances: the flavone glycosides (flavonoid fraction, 24%) and the terpene lactones (terpenoid fraction, 6%) [16]. The amount of isorhamnetin in dry Ginkgo leaf could reach 0.85 ± 0.02 mg/g [17]. Isorhamnetin has been proved to have the activities of antitumor [18], antioxidation [3, 19], reducing the superoxide anion in liver cells [20], and decreasing the risk of many disorders, for example, diabetes, hypertension, and heart disease [21]. In nervous system, isorhamnetin was also shown to have the protective effect against the oxidative stress induced by simulated microgravity *in vitro* [22]. Besides isorhamnetin, other flavonoids, or natural compounds, have also been shown to induce neuronal differentiation and neurite outgrowth, for example, wogonin isolated from *Scutellaria baicalensis* [23] and euxanthone isolated from *Polygala caudate* [24]. In addition, the NGF-potentiating flavonoids have also been reported, for example, liquiritin from *Glycyrrhizae* root [25] and littorachalcone from *Verbena litoralis* [26].

Neurofilaments are the key components during the extension of neurite, and their expression level could serve as a marker for neuronal differentiation. The application of isorhamnetin in cultured PC12 cells could increase significantly the expression levels of NF68 and NF160. Both NF68 and NF160 are the protein markers for the early stage of the differentiation. In contrast, the expression of NF200, a

marker protein for late stage of neuron differentiation [27], was also altered but at a less extent as compared to that of NF68 or NF160 at the isorhamnetin-treated cultures. Under this scenario, the involvement of isorhamnetin in neuronal differentiation could be mainly at the early stage, which however could not fully support the entire differentiation process at late stage. The potentiating effect of isorhamnetin in the NGF-induced neurite outgrowth also supported this notion. The increased expressions of NF68 and NF160 in cultured cells, induced by isorhamnetin, could be a prelude for the expression of NF200, and the neurite outgrowth could be the final outcome of increased protein expressions.

NGF is one of the key modulators of neurite outgrowth during development and into adulthood, many diseases of nervous system are associated with NGF insufficiency, especially some neurodegenerative diseases [28], for example, depression [29] and Alzheimer's disease [30]. For the property of potentiating effect on NGF-induced neurite outgrowth, isorhamnetin would have potential to be used to treat the differentiation problem caused by NGF insufficiency. Therefore, the NGF-potentiating effect of isorhamnetin could be considered as a new direction in developing drugs or health food supplements to help the prevention and recovery of neurodegenerative diseases. NGF achieves its function by binding and activating TrkA receptor on neuronal cells. The NGF-activated TrkA stimulates downstream signaling pathways, which results in neuronal differentiation and promoting cell survival [13]. The NGF-induced neurite outgrowth is mediated by activation of Ras/ERK, PI3K/Akt, and phospholipase-C-γ (PLC-γ1) [14]. Various classes of flavonoids were demonstrated to induce the neurite outgrowth, or to potentiate the NGF-induced neurite outgrowth, in cultured neurons, and the signal could be mediated by a MEK pathway [31–33]. Here, isorhamnetin can neither directly activate these signaling molecules by phosphorylation, nor potentiated NGF-induced activation of the signaling pathways, which may tell us that even though different flavonoids have the similar effects in neurite outgrowth, their mechanism may be totally different. The signal triggered by isorhamnetin in cultured PC12 cells is being determined currently in our laboratory.

5. Conclusion

Flavonoids are a group of natural compounds with multiple biofunctions. In this study, we aimed to investigate their effects on neuronal differentiation of cultured PC12 cells. Sixty-five flavonoids from different subclasses were screened for their differentiating effect on cultured PC12 cells. Among these flavonoids, a flavonol aglycone, isorhamnetin was found to have the best effect in inducing the expression of neurofilaments, and which potentiated the NGF-induced neurite outgrowth and neurofilament expression. Although the mechanism has not been revealed, this property of isorhamnetin could be a new direction in searching potential candidates as new drugs or food supplements for neurodegenerative diseases.

Conflict of Interests

The authors declare that there are no conflict of interests in the current study.

Acknowledgments

This research was supported by Grants from Research Grants Council of Hong Kong (N_HKUST629/07, 662608, 661110, 662911) and Croucher Foundation (CAS-CF07/08.SC03) to Karl W. K. Tsim and David T. W. Lau.

References

[1] R. J. Miksicek, "Commonly occurring plant flavonoids have estrogenic activity," *Molecular Pharmacology*, vol. 44, no. 1, pp. 37–43, 1993.

[2] A. L. Murkies, G. Wilcox, and S. R. Davis, "Phytoestrogens," *Journal of Clinical Endocrinology and Metabolism*, vol. 83, no. 2, pp. 297–303, 1998.

[3] J. T. T. Zhu, R. C. Y. Choi, G. K. Y. Chu et al., "Flavonoids possess neuroprotective effects on cultured pheochromocytoma PC12 cells: a comparison of different flavonoids in activating estrogenic effect and in preventing β-amyloid-induced cell death," *Journal of Agricultural and Food Chemistry*, vol. 55, no. 6, pp. 2438–2445, 2007.

[4] R. C. Y. Choi, J. T. T. Zhu, K. W. Leung et al., "A flavonol glycoside, isolated from roots of panax notoginseng, reduces amyloid-β-induced neurotoxicity in cultured neurons: signaling transduction and drug development for Alzheimer's disease," *Journal of Alzheimer's Disease*, vol. 19, no. 3, pp. 795–811, 2010.

[5] J. T. T. Zhu, R. C. Y. Choi, H. Q. Xie et al., "Hibifolin, a flavonol glycoside, prevents β-amyloid-induced neurotoxicity in cultured cortical neurons," *Neuroscience Letters*, vol. 461, no. 2, pp. 172–176, 2009.

[6] A. J. Y. Guo, R. C. Y. Choi, A. W. H. Cheung et al., "Baicalin, a flavone, induces the differentiation of cultured osteoblasts: an action via the Wnt/β-catenin signaling pathway," *Journal of Biological Chemistry*, vol. 286, no. 32, pp. 27882–27893, 2011.

[7] L. A. Greene and A. S. Tischler, "Establishment of a noradrenergic clonal line of rat adrenal pheochromocytoma cells which respond to nerve growth factor," *Proceedings of the National Academy of Sciences of the United States of America*, vol. 73, no. 7, pp. 2424–2428, 1976.

[8] D. K. Fujii, S. L. Massoglia, N. Savion, and D. Gospodarowicz, "Neurite outgrowth and protein synthesis by PC12 cells as a function of substratum and nerve growth factor," *Journal of Neuroscience*, vol. 2, no. 8, pp. 1157–1175, 1982.

[9] C. F. Blackman, S. G. Benane, D. E. House, and M. M. Pollock, "Action of 50 Hz magnetic fields on neurite outgrowth in pheochromocytoma cells," *Bioelectromagnetics*, vol. 14, no. 3, pp. 273–286, 1993.

[10] J. Schimmelpfeng, K. F. Weibezahn, and H. Dertinger, "Quantification of NGF-dependent neuronal differentiation of PC-12 cells by means of neurofilament-L mRNA expression and neuronal outgrowth," *Journal of Neuroscience Methods*, vol. 139, no. 2, pp. 299–306, 2004.

[11] M. K. Lee and D. W. Cleveland, "Neuronal intermediate filaments," *Annual Review of Neuroscience*, vol. 19, pp. 187–217, 1996.

[12] T. Mosmann, "Rapid colorimetric assay for cellular growth and survival: application to proliferation and cytotoxicity

assays," *Journal of Immunological Methods*, vol. 65, no. 1-2, pp. 55–63, 1983.

[13] D. Vaudry, P. J. S. Stork, P. Lazarovici, and L. E. Eiden, "Signaling pathways for PC12 cell differentiation: making the right connections," *Science*, vol. 296, no. 5573, pp. 1648–1649, 2002.

[14] J. Hur, P. Lee, E. Moon et al., "Neurite outgrowth induced by spicatoside A, a steroidal saponin, via the tyrosine kinase A receptor pathway," *European Journal of Pharmacology*, vol. 620, no. 1-3, pp. 9–15, 2009.

[15] V. S. Sierpina, B. Wollschlaeger, and M. Blumenthal, "Ginkgo biloba," *American Family Physician*, vol. 68, no. 5, pp. 923–926, 2003.

[16] B. Ahlemeyer and J. Krieglstein, "Neuroprotective effects of Ginkgo biloba extract," *Cellular and Molecular Life Sciences*, vol. 60, no. 9, pp. 1779–1792, 2003.

[17] G. Haghi and A. Hatami, "Simultaneous quantification of flavonoids and phenolic acids in plant materials by a newly developed isocratic high-performance liquid chromatography approach," *Journal of Agricultural and Food Chemistry*, vol. 58, no. 20, pp. 10812–10816, 2010.

[18] B. S. Teng, Y. H. Lu, Z. T. Wang, X. Y. Tao, and D. Z. Wei, "In vitro anti-tumor activity of isorhamnetin isolated from *Hippophae rhamnoides* L. against BEL-7402 cells," *Pharmacological Research*, vol. 54, no. 3, pp. 186–194, 2006.

[19] L. Pengfei, D. Tiansheng, H. Xianglin, and W. Jianguo, "Antioxidant properties of isolated isorhamnetin from the sea buckthorn marc," *Plant Foods for Human Nutrition*, vol. 64, no. 2, pp. 141–145, 2009.

[20] K. Igarashi and M. Ohmuma, "Effects of isorhamnetin, rhamnetin, and quercetin on the concentrations of cholesterol and lipoperoxide in the serum and liver and on the blood and liver antioxidative enzyme activities of rats," *Bioscience, Biotechnology and Biochemistry*, vol. 59, no. 4, pp. 595–601, 1995.

[21] J. Lee, E. Jung, J. Lee et al., "Isorhamnetin represses adipogenesis in 3T3-L1 cells," *Obesity*, vol. 17, no. 2, pp. 226–232, 2009.

[22] L. Qu, H. Chen, C. Wang et al., "Protection of isorhamnetin and luteolin against simulated microgravity induced oxidative stress in SH-SY5Y cells," in *Proceedings of the 60th International Astronautical Congress (IAC '09)*, pp. 184–190, October 2009.

[23] J. S. Lim, M. Yoo, H. J. Kwon, H. Kim, and Y. K. Kwon, "Wogonin induces differentiation and neurite outgrowth of neural precursor cells," *Biochemical and Biophysical Research Communications*, vol. 402, no. 1, pp. 42–47, 2010.

[24] W. Y. Ha, P. K. Wu, T. W. Kok et al., "Involvement of protein kinase C and E2F-5 in euxanthone-induced neurite differentiation of neuroblastoma," *International Journal of Biochemistry and Cell Biology*, vol. 38, no. 8, pp. 1393–1401, 2006.

[25] Z. A. Chen, J. L. Wang, R. T. Liu et al., "Liquiritin potentiate neurite outgrowth induced by nerve growth factor in PC12 cells," *Cytotechnology*, vol. 60, no. 1-3, pp. 125–132, 2009.

[26] Y. Li, M. Ishibashi, X. Chen, and Y. Ohizumi, "Littorachalcone, a new enhancer of NGF-mediated neurite outgrowth, from Verbena littoralis," *Chemical and Pharmaceutical Bulletin*, vol. 51, no. 7, pp. 872–874, 2003.

[27] M. J. Carden, J. Q. Trojanowski, W. W. Schlaepfer, and V. M. Y. Lee, "Two-stage expression of neurofilament polypeptides during rat neurogenesis with early establishment of adult phosphorylation patterns," *Journal of Neuroscience*, vol. 7, no. 11, pp. 3489–3504, 1987.

[28] A. Kruttgen, S. Saxena, M. E. Evangelopoulos, and J. Weis, "Neurotrophins and neurodegenerative diseases: receptors stuck in traffic?" *Journal of Neuropathology and Experimental Neurology*, vol. 62, no. 4, pp. 340–350, 2003.

[29] Y. Dwivedi, A. C. Mondal, H. S. Rizavi, and R. R. Conley, "Suicide brain is associated with decreased expression of neurotrophins," *Biological Psychiatry*, vol. 58, no. 4, pp. 315–324, 2005.

[30] G. A. Higgins and E. J. Mufson, "NGF receptor gene expression is decreased in the nucleus basalis in Alzheimer's disease," *Experimental Neurology*, vol. 106, no. 3, pp. 222–236, 1989.

[31] C. W. Lin, M. J. Wu, I. Y. C. Liu, J. D. Su, and J. H. Yen, "Neurotrophic and cytoprotective action of luteolin in PC12 cells through ERK-dependent induction of Nrf2-Driven HO-1 expression," *Journal of Agricultural and Food Chemistry*, vol. 58, no. 7, pp. 4477–4486, 2010.

[32] U. Gundimeda, T. H. McNeill, J. E. Schiffman, D. R. Hinton, and R. Gopalakrishna, "Green tea polyphenols potentiate the action of nerve growth factor to induce neuritogenesis: possible role of reactive oxygen species," *Journal of Neuroscience Research*, vol. 88, no. 16, pp. 3644–3655, 2010.

[33] H. Nagase, N. Omae, A. Omori et al., "Nobiletin and its related flavonoids with CRE-dependent transcription-stimulating and neuritegenic activities," *Biochemical and Biophysical Research Communications*, vol. 337, no. 4, pp. 1330–1336, 2005.

Hindawi Publishing Corporation
Evidence-Based Complementary and Alternative Medicine
Volume 2012, Article ID 414536, 10 pages
doi:10.1155/2012/414536

Research Article

Therapeutic Effect of Yi-Chi-Tsung-Ming-Tang on Amyloid β_{1-40}-Induced Alzheimer's Disease-Like Phenotype via an Increase of Acetylcholine and Decrease of Amyloid β

Chung-Hsin Yeh,[1,2,3] Ming-Tsuen Hsieh,[4] Chi-Mei Hsueh,[2] Chi-Rei Wu,[4] Yi-Chun Huang,[5] Jiunn-Wang Liao,[6] and Kuan-Chih Chow[7]

[1] *Department of Neurology, Show Chwan Memorial Hospital, Changhua, Taiwan*
[2] *Graduate Institute of Life Sciences, National Chung Hsing University, Taichung 40001, Taiwan*
[3] *Department of Nursing, College of Medicine & Nursing, HungKuang University (HKU), Taichung 40001, Taiwan*
[4] *School of Chinese Pharmaceutical Sciences and Chinese Medicine Resources, College of Pharmacy, China Medical University, Taichung 40001, Taiwan*
[5] *School of Health, National Taichung University of Science and Technology, Taichung 40401, Taiwan*
[6] *Department of Veterinary Medicine, National Chung Hsing University, Taichung 40001, Taiwan*
[7] *Graduate Institute of Biomedical Sciences, National Chung Hsing University, Taichung 40001, Taiwan*

Correspondence should be addressed to Kuan-Chih Chow, kcchow@dragon.nchu.edu.tw

Received 13 March 2012; Accepted 23 April 2012

Academic Editor: Paul Siu-Po Ip

Alzheimer's disease (AD) is an irreversible neurodegenerative disorder characterized by amyloid accumulation, neuronal death, and cognitive impairments. Yi-Chi-Tsung-Ming-Tang (YCTMT) is a traditional Chinese medicine and has never been used to enhance cognitive function and treat neurodegenerative disorders such as senile dementia. Whether YCTMT has a beneficial role in improving learning and memory in AD patients remains unclear. The present study showed that oral administration of YCTMT ameliorated amyloid-β- ($A\beta_{1-40}$) injection-induced learning and memory impairments in rats, examined using passive avoidance and Morris water-maze tests. Immunostaining and Western Blot results showed that continuous $A\beta_{1-40}$ infusion caused amyloid accumulation and decreased acetylcholine level in hippocampus. Oral administration of medium and high dose of YCTMT 7 days after the $A\beta_{1-40}$ infusion decreased amyloid accumulation area and reversed acetylcholine decline in the $A\beta_{1-40}$-injected hippocampus, suggesting that YCTMT might inhibit $A\beta$ plague accumulation and rescue reduced acetylcholine expression. This study has provided evidence on the beneficial role of YCTMT in ameliorating amyloid-induced AD-like symptom, indicating that YCTMT may offer an alternative strategy for treating AD.

1. Introduction

Alzheimer's disease (AD) is a progressive neurodegenerative disorder that gradually impairs memory and cognition [1]. It has been estimated that about 5% of the population older than 65 years is affected by AD [2]. The incidence of AD doubles every 5 years and 1275 new cases diagnosed yearly per 100,000 persons older than 65 [3]. In 2010, the number of worldwide AD patients has reached 35 million [4, 5]. The high cost spending on AD treatment and patient care makes AD become one of the most challenging brain disorders in elder human and causes tremendous financial burden.

AD is characterized by cognitive impairment, memory loss, dementia in neuropsychology, and intracellular neurofibrillary tangles and senile plaques in histopathology [6, 7]. During the progress of AD, short-term memory is first affected due to neuronal dysfunction and degeneration in the hippocampus and amygdala. The pathogenic mechanisms of AD include impaired cholinergic function, increased oxidative stress, induction of the amyloid cascade (i.e., amyloid

beta, Aβ, deposition, and plaque formation), expression of inflammatory mediators, deficiencies in steroid hormones, and appearance of glutamate-mediated excitotoxicity [2]. The amyloid cascade hypothesis, which suggests a pivotal role for Aβ in the pathogenesis of AD, is accepted by most investigators in this field [8]. Aβ is the major component of the senile plaques [9–11], and extensive studies have indicated that Aβ peptides contribute to the neuronal cell loss and pathogenesis of AD [12, 13].

Aβ_{1-40} is a prone-to-aggregation product of amyloid precursor protein (APP) proteolytic cleavage [14, 15] and has been shown to have a toxic effect on endothelial cells in cerebral circulation in vitro [16]. Direct injection of synthetic Aβ_{1-40} into particular brain regions has been used to induce AD-like pathological changes in animal model [17]. Recently, Passos and colleagues described a mouse model of acute inflammation induced by Aβ_{1-40} intracerebroventricular injection that appears to mimic the early phase of AD progression [18, 19]. Increased oxidative stress owning to lipid peroxidation, protein oxidation, and hydrogen peroxide formation may also be involved in Aβ-induced neurotoxicity [20]. Indeed, antioxidant therapy prevents the learning and memory deficits induced by Aβ in rats [21], and it also delays the clinical progression of the disease in humans [22]. Proteomic analysis using peptide mass fingerprint (PMF) has also revealed Aβ_{1-40}-induced changes in protein expression in the rat hippocampus [23].

Acetylcholine (Ach), a neurotransmitter of cholinergic system, influences neuron plasticity and plays an important role in cognition and memory [24, 25]. Aβ deposition is closely associated with dysfunction and degeneration of cholinergic neuronal circuits in the basal forebrain nuclei and also results in deficit of Ach in cortical and hippocampal areas [26]. Consistently, upregulation of acetylcholinesterase, an enzyme that catalyzes the hydrolysis of Ach, has been reported within and around amyloid plaques [27], and upregulation of its activity has also been shown to encourage the assembly of Aβ into fibrils that lead to Aβ toxicity [28]. The level of Ach has also been shown to be related to the degree of amnesia and Aβ depositions in the AD brain [29]. All these studies suggest that Ach plays an important role in AD [30, 31].

While up to now there has been no effective treatment for AD, targeting Aβ production and reversing Ach diminution are attractive therapeutic strategies for AD [32, 33]. In addition, alternative medicines that improve AD symptom have also been recently identified and they are natural and may be safer and more effective than currently commercialized drugs for AD [32, 33]. YCTMT was first introduced by an ancient Chinese physician, Dong-Yuan Li, in Jin Dynasty (AD 1200s). YCTMT is a decoction made of various Chinese herbs including *Astragali radix*, *Ginseng radix*, *Puerariae radix*, *Paeoniae lactiforae*, *Phellodendri contex*, *Viticis fructus*, *Cimicifugae uralensis*, and *Glycyrrhiza uralensis*. Ginseng can reduce oxidative stress that damages neuroplasticity, neurogenesis, and memory formation [34, 35]. In addition, Ginseng has also been shown to promote axonal and dendritic extension [36]. Astragalus promotes axonal maturation and prevents memory loss in mice [37]. Puerarin and Glycyrrhiza have been shown to have neuroprotective effects against Aβ treatment in mouse model [38, 39]. According to the theory of Dr. Li, Yi-Chi-Tsung-Ming-Tang (YCTMT, also known as Yiqicongming decoction) treats or prevents dizziness, tinnitus, and blurred vision. Therefore, it is intriguing to know whether YCTMT also has a beneficial effect on ameliorating AD-related symptoms. The aim of this study was to evaluate the effect of YCTMT treatment on Aβ_{1-40}-induced AD-like symptoms and possible underlying mechanism.

2. Materials and Methods

2.1. Drugs and Reagents. YCTMT is composed of *Astragali radix*, *Ginseng radix*, *Puerariae radix*, *Paeoniae lactiforae*, *Phellodendri contex*, *Viticis fructus*, *Cimicifugae uralensis*, and *Glycyrrhiza uralensis* in a ratio of 5 : 5 : 5 : 1 : 1 : 1.5 : 3 : 5 (dry weight). All components were purchased from a Chinese herbal shop in Taichung city, Taiwan, and confirmed by Professor Ming-Tsuen Hsieh. YCTMT (0.5 kg) was prepared as a mixture of all above components and extracted with 5 L distilled water at 100°C. The liquid extract was powdered by heating in a rotary vacuum evaporator. In the study, YCTMT powder was dissolved in distilled water to make the final concentrations at 0.5, 1.0, and 2.0 g/mL. Aβ_{1-40} was purchased from Tocris Bioscience (Ellisville, MO, USA) and dissolved in a vehicle containing 35% acetonitrile and 0.1% trifluoroacetic acid. Other chemicals were purchased from Sigma-Aldrich (St Louis, MO, USA).

2.2. Animals. Adult male Sprague-Dawley (S.D.) rats (200–250 g) were purchased from BioLASCO (Taipei, Taiwan). The rats were maintained on a standard diet with water *ad libitum* and housed under a 12 : 12 light-dark cycle in a temperature-controlled environment (23 ± 1°C). The animals were cared in accordance with guidelines provided by the Institutional Animal Ethics Committee of China Medical University (Taichung, Taiwan).

2.3. Rat Model with AD-Like Phenotype. Rat model with AD-like phenotype was developed by infusing Aβ_{1-40} into cerebral ventricle in the brain as described previously [18, 19, 40]. Briefly, one week before experiment, animals were randomly divided into five groups ($n = 9$ for each group). At day 0, rats were anaesthetized with phenobarbital (45 mg/kg, i.p.), placed in a Narishige stereotaxic instrument with the head being fixed. The skull was opened carefully, and a cannula was implanted into the right ventricle at coordinates: A − 1.4, L ± 2.4, and V 7.2, using an atlas [41]. At day 1, vehicle or Aβ_{1-40} was continuously administered (25 pM/day) intraventricularly at an infusion rate of 0.5 μL/h for three weeks via the cannula that was powered by a miniosmotic pump (model 2002, Alzet, CA, USA). The control rats were infused with the vehicle only. From the 8th day, rats were fed with YCTMT (0.5, 1.0, and 2.0 g/kg/day) orally once a day. The experimental scheme was presented in Figure 1.

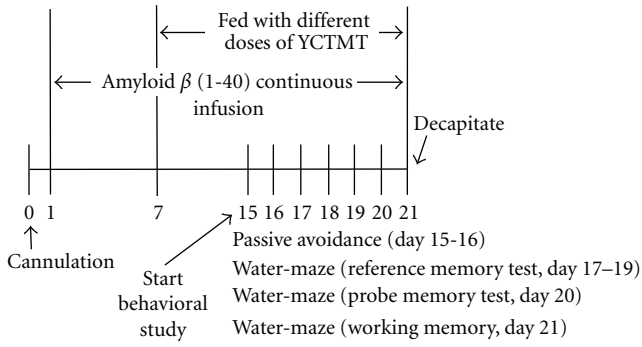

Figure 1: Experimental scheme.

2.4. Passive Avoidance Test. The passive avoidance test was performed at day 15 and 16 after surgery according to step-through passive avoidance task previously described [42]. Briefly, the guillotine door connecting the light and dark space was closed during the trial training. When a rat was placed in the light space, with its back facing the guillotine door, the door was opened. The time of step-through latency (STL) taken by the rat to enter the light space was measured with a stopwatch. Once the rat entered the dark space, the door was closed. An inescapable scrambled foot-shock (1.0 mA for 2 s) was then delivered through the grid floor. The rat was removed from the dark space 5 seconds after the shock was administered. Then, the rat was put back into the home cage until the retention trial was over.

2.5. Morris Water-Maze Test. A Morris water-maze test was used in the study to assess the memory capability [43, 44]. In brief, the apparatus consisted of a circular water tank (180 cm in diameter, 60 cm in height, filled with water in a depth of 50 cm, at 28 ± 1°C) with a platform (11 cm in diameter) set under the water. Morris water-maze is a swimming-based model in which animals must learn to escape from water and step onto the platform. An escape platform was placed in a constant position in the center of one of the four quadrants of the tank and 1 cm below the water surface. For reference memory test, the rats were trained for 3 days (starting from day 17 to 19), 120 s per trial, and 4 trials per day starting at four different positions with 30 min intervals (Figure 1). If the rats could not find the hidden platform within each training session (120 s), the animals were led to it. If the rats swam onto the platform within 120 s, the rat was allowed to stay on the platform for 30 s then returned to home cage. In each training session, the latency to escape onto the hidden platform was recorded. For probe memory test, the hidden platform was removed on day 20, and memory retrieval was examined by a probe trail that lasted for 120 s in the pool. The time at which the animals crossed the annulus where the platform had been located was assigned. Twenty-four hours after probe trial, working memory (reacquisition) test was performed by measuring the time each rat spent in the new quadrant of the target platform.

2.6. Immunohistochemical Detection for Aβ and Ach Expression in Brain. Rats were sacrificed at day 21 with pentobarbital (90 mg/kg, i.p.) and perfused transcardially with saline, followed by 4% paraformaldehyde in saline. After postfixation, the whole brain was removed and prepared for paraffin slice. Brain sections with 5 μm thickness were obtained on a microtome (Leica 2030 Biocut) at 1-mm interval from the stereotaxic coordinates between −1.46 mm and −3.40 mm Bregma. Brain sections were deparaffinized in xylene, rehydrated in a series of ethanol, and endogenous peroxidase quenched with 1% (v/v) H_2O_2 in methanol and microwaved for 15 min (with 650 W) in 0.01 M citrate buffer (pH 6.0). Nonspecific binding sites were blocked by blocking buffer containing 10% (v/v) goat normal serum and 0.1% Triton X-100 in PBS for 60 min at room temperature. Antibodies against Aβ (1 : 300 dilution, Convance, no. SIG-39220) and Ach (1 : 300 dilution, Chemicon, Billerica, MA, USA) were applied to sections overnight at 4°C. Sections were washed with PBS, incubated with biotinylated secondary antibody for 2 hr at 25°C, washed, and placed in avidin-peroxidase conjugate solution for 1 hr. The horseradish peroxidase reaction was detected with 0.05% diaminobenzidine and 0.03% H_2O_2. The reaction was stopped with H_2O, and sections were dehydrated in an ethanol series, cleared in xylene, and coverslipped in permanent mounting solution. Protein expression area in each brain section was measured according to Lim et al. [45] and Liao et al. [46] with slight modification. Briefly, a full brain middle section area was measured by an image analyzer (Leica, Q500MC, Nussloch, Germany). Brain sections of each rat group were measured under 40x magnification, and at least 20 fields from each brain section were counted. The permillage of Aβ- or Ach-positive areas was calculated using the following equation: ‰of Aβ or Ach area = (sum of Aβ- or Ach-positive area/total area of brain section) ×1000‰.

2.7. Western Blot. Protein extraction was performed in RIPA lysis Buffer 50 mM Tris, pH 7.4, 150 mM NaCl, 1% NP-40, 0.5% sodium deoxycholate, 0.1% SDS, protease inhibitor cocktail (sodium orthovanadate, sodium fluoride, EDTA, leupeptin), and 1 mM PMSF. Quantification of protein was performed using the BCA Protein Assay Kit (Beyotime). Equal amounts of protein samples were separated on 12% SDS-PAGE gels and transferred onto a PVDF membrane at 0.8 mA/cm^2 for 1.5 h. The membrane was blocked with 5% nonfat milk in a 20 mM Tris-HCl (pH 7.4) containing 150 mM NaCl and 0.05% Tween20 (TBS-T) for 1 h at RT and incubated with the primary antibodies: β-amyloid antibody (1 : 1000 dilution, Abcam, Cambridge, MA, USA), antiacetylcholine (Chemicon, no. MAB5302.), and β-actin (abs, no. abs-24) at 4°C overnight. After being washed with TBS-T, the membrane was incubated with HRP-conjugated IgG (MILLIPORE, Chemiluminescent HRP Substrate, no. WBKLS0500) for 1 h at RT, washed with TBS-T again, and detected by ECL (Thermo Scientific). Densitometric quantitation was analyzed with FUJIFILM, Multi Gauge V3.0 Software, and standardized with β-actin. All Western Blotting samples were run in triplicate.

2.8. Statistical Analysis. All of the data obtained were expressed as mean ± standard errors of means (SEM) and analyzed using one-way analysis of variance (ANOVA), followed by post hoc between-group analyses using Scheffé's test for multigroup comparisons. The criterion for statistical significance was $P < 0.05$ in all evaluation.

3. Results

3.1. YCTMT Posttreatment Reversed $A\beta_{1-40}$-Mediated Impairment in Memory Retention. Result from passive avoidance test showed that at day 15 after $A\beta_{1-40}$ infusion significantly reduced the step through latency (STL) of treated mice compared to the vehicle injection ($P < 0.05$, Figure 2), suggesting an $A\beta_{1-40}$-induced impairment in memory retention after 2-week continuous injection. YCTMT posttreatment for 7 days with doses of 1.0 and 2.0 g/kg/day, but not 0.5 g/kg/day, significantly attenuated $A\beta_{1-40}$-mediated reduction in STL ($P < 0.05$, Figure 2), indicating that YCTMT reversed $A\beta_{1-40}$-mediated impairment in a dose-dependent manner. There was no significant difference between the control and YCTMT-treated groups at 1.0 and 2.0 g/kg/day. This result suggested that treatment with YCTMT recovered $A\beta_{1-40}$-induced deficit in memory retention in rats.

3.2. YCTMT Effectively Reversed $A\beta_{1-40}$-Induced Impairments in Learning and Memory. To further evaluate the therapeutic effect of YCTMT on $A\beta_{1-40}$-induced impairments in learning and memory, Morris water maze test was conducted. In reference memory test, these $A\beta_{1-40}$-treated animals showed significantly longer escape latency than normal control animals at day 17, 18, and 19 postinfusion of amyloid (Figure 3(a)). Posttreatment of YCTMT with the lowest dose of 0.5 g/kg/day showed no effect on $A\beta_{1-40}$-caused deficits. However, YCTMT treatment at dose of 1.0 g/kg/day significantly reduced escape latency in $A\beta_{1-40}$-treated rats at day 17 and 19, but not at day 18. Posttreatment with 2.0 g/kg/day YCTMT reversed increased escape latency caused by $A\beta_{1-40}$ injection at all three test days (day 17 to 19), and the latency reached the level as short as that of normal control. These results indicated that $A\beta_{1-40}$-induced impairments in spatial learning memory were reversed by posttreatment with YCTMT in a dose-dependent manner.

The beneficial effect of YCTMT on $A\beta_{1-40}$-induced learning deficit was further analyzed using probe and working memory tests. The number of annulus crossing, referred to the number of passing over the previous platform site, was measured at day 20. Result showed that number of annulus crossings in $A\beta_{1-40}$-treated group was significantly lower than that of control group, whereas YCTMT posttreatment significantly elevated the number in a dose-dependent manner and showed significance at 1.0 and 2.0 g/kg/day ($P < 0.05$, Figure 3(b)). Compared to the control group, $A\beta_{1-40}$-treated group also showed significantly longer escape latency to found the platform at a constant location and to find the hidden platform at a new location during the reference memory test (day 17–19, Figure 3(a)) and during the working memory test (day 21, Figure 3(c)), respectively,

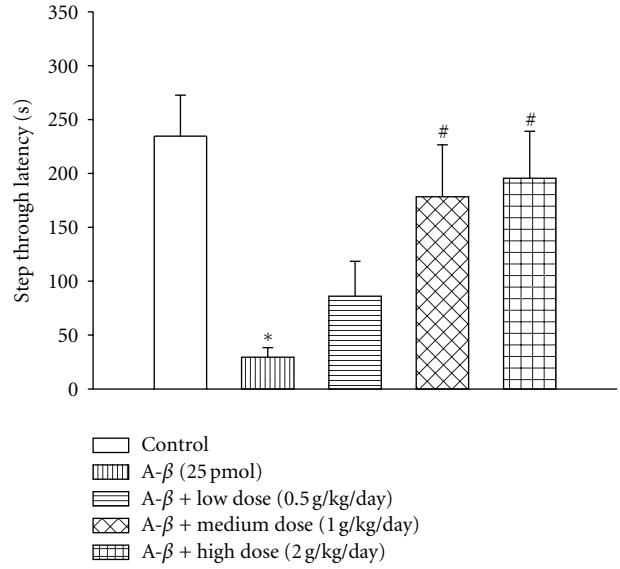

Figure 2: Passive avoidance test at day 15 after $A\beta_{1-40}$ infusion. $A\beta_{1-40}$ infusion reduced step-through latency of rats, and it was restored by YCTMT posttreatment ($n = 9$ for each group). YCTMT (0.5, 1.0, and 2.0 g/kg/day) was administrated for a week before test. *Represents significant difference between the indicated and normal control group; #between the indicated and $A\beta_{1-40}$ group, $P < 0.05$.

suggesting the $A\beta_{1-40}$-induced impairments in reference and working memory in injected rats. Posttreatment with YCTMT at dose of 1.0 and 2.0 g/kg/day significantly reversed $A\beta_{1-40}$-caused increase of escape latency. These results again demonstrated that YCTMT was able to ameliorate $A\beta_{1-40}$-caused impairment in learning and memory in a variety of forms.

3.3. YCTMT Significantly Decreased $A\beta_{1-40}$-Induced Aβ Plaque Area. To investigate the effect of YCTMT posttreatment on amyloid protein burden in the brain, sections were analyzed with immunohistochemical staining. 4G8 antibody against amino acid residues 17–24 of beta-amyloid was used in the study (Figures 4(a)–4(e)). Intracerebroventricular (i.c.v.) administration of $A\beta_{1-40}$significantly increased Aβ plaque area (arrow in Figure 4(b)) in hippocampus compared with vehicle injection in the control group (Figure 4(a)). Amyloid accumulation was shown in brown and located in the hippocampus. Treatment with 1.0 and 2.0 g/kg/day YCTMT reduced the amyloid-accumulated area, showing as decreased size of 4G8-positive area in hippocampus (Figures 4(d) and 4(e)). Quantitative analysis showed that YCTMT treatment reduced Aβ plaque area in hippocampus in a concentration-dependent manner (Figure 4(f)). This result suggests that the beneficial effect of YCTMT on $A\beta_{1-40}$-induced impairment in cognition might be mediated by reducing Aβ accumulation in the hippocampus.

3.4. YCTMT Significantly Reversed $A\beta_{1-40}$-Induced Decrement of Ach Area. Ach is an important neurotransmitter and

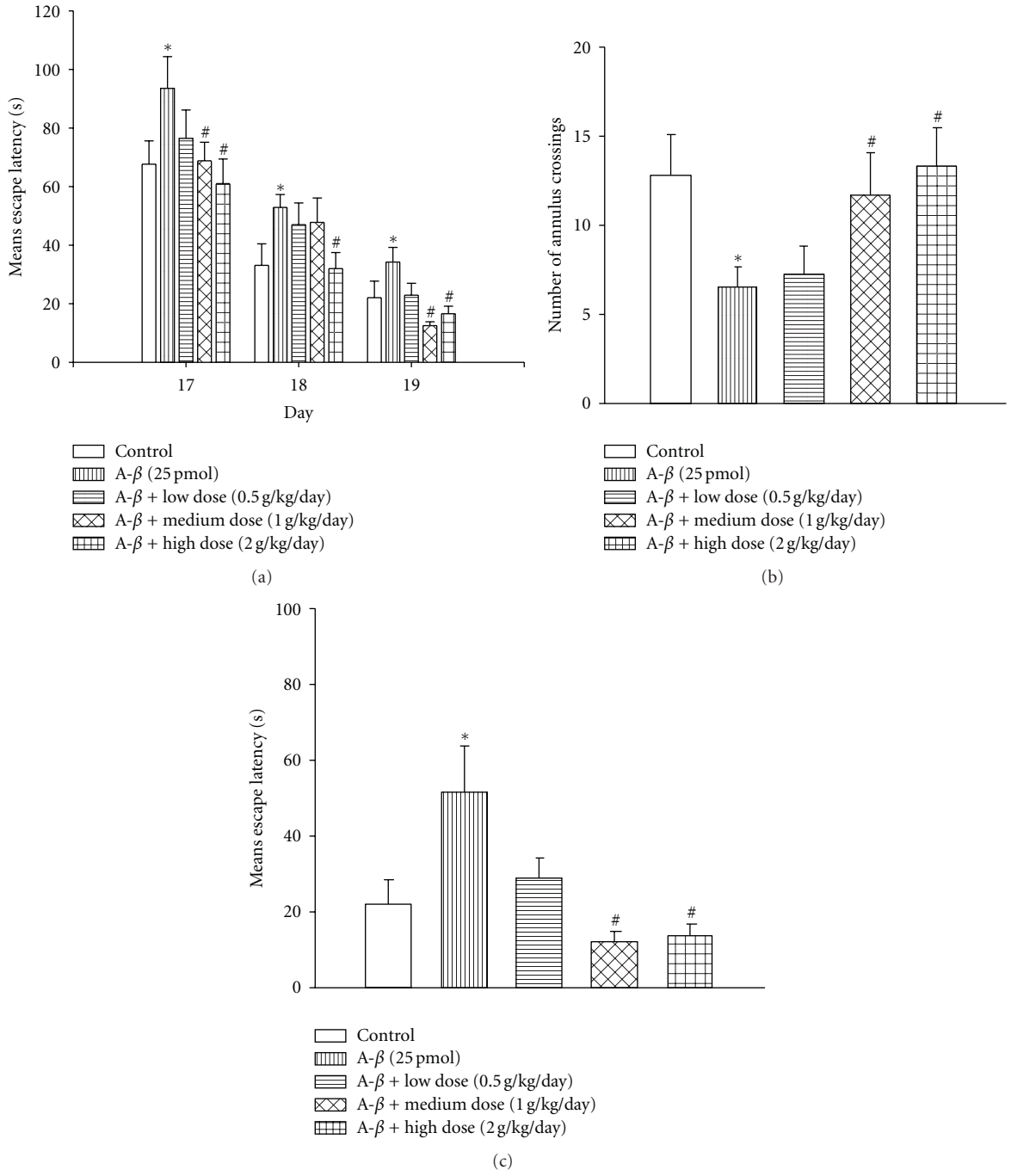

Figure 3: YCTMT posttreatment improved memory of $A\beta_{1-40}$-infused rat in Morris water-maze test. (a) Reference memory test at day 17–19. (b) Probe test at day 20. (c) Working memory test at day 21. $A\beta_{1-40}$-infused rats were administrated with YCTMT (0.5, 1.0, and 2.0 g/kg/day) before tests. *Represents significant difference between the sham and $A\beta_{1-40}$ on the same day; #is for the comparison between $A\beta_{1-40}$ and $A\beta_{1-40}$ + YCTMT on the same day, $P < 0.05$.

plays critical roles in the formation of learning/memory and etiology of Alzheimer's disease [47]. To explore the possible mechanism of YCTMT-mediated beneficial role in relieving AD-like symptom, we further evaluated Ach expression using immunohistochemical analysis (Figure 5) and Western Blot (Figure 6). Injection of $A\beta_{1-40}$ significantly decreased Ach expression in hippocampus compared with the control group (Figures 5(a) and 5(b)). Quantitative data showed that YCTMT reversed Ach area in a concentration-dependent manner in the whole brain. Treatment with 1.0 and 2.0 g/kg/day YCTMT significantly reversed the expression of Ach in the brain (Figures 5(d) and 5(e)). YCTMT-induced reversal of Ach expression level after $A\beta_{1-40}$ injection was also confirmed with Western Blot. Quantitative

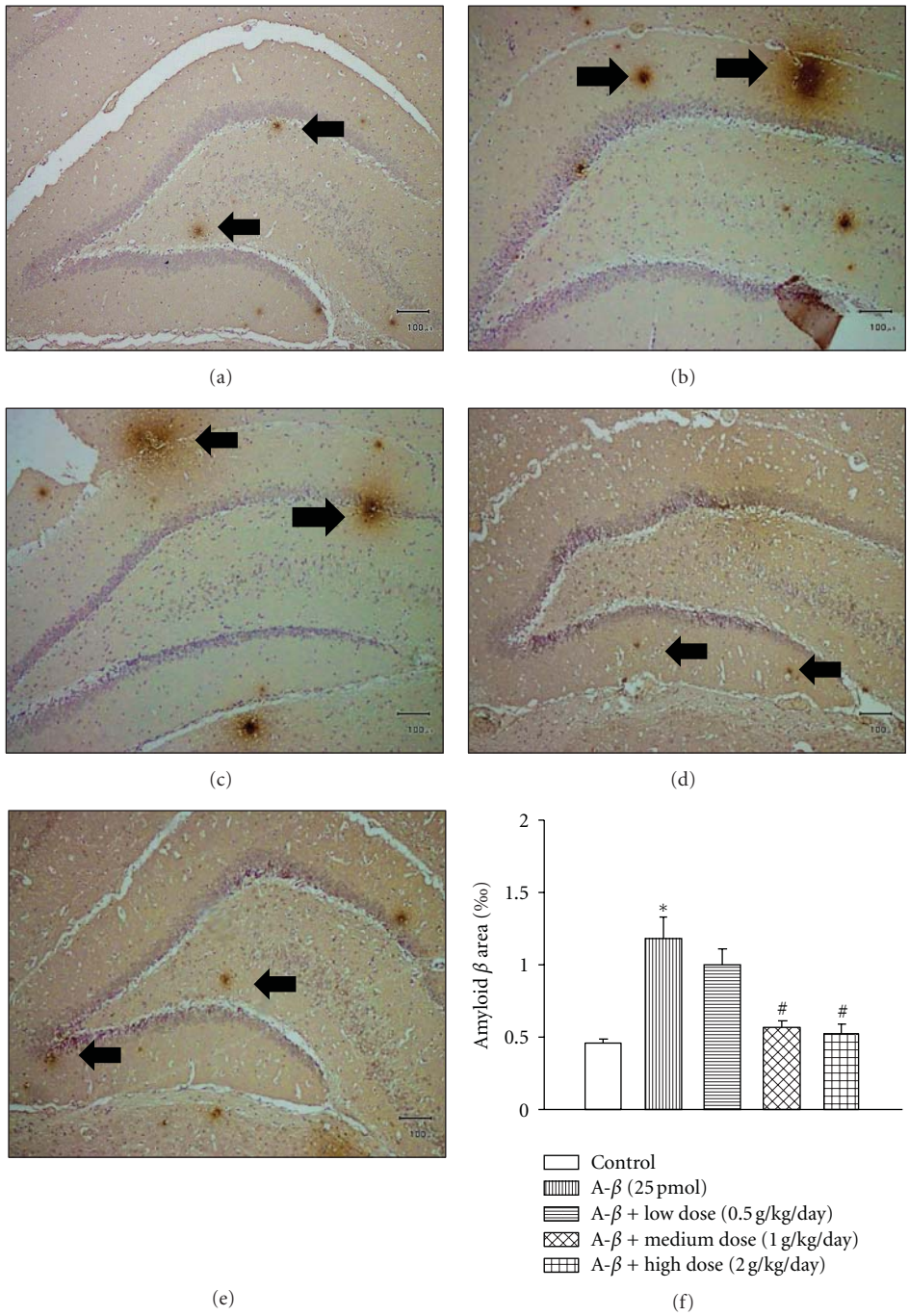

FIGURE 4: YCTMT posttreatment decreased Aβ_{1-40}-induced amyloid accumulation. (a) Control. (b) Aβ_{1-40} infusion (25 pmol). (c)–(e) YCTMT treatment with doses of 0.5, 1.0, and 2.0 g/kg/day. (f) Quantification of amyloid accumulation area. *Represents significant difference between the indicated and normal control group; #between the indicated and Aβ_{1-40} group, $P < 0.05$. The scale bar represents 100 μm.

result of Western Blot showed that medium- and high-dose YCTMT treatment rescued reduced Ach expression (Figure 6(c)), suggesting the beneficial effect of YCTMT on AD-like symptom. This result suggested that posttreatment with YCTMT could reverse Aβ_{1-40}-reduced diminish of Ach expression correlated with functional deficit in the AD brain.

We also found that there was a correlation between amyloid plaque area and acetylcholine expression site ($R = 0.719$).

4. Discussion

In this study, we observed a beneficial effect of YCTMT posttreatment on Aβ_{1-40}-induced AD-like symptoms. YCTMT treatment decreased Aβ_{1-40}-induced amyloid burden and reversed declined Ach level in hippocampus. It also improved learning and memory function in treated rats in a dose-dependent manner. These results provide evidence of the

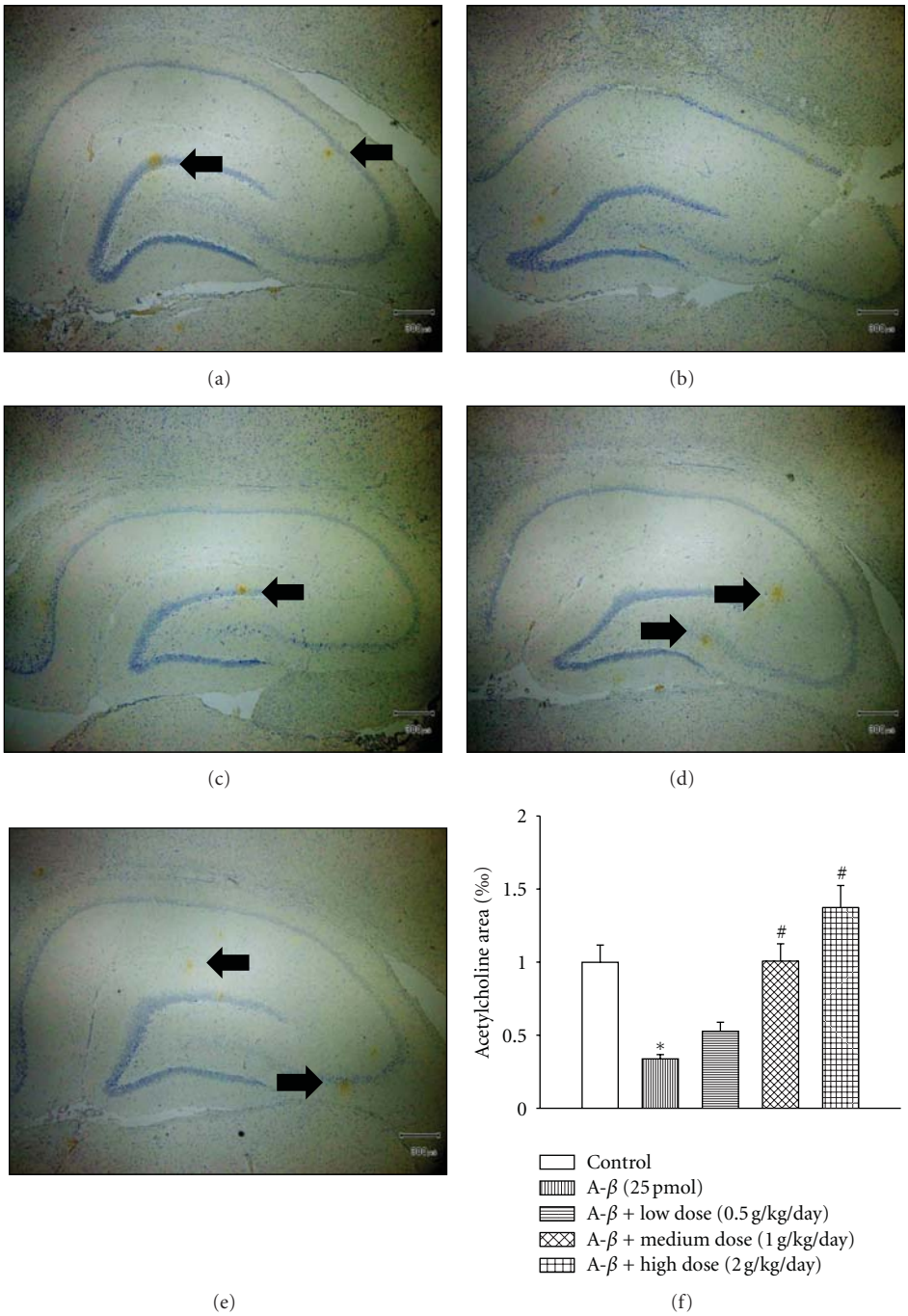

Figure 5: YCTMT posttreatment reversed $A\beta_{1-40}$-induced decreases of Ach level. (a) Control. (b) $A\beta_{1-40}$ infusion (25 pmol). (c)–(e) YCTMT treatment with doses of 0.5, 1.0, and 2.0 g/kg/day, respectively. (f) Quantification of Ach expression. *Represents significant difference between the indicated and normal control group; #between the indicated and $A\beta_{1-40}$ group, $P < 0.05$. The scale bar represents 100 μm.

therapeutic effect of YCTMT on AD and suggest a potential treatment strategy.

Investigators have established that toxic Aβ is the major player in neuronal damage and dementia in both in vitro culture assays and in the intact brain of animal [48]. Notably, i.c.v. injections of $A\beta_{1-40}$ into rats produced learning disability, brain morphological changes, and cholinergic neuronal degeneration [49]. In addition, $A\beta_{1-40}$ induces spatial learning and spatial working memory deficits in animal model [50]. In the present study, we confirmed that continuous infusion of $A\beta_{1-40}$ into the cerebral ventricle induced deficits in memory retention, spatial learning memory, probe memory, and working memory in the rats. Moreover, posttreatment with YCTMT reversed various types of learning

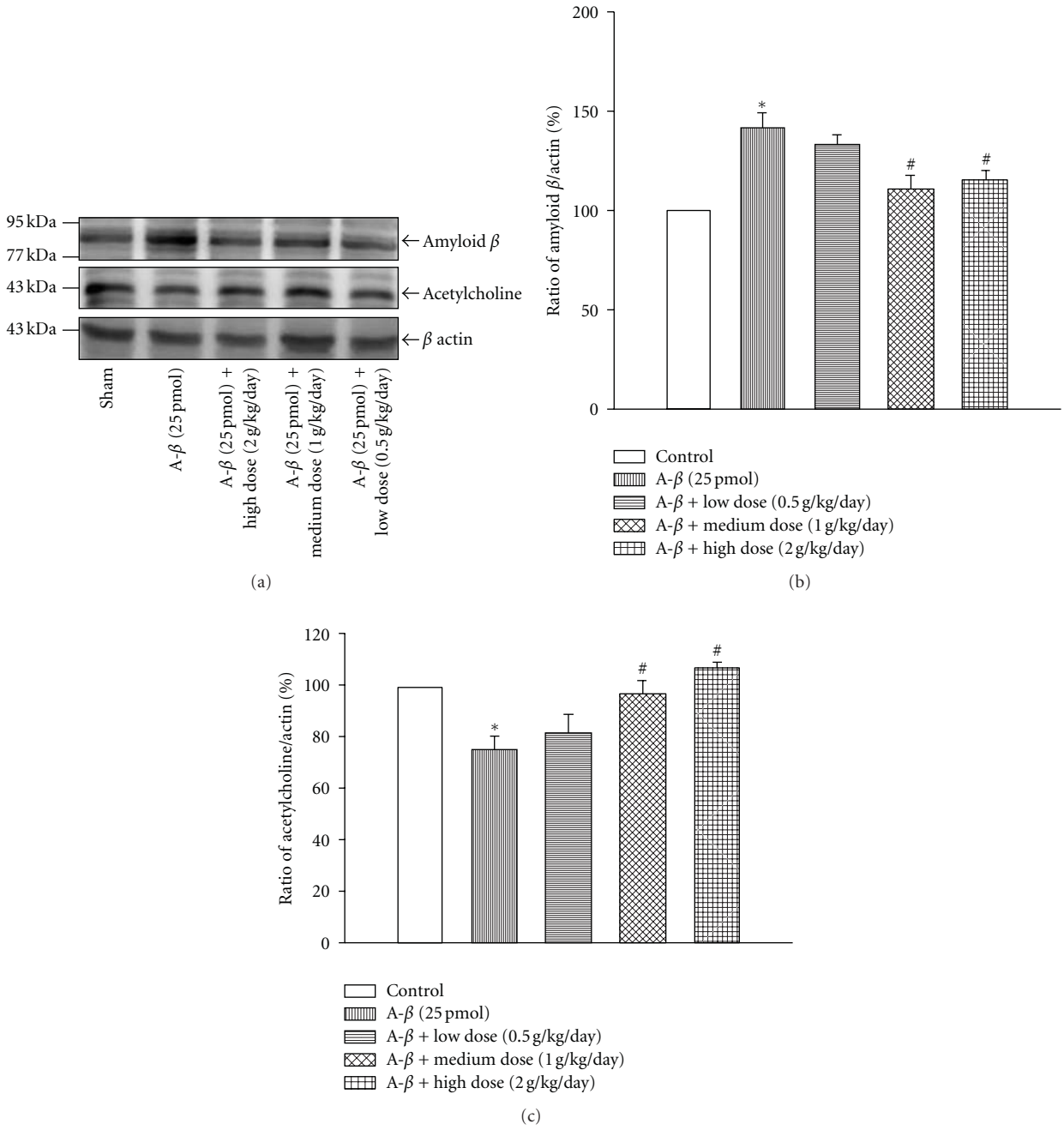

Figure 6: YCTMT posttreatment reversed $A\beta_{1-40}$ and Ach protein level. (a) Comparison of protein level of beta-amyloid and Ach using Western Blot. (b) Quantification of amyloid protein level. (c) Quantification of Ach protein level. *represents significant difference between the indicated and normal control group; #between the indicated and $A\beta_{1-40}$ group, $P < 0.05$.

and memory loss caused by $A\beta_{1-40}$. These results indicated that YCTMT might have beneficial anti-Alzheimer's disease effects on $A\beta_{1-40}$-induced AD animal model.

We also found that i.c.v. administration of $A\beta_{1-40}$-induced $A\beta$ plague formation was consistent with previous report [15, 18–20, 22]. Both WB and immunostaining results showed that posttreatment with YCTMT for 7 days downregulated $A\beta$ burden in the rat brain. $A\beta_{1-40}$ contributes to the progression of AD and directly impairs cholinergic signaling and Ach release [51]. Activities of choline acetyltransferase and acetylcholinesterase, one for synthesis and the other for hydrolysis of acetylcholine, decrease significantly and correlate with the extent of intellectual impairment in Alzheimer's dementia patients [52]. Coincidently, we also found that posttreatment with YCTMT recovered the expressions of Ach in the rat brains that were challenged with $A\beta_{1-40}$. These results implied that YCTMT might reduce the production of $A\beta$ plaque, possibly through increasing the expression of

Ach. However, the mechanisms underlying the influence of Ach expression need further study.

Traditional Chinese Medicine (TCM) has been around for thousands of years and extensively used in the prevention, diagnosis, and treatment of diseases in China. There are several TCMs that have been used to enhance cognitive function and senile dementia [53]. YCTMT is one of the TCMs and has been conventionally used in the improvement of visual acuity and hearing in purpose. Our results provided new evidence of the beneficial role of YCTMT in AD-associated learning and memory deficits. Oral administration of YCTMT in S.D. rats appeared to reverse the $A\beta_{1-40}$-impaired memory, spatial learning memory, probe memory, and working memory deficits. YCTMT might inhibit $A\beta$ plague accumulation and reverse Ach decline. This study suggests a potential use of YCTMT as a potential therapeutic agent for treating AD.

5. Conclusion

We have shown that YCTMT inhibits $A\beta$ plague accumulation and rescues reduced acetylcholine expression. This study has provided evidence on the beneficial role of YCTMT in ameliorating amyloid-induced AD-like symptom, indicating that YCTMT may offer an alternative strategy for treating AD.

Acknowledgment

This study was supported by the Show Chwan Memorial Hospital, Changhua, Taiwan (Grants RD96007 and RD97022).

References

[1] G. Stuchbury and G. Münch, "Alzheimer's associated inflammation, potential drug targets and future therapies," *Journal of Neural Transmission*, vol. 112, no. 3, pp. 429–453, 2005.

[2] R. S. Shah, H. G. Lee, Z. Xiongwei, G. Perry, M. A. Smith, and R. J. Castellani, "Current approaches in the treatment of Alzheimer's disease," *Biomedicine and Pharmacotherapy*, vol. 62, no. 4, pp. 199–207, 2008.

[3] D. Hirtz, D. J. Thurman, K. Gwinn-Hardy, M. Mohamed, A. R. Chaudhuri, and R. Zalutsky, "How common are the "common" neurologic disorders?" *Neurology*, vol. 68, no. 5, pp. 326–337, 2007.

[4] T. Mura, J. F. Dartigues, and C. Berr, "How many dementia cases in France and Europe? Alternative projections and scenarios 2010–2050," *European Journal of Neurology*, vol. 17, no. 2, pp. 252–259, 2010.

[5] H. W. Querfurth and F. M. LaFerla, "Alzheimer's disease," *The New England Journal of Medicine*, vol. 362, no. 4, pp. 329–344, 2010.

[6] G. Münch, R. Schinzel, C. Loske et al., "Alzheimer's disease—synergistic effects of glucose deficit, oxidative stress and advanced glycation endproducts," *Journal of Neural Transmission*, vol. 105, no. 4-5, pp. 439–461, 1998.

[7] W. Retz, W. Gsell, G. Münch, M. Rösler, and P. Riederer, "Free radicals in Alzheimer's disease," *Journal of Neural Transmission, Supplement*, vol. 54, pp. 221–236, 1998.

[8] H. W. Klafki, M. Staufenbiel, J. Kornhuber, and J. Wiltfang, "Therapeutic approaches to Alzheimer's disease," *Brain*, vol. 129, no. 11, pp. 2840–2855, 2006.

[9] G. Habicht, C. Haupt, R. P. Friedrich et al., "Directed selection of a conformational antibody domain that prevents mature amyloid fibril formation by stabilizing $A\beta$ protofibrils," *Proceedings of the National Academy of Sciences of the United States of America*, vol. 104, no. 49, pp. 19232–19237, 2007.

[10] R. Rönicke, A. Klemm, J. Meinhardt, U. H. Schröder, M. Fändrich, and K. G. Reymann, "$A\beta$ mediated diminution of MTT reduction—an artefact of single cell culture?" *PLoS ONE*, vol. 3, no. 9, Article ID e3236, 2008.

[11] A. Eckert, S. Hauptmann, I. Scherping et al., "Oligomeric and fibrillar species of β-amyloid ($A\beta$42) both impair mitochondrial function in P301L tau transgenic mice," *Journal of Molecular Medicine*, vol. 86, no. 11, pp. 1255–1267, 2008.

[12] H. C. Huang and Z. F. Jiang, "Accumulated amyloid-β peptide and hyperphosphorylated tau protein: relationship and links in Alzheimer's disease," *Journal of Alzheimer's Disease*, vol. 16, no. 1, pp. 15–27, 2009.

[13] M. Sánchez-Alavez, R. A. Gallegos, M. A. Kalafut, D. Games, S. J. Henriksen, and J. R. Criado, "Loss of medial septal modulation of dentate gyrus physiology in young mice overexpressing human β-amyloid precursor protein," *Neuroscience Letters*, vol. 330, no. 1, pp. 45–48, 2002.

[14] S. S. Sisodia and P. H. St George-Hyslop, "γ-secretase, Notch, $A\beta$ and Alzheimer's disease: where do the presenilins fit in?" *Nature Reviews Neuroscience*, vol. 3, no. 4, pp. 281–290, 2002.

[15] E. Tamagno, M. Guglielmotto, M. Aragno et al., "Oxidative stress activates a positive feedback between the γ- and β-secretase cleavages of the β-amyloid precursor protein," *Journal of Neurochemistry*, vol. 104, no. 3, pp. 683–695, 2008.

[16] K. Niwa, G. A. Carlson, and C. Iadecola, "Exogenous Aβ1-40 reproduces cerebrovascular alterations resulting from amyloid precursor protein overexpression in mice," *Journal of Cerebral Blood Flow and Metabolism*, vol. 20, no. 12, pp. 1659–1668, 2000.

[17] G. Cantarella, D. Uberti, T. Carsana, G. Lombardo, R. Bernardini, and M. Memo, "Neutralization of TRAIL death pathway protects human neuronal cell line from β-amyloid toxicity," *Cell Death and Differentiation*, vol. 10, no. 1, pp. 134–141, 2003.

[18] R. Medeiros, R. D. S. Prediger, G. F. Passos et al., "Connecting TNF-α signaling pathways to iNOS expression in a mouse model of Alzheimer's disease: relevance for the behavioral and synaptic deficits induced by amyloid β protein," *Journal of Neuroscience*, vol. 27, no. 20, pp. 5394–5404, 2007.

[19] R. D. S. Prediger, R. Medeiros, P. Pandolfo et al., "Genetic deletion or antagonism of kinin B1 and B2 receptors improves cognitive deficits in a mouse model of Alzheimer's disease," *Neuroscience*, vol. 151, no. 3, pp. 631–643, 2008.

[20] D. A. Butterfield and C. M. Lauderback, "Lipid peroxidation and protein oxidation in Alzheimer's disease brain: potential causes and consequences involving amyloid β-peptide-associated free radical oxidative stress," *Free Radical Biology and Medicine*, vol. 32, no. 11, pp. 1050–1060, 2002.

[21] T. Nabeshima, "Protectiye effects of idebenone and α-tocopherol on β-amyloid-(1–42)-induced learning and memory deficits in rats: implication of oxidative stress in β-amyloid-induced neurotoxicity in vivo," *European Journal of Neuroscience*, vol. 11, no. 1, pp. 83–90, 1999.

[22] M. Sano, C. Ernesto, R. G. Thomas et al., "A controlled trial of selegiline, alpha-tocopherol, or both as treatment for

Alzheimer's disease," *The New England Journal of Medicine*, vol. 336, no. 17, pp. 1216–1222, 1997.

[23] X. Shi, X. Lu, L. Zhan et al., "Rat hippocampal proteomic alterations following intrahippocampal injection of amyloid beta peptide (1–40)," *Neuroscience Letters*, vol. 500, no. 2, pp. 87–91, 2011.

[24] Q. Gu, "Contribution of acetylcholine to visual cortex plasticity," *Neurobiology of Learning and Memory*, vol. 80, no. 3, pp. 291–301, 2003.

[25] M. Sarter, M. E. Hasselmo, J. P. Bruno, and B. Givens, "Unraveling the attentional functions of cortical cholinergic inputs: interactions between signal-driven and cognitive modulation of signal detection," *Brain Research Reviews*, vol. 48, no. 1, pp. 98–111, 2005.

[26] R. T. Bartus, R. L. Dean, B. Beer, and A. S. Lippa, "The cholinergic hypothesis of geriatric memory dysfunction," *Science*, vol. 217, no. 4558, pp. 408–417, 1982.

[27] R. Jazi, R. Lalonde, S. Qian, and C. Strazielle, "Regional brain evaluation of acetylcholinesterase activity in PS1/A246E transgenic mice," *Neuroscience Research*, vol. 63, no. 2, pp. 106–114, 2009.

[28] J. B. Melo, P. Agostinho, and C. R. Oliveira, "Involvement of oxidative stress in the enhancement of acetylcholinesterase activity induced by amyloid beta-peptide," *Neuroscience Research*, vol. 45, no. 1, pp. 117–127, 2003.

[29] F. A. Ling, D. Z. Hui, and S. M. Ji, "Protective effect of recombinant human somatotropin on amyloid β-peptide induced learning and memory deficits in mice," *Growth Hormone and IGF Research*, vol. 17, no. 4, pp. 336–341, 2007.

[30] N. Toda, T. Kaneko, and H. Kogen, "Development of an efficient therapeutic agent for alzheimer's disease: design and synthesis of dual inhibitors of acetylcholinesterase and serotonin transporter," *Chemical and Pharmaceutical Bulletin*, vol. 58, no. 3, pp. 273–287, 2010.

[31] K. Imahori, "The biochemical study on the etiology of Alzheimer's disease," *Proceedings of the Japan Academy B*, vol. 86, pp. 54–61, 2010.

[32] B. R. Ott and N. J. Owens, "Complementary and alternative medicines for Alzheimer's disease," *Journal of Geriatric Psychiatry and Neurology*, vol. 11, no. 4, pp. 163–173, 1998.

[33] M. T. Hsieh, W. H. Peng, C. R. Wu, K. Y. Ng, C. L. Cheng, and H. X. Xu, "Review on experimental research of herbal medicines with anti-amnesic activity," *Planta Medica*, vol. 76, no. 3, pp. 203–217, 2010.

[34] G. Zhang, A. Liu, Y. Zhou, X. San, T. Jin, and Y. Jin, "Panax ginseng ginsenoside-Rg2 protects memory impairment via anti-apoptosis in a rat model with vascular dementia," *Journal of Ethnopharmacology*, vol. 115, no. 3, pp. 441–448, 2007.

[35] J. T. Zhang, "Nootropic mechanisms of ginsenoside Rg1 influence on neuronal plasticity and neurogenesis," *Yaoxue Xuebao*, vol. 40, no. 5, pp. 385–388, 2005.

[36] C. Tohda, N. Matsumoto, K. Zou, M. R. Meselhy, and K. Komatsu, "Axonal and dendritic extension by protopanaxadiol-type saponins from Ginseng drugs in SK-N-SH cells," *Japanese Journal of Pharmacology*, vol. 90, no. 3, pp. 254–262, 2002.

[37] C. Tohda, T. Tamura, S. Matsuyama, and K. Komatsu, "Promotion of axonal maturation and prevention of memory loss in mice by extracts of Astragalus mongholicus," *British Journal of Pharmacology*, vol. 149, no. 5, pp. 532–541, 2006.

[38] J. Ahn, M. Um, W. Choi, S. Kim, and T. Ha, "Protective effects of Glycyrrhiza uralensis Fisch. on the cognitive deficits caused by β-amyloid peptide 25–35 in young mice," *Biogerontology*, vol. 7, no. 4, pp. 239–247, 2006.

[39] Y. Wu and H. Y. Wan, "Protective effect of puerarin on anoxia-reoxygenation induced cerebral cell injury in culture," *Chinese Pharmacological Bulletin*, vol. 22, no. 9, pp. 1130–1133, 2006.

[40] F. S. Tsai, H. Y. Cheng, M. T. Hsieh, C. R. Wu, Y. C. Lin, and W. H. Peng, "The ameliorating effects of luteolin on beta-amyloid-induced impairment of water maze performance and passive avoidance in rats," *American Journal of Chinese Medicine*, vol. 38, no. 2, pp. 279–291, 2010.

[41] G. Paxinos and C. Watson, *The Rat Brain in Stereotaxic Coordinates*, Elsevier, San Diego, Calif, USA, 2006.

[42] E. Suits and R. L. Isaacson, "The effects of scopolamine hydrobromide on one-way and two-way avoidance learning in rats," *Neuropharmacology*, vol. 7, no. 5, pp. 441–446, 1968.

[43] R. Morris, "Developments of a water-maze procedure for studying spatial learning in the rat," *Journal of Neuroscience Methods*, vol. 11, no. 1, pp. 47–60, 1984.

[44] M. Parle and N. Singh, "Animal models for testing memory," *Asia Pacific Journal of Pharmacology*, vol. 16, no. 2, pp. 101–120, 2004.

[45] G. P. Lim, F. Yang, T. Chu et al., "Ibuprofen suppresses plaque pathology and inflammation in a mouse model for alzheimer's disease," *Journal of Neuroscience*, vol. 20, no. 15, pp. 5709–5714, 2000.

[46] J. W. Liao, C. K. Hsu, M. F. Wang, W. M. Hsu, and Y. C. Chan, "Beneficial effect of Toona sinensis Roemor on improving cognitive performance and brain degeneration in senescence-accelerated mice," *British Journal of Nutrition*, vol. 96, no. 2, pp. 400–407, 2006.

[47] H. R. Parri and K. T. Dineley, "Nicotinic acetylcholine receptor interaction with β-amyloid: molecular, cellular, and physiological consequences," *Current Alzheimer Research*, vol. 7, no. 1, pp. 27–39, 2010.

[48] C. Haass and D. J. Selkoe, "Soluble protein oligomers in neurodegeneration: lessons from the Alzheimer's amyloid β-peptide," *Nature Reviews Molecular Cell Biology*, vol. 8, no. 2, pp. 101–112, 2007.

[49] A. Nitta, T. Fukuta, T. Hasegawa, and T. Nabeshima, "Continuous infusion of β-amyloid protein into the rat cerebral ventricle induces learning impairment and neuronal and morphological degeneration," *Japanese Journal of Pharmacology*, vol. 73, no. 1, pp. 51–57, 1997.

[50] Y. Peng, C. Xing, S. Xu et al., "l-3-n-butylphthalide improves cognitive impairment induced by intracerebroventricular infusion of amyloid-β peptide in rats," *European Journal of Pharmacology*, vol. 621, no. 1–3, pp. 38–45, 2009.

[51] S. Kar, A. M. Issa, D. Seto, D. S. Auld, B. Collier, and R. Quirion, "Amyloid β-peptide inhibits high-affinity choline uptake and acetylcholine release in rat hippocampal slices," *Journal of Neurochemistry*, vol. 70, no. 5, pp. 2179–2187, 1998.

[52] E. K. Perry, B. E. Tomlinson, G. Blessed et al., "Correlation of cholinergic abnormalities with senile plaques and mental test scores in senile dementia," *British Medical Journal*, vol. 2, no. 6150, pp. 1457–1459, 1978.

[53] H. Yan, L. Li, and X. C. Tang, "Treating senile dementia with traditional Chinese medicine," *Clinical Interventions in Aging*, vol. 2, no. 2, pp. 201–208, 2007.

Hindawi Publishing Corporation
Evidence-Based Complementary and Alternative Medicine
Volume 2012, Article ID 795843, 9 pages
doi:10.1155/2012/795843

Research Article

The Components of *Flemingia macrophylla* Attenuate Amyloid β-Protein Accumulation by Regulating Amyloid β-Protein Metabolic Pathway

Yun-Lian Lin,[1] Huey-Jen Tsay,[2] Yung-Feng Liao,[3] Mine-Fong Wu,[3] Chuen-Neu Wang,[4] and Young-Ji Shiao[3,4]

[1] *Division of Medicinal Chemistry, National Research Institute of Chinese Medicine, Taipei 112, Taiwan*
[2] *Institute of Neuroscience, National Yang-Ming University, Taipei 112, Taiwan*
[3] *Institute of Biopharmaceutical Science, National Yang-Ming University, Taipei 112, Taiwan*
[4] *Division of Basic Chinese Medicine, National Research Institute of Chinese Medicine, Taipei 112, Taiwan*

Correspondence should be addressed to Young-Ji Shiao, yshiao@nricm.edu.tw

Received 10 January 2012; Revised 6 March 2012; Accepted 13 March 2012

Academic Editor: Karl Wah-Keung Tsim

Flemingia macrophylla (Leguminosae) is a popular traditional remedy used in Taiwan as anti-inflammatory, promoting blood circulation and antidiabetes agent. Recent study also suggested its neuroprotective activity against Alzheimer's disease. Therefore, the effects of *F. macrophylla* on Aβ production and degradation were studied. The effect of *F. macrophylla* on Aβ metabolism was detected using the cultured mouse neuroblastoma cells N2a transfected with human Swedish mutant APP (swAPP-N2a cells). The effects on Aβ degradation were evaluated on a cell-free system. An ELISA assay was applied to detect the level of Aβ1-40 and Aβ1-42. Western blots assay was employed to measure the levels of soluble amyloid precursor protein and insulin degrading enzyme (IDE). Three fractions of *F. macrophylla* modified Aβ accumulation by both inhibiting β-secretase and activating IDE. Three flavonoids modified Aβ accumulation by activating IDE. The activated IDE pool by the flavonoids was distinctly regulated by bacitracin (an IDE inhibitor). Furthermore, flavonoid 94-18-13 also modulates Aβ accumulation by enhancing IDE expression. In conclusion, the components of *F. macrophylla* possess the potential for developing new therapeutic drugs for Alzheimer's disease.

1. Introduction

Flemingia macrophylla (Leguminosae) is a popular traditional remedy used in Taiwan [1] and India [2]. The stems or leaves have been used as an anti-inflammatory, blood circulation promotion and antidiabetic agent, all of which were relevant to the pathogenesis of Alzheimer's disease (AD). Recent research has suggested its neuroprotective activity against amyloid β (Aβ) [3], hepatoprotective activity [4], antiinflammatory activity [5], and antiosteoporosis activity [6].

AD is a complex mental illness characterized by the accumulation of extracellular senile plaques and intracellular neurofibrillary tangles. Senile plaques are composed of deposited Aβ, derived from the processing of amyloid precursor protein (APP) by two enzymes: β-site APP cleaving enzyme (BACE or β-secretase) and γ-secretase [7]. According to the amyloid hypothesis, abnormal accumulation of Aβ in the brain is the primary causative factor contributing to AD pathogenesis, whereby the disease process is believed to result from an imbalance between Aβ production (anabolic activity) and clearance (catabolic activity) [8–10]. APP molecules are cleaved by secretases at the cell surface, the Golgi complex, and along the endosomal/lysosomal pathway [11, 12]. Most cell surface β-secretase is reinternalized into early endosomal compartments, from where it can be recycled back to the cell surface or later be redirected to endosomal/lysosomal compartments and/or to the *trans*-Golgi [13]. It is generally believed that removal of Aβ from the brain might be of great therapeutic benefit [14]. Consequently, therapeutic strategies aiming to decrease Aβ levels, such as inhibition of either β-secretase or γ-secretase and Aβ immunization, are currently a major focus of AD research [15–17]. Much more attention has been paid to abnormal Aβ production, but recently, the role of Aβ degradation in Aβ

homoeostasis has been increasingly recognized, as several enzymes that degrade Aβ have been identified, such as insulin degrading enzyme (IDE), neprilysin (NEP), and matrix metalloproteins (MMPs) [18].

Clinical and epidemiological studies have found that type 2 diabetes and hyperinsulinemia increased the risk of developing AD, and the link between these two diseases may be IDE [19, 20]. IDE is a zinc metalloendopeptidase that is highly expressed in the liver, testis, muscle, and brain. Although it is predominantly cytosolic, a secreted form of IDE in extracellular compartments such as cerebrospinal fluid was also identified [21]. IDE degrades a wide range of substrates that include insulin, amylin, insulin-like growth factors, and Aβ [18]. Furthermore, previous work has reported that the IDE level in AD is reduced [22].

In this study, we investigate the effect of *F. macrophylla* extracts or isolated pure compounds on Aβ accumulation and found that they decrease extracellular accumulation of Aβ1-40 in the cultured mouse neuroblastoma cells N2a transfected with human Swedish mutant APP (swAPP-N2a cells) by inhibiting β-secretase or enhancing Aβ degradation.

2. Methods

2.1. Reagents. Medium for cell culture, heparin, Lipofectamine, and human β amyloid 1-40 and 1-42 kits were purchased from Invitrogen (Carlsbad, CA, USA). Mouse anti-actin antibody and anti-IDE polyclonal antibody, rabbit polyclonal anti-APP (KPI domain) antibody, and synthetic Aβ1-40 were purchased from Millipore (Billerica, MA, USA). Anti-Aβ1-17 antibody (clone 6E10) was from Signet (Dedham, MA). Enhanced chemiluminescence detection reagents, anti-rabbit and anti-mouse IgG antibody conjugated with horseradish peroxidase were obtained from GE Healthcare (Buckinghamshire, UK). Insulin, progesterone, putrescine, sodium selenite, and transferrin were purchased from Sigma (St. Louis, MO, USA). All other reagents were purchased from Sigma (St. Louis, MO, USA) or Merck (Darmstadt, Germany).

2.2. Plant Material, Extraction, and Isolation. The aerial parts of *F. macrophylla* were collected from Kaohsiung County, Taiwan in May, 2002. The plant was identified by Mr. Jun-Chih Ou, former associate investigator of National Research Institute of Chinese Medicine, and comparison with the voucher specimens was deposited earlier at the Herbarium of the Department of Botany, National Taiwan University, Taipei, Taiwan (no. TAI219262, April, 1988). The extraction and isolation of each fraction for this assay is listed in Table 1, and the structure and chemical name of the flavonoids isolated from *F. macrophylla* were displayed in Figure 1.

2.3. Cell Culture and Transfection. Neuro-2a (N2a) cells were cultured in minimal essential medium (MEM) containing 10% fetal bovine serum (FBS). Confluent 90% N2a cells were transfected with plasmid containing human Swedish mutant of amyloid precursor protein (pCGR/APP_{770}) by using Lipofectamine 2000. After transfection for 6 h, the cells were incubated with chemical defined medium (DMEM/F12 medium containing 5 mM Hepes pH 7.4, 0.6% glucose, 2.5 mM glutamine, 3 mM $NaHCO_3$, 100 μg/mL, transferring, 20 nM progesterone, 60 μM putrescine, 30 nM sodium selenite, 2 μg/mL heparin, and 100 nM insulin) for 20 h. For treatment with cells, the fractions or flavanoids of *F. macrophylla* were introduced into the chemical defined medium.

Table 1: Extraction and isolation of *F. macrophylla*. The ground aerial parts of *F. macrophylla* (12 kg) were extracted following the protocol, and the fractions were named.

Fraction name	The protocol of extraction and fractionation
EtOH	The aerial parts of *F. macrophylla* were extracted three times with 95% ethanol (EtOH) at 60°C overnight. The combined EtOH extract was evaporated under reduced pressure.
H_2O	EtOH extract was taken up in water as water-soluble fraction.
H25M H50M H75M H100M	The water-soluble fraction (H_2O) was chromatogramed over Diaion HP-20 column and eluted with 25%-, 50%-, 75%-, and 100%-methanol to give four fractions: H25M, H50M, H75M, and H100M, respectively.
EA n-BuOH	The water-soluble fraction (H_2O) was partitioned with ethyl acetate and n-butanol successively to get two fractions: EA and n-BuOH, respectively.
B25M B50M B75M B100M	The n-BuOH fraction was chromatogramed over Diaion HP-20 column and eluted with 25%-, 50%-, 75%-, and 100%-methanol to give four fractions: B25M, B50M, B75M, B100M, respectively.
EA-n	EA and n-BuOH fractions were subjected to silica gel column chromatography using a hexane-EA-methanol gradient and EA-methanol gradient, respectively. Eleven fractions were collected as EA-n (n = 4, 35, 52, 55, 74, 79, 85, 94, 103, 121, 165).
Flavonoids	The fractions rich in flavonoids were separated first over a silica gel column with a 25%–60% EA/hexane gradient as eluent and then over Sephadex LH-20 columns with EA or methanol to afford flavonoids.

2.4. MTT Assay. The reduction of 3-[4,5-dimethylthiazol-2-yl]-2,5-diphenyl-tetrazolium bromide (MTT) was used to evaluate cell viability. Cells were incubated with 0.5 mg/mL MTT for 1 h. The formazan particles were dissolved with DMSO. $OD_{600\,nm}$ was measured using an ELISA reader.

2.5. The Cell-Free Assay of Aβ1-40 Degradation. The conditioned medium of N2a cells containing the proteases to degrade Aβ was collected and used for the cell-free assay of Aβ degradation. Ten ng of synthetic Aβ1-40 (Invitrogen, 03-138) were added into 300 μL N2a-conditioned medium containing various reagents and incubated at 37°C for 24 h. The remaining Aβ were then quantified by ELISA assay kit.

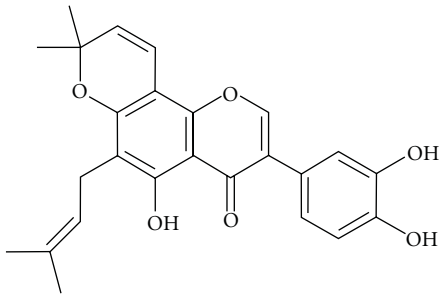

49-3

Isolation number	Chemical name
49-3	Promiferin
52-11	Lespedezaflavanone B
85-29	Flemingichromone
92-26	Genistein
94-18-13	Prunetin

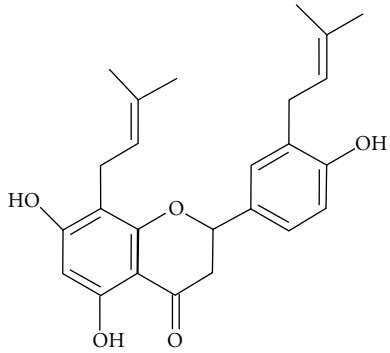

52-11

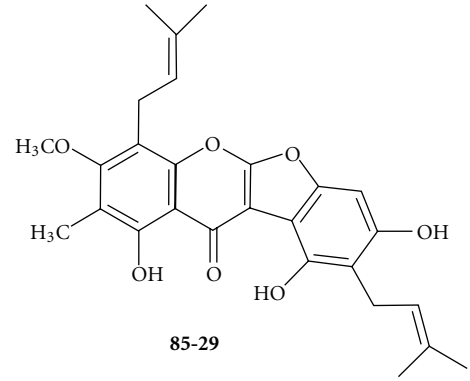

85-29

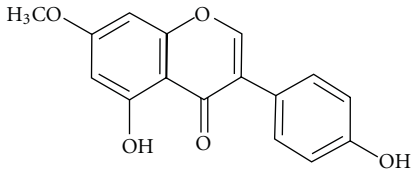

94-18-13

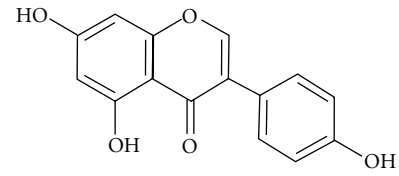

92-26

Figure 1: The structure and chemical name of the flavonoids isolated from *F. macrophylla*.

2.6. Quantification of Aβ1-40 in Cells and Culture Medium. After treatment, culture media and cell were collected separately and subjected to determining the levels of Aβ1-40 using assay kits. The detailed experiments were performed according to the manufacturer's protocol.

2.7. Immunoblotting. After treatment, culture media were collected and cells were washed with ice-cold phosphate buffered saline (PBS) three times. Cells were harvested in lysis buffer (50 mM Hepes pH7.5, 2.5 mM EDTA, 1 mM phenylmethylsulfonyl fluoride, 5 μg/mL aprotinin, and 10 μg/mL leupeptin), and cell lysates were prepared. Equal protein amounts of cell lysate and equal volume of culture medium were subjected to SDS-polyacrylamide gel electrophoresis and immunoblotting. Fujifilm LAS-3000 (Tokyo, Japan) was used to detect and quantify the immunoreactive protein.

2.8. Statistical Analysis. Results are expressed as mean ± SD and were analyzed by ANOVA with post hoc multiple comparisons with a Bonferroni test.

3. Results

3.1. The Effects of Insulin and Bacitracin on Aβ1-40 Level in swAPP-N2a Cells Culture. To determine the importance of IDE activity on the levels of both extracellular and intracellular Aβ1-40 in swAPP-N2a cell culture, various concentrations of insulin (the substrate of IDE) and/or 2 nM bacitracin (a competitive inhibitor of IDE) were subjected into swAPP-N2a cell culture, and the Aβ1-40 accumulation was assayed. The results showed that insulin promotes Aβ1-40 accumulation in a concentration-dependent manner. Extracellular Aβ1-40 was hardly detected (i.e., 0.88 ± 1.07 ng/mL) in the culture medium without containing insulin. Insulin at

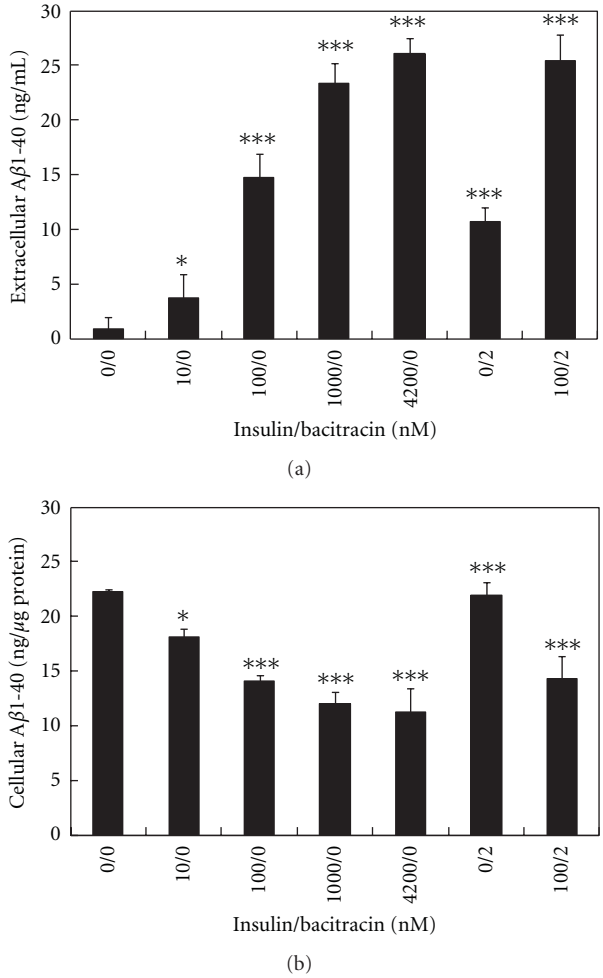

Figure 2: The effect of insulin and bacitracin on the level of extracellular and intracellular Aβ1-40. APP-transfected N2a cells were treated with indicated concentrations of insulin and bacitracin for 20 h. The level of extracellular (a) and intracellular (b) Aβ1-40 was determined by ELISA. Results are means ± SD from three independent experiments. Significant differences between control and treated cells are indicated by $^{*}P < 0.05$, $^{***}P < 0.001$.

10, 100, 1000, and 4200 nM increased the level of extracellular Aβ1-40 to 3.70 ± 2.18 ng/mL, 14.78 ± 2.17 ng/mL, 23.38 ± 1.83 ng/mL, and 26.02 ± 1.45 ng/mL, respectively (Figure 2(a)). The results suggested that about 26 ng/mL of extracellular Aβ1-40 in the cultured medium regulated by insulin sensitive peptidase(s), including IDE. Therefore, bacitracin was employed to verify the IDE-sensitive pool of extracellular Aβ1-40 in the cultured medium. The results showed that 2 nM bacitracin increased the level of extracellular Aβ1-40 to 10.66 ± 1.32 ng/mL (Figure 2(a)), and higher concentration of bacitracin did not significantly enhance this effect, suggesting that about 11 ng/mL of extracellular Aβ1-40 in the cultured medium was regulated by IDE.

Insulin may regulate the extracellular Aβ1-40 by enhancing exocytosis of the intracellular Aβ1-40. Therefore, the level of intracellular Aβ1-40 was assayed. The results showed that the level of intracellular Aβ1-40 was concentration

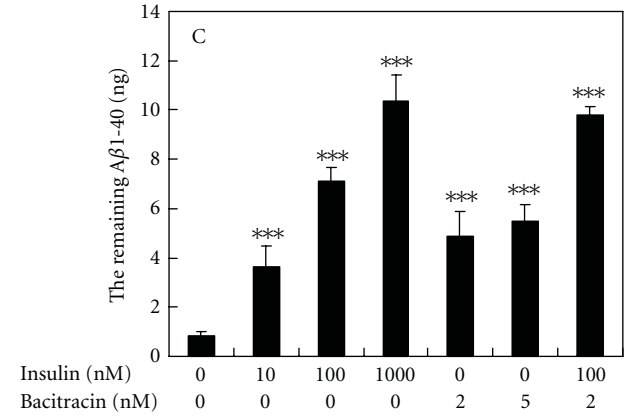

Figure 3: The effect of insulin and bacitracin on Aβ1-40 degradation in the N2a-conditioned medium. Aβ1-40 (10 ng) were incubated in the N2a-conditioned medium with indicated concentrations of insulin and bacitracin, at 37°C for 16 h. The level of remaining Aβ1-40 was determined by ELISA. Results are means ± SD from three independent experiments. Significant differences between control and FM fractions-treated cells are indicated by $^{***}P < 0.001$.

dependently reduced by insulin, but not by bacitracin (Figure 2(b)). The results suggested that insulin may promote the level of extracellular Aβ1-40 by inhibiting IDE and by accelerating the exocytosis of intracellular Aβ1-40. Alternately, bacitracin did not affect the exocytosis of intracellular Aβ1-40. The similar effects of insulin and bacitracin were found on Aβ1-42 (data not shown).

3.2. The Effects of Insulin and Bacitracin on the Degradation of Synthetic Aβ1-40 in the N2a-Conditioned Medium. For bypassing the involvement of Aβ anabolic and trafficking pathway, a cell-free Aβ degradation assay using N2a cell-conditioned medium as the source of secreted protease and the synthetic Aβ1-40 was employed as the substrate. The results showed that Aβ degradation was inhibited by insulin in a concentration-dependent manner (Figure 3). The added synthetic Aβ1-40 (10 ng) was degraded to 0.83 ± 0.17 ng in the conditioned medium without containing insulin, and 10, 100, and 1000 nM insulin increased the level of remaining Aβ1-40 to 3.65 ± 0.82 ng, 7.13 ± 0.55 ng, and 10.34 ± 1.11 ng, respectively, indicating that the degradation of 10 ng Aβ was completely abolished by 1 μM insulin (Figure 3). Treatment with 2 nM, 5 nM bacitracin, or 2 nM bacitracin combined with 100 nM insulin increased the remaining level of Aβ1-40 to 4.83 ± 0.96, 5.51 ± 0.65, and 9.81 ± 0.35 ng, respectively (Figure 3), suggesting a synergism of insulin and bacitracin on inhibiting Aβ degradation.

3.3. The Effects of the Fractions and Flavonoids Isolated from F. macrophylla on the Level of Aβ1-40. To determine the effects of the fractions and flavonoids isolated from *F. macrophylla* on the level of extracellular Aβ1-40, the cell toxicity of the fractions and flavonoids was detected, and was then the subtoxic concentration (STC) of the fractions and flavonoids

Table 2: The effects of the fractions of *F. macrophylla* on the levels of extracellular and intracellular Aβ1-40. APP-transfected N2a cells were treated with the fractions of *F. macrophylla* at the STC for 20 h. The level of extracellular and intracellular Aβ1-40 was determined by ELISA. Results are means ± SD from three independent experiments. Significant differences between control and fractions-treated cells are indicated by $^{*}P < 0.05$, $^{**}P < 0.01$, and $^{***}P < 0.001$.

Fractions	STC (μg/mL)	Aβ1-40 (% of control)	
		Extracellular	Intracellular
EtOH	10	46.18 ± 8.19***	94.92 ± 21.28
H_2O	100	28.16 ± 7.38***	155.62 ± 13.79***
H25M	1	78.70 ± 5.21*	nd[a]
H50M	1	86.05 ± 24.57	nd
H75M	50	13.75 ± 5.56***	212.47 ± 47.25***
H100M	1	69.98 ± 13.68**	nd
BuOH	1	63.49 ± 8.09***	nd
B25M	1	66.19 ± 18.86*	nd
B50M	10	18.66 ± 2.77***	100.36 ± 16.35
B75M	50	9.40 ± 3.05***	238.75 ± 60.32***
B100M	50	64.95 ± 9.02**	nd
EA	1	124.57 ± 35.93	nd
EA-1	10	55.16 ± 6.27**	nd
EA-4	1	119.70 ± 24.55	nd
EA-35	10	71.64 ± 13.65*	nd
EA-52	1	64.57 ± 6.94*	nd
EA-55	1	54.14 ± 22.13**	nd
EA-74	1	52.65 ± 12.65**	96.21 ± 4.71
EA-79	1	107.02 ± 10.67	nd
EA-85	1	111.94 ± 26.00	nd
EA-94	1	98.63 ± 27.61	nd
EA-103	1	77.66 ± 4.73*	nd
EA-121	1	60.82 ± 18.82**	nd
EA-165	1	69.57 ± 19.16*	nd

[a]nd, not determined.

was subjected into the extracellular Aβ1-40 accumulation assay. The results indicated that five highly polar fractions (i.e., EtOH, H_2O, H75M, B50M, and B75M) attenuated the accumulation of medial Aβ1-40 by more than 50% (Table 2). Among the lesser polar fractions, EA-74 is the most effective fraction which attenuated the accumulation of medial Aβ1-40 to 52.62 ± 12.56% of control (Table 2). Three flavonoids (i.e., 49-2, 52-11, and 94-18-13) attenuated the accumulation of extracellular Aβ1-40 by more than 30% (Table 3).

The effects of the fractions and flavonoids on the intracellular Aβ1-40 accumulation were further evaluated. The result showed that the fraction H_2O, H75M, and B75M elevated the intracellular level of Aβ1-40 to 155.6 ± 13.4, 213.5 ± 47.3, and 238.8 ± 60.3% of the control, respectively, and the fraction EtOH, B50M, and EA-74 and the flavonoid 49-2, 52-11, and 94-18-13 did not exert significant effects on the intracellular Aβ1-40 accumulation (Tables 2 and 3). Those were therefore selected for further investigation.

Table 3: The effects of the flavonoids isolated from *F. macrophylla* on the levels of extracellular and intracellular Aβ1-40. APP-transfected N2a cells were treated with the flavonoids at STC for 20 h. The level of extracellular and intracellular Aβ1-40 was determined by ELISA. Results are means ± SD from three independent experiments. Significant differences between control and flavonoid-treated cells are indicated by $^{*}P < 0.05$, and $^{**}P < 0.01$.

Flavonoid	STC (μg/mL)	Aβ1-40 (% of control)	
		Extracellular	Intracellular
49-3	0.1	66.93 ± 11.16*	96.03 ± 5.64
52-11	0.1	65.41 ± 16.90*	99.36 ± 9.81
85-29	0.1	94.26 ± 18.15	nd
92-26	1	87.00 ± 29.13	nd
94-18-13	0.1	56.83 ± 7.52**	104.23 ± 12.40

[a]nd, not determined.

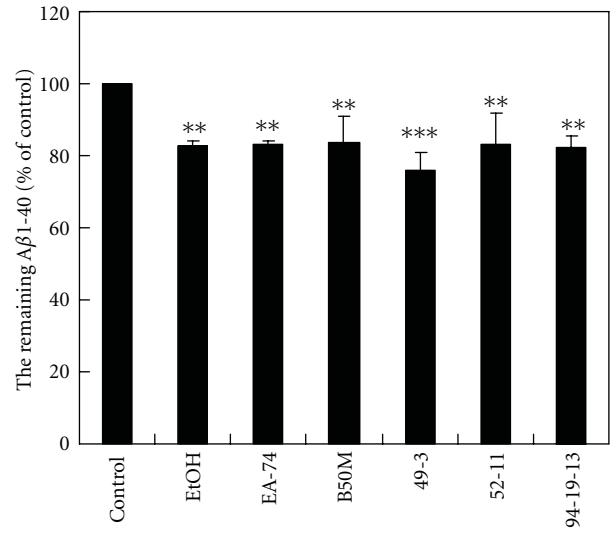

Figure 4: The effects of the fractions and flavonoids of *F. macrophylla* on Aβ1-40 degradation in the N2a-conditioned medium. Aβ1-40 (10 ng) were incubated in the N2a-conditioned medium with 100 nM insulin and the fractions and flavonoids of *F. macrophylla* at NTC, 37°C for 20 h. The level of remaining Aβ1-40 was determined by ELISA. Results are means ± SD from three independent experiments. Significant differences between control and the treated cells are indicated by $^{**}P < 0.01$, $^{***}P < 0.001$.

3.4. The Effects of the Fractions and Flavonoids Isolated from F. macrophylla on the Aβ1-40 Degradation in the N2a-Conditioned Medium. The fraction EtOH, EA-47, B50M, and flavonoid 49-3, 52-11, and 94-19-13 decreased the remaining synthetic Aβ1-40 to 82.66 ± 1.26%, 83.25 ± 0.74%, 83.50 ± 7.30%, 76.02 ± 4.88%, 83.24 ± 8.60%, and 82.31 ± 8.04% of the control, respectively (Figure 4). The results suggesting that the fractions and flavonoids may ameliorate Aβ accumulation by promoting Aβ degradation. The similar effects were found on Aβ1-42 (data not shown).

3.5. The Level of Secreted IDE Was Promoted by Flavonoid 94-18-13. Treatment with the fraction B50M, EA-74, and

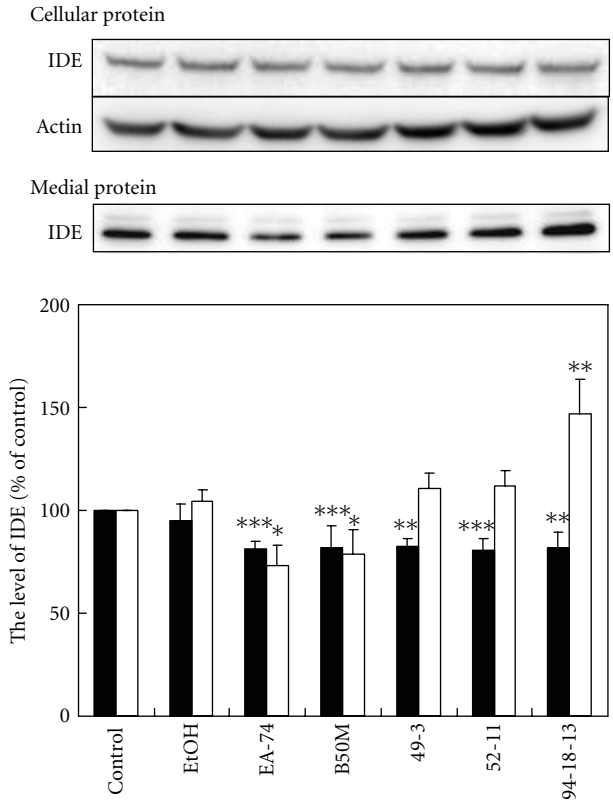

Figure 5: The level of IDE was differentially affected by the fractions and flavonoids of *F. macrophylla*. N2a cells were treated with fractions and flavonoids for 20 h at NTC. The level of IDE in cell lysate and medium was determined by immunoblotting. The upper panel is the representative blot. The lower panel is the relative level of IDE in cell lysate (closed column) and medium (opened column) exhibited as percentage of the control. Results are means ± SD from three independent experiments. Significant differences between control and the treated cells are indicated by $^{*}P < 0.05$, $^{**}P < 0.01$ and $^{***}P < 0.001$.

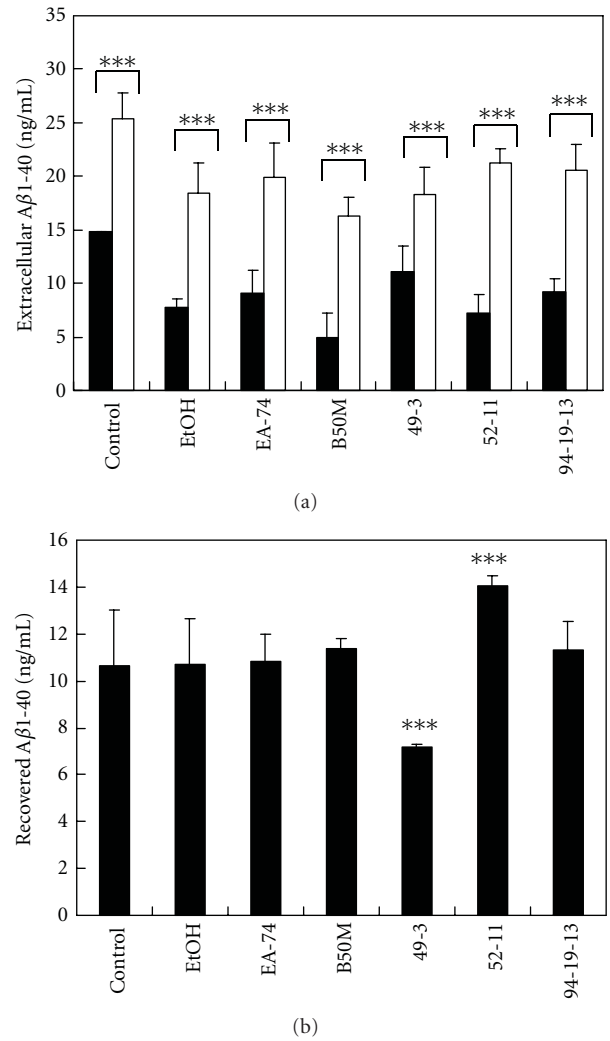

Figure 6: Aβ1-40 accumulation reduced by the fractions and flavonoids was differentially recovered by bacitracin. (a) swAPP$_{770}$-transfected N2a cells were treated with the fractions and flavonoids for 20 h at NTC, in the absence (closed columns) and presence (opened columns) of 2 nM bacitracin. The level of extracellular Aβ1-40 was determined by ELISA. (b) The recovery effect of bacitracin was calculated by the subtraction between the levels of the cells treated with and without bacitracin. Results are means ± SD from three independent experiments. Significant differences between control and FM fractions-treated cells are indicated by $^{***}P < 0.001$.

flavonoid 49-2, 52-11, and 94-18-13 attenuated the level of cellular IDE by about 20%, whereas the fraction EtOH failed to show significant effect on the level of cellular IDE (Figure 5). Treatment with the faction B50M and EA-74 eliminated the level of medial IDE by 21.3 ± 12.0 and 26.6 ± 9.9%, respectively. On the contrary, flavonoid 94-18-13 increased the level of medial IDE to 146.9 ± 16.7% of the control. The result suggested that only flavonoid 94-18-13 may accelerate Aβ degradation by promoting IDE expression. The change in enzyme activity may also be involved although it is not detected in this study.

3.6. The Recovery Effect of Bacitracin on the Treatment-Reduced Accumulation of Extracellular Aβ1-40. The promoting activity of the fractions and flavonoids on Aβ degradation by IDE may include bacitracin-sensitive and -insensitive pools. The bacitracin-sensitive pools in the cultures treated with the fraction EtOH, EA-74, B50M, and flavonoid 94-19-13 were 10.71, 10.83, 11.35, and 11.29 ng/mL, respectively (Figure 6). The results suggested that these treatments did not affect the bacitracin-sensitive pool. The bacitracin-sensitive pools in the cultures treated with the flavonoid 49-3 and 52-11 were 7.18 and 14.05 ng/mL, suggesting that flavonoid 49-3 and 52-11 reduce and enhance the bacitracin-sensitive pool, respectively.

3.7. The Level of Soluble APPβ Was Decreased by the Fractions of F. macrophylla. The anabolic pathway of Aβ may also be affected by the fractions of *F. macrophylla* which resulted in

the decrease of extracellular Aβ. Two categories of soluble APP (sAPP) including α-secretase-derived sAPP (sAPPα) and β-secretase-derived sAPP (sAPPβ) may be detected in the swAPP-N2a-conditioned medium. Two antibodies were used to detect these two sAPPs. The anti-Aβ1-17 (6E10) antibody may recognize sAPPα (this fragment contains Aβ1-17), and the anti-APP (KPI domain) antibody may recognize both sAPPα and sAPPβ on immunoblot. The result showed that 6E10 antibody-recognized sAPPα was not significantly affected by the fractions of *F. macrophylla*. By contrast, the anti-APP (KPI domain) antibody-recognized sAPPα and sAPPβ were significantly decreased. The fractions of EtOH, EA-47, and B50M decreased the level of sAPPs to 76.73 ± 9.11%, 78.99 ± 7.02%, and 79.44 ± 8.48%, respectively. The result indicated that the fractions may inhibit the activity of β-secretase and then decrease the level of sAPPβ (Figure 7), which may reflect the effects of these fractions on attenuating Aβ accumulation.

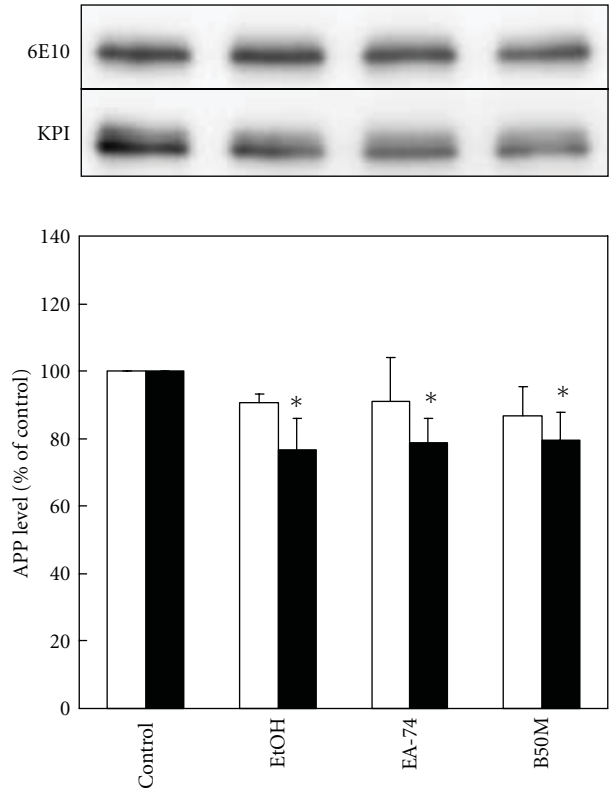

Figure 7: The effect of the fractions of *F. macrophylla* on the level of secreted APP in swAPP770-transfected N2a cell. swAPP$_{770}$-transfected N2a cells were treated with the fractions for 20 h at NTC of 10, 1, and 10 μg/mL, respectively. The level of 6E10 antibody-stained sAPP (i.e., sAPPα) and KPI antibody-stained sAPPs (i.e., sAPPα plus sAPPβ) in conditioned medium was determined by immunoblotting. The upper part is the representative image of immunoblot. The lower part is the relative level of 6E10 antibody-stained sAPPα (opened column) and KPI antibody-stained sAPPs (closed column). Results are means ± SD from three independent experiments. Significant differences between control and FM fractions-treated cells are indicated by $^*P < 0.05$.

4. Discussion

It is generally believed that removal of Aβ from the brain might be of great benefit for AD therapy [14, 23]. To find the reagents which are capable of reducing Aβ levels is required for improving the treatment of AD. Aβ level are determined by the metabolic balance between anabolic and catabolic activities. Among the catabolic enzymes, insulin degrading enzyme (IDE) is thought to be the principal secreted enzyme responsible for the degradation of Aβ in the extracellular space [18, 21, 24]. An interesting link between insulin and Aβ is that they both are IDE substrates [20, 25, 26], and the patients with type 2 diabetes have an increased risk of AD [27]. Since IDE is more efficient on degrading insulin than Aβ, the concomitant increase in insulin and Aβ levels may lead to a redistribution of available IDE away from its function as an Aβ-degrading enzyme [25]. Thus, the involvement of IDE on Aβ degradation in our experimental system was verified by insulin and bacitracin, an IDE competitive inhibitor [28], to promote Aβ accumulation. Aβ degradation was completely abolished by 1 μM Insulin, which was only partially inhibited by bacitracin. The results suggesting that IDE may be the major enzyme contribute to degrade the extracellular Aβ.

By using swAPP-N2a as cell model, we investigated the effects of *F. macrophylla* on reducing Aβ accumulation in the present of 100 nM insulin. Previous studies have indicated that some herbal medicine-derived compounds reduced Aβ accumulation in the similar cell models [29–33]. *F. macrophylla* is a popular traditional remedy used in Taiwan [1] and India [2]. The stems have been used in folk medicine for antirheumatic and anti-inflammatory agent, promoting blood circulation and antidiabetes. Our recent research has suggested the AD-relative neuroprotective effects of *F. macrophylla* on the primary cultures of neonatal cortical neurons against Aβ-mediated neurotoxicity [3]. However, the effect of *F. macrophylla* on Aβ accumulation and the underlying mechanism has not been studied. To investigate whether *F. macrophylla* affects Aβ metabolism, we detect the extracellular and intracellular Aβ1-40 levels of the treated swAPP-N2a cells by ELISA assay and found that fraction EtOH, EA-74, and B50M and flavonoid 49-3, 52-11, and 94-19-13 significantly reduced the extracellular Aβ1-40 accumulation without promoting the intracellular Aβ1-40 accumulation.

Several target sites including Aβ anabolic, trafficking, and catabolic pathways could be considered as the targets of the fractions or flavonoids on Aβ accumulation in swAPP-N2a cells. Therefore, a cell-free Aβ degradation system using N2a cell-conditioned medium as protease source and the synthetic Aβ1-40 as subtract was used to bypass the involvement of Aβ anabolic and trafficking pathway. The results showed that Aβ degradation was inhibited by insulin in a concentration-dependent manner. Aβ degradation was completely abolished by 1 μM insulin. Bacitracin partially inhibited the degradation of Aβ1-40 alone or combined with insulin. It has been proposed that both microglia and

astrocytes secrete protease, including IDE that mediates the degradation of Aβ in the extracellular milieu [21, 34] which may be similar to our system.

Aβ degradation by IDE was promoted by the fractions and flavonoids. In the presence of 100 nM insulin, the fractions and flavonoids decreased the remaining Aβ1-40 to about 80% of the control. The results suggest that the fractions and flavonoids may ameliorate Aβ accumulation by promoting Aβ degradation.

To study the mechanism underlying the effect of the fractions and flavonoids on the level of IDE, we first performed western blot analysis to detect IDE expression. The results showed that only flavonoid 94-18-13 significantly improved IDE expression. Nevertheless, the underlying mechanism required further investigation, although recent studies have indicated that IDE expression may be regulated through liver X receptor [35], NMDA receptor [36], β2 adrenergic receptor [37], insulin receptor [38], dopamine receptor [39], and glucocorticoid receptor [40].

To study the effect of the fractions and compounds on the IDE-dependent degradation pool of extracellular Aβ, we then detected extracellular Aβ1-40 levels with ELISA after treating swAPP-N2a cells with the fractions or flavonoids in the absence or presence of 2 nM bacitracin. We found that three fractions and flavonoid 94-19-13 activated IDE without affecting the bacitracin-sensitive pool, which was partially compressed and extended by flavonoid 49-3 and 52-11, respectively, through the allosteric regulatory effect. In the previous study, Cabrol et al. [41] discovered two small molecule activators of IDE through high-throughput compound screening. They established the putative ATP-binding domain as a key modulator of IDE proteolytic activity. ATP inhibits IDE-mediated insulin degradation at physiological concentration [42]. On the other hand, ATP was found to activate IDE-mediated fluorogenic substrate by conformational switch through its triphosphate moiety [43, 44]. Recently, the allosteric regulatory sites of IDE were identified [45]. Therefore, the fractions and flavonoids may activate IDE by occupying the allosteric binding site.

To determine whether the fractions affect Aβ anabolism, the western blot of medial sAPPs (sAPPα and sAPPβ) was performed. The results showed that all three fractions ameliorated the production of sAPPs but not sAPPα, suggesting that sAPPβ was affected by these three fractions through inhibiting the activity of β-secretase. The previous studies have demonstrated that the tenuigenin isolated from *Polygala tenuifolia* and berberine isolated from *Coptidis rhizome* can inhibit the secretion of Aβ via β-secretase inhibition [30–32].

5. Conclusion

The results suggested that the fraction EtOH, EA-74, and B50M of *F. macrophylla* may modify Aβ accumulation by both inhibiting β-secretase and activating IDE. The three flavonoids may modify Aβ accumulation by activating IDE. The activated IDE poor by these three flavonoids was distinctly regulated by bacitracin. Furthermore, flavonoid 94-18-13 also modulates Aβ accumulation by enhancing IDE expression. Change in Aβ accumulation may prevent Aβ aggregation and the subsequent neurotoxicity on AD. Such information could be exploited to develop the new therapeutic drugs for sporadic AD.

Acknowledgments

This study was supported by Grant no. NSC-97-2320-B-077-003-MY3 from National Science Council, Grant no, NRICM-98-DBCM-06 from National Research Institute of Chinese Medicine, Taiwan, and the Ministry of Education-Aim for the Top University Plan (010AC-B5).

References

[1] T. C. Huang and H. Ohashi, "Leguminosae," in *Flora of Taiwan*, vol. 3, pp. 160–396, Editorial Committee of Flora of Taiwan, Taipei, Taiwan, 2nd edition, 1993.

[2] D. Syiem and P. Z. Khup, "Evaluation of *Flemingia macrophylla* L., a traditionally used plant of the north eastern region of India for hypoglycemic and anti-hyperglycemic effect on mice," *Pharmacologyonline*, vol. 2, pp. 355–366, 2007.

[3] Y. J. Shiao, C. N. Wang, W. Y. Wang, and Y. L. Lin, "Neuroprotective flavonoids from *Flemingia macrophylla*," *Planta Medica*, vol. 71, no. 9, pp. 835–840, 2005.

[4] P. C. Hsieh, Y. L. Ho, G. J. Huang et al., "Hepatoprotective effect of the aqueous extract of *Flemingia macrophylla* on carbon tetrachloride-induced acute hepatotoxicity in rats through anti-oxidative activities," *American Journal of Chinese Medicine*, vol. 39, no. 2, pp. 349–365, 2011.

[5] Y. J. Ko, T. C. Lu, S. Kitanaka et al., "Analgesic and anti-inflammatory activities of the aqueous extracts from three flemingia species," *American Journal of Chinese Medicine*, vol. 38, no. 3, pp. 625–638, 2010.

[6] W. C. Lin, H. Y. Ho, and J. B. Wu, "*Flemingia macrophylla* extract ameliorates experimental osteoporosis in ovariectomized rats," *Evidence-Based Complementary and Alternative Medicine*, vol. 2011, Article ID 752302, 9 pages, 2011.

[7] D. J. Selkoe, "Alzheimer's disease results from the cerebral accumulation and cytotoxicity of amyloid β-protein," *Journal of Alzheimer's Disease*, vol. 3, no. 1, pp. 75–81, 2001.

[8] M. Citron, "β-Secretase inhibition for the treatment of Alzheimer's disease-promise and challenge," *Trends in Pharmacological Sciences*, vol. 25, no. 2, pp. 92–97, 2004.

[9] M. P. Mattson, "Pathways towards and away from Alzheimer's disease," *Nature*, vol. 430, no. 7000, pp. 631–639, 2004.

[10] G. K. Gouras, D. Tampellini, R. H. Takahashi, and E. Capetillo-Zarate, "Intraneuronal β-amyloid accumulation and synapse pathology in Alzheimer's disease," *Acta Neuropathologica*, vol. 119, no. 5, pp. 523–541, 2010.

[11] O. Isacson, H. Seo, L. Lin, D. Albeck, and A. C. Granholm, "Alzheimer's disease and Down's syndrome: roles of APP, trophic factors and ACh," *Trends in Neurosciences*, vol. 25, no. 2, pp. 79–84, 2002.

[12] L. Gasparini, W. J. Netzer, P. Greengard, and H. Xu, "Does insulin dysfunction play a role in Alzheimer's disease?" *Trends in Pharmacological Sciences*, vol. 23, no. 6, pp. 288–293, 2002.

[13] R. A. Nixon, "Endosome function and dysfunction in Alzheimer's disease and other neurodegenerative diseases," *Neurobiology of Aging*, vol. 26, no. 3, pp. 373–382, 2005.

[14] K. A. Bates, G. Verdile, Q. X. Li et al., "Clearance mechanisms of Alzheimer's amyloid-β peptide: implications for therapeutic

design and diagnostic tests," *Molecular Psychiatry*, vol. 14, no. 5, pp. 469–486, 2009.

[15] A. K. Ghosh, S. Gemma, and J. Tang, "β-secretase as a therapeutic target for Alzheimer's disease," *Neurotherapeutics*, vol. 5, no. 3, pp. 399–408, 2008.

[16] M. S. Wolfe, "Inhibition and modulation of γ-secretase for Alzheimer's disease," *Neurotherapeutics*, vol. 5, no. 3, pp. 391–398, 2008.

[17] C. A. Lemere and E. Masliah, "Can Alzheimer disease be prevented by amyloid-β immunotherapy?" *Nature Reviews Neurology*, vol. 6, no. 2, pp. 108–119, 2010.

[18] J. S. Miners, S. Baig, J. Palmer, L. E. Palmer, P. G. Kehoe, and S. Love, "Aβ-degrading enzymes in Alzheimer's disease," *Brain Pathology*, vol. 18, no. 2, pp. 240–252, 2008.

[19] J. S. Roriz-Filho, T. M. Sá-Roriz, I. Rosset et al., "(Pre)diabetes, brain aging, and cognition," *Biochimica et Biophysica Acta*, vol. 1792, no. 5, pp. 432–443, 2009.

[20] W. Q. Qiu and M. F. Folstein, "Insulin, insulin-degrading enzyme and amyloid-β peptide in Alzheimer's disease: review and hypothesis," *Neurobiology of Aging*, vol. 27, no. 2, pp. 190–198, 2006.

[21] W. Q. Qiu, D. M. Walsh, Z. Ye et al., "Insulin-degrading enzyme regulates extracellular levels of amyloid β- protein by degradation," *Journal of Biological Chemistry*, vol. 273, no. 49, pp. 32730–32738, 1998.

[22] A. Perez, L. Morelli, J. C. Cresto, and E. M. Castano, "Degradation of soluble amyloid beta-peptides 1–40, 1–42, and the Dutch variant 1–40Q by insulin degrading enzyme from Alzheimer disease and control brains," *Neurochem Research*, vol. 25, no. 2, pp. 247–255, 2000.

[23] M. S. Forman, J. Q. Trojanowski, and V. M. Y. Lee, "Neurodegenerative diseases: a decade of discoveries paves the way for therapeutic breakthroughs," *Nature Medicine*, vol. 10, no. 10, pp. 1055–1063, 2004.

[24] W. Farris, S. Mansourian, Y. Chang et al., "Insulin-degrading enzyme regulates the levels of insulin, amyloid β-protein, and the β-amyloid precursor protein intracellular domain in vivo," *Proceedings of the National Academy of Sciences of the United States of America*, vol. 100, no. 7, pp. 4162–4167, 2003.

[25] G. Taubes, "Insulin insults may spur Alzheimer's disease," *Science*, vol. 301, no. 5629, pp. 40–41, 2003.

[26] W. Farris, S. Mansourian, M. A. Leissring et al., "Partial loss-of-function mutations in insulin-degrading enzyme that induce diabetes also impair degradation of amyloid β-protein," *American Journal of Pathology*, vol. 164, no. 4, pp. 1425–1434, 2004.

[27] G. S. Watson, E. R. Peskind, S. Asthana et al., "Insulin increases CSF Aβ42 levels in normal older adults," *Neurology*, vol. 60, no. 12, pp. 1899–1903, 2003.

[28] T. Shiiki, S. Ohtsuki, A. Kurihara et al., "Brain insulin impairs amyloid-β(1–40) clearance from the brain," *Journal of Neuroscience*, vol. 24, no. 43, pp. 9632–9637, 2004.

[29] H. Y. Zhang, H. Yan, and X. C. Tang, "Huperzine A enhances the level of secretory amyloid precursor protein and protein kinase C-α in intracerebroventricular β-amyloid-(1–40) infused rats and human embryonic kidney 293 Swedish mutant cells," *Neuroscience Letters*, vol. 360, no. 1-2, pp. 21–24, 2004.

[30] H. Jia, Y. Jiang, Y. Ruan et al., "Tenuigenin treatment decreases secretion of the Alzheimer's disease amyloid β-protein in cultured cells," *Neuroscience Letters*, vol. 367, no. 1, pp. 123–128, 2004.

[31] J. Lv, H. Jia, Y. Jiang et al., "Tenuifolin, an extract derived from tenuigenin, inhibits amyloid-β secretion in vitro," *Acta Physiologica*, vol. 196, no. 4, pp. 419–425, 2009.

[32] M. Asai, N. Iwata, A. Yoshikawa et al., "Berberine alters the processing of Alzheimer's amyloid precursor protein to decrease Aβ secretion," *Biochemical and Biophysical Research Communications*, vol. 352, no. 2, pp. 498–502, 2007.

[33] L. Yang, J. Hao, J. Zhang et al., "Ginsenoside Rg3 promotes beta-amyloid peptide degradation by enhancing gene expression of neprilysin," *Journal of Pharmacy and Pharmacology*, vol. 61, no. 3, pp. 375–380, 2009.

[34] I. V. Kurochkin and S. Goto, "Alzheimer's β-amyloid peptide specifically interacts with and is degraded by insulin degrading enzyme," *FEBS Letters*, vol. 345, no. 1, pp. 33–37, 1994.

[35] Q. Jiang, C. Y. D. Lee, S. Mandrekar et al., "ApoE promotes the proteolytic degradation of Aβ," *Neuron*, vol. 58, no. 5, pp. 681–693, 2008.

[36] J. Du, J. Chang, S. Guo, Q. Zhang, and Z. Wang, "ApoE 4 reduces the expression of Aβ degrading enzyme IDE by activating the NMDA receptor in hippocampal neurons," *Neuroscience Letters*, vol. 464, no. 2, pp. 140–145, 2009.

[37] Y. Kong, L. Ruan, L. Qian, X. Liu, and Y. Le, "Norepinephrine promotes microglia to uptake and degrade amyloid β peptide through upregulation of mouse formyl peptide receptor 2 and induction of insulin-degrading enzyme," *Journal of Neuroscience*, vol. 30, no. 35, pp. 11848–11857, 2010.

[38] D. Luo, X. Hou, L. Hou et al., "Effect of pioglitazone on altered expression of Aβ metabolism-associated molecules in the brain of fructose-drinking rats, a rodent model of insulin resistance," *European Journal of Pharmacology*, vol. 664, no. 1–3, pp. 14–19, 2011.

[39] E. Himeno, Y. Ohyagi, L. Ma et al., "Apomorphine treatment in Alzheimer mice promoting amyloid-β degradation," *Annals of Neurology*, vol. 69, no. 2, pp. 248–256, 2011.

[40] Y. Wang, M. Li, J. Tang et al., "Glucocorticoids facilitate astrocytic amyloid-β peptide deposition by increasing the expression of APP and BACE1 and decreasing the expression of amyloid-β-degrading proteases," *Endocrinology*, vol. 152, no. 7, pp. 2704–2715, 2011.

[41] C. Cabrol, M. A. Huzarska, C. Dinolfo et al., "Small-molecule activators of insulin-degrading enzyme discovered through high-throughput compound screening," *PloS one*, vol. 4, no. 4, p. e5274, 2009.

[42] M. C. Camberos, A. A. Pérez, D. P. Udrisar, M. I. Wanderley, and J. C. Cresto, "ATP inhibits insulin-degrading enzyme activity," *Experimental Biology and Medicine*, vol. 226, no. 4, pp. 334–341, 2001.

[43] E. S. Song, M. A. Juliano, L. Juliano, M. G. Fried, S. L. Wagner, and L. B. Hersh, "ATP effects on insulin-degrading enzyme are mediated primarily through its triphosphate moiety," *Journal of Biological Chemistry*, vol. 279, no. 52, pp. 54216–54220, 2004.

[44] H. Im, M. Manolopoulou, E. Malito et al., "Structure of substrate-free human insulin-degrading enzyme (IDE) and biophysical analysis of ATP-induced conformational switch of IDE," *Journal of Biological Chemistry*, vol. 282, no. 35, pp. 25453–25463, 2007.

[45] N. Noinaj, S. K. Bhasin, E. S. Song et al., "Identification of the allosteric regulatory site of insulysin," *PLoS ONE*, vol. 6, no. 6, Article ID e20864, 2011.

Hindawi Publishing Corporation
Evidence-Based Complementary and Alternative Medicine
Volume 2012, Article ID 245091, 5 pages
doi:10.1155/2012/245091

Research Article

Effect of Toki-Shakuyaku-San on Regional Cerebral Blood Flow in Patients with Mild Cognitive Impairment and Alzheimer's Disease

Teruyuki Matsuoka,[1] Jin Narumoto,[1] Keisuke Shibata,[1] Aiko Okamura,[1] Shogo Taniguchi,[1] Yurinosuke Kitabayashi,[2] and Kenji Fukui[1]

[1] *Department of Psychiatry, Graduate School of Medical Science, Kyoto Prefectural University of Medicine, 465 Kajii-cho, Kawaramachi-Hirokoji, Kamigyo-ku, Kyoto 602-8566, Japan*
[2] *Department of Psychiatry, Gojouyama Hospital, 4-6-3 Rokujo-Nishi, Nara 630-8044, Japan*

Correspondence should be addressed to Teruyuki Matsuoka, tmms2004@koto.kpu-m.ac.jp

Received 12 October 2011; Accepted 18 November 2011

Academic Editor: Paul Siu-Po Ip

The aim of this study was to examine the effect of toki-shakuyaku-san (TSS) on mild cognitive impairment (MCI) and Alzheimer's disease (AD) using single-photon emission computed tomography (SPECT). All subjects were administered TSS (7.5 g/day) for eight weeks. SPECT and evaluations using the Mini Mental State Examination (MMSE), Neuropsychiatric Inventory, and Physical Self-Maintenance Scale were performed before and after treatment with TSS. Three patients with MCI and five patients with AD completed the study. No adverse events occurred during the study period. After treatment with TSS, regional cerebral blood flow (rCBF) in the posterior cingulate was significantly higher than that before treatment. No brain region showed a significant decrease in rCBF. TSS treatment also tended to improve the score for orientation to place on the MMSE. These results suggest that TSS could be useful for treatment of MCI and AD.

1. Introduction

Cholinesterase inhibitors (ChEIs) and memantine, an N-methyl-D-aspartate antagonist, are commonly used in treatment of Alzheimer's disease (AD). These drugs slow the progression of the disease and improve cognition, function, and behavior impairment but often have to be discontinued because of adverse events [1, 2]. There are no approved drugs for treatment of mild cognitive impairment (MCI). A systematic review showed that ChEIs were ineffective in preventing progression of MCI to AD or improving cognitive functions and led to adverse events [3].

There has been a recent increase in the use of traditional herbal medicine for treatment of dementia. Yokukan-san has been shown to improve behavioral and psychological symptoms of dementia (BPSD) [4, 5], hachimi-jio-gan improved cognitive function and activity of daily living (ADL) in AD [6], and choto-san was effective for patients with vascular dementia [7, 8]. Moreover, combination treatment with kami-untan-to and donepezil improved cognitive function and increased regional cerebral blood flow (rCBF) in the bilateral frontal lobes [9].

Toki-shakuyaku-san (TSS) is mainly used for gynecologic disorders but has also been used for treatment of cognitive impairment based on accumulated evidence of its neuroactive and neuroprotective effects. TSS activates cholinergic [10–14] and monoaminergic [12, 13, 15] neurons and has a protective effect on amyloid β [16, 17], an antioxidant effect [18, 19], and an antiapoptosis action [12]. Several clinical studies have also suggested that TSS improves cognitive impairment in dementia, MCI, and poststroke patients [20–22]. Brain imaging may be useful to examine the effects of TSS. Therefore, the aim of this study was to identify the effects of TSS in patients with MCI and AD using single-photon emission computed tomography (SPECT).

2. Methods

2.1. Subjects. The subjects were 13 patients treated at the Center for Diagnosis of Dementia at the Kyoto Prefectural University of Medicine. Four patients were diagnosed with MCI and 9 with AD, based on Petersen et al. [23] and the National Institute of Neurological and Communicative Disease and Stroke-Alzheimer's Disease and Related Disorders Association (NINCDS-ADRDA) criteria for probable AD [24]. We excluded patients with a significant history of psychiatric or neurological disorders (other than MCI and AD), including stroke, head injury, epilepsy, psychiatric disorders, alcohol abuse, or a serious medical condition. Participants had not been prescribed ChEIs or memantine since our center examines patients who have not been diagnosed with dementia. This study was approved by the Ethics Committee of the Kyoto Prefectural University of Medicine. Informed consent was obtained from all of the patients.

2.2. Study Protocol. Subjects were treated with TSS given as a daily dose of 7.5 g of powder for eight weeks. During this period, new medications were not introduced. TSS is registered in the Pharmacopoeia of Japan as Kampo Medicine TJ-23. The TSS used in the study was provided by Tsumura (Tokyo, Japan) and was prepared from the extract of a mixture of dried plants: 4.0 g Paeoniae radix, 4.0 g Atractylodis lanceae rhizoma, 4.0 g Alismatis rhizoma, 4.0 g Hoelen, 3.0 g Cnidii rhizome, and 3.0 g Angelicae radix. All subjects underwent magnetic resonance imaging (MRI) or computed tomography (CT) before treatment. SPECT was performed before and after treatment.

Cognitive impairment was evaluated using the Mini Mental State Examination (MMSE) [25] before and after the study period. The MMSE has 11 subscales including orientation to time, orientation to place, registration, attention, recall, naming, repetition, auditory comprehension/command, reading comprehension, sentence construction, and constructional praxis. BPSD were evaluated before and after the study period using the Neuropsychiatric Inventory (NPI) [26]. The NPI is a caregiver-based clinical instrument that evaluates 10 domains of neuropsychiatric symptoms in dementia: delusions, hallucinations, agitation, depression, anxiety, euphoria, apathy, disinhibition, irritability, and aberrant motor behavior. The frequency score ranges from 0 to 4 points, and the severity score ranges from 0 to 3 points. The NPI score for each subscale is created by multiplying the frequency and severity scores, with a maximum score of 12. Therefore, the NPI total score ranges from 0 to 120. Higher scores denote a greater severity of a symptom. ADL before and after the study period were evaluated using the Physical Self-Maintenance Scale (PSMS) [27], which consists of 6 items related to physical activities: toileting, feeding, dressing, grooming, ambulating, and bathing. A lower total score indicates greater impairment of ADL.

2.3. Image Acquisition and Analysis. Brain perfusion SPECT was performed by intravenous injection of 185 MBq of N-isopropyl-p-[^{123}I]iodoamphetamine (I-123-IMP) (Nihon Mediphysics, Hyogo, Japan) in subjects seated at rest with their eyes open. SPECT imaging commenced 22 min after the injection and continued for 16 min. A triple-head gamma camera (Prism Irix, Picker International, Cleveland, OH, USA) and a low-energy, high-resolution, and parallel collimator were used. Projection data from each camera were obtained in a 128×128 format for 40 angles of 1201 at 8 s per angle (voxel size: $2 \times 2 \times 2$ mm).

Image analysis was performed using Statistical Parametric Mapping (SPM) 8 (Wellcome Department of Cognitive Neurology, University College, London, UK) in Matlab 7.5 (Mathworks Inv., Sherborn, MA, USA). After confirmation of no significant artifacts due to atrophy using MRI or CT scans, all SPECT images were anatomically normalized using the I-123-IMP template (Fujifilm RI Pharma, Tokyo, Japan) matched to the Montreal Neurological Institute (MNI) template. The normalized images were smoothed using a 12-mm full-width half-maximum (FWHM) isotropic Gaussian kernel. To examine regional differences, the images were scaled to a mean global cerebral blood flow of 50 mL/100 g/min.

2.4. Statistical Analysis. A Wilcoxon signed rank test was used to analyze the changes in MMSE, NPI, and PSMS scores. Data were analyzed using SPSS 12.0 J for Windows (SPSS Inc., Chicago, IL, USA). $P < 0.05$ was considered statistically significant. A paired t-test was performed to determine whether TSS affected rCBF in patients with MCI and AD. The X, Y, and Z coordinates provided by SPM approximate the MNI brain space. The statistical thresholds were set to a family-wise error (FWE)-corrected P value of 0.05 at the voxel level.

3. Results

3.1. Subject Characteristics. Eight of the 13 subjects completed the study. Five were discontinued because of poor compliance ($n = 3$), a move to another area ($n = 1$), and refusal to continue ($n = 1$). None of the subjects had adverse events. The characteristics of the 8 subjects who completed the study are shown in Table 1. Six had not been prescribed with a psychoactive drug, 1 had taken risperidone (1 mg/day), and 1 had taken rilmazafone (0.5 mg/day) before the start of the study. Both subjects continued to take these drugs during the study.

3.2. Changes in MMSE, NPI, and PSMS Scores. Changes in MMSE, NPI, and PSMS scores are shown in Table 2. At baseline, cognitive impairment and BPSD were mild, and ADL was high. Scores for the MMSE, NPI total, and PSMS did not change significantly after TSS treatment. Among the MMSE subscales, the score for orientation to place showed a tendency to improve ($P = 0.025$), but the change was not significant using a Bonferroni correction ($P = 0.025 > 0.05/11$) (Table 3).

3.3. Paired t-Test Using SPM. The paired t-test showed a significant increase in rCBF in the posterior cingulate after TSS treatment compared to before treatment (Table 4).

Table 1: Clinical characteristics of subjects who completed the study.

Item	Value
Sex, M/F	3/5
Handedness, R/L	8/0
Age, y.o.	77.8 ± 4.9
Diagnosis, MCI/AD	3/5
Age at onset, y.o.	76.3 ± 4.3
Duration of illness, years	1.6 ± 1.6
Education, years	12.0 ± 1.7

AD: Alzheimer's disease; F: female; L: left; M: male; MCI: mild cognitive impairment; R: right; SD: standard deviation; y.o.: years old.
Values are shown as a number ratio or as the mean ± SD.

Table 2: Changes in MMSE, NPI and PSMS scores from before to after TSS treatment for 8 weeks.

	Baseline mean ± SD	8 weeks mean ± SD	*P* value
MMSE	23.4 ± 3.6	23.9 ± 3.8	0.279
NPI total score	5.5 ± 5.9	3.9 ± 4.6	0.180
PSMS	5.9 ± 0.4	5.4 ± 1.4	0.414

MMSE: Mini Mental State Examination; NPI: Neuropsychiatric Inventory; PSMS: Physical Self-Maintenance Scale; SD: standard deviation.

Table 3: Changes in MMSE subscale scores from before to after TSS treatment for 8 weeks.

	Baseline mean ± SD	8 weeks mean ± SD	*P* value
Orientation to time	3.5 ± 1.6	3.1 ± 2.1	0.414
Orientation to place	3.9 ± 0.4	4.5 ± 0.5	0.025
Registration	3.0 ± 0.0	3.0 ± 0.0	1.000
Attention	3.5 ± 1.6	3.4 ± 1.6	0.655
Recall	1.0 ± 1.2	1.0 ± 0.9	0.891
Naming	2.0 ± 0.0	2.0 ± 0.0	1.000
Repetition	0.9 ± 0.4	1.0 ± 0.0	0.317
Auditory comprehension/command	2.8 ± 0.5	3.0 ± 0.0	0.157
Reading comprehension	1.0 ± 0.0	1.0 ± 0.0	1.000
Sentence construction	1.0 ± 0.0	1.0 ± 0.0	1.000
Constructional praxis	0.9 ± 0.4	0.9 ± 0.4	1.000

MMSE: Mini Mental State Examination; SD: standard deviation.

When the statistical thresholds were set to an uncorrected *P* value of 0.001 at the voxel level and a corrected *P* value of 0.05 at the cluster level, the posterior cingulate was the only brain region that showed a significant increase in rCBF (Figure 1). No brain region showed a significant decrease in rCBF.

4. Discussion

In this study, rCBF in the posterior cingulate was significantly increased after eight weeks of treatment with TSS. The MMSE, NPI total, and PSMS scores did not worsen and adverse events did not occur during the treatment. Moreover, TSS treatment tended to improve the score for orientation to place on the MMSE.

Some clinical studies have demonstrated improvement in cognitive impairment by TSS in dementia and poststroke patients. Inanaga et al. reported improvement in orientation to time and place, spontaneous activity, emotional lability, and motivation in 80 dementia patients (40 with vascular dementia, 38 with AD, and 2 with mixed dementia) after 12 weeks of TSS treatment [20], while Goto et al. demonstrated that TSS is effective in suppressing impairment of visuospatial perception and the lower limbs in poststroke patients [22]. In our subjects, orientation to place tended to improve while other cognitive impairments and BPSD were unchanged. These findings are partly consistent with previous studies and suggest that TSS might be particularly effective for improvement of spatial perception.

TSS treatment in this study was associated with a change in rCBF in the posterior cingulate. This brain region plays an important role in many cognitive functions, including visuospatial orientation, topokinesis, navigation of the body in space, self reflection, autobiographical memory, and assessment of objects in space in terms of first-person orientation [28]. Connections between the posterior cingulate and the parahippocampus are likely to play a major role in memory-related functions [29], and these connections may be disturbed in MCI and AD [30, 31]. Moreover, hypofunction in the posterior cingulate is associated with visuoperceptual deficits in MCI and AD [32], as well as disorientation to time and place in AD [33]. In this study, TSS increased rCBF in the posterior cingulate and improved orientation to place based on the MMSE. Therefore, TSS might be useful for treatment of cognitive impairment associated with the posterior cingulate.

Previous studies have shown that donepezil increases or maintains rCBF, mainly in the frontal lobes [34–37]. In contrast, in this study, TSS increased rCBF in the posterior cingulate. In addition to the cholinergic effect, TSS also has monoaminergic, antiamyloid, antioxidant and antiapoptosis effects [10–19]. Collectively, these results suggest that TSS has different effects on cognitive impairment compared to those of donepezil. Therefore, combining TSS with donepezil might have an additional benefit in treatment of MCI and AD.

The study has several limitations, since it was performed with an open label design with no control group, the observation period was short, and the sample size was small. These limitations may reduce the strength of the results, but the findings were partly consistent with previous studies. Moreover, to our knowledge, this is the first study to demonstrate an effect of TSS on rCBF in patients with MCI and AD.

5. Conclusions

Treatment with TSS significantly increased rCBF in the posterior cingulate and tended to improve orientation to place in MCI and AD patients. Therefore, TSS might be useful for treatment of MCI and AD. Moreover, since the effects of TSS on rCBF may differ from those of donepezil, combination

Table 4: Results of paired t-tests.

Brain area	MNI coordinates at the center of the cluster			Z value at the local maximum	Voxel P value (corrected)	Cluster size	Cluster P value (corrected)
	X	Y	Z				
Posterior cingulate	2	−32	40	5.66	0.002	6	<0.001
	4	−24	44	5.08	0.039	1	0.015

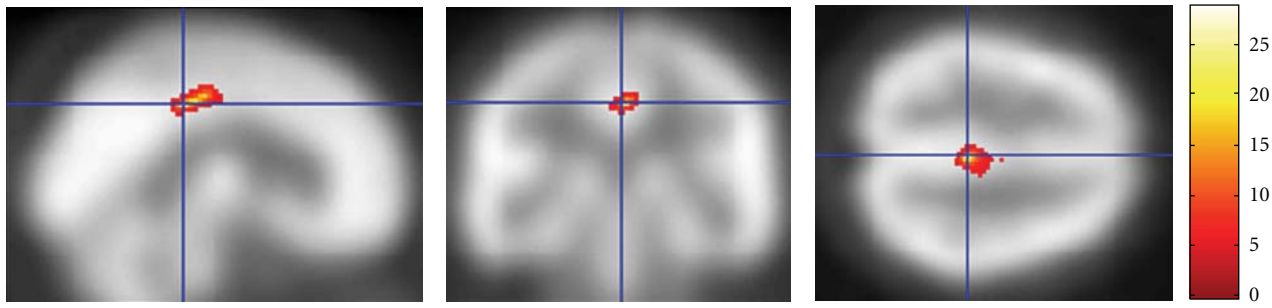

Figure 1: Regions showing a significant increase in rCBF after TSS treatment. The statistical thresholds were set to an uncorrected P value of 0.001 at the voxel level and to a corrected P value of 0.05 at the cluster level.

therapy of TSS and donepezil might be particularly effective. A study in a large number of MCI and AD patients is needed to confirm the effects of TSS.

Conflict of Interests

The authors declare that there is no conflict of interests.

Acknowledgments

This study was supported by a Grant-in-Aid for Young Scientists (B) (19790829) from the Ministry of Education, Culture, Sports, Science and Technology (MEXT) (to Dr. Y. Kitabayashi) and by the research fund of the Institute of Kampo Medicine.

References

[1] R. A. Hansen, G. Gartlehner, A. P. Webb, L. C. Morgan, C. G. Moore, and D. E. Jonas, "Efficacy and safety of donepezil, galantamine, and rivastigmine for the treatment of Alzheimer's disease: a systematic review and meta-analysis," *Clinical Interventions in Aging*, vol. 3, no. 2, pp. 211–225, 2008.

[2] S. J. Thomas and G. T. Grossberg, "Memantine: a review of studies into its safety and efficacy in treating Alzheimer's disease and other dementias," *Clinical Interventions in Aging*, vol. 4, pp. 367–377, 2009.

[3] R. Raschetti, E. Albanese, N. Vanacore, and M. Maggini, "Cholinesterase inhibitors in mild cognitive impairment: a systematic review of randomised trials," *PLoS Medicine*, vol. 4, no. 11, article 338, 2007.

[4] K. Iwasaki, T. Satoh-Nakagawa, M. Maruyama et al., "A randomized, observer-blind, controlled trial of the traditional Chinese medicine Yi-Gan San for improvement of behavioral and psychological symptoms and activities of daily living in dementia patients," *Journal of Clinical Psychiatry*, vol. 66, no. 2, pp. 248–252, 2005.

[5] K. Mizukami, T. Asada, T. Kinoshita et al., "A randomized cross-over study of a traditional Japanese medicine (kampo), yokukansan, in the treatment of the behavioural and psychological symptoms of dementia," *International Journal of Neuropsychopharmacology*, vol. 12, no. 2, pp. 191–199, 2009.

[6] K. Iwasaki, S. Kobayashi, Y. Chimura et al., "A randomized, double-blind, placebo-controlled clinical trial of the Chinese herbal medicine "ba wei di huang wan" in the treatment of dementia," *Journal of the American Geriatrics Society*, vol. 52, no. 9, pp. 1518–1521, 2004.

[7] Y. Shimada, K. Terasawa, T. Yamamoto et al., "A well-controlled study of Choto-san and placebo in the treatment of vascular dementia," *Journal of Traditional Medicines*, vol. 11, pp. 246–255, 1994.

[8] K. Terasawa, Y. Shimada, T. Kita et al., "Choto-san in the treatment of vascular dementia: a double-blind, placebo-controlled study," *Phytomedicine*, vol. 4, no. 1, pp. 15–22, 1997.

[9] M. Maruyama, N. Tomita, K. Iwasaki et al., "Benefits of combining donepezil plus traditional Japanese herbal medicine on cognition and brain perfusion in Alzheimer's disease: a 12-week observer-blind, donepezil monotherapy controlled trial," *Journal of the American Geriatrics Society*, vol. 54, no. 5, pp. 869–871, 2006.

[10] M. Fujiwara and K. Iwasaki, "Toki-Shakuyaku-San and Oren-Gedoku-To improve the disruption of spatial cognition induced by cerebral ischaemia and central cholinergic dysfunction in rats," *Phytotherapy Research*, vol. 7, no. 7, pp. S60–S62, 1993.

[11] T. Itoh, S. Michijiri, S. Murai et al., "Regulatory effect of danggui-shaoyao-san on central cholinergic nervous system dysfunction in mice," *American Journal of Chinese Medicine*, vol. 24, no. 3-4, pp. 205–217, 1996.

[12] N. Hagino, "Kampo medicine and neuroendocrine—from here to molecular biology," *Journal of Traditional Medicines*, vol. 13, pp. 105–117, 1996.

[13] K. Toriizuka, P. Hou, T. Yabe, K. Iijima, T. Hanawa, and J. C. Cyong, "Effects of Kampo medicine, Toki-shakuyaku-san (Tang-Kuei-Shao-Yao-San), on choline acetyltransferase

activity and norepinephrine contents in brain regions, and mitogenic activity of splenic lymphocytes in ovariectomized mice," *Journal of Ethnopharmacology*, vol. 71, no. 1-2, pp. 133–143, 2000.

[14] I. Hatip-Al-Khatib, F. B. Hatip, Y. Yoshimitsu et al., "Effect of Toki-Shakuyaku-San on acetylcholine level and blood flow in dorsal hippocampus of intact and twice-repeated ischemic rats," *Phytotherapy Research*, vol. 21, no. 3, pp. 291–294, 2007.

[15] Q. H. Song, K. Toriizuka, G. B. Jin, T. Yabe, and J. C. Cyong, "Long term effects of Toki-shakuyaku-san on brain dopamine and nerve growth factor in olfactory-bulb-lesioned mice," *Japanese Journal of Pharmacology*, vol. 86, no. 2, pp. 183–188, 2001.

[16] N. Egashira, K. Iwasaki, Y. Akiyoshi et al., "Protective effect of Toki-shakuyaku-san on amyloid β25-35- induced neuronal damage in cultured rat cortical neurons," *Phytotherapy Research*, vol. 19, no. 5, pp. 450–453, 2005.

[17] Y. Y. Liu and T. Kojima, "Protective effects of Toki-Shakuyaku-San Tsumra Japan-23 (TJ-23) on β-amyloid protein (β40)-induced apoptosis in pheochromocytoma-12 (PC12) cells," *Journal of Health Science*, vol. 53, no. 2, pp. 196–201, 2007.

[18] Y. Ueda, M. Komatsu, and M. Hiramatsu, "Free radical scavenging activity of the Japanese herbal medicine Toki-Shakuyaku-San (TJ-23) and its effect on superoxide dismutase activity, lipid peroxides, glutamate, and monoamine metabolites in aged rat brain," *Neurochemical Research*, vol. 21, no. 8, pp. 909–914, 1996.

[19] M. Ito, M. Ohbayashi, M. Furukawa, and S. Okoyama, "Neuroprotective effects of TJ-23 (Tokishakuyakusan) on adult rat motoneurons following peripheral facial nerve axotomy," *Otolaryngology-Head and Neck Surgery*, vol. 136, no. 2, pp. 225–230, 2007.

[20] K. Inanaga, K. Dainoson, Y. Ninomiya et al., "Effects of Toki-Shakuyaku-San in patients with senile cognitive disorders," *Progress in Medicine*, vol. 16, pp. 293–300, 1996 (Japanese).

[21] Y. Kitabayashi, K. Shibata, T. Nakamae, J. Narumoto, and K. Fukui, "Effect of traditional Japanese herbal medicine toki-shakuyaku-san for mild cognitive impairment: SPECT study," *Psychiatry and Clinical Neurosciences*, vol. 61, no. 4, pp. 447–448, 2007.

[22] H. Goto, N. Satoh, Y. Hayashi et al., "A Chinese herbal medicine, tokishakuyakusan, reduces the worsening of impairments and independence after stroke: a 1-year randomized, controlled trial," *Evidence-based Complementary and Alternative Medicine*, vol. 2011, article 194046, 2011.

[23] R. C. Petersen, G. E. Smith, S. C. Waring, R. J. Ivnik, E. G. Tangalos, and E. Kokmen, "Mild cognitive impairment: clinical characterization and outcome," *Archives of Neurology*, vol. 56, no. 3, pp. 303–308, 1999.

[24] G. McKhann, D. Drachman, and M. Folstein, "Clinical diagnosis of Alzheimer's disease: report of the NINCDS-ADRDA work group under the auspices of Department of Health and Human Services Task Force on Alzheimer's disease," *Neurology*, vol. 34, no. 7, pp. 939–944, 1984.

[25] M. F. Folstein, S. E. Folstein, and P. R. McHugh, ""Mini mental state". A practical method for grading the cognitive state of patients for the clinician," *Journal of Psychiatric Research*, vol. 12, no. 3, pp. 189–198, 1975.

[26] J. L. Cummings, M. Mega, K. Gray, S. Rosenberg-Thompson, D. A. Carusi, and J. Gornbein, "The neuropsychiatric inventory: comprehensive assessment of psychopathology in dementia," *Neurology*, vol. 44, no. 12, pp. 2308–2314, 1994.

[27] M. P. Lawton and E. M. Brody, "Assessment of older people: self-maintaining and instrumental activities of daily living," *Gerontologist*, vol. 9, no. 3, pp. 179–186, 1969.

[28] B. A. Vogt and S. Laureys, "Posterior cingulate, precuneal and retrosplenial cortices: cytology and components of the neu ral network correlates of consciousness," *Progress in Brain Research*, vol. 150, pp. 205–217, 2005.

[29] B. A. Vogt, D. M. Finch, and C. R. Olson, "Functional heterogeneity in cingulate cortex: the anterior executive and posterior evaluative regions," *Cerebral Cortex*, vol. 2, no. 6, pp. 435–443, 1992.

[30] Y. Zhou, J. H. Dougherty Jr., K. F. Hubner, B. Bai, R. L. Cannon, and R. K. Hutson, "Abnormal connectivity in the posterior cingulate and hippocampus in early Alzheimer's disease and mild cognitive impairment," *Alzheimer's and Dementia*, vol. 4, no. 4, pp. 265–270, 2008.

[31] R. Heun, K. Freymann, M. Erb et al., "Successful verbal retrieval in elderly subjects is related to concurrent hippocampal and posterior cingulate activation," *Dementia and Geriatric Cognitive Disorders*, vol. 22, no. 2, pp. 165–172, 2006.

[32] M. Alegret, G. Vinyes-Junqué, M. Boada et al., "Brain perfusion correlates of visuoperceptual deficits in mild cognitive impairment and mild Alzheimer's disease," *Journal of Alzheimer's Disease*, vol. 21, no. 2, pp. 557–567, 2010.

[33] N. Hirono, E. Mori, K. Ishii et al., "Hypofunction in the posterior cingulate gyrus correlates with disorientation for time and place in Alzheimer's disease," *Journal of Neurology Neurosurgery and Psychiatry*, vol. 64, no. 4, pp. 552–554, 1998.

[34] R. T. Staff, H. G. Gemmell, M. F. Shanks, A. D. Murray, and A. Venneri, "Changes in the rCBF images of patients with Alzheimer's disease receiving Donepezil therapy," *Nuclear Medicine Communications*, vol. 21, no. 1, pp. 37–41, 2000.

[35] S. Nakano, T. Asada, H. Matsuda, M. Uno, and M. Takasaki, "Donepezil hydrochloride preserves regional cerebral blood flow in patients with Alzheimer's disease," *Journal of Nuclear Medicine*, vol. 42, no. 10, pp. 1441–1445, 2001.

[36] Y. Ushijima, C. Okuyama, S. Mori, T. Kubota, T. Nakai, and T. Nishimura, "Regional cerebral blood flow in Alzheimer's disease: comparison between short and long-term donepezil therapy," *Annals of Nuclear Medicine*, vol. 20, no. 6, pp. 425–429, 2006.

[37] S. Shimizu, H. Hanyu, T. Iwamoto, K. Koizumi, and K. Abe, "SPECT follow-up study of cerebral blood flow changes during Donepezil therapy in patients with Alzheimer's disease," *Journal of Neuroimaging*, vol. 16, no. 1, pp. 16–23, 2006.